Impact de l'infection par Porphyromonas gingivalis sur la réponse inflammatoire locale et systémique

Isaac Maximiliano Bugueno Valdbenito

UNIVERSITÉ DE STRASBOURG

École Doctorale Sciences de la Vie et de la Santé

Unité de recherche Inserm-Unistra UMR 1260 « Nanomédecine Régénérative »

« Impact de l'infection par *Porphyromonas gingivalis* sur la réponse inflammatoire locale et systémique »

THÈSE

Présentée et soutenue publiquement le **22 Novembre 2019** par

Isaac Maximiliano Bugueno Valdebenito

Pour obtenir le grade de **Docteur de l'Université de Strasbourg**

Directeur de Thèse	**Dr Olivier HUCK** *Professeur des Universités, Université de Strasbourg.*
Rapporteurs Externes	**Dr Assem SOUEIDAN** *Professeur des Universités, Université de Nantes.*
	Dr Kerstin GRITSCH *Professeur des Universités, Université Claude Bernard Lyon 1.*
Examinateur Interne	**Dr Agnès BLOCH-ZUPAN** *Professeur des Universités, Université de Strasbourg.*
Membre invité	**Dr Nadia BENKIRANE-JESSEL**

"Vale más actuar exponiéndose
a arrepentirse de ello,
que arrepentirse
de no haber hecho nada"
(Boccacio)

« Mieux vaut agir en s'exposant
au regret
que regretter de n'avoir rien fait »
(Boccacio)

Remerciements

***J**e tiens à adresser mes remerciements et ma reconnaissance au Dr Assem Soueidan, au Dr Kerstin Gritsch et au Dr Agnès Bloch - Zupan, qui m'ont fait l'honneur de consentir à l'évaluation de ces travaux de thèse et de participer à mon jury lors de ma soutenance de thèse. Un grand merci pour l'intérêt que vous avez porté à cette recherche.*

Cette thèse de doctorat a été réalisée au sein de l'unité de recherche INSERM UMR 1260 « Nanomédecine Régénérative », dirigée par le Dr Nadia Benkirane - Jessel, à qui je souhaite exprimer mes remerciements pour m'avoir donné l'opportunité d'intégrer cette unité de recherche pendant cinq ans et demi, et d'avoir pu y réaliser ma thèse.

Je tiens ensuite à remercier particulièrement le Dr Olivier Huck, pour son soutien à tout moment dès mon arrivée à Strasbourg, pour son enseignement, sa disponibilité, son encadrement, surtout pour son énorme sympathie et bonne humeur et d'avoir cru en moi, d'un point de vue professionnel et humain.

Je tiens également à remercier très chaleureusement tous les membres de l'équipe du laboratoire qui m'ont accompagné depuis mon arrivée à Strasbourg, lorsque j'ai réalisé mon stage en 2014, puis mes stages de Master et jusqu'à aujourd'hui où je franchis cette nouvelle étape. Merci pour les bons moments de rire et d'écoute.

Merci Sabine, pour toute ton aide et ta disponibilité, pour les rires partagés et nos envies de voyager, pendant toutes ces années. Merci Arielle, pour tous tes conseils, pour ton soutien pendant ces années, et pour toujours croire en moi. Merci Hervé, pour ta patience, pour ton écoute et pour être toujours prêt à m'aider.

Je remercie spécialement mon « Team Pg Strasbourg ». Merci Linda pour toute ta joie et ta merveilleuse sympathie, ainsi que pour la confiance et l'admiration que tu m'as toujours données. Merci Fareeha pour tous les moments partagés avec du bonheur et pour être ma collègue de doctorat toutes ces années. Merci Catherine pour ton aide précieuse pendant ces années à Strasbourg, pour prendre soin de mon chien avec amour et pour ton sourire dans toutes les situations. Merci à Porphyromonas gingivalis pour nous avoir accompagnés au cours de cette grande étape de nos vies et avoir rendu possible l'union de ce groupe.

Un grand merci à mes divers collègues de bureau, qui déménageaient en continu et sans qui mes journées n'auraient pas été aussi sympathiques. À David, qui a été mon premier collègue à mon arrivée et les 3 années suivantes et qui m'a permis de découvrir la véritable Alsace et l'amitié. À Quentin, avec qui nous avons partagé des conversations profondes et qui m'a toujours remonté le moral dans des moments difficiles, à Damien qui n'était pas souvent avec nous, mais toujours avec son énorme sympathie et charisme. Enfin, mes innombrables collègues, Aggeliki, Merve, Rana, Ryan parmi tant d'autres, qui m'ont permis à l'heure actuelle d'avoir de beaux souvenirs de mes journées au laboratoire et de nos pauses déjeuner.

Enfin, je tiens à remercier mon ex-équipe de recherche du laboratoire de Microbiologie Orale de l'Université du Chili, les professeurs Denisse Bravo, Anilei Hoare, Leyla Gomez, Patricia Palma, Nora Silva et Marta Gajardo, ainsi que mes collègues Darna Venegas, Daniela Salinas, Cristopher Soto y

Leonor Diaz, qui m'ont vu m'initier à la recherche et m'ont vu grandir à la faculté de chirurgie dentaire. C'est ainsi, grâce au soutien et au financement du Chili, que je suis actuellement en train de franchir cette nouvelle étape du doctorat.

J'adresse un gigantesque merci particulièrement à ma mère Noemí Valdebenito et à mes chers grands-parents, Audelio et Rosario, pour tout leur soutien et toute leur affection dont ils ont fait preuve à mon égard tout au long des années où ils m'ont vu grandir. Pour toutes les peines infligées et surtout les joies. Grâce à eux et à Dieu, je suis aussi arrivé où je suis maintenant.

Finalement, je tiens à remercier mes amis et ceux que j'aime sans avoir de lien sanguin, ceux qui ont été présents depuis le début de cette thèse ou même ceux qui sont arrivés à la fin, mais que je souhaite remercier le plus chaleureusement possible : Marion, pour tous ces longs et merveilleux voyages ensemble, pour être apparue sur mon chemin à Strasbourg et pour avoir partagé ensemble des chagrins et surtout des joies. Merci à John, d'avoir été le meilleur colocataire que j'ai pu avoir et d'être toujours un ami inconditionnel. À David et Laetitia, pour toujours être là pour moi, surtout pour m'écouter aux moments difficiles. À Liliane pour être une amie inconditionnelle et même si nos chemins se sont croisés depuis pas longtemps, tu es devenue quelqu'un de précieux dans ma vie. Ainsi, spécialement à Raphaël, que j'ai eu la grande chance de croiser cette année et qui m'a donné son soutien et son affection. Enfin à Maxime, Pierre, Lola, Mathieu, Quentin, Anvita, Terry, Celine, Pascale, Arnold, Kevin, Catalina, Josefina, Tomi, Cécile, Marion la Chilienne, Heidy, Barbara, Alvini, Ionna, Penny, Gabrielle, AFI, Claudio, Mykolas, Alexandra, Clément, parmi d'autres, avec qui j'ai partagé des moments inoubliables à Strasbourg. Je souhaite que cela continue ainsi dans le futur.

Je souhaiterais enfin remercier tous mes proches, mon frère, ma sœur, et tous ceux qui de loin m'ont toujours épaulé tout au long de ma vie et de ma thèse.

Table des matières

Liste des abréviations

Aa : *Aggregatibacter actinomycetemcomitans*
AE : Attache épithélial
Apaf-1 : Facteur apoptotique activant la protéase-1
ARNdb : ARN synthétique double-brin viral
ARNss : ARN simple brin viraux
BH3 : Famille de protéines Blc-2-Homologue-3
C : Cément radiculaire
CA : Crête alvéolaire
CATB : Cathepsin B
CARD : Domaines de recrutement des caspases
CDK4 : Kinase dépendante des cyclines 4
CML : Cellules musculaires lisses
COX-2 : Cyclooxygénase-2
CpG : Segment d'ADN de deux nucléotides CG
CR1 : Récepteur C3b du complément 1
CRP : Protéine C réactive
DISC : Complexe de signalisation induisant la mort
EC : Cellules endothéliales
EJ : Épithélium jonctionnel
EMV : Microvésicules d'origine endothéliale
eNOS : Oxyde nitrique synthase endothéliale
FADD: Domaine Fas associée à la mort
GA : Gencive attachée
GCF : Fluide gingival
GEC : Cellules épithéliales gingivales
GL : Gencive libre
IAP: Inhibiteurs de l'apoptose
Icam : Protéine d'adhésion intercellulaire
IFN : Interféron
IKK : Kinase inhibitrice du complexe NF-κB
IL-(n) : Interleukine (n°)
ILGF : Facteurs de croissance analogues à l'insuline
iNOS : Oxyde nitrique inductible
IRAK(n) : La kinase (n°) associée au récepteur de l'interleukine-1
IRF : Facteur de régulation de l'interféron
JAC : Jonction amélo-cémentaire
JNK : Kinase JUN N-terminale
LDL : Lipoprotéines de basse densité
LMG : Ligne muco-gingivale
LP : Ligament parodontal
LPS : Lipopolysaccharide
MAL: Analogue de l'adaptateur de la réponse primaire de différenciation myéloïde 88
MAPK : Protéines kinases activées par des mitogènes
mDC : Cellule dendritique myéloïde
miRNA : microRNAs
MKK : Protéine kinase activée par un mitogène
MMP : Métalloprotéases matricielles
MMP-9 : Métalloprotéase 9
MMV : Microvésicules provenant de monocytes
MOI : Multiplicité d'infection
MV : Microvésicules
Myd88 : La réponse primaire de différenciation myéloïde 88
NOD / NB-ARC : Domaine de liaison et d'oligomérisation des nucléotides
NO : Oxyde nitrique
OA : Os alvéolaire
PAMP : Motifs moléculaires associés aux pathogènes
PDGF : Facteur de croissance dérivé des plaquettes

PhtdSer : Phosphatidylsérine
***Pg*-LPS :** Lipopolysaccharide de *Porphyromonas gingivalis*
PI3K : Phosphatidylinositol-3-kinase
PMV : Microvésicules plaquettaires
PNN : Neutrophiles polynucléaires
PSD : Synergie polymicrobienne et dysbiose
RANK-L : Récepteur activateur du facteur nucléaire kappa-B - ligand
RE : Réticulum endoplasmique
RTqPCR: Réaction quantitative en chaîne par polymérase en temps réel
SARM : Protéine stérile contenant un motif « tatou » et un motif α
Smac : Deuxième activateur mitochondrial des caspases
SOD-1 : Superoxyde dismutase 1
TAB : protéine de liaison à TAK1
TC : Tissu conjonctif
TGFβ : Facteur de croissance transformant bêta
TIR : Domaine du récepteur Toll / interleukine-1
TLR : Récepteur “Toll-like”
TNF-α : Facteur de nécrose tumorale
TRAF6 : Facteur 6 associé au récepteur du facteur de nécrose tumorale
TRAM : Molécule adaptatrice liée au TRIF
TRIF : Adaptateur contenant le domaine TIR induisant l’nterféron-β
Ub : Ubiquitin
Vcam : Protéine d'adhésion cellulaire vasculaire
VM : Vésicules membranaires
WD40 : Motif structurel court d'environ 40 acides aminés
XIAP : Protéine inhibitrice de l'apoptose liée au chromosome X

Liste des figures

Liste des annexes

I. Liste des publications scientifiques

II. Conférences scientifiques nationales et internationales

III. Annexe n°1

Bugueno IM., Khelif Y., Seelam N., Morand DN., Tenenbaum H., Davideau JL., Huck O. *"Porphyromonas gingivalis* Differentially modulates Cell death profile in Ox-LDL and TNF-a pre- treated Endothelial Cells". **PLoS One 2016, 11(4): e0154590.**

IV. Annexe n°2

Korah L., Amri N., **Bugueno I.M**., Hotton E., Tenenbaum H., Huck O., Berdal A., Davideau J.L. Experimental periodontitis in Msx2 mutant mice induces alveolar bone necrosis. **Journal of Periodontology 2019, Doi:10.1002/JPER.16-0435**

V. Annexe n°3

Lapérine O., Cloitre A., Caillon J., Huck O., **Bugueno I.M.,** Sourice S., Le Tilly E., Palmer G., Davideau J.L., Geoffroy V., Guicheux J., Beck-Cornier S., Lesclous P. "Interleukin-33 and RANK-L Interplay in the Alveolar Bone Loss Associated to Periodontitis", **PLoS ONE 11(12): e0168080. doi:10.1371/journal.pone.0168080.**

VI. Annexe n°4

Cloitre A., Halgand B., Sourice S., Caillon J., Huck O., **Bugueno I.M.**, Batool F., Guicheux J., Geoffroy V., Lesclous P. "IL-36γ is a pivotal inflammatory player in periodontitis-associated bone loss", **Scientific Reports** *(2019) 9:19257.*

1. INTRODUCTION

I. Le parodonte

Le parodonte est composé par l'ensemble des tissus de soutien dentaires. Il comprend : l'os alvéolaire, le ligament alvéolo-dentaire ou desmodonte, la gencive, le cément radiculaire ainsi que des éléments nerveux et sanguins (Bosshardt and Lang, 2005 ; Pihlstrom et al., 2005 ; Auriol et al., 2000) **(Figure n°1).**

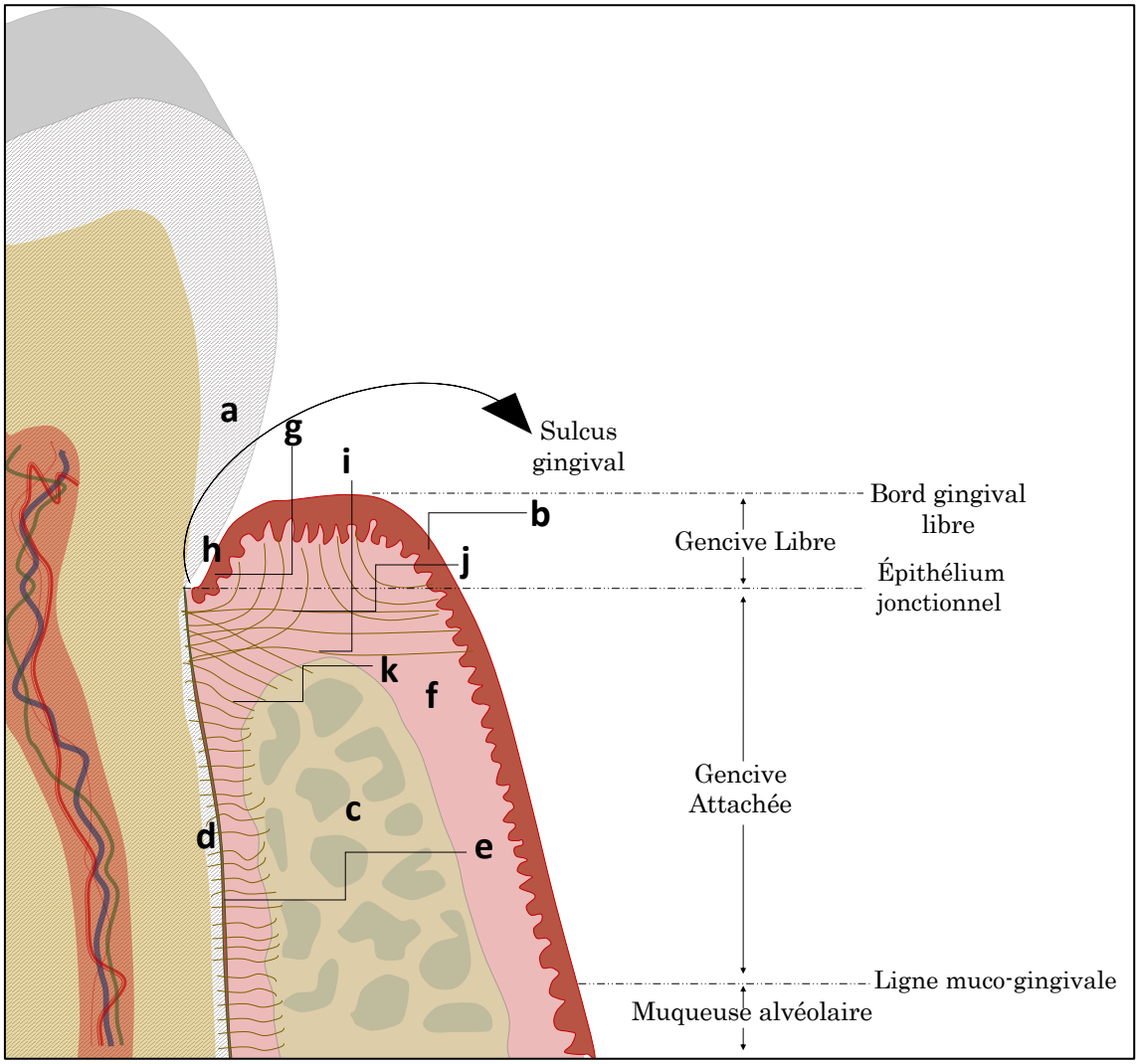

Figure n°1. Schéma du parodonte. *Il représente les tissus de soutien dentaires et est constitué par l'os alvéolaire (c), le ligament alvéolo-dentaire ou desmodonte (e), la gencive (f) et le cément radiculaire (d). La gencive est classiquement subdivisée en différentes zones topographiques, la gencive libre, la gencive attachée et la gencive interdentaire. Plus précisément, la gencive est composée par l'épithélium gingival buccal (b), l'épithélium sulculaire (g), l'épithélium jonctionnel (h) et le tissu conjonctif (k).*

I.A. La gencive

La gencive est en continuité avec la muqueuse buccale et constitue la partie la plus superficielle du parodonte. Elle débute au niveau de la ligne muco-gingivale (LMG) et recouvre la partie coronaire des procès alvéolaires. La LMG est absente au niveau du palais. Elle fait, à cet endroit, partie de la muqueuse palatine kératinisée, non mobile. La gencive se termine au niveau du collet des dents où elle les entoure et forme un anneau épithélial, l'épithélium jonctionnel (EJ). Elle assure ainsi la continuité du recouvrement épithélial de la cavité buccale (Bosshardt, 2018 ; Bosshardt and Lang, 2005 ; Pöllänen et al., 2012 ; Auriol et al., 2000).

I.A.1. Zones topographiques de la gencive

La gencive est classiquement subdivisée en différentes zones topographiques : la gencive libre, la gencive attachée et la gencive interdentaire (Bosshardt and Lang, 2005).

i. **La gencive libre ou marginale :** c'est la portion de gencive étroite, mobile, festonnée et sans soutien osseux qui se termine coronairement par un bord effilé en lame de couteau ou bord gingival libre. Elle est recouverte par un épithélium kératinisé. Elle est séparée de la surface dentaire par un espace virtuel que l'on appelle sillon gingivo-dentaire ou sulcus. Cette gencive se termine apicalement par le sillon gingival libre ou sillon marginal qui la sépare de la gencive attachée. Ce sillon se situe au niveau de la jonction amélo-cémentaire. Cette partie de gencive n'est donc pas fixée mécaniquement à la dent mais est fixée par simple adhésion.

ii. **La gencive attachée :** elle est limitée en direction apicale par la LMG qui la sépare de la muqueuse alvéolaire. Elle possède une consistance ferme, une couleur rose corail et présente souvent une surface finement granitée qui lui donne l'aspect d'une peau d'orange. La hauteur de la gencive attachée augmente avec l'âge (Srivastava et al., 1990 ; Tenenbaum and Tenenbaum, 1986). Elle varie selon les individus, entre les différents types de dents, de la position sur l'arcade et de la localisation des freins ou attaches musculaires. Elle sert de rupteur de force pour la gencive libre contre les sollicitations musculaires qui s'étendent au sein de la muqueuse alvéolaire car elle est fermement solidarisée à la dent par les fibres du tissu conjonctif et à l'os alvéolaire sous-jacent.

iii. **La papille interdentaire :** la gencive interdentaire s'enfonce contre le septum interdentaire apicalement par rapport au point de contact (ou à la surface de contact). Dans les secteurs antérieurs, la papille interdentaire est lancéolée tandis que dans les zones molaires, les papilles sont plus aplaties, pyramidales dans le sens vestibulo-

lingual. Comme la papille interdentaire a un profil qui suit le contour des surfaces de contact interproximales, une dépression ou col se situe entre la papille vestibulaire et la papille linguale (Berglundh et al., 1991 ; Dale, 2002).

I.A.2. L'histomorphologie de la gencive

D'un point de vue histomorphologique, la gencive est constituée d'une composante épithéliale et d'une composante conjonctive (Berglundh et al., 1991 ; Bosshardt, 2018; Bosshardt and Lang, 2005 ; Pöllänen et al., 2012) **(Figures n°2 et 3).**

i. L'épithélium

L'épithélium qui recouvre la gencive peut être différencié en trois types :

a. L'épithélium buccal

Il s'agit d'un épithélium pavimenteux, stratifié, kératinisé qui présente des digitations épithéliales dans le chorion gingival. Il comprend quatre couches. On distingue de la lame basale vers la partie la plus externe (Pöllänen et al., 2003 ; Salonen and Santti, 1985) (Figure n°2) :

- Les cellules de la couche basale (*stratum germinatum*) sont soit cylindriques, soit cuboïdes et sont en contact avec la membrane basale. Les cellules basales possèdent la capacité de se diviser. La couche basale peut être considérée comme le réservoir des cellules progénitrices.
- La couche épineuse (*stratum spinosum*) de l'épithélium est constituée de 10 à 20 couches de cellules relativement larges, polyédriques, munies de prolongements cytoplasmiques courts. Les cellules sont attachées entre elles par de nombreux hémidesmosomes.
- La couche granuleuse (*stratum granulosum*) est formée de cellules comportant des corps électro-denses de kérato-hyaline et des amas de granules contenant du glycogène commencent à apparaître. Ces granules semblent en relation avec la synthèse de kératine.
- Les cellules de la couche cornée (*stratum corneum*) possèdent un cytoplasme rempli de kératine et la totalité de l'appareil de synthèse protéique et de production d'énergie a disparu (noyau, mitochondries, réticulum endoplasmique et appareil de Golgi).

b. L'épithélium sulculaire

Il fait face à la dent. Il s'agit d'un épithélium pavimenteux stratifié non kératinisé (Pöllänen et al., 2003 ; Salonen and Santti, 1985).

c. L'épithélium jonctionnel

L'EJ dont la hauteur peut atteindre 2 mm, entoure le collet de la dent comme un anneau (Crawford and Hopp, 1990 ; Pöllänen et al., 2003). Cet EJ est en continuité avec l'épithélium sulculaire et participe à l'attache entre la gencive et la dent. Dans sa partie apicale, il n'est constitué que de quelques couches cellulaires alors que coronairement il est composé de 15 à 30 couches. L'EJ est composé de deux couches, la couche basale (active sur le plan de la division cellulaire) et la couche supra-basale (cellules filles). Les cellules basales ainsi que les cellules supra-basales sont allongées selon un axe parallèle à la surface de la dent. La membrane des cellules de l'EJ présente des hémidesmosomes en direction de l'émail (Crawford and Hopp, 1990 ; Dale, 2002 ; Olsson and Lindhe, 1991 ; Pöllänen et al., 2003 ; Salonen and Santti, 1985) **(Figure n°2).**

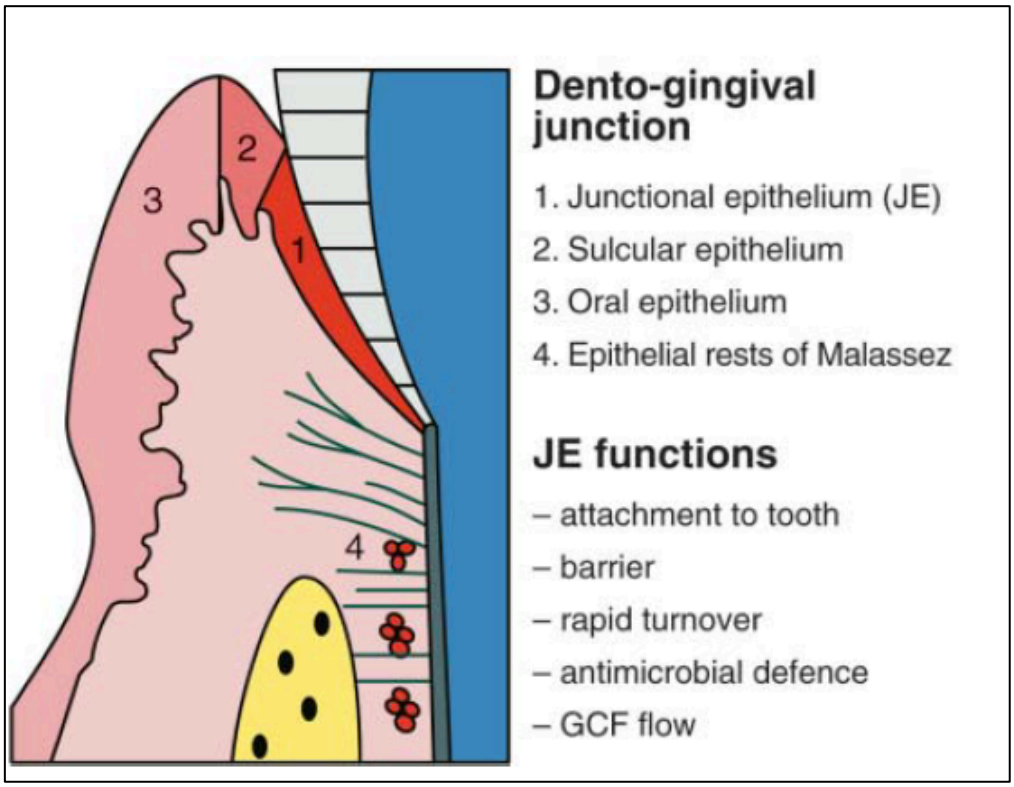

Figure n°2. Illustration schématique des différents types d'épithélium à la jonction dento-gingivale. *L'épithélium de jonction présente un phénotype différent qui permet au tissu de se fixer à la surface de la dent et de participer à la défense de l'hôte (Pöllänen et al., 2003).*

ii. Le tissu conjonctif gingival

C'est le tissu prédominant de la gencive. Il est composé de fibres de collagène (60% du volume tissulaire, de fibroblastes (5%), de vaisseaux et de nerfs enchâssés dans une matrice extracellulaire (35%) (Berglundh et al., 1991 ; Olsson and Lindhe, 1991 ; Pöllänen et al., 2003).

a. Les cellules du tissu conjonctif

Les cellules du tissu conjonctif sont les fibroblastes (65% de la population cellulaire totale). Les fibroblastes sont situés entre les fibres de collagène, leur orientation spatiale étant conditionnée par l'organisation des faisceaux fibrillaires. Le fibroblaste est impliqué dans la production de divers types de fibres retrouvées dans le tissu conjonctif et dans la synthèse de la matrice extracellulaire du tissu conjonctif (Higa et al., 2017). Des cellules immunitaires, myéloïdes (monocytes, macrophages, leucocytes), lymphoïdes (lymphocytes T et B, plasmocytes), mastocytes (responsables de la production de certains composants de la matrice extracellulaire) et cellules accessoires (les cellules présentant l'antigène, les plaquettes, les cellules endothéliales, les cellules dendritiques) sont également retrouvées (Moutsopoulos and Konkel, 2018 ; Wu et al., 2014).

b. Les fibres du tissu conjonctif

Ce sont les fibres de collagène, de réticuline, d'oxytalane et les fibres élastiques. Les fibres collagènes constituent la composante essentielle du parodonte. Elles possèdent de nombreuses propriétés biophysiques et biochimiques qu'elles confèrent aux tissus (résistance aux tractions et aux forces mécaniques, souplesse, digestion par des enzymes protéolytiques (collagénases, protéases)). Ces fibres confèrent à la gencive une forme stable, et si elles se fixent en dessous de l'EJ, elles les protègent contre les forces de cisaillement et stabilisent les dents. Au sens large, les fibres périosto-gingivales peuvent également être comptées parmi les fibres gingivales. Elles fixent la gencive sur le procès alvéolaire. Selon leur insertion et leur trajet à travers les tissus, les faisceaux orientés dans la gencive peuvent être divisés en plusieurs groupes (Berglundh et al., 1991 ; Dale, 2002 ; Lopez et al., 1976 ; Palmer and Lubbock, 1995 ; Romanos and Bernimoulin, 1990).

Les fibres dento-gingivales comprennent les fibres circulaires et semi-circulaires, les fibres dento-périostées, les fibres transeptales et on trouve aussi les fibres alvéolo-gingivales, interpapillaires, transgingivales, périosto-gingivales, intercirculaires et intergingivales.

Les fibres de réticuline sont des fibres qui se trouvent normalement connectées aux fibres de collagène les plus fortes. Elles correspondent à des fibrilles de collagène récemment formées, qui peuvent poursuivre leur polymérisation et se transformer en fibres et en faisceaux. Elles sont présentes aux interfaces entre l'épithélium et le tissu conjonctif (Lopez et al., 1976 ;

Lorencini et al., 2009 ; Romanos and Bernimoulin, 1990). Les fibres élastiques n'ont pas une structure homogène. Elles comportent invariablement deux composantes étroitement liées : une composante centrale amorphe, l'élastine (90% de la fibre élastique mature) et une composante microfibrillaire périphérique (Lopez et al., 1976 ; Lorencini et al., 2009 ; Palmer and Lubbock, 1995).

c. La matrice extracellulaire

La matrice extracellulaire est essentiellement produite par les fibroblastes bien que certains constituants le soient par les mastocytes et d'autres composants dérivés du sang. Elle constitue le milieu dans lequel les cellules du tissu sont incluses et elle est essentielle au maintien des fonctions normales du tissu. C'est en son sein qu'a lieu le transport des fluides biologiques, des électrolytes, des nutriments, des métabolites vers et à partir des cellules du tissu conjonctif. Le constituant majeur de cette matrice extracellulaire est représenté par les macromolécules telles que certaines protéines polysaccharidiques, glycoprotéines et protéoglycanes (Romanos and Bernimoulin, 1990).

I.B. La muqueuse alvéolaire

La gencive se termine au niveau de la jonction muco-gingivale et continue du côté alvéolaire par la muqueuse alvéolaire qui recouvre la face interne des lèvres et des joues. La muqueuse alvéolaire se distingue de la gencive par sa couleur plus rouge, son aspect plus lisse et sa mobilité relative par rapport aux plans sous-jacents. Elle est attachée de manière lâche au périoste de l'os alvéolaire vestibulaire et lingual sous-jacent. Elle effectue sa jonction avec la muqueuse jugale et labiale au fond du vestibule. Le vestibule est un espace virtuel délimité apicalement par la zone de déflexion entre la muqueuse alvéolaire et les muqueuses jugales et labiales et, coronairement, par la face externe de la gencive kératinisée (Karring et al., 1975 ; Katafuchi et al., 2007 ; Palmer and Lubbock, 1995). Histologiquement, elle est composée d'un épithélium non kératinisé dont l'épaisseur varie entre 0,005 et 0,3 mm et d'un tissu conjonctif riche en fibres élastiques (Chavrier, 1990 ; Lopez et al., 1976).

I.C. L'os alvéolaire

Il est défini comme la partie du maxillaire et de la mandibule qui forme et supporte les procès alvéolaires. Ces procès alvéolaires sont des structures qui dépendent des dents. Ils se développent lors du développement et de l'éruption dentaire et se résorbent largement lors de la perte de l'organe dentaire. Les parois alvéolaires sont bordées d'os compact et les zones inter-

alvéolaires contiennent de l'os spongieux. L'os alvéolaire comprend une corticale externe, un os spongieux médian et une corticale alvéolaire interne que l'on appelle aussi lame cribriforme ou *lamina dura* (Filipowska et al., 2017 ; Florencio-Silva et al., 2015 ; Ho et al., 2013 ; Mori et al., 2015) **(Figure n°3).**D'un point de vue histologique, la paroi alvéolaire présente une épaisseur de 0,1-0,4 mm et est criblée de nombreux petits trous (les canaux de Volkmann) par lesquels les vaisseaux et les fibres nerveuses entrent et sortent de l'espace desmodontal (Filipowska et al., 2017 ; Mori et al., 2015).

I.C.1. Les cellules osseuses

Les ostéoblastes quiescents ou actifs et les ostéoclastes sont présents :

- à la surface des trabécules osseuses dans l'os spongieux,
- sur les surfaces de l'os cortical,
- à l'intérieur de l'os spongieux au niveau des espaces médullaires.

Au cours du processus de maturation et de minéralisation de l'os ostéoïde, quelques ostéoblastes sont enchâssés dans le tissu ostéoïde, les ostéocytes. L'ostéoblaste est impliqué dans l'ostéogenèse de la paroi alvéolaire, en synthétisant le collagène et la substance fondamentale de l'os. L'ostéoclaste (cellule géante spécialisée dans la résorption des tissus minéralisés tels que la dentine, le cément et l'os), est rencontré dans les lacunes de Howship et résorbe la matrice osseuse au cours des remaniements osseux (Saffar et al., 1997 ; Schwartz et al., 1997).

I.C.2. La matrice extracellulaire osseuse

La composition de l'os dépend de ses cellules (ostéoblastes, ostéoclastes et ostéocytes) dont l'activité est partiellement gouvernée par des hormones (PTH, calcitonine, vitamine D, androgènes, œstrogènes…), des facteurs de croissance (TGFβ, PDGF, ILGF, …), des cytokines (interleukines (IL), lymphokines, …), des facteurs locaux (prostaglandines), de la nutrition (calcium) et des facteurs mécaniques. L'os est riche en minéraux tels que le calcium et le phosphate, ainsi que l'hydroxyle de carbonate et de citrate, avec des traces d'autres ions tels que le sodium, le magnésium et le fluor. Les sels minéraux sont répartis en cristaux d'hydroxyapatite. Les espaces situés entre les cristaux sont remplis de matrice organique avec une prédominance de collagène, ainsi que d'eau et de petites quantités de mucopolysaccharides, en particulier la chondroïtine sulfate. Le collagène osseux, qui est seulement produit par les ostéoblastes, est composé essentiellement de collagène de type I avec de petites quantités de

collagène de type III et IV (Foster et al., 2018 ; Ho et al., 2013 ; Mori et al., 2015; Saffar et al., 1997 ; Vignery and Baron, 1980).

I.D. Le ligament alvéolo-dentaire

Le ligament alvéolo-dentaire ou desmodonte permet la jonction entre la dent et l'os alvéolaire. Le desmodonte se définit comme la structure conjonctive située entre le cément radiculaire et l'os alvéolaire, reliant ainsi les dents aux maxillaires par les fibres de Sharpey. Contrairement aux autres structures ligamentaires, ce ligament possède une activité métabolique intense et son potentiel réparateur est plus élevé qu'aucun autre tissu du parodonte (Jönsson et al., 2011 ; Seo et al., 2004 ; Somerman et al., 1990) **(Figure n°3).**

Les processus de cytodifférenciation puis d'histodifférenciation qui aboutiront à la mise en place des tissus parodontaux se produisent au sein du sac folliculaire, à partir des éléments cellulaires (cellules mésenchymateuses indifférenciées de type fibroblastique) d'une part, et à partir des éléments fibrillaires (fibres de collagène) d'autre part. Au cours de l'édification radiculaire, les insertions ligamentaires se mettent en place au fur et à mesure des progrès de la cémentogénèse et de l'ostéogénèse (Bosshardt and Schroeder, 1991 ; Kim et al., 2010 ; Lézot et al., 2000 ; Ripamonti et al., 2009 ; Yu et al., 2011). D'un point de vue histologique, le ligament parodontal est un tissu conjonctif fibreux comprenant des fibroblastes, de la substance fondamentale et des fibres en très grand nombre.

I.D.1. Les cellules du ligament parodontal

Elles peuvent être classées en trois grands groupes en fonction de leur origine et de leur rôle : les cellules conjonctives, les cellules épithéliales et les cellules immunitaires (Jönsson et al., 2011 ; Kim et al., 2010 ; Seo et al., 2004 ; Somerman et al., 1990 ; Yu et al., 2011).

i. **Les cellules conjonctives**
   - le pool fibroblastique (fibroblastes, fibrocytes et myofibroblastes),
   - les cellules osseuses (ostéoblastes, ostéocytes et ostéoclastes),
   - les cellules cémentaires (cémentoblastes, cémentocytes et cémentoclastes),
   - les cellules mésenchymateuses pluripotentes qui seraient capables par division et différenciation de remplacer chacun des types cellulaires présents dans l'espace desmodontal.

ii. **Les cellules épithéliales** (restes épithéliaux de Malassez) : ce sont des reliquats de la gaine de Hertwig et dont la fonction est encore peu connue.

iii. **Les cellules de défense** : elles sont identiques à celles décrites pour le tissu gingival.

I.D.2. La matrice extracellulaire du ligament

Elle se compose de quatre familles de macromolécules principales : les collagènes (dont la réticuline), l'élastine qui représente la partie fibreuse de la matrice extracellulaire. Les protéoglycanes et les glycoprotéines de structure en constituent la partie gélatineuse, appelée substance fondamentale (Palmer and Lubbock, 1995 ; Somerman et al., 1990).

- Système fibreux du ligament **:** les fibres constituent l'élément majeur de la matrice extracellulaire du ligament parodontal en représentant 70 à 80% de son volume. Elles sont responsables des propriétés physiques, et notamment, de l'ancrage de la dent au sein de son alvéole. Elles comportent essentiellement des faisceaux de fibres de collagène (90%) mais également des fibres de réticuline et des fibres élastiques. On rencontre 6 types différents : du collagène fibrillaire (types I, III et V) et non fibrillaire (types IV, VI et XII) formant un ensemble très hétérogène. Les fibres de réticuline sont arrangées d'une manière nette et organisée pour former un treillis dans lequel les principales fibres collagènes se développent, s'orientent et réalisent un support pour les cellules. Les fibres élastiques sont de longues fibres linéaires dépourvues de striations périodiques, anastomosées les unes aux autres, extensibles et reprenant leur longueur initiale lorsque la traction cesse (El-Awady et al., 2013, 2010 ; Seo et al., 2004).
- Substance fondamentale : la substance fondamentale, du fait de ses déplacements et de sa compressibilité, et de par la structure des macromolécules qui la composent, joue le rôle d'amortisseur vis-à-vis des forces de pression développées lors de la mastication ou d'autres fonctions orales (phonation, déglutition) et parafonctions (bruxisme). Elle présente d'autres fonctions aussi importantes : liaison et échanges des ions et de l'eau, contrôle de la synthèse des fibres collagènes et de l'orientation fibrillaire. Elle comprend principalement les protéines non collagéniques, telles que les protéoglycanes et les glycoprotéines de structure (El-Awady et al., 2013 ; Palmer and Lubbock, 1995).

I.E. Le fluide gingival (GCF)

Il se définit comme le liquide qui suinte du sillon gingivo-dentaire. On y observe des cellules épithéliales desquamées, des polymorphonucléaires, des lymphocytes et des plasmocytes qui migrent à travers l'attache épithéliale et aussi la présence d'éléments bactériens provenant de la plaque sous-gingivale. Les principales protéines sont des albumines, des

globulines et du fibrinogène. Les immunoglobulines se présentent dans des proportions comparables à celles qui existent au niveau du sérum. Des enzymes d'origine bactérienne ou lysosomiales en font aussi partie. Les principales sont des protéases, des phosphatases acides et alcalines, des hyaluronidases et du lysozyme (Barros et al., 2016 ; Goodson, 2003 ; Taylor and Preshaw, 2016). Le GCF permet une certaine défense de l'organisme face à l'agression bactérienne, mais cette défense apparaît comme largement insuffisante (Barros et al., 2016). Cette protection est pour une part mécanique ceci est dû au fait qu'il s'écoule continuellement à travers le sillon. Une autre protection antibactérienne s'y trouve cependant rassemblée constituée de tout un arsenal de polymorphonucléaires neutrophiles, d'immunoglobulines et d'enzymes (Goodson, 2003 ; Taylor and Preshaw, 2016).

I.F. La vascularisation du parodonte

Les tissus parodontaux sont richement vascularisés. C'est particulièrement le cas du ligament parodontal (Griffin, 1965 ; Griffin and Spain, 1972 ; Schroeder and Listgarten, 1997). Les principaux vaisseaux irriguant les procès alvéolaires et le parodonte sont :

- au niveau du maxillaire, les artères alvéolaires postérieure et antérieure, l'artère infraorbitale et l'artère palatine,
- au niveau de la mandibule, l'artère mandibulaire, l'artère mentale, l'artère buccale et l'artère faciale.

I.G. L'innervation du parodonte

La sensibilité du maxillaire est assurée par la deuxième branche du nerf trijumeau, celle de la mandibule par sa troisième branche. Le parodonte (plus particulièrement la gencive et le ligament parodontal) est innervé non seulement par les branches ubiquitaires du sympathique, mais aussi par des mécanorécepteurs « semblables aux corpuscules de Ruffini » et des fibres nerveuses nociceptives (Griffin and Harris, 1974a ; Griffin and Spain, 1972 ; Schroeder and Listgarten, 1997). Le fonctionnement de cette innervation est coordonné avec celui de la pulpe et de la dentine (Bosshardt, 2018 ; Griffin and Harris, 1974b ; Schroeder and Listgarten, 1997). Ces deux systèmes afférents fournissent des informations sur les positions des mâchoires et les migrations / mouvements des dents et les contacts occlusaux lors de la mastication et de la déglutition. L'EJ, ainsi que les épithéliums de la gencive libre et de la gencive attachée, qui ne sont pas tous vascularisés, sont alimentés par un réseau dense de terminaisons nerveuses nociceptives et tactiles. Il en est de même pour le tissu conjonctif gingival subépithélial et

supracrestal. Les perceptions somatosensorielles dans le cas de certaines gingivopathies, de même que les sensations de pression et de douleur lors du sondage du sillon sain ou de la poche, sont l'expression clinique de l'innervation des tissus gingivaux (Griffin and Harris, 1974a ; Sakallioğlu et al., 2006 ; Schroeder and Listgarten, 1997).

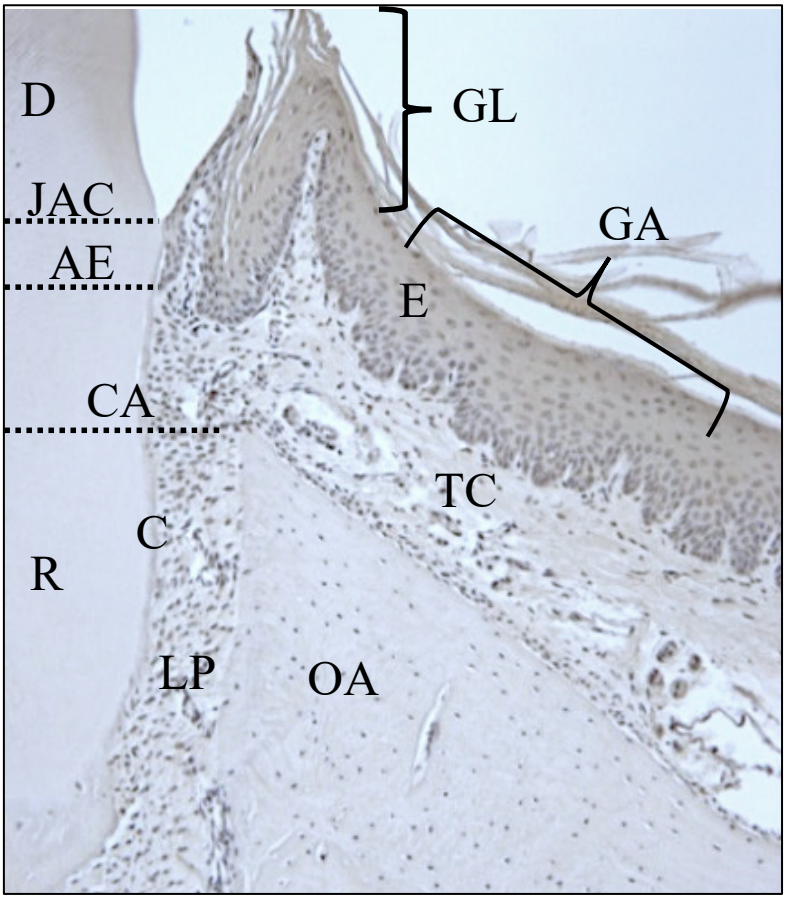

Figure n°3. Histomorphologie des tissus parodontaux*. Coupe histologique d'une première molaire d'une souris et présentant les éléments du parodonte (20x). Gencive libre (GL), gencive attachée (GA), jonction amélo-cémentaire (JAC), épithélium jonctionnel (EJ), crête alvéolaire (CA), épithélium gingival (E), tissu conjonctif (TC), ligament parodontal (LP), racine dentaire (R), dentine (D), cément radiculaire (C), os alvéolaire (OA, attache épithéliale (AE).*

II. Les maladies parodontales

La parodontite est une maladie d'étiologie infectieuse caractérisée par une réponse inflammatoire exacerbée entraînant la destruction du parodonte **(Figure n°4).** La destruction de ces tissus de soutien peut entraîner, pour les formes les plus avancées, la perte des dents touchées (Hajishengallis, 2015a ; Hajishengallis and Lamont, 2012).

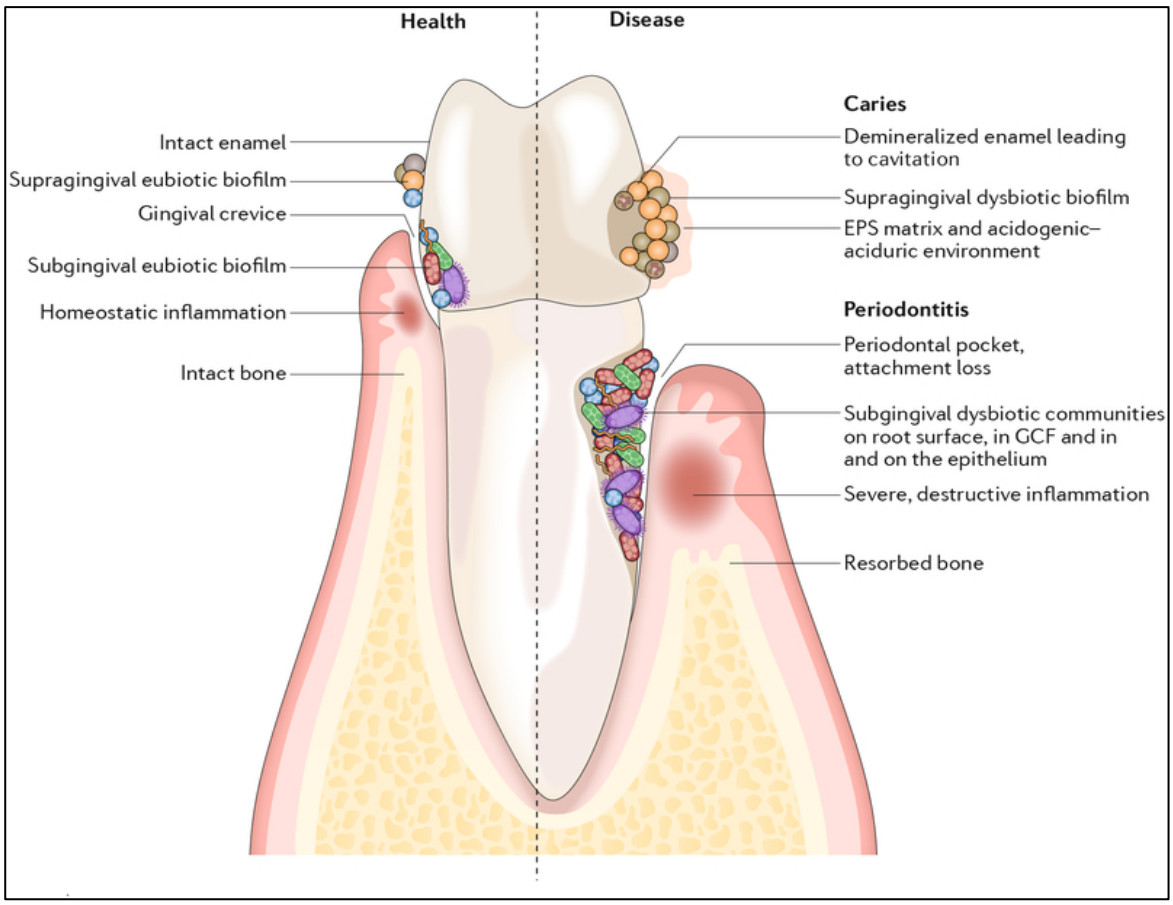

Figure n°4. Biogéographie de la colonisation du microbiote oral dans les divers microenvironnements de la cavité buccale*. La colonisation microbienne se produit sur toutes les surfaces disponibles et les micro-organismes peuvent également pénétrer dans les tissus et cellules épithéliales. Le microbiote s'assemble dans des communautés de biofilms sur les surfaces abiotiques et biotiques. En bonne santé (à gauche), les biofilms eubiotiques maintiennent un équilibre homéostatique avec l'hôte. Malade (à droite), les biofilms deviennent dysbiotiques, provoquant des caries et des maladies parodontales, entraînant l'induction de réponses inflammatoires exacerbées et destructrices. EPS, substance polymérique extracellulaire; GCF, liquide créviculaire gingival (Lamont et al., 2018).*

Selon l'Organisation mondiale de la santé, la parodontite représente un problème de santé publique majeur qui affecte 35 à 50% de la population adulte dans le monde (Petersen and Ogawa, 2012) et dont la prévalence des formes sévères est estimée à environ 11%, avec un pic d'incidence maximal autour de 38 ans (Kassebaum et al., 2014). En France, 82,2 % de la population française adulte présente au moins une poche parodontale et 10,2 % présente une poche parodontale de plus de 5 mm de profondeur au sondage (Bourgeois et al., 2007).

Ce processus infectieux complexe est caractérisé par la formation de poches parodontales. Ceci est reconnu comme la manifestation pathognomonique de la parodontite et

peut affecter un nombre variable de dents avec des taux de progression variables. Bien que son apparition puisse avoir lieu à tout âge - elle est plus fréquente chez les adultes - la prévalence et la sévérité de la maladie augmentent avec l'âge et en fonction de plusieurs facteurs associés à l'hôte et à l'environnement (Armitage, 1999 ; Caton et al., 2018). Ainsi, l'initiation et le développement des parodontites sont influencées par la présence de nombreux facteurs de risque locaux et/ou systémiques. À côté des facteurs environnementaux comme le stress et le tabac (Akcali et al., 2013), et des facteurs génétiques (Korah et al., 2019), les maladies systémiques occupent une place très importante. Parmi ces maladies systémiques, le diabète est une des pathologies majeures (Lockhart et al., 2012 ; Rydén et al., 2016). Enfin, dans le sens inverse, les parodontites sont également considérées comme facteur de risque pour certaines pathologies telles que les maladies cardiovasculaires (Huck et al., 2011), les complications de la grossesse (Rakoto-Alson et al., 2010) ou certaines pathologies auto-immunes (Jung et al., 2017 ; Perricone et al., 2019).

II.A. Pathogenèse de la parodontite : la dysbiose du microbiote sous-gingival

La présence d'une communauté bactérienne sous-gingivale complexe dans laquelle coexistent différents genres et espèces microbiennes est nécessaire à l'établissement de la parodontite (Haffajee and Socransky, 2005 ; Hajishengallis and Lamont, 2014 ; Singh et al., 2011 ; Socransky and Haffajee, 2002). Certaines bactéries interagissent de manière complexe avec les tissus parodontaux, adhérant et envahissant les cellules épithéliales pour établir l'infection (Yilmaz et al., 2003). Lors de la première interaction avec les cellules épithéliales, des facteurs de virulence bactériens tels que le lipopolysaccharide (LPS), les fimbriae et l'antigène K ou capsule, sont essentiels (Kocgozlu et al., 2009 ; Singh et al., 2011; Vernal et al., 2009). Ces facteurs sont également susceptibles de déclencher des processus immunitaires, en modulant la réponse inflammatoire et en induisant la libération d'enzymes protéolytiques, ces deux phénomènes étant impliqués dans la destruction tissulaire (Elkaim et al., 2008 ; Kocgozlu et al., 2009). Cette réponse inflammatoire est initiée au niveau des tissus mous et s'étend ensuite aux tissus parodontaux profonds (Armitage, 2004 ; Asman et al., 1997 ; Haffajee and Socransky, 2005 ; Lapérine et al., 2016 ; Loesche and Grossman, 2001 ; Slots and Chen, 1999).

Les données récentes indiquent que la parodontite est initiée par une dysbiose de l'écosystème oral et la présence d'un microbiote synergique, ceci contrairement aux hypothèses physiopathologiques précédentes considérant le rôle d'un nombre réduit de microorganismes (Hajishengallis and Lamont, 2012). Sur la base de cette diversité d'espèces associées à la

parodontite, il est possible qu'il existe souvent des communautés potentiellement pathogènes ainsi qu'une immense variété de microorganismes qui contribuent aux facteurs nécessaires pour que ces conditions de dysbiose et de synergie puissent être réunies (Abusleme et al., 2013 ; Hajishengallis and Lamont, 2012). L'interaction entre les composants microbiens et non microbiens de l'écosystème oral conduit à une forme de stabilisation dans laquelle des microorganismes et des structures non microbiennes (les cellules et d'autres composants de l'hôte) coexistent en harmonie et en équilibre avec leur environnement. Cet équilibre reste stable dans le temps et reflète une situation dynamique dans laquelle les cellules meurent et sont remplacées. Cette communauté, appelée « climax », peut être modifiée ponctuellement par des forces exogènes. L'équilibre a tendance à être restauré lorsque l'habitat revient à son état d'origine. Dans d'autres situations, les environnements peuvent être modifiés de façon irréversible, donnant lieu à un état altéré et à une communauté microbienne différente dans laquelle une succession de microorganismes se développe et favorise la colonisation de certains microorganismes au détriment d'autres, en provoquant une altération de l'homéostasie sous-gingivale (dysbiose) (Abusleme et al., 2013 ; Hajishengallis and Lamont, 2014, 2012). Dans cette synergie polymicrobienne, différents membres ou combinaisons d'espèces spécifiques au sein du microbiote remplissent des rôles distincts qui convergent pour former et établir un micro-environnement provoquant la maladie (Abusleme et al., 2013). L'une des conditions essentielles à l'apparition d'une telle communauté potentiellement pathogène concerne la capacité de certaines espèces, appelées agents pathogènes clés (« *keystone pathogens* »), de moduler la réponse de l'hôte de manière à échapper à la surveillance immunitaire et à faire pencher la balance de l'homéostasie vers la dysbiose. Les agents étiologiques les plus impliqués et considérés clés sont *Aggregatibacter actinomycetemcomitans (Aa), Tannerella forsythia (T.forsythia), Treponema denticola (T.denticola) et Porphyromonas gingivalis* (*P.gingivalis*) (Abusleme et al., 2013 ; Hajishengallis, 2015a) **(Figure n°5).** Ces agents pathogènes clés augmentent également la virulence de l'ensemble de la communauté microbienne grâce à une communication interactive avec des agents pathogènes accessoires (Plančak et al., 2015). D'autres fonctions essentielles importantes pour la pathogénicité nécessitent l'expression de facteurs de virulence (adhésines, fimbriae, lipopolysaccharide, protéases, …), qui, en combinaison, agissent en tant que facteurs de virulence communautaire pour soutenir nutritionnellement une communauté microbienne hétérotypique, compatible et pro-inflammatoire induisant une réponse de l'hôte non résolutive et destructrice des tissus (Hajishengallis and Lamont, 2014, 2012 ; Lamont et al., 2018) **(Figure n°6 et 7).**

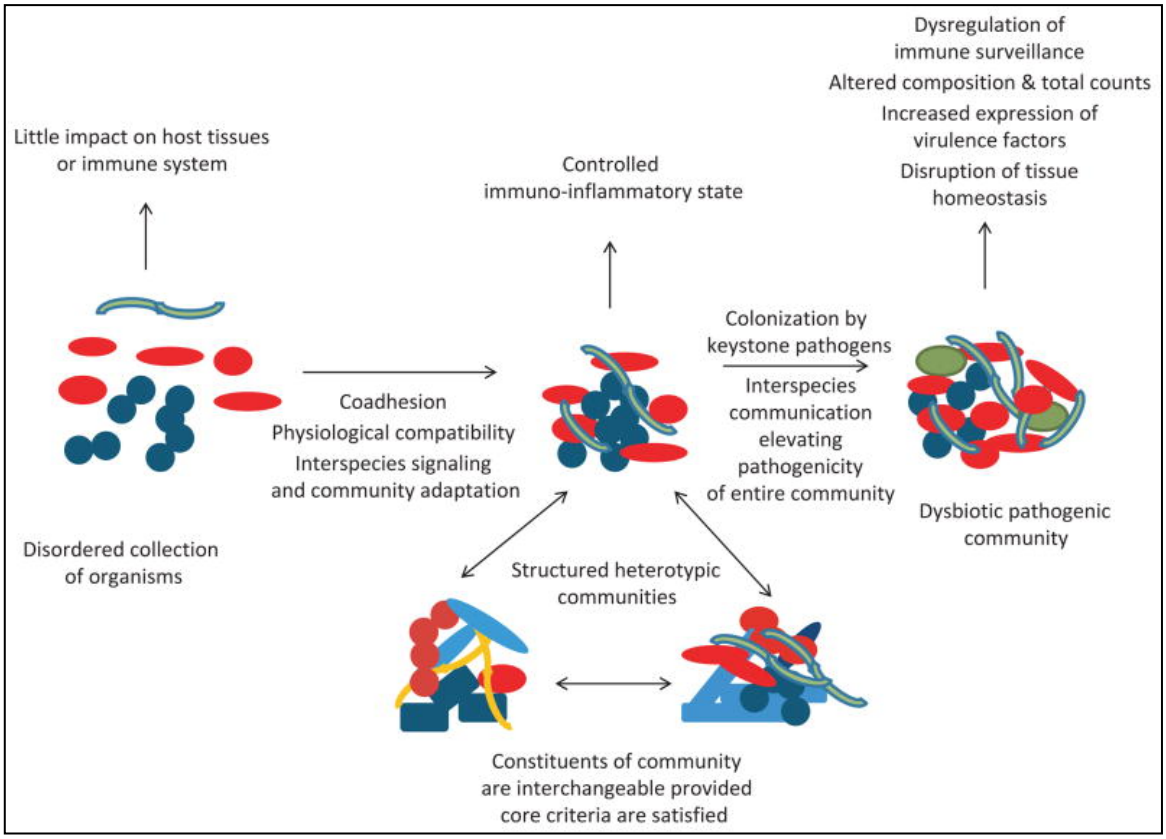

Figure n°5. Synergie polymicrobienne et dysbiose (PSD). *Le sulcus gingival est colonisé par un microbiote riche en espèces bactériennes et des organismes compatibles s'assemblent en communautés hétérotypiques. Ces communautés sont en équilibre avec l'hôte. Bien qu'ils soient pro-inflammatoires et qu'ils puissent produire des produits toxiques tels que les protéases, leur prolifération et leur pathogénicité sont également dépendantes de l'hôte. Les compositions microbiennes peuvent varier dans le temps, d'une personne à l'autre et d'un site à l'autre. La colonisation par des agents pathogènes clés tels que P.gingivalis augmente la virulence de l'ensemble de la communauté à la suite d'une communication interactive avec d'autres espèces bactériennes accessoires tels que les streptocoques du groupe mitis. La surveillance immunitaire de l'hôte est altérée et le nombre de microorganismes dysbiotiques augmente, ce qui finit par perturber l'homéostasie tissulaire et entraîner la destruction des tissus parodontaux (Hajishengallis and Lamont, 2012).*

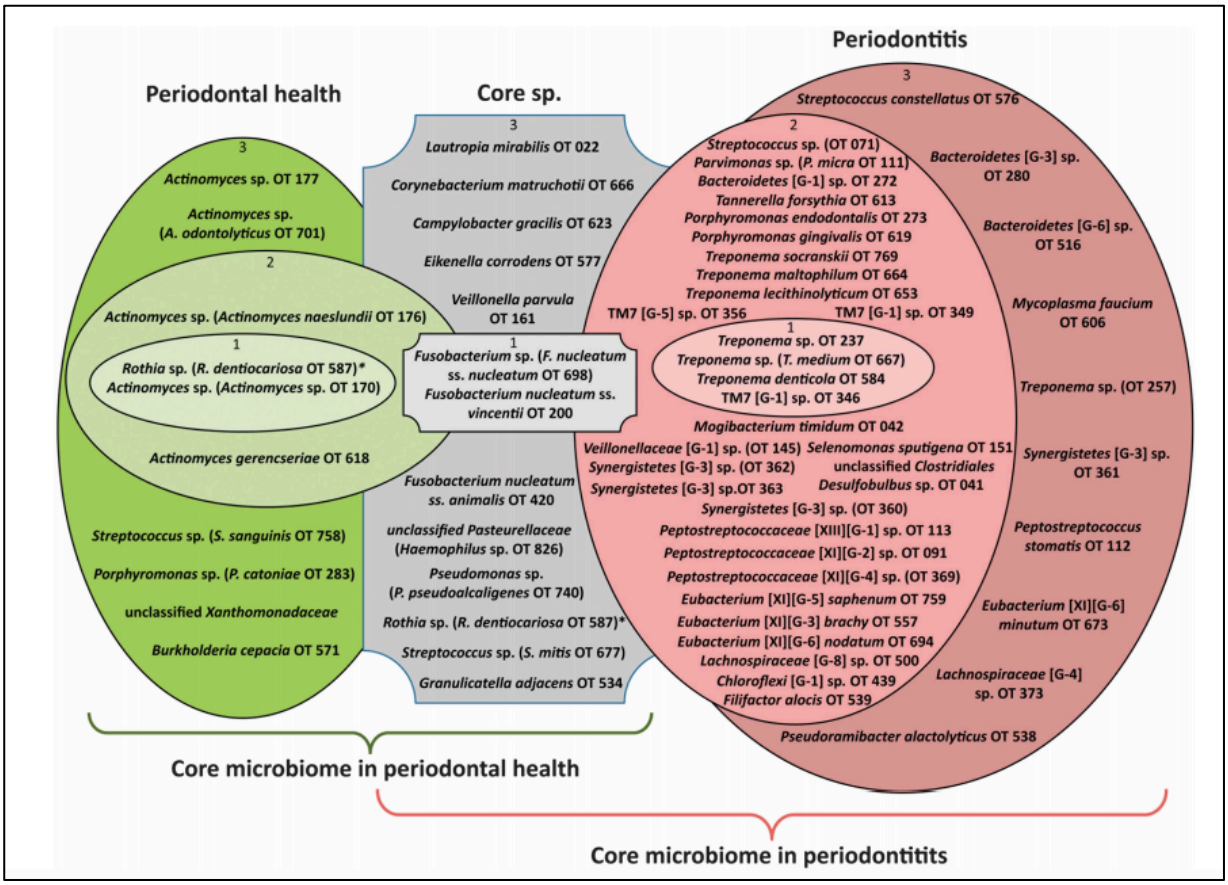

Figure N°6. Le microbiome sous-gingival dans la santé et la parodontite. *Les microorganismes faisant partie du microbiome principal (gris) ont d'abord été définis comme ceux présents chez au moins 50% des sujets des groupes sain et parodontite. Le microbiome décrit dans le groupe vert correspond aux microorganismes retrouvés chez au moins 50% des sujets en bonne santé et pour le groupe rouge, ceux présents chez au moins 50% des patients atteints de parodontite. Les microorganismes en vert représentent les principales espèces associées à la santé et apparaissent avec une prévalence accrue et une abondance relative en santé comparée à la maladie. Les composants en rouge représentent les principales espèces associées à la parodontite, présentes avec une prévalence accrue et une abondance relative dans la parodontite par rapport à l'état de santé (Abusleme et al., 2013).*

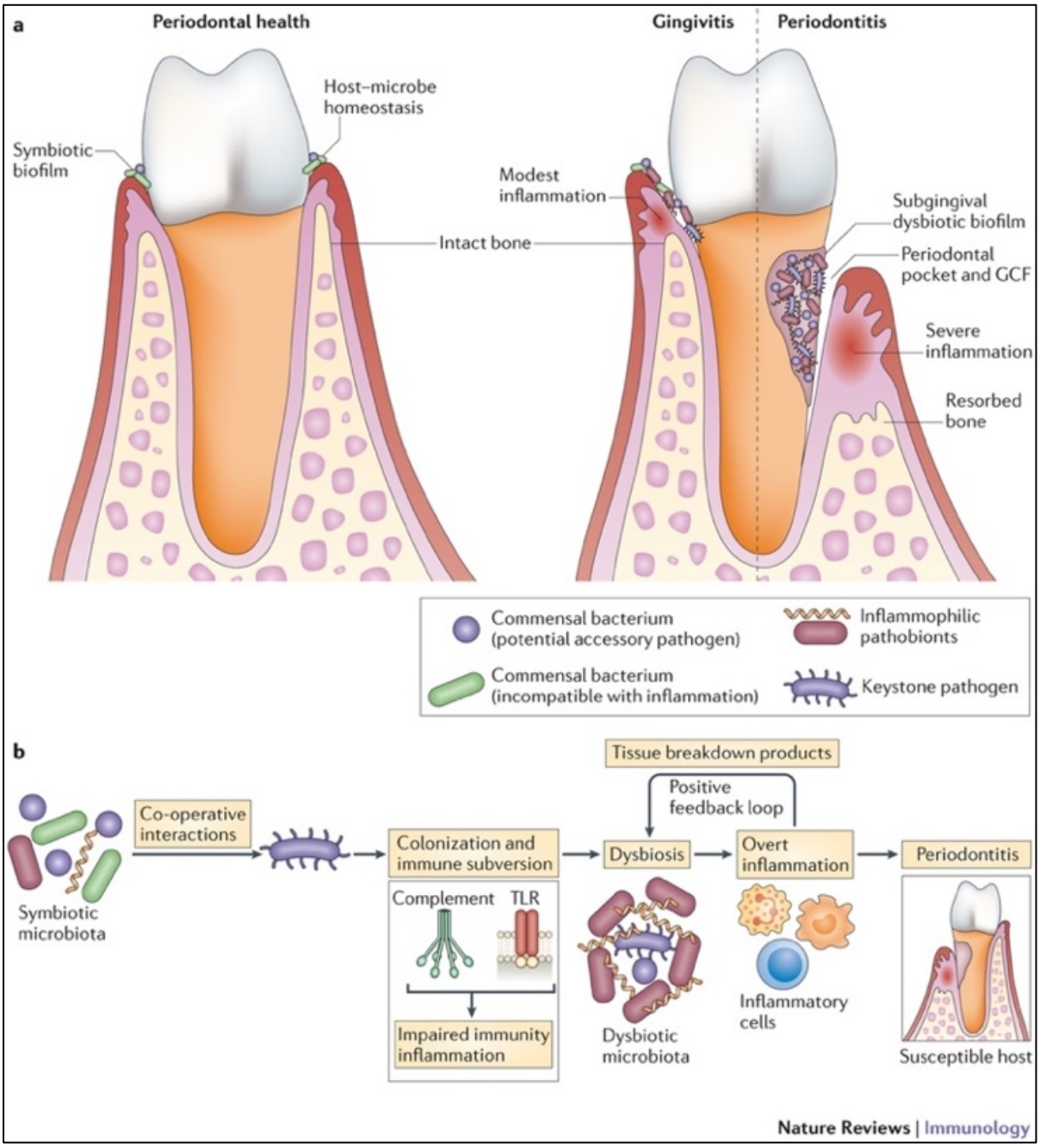

Figure n°7 : Synergie polymicrobienne et dysbiose au cours de la parodontite. ***a.*** *La figure montre la progression d'un état de santé parodontale à la gingivite, qui est définie comme une inflammation des tissus mous sans perte osseuse associée. La parodontite se développe lorsqu'il y a formation des poches parodontales et perte d'os alvéolaire.* ***b****. La parodontite est induite chez des hôtes sensibles par une communauté polymicrobienne, dont les différents membres ont des rôles distincts synergiques pouvant induire une inflammation destructrice. Les pathogènes clés (keystone-pathogens) sont des microorganismes pour lesquels la colonisation est facilitée par des agents pathogènes secondaires. L'inflammation favorise la dysbiose via les produits de dégradation utilisés comme les nutriments par les différentes espèces bactériennes (Hajishengallis, 2015a).*

Il est maintenant bien reconnu que la présence d'espèces bactériennes est nécessaire mais pas suffisante pour l'apparition et la progression de la parodontite. La reconnaissance des composants microbiens en tant que « signaux de danger » par les cellules immunitaires de l'hôte et la production ultérieure de médiateurs inflammatoires sont une étape essentielle dans la pathogenèse parodontale (Graves et al., 2012). La production de cytokines pro-inflammatoires (y compris IL-1β, IL-6 et TNF-α) par des cellules inflammatoires résidentes et recrutées agissant en synergie semble revêtir une importance particulière dans ce processus. En effet, ces cytokines augmentent le recrutement et l'activité des cellules de résorption osseuse, les ostéoclastes, en augmentant la production d'un facteur ostéoclastogénique crucial, le ligand des récepteurs du facteur nucléaire $_{K}$B (RANK-L) et favorisent la destruction osseuse (Hienz et al., 2015 ; Lapérine et al., 2016). Cependant, des traitements ciblés contre ces 3 molécules ne présentaient pas d'effet thérapeutique convaincant dans la parodontite suggérant ainsi fortement que d'autres médiateurs inflammatoires pourraient être impliqués (Preshaw et al., 2012). Récemment, il a été démontré que parmi les médiateurs inflammatoires impliqués dans la parodontite, des membres de la famille des IL-1pourraient jouer un rôle dans l'initiation et la progression de la parodontite. Par exemple, il a été démontré que la surexpression de l'IL-33 par les cellules épithéliales gingivales est associée à l'initiation de la parodontite et peut déclencher l'expression de RANK-L favorisant la résorption osseuse induite par l'infection par *P.gingivalis* (Lapérine et al., 2016).

De nouveaux membres de cette famille des IL-1 telle que l'IL-36, pourraient également jouer un rôle clé dans la réponse immunitaire médiée par *P.gingivalis* au cours d'une parodontite (Huynh et al., 2017). Récemment, une étude a démontré à partir d'échantillons gingivaux humains et de cellules gingivales primaires, une implication pathologique d'IL-36, en particulier d'IL-36γ, dans la pathogenèse de la parodontite. L'IL-36γ semble jouer un rôle central dans la réponse immunitaire innée induite par *P.gingivalis* (Cloître et al., 2019).

III. *Porphyromonas gingivalis,* un parodontopathogène majeur

Au sein des espèces pathogènes impliquées dans l'étiologie des parodontites, *P.gingivalis* a été décrit comme étant l'un des agents étiologiques majeurs (Bugueno et al., 2016 ; Byrne et al., 2009 ; Hajishengallis and Lamont, 2012 ; Huck et al., 2012; Lamont and Jenkinson, 1998 ; Socransky and Haffajee, 2002).

Cette bactérie parodontopathogène a été trouvée dans 85,75% des échantillons de plaque sous-gingivale de patients atteints de parodontite chronique (Rafiei et al., 2018). C'est une

bactérie gram-négative assaccharolytique non-motile anaérobie obligatoire qui forme des colonies pigmentées en noir en culture sur gélose au sang. La présence de fer est une nécessité absolue pour sa croissance (How et al., 2016). Le principal habitat de *P.gingivalis* est le sulcus sous-gingival de la cavité buccale humaine et on retrouve cette bactérie en quantité importante au sein des poches parodontales, notamment au niveau des lésions profondes et des formes pathologiques sévères, cet environnement anaérobie étant propice à sa croissance (Lamont et al., 2018). Elle repose sur la fermentation des acides aminés pour la production d'énergie, une propriété nécessaire à sa survie dans les poches parodontales profondes où la disponibilité en sucre est faible (Bostanci and Belibasakis, 2012). En tant que bactérie anaérobie stricte, *P.gingivalis* est un colonisateur secondaire de la plaque dentaire, adhérant aux colonisateurs primaires tels que *Streptococcus gordonii* et *Prevotella intermedia*. Pratiquement tous les chercheurs s'accordent à dire que les taux sériques d'anticorps anti - *P.gingivalis* sont plus élevés chez les patients atteints de parodontite (Casarin et al., 2010 ; Mahanonda et al., 1991). Récemment, de nouvelles variations des composants de surface, tels que le LPS, pourraient être associées à des différences de virulence bactérienne et de progression de la parodontite (Díaz et al., 2015 ; Soto et al., 2016).

Bien que le rôle précis joué par cette bactérie dans l'établissement de la lésion ne soit pas encore totalement compris, il a été démontré qu'elle est capable d'envahir les cellules épithéliales humaines ainsi que de persister et de se répliquer par voie intracellulaire, ce qui empêcherait sa détection par le système immunitaire (Bugueno et al., 2016 ; Díaz et al., 2015 ; Inaba et al., 2009 ; Sandros et al., 1994 ; Yilmaz, 2008 ; Yilmaz et al., 2006, 2002). Du fait de l'importance de cette étape dans l'infection, de nombreuses études ont tenté de clarifier les mécanismes impliqués dans l'internalisation de la bactérie par la cellule hôte, notamment épithéliale, et ceux impliqués dans l'échappement à la réponse immunitaire **(Figure n°8)**.

III.A. La gencive, une barrière immunitaire

Dans la cavité buccale, les cellules épithéliales représentent la plus grande surface de contact et sont les sites d'entrée préférentiels pour l'invasion de l'hôte par des bactéries (Amano, 2007 ; Tribble and Lamont, 2010). Par conséquent, l'interaction entre les cellules épithéliales gingivales (GEC) et les bactéries parodontales déterminerait si le processus de colonisation aboutirait ou non. Des études ont montré comment certaines GEC présentent des taux intracellulaires élevés de *P.gingivalis* (Noiri et al., 1997 ; Vitkov et al., 2005) indiquant que cette bactérie persiste et survit dans ces cellules (Madianos et al., 1997 ; Nakhjiri et al., 2001).

La persistance intracellulaire est une stratégie développée par la bactérie pour échapper à la réponse immune contribuant ainsi au processus pathologique des maladies parodontales (Lamont et al., 2018). *P.gingivalis* est capable de moduler le cycle cellulaire et la mort cellulaire programmée dans le but de promouvoir son développement et sa propagation à des sites distants (Furuta et al., 2009 ; Pan et al., 2014). Ainsi, il a été observé que l'invasion épithéliale par *P.gingivalis* régule l'apoptose et stimule la prolifération cellulaire par la modulation de plusieurs cascades moléculaires impliquant p53 et JaK kinase/Stat (Kuboniwa et al., 2008 ; Mao et al., 2007). Cependant, les mécanismes précis impliqués restent à déterminer et plusieurs résultats contradictoires ont été observés concernant l'influence de *P.gingivalis* sur la régulation de l'apoptose et la viabilité cellulaire, certaines études confirmant l'induction de l'apoptose par l'infection bactérienne (Brozovic et al., 2006 ; Stathopoulou et al., 2009), d'autres décrivant sa capacité à inhiber un tel processus (Mao et al., 2007 ; Nakhjiri et al., 2001).

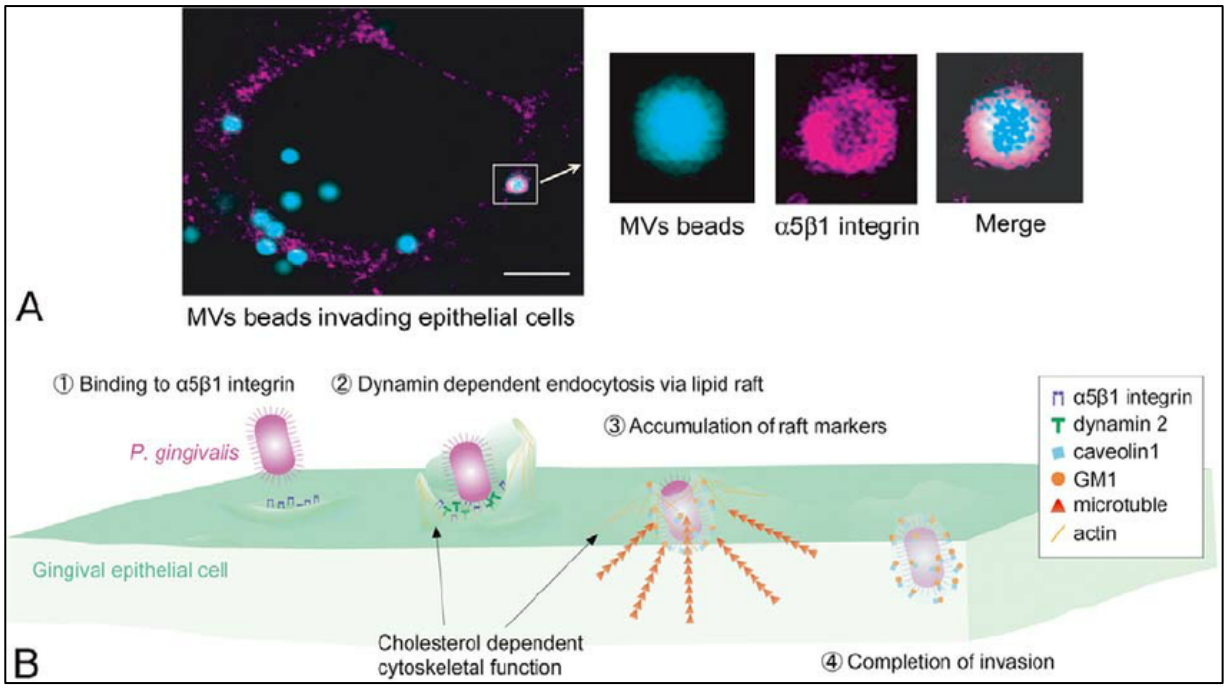

Figure n°8. Invasion des cellules épithéliales par P.gingivalis. *A. Invasion de cellules épithéliales par des billes de polystyrène fluorescentes couplées à des vésicules membranaires (VM) de P.gingivalis. La zone encadrée montre que l'intégrine α5-β1 (magenta) a été recrutée autour des billes revêtues de Vm (cyan) (Tsuda et al., 2005). Barre = 5 µm. B. Schéma suggéré du mécanisme d'invasion de P.gingivalis en ce qui concerne la machinerie cellulaire de l'hôte, le cytosquelette et les rayons lipidiques. Les fimbriae de P.gingivalis adhèrent à l'intégrine α5-β1, après quoi la bactérie est ensuite entourée par l'intégrine α5-β1 et invaginée par la voie médiée par l'actine contrôlée par la phosphatidylinositol-3-kinase (PI3K). L'événement invasif nécessite la dynamique du cytosquelette cellulaire, des fibres d'actine et des microtubules. La*

dynamique de l'assemblage et du désassemblage des microtubules est essentielle à ce processus (Amano, 2007).

IV. La réponse cellulaire médiée par les « Toll-Like receptors »

Les récepteurs « Toll-like » (TLRs) jouent un rôle primordial dans l'initiation de l'immunité innée contre les agents pathogènes envahissants (Akira, 2006 ; O'Neill and Bowie, 2007). Les voies de signalisation activées par différents TLRs ont donc fait l'objet de nombreuses recherches. Les TLRs activent une réponse immunostimulante puissante, en favorisant le recrutement de plusieurs protéines adaptatrices pour activer le facteur nucléaire-$_{K}$B (NF-$_{K}$B), ce qui induit l'expression de gènes pro-inflammatoires, de cytokines inflammatoires telles que IL-1β, IL-6, TNF-α, ainsi que d'autres molécules impliquées dans la mort cellulaire (Akira, 2006 ; Sobrino et al., 2017).

Le signal transmis par les TLRs doit donc être étroitement contrôlé, et il est clairement établi que si les TLRs sont suractivés, des maladies infectieuses et inflammatoires peuvent se développer (Maekawa et al., 2014 ; Nativel et al., 2017 ; Wang et al., 2006). Une étude portant sur le LPS de *P.gingivalis* a montré que la région de l'antigène O du LPS de cette bactérie est nécessaire pour augmenter la viabilité des GEC lors d'une infection bactérienne et cette augmentation est imputable à une réduction de l'apoptose. De plus, bien que l'internalisation bactérienne soit nécessaire, les effets observés ne sont pas dus à des altérations de l'adhésion, de l'invasion ou de la survie intracellulaire de *P.gingivalis*. Fait intéressant, l'inhibition de l'apoptose est corrélée à une expression accrue de TLR-4, suggérant un rôle pour ce récepteur dans ce processus (Soto et al., 2016). *P.gingivalis* est capable d'activer ou moduler les voies de signalisation initiées par les TLRs et ceci représente un rôle crucial dans l'inflammation et l'activation et/ou inactivation d'autres processus, tels que l'apoptose, dans différentes lignées cellulaires. De nombreuses études ont montré les effets de l'infection par *P.gingivalis* sur l'activation des cascades pro-inflammatoires *via* les TLR-2 et TLR-4 (Kocgozlu et al., 2009 ; Singh et al., 2011). Cet effet médié par les TLRs peut être retrouvé dans différents types cellulaires. Il a été démontré que l'infection par *P.gingivalis* affecte rapidement les cellules endothéliales et module l'activité de la cathepsine B (CATB) via ces récepteurs (Huck et al., 2012).

La signalisation par les TLRs implique une famille de cinq protéines adaptatrices, qui se couplent aux protéines kinases en aval et qui conduisent finalement à l'activation de facteurs de transcription tels que NF-$_{K}$B et des membres de la famille du facteur de régulation de l'interféron (IFN) (IRF). Le domaine de signalisation clé, unique au système des TLRs, est le

domaine du récepteur Toll / interleukine-1 (IL-1) (TIR), situé sur la face cytosolique de chaque TLR ainsi que dans les adaptateurs (O'Neill et al., 2003 ; O'Neill and Bowie, 2007). Semblables aux TLRs, les adaptateurs sont conservés chez de nombreuses espèces (O'Neill, 2008; Rast et al., 2006). Ces adaptateurs sont MyD88, MyD88-adaptor-like (MAL), (également connus sous le nom de TIRAP), une protéine adaptatrice contenant un domaine TIR induisant l'IFN-β (TRIF; également connu sous le nom de TICAM1), une molécule adaptatrice liée au TRIF (TRAM; également connue sous le nom de TICAM2), et une protéine appelée « sterile α- and armadillo motif-containing protein" (SARM) (O'Neill et al., 2003 ; O'Neill and Bowie, 2007) **(Figure n°9)**. Il a été démontré que SARM interagissait avec TRIF et interférait ainsi avec la fonction de TRIF. Cette découverte, ainsi que d'autres données relatives à la régulation biochimique de MAL et de TRAM, a permis de tirer des conclusions sur le rôle de ces cinq adaptateurs dans la signalisation des TLRs et de fournir une compréhension plus large des mécanismes moléculaires dans la phase de transduction du signal TLR et donc de l'initiation de l'immunité innée (O'Neill, 2008; O'Neill and Bowie, 2007, 2007).

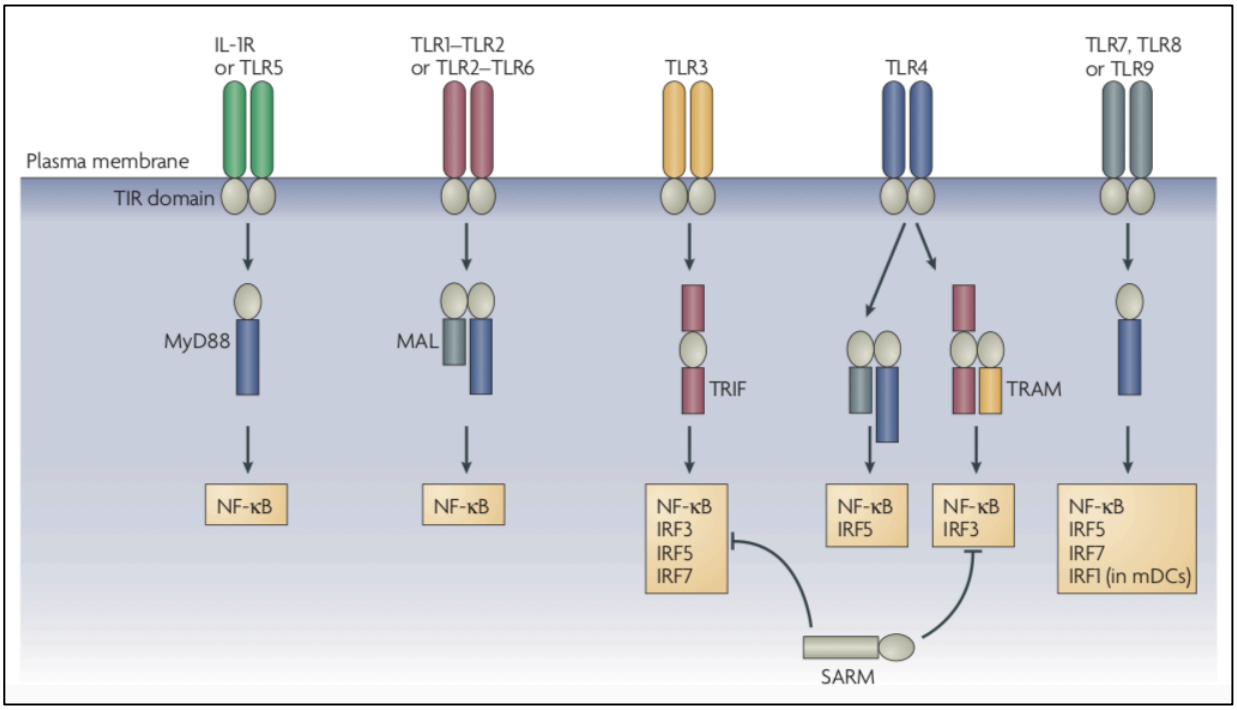

Figure n°9. Vue d'ensemble des adaptateurs contenant le domaine TIR de la superfamille TLR / IL-1 dans l'activation des facteurs de transcription*. Chaque adaptateur est utilisé différentiellement par les complexes de récepteurs TLRs pour réguler positivement l'activation du facteur de transcription. La seule exception concerne SARM (« sterile α- and armadillo-motif-containing protein ») qui inhibe l'activation du facteur de transcription induit par une protéine adaptatrice contenant un domaine Toll / IL-1R (TIR) induisant l'interféron-β (IFNβ). IL-1R : récepteur de l'interleukine-1; IRF : facteur de régulation d'IFN; mDC : cellule*

dendritique myéloïde; MAL : protéine « adaptor-like MyD88 » (gène de réponse primaire de différenciation myéloïde 88); NF-κB: facteur nucléaire-κB; TLR : récepteur Toll-like; TRAM : molécule adaptatrice liée au TRIF (O'Neill and Bowie, 2007).

IV.A. Activation des voies TLRs

Les TLRs se présentent sous forme de dimères (Bell et al., 2006 ; O'Neill and Bowie, 2007). Ces récepteurs reconnaissent principalement des motifs moléculaires associés aux pathogènes. Ces motifs moléculaires associés aux pathogènes (PAMP, acronyme pour Pathogen-associated molecular pattern) sont des molécules associées aux bactéries, virus champignons, parasites reconnus par le système immunitaire inné (Akira, 2006).

Chaque récepteur TLR va pouvoir être activé par différents stimuli et en fonction de l'activation par les ligands d'origine microbienne, diverses réactions sont possibles. Par exemple, TLR-1 et TLR-2 hétérodimérisent et le dimère résultant détecte les lipopeptides triacylés bactériens. TLR-2 hétérodimérise avec TLR-6, qui reconnaît les lipopeptides bactériens diacylés. TLR-4 (le récepteur du produit bactérien lipopolysaccharide (LPS) des espèces à gram négatif) et TLR-9 (le récepteur des motifs d'ADN non méthylés contenant CpG, présents dans l'ADN bactérien et viral) sont homodimères. Ceci est également supposé être le cas de TLR-3 (qui détecte l'ARN synthétique double-brin viral (ARNdb)) et de TLR-5 (qui détecte la flagelline des bactéries). Plus récemment, il a été montré que TLR-8 (qui, comme le TLR-7, peut détecter des ARN simple brin viraux (ARNss) et des composés synthétiques d'imidazoquinolène tels que l'imiquimod) se dimérise avec TLR-7 et TLR-9, et les ligands du TLR-8 sont censés être antagonisés en signalant TLR-7 ou TLR-9. Il a également été démontré que TLR-9 interagit et au même temps, il inhibe la signalisation par le biais de TLR-7 (O'Neill and Bowie, 2007 ; Wang et al., 2006). On pense que les dimères de TLRs sont pré-assemblés dans un complexe de faible affinité avant la liaison du ligand. Une fois que le ligand se lie, il induit un changement conformationnel qui rapproche les deux domaines TIR situés sur la face cytosolique de chaque récepteur créant ainsi une nouvelle plateforme sur laquelle s'active un complexe de signalisation (Bell et al., 2006). Cette dimérisation symétrique va associer les domaines TIR cytosoliques de manière symétrique et les contraindre par conséquent à se réorganiser structurellement créant ainsi la plateforme de signalisation nécessaire au recrutement d'adaptateurs. Une fois que la signalisation est initiée, chaque adaptateur conduira finalement à l'activation de facteurs de transcription spécifiques (tels que NF-κB) **(Figure n°10)**. La signalisation des TLRs dépend de l'utilisation sélective de différentes combinaisons d'adaptateurs par différents TLRs. Des informations récentes sur la régulation covalente de

TRAM et de MAL, ainsi que sur le rôle inhibiteur de SARM en ce qui concerne la signalisation TRIF, soulignent la complexité de l'utilisation de l'adaptateur et de la régulation dans l'action des TLRs (Naiki et al., 2005). Des modèles clairs de cette régulation qui identifient les principaux points de contrôle peuvent maintenant être dessinés. Le rôle des adaptateurs dans les maladies inflammatoires et infectieuses devient également plus évident, des études portant sur une mutation de MAL ayant démontré une protection contre de multiples maladies infectieuses (Horng et al., 2002 ; Jeyaseelan et al., 2005 ; Yamamoto et al., 2002). La possibilité de cibler les adaptateurs de manière thérapeutique devient une possibilité réaliste notamment dans le contexte des parodontites. Plus spécifiquement, les connaissances acquises dans les régions des adaptateurs impliqués dans les interactions protéine-protéine (telles que certaines régions dans MyD88) pourraient permettre le développement d'agents spécifiques pour perturber ces interactions et limiter ainsi leur capacité de signalisation (Castrillo et al., 2001 ; McGettrick et al., 2006).

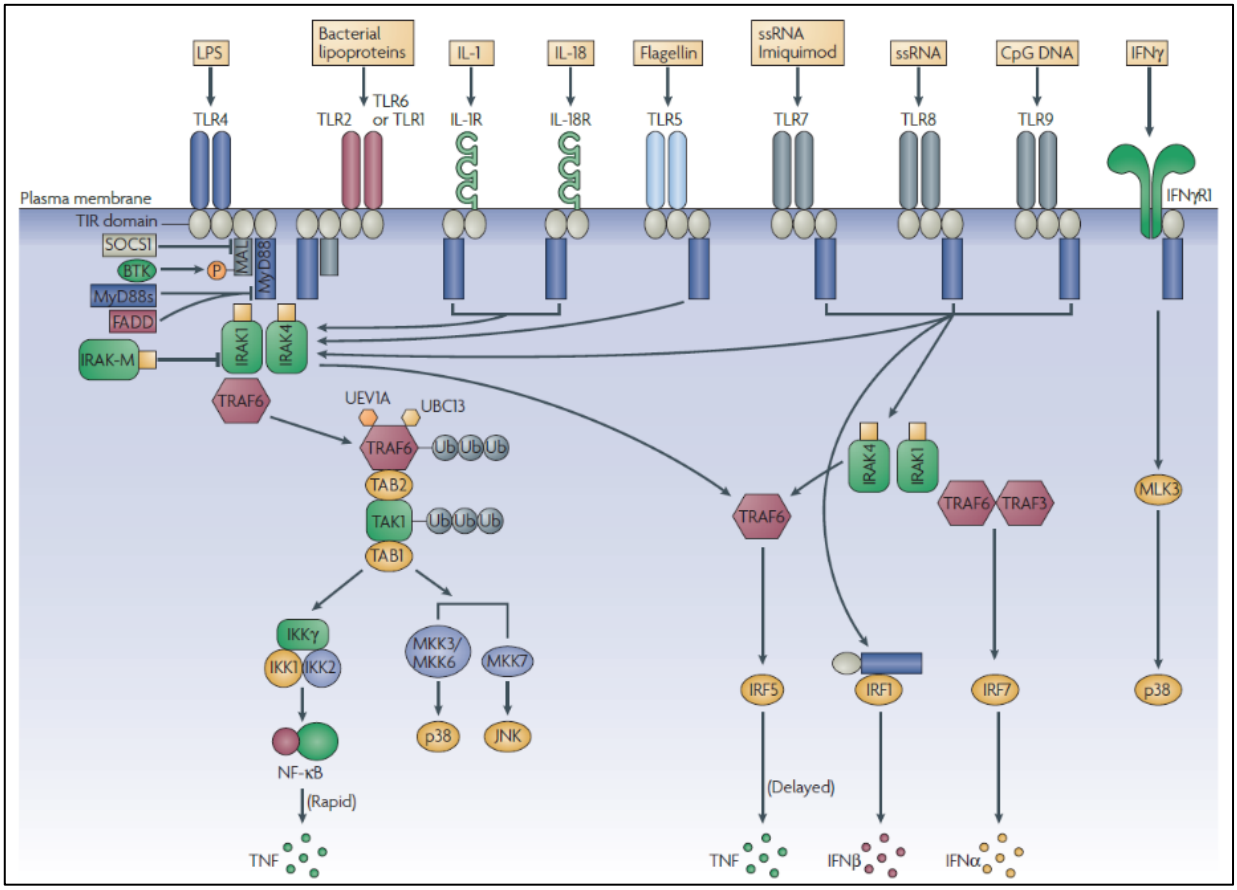

Figure n°10. Activation de la signalisation intracellulaire par les différents TLRs via l'adaptateur MyD88. *Myd88 est l'adaptateur de signalisation clé pour tous les récepteurs de type Toll (TLR; à l'exception de TLR3 et de certains signaux de TLR-4), IL-1R et IL-18R. Son rôle principal est l'activation de NF-κB (facteur nucléaire-κB). Il est directement recruté par*

les domaines TIR dans certains TLRs et permet de recruter la protéine IRAK4 (kinase 4 associée à IL-1R). Cela conduit à une voie impliquant l'IRAK1, le facteur TRAF6 (facteur 6 associé au récepteur du facteur de nécrose tumorale), et plusieurs autres protéines-kinases. Ceci conduit à l'activation de la kinase 'inhibitrice du complexe NF-$_K$B (IKK) et de NF-$_K$B, et des kinases en amont pour p38 et JNK (kinase JUN N-terminale). MKK : protéine kinase activée par un mitogène; TAB : protéine de liaison à TAK1 : TNF, facteur de nécrose tumorale; Ub : Ubiquitin (O'Neill and Bowie, 2007).

V. L'apoptose et les maladies parodontales

L'apoptose est un processus physiologique et hautement régulé. Sa dérégulation est donc associée au développement de pathologies telles que le cancer et certaines maladies du système immunitaire (Fadeel and Orrenius, 2005). L'apoptose peut être activée par deux voies principales, les voies intrinsèque et extrinsèque, qui déclenchent des phénomènes cellulaires tels que l'activation des caspases, la fragmentation des mitochondries et de l'ADN chromosomique, la condensation de la chromatine (picnose), et enfin, la formation de corps apoptotiques qui sont éliminés par la phagocytose (Elmore, 2007). L'activation des voies apoptotiques se produit par l'action de protéines inductrices (pro-apoptotiques) ou inhibitrices (anti-apoptotiques) (Elmore, 2007 ; Fadeel and Orrenius, 2005) **(Figure n°11)**. Le processus apoptotique lui-même n'est généralement pas préjudiciable car, contrairement à la nécrose, la dégradation des composants cellulaires étant fortement régulée et le contenu cellulaire ne fuyant pas dans l'espace extracellulaire. Au lieu de cela, des corps apoptotiques formés sont reconnus et efficacement phagocytés par les macrophages (Lawen, 2003). En revanche, lorsque les cellules sont soumises à la nécrose, le contenu de celles-ci s'infiltre dans l'environnement, ce qui entraîne une réponse inflammatoire aiguë. Au cours du développement, l'apoptose est essentielle à l'établissement des structures corporelles, comme par exemple, la résorption d'espaces interdigitaux chez les mammifères (Fadeel and Orrenius, 2005). L'apoptose est également cruciale pour la formation de systèmes physiologiques fonctionnels. Dans les tissus adultes, l'homéostasie est obtenue par l'équilibre entre prolifération cellulaire et apoptose. Une bonne régulation de l'apoptose est cruciale pour prévenir l'hypo- ou l'hyperplasie dans les tissus mais est également essentielle dans un certain nombre d'événements physiologiques dynamiques qui coïncident avec une accumulation temporelle et locale de certains types cellulaires (Degterev et al., 2003). Par exemple, les neutrophiles servent de première ligne de défense contre les micro-organismes et sont recrutés sur les sites d'inflammation par chimiotactisme. Afin de prévenir les lésions tissulaires, une résolution efficace de l'inflammation est essentielle et passe par l'apoptose des neutrophiles (Kooijman, 2006 ; Savill,

1997). Enfin, le processus d'apoptose est utilisé pour éliminer des cellules nuisibles telles que des cellules infectées par un virus et des cellules cancéreuses par des lymphocytes cytotoxiques T et Natural Killer cells (NK) (Degterev et al., 2003).

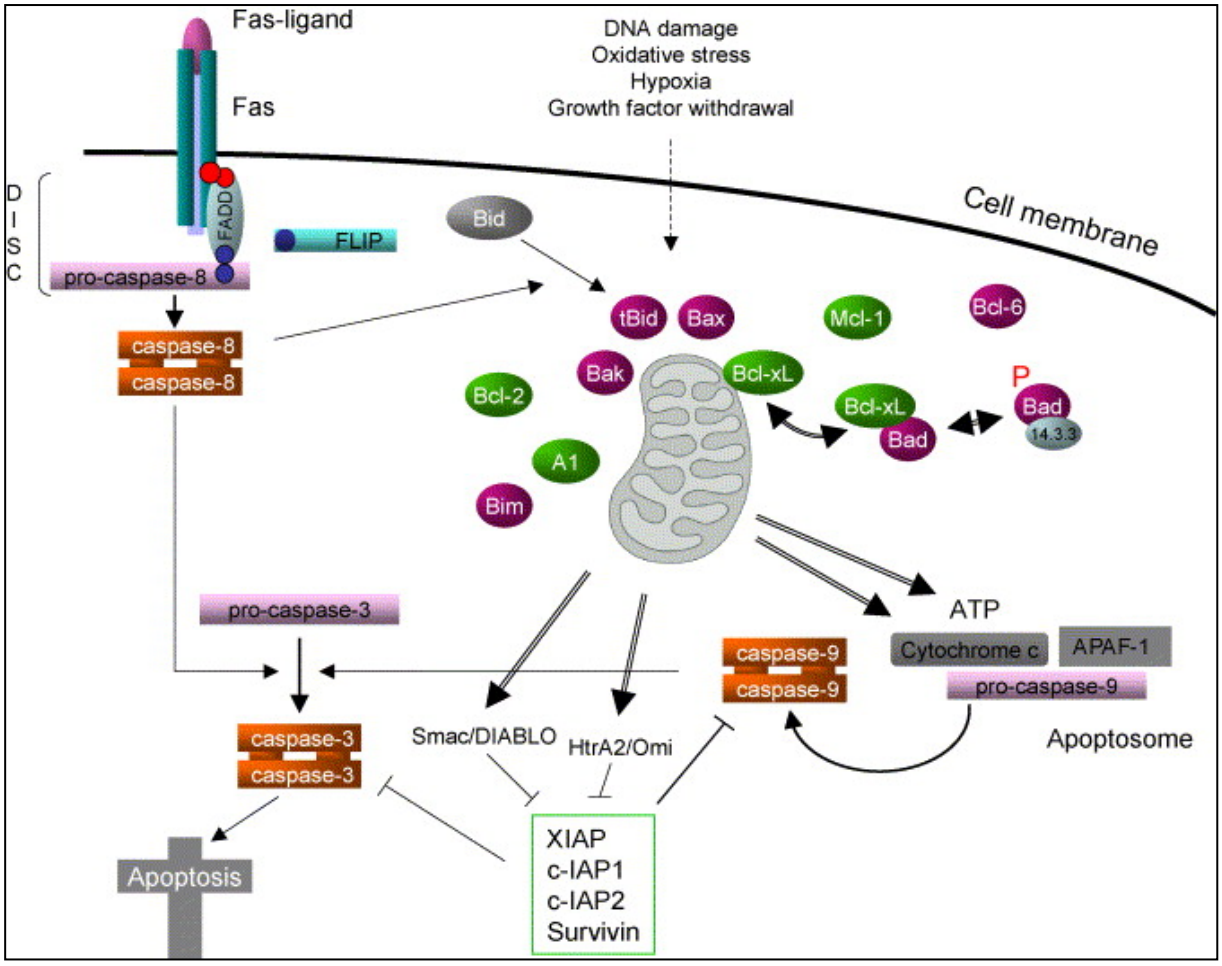

Figure n°11. Schéma de la voie de l'apoptose cellulaire*. La figure montre les deux voies principales, extrinsèque et intrinsèque de l'apoptose, et d'autre part les composants des voies apoptotiques intrinsèques et extrinsèques. Les facteurs apoptogènes sont des ligands des récepteurs induisant la mort, qui déclenchent la voie apoptotique extrinsèque, et des facteurs de stress tels que les agents endommageant l'ADN, les espèces réactives de l'oxygène et l'inhibition du facteur de croissance, qui évoquent la voie intrinsèque via la déstabilisation de la membrane externe mitochondriale (Kooijman, 2006).*

La voie intrinsèque est largement conservée chez les vers et les mouches. Chez les mammifères, elle est déclenchée en réponse à des facteurs de stress cellulaire distincts, notamment l'inhibition du facteur de croissance, des dommages à l'ADN et le stress du réticulum endoplasmique (RE), et est transduit par des membres de la famille Bcl-2. Seuls les

membres de cette famille Blc-2-Homologue-3 (BH3), activent directement les membres pro-apoptotiques de la famille Bcl-2, BAX et BAK, ou agissent afin d'inhiber les membres de la famille anti-apoptotique Bcl-2 (Brunelle and Letai, 2009). Il est démontré que les molécules BAX et BAK s'homo-oligomérisent pour former des pores dans la membrane mitochondriale externe, à travers lesquels les protéines pro-apoptotiques, y compris le cytochrome c et le deuxième activateur mitochondrial des caspases (Smac; également appelé DIABLO), peuvent passer vers le cytoplasme. Le cytochrome c, en particulier, est un médiateur crucial de la voie intrinsèque, car il active encore une autre protéine adaptatrice, connue sous le nom de facteur apoptotique activant la protéase-1 (Apaf-1), qui homo-oligomérise en un complexe moléculaire activant le recrutement des caspases (active la caspase-9 initiatrice et les caspases-3 et -7 effectrices) (Bratton et al., 2001 ; Bratton and Salvesen, 2010 ; Zou et al., 1997). Le complexe Apaf-1 / caspase-9 est appelé l'apoptosome et présente un mécanisme moléculaire très différent de celui du complexe de signalisation induisant la mort (DISC, domaine intracellulaire dans la face cytosolique, voie extrinsèque), bien que l'apoptosome et le DISC partagent la même fonction d'activation de leurs caspases terminales respectives pour initier l'apoptose (Bratton and Salvesen, 2010 ; Riedl and Salvesen, 2007). Les homologues d'Apaf-1 et de caspase-9 sont conservés chez tous les organismes multicellulaires (Dunn et al., 2007).

V.A. L'apoptose et le complexe de l'apoptosome

La voie intrinsèque de l'apoptose nécessite la libération de facteurs pro-apoptotiques des mitochondries, en particulier du cytochrome c vers le cytosol, qui active les composants liés à l'apoptosome (Ledgerwood and Morison, 2009). Le complexe de l'apoptosome est une plate-forme de signalisation en forme de roue cytosolique, constituée par l'oligomérisation du facteur Apaf-1 (Bratton and Salvesen, 2010 ; Riedl and Salvesen, 2007), induite par la libération du cytochrome c, conduisant à l'activation de plusieurs caspases, dont les caspases 9 et 3, et finalement à l'apoptose (Yuan and Akey, 2013) **(Figure n°12)**. L'activité de l'apoptosome Apaf-1 est contrôlée par plusieurs protéines telles que la protéine inhibitrice de l'apoptose liée au chromosome X (XIAP) (Shiozaki et al., 2003). Xiap fait partie des inhibiteurs des protéines de l'apoptose (IAPs) capables d'interagir à la fois directement avec les caspases activées et sous le contrôle des activateurs des caspases (indirectement) (Elmore, 2007). XIAP agit comme un garde-fou contre l'induction accidentelle du programme de mort cellulaire (Bratton and Salvesen, 2010 ; Cain, 2003) et peut également être ciblé par des agents pathogènes (Greenberg et al., 2015).

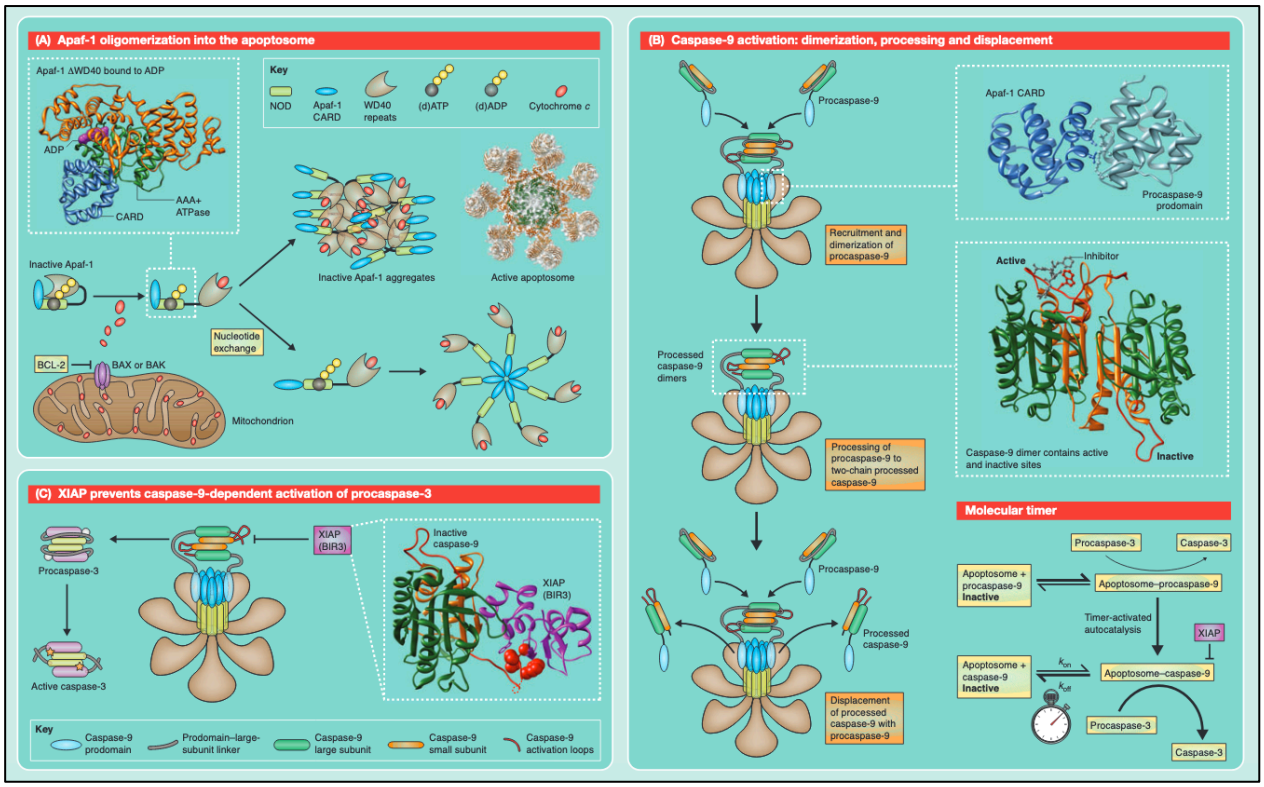

Figure n°12. Régulation de l'apoptosome Apaf-1-Caspase-9*. Apaf-1 est une protéine adaptatrice multidomaine contenant un domaine de recrutement des caspases N-terminal (CARD), suivi d'un domaine de liaison et d'oligomérisation des nucléotides (NOD, également connu sous le nom de NB-ARC), et un domaine Y de régulation C-terminal composé de 12 à 13 répétitions de la molécule WD40, qui forment des hélices β à sept et six rayons. Apaf-1 est normalement présent en tant que monomère dans une conformation verrouillée inactive liée au dATP ou à l'ATP. Cependant, lors de la liaison du cytochrome c à WDR40, Apaf-1 subirait un changement de conformation, entraîné par l'hydrolyse de l'ATP (d). Bien que les détails spécifiques ne soient pas clarifiés, après l'échange de nucléotides, les domaines CARD et les domaines hélicoïdaux auxiliaires d'Apaf-1 subissent des changements conformationnels supplémentaires pour exposer son domaine AAA + ATPase et permettre à de multiples protéines Apaf-1 de s'oligomériser en un complexe apoptosome heptamérique circulaire. Lorsque ces complexes sont incubés avec la procaspase-9, les domaines CARD d'Apaf-1 et de procaspase-9 forment un disque' attaché de manière flexible qui se trouve au-dessus du concentrateur central et chacun des domaines WDR40 sont connectés au noyau par le biais du domaine ultra-hélicoïdal. Globalement, cela donne l'apparence d'une particule en forme de roue dans laquelle sept rayons coudés rayonnent vers l'extérieur du noyau central et où se trouvent les enzymes procaspase-9 (ou au moins leurs CARD) au sommet du complexe (Bratton and Salvesen, 2010).*

V.B. *P.gingivalis* et l'apoptose des cellules

L'apoptose a été décrite comme un mécanisme potentiel impliqué dans la destruction tissulaire étendue associée à des maladies infectieuses et inflammatoires telles que l'ulcère

gastrique lié à *Helicobacter pylori* (Koeppel et al., 2015), l'athérosclérose (Yamada et al., 2016) et la parodontite chronique (Stathopoulou et al., 2009). Ainsi, un dérèglement de l'expression des gènes liés à l'apoptose, tels que Bax, Bcl2, Nlrp3 ou Smad2, a été observé dans les tissus gingivaux de patients atteints de parodontite (Song et al., 2015). Comme le processus d'apoptose est impliqué dans l'homéostasie et se caractérise par des modifications morphologiques cellulaires sous l'influence de plusieurs régulateurs (Zamaraev et al., 2015), il a été proposé précédemment que la persistance intracellulaire est une stratégie développée par la plupart des bactéries intracellulaires pour échapper à la réponse immune, contribuant ainsi au processus pathologique des maladies infectieuses et inflammatoires, telles que les maladies parodontales (Díaz et al., 2015 ; Hajishengallis, 2015a ; Lamont et al., 2018). *P.gingivalis* serait alors capable de moduler différentiellement l'apoptose des cellules (Mao et al., 2007 ; Roth et al., 2007 ; Stathopoulou et al., 2009; Yao et al., 2010). Plusieurs auteurs ont lié cette augmentation de la viabilité cellulaire à l'inhibition des mécanismes apoptotiques induits par *P.gingivali*s. L'une de ces études a montré que l'infection par *P.gingivalis* modulait un total de 55 gènes liés à l'apoptose dans les cellules épithéliales, en augmentant la survie et la prolifération de ces cellules (Handfield et al., 2005). Ainsi, *P.gingivalis* serait capable d'inhiber l'apoptose dans d'autres types cellulaires, y compris certaines cellules immunitaires (Murray and Wilton, 2003), les fibroblastes (Urnowey et al., 2006) et les cultures primaires de GEC (Mao et al., 2007).

À ce jour, les mécanismes et facteurs de virulence impliqués dans l'inhibition de l'apoptose au niveau des cellules épithéliales n'ont pas été complétement élucidés. Malgré cela, il a été rapporté que le LPS de *P.gingivalis* inhibe l'apoptose de certaines cellules immunitaires (Jain et al., 2013). Il semble donc raisonnable de suggérer que ce facteur de virulence pourrait participer à l'inhibition de l'apoptose dans l'épithélium, à travers la modulation des voies de signalisations initiées par les TLRs (Kocgozlu et al., 2009 ; Singh et al., 2011). À ce jour, il a été observé que la bactérie adhère et envahit les cellules hôtes en remodelant le cytosquelette et en reprogrammant diverses voies de transduction du signal liées à la survie, telles que la régulation du cycle cellulaire et l'apoptose (Gruenheid and Finlay, 2003 ; Inaba et al., 2009; Pan et al., 2014).

Fait intéressant, il a déjà été démontré que *P.gingivalis* modulait l'expression de l'apoptosome dans les cellules endothéliales (Bugueno et al., 2016) avec une influence potentielle sur l'aggravation de l'athérosclérose (Lalla et al., 2003). Cependant, l'effet d'une telle infection au niveau parodontal n'a pas encore été étudié. Par conséquent, il reste intéressant d'identifier de nouveaux mécanismes moléculaires associés à l'initiation de la parodontite, tels

que ceux associés aux protéines cytosoliques adaptatrices liées au domaine TIR, impliquées dans la reconnaissance des pathogènes par les TLRs **(Figure n°17)**.

VI. Implication systémique des parodontites

Au cours des dernières décennies, les maladies parodontales ont été associées à diverses maladies chroniques telles que le diabète, la polyarthrite rhumatoïde, les complications de la grossesse et les maladies cardio-vasculaires, suggérant un impact systémique (Huck et al., 2011 ; Linden et al., 2013 ; Lockhart et al., 2012 ; Pothineni et al., 2017 ; Rosenfeld and Campbell, 2011 ; Tonetti et al., 2007). Sur le plan cardio-vasculaire, les patients atteints de parodontite semblent plus prédisposés à la dysfonction endothéliale, à la progression de la maladie anévrysmale (Salhi et al., 2019), au rétrécissement des artères coronaires et à une augmentation de la mortalité associée aux troubles cardio-vasculaires (Buhlin et al., 2002; Xu and Lu, 2011). Ceci a notamment été confirmé lors d'un essai clinique où un traitement parodontal intensif chez des patients atteints de parodontite sévère a amélioré la fonction endothéliale à 6 mois, un marqueur reconnu des lésions vasculaires (Tonetti et al., 2007), renforçant ainsi ce lien de causalité.

Parmi les mécanismes biologiques proposés (Hajishengallis, 2015b ; Huck et al., 2011; Liljestrand et al., 2018 ; Salhi et al., 2019), l'impact des bactéries buccales et plus particulièrement parodontales sur l'homéostasie artérielle (Zelkha et al., 2010) est suggéré par leur dissémination éventuelle dans le flux sanguin à partir de la poche parodontale, puisqu'elles ont été détectées dans des plaques athéromateuses ainsi que dans la paroi des vaisseaux sains chez les patients atteints de parodontite légère à sévère (Amar and Engelke, 2015 ; Elkaim et al., 2008).

VII. L'athérosclérose

Les maladies cardio-vasculaires sont responsables de la plupart des décès dans le monde et représentent environ 32% de tous les décès en 2010 aux États-Unis et 28% en France. Elles sont considérées comme la deuxième cause de mortalité dans le monde juste après les cancers. Ces maladies exposent à de nombreuses complications aiguës ou chroniques telles que les infarctus du myocarde, les accidents vasculaires cérébraux, l'insuffisance cardiaque ou encore l'atteinte des extrémités des membres inférieurs. Bien que la morbidité et la mortalité liées aux maladies cardio-vasculaires aient diminué au cours des deux dernières décennies, l'augmentation du nombre de patients diabétiques et/ou obèses fait craindre une augmentation

de celle-ci dans le futur. Ainsi, la mise en évidence de facteurs de risque modifiables est primordiale pour améliorer la prise en charge des patients (Dimmeler, 2011).

Sur le plan physiopathologique, les maladies cardio-vasculaires constituent un ensemble de troubles affectant le cœur et les vaisseaux sanguins dont la cause la plus fréquente est l'athérosclérose. L'athérosclérose est une pathologie inflammatoire chronique caractérisée par un rétrécissement de la lumière artérielle. Le développement de la plaque d'athérome est un phénomène complexe induit par un grand nombre de phénomènes cellulaires et moléculaires tels que l'accumulation de lipoprotéines de basse densité (LDL), le recrutement et l'activation de cellules inflammatoires, la modification phénotypique des cellules musculaires lisses (VSMC), la dysfonction endothéliale ainsi que la migration des VSMC et leur prolifération dans l'*intima* (Karki et al., 2013 ; Lee et al., 2015). Le développement de la plaque d'athérome est orchestré par de nombreuses molécules, notamment les cytokines ainsi que certains facteurs chimiotactiques sécrétés au niveau des cellules endothéliales. Ces facteurs chimiotactiques vont induire le recrutement de monocytes et leur infiltration dans l'*intima*. Dans l'*intima*, les monocytes se différencient en macrophages et après phagocytose des LDLs se transforment en macrophages spumeux. Certaines molécules sont ainsi particulièrement étudiées du fait de leur influence sur l'ensemble de ces étapes, notamment au niveau endothélial, telles que la cyclooxygénase-2 (COX-2), la synthase de l'oxyde nitrique inductible (iNOS), TNF-α et certaines voies des protéines kinases activées par des mitogènes (MAPK) (Karki et al., 2013). Dans les stades ultimes d'évolution de la plaque, la rupture de la plaque d'athérome va entraîner la formation d'un caillot induisant une obturation de la lumière artérielle, une réduction du flux sanguin et donc un accident ischémique **(Figure n°13)**. A l'heure actuelle, l'ensemble des facteurs de risque pouvant influer sur le développement de la plaque d'athérome ne sont pas encore tous connus et un rôle particulier a été proposé pour l'infection (Rosenfeld and Campbell, 2011).

De nombreuses études ont mis en évidence le rôle de l'infection sur le développement de l'athérosclérose et plusieurs agents infectieux ont été identifiés tels que *Chlamydia pneumoniae (C.pneumoniae)*, *H.pylori* et *P.gingivalis* (Elkaim et al., 2008 ; Lockhart et al., 2012; Yilmaz, 2008). Cependant, les mécanismes moléculaires associés à chaque pathogène ne sont pas suffisamment décrits et l'impact pathologique spécifique de chacun d'entre eux reste sujet à discussion.

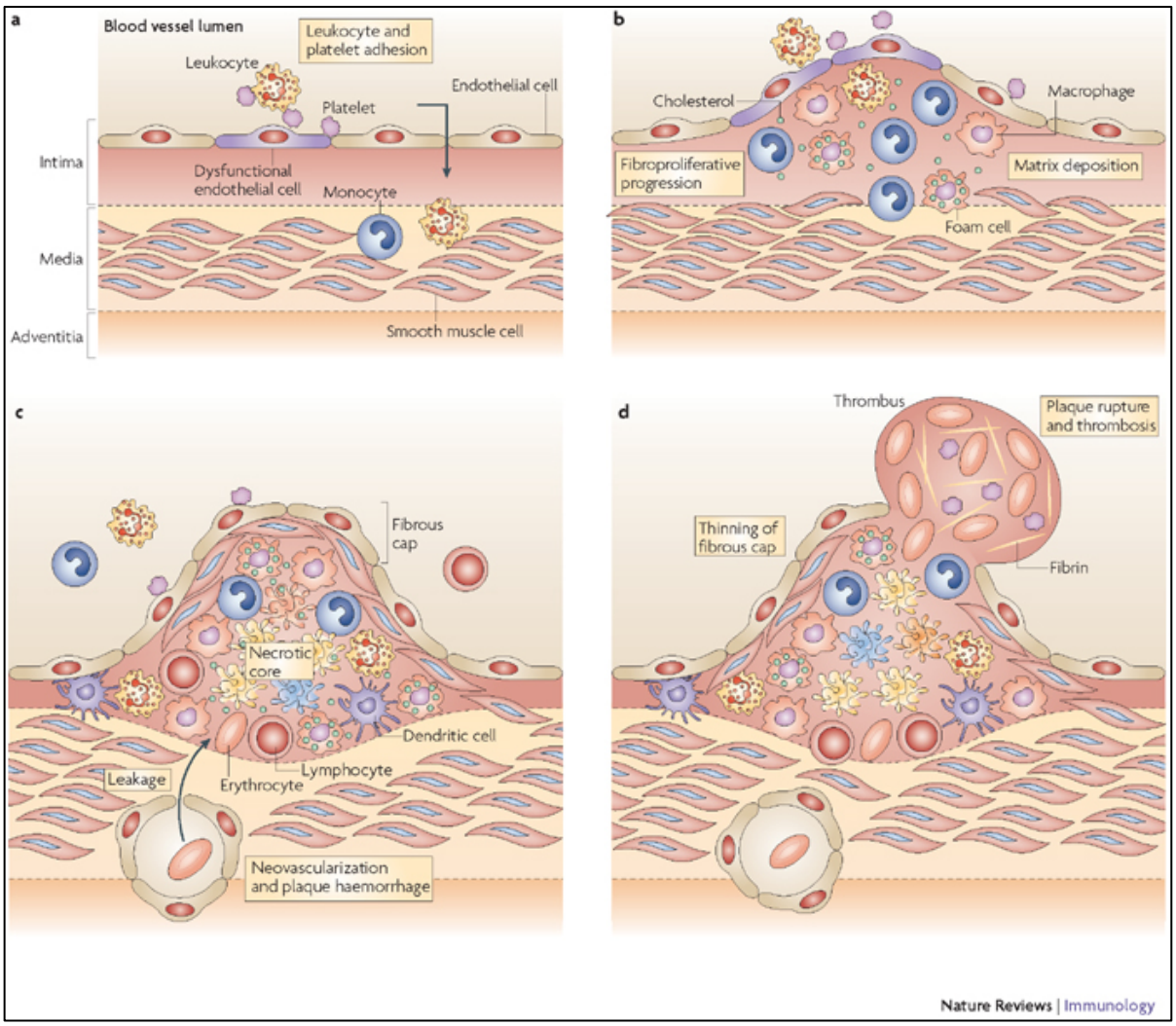

Figure n°13. Stade d'évolution de l'athérosclérose. *(a) Le dysfonctionnement des cellules endothéliales et leur activation dans des conditions pro-inflammatoires entraînent une adhérence précoce des plaquettes et des leucocytes et une perméabilité accrue de l'endothélium. (b) Les monocytes qui sont recrutés dans l'intima et la media accumulent les lipides et se transforment en cellules spumeuses, constituant des stries grasses. L'afflux continu de cellules mononucléaires, le dépôt des composants de la matrice et le recrutement des cellules musculaires lisses donnent lieu à la progression fibro-prolifération des plaques. (c) L'apoptose des macrophages et d'autres cellules de la plaque crée un noyau nécrotique et une coque fibreuse qui se compose d'une matrice et d'une couche de cellules musculaires lisses. (d) L'amincissement et l'érosion de la coque fibreuse dans des plaques instables, par exemple, en raison de la dégradation de la matrice par les protéases, aboutit finalement à une rupture de la plaque, à la libération des débris, à l'activation du système de coagulation et à la thrombose artérielle (Weber and Noels, 2011).*

VIII. Impact de l'infection par *Porphyromonas gingivalis* sur les cellules endothéliales

Les cellules endothéliales (EC) sont des cellules clés dans l'homéostasie vasculaire et leur dysfonctionnement est associé avec différentes phases de développement de la plaque d'athérome (Bugueno et al., 2016 ; Huck et al., 2012 ; Lockhart et al., 2012 ; Rydén et al., 2016) du fait notamment de leur localisation à l'interface entre flux sanguin et paroi artérielle. Ces cellules sont ainsi sous l'influence directe de plusieurs facteurs de stress comme les bactéries pathogènes lors d'épisodes de bactériémie **(Figure n°14)**. Plusieurs bactéries ont été décrites comme étant capable d'aggraver l'athérosclérose par l'induction de la mort des EC y compris *C.pneumoniae*, comme cela a été démontré *in vitro* (Birck et al., 2013) et *in vivo* (Roth et al., 2007). Si l'on considère plus particulièrement *P.gingivalis*, cette bactérie via l'action de ses facteurs de virulence tel que le lipopolysaccharide (LPS) est susceptible d'augmenter la mort cellulaire endothéliale par apoptose et nécrose (Bugueno et al., 2016), mais également d'activer différentes voies moléculaires associées aux TLRs et à la réponse immunitaire innée (Huck et al., 2015). Cette bactérie active également différentes enzymes impliquées dans le remodelage de la matrice extracellulaire telles que la CATB (Huck et al., 2012), l'inflammasome NLRP3 (Huck et al., 2015), la sécrétion de cytokines pro-inflammatoires (Rodrigues et al., 2012), favorisant ainsi l'évolution et la rupture de la plaque **(Figure n°14**.

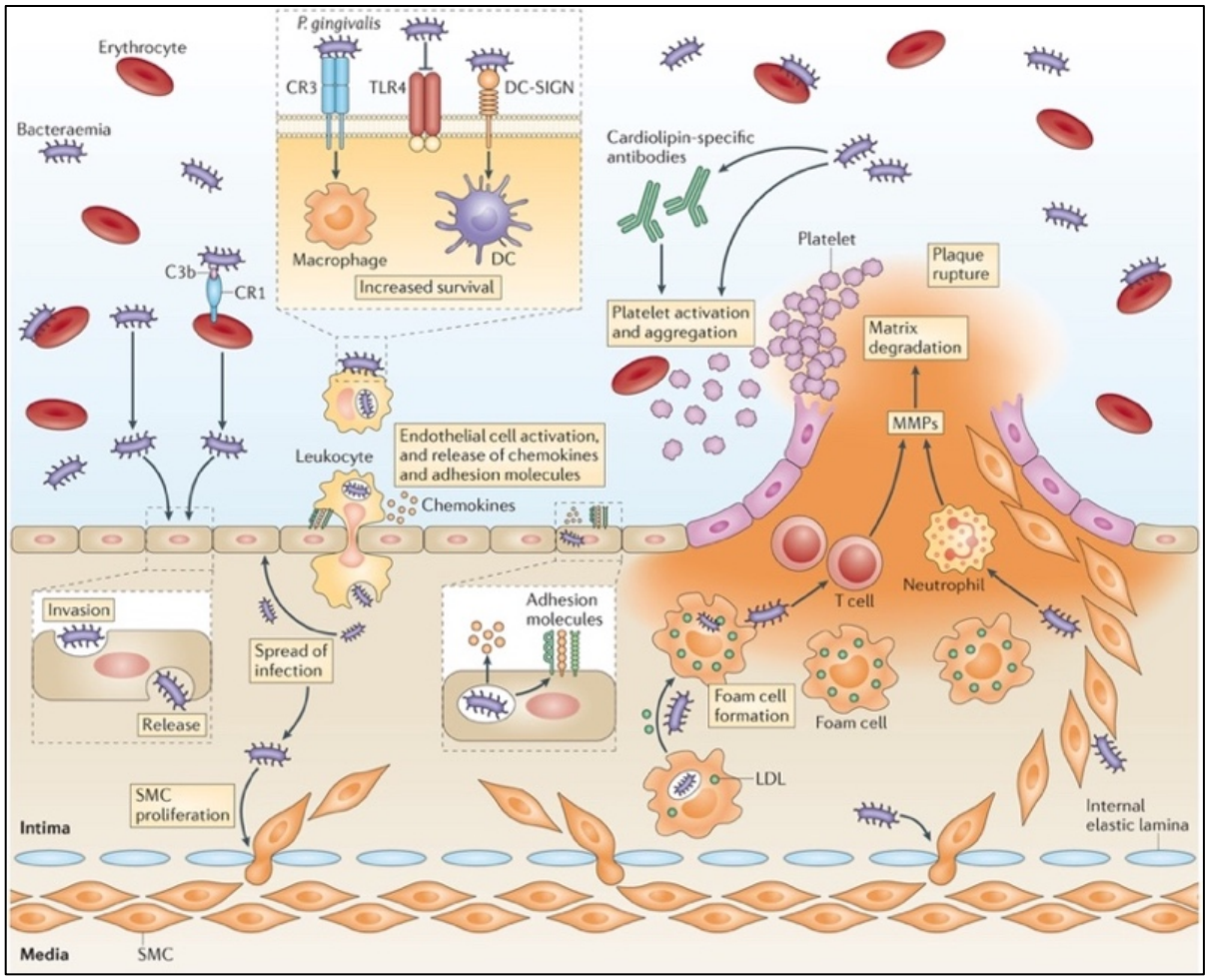

Figure n° 14. La dissémination de P.gingivalis dans la circulation systémique. *En plus d'une voie bactérienne, les bactéries parodontales peuvent envahir des leucocytes ou des érythrocytes, auxquels ils se fixent par l'interaction avec un récepteur C3b du complément 1 (CR1), et diffusent à partir de la muqueuse buccale aux tissus aortiques. Les bactéries envahissent, mais aussi activent les cellules endothéliales par l'augmentation de l'expression des molécules d'adhésion cellulaires et chimiokines, qui peuvent favoriser la transmigration des leucocytes pouvant abriter des bactéries intracellulaires viables. Les bactéries peuvent se propager aux tissus plus profonds où elles peuvent induire la prolifération des cellules musculaires lisses (CML) dans l'intima. L'absorption de lipoprotéines de basse densité (LDL) par les macrophages est augmentée en présence de bactéries, conduisant à une accélération de la formation des cellules spumeuses et à l'athérogenèse. Au stade ultime, la rupture de la plaque peut être facilitée par les bactéries, via la production de métalloprotéases matricielles (MMP) par les cellules vasculaires. L'agrégation plaquettaire induite contribuera à une occlusion thrombotique des vaisseaux (Hajishengallis, 2015a).*

Par ailleurs, il a également été démontré que l'infection par *P.gingivalis* et *C.pneumoniae* peut amplifier de manière synergique, l'impact d'autres facteurs de risque tels que les LDL ou encore certaines cytokines pro-inflammatoires (TNF-α). Par exemple, l'infection par *P.gingivalis* va augmenter de manière significative la mort cellulaire endothéliale induite par LDL en activant certaines voies moléculaires spécifiques régulant l'apoptose/nécrose caspase-dépendantes (Bugueno et al., 2016). La mort cellulaire endothéliale est un élément important de l'athérogenèse puisque ces cellules vont présenter certains facteurs membranaires pouvant activer notamment la réponse thrombogénique et faciliter le recrutement/diapédèse de certains types cellulaires de type polynucléaires neutrophiles (PNN) (Choy et al., 2001 ; Zhang et al., 2015). Plus précisément, le processus d'apoptose des ECs est impliqué dans la phase précoce de l'athérogenèse (Pirillo et al., 2013). Elle augmente la perméabilité vasculaire, la coagulation et favorise la prolifération des cellules musculaires lisses (Hopkins, 2013). En outre, les cellules apoptotiques non phagocytées peuvent devenir nécrotiques contribuant à l'inflammation vasculaire (Napoli, 2003). Récemment, l'apoptosome a été reconnue comme une cible thérapeutique potentielle dans plusieurs maladies telles que le diabète et l'obésité (Gupta et al., 2009 ; Tang et al., 2015). Son implication dans l'athérosclérose a été proposée (Maiolino et al., 2013) et certaines bactéries dont *P.gingivalis* ont été démontrées comme pouvant moduler son activité. Récemment, il a été proposé que le rôle pathogène associé à l'infection puisse être la répercussion de la réponse cellulaire paracrine médiée par certaines cytokines mais également par certaines microvésicules d'origine endothéliale **(Figure n°16)**.

IX. Les microvésicules d'origine endothéliale

Les microvésicules (MV), également appelées microparticules, sont des vésicules membranaires plasmatiques allant de 50 nm à 1 µm libérées par les cellules stimulées. Elles contiennent une variété de molécules actives telles que des lipides, des enzymes, des récepteurs, des microARN (miARN) (VanWijk et al., 2003). Les MV sont sécrétées par les cellules lors d'un stress cellulaire pouvant être induit par un grand nombre de stimuli **(Figure n° 15)**.

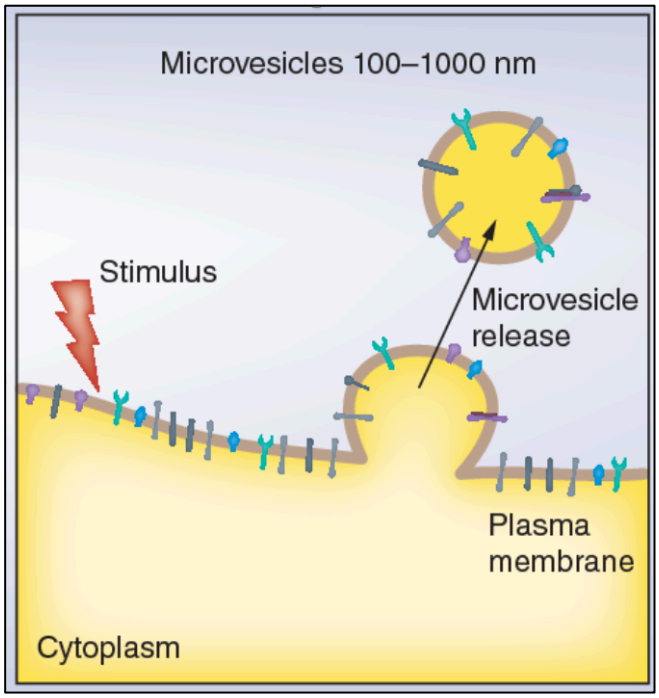

Figure n°15. Schéma des principaux mécanismes de biogenèse des microvésicules*. Les microvésicules sont générées par le soufflage de la membrane plasmique cellulaire à la suite d'un grand nombre de stimuli. Elles portent des molécules potentiellement bioactives, notamment des récepteurs, des ligands, des enzymes et des ARN fonctionnels (Vítková et al., 2018).*

A ce jour, les MV ont été principalement identifiées comme étant des vésicules membranaires libérées par les cellules vasculaires telles que les EC, les CML, des plaquettes, des érythrocytes et des leucocytes (Angelillo-Scherrer, 2012). Historiquement, les MV étaient considérées comme « des débris cellulaires sans intérêt biologique » mais certaines études ont mis en évidence leurs propriétés pathogéniques importantes notamment dans le domaine de l'athérosclérose (Patz et al., 2013). Dans la circulation sanguine, les MV endothéliales (EMV) constituent une sous-population de la famille des MV associées à la pathogenèse de diverses maladies cardio-vasculaires, principalement déclenchées par une dysfonction endothéliale. Les recherches ont démontré le rôle clé des EMV dans la croissance, la division et la maturation des précurseurs des ECs, importantes pour la régénération des vaisseaux sanguins (Hristov et al., 2004), ce qui suggère un rôle potentiel des EMV sur l'homéostasie vasculaire (Dignat-George and Boulanger, 2011) **(Figure n°16)**. Une des caractéristiques des EMV est qu'elles exposent dans leur surface la phosphatidylsérine (PhtdSer), un phospholipide anionique transféré du côté interne au côté externe de la membrane plasmique avant leur libération. De plus, les protéines membranaires présentes à la surface de la cellule mère permettent de caractériser leur origine cellulaire dans les fluides corporels. Les EMV circulantes

procoagulantes ont été démontrées comme des biomarqueurs des atteintes vasculaires d'origine athérothrombotique, inflammatoire ou mécanique, y compris l'ischémie de reperfusion. Quelle que soit leur origine cellulaire, les MV en circulation émergent en tant que nouveaux acteurs de la dysfonction cellulaire agissant en tant que messagers procoagulants, pro-inflammatoires, apoptotiques ou pro-sénescence dans des conditions pathologiques. En effet, le stress cellulaire initial à l'origine de l'excrétion des MV apparaît pertinent pour l'induction d'un dysfonctionnement cellulaire spécifique (Vítková et al., 2018).

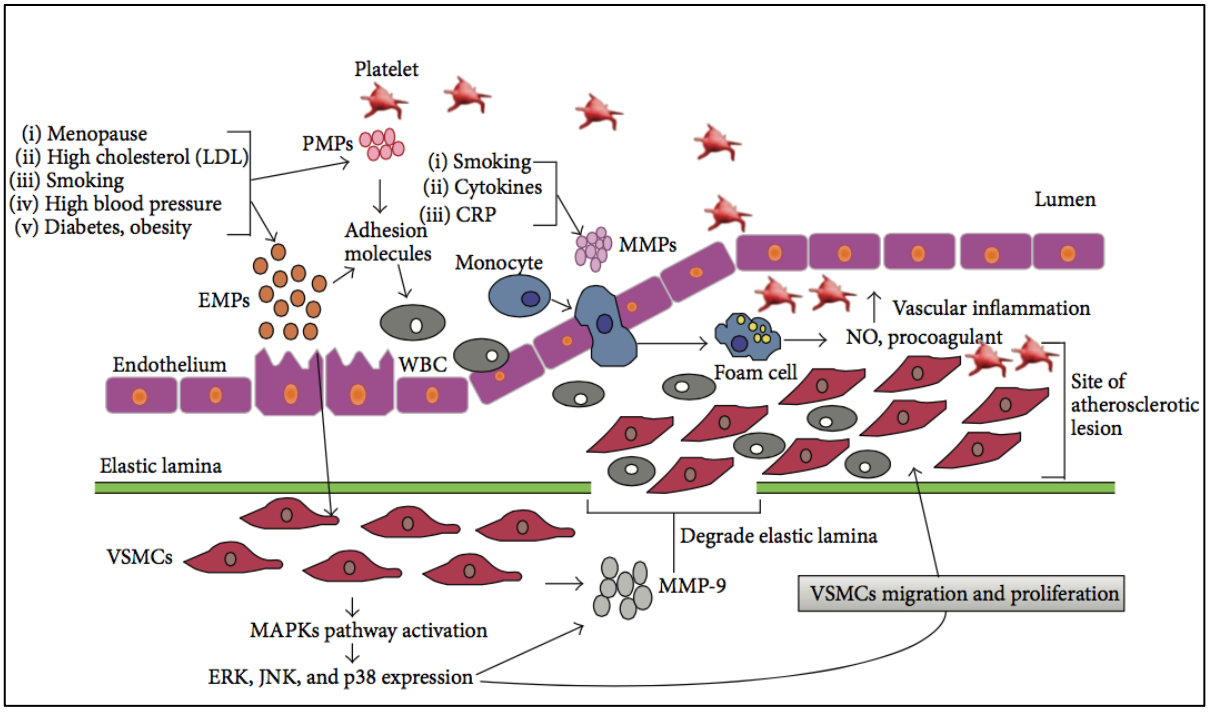

Figure n°16 : Principales hypothèses relatives au rôle des microvésicules (MV) dans la physiopathologie de l'athérosclérose. *Les microvésicules endothéliales (EMV) et les microvésicules plaquettaires (PMV) sont générées par l'activation de l'endothélium par un certain nombre de facteurs comme le tabagisme, le stress oxydatif, l'obésité et l'hypertension artérielle alors que les microvésicules provenant de monocytes (MMV) sont générées par les cytokines pro-inflammatoires (TNF-α, IL 1-β), le tabagisme et la protéine C réactive (CRP). Les EMV peuvent activer les cellules musculaires lisses vasculaires (CML) pour exprimer la MMP-9 qui peut dégrader la barrière élastique "la lamina", pour faciliter la migration des CML depuis la couche media vers l'intima sur le site de la lésion athérothrombotique. En outre, les EMV sont aussi capables d'augmenter l'expression d'ERK, JNK et p38 via la voie des MAPK, entraînant la prolifération et la migration des CML, pour développer la plaque d'athérome. Les molécules d'adhésion cellulaire, exprimées par les EMV et les PMV, facilitent*

l'adhérence des leucocytes et des plaquettes à la surface endothéliale, en développant ainsi l'épaississement de l'intima et d'une lésion vasculaire. Les MMV peuvent activer la voie de la synthase de l'oxyde nitrique inductible pour libérer de l'oxyde nitrique (NO), qui est un pro-coagulant responsable de l'inflammation vasculaire et de la dysfonction endothéliale. Collectivement, tous ces événements conduisent à l'athérosclérose (Paudel et al., 2016).

Il apparaît ainsi important de pouvoir connaître le phénotype d'EMV entre un état sain et pathologique, ceci afin d'une part de mieux comprendre leur rôle physiopathologique mais également de pouvoir évaluer leur potentiel intérêt clinique comme marqueur de la souffrance vasculaire. Ainsi, Markiewicz *et al*., 2013 ont réalisé une étude afin de mettre en évidence les différentes stades associés à l'angiogenèse et la sécrétion de EMV par dosage *in vivo* (VanWijk et al., 2003). Cette étude a ainsi mis en évidence, d'une part l'augmentation de la concentration d'EMV chez les patients malades, mais a également mis en évidence une corrélation entre l'angiogenèse et la concentration d'EMV. Une autre étude réalisée par Koga et al. a démontré la présence des EMV positives à CD-144, également connu sous le nom de « vascular endothelial- (VE-) cadherin » dans la circulation humaine, avec des niveaux plus élevés observés chez les personnes souffrant de diabète et de maladies coronariennes (Koga et al., 2005). Ces données permettent ainsi d'utiliser l'évaluation des EMV CD-144 comme marqueurs diagnostiques et/ou thérapeutiques (Koga et al., 2005).

2. OBJECTIFS

Les mécanismes impliqués dans l'initiation et le développement des parodontites restent peu connus. A l'heure actuelle, le rôle prépondérant joué par *P.gingivalis* est considéré comme majeur dans les phénomènes associés. De ce fait, la mise en évidence de nouveaux mécanismes ou de nouvelles cibles cellulaires affectées par ce pathogène pourrait permettre de développer de nouvelles stratégies thérapeutiques. L'objectif de ce travail de thèse a donc été de déterminer l'impact de *P.gingivalis* sur l'homéostasie des tissus mous gingivaux et de l'endothélium. Pour cela, différentes stratégies ont été utilisées :

❖ Chapitre 1 : **Contribution de *P.gingivalis* à la modulation de la mort cellulaire épithéliale et fibroblastique.**

Dans ce premier chapitre, nous avons cherché à déterminer les mécanismes impliqués dans l'invasion et la modulation de la réponse immunitaire de l'hôte par *P.gingivalis* pour favoriser sa survie. Il a été décrit que cette bactérie est capable de moduler le cycle cellulaire et la mort cellulaire programmée contribuant à l'aggravation de la lésion parodontale.

Un domaine émergent dans la pathogenèse bactérienne est la capacité des bactéries à inhiber l'apoptose dans les cellules eucaryotes. L'inhibition de l'apoptose fournit un avantage de survie car elle permet aux bactéries de se loger ainsi que de se répliquer dans les cellules hôtes. Des résultats controversés sont trouvés dans la littérature concernant l'effet induit par *P.gingivalis* sur l'apoptose et la prolifération des GEC. Plusieurs voies moléculaires ont été identifiées comme déclencheurs clés de l'apoptose, notamment l'apoptosome Apaf-1 et ses inhibiteurs, telle que la protéine XIAP, qui semble être intéressante d'un point de vue physiopathologique et thérapeutique.

❖ Chapitre 2 : **Implication des microvésicules d'origine endothéliale induites par l'infection par *P.gingivalis* dans l'inflammation endothéliale.**

Dans une deuxième partie, nous nous sommes intéressés à la réponse de l'endothélium face à l'infection parodontale, lors de la dissémination des parodontopathogènes *via* la circulation systémique. L'infection chronique a été décrite comme un mécanisme potentiel

impliqué dans l'aggravation de l'athérothrombose. Récemment, il a été suggéré que le rôle pathogène associé à une infection bactérienne pourrait être induit par la réponse paracrine des cellules endothéliales (EC) induite par les cytokines sécrétées mais également par des microvésicules d'origine endothéliale (EMV). Nous avons ainsi voulu déterminer le rôle de *P.gingivalis* sur la sécrétion des EMV et leurs propriétés pro-inflammatoires. La mise en évidence d'un nouveau mécanisme contribuerait à une meilleure compréhension des phénomènes impliqués dans l'interaction entre parodontite et maladies cardio-vasculaires.

❖ Chapitre 3 : **Développement d'un nouveau modèle 3D sphéroïde *in vitro* permettant l'évaluation de l'impact de l'infection par *P.gingivalis* sur les interactions épithélio-fibroblastiques.**

La troisième partie concerne plus particulièrement le développement d'un nouveau modèle cellulaire 3D *in vitro*. Dans le but de mieux comprendre l'impact des interactions entre les tissus mous gingivaux et les agents pathogènes parodontaux, tel que *P.gingivalis*, un nouveau modèle 3D *in vitro* de gencive a été développé en utilisant la méthode des gouttes suspendues, formant des microtissus comprenant 2 types cellulaires distincts et mimant ainsi l'interface épithélium-conjonctif. Ce modèle doit nous permettre, à terme, de prendre en compte les interactions épithélio-fibroblastiques dans les phénomènes inflammatoires induits par *P.gingivalis*, et donc de se rapprocher au plus près de la situation *in vivo*.

❖ Chapitre 4 : **Impact de *P.gingivalis* sur la modulation des protéines « TIR-domain-containing adaptors (TIR) » dans la signalisation médiée par les « Toll-like receptors ».**

Dans un ultime chapitre, nous nous sommes intéressés à l'identification des voies moléculaires précocement modulées par *P.gingivalis*. Les TLRs constituant la voie classique d'activation cellulaire face à l'infection, une analyse de la modulation de l'expression des molécules impliquées dans la signalisation intracellulaire et associée au recrutement des protéines adaptatrices contenant le domaine du récepteur Toll/interleukine-1 (TIR) a été effectué. Le but de cette étude est d'évaluer les effets de l'infection par *P.gingivalis* sur

l'expression et les interactions protéine-protéine parmi 5 TIR (MAL, Myd88, Trif, TRAM et Sarm), ceci afin de mettre en évidence de potentielles cibles thérapeutiques.

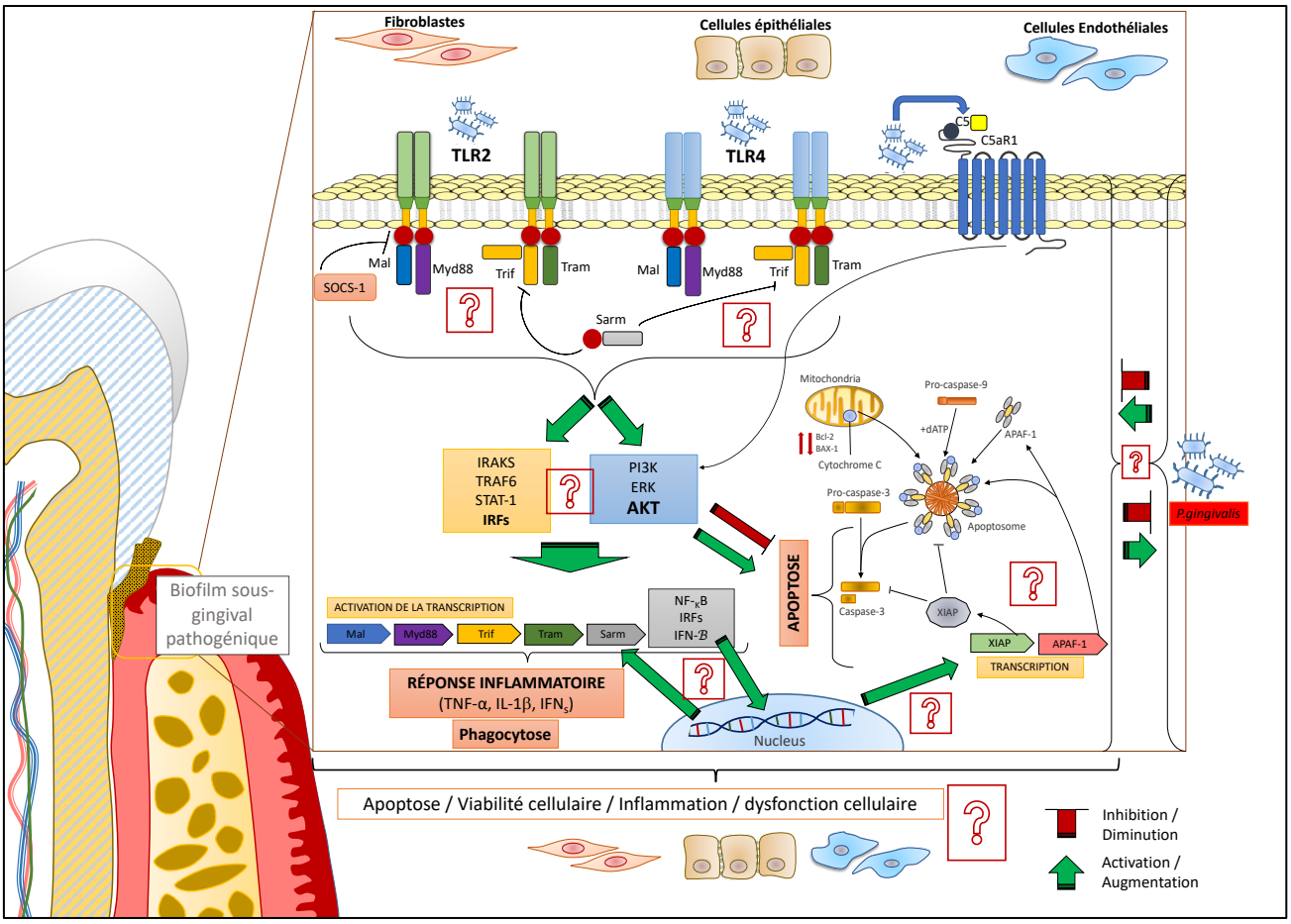

Figure n°17. Schéma représentant les voies moléculaires potentiellement modulées par P.gingivalis au niveau des cellules épithéliales, des fibroblastes et des cellules endothéliales. *Ces mécanismes, liés à l'initiation et au développement des parodontites, restent encore peu connus. Ces processus sont principalement l'apoptose, la reconnaissance des pathogènes et des facteurs de virulence via la signalisation par les TLRs, la réponse inflammatoire et l'invasion intracellulaire. A l'heure actuelle, le rôle prépondérant joué par P.gingivalis est considéré comme majeur dans la physiopathologie des parodontites. Dans ces travaux de thèse, nous nous intéressons à mettre en évidence de nouveaux mécanismes ou de nouvelles cibles cellulaires affectées par ce pathogène, ce qui pourrait permettre de développer de nouvelles stratégies thérapeutiques.*

3. RÉSULTATS ET DISCUSSION

CHAPITRE 1

Contribution de *P.gingivalis* à la modulation de la mort cellulaire cellulaire épithéliale et fibroblastique.

❖ **Bugueno I.M.,** Batool F., Benkirane- Jessel N., Huck N. "*Porphyromonas gingivalis* differentially modulates apoptosome Apoptotic Peptidase Activating Factor 1 in epithelial cells and fibroblasts", **The American Journal of Pathology 2017, 188(2): 404-416.**

Contexte et objectifs

Les bactéries parodontopathogènes, telles que *P.gingivalis, T.forsythia et T.denticola*, interagissent avec les cellules hôtes, y compris les cellules épithéliales et les fibroblastes, afin de coloniser et d'envahir les zones profondes du parodonte (Costalonga and Herzberg, 2014). *P.gingivalis*, une bactérie considérée comme l'un des agents pathogènes clés impliqués dans la transition d'un état de santé parodontale vers la maladie (Abusleme et al., 2013), présente un large éventail de facteurs de virulence, notamment le lipopolysaccharide (*Pg*-LPS) et plusieurs protéases extracellulaires contribuant à sa capacité d'invasion (Soto et al., 2015 ; Diaz et al., 2014). La persistance intracellulaire est une stratégie développée par la bactérie pour échapper à la réponse immune innée favorisant la dysbiose au niveau sous-gingival (Lamont et al., 2018).

L'apoptose a été décrite comme un mécanisme potentiel impliqué dans la destruction tissulaire associée à des nombreuses maladies infectieuses et inflammatoires (Lin et al., 2014 ; Yamada et al., 2016). La dérégulation de l'expression des gènes liés à la voie intrinsèque de l'apoptose, tels que Bax ou Bcl2, a été observée dans les tissus gingivaux de patients atteints de parodontite (Song et al., 2016). L'apoptose est impliquée dans l'homéostasie tissulaire et est sous l'influence de régulateurs, y compris des caspases, qui pourraient être qualifiées d'exécuteurs clés du mécanisme de la mort cellulaire (Zamaraev et al., 2015). Même s'il existe deux voies d'activation de l'apoptose, nous nous sommes intéressés principalement à la voie intrinsèque. La voie intrinsèque de l'apoptose nécessite la libération vers le cytosol de facteurs pro-apoptotiques des mitochondries, en particulier du cytochrome c, qui activent les composants liés à l'apoptosome (Lergedwood et al., 2009). Le complexe de l'apoptosome est une plate-forme de signalisation en forme de roue cytosolique, constituée par l'oligomérisation du facteur activant l'apoptose de la peptidase 1 (Apaf-1) (Riedl et al., 2007) induite par la libération du cytochrome c conduisant à l'activation de plusieurs caspases, y compris des caspase-9 et -3 (Yuan et al., 2013). L'activité de l'apoptosome Apaf-1 est contrôlée par plusieurs protéines telles que l'inhibiteur lié à la protéine de l'apoptose X (XIAP) (Shiozaki et al., 2003). Nous avons précédemment démontré que *P.gingivalis* modulait l'expression de l'apoptosome

dans les cellules endothéliales (Bugueno et al., 2016). Cependant, l'impact au niveau des cellules du parodonte est méconnu.

Par conséquent, le but de cette étude était d'évaluer l'expression d'Apaf-1 dans les tissus gingivaux provenant de patients sains ou présentant une parodontite et *in vivo* dans un modèle expérimental murin de parodontite. Simultanément, l'expression et les activités enzymatiques de molécules clés liées à l'apoptosome ont été examinées en réponse à l'infection par *P.gingivalis* dans deux lignées cellulaires *in vitro*, les cellules épithéliales gingivales (GEC) et les fibroblastes oraux (FB) dans le but d'identifier de nouveaux mécanismes moléculaires associés à l'initiation de la parodontite.

Résultats et discussion

Une expression différentielle de l'ARNm d'Apaf-1 et de Xiap a été observé entre les échantillons gingivaux humains soulignant leurs rôles potentiels dans la parodontite. Cette modulation de l'expression d'Apaf-1 a également été observée dans un modèle de parodontite expérimentale murine induite par des ligatures infectées par *P.gingivalis*. *In vitro*, *P.gingivalis* cible les molécules Apaf-1, XIAP, caspase-3 et caspase-9 au niveau de l'ARNm et protéique, entrainant une inhibition de la mort des GEC. L'effet inverse a été observé au niveau des FB dans lesquels *P.gingivalis* a induit une augmentation de la mort cellulaire via apoptose. Pour évaluer si les effets observés étaient associés à la protéine Apaf-1, les GEC et les FB ont été transfectés avec un siRNA ciblant cette même protéine confirmant les observations précédentes. Enfin, les effets de *P.gingivalis* sur l'activation de l'apoptose, par inhibition de XIAP, ont été évalués confirmant son implication.

Conclusion

Cette étude a démontré le rôle joué par Apaf-1 et XIAP dans la pathogenèse des parodontites. Ainsi, l'infection par *P.gingivalis* module l'activation de l'apoptosome Apaf-1 et de XIAP de manière différentielle en fonction du type cellulaire. Ceci pourrait constituer l'un des mécanismes expliquant la subversion de la réponse immunitaire innée de *P.gingivalis*. Cependant, d'autres expériences portant sur l'activation d'Apaf-1 devraient être menées afin d'évaluer son impact potentiel dans la prévention ou le traitement des parodontites. Ceci

pourrait contribuer à la mise en évidence de médicaments spécifiques prenant en compte le risque d'effets secondaires associés.

The American Journal of Pathology, Vol. 188, No. 2, February 2018

The American Journal of
PATHOLOGY
ajp.amjpathol.org

IMMUNOPATHOLOGY AND INFECTIOUS DISEASES

Porphyromonas gingivalis Differentially Modulates Apoptosome Apoptotic Peptidase Activating Factor 1 in Epithelial Cells and Fibroblasts

Isaac M. Bugueno,* Fareeha Batool,* Linda Korah,* Nadia Benkirane-Jessel,* and Olivier Huck*†

From INSERM 1260 Regenerative Nanomedicine, Fédération de Médecine Translationnelle de Strasbourg (FMTS), Strasbourg; and the Faculty of Dental Surgery, Periodontology,† Université de Strasbourg, Strasbourg, France*

Accepted for publication October 3, 2017.

Address correspondence to Olivier Huck, D.D.S., Ph.D., Periodontology, Dental Faculty, 8 rue Sainte-Elisabeth, 67000 Strasbourg, France. E-mail: o.huck@unistra.fr.

Porphyromonas gingivalis is able to invade and modulate host–immune response to promote its survival. This bacterium modulates the cell cycle and programed cell death, contributing to periodontal lesion worsening. Several molecular pathways have been identified as key triggers of apoptosis, including apoptosome apoptotic peptidase activating factor 1 (APAF-1). Apaf-1 and X-linked inhibitor of apoptosis protein (Xiap) mRNA were differentially expressed between gingival samples harvested from human healthy and chronic periodontitis tissues (Apaf-1, 19.2-fold; caspase-9, 14.5-fold; caspase-3, 6.8-fold; Xiap: 2.5-fold in chronic periodontitis) ($P < 0.05$), highlighting their potential role in periodontitis. An increased proteic expression of APAF-1 was also observed in a murine experimental periodontitis model induced by *P. gingivalis*–soaked ligatures. *In vitro*, it was observed that *P. gingivalis* targets APAF-1, XIAP, caspase-3, and caspase-9, to inhibit epithelial cell death at both mRNA and protein levels. Opposite effect was observed in fibroblasts in which *P. gingivalis* increased cell death and apoptosis. To assess if the observed effects were associated to APAF-1, epithelial cells and fibroblasts were transfected with siRNA targeting Apaf-1. Herein, we confirmed that APAF-1 is targeted by *P. gingivalis* in both cell types. This study identified APAF-1 apoptosome and XIAP as intracellular targets of *P. gingivalis*, contributing to the deterioration of periodontal lesion through an increased persistence of the bacteria within tissues and the subversion of host–immune response. *(Am J Pathol 2018, 188: 404–416; https://doi.org/10.1016/j.ajpath.2017.10.014)*

Periodontitis is a group of common chronic inflammatory diseases characterized by the destruction of tooth-supporting tissues and affecting >30% to 50% of the adult population worldwide.[1] The pathogenesis of periodontitis is related to the disruption of homeostasis between host–immune response and dysbiotic microbial flora at the lesion site.[2] Periodontopathogenic bacteria, such as *Porphyromonas gingivalis*, *Tannerella forsythia*, and *Treponema denticola* interact with the host cells, including epithelial cells (ECs) and fibroblasts (FBs), aiming to colonize and bypass this barrier for invading the profound periodontal tissues.[3] *P. gingivalis*, a Gram-negative assacharolytic bacteria, is considered as one of the keystone pathogens involved in the transition from periodontal health to disease.[4] This bacterium exhibits a wide array of virulence factors, including lipopolysaccharide (*Pg*-LPS), extracellular proteases, and several factors that contribute to its capability of cellular invasion such as fimbriae.[5] Intracellular persistence is one strategy developed by the bacteria to escape the host–immune response, contributing to the pathologic process of periodontal diseases.[6] This bacterium is also able to modulate cell cycle and programed cell death in an attempt to avoid the host–cell response and to promote its spread to distant sites.[7,8] For instance, it has been observed that epithelial invasion by *P. gingivalis* subdues apoptosis and stimulates cell proliferation through modulation of several molecular triggers such as p53 and Janus kinase/Stat.[9,10] However, the

Supported by INSERM and Faculté de Chirurgie Dentaire, Université de Strasbourg.

Disclosures: None declared.

https://doi.org/10.1016/j.ajpath.2017.10.014

mechanisms involved remain under investigation, and several contradictory results have been observed about the influence of *P. gingivalis* on apoptosis and cell viability with some studies endorsing induction of apoptosis by infection.[11,12] However, others have described its ability to inhibit such a process as a mechanism leading to induction of apoptosis.[10,13]

Apoptosis has been described as a potential mechanism involved in the extensive tissue destruction associated to infectious and inflammatory diseases such as gastric ulcer related to *Helicobacter pylori*,[14] atherosclerosis,[15] and chronic periodontitis (CP).[12] Dysregulation of apoptosis-related genes, such as *Bax*, *Bcl2*, *Nlrp3*, or *Smad2*, has been observed in the gingival tissues of patients with periodontitis.[16] Apoptosis is involved in homeostasis and is characterized by cellular morphologic changes, including cell shrinkage, DNA fragmentation, and engulfment by macrophages or neighboring cells. It is under the influence of regulators, including caspases that could be stated as key executioners of the cell death machinery.[17] Apoptosis is induced by both extrinsic and intrinsic pathways. The intrinsic apoptosis pathway requires the release of proapoptotic factors from mitochondria, especially cytochrome c to the cytosol, which activates apoptosome-related components.[18] The apoptosome complex is a cytosolic wheel-shaped signaling platform, constituted by the oligomerization of apoptotic peptidase activating factor 1 (APAF-1)[19] induced by cytochrome c release that leads to the activation of several caspases, including caspase-9 and -3, and ultimately to apoptosis.[20] APAF-1 apoptosome activity is controlled by several proteins such as X-linked inhibitor of apoptosis protein (XIAP).[21] XIAP is a member of inhibitors of apoptosis proteins (IAPs) that is able to interact both directly with the activated caspases and under the control of activator of caspases such as second mitochondria-derived activator of caspase/direct inhibitor of apoptosis-binding protein with low pI.[22] XIAP acts as a guard against accidental induction of the cell death program[23] and may also be targeted by pathogens.[24] Interestingly, it was already demonstrated that apoptosome expression is modulated by *P. gingivalis* in an endothelial cell model[25] with potential influence on atherosclerosis worsening.[26] However, the effect of such infection at the periodontal level has not been investigated so far.

Therefore, the aim of this study was to evaluate the expression of APAF-1 in CP tissues *in vivo*. Simultaneously, the expression and enzymatic activities of key molecules related to apoptosome were examined in response to *P. gingivalis* infection in ECs and FBs *in vitro*, in an attempt to identify new molecular mechanisms associated to periodontitis onset.

Materials and Methods

Ethics Statement

A total of 20 patients accepted to participate in this study that received approval from the Ethic Committee (French Ministry of Research, Bioethic department authorization DC-2014-2220). All patients gave written and informed consent before enrollment. Complete medical and dental histories were taken from all of the subjects.

Study Population and Clinical Examination

None of the patients had systemic diseases or cigarette smoking habit and had not taken any prior medications such as antibiotics in the past 3 months. Clinical periodontal examination included measurement of pocket probing depth and bleeding on probing at six sites around each tooth with a manual periodontal probe. The healthy group consisted of nine patients (five men and four women; mean age, 37.8 ± 17.3 years), and the CP group consisted of 11 patients (four men and seven women; mean age, 62.4 ± 7.3 years). Periodontal diagnosis of CP was based on the 1999 International World Workshop for a Classification of Periodontal Disease and Conditions.[27]

Collection of Gingival Tissue Samples

Gingival samples were obtained during periodontal surgeries (open access flap) or dental extractions. Samples were inserted immediately in a sterile tube and stored at −80°C until RNA extraction.

Bacterial Culture

Porphyromonas gingivalis ATCC 33277 (ATCC, Manassas, VA) was cultured under strict anaerobic conditions at 37°C in brain–heart infusion medium (Sigma-Aldrich, St. Louis, MO), supplemented with 5 mg/mL hemin and 1 mg/mL menadione. On the day of infection, bacteria were collected and counted as previously described.[25] To inactivate *P. gingivalis* (heat-killed *P. gingivalis*; H*Pg*), bacteria were heated at 85°C for 10 minutes before the beginning of the experiment. Commercial ultrapure *Pg*-LPS was purchased from InvivoGen (San Diego, CA).

Experimental Periodontitis

After anesthesia, *P. gingivalis*–infected ligature was placed at the cervical palatal site of first and second maxillary molars of mice (C57/BL6; Charles River, Larbresle, France). Ligatures were replaced twice a week during 30 days as described previously.[28] All procedures were approved by the local ethical committee and performed according to the regulations for animal experimentation. Mice were examined to evaluate pain and stress, and their weight was monitored daily.

Immunohistochemistry

Immunohistochemistry for APAF-1 has been performed on sections from *P. gingivalis*–infected mice and controls. Slides were treated as described in Saadi-Thiers et al.[28]

Briefly, after preliminary treatment, slides were incubated with primary antibody against APAF-1 (rabbit; PA5-19894; ThermoFischer, Illkirch, France) (dilution 1:200) at 4°C for 24 hours and then with peroxidase dog anti-rabbit IgG (dilution 1:200) for 30 minutes (ImmunoCruzTM rabbit ABC Staining System; Santa Cruz Biotechnology, Heidelberg, Germany). As a negative control, sections were treated with phosphate-buffered saline or with IgG as the primary antibody to rule out nonspecific binding. Finally, the sections were treated with diaminobenzadine as a substrate chromogen and counterstained with hematoxylin. The slides were then mounted and observed under a light microscope. ImageJ software version 1.5 (NIH, Bethesda, MD; *http://imagej.nih.gov/ij*) was used to evaluate the relative protein expression of APAF-1 on both healthy and diseased tissues.

Cell Culture

Human oral ECs (GECs) used in this study derived from the TERT-2/OKF-6 cell line (BWH Cell Culture and Microscopy Core, Boston, MA). Cells were cultured at 37°C in a humidified atmosphere with 5% CO_2 in Defined Keratinocyte-serum-free basal medium supplemented with a cocktail of growth supplements (InvitroGen). Human oral FBs were isolated from gingival biopsy and cultivated in RPMI 1640 medium supplemented with 10% fetal bovine serum (Life Technologies, Saint-Aubin, France), 2 mmol/L glutamine, 250 U/mL fungizone, and 10 U/mL antibiotics (10 U/mL penicillin and 100 μg/mL streptomycin).

Infection of GECs with *P. gingivalis* and Stimulation by Its LPS

Twenty-four hours before the experiment, 2×10^5 cells were plated in each well of a 24-well plate. At the day of the experiment, cells were washed twice with phosphate-buffered saline and infected for 24 to 48 hours with *P. gingivalis* at a multiplicity of infection (MOI) of 100 and 10 bacteria/cell or stimulated by 1 μg/mL *Pg*-LPS and 1 μg/mL *Escherichia coli*-LPS for 24 to 48 hours.

Metabolic Activity of Cells

Metabolic activity/cell viability was measured with colorimetric AlamarBlue test (resazurin reduction test)[29] (ThermoFischer). After 24 hours of infection, stimulation, or transfection, 300 μL of incubation media was transferred to 96-well plates and measured at 570 and 600 nm to determine the percentage of AlamarBlue reduction.

Flow Cytometric Analysis

GECs and FBs were treated according to experimental design (infection, stimulation) as described. To measure apoptotic and necrotic cells, Annexin V−propidium iodide staining and flow cytometric analyses were performed. Briefly, after removal of the supernatant, cells were centrifuged and re-suspended. Cells were stained with Annexin-V-FLUOS Staining Kit (Roche Applied Science, Meylan, France) according to the manufacturer's instructions. For each condition, a total of 10,000 isolated cells were considered, using a wavelength of 488 nm for fluorescein and a wavelength of 617 nm for propidium iodide. BD LSR II was used for fluorimetric analysis. The percentage of Annexin V-positive cells was calculated from the quadrants (Qs) as follows: percentage of Q1: positive cells for IP^{PE} (necrosis), Q2: positive cells for Annexin V^{FITC} and IP^{PE} (late apoptosis), Q3: annexin-positive cells V^{FITC} (apoptosis), Q4: unlabeled (viable cells).

RNA Isolation and Reverse Transcription

Total RNA from gingival samples and cells was extracted using Tri reagent (Sigma-Aldrich) according to the manufacturer's instructions. The total RNA concentration was quantified with NanoDrop 1000 (ThermoFischer). Reverse transcription was performed with the iScript Reverse Transcription Supermix (Bio-Rad, Miltry-Mory, France) according to the manufacturer's instructions.

Real-Time Quantitative PCR Analysis

To quantify mRNA expression, real-time quantitative PCR was performed on the cDNA samples. PCR amplification and analysis were performed with CFX Connect Real-Time PCR Detection System (Bio-Rad). Amplification reactions have been performed using iTAq Universal SYBR Green Supermix (Bio-Rad). β-actin was used as endogenous RNA control (housekeeping gene) in all samples. Primer sequences related to *Bcl2*, Bax1, Caspase-3, Caspase-9 were purchased from Qiagen (Les Ulis, France) and sequence for *Apaf*1 (3′-GTCTGCTGATGGTGCAAGGA-5′; 5′-GATGGCCCGTGTG-GATTTC-3′), keratin-10 (3′-CATGAGTGTCCCCCGGTATC-5′; 5′-CAGTATCAGCCGCTTTCAGA-3′), and *Xiap* (3′-TGGGA-CATGGATATACTCAGTTAACAA-5′; 5′-GTTAGCCCTCCTC-CACAGTGAA-3′) were synthesized (ThermoFischer). The specificity of reaction was controlled with the melting curve analysis. The expression level was calculated after normalization to the housekeeping gene. All PCR assays were performed in triplicate, and results were represented by the mean values.

Caspase Activity Fluorogenic Assays

Caspase-3 and -9 enzymatic activities were determined with specific fluorogenic enzymatic assays. Cells were sonicated, and lysates were incubated with 200 μL of substrate solution (20 mmol/L HEPES, pH 7.4, 2 mmol/L EDTA, 0.1% 3-[(3-cholamidopropyl)dimethylammonio]-1-propanesulfonate, 5 mmol/L dithiothreitol, and 0.75 μm of caspase substrate) for 1 hour at 37°C as previously described.[30,31] The activity of

each caspase was calculated from the cleavage of the respective specific fluorigenic substrate (AC-DEVD-AMC for caspase-3 and AC-LEHD-AMC for caspase-9) (Bachem, Bobendorf, Switzerland). Substrate cleavage was measured with a fluorescence spectrophotometer with excitation wavelength of 360 nm and emission at 460 nm. Results were expressed as fluorescence units per milligram of total protein.

Western Blot Analysis

Proteins were separated by SDS/PAGE and transferred to a nitrocellulose membrane (Hybond ECL; Fischer Scientific, Illkirch, France). Primary antibodies were directed against APAF-1 (PA5-19894; ThermoFischer), XIAP (SC-11426; Santa Cruz Biotechnology), and β-actin (SC-130301; Santa Cruz Biotechnology). Proteins were visualized with secondary antibody conjugated to alkaline phosphatase (anti-mouse REF: A120-101AP; anti-rabbit REF: A90- 116-AP; Bethyl Laboratories, Montgomery, TX). All antibodies were used at the dilutions recommended by the manufacturer.

Terminal Deoxynucleotidyl Transferase Fluorescein-dUTP Nick End Labeling

Direct terminal deoxynucleotidyl transferase fluorescein-dUTP nick end labeling assay was performed using a commercially available kit (TACS 2 TdTDAB *in situ* apoptosis detection kit; Trevigen Inc., Gaithersburg, MD), according to the manufacturer's instructions.

siRNA Transfection and XIAP Inhibition

One day before the transfection, 5×10^6 cells were seeded in a 6-well plate. Transfection with 5 nmol/L of siRNA targeted against APAF-1 (SI00022792) or with negative control (Qiagen) was performed with a HiPerfect Transfection reagent, according to the manufacturer's protocol.

To inhibit XIAP, cells were pretreated with 50 mmol/L of Embelin (S7025; Selleckchem, Munich, Germany) diluted in 0.3% dimethyl sulfoxide 48 hours before infection. Cells were then infected according to the experimental design.

Statistical Analysis

Statistical analysis was performed with pairwise analysis of variance test and post hoc Tukey test. Statistical significance level was considered as $P < 0.05$. Data were analyzed with Prism 6.0 (GraphPad Software, La Jolla, CA). All experiments have been performed in triplicate and in at least three sets of experiments.

Results

Expression Levels of Apoptosome-Related Components Are Modulated in Chronic Periodontitis

The expression of mRNAs related to Apaf-1, Xiap, caspase-3, and -9 was evaluated in gingival biopsies from healthy and CP patients to assess their potential relationship with periodontal lesion. Analysis showed that the expression of Apaf-1, caspase-3, and -9 mRNAs was significantly increased in the CP group (Apaf-1, 19.2-fold; caspase-9, 14.4-fold; caspase-3, 6.8-fold) ($P < 0.05$) (Figure 1, A, C, and D). However, the expression of the apoptosome inhibitor Xiap was decreased in the CP group (2.5-fold) (Figure 1B). The decrease of Xiap expression correlated with the increased expression of Apaf-1 as estimated with Spearman correlation test ($R = -0.5$; $P < 0.05$).

These results were also observed *in vivo*, in a murine model of experimental periodontitis associated to *P. gingivalis* infection (Figure 1, E–L). In the control group, Apaf-1 was detected mainly in soft tissues, especially within the epithelium (Figure 1, E–H). At the diseased site, Apaf-1 was still observed within the sulcular epithelium and also in the underlying connective tissue (Figure 1, I–L). No significant staining was observed in alveolar bone, suggesting a role for apoptosome mainly in the soft tissue compartment during CP pathogenesis.

Infection with *P. gingivalis* Modulates Metabolic Activity in a Dose- and Cell-Dependent Manner

To evaluate the impact of *P. gingivalis* infection on gingival cells, assessment of the metabolic activity of cells was evaluated in GECs and FBs (Figure 2). A dose-related effect has been observed in GECs regarding the metabolic activity of cells. At a high MOI (100), *P. gingivalis* increased significantly the metabolic activity of the GECs, whereas such an effect could not be observed with a low MOI (10) and H*Pg* after 24 and 48 hours (Figure 2A). A cell-specific response has been observed. In FBs, infection with *P. gingivalis* reduced significantly the metabolic activity for each tested MOI (Figure 2B). In both cell types, *Pg*-LPS displayed toxic effects at 48 hours (Figure 2, A and B).

Increased EC Viability Is Correlated with Decreased Apoptotic Rate

To evaluate the qualitative impact of *P. gingivalis* infection on cell death, apoptotic or necrotic state of infected cells was evaluated by flow cytometry. After 24 hours of infection, at high MOI (100), the increase of metabolic activity induced by *P. gingivalis* infection was correlated with a decrease in the apoptotic rate in GECs. No differences were observed between infection at MOI of 10 and uninfected cells (Figure 2, C and E). A cell-specific response has been

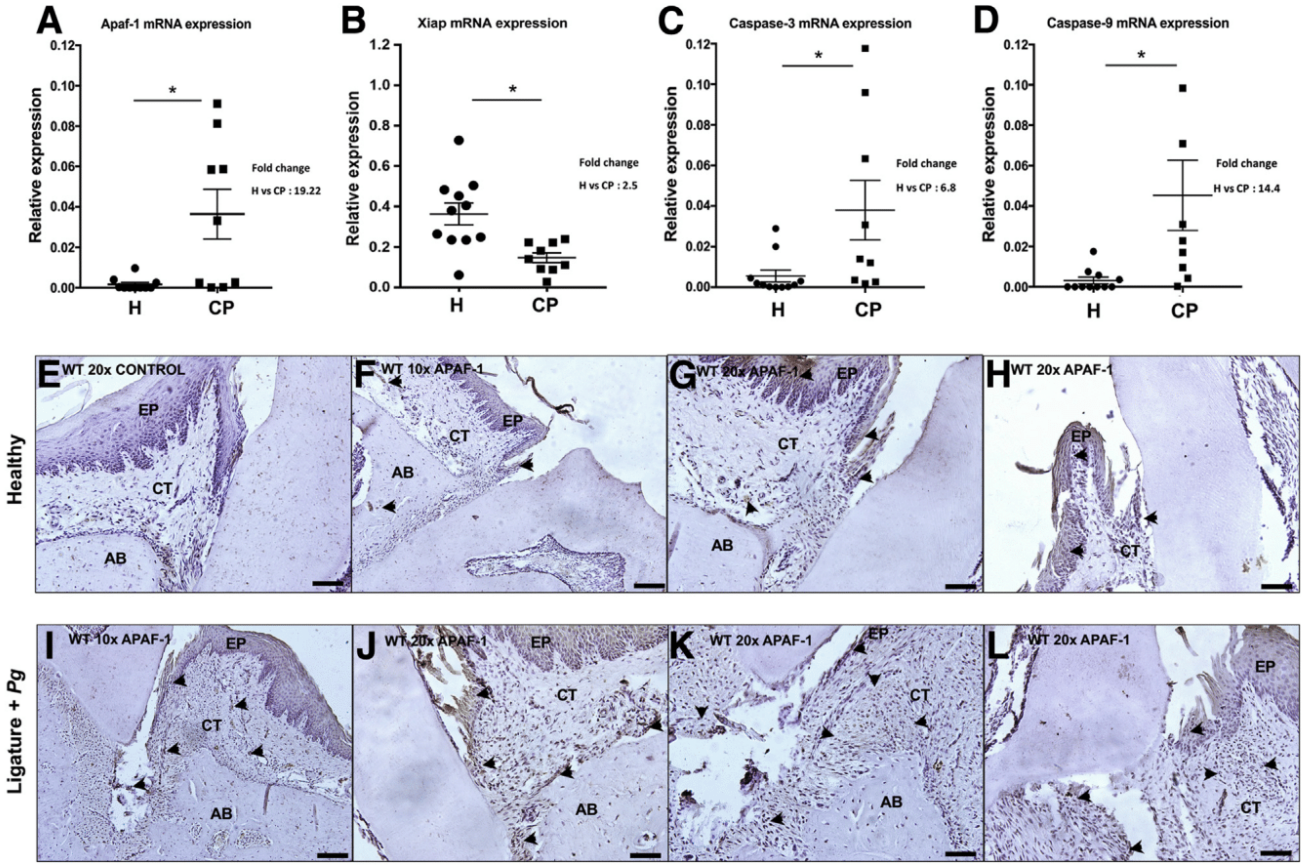

Figure 1 Apoptotic peptidase activating factor 1 (Apaf-1), caspase-3, caspase-9, and X-linked inhibitor of apoptosis protein (Xiap) mRNA expression in chronic periodontitis (CP). The mRNA expression levels were evaluated in the healthy (H) and CP groups. mRNA expression was normalized against the expression level of β-actin. **A**–**D:** Relative expression of Apaf-1 (**A**), Xiap (**B**), caspase-3 (**C**), and caspase-9 (**D**). **E**–**L:** Apaf-1 expression in healthy periodontal tissue (left first molar) (**E**–**H**) and in experimental periodontitis induction (right first molar) (**I**–**L**), in wild-type mouse. **Arrowheads** indicate the zones of Apaf-1 expression. $n = 10$ in the H group (**A**–**D**); $n = 9$ in the CP group (**A**–**D**). $^*P < 0.05$. Scale bars = 100 μm. AB, alveolar bone; CT, connective tissue; EP, epithelium; WT, wild-type.

observed, whereas, unlike GECs, the same conditions of infection and *Pg*-LPS stimulation significantly increased apoptosis in FBs (Figure 2, D and F).

Modulation of Apoptosome-Related mRNA Expression by *P. gingivalis* Infection

To evaluate if intrinsic apoptosis-related pathways, especially associated to APAF-1 apoptosome, were modulated by *P. gingivalis* infection, mRNA expression was analyzed in infected GECs and FBs at 24 hours (Figure 3).

In GECs, *P. gingivalis* infection (MOI = 100) decreased significantly Apaf-1 and caspase-3 mRNA expression ($P < 0.05$), and a descending trend was observed regarding caspase-9 mRNA expression as well (Figure 3, A and E). Of interest, the antiapoptotic B-cell lymphoma 2 (Bcl-2) and Xiap mRNAs were concomitantly increased and proapoptotic Bcl-2–associated X protein (Bax-1) was decreased (Figure 3A). An increase in keratin-10 expression has also been recorded, confirming the increased proliferation of GECs. When GECs were infected with a lower MOI (MOI = 10), opposite effects compared with those obtained with MOI of 100 have been observed, especially regarding Apaf-1 and caspase-3 expression (Figure 3, A and C). *Pg*-LPS may be implicated in the observed effect because it induced a significant increase in the expression of Apaf-1 and caspase-3 mRNAs (Figure 3, C and E).

In FBs, *P. gingivalis* infection, at each tested MOI (10 and 100), increased significantly *Apaf1*, caspase-3, and -9 gene expression (Figure 3, B–F). The same proapoptotic effects have been observed regarding Bcl-2/Bax-1 mRNA expression because infection leads to a decrease in Bcl-2 and an increase in Bax-1 mRNA expression. Interestingly, a toxic effect of *Pg*-LPS has also been highlighted (Figure 3D).

Infection with *P. gingivalis* Modulates APAF-1 and XIAP Protein Levels and Enzymatic Activity of Caspases

To corroborate the results obtained at the gene level, protein concentrations of APAF-1, XIAP, and caspase-3 and -9 enzymatic activities have been measured. In GECs,

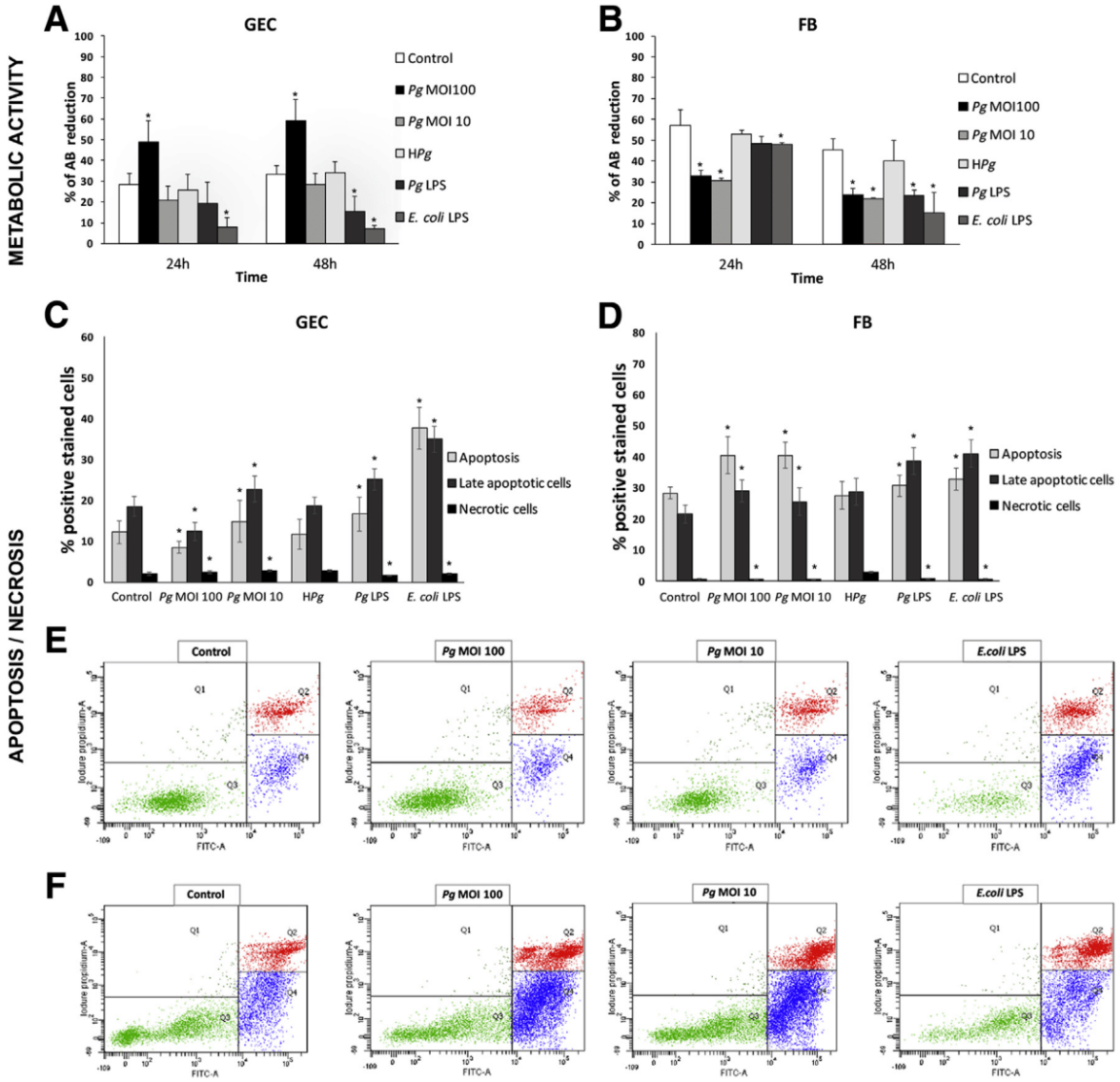

Figure 2 Effects of *Porphyromonas gingivalis* infection on cell metabolic activity and cell death. **A:** Metabolic activity of human oral epithelial cells (GECs) infected with *P. gingivalis* with multiplicity of infection (MOI) of 100 and MOI of 10, heat-killed *P. gingivalis* (H*Pg*), and stimulated by *Pg*-lipopolysaccharide (LPS) and *Escherichia coli*-LPS at 24 and 48 hours. **B:** Metabolic activity of fibroblasts (FBs) infected with *P. gingivalis* with MOI of 100 and MOI of 10, H*Pg*, and stimulated by *Pg*-LPS and *E. coli*-LPS (1 μg/mL) at 24 and 48 hours. **C:** Analysis of cell death of GECs infected with *P. gingivalis* with MOI of 100 and MOI of 10, H*Pg*, and stimulated by *Pg*-LPS and *E. coli*-LPS at 24 hours, by Annexin V^{FITC} and IP^{PE} labeling measured by flow cytometry, showing apoptotic, late apoptotic, and necrotic cell populations. **D:** Analysis of cell death of FBs infected with *P. gingivalis* with MOI of 100 and MOI of 10, H*Pg*, and stimulated by *Pg*-LPS and *E. coli*-LPS at 24 hours, by Annexin V^{FITC} and IP^{PE} labeling measured by flow cytometry, showing apoptotic, late apoptotic, and necrotic cell populations. **E** and **F:** Histogram of Annexin V^{FITC} and IP^{PE} labeling on GECs and FBs [quadrant (Q)1: IP^{PE} positive cells; Q2: Annexin V^{FITC}/IP^{PE} positive cells; Q3: Annexin V^{FITC} positive cells; Q4: no labeled/viable cells]. Data are expressed as means ± SD. $^*P < 0.05$ versus control. AB, alveolar bone; FITC, fluorescein isothiocyanate.

P. gingivalis (MOI = 100) decreased significantly APAF-1 and increased XIAP concentrations, whereas *P. gingivalis* infection at MOI of 10 and H*Pg* did not induce any modification (Figure 4, A, C and E). Similar to the trend observed for mRNA level, opposite results were obtained for APAF-1 in FBs because infection at both tested MOIs increased APAF-1 concentration (Figure 4, B, D and F). *Pg*-LPS may be involved because XIAP concentration was decreased after *Pg*-LPS stimulation in GECs.

Caspases are major components of apoptosome-related pathways because they are key activators of apoptosis. In our model, infection modulated caspase-9 and -3 enzymatic activities in a dose-dependent manner. In GECs, for MOI of 100, the enzymatic activity of both caspases was decreased, whereas at MOI of 10, an increase was measured. Intriguingly, *Pg*-LPS did not modify caspase-3 enzymatic activity; however, it seemed to be implicated in the activation of caspase-9. In FBs, *P. gingivalis* infection increased caspase-3 significantly. Of interest, an

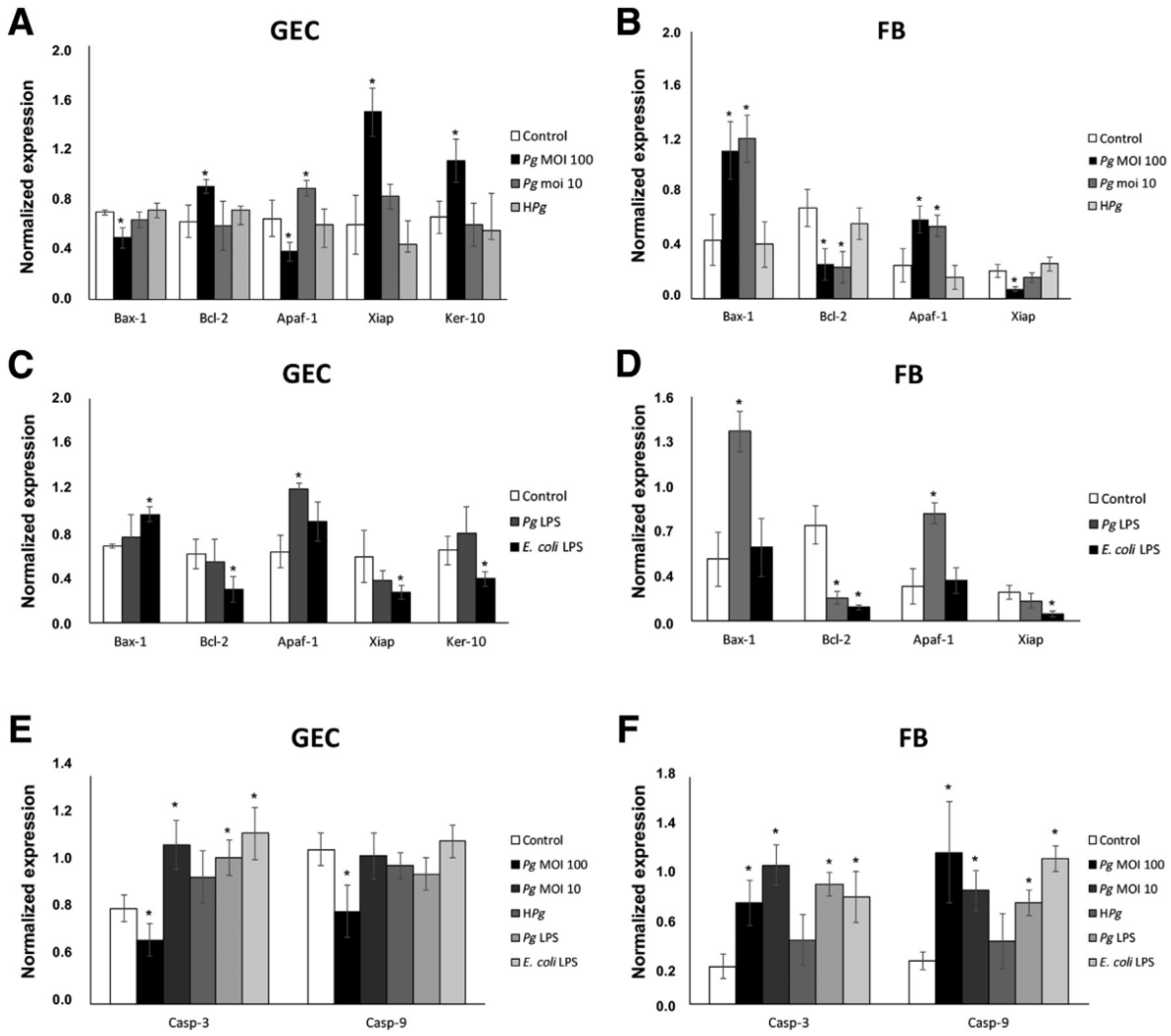

Figure 3 *Porphyromonas gingivalis* and its lipopolysaccharide (LPS) differentially modulates apoptosis-related gene expression in human oral epithelial cells (GECs) and human oral fibroblasts (FBs). **A:** Gene expression of Bax-1, Bcl-2, Apaf-1, Xiap, and Ker-10 in GECs infected with *P. gingivalis* with multiplicity of infection (MOI) of 100 and MOI of 10 and heat-killed *P. gingivalis* (H*Pg*) at 24 hours. **B:** Gene expression of Bax-1, Bcl-2, APAF-1, and Xiap in FBs infected with *P. gingivalis* with MOI of 100 and MOI of 10 and H*Pg* at 24 hours. **C:** Gene expression of Bax-1, Bcl-2, Apaf-1, Xiap, and Ker-10 in GECs stimulated by *Pg*-LPS and *Escherichia coli*-LPS (1 μg/mL) at 24 hours. **D:** Gene expression of Bax-1, Bcl-2, Apaf-1, and Xiap in FBs stimulated by *Pg*-LPS and *E. coli*-LPS (1 μg/mL) at 24 hours. **E:** Gene expression of caspase-1, -3, and -9 in GECs infected with *P. gingivalis* with MOI of 100 and MOI of 10, H*Pg*, and stimulated by *Pg*-LPS and *E. coli*-LPS (1 μg/mL) at 24 hours. **F:** Gene expression of caspase-1, -3, and -9 in FBs infected with *P. gingivalis* with MOI of 100 and MOI of 10, H*Pg*, and stimulated by *Pg*-LPS and *E. coli*-LPS (1 μg/mL) at 24 hours. Data are expressed as means ± SD. $^*P < 0.05$ versus control. Casp, caspase.

increase in caspase-9 activity was also observed after *Pg*-LPS stimulation (Figure 5).

P. gingivalis Modulates Cell Survival and Cell Death in Infected GECs and FBs through APAF-1 and XIAP Modulation

To evaluate if APAF-1 was a key effector of cell death associated to *P. gingivalis* infection, RNA silencing was performed with siRNA targeting APAF-1 in GECs and FBs. Metabolic activity, ratio of apoptosis and necrosis, and enzymatic activity of caspases were measured after Apaf-1 RNA silencing in GECs and FBs.

In transfected GECs, infection at high MOI did not increase metabolic activity. Furthermore, the inhibition of APAF-1 was associated to an increase in the metabolic activity of cells at low MOI, highlighting the role of apoptosome in the response of cells to *P. gingivalis* (Figure 6A). In FBs, an opposite effect was observed, confirming the differential mechanisms involved in relation to cell type (Figure 6B). A qualitative change has also been observed regarding the type of cell death induced. When transfected cells were infected with *P. gingivalis*, an increase in apoptosis was observed in comparison with the negative control and H*Pg* in GECs (Figure 6C). Of interest, such result was correlated with an increase in caspase-3 activity (Figure 6E). As observed for metabolic activity, contradictory effects were observed in FBs compared with that in GECs (Figure 6, B, D and F).

To determine the implication of XIAP, cells were treated with Embelin, an XIAP inhibitor, before infection. In

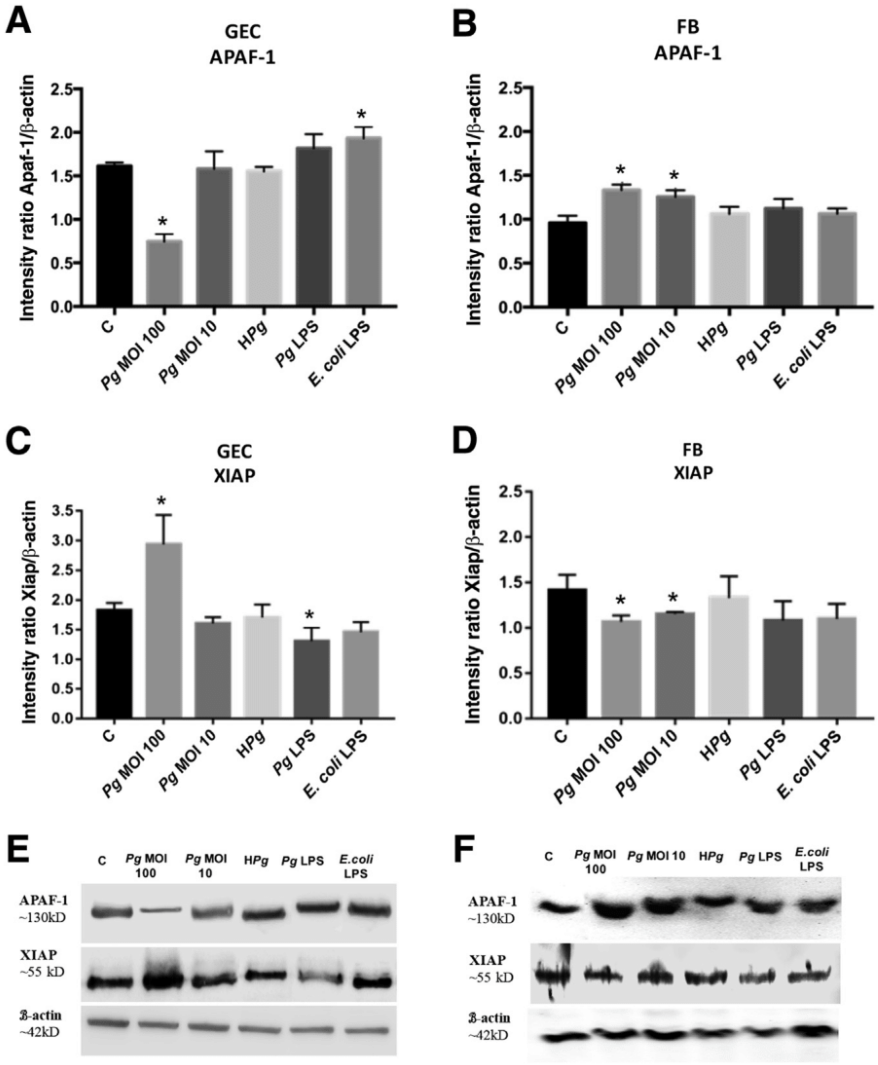

Figure 4 *Porphyromonas gingivalis* modulates apoptotic peptidase activating factor 1 (APAF-1) and X-linked inhibitor of apoptosis protein (XIAP) protein concentration in human oral epithelial cells (GECs) and human oral fibroblasts (FBs). **A**, **C**, and **E:** Western blot analysis for APAF-1 and XIAP in GECs infected with *P. gingivalis* with multiplicity of infection (MOI) of 100 and MOI of 10, heat-killed *P. gingivalis* (H*Pg*), and stimulated by *Pg*-lipopolysaccharide (LPS) and *Escherichia coli*-LPS (1 μg/mL) at 24 hours. **B**, **D**, and **F:** Western blot analysis for APAF-1 and XIAP proteins in FBs infected with *Pg* with MOI of 100 and MOI of 10, H*Pg*, and stimulated by *Pg*-LPS and *E. coli*-LPS (1 μg/mL) at 24 hours. $*P < 0.05$ versus control. C, control.

GECs, the increase of metabolic activity induced by *P. gingivalis* (MOI = 100) infection was inhibited (Figure 7A) and was correlated with increased apoptosis and caspases activity (Figure 7, C and E). In FBs, pretreatment with Embelin did not modulate cellular metabolic activity (Figure 7B) in infected cells. However, a qualitative change related to the type of cell death induced was observed (Figure 7D).

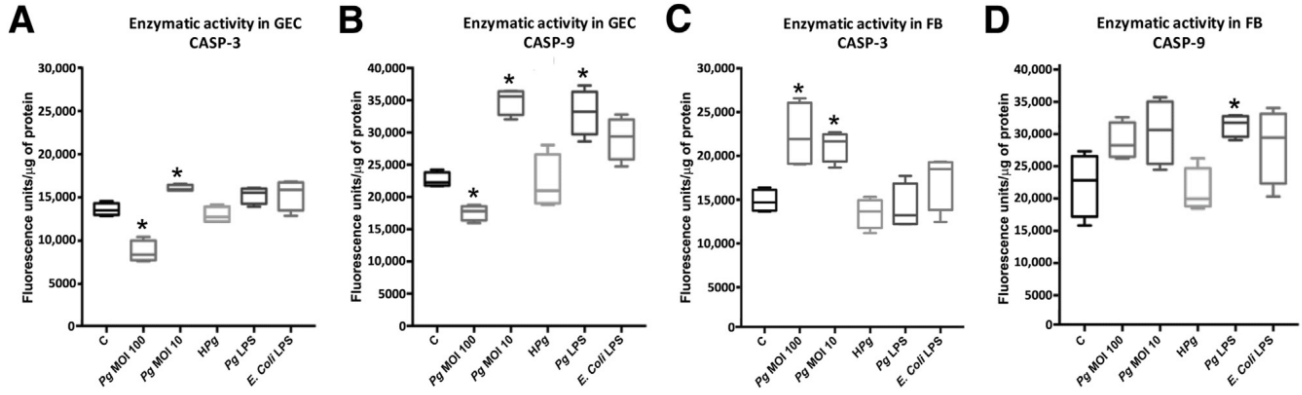

Figure 5 *Porphyromonas gingivalis* and its lipopolysaccharide (LPS) modulate enzymatic activity of caspases in a dose- and cell-dependent manner. Enzymatic activity of caspase-3 (**A** and **C**) and caspase-9 (**B** and **D**) in human oral epithelial cells (GECs) and human oral fibroblasts (FBs) infected with *P. gingivalis* with multiplicity of infection (MOI) of 100 and MOI of 10, heat-killed *P. gingivalis* (H*Pg*), and stimulated by *Pg*-LPS and *Escherichia coli*-LPS (1 μg/mL) at 24 hours. Data are expressed as means ± SD. $*P < 0.05$ versus control. C, control; CASP, caspase.

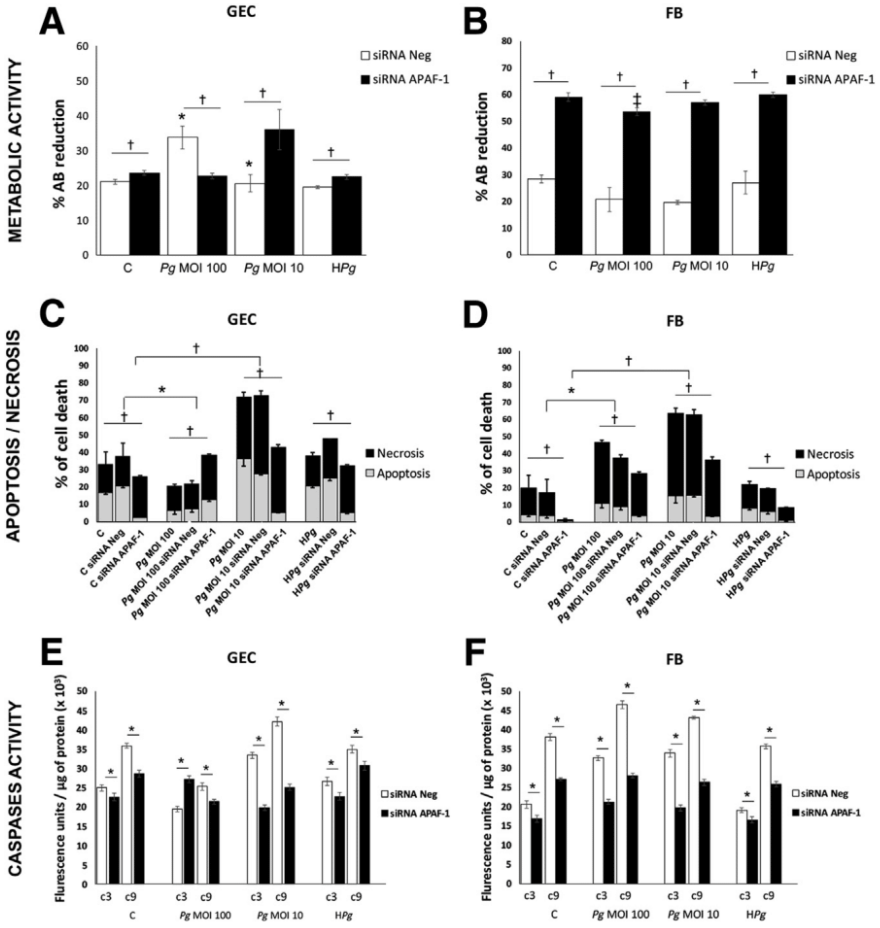

Figure 6 *Porphyromonas gingivalis* modulates cell survival and apoptosis rate in infected human oral epithelial cells (GECs) and human oral fibroblasts (FBs) through apoptosome-related proteins. **A** and **B:** Metabolic activity of GECs and FBs transfected with siRNA targeting apoptotic peptidase activating factor 1 (APAF-1) and infected with *P. gingivalis* with multiplicity of infection (MOI) of 100, MOI of 10, and heat-killed *P. gingivalis* (H*Pg*) at 24 hours. **C** and **D:** Apoptosis/necrosis ratio, in transfected GECs and FBs and infected with *P. gingivalis* with MOI of 100, MOI of 10, and H*Pg* at 24 hours. **E** and **F:** Enzymatic activity of caspase-3 (c3) and caspase-9 (c9) in transfected GECs and FBs and infected with *P. gingivalis* with MOI of 100, MOI of 10, and H*Pg* at 24 hours. Data are expressed as means ± SD. $^{*}P < 0.05$ versus control; $^{\dagger}P < 0.05$; $^{\ddagger}P < 0.05$ versus transfected control. AB, alveolar bone; C, control.

Discussion

This study aimed at determining the ability of *P. gingivalis* to modulate APAF-1 apoptosome activity and programed cell death in the periodontal soft tissue cells. First, in gingival samples from periodontitis patients, an increase of Apaf-1 expression and a decrease of its inhibitor, Xiap, was demonstrated, showing that APAF-1 apoptosome may be involved in the periodontal lesion. However, this difference in terms of gene expression may also be related to changes of the cellular composition of the analyzed samples with CP samples exhibiting more inflammatory cells than healthy ones. In an *in vivo* model of experimental periodontitis, an increased expression of APAF-1 was observed at the diseased site, especially at the connective tissue level, consolidating our hypothesis.

In vitro, *P. gingivalis* acted differentially on this specific pathway according to the MOI and cell type. Herein, we observed an augmentation in EC viability, correlated with a decrease in apoptosis triggers (APAF-1, caspases) and an increase of apoptosis inhibitors (XIAP), when cells were infected at a high MOI. In addition, when XIAP was inhibited, the increased proliferation of GECs was counteracted. Such effect was not observed in FBs.

Because of their specific location at the interface between subgingival biofilms and gingival sulcus, ECs constitute the first line of host defense. Integrity of the epithelial barrier is a key factor for periodontal health because ECs play a key role in the overall tissue homeostasis and initiation of innate immune response.[5] Not only do these cells release soluble mediators such as cytokines[32] that sustain the inflammatory process but also antimicrobial peptides such as β-defensins.[33] *P. gingivalis* is considered as one of the keystone pathogens and is able to modulate cell cycle and programed cell death to favor its survival.[7,34] Cellular invasion by *P. gingivalis* is followed by intracellular persistence, bacterial multiplication, and leads to bacterial spread to adjacent tissues, including connective tissue and bone.[35] Moreover, several studies showed that this bacterium uses a panel of strategies to hijack host mechanisms such as autophagy.[36] In this study, it was confirmed that *P. gingivalis* infection inhibits apoptosis and increases the proliferation rate of ECs. This result is in accordance with the previous studies[7,9,10,13] that implicated the dysregulation of cell cycle by bacteria during the pathogenic process.[8,25] Recently, the importance of cell cycle in the invasion process of *P. gingivalis* has been demonstrated, because the bacteria preferentially target cells in the S phase.[37] This

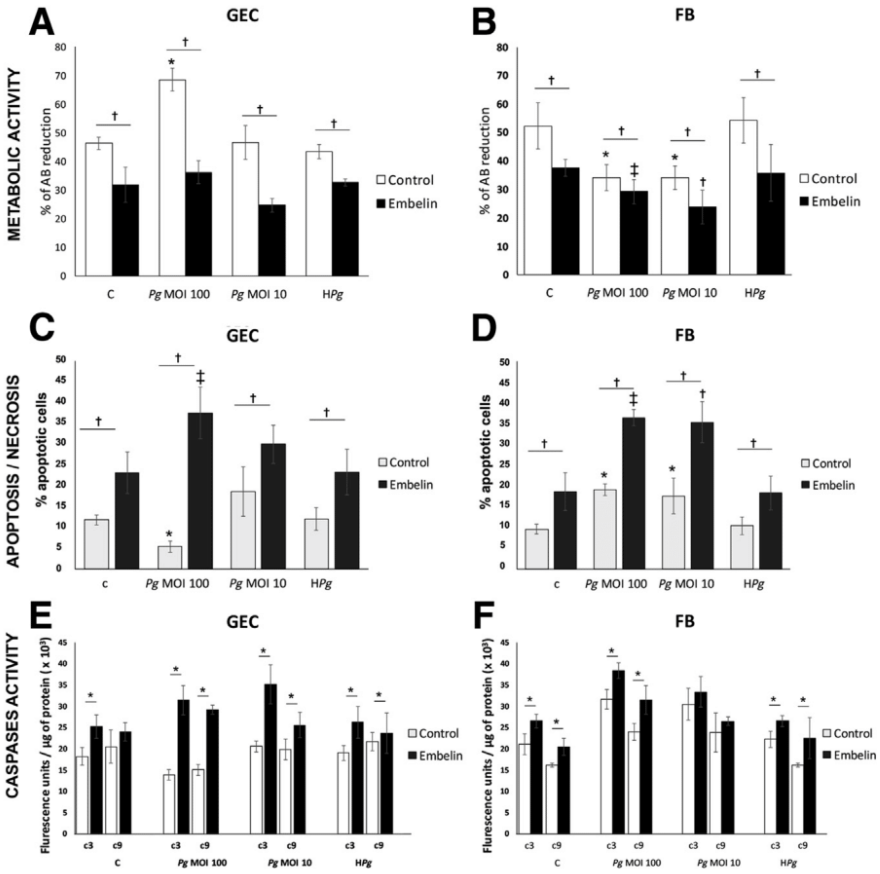

Figure 7 *Porphyromonas gingivalis* modulates cell survival and apoptotic rate in human oral epithelial cells (GECs) and human oral fibroblasts (FBs) through apoptosome-related proteins. **A** and **B:** Metabolic activity of GECs and FBs treated with Embelin during 48 hours and infected with *P. gingivalis* with multiplicity of infection (MOI) of 100, MOI of 10, and heat-killed *P. gingivalis* (H*Pg*) at 24 hours. **C** and **D:** Apoptosis evaluation by terminal deoxynucleotidyl transferase-mediated dUTP nick-end labeling assay in transfected GECs and FBs and infected with *P. gingivalis* with MOI of 100, MOI of 10, and H*Pg* at 24. **E** and **F:** Enzymatic activity of caspase-3 (c3) and caspase-9 (c9) in transfected GECs and FBs and infected with *P. gingivalis* with MOI of 100, MOI of 10, and H*Pg* at 24 hours. Data are expressed as means ± SD. $^{*}P < 0.05$ versus control; $^{\dagger}P < 0.05$ for differences between pretreated and nontreated cells; $^{\ddagger}P < 0.05$ versus pretreated control. AB, alveolar bone; C, control.

increase, in terms of proliferation rate, has prominent clinical consequences because it was suggested that fast turnover of ECs may reduce immune response at the sulcular level.[9] Moreover, this may also have influence on cellular senescence that has been associated to impaired innate immune response, increased oxidative stress and that reduce bacterial clearance.[38–40] Contradictory results could also be found, and some studies described an increased EC death induced by *P. gingivalis* infection. Such discrepancies were already observed by Stathopoulou et al[12] and might be explained by the different protocols used (MOI, bacterial strain, length of exposure, cell type).[11]

In FBs, the effects observed were similar to those in endothelial cells,[25] whereas opposite outcomes in comparison with GECs were noticed, highlighting the differential effect of the infection according to cell type. This result is in accordance with previous studies that showed the cytotoxic effect of *P. gingivalis* on FBs[41] but differs from those observed in periodontal ligament fibroblasts.[42] This reduction of proliferation rate diminishes the capability of the host to regenerate or to repair the injured tissues and contributes to worsening of periodontal lesions.[43]

Apoptosis is a well-described cellular process and plays a key role in homeostasis, and its dysregulation has been associated to periodontitis.[16] Modulation of apoptosis or programed cell death by periodontal pathogens is an important feature of the disease, especially at the epithelial level where antiapoptotic effects and therefore prosurvival cellular phenotype will be a key mechanism of bacterial colonization[10] and to sustained inflammation. For instance, reduced apoptosis within periodontal tissues correlates with chronic persistence of inflammatory cells.[44] It has been described that *P. gingivalis*–induced effects on apoptosis regulation depend on cell type and associated with the modulation of several pathways such as phosphatidylinositol 3-kinase/Akt or Janus kinase/Stat pathways.[10,34] In this study, we focused on the APAF-1–related pathway that has been described as an important component of the mitochondria-mediated intrinsic pathway.[45] It was observed that *P. gingivalis* modulates significantly the expression of APAF-1 in a cell- and dose-dependent manner. In ECs, at high dose, *P. gingivalis* blocked cell death through a decrease in APAF-1 expression, reduction in the enzymatic activity of caspases, and an increase in XIAP expression. APAF-1 has already been described as a target of several pathogens, including bacteria such as *Chlamydia pneumoniae*[46] or viruses such as Influenza A virus.[47] The decrease of APAF-1, at both mRNA and protein levels, may explain the increased metabolic activity observed. Therefore, it can be hypothesized that such dysregulation may be a specific bacterial strategy to avoid clearance from the organism with potential consequences regarding induction of inflammatory

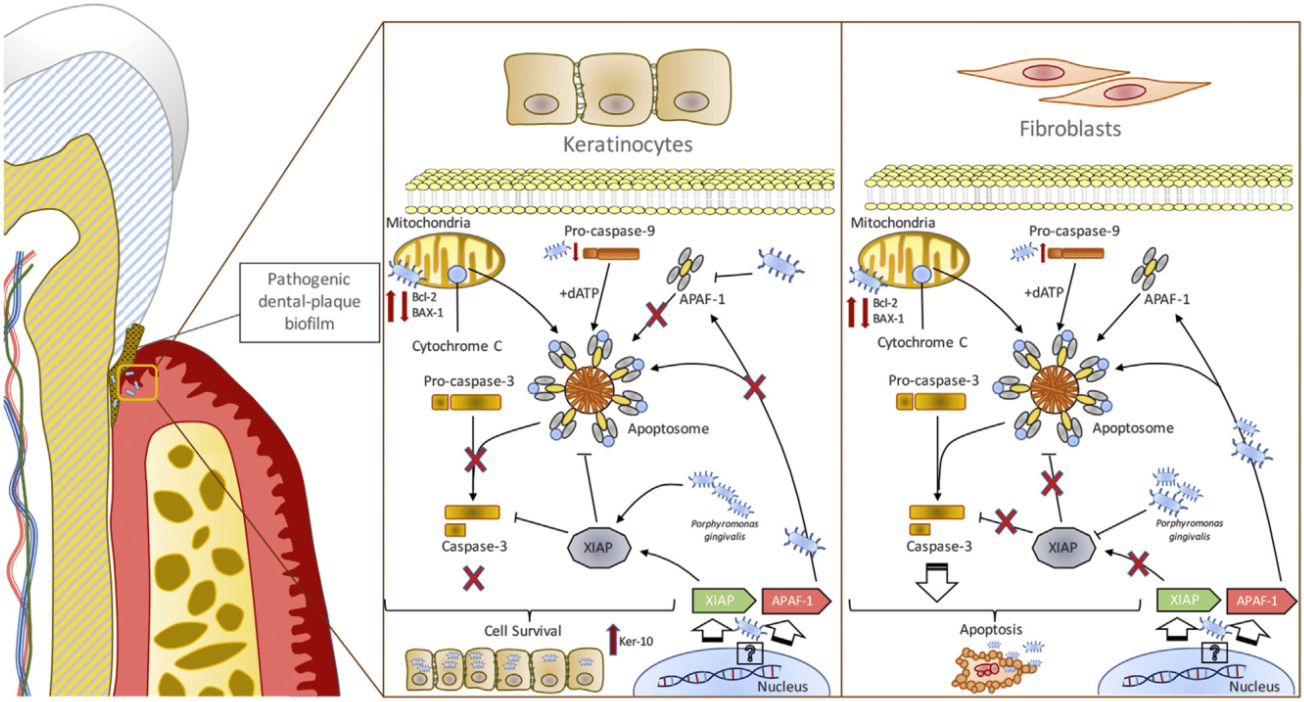

Figure 8 Cell death and activation of apoptotic peptidase activating factor 1 (APAF-1)—related pathway in response to *Porphyromonas gingivalis* infection in epithelial cells and fibroblasts. Cell-specific modulation of apoptosis by *P. gingivalis* in epithelial cells and fibroblasts. In epithelial cells, *P. gingivalis* decreases APAF-1 and increases X-linked inhibitor of apoptosis protein (XIAP) expression, leading to an augmented cell survival. However, in fibroblasts, bacteria stimulate APAF-1 pathway and reduce XIAP expression, inducing apoptosis. Bax-1, Bcl-2—associated X protein; Bcl-2, B-cell lymphoma 2.

cell death through necrosis or necroptosis as suggested in a mouse model.[48] The regulatory role of XIAP has also been investigated by using an inhibitor. In our model of ECs, inhibition of XIAP inhibited the *P. gingivalis*—induced increase of cell viability. This effect was associated with an elevated caspase-3 and -9 enzymatic activity, as already demonstrated in other cellular models.[22,49] IAPs, such as cIAP1, cIAP2, and XIAP, are key elements of homeostasis because their loss or inhibition sensitizes the cell to death associated to inducers such as tumor necrosis factor (TNF).[50] A better understanding of mechanisms involved between IAP and regulation of cell death will be instrumental in developing therapeutic strategies. In FBs, inhibition of XIAP did not affect *P. gingivalis*—associated cell death as hypothesized. However, it is important to consider the multitude of pathways that control apoptosis process and crosstalk between them especially in the context of *P. gingivalis* infection. For instance, *P. gingivalis* is able to modulate NLR family pyrin domain containing 3 (NLRP3) inflammasome expression.[51,52] NLRP3 inflammasome is implicated in the release of mature IL-1β and IL-18 and to pyroptosis but also in the control of apoptosis as demonstrated in osteoblasts infected by *Aggregatibacter actinomycetemcomitans*.[53] Interestingly, inflammasome and apoptosome are similar in their structure and are subject to crosstalk mediated by cytochrome c.[54] Future studies need to focus on the effect induced by apoptosome modulation by *P. gingivalis* on inflammasome activity and especially on its impact on sustained periodontal inflammation.

A differential cellular effect was also observed between high and low doses of infection. To date no MOI has been regarded as the most relevant to the *in vivo* situation, even if MOI of 100 corresponds to the optimal dose for *P. gingivalis* invasion[6]; however, the use of a low and high MOI may give some data relevant to low-grade versus acute infection. We could hypothesize that in case of high bacterial load, as observed in deep pockets that occur during severe forms of periodontitis, host defense is submerged by the bacterial aggression, leading to an unregulated cellular proliferation. In case of low bacterial charge, host defense is able to control bacterial spreading and to eliminate infected cells more efficiently. Hence, it may be considered that apoptosome may be positive in the case of mild infection but detrimental in the case of severe infection. Such effect has already been observed with regard to another molecular platform, the inflammasome,[55] in an infectious context. Here, we showed that APAF-1 was increased in periodontitis, based on clinical biopsies and ligature-induced experimental periodontitis analyses. However, even if we can suppose that high bacterial load was associated to the analyzed tissues, no bacterial sampling was available, restraining the possibility to directly assess the correlation between *P. gingivalis* presence and APAF-1 expression. Furthermore, even if relevant to study periodontal pathogenesis,[56] the local trauma that occurs while using ligature-induced periodontitis should be considered because observed modulatory effects could not be solely associated to *P. gingivalis* in this model. However, to date, no data are

available regarding the specific effect induced by chronic mechanical trauma on programed cell death at the periodontal lesion site.

To better understand the bacterial mechanisms involved, the effects induced by *P. gingivalis* LPS were investigated. *Pg*-LPS is a well-described virulence factor that activates host inflammatory response. It has already been shown that *Pg*-LPS induces secretion of several proinflammatory cytokines such as TNF-α or IL-1[57] or extracellular matrix proteases such as cathepsins.[58] In this study, *Pg*-LPS exhibits cytotoxic effects in both cell types as observed in endothelial cells.[25] As for the bacteria, cytotoxicity of LPS has been demonstrated to depend on the strain and structure, such as the presence of O-antigen,[59] and also the cell type.[60] Appealingly, LPS was found to modulate apoptosome-related pathway by increasing APAF-1 expression and caspases activity as observed in endothelial cells.[25] *Pg*-LPS acts through toll-like receptors (TLRs) such as TLR-2[57] and TLR-4.[59,61] Besides, TLRs have already been linked to apoptosis in several infectious models such as in macrophages simulated with *Mycobacterium* proteins.[62,63] However, specific mechanisms associated with *Pg*-LPS need to be elucidated.

Finally, this study demonstrated the putative role of APAF-1/XIAP in periodontal pathogenesis within soft tissues. Infection with *P. gingivalis* modulates APAF-1 apoptosome and XIAP activities in a cell type–dependent manner (Figure 8). These mechanisms may be one of those explaining the subversion of innate immune response by *P. gingivalis* that occurs during periodontitis. However, further experiments such as knock-in of *Apaf-1* should be conducted to evaluate its potential impact on the prevention or management of *P. gingivalis*–associated diseases. Targeting programed cell death in a time-controlled manner may be a promising tool, as suggested for autophagy; however, specific drugs should be developed with limited risk of side effect.

Acknowledgment

We thank Dr. Thomas Décoville for his help with flow cytometric experiments.

References

1. Petersen PE, Baehni PC: Periodontal health and global public health. Periodontol 2000 2012, 60:7–14
2. Hajishengallis G: Periodontitis: from microbial immune subversion to systemic inflammation. Nat Rev Immunol 2015, 15:30–44
3. Costalonga M, Herzberg MC: The oral microbiome and the immunobiology of periodontal disease and caries. Immunol Lett 2014, 162: 22–38
4. Hajishengallis G, Lamont RJ: Breaking bad: manipulation of the host response by Porphyromonas gingivalis. Eur J Immunol 2014, 44: 328–338
5. Yilmaz O: The chronicles of Porphyromonas gingivalis: the microbium, the human oral epithelium and their interplay. Microbiology 2008, 154:2897–2903
6. Lamont RJ, Chan A, Belton CM, Izutsu KT, Vasel D, Weinberg A: Porphyromonas gingivalis invasion of gingival epithelial cells. Infect Immun 1995, 63:3878–3885
7. Pan C, Xu X, Tan L, Lin L, Pan Y: The effects of Porphyromonas gingivalis on the cell cycle progression of human gingival epithelial cells. Oral Dis 2013, 20:100–108
8. Furuta N, Takeuchi H, Amano A: Entry of Porphyromonas gingivalis outer membrane vesicles into epithelial cells causes cellular functional impairment. Infect Immun 2009, 77:4761–4770
9. Kuboniwa M, Hasegawa Y, Mao S, Shizukuishi S, Amano A, Lamont RJ, Yilmaz O: P. gingivalis accelerates gingival epithelial cell progression through the cell cycle. Microbes Infect 2008, 10:122–128
10. Mao S, Park Y, Hasegawa Y, Tribble GD, James CE, Handfield M, Stavropoulos MF, Yilmaz O, Lamont RJ: Intrinsic apoptotic pathways of gingival epithelial cells modulated by Porphyromonas gingivalis. Cell Microbiol 2007, 9:1997–2007
11. Brozovic S, Sahoo R, Barve S, Shiba H, Uriarte S, Blumberg RS, Kinane DF: Porphyromonas gingivalis enhances FasL expression via up-regulation of NFkappaB-mediated gene transcription and induces apoptotic cell death in human gingival epithelial cells. Microbiology 2006, 152:797–806
12. Stathopoulou PG, Galicia JC, Benakanakere MR, Garcia CA, Potempa J, Kinane DF: Porphyromonas gingivalis induce apoptosis in human gingival epithelial cells through a gingipain-dependent mechanism. BMC Microbiol 2009, 9:107
13. Nakhjiri SF, Park Y, Yilmaz O, Chung WO, Watanabe K, El-Sabaeny A, Park K, Lamont RJ: Inhibition of epithelial cell apoptosis by Porphyromonas gingivalis. FEMS Microbiol Lett 2001, 200:145–149
14. Lin W-C, Tsai H-F, Liao H-J, Tang C-H, Wu Y-Y, Hsu P-I, Cheng A-L, Hsu P-N: Helicobacter pylori sensitizes TNF-related apoptosis-inducing ligand (TRAIL)-mediated apoptosis in human gastric epithelial cells through regulation of FLIP. Cell Death Dis 2014, 5:e1109
15. Yamada S, Noguchi H, Tanimoto A: Critical and diverse in vivo roles of apoptosis signal-regulating kinase 1 in animal models of atherosclerosis and cholestatic liver injury. Histol Histopathol 2016, 32: 43–444
16. Song B, Zhou T, Yang WL, Liu J, Shao LQ: Programmed cell death in periodontitis: recent advances and future perspectives. Oral Dis 2016, 23:609–619
17. Zamaraev AV, Kopeina GS, Zhivotovsky B, Lavrik IN: Cell death controlling complexes and their potential therapeutic role. Cell Mol Life Sci 2015, 72:505–517
18. Ledgerwood EC, Morison IM: Targeting the apoptosome for cancer therapy. Clin Cancer Res 2009, 15:420–424
19. Riedl SJ, Salvesen GS: The apoptosome: signalling platform of cell death. Nat Rev Mol Cell Biol 2007, 8:405–413
20. Yuan S, Akey CW: Apoptosome structure, assembly, and procaspase activation. Structure 2013, 21:501–515
21. Shiozaki EN, Chai J, Rigotti DJ, Riedl SJ, Li P, Srinivasula SM, Alnemri ES, Fairman R, Shi Y: Mechanism of XIAP-mediated inhibition of caspase-9. Mol Cell 2003, 11:519–527
22. Ho AT, Li QH, Okada H, Mak TW, Zacksenhaus E: XIAP activity dictates Apaf-1 dependency for caspase 9 activation. Mol Cell Biol 2007, 27:5673–5685
23. Cain K: Chemical-induced apoptosis: formation of the Apaf-1 apoptosome. Drug Metab Rev 2003, 35:337–363
24. Greenberg DE, Sturdevant DE, Marshall-Batty KR, Chu J, Pettinato AM, Virtaneva K, Lane J, Geller BL, Porcella SF, Gallin JI, Holland SM, Zarember KA: Simultaneous host-pathogen transcriptome analysis during Granulibacter bethesdensis infection of neutrophils from healthy subjects and patients with chronic Granulomatous disease. Infect Immun 2015, 83:4277–4292
25. Bugueno IM, Khelif Y, Seelam N, Morand D-N, Tenenbaum H, Davideau J-L, Huck O: Porphyromonas gingivalis differentially modulates cell death profile in Ox-LDL and TNF-alpha pre-treated endothelial cells. PLoS One 2016, 11:e0154590

26. Tucka J, Yu H, Gray K, Figg N, Maguire J, Lam B, Bennett M, Littlewood T: Akt1 regulates vascular smooth muscle cell apoptosis through FoxO3a and Apaf1 and protects against arterial remodeling and atherosclerosis. Arterioscler Thromb Vasc Biol 2014, 34: 2421−2428
27. Armitage GC: Development of a classification system for periodontal diseases and conditions. Ann Periodontol 1999, 4:1−6
28. Saadi-Thiers K, Huck O, Simonis P, Tilly P, Fabre J-E, Tenenbaum H, Davideau J-L: Periodontal and systemic responses in various mice models of experimental periodontitis: respective roles of inflammation duration and Porphyromonas gingivalis infection. J Periodontol 2013, 84:396−406
29. Rampersad SN: Multiple applications of Alamar Blue as an indicator of metabolic function and cellular health in cell viability bioassays. Sensors (Basel) 2012, 12:12347−12360
30. Hasegawa J, Kamada S, Kamiike W, Shimizu S, Imazu T, Matsuda H, Tsujimoto Y: Involvement of CPP32/Yama(-like) proteases in Fas-mediated apoptosis. Cancer Res 1996, 56:1713−1718
31. Rosado JA, Lopez JJ, Gomez-Arteta E, Redondo PC, Salido GM, Pariente JA: Early caspase-3 activation independent of apoptosis is required for cellular function. J Cell Physiol 2006, 209:142−152
32. Ramage G, Lappin DF, Millhouse E, Malcolm J, Jose A, Yang J, Bradshaw DJ, Pratten JR, Culshaw S: The epithelial cell response to health and disease associated oral biofilm models. J Periodont Res 2016, 52:325−333
33. Liu J, Chen J, Du X, Hu L, Chen L: The expression of hBDs in the gingival tissue and keratinocytes from healthy subjects and periodontitis patients. Arch Oral Biol 2014, 59:193−198
34. Yilmaz O, Jungas T, Verbeke P, Ojcius DM: Activation of the phosphatidylinositol 3-kinase/Akt pathway contributes to survival of primary epithelial cells infected with the periodontal pathogen Porphyromonas gingivalis. Infect Immun 2004, 72:3743−3751
35. Sakanaka A, Takeuchi H, Kuboniwa M, Amano A: Dual lifestyle of Porphyromonas gingivalis in biofilm and gingival cells. Microb Pathog 2016, 94:42−47
36. Takeuchi H, Furuta N, Morisaki I, Amano A: Exit of intracellular Porphyromonas gingivalis from gingival epithelial cells is mediated by endocytic recycling pathway. Cell Microbiol 2011, 13:677−691
37. Al-Taweel FB, Douglas CW, Whawell SA: The periodontal pathogen Porphyromonas gingivalis preferentially interacts with oral epithelial cells in S phase of the cell cycle. Infect Immun 2016, 84:1966−1974
38. Shaik-Dasthagirisaheb YB, Huang N, Weinberg EO, Shen SS, Genco CA, Gibson FC III: Aging and contribution of MyD88 and TRIF to expression of TLR pathway-associated genes following stimulation with Porphyromonas gingivalis. J Periodont Res 2015, 50:89−102
39. Wu Y, Dong G, Xiao W, Xiao E, Miao F, Syverson A, Missaghian N, Vafa R, Cabrera-Ortega AA, Rossa C Jr, Graves DT: Effect of aging on periodontal inflammation, microbial colonization, and disease susceptibility. J Dent Res 2016, 95:460−466
40. Ebersole JL, Kirakodu S, Novak MJ, Exposto CR, Stromberg AJ, Shen S, Orraca L, Gonzalez-Martinez J, Gonzalez OA: Effects of aging in the expression of NOD-like receptors and inflammasome-related genes in oral mucosa. Mol Oral Microbiol 2016, 31:18−32
41. Desta T, Graves DT: Fibroblast apoptosis induced by Porphyromonas gingivalis is stimulated by a gingipain and caspase-independent pathway that involves apoptosis-inducing factor. Cell Microbiol 2007, 9:2667−2675
42. Liu J, Tang X, Li C, Pan C, Li Q, Geng F, Pan Y: Porphyromonas gingivalis promotes the cell cycle and inflammatory cytokine production in periodontal ligament fibroblasts. Arch Oral Biol 2015, 60: 1153−1161
43. Chang M-C, Tsai Y-L, Chen Y-W, Chan C-P, Huang C-F, Lan W-C, Lin CC, Lan W-H, Jeng J-H: Butyrate induces reactive oxygen species production and affects cell cycle progression in human gingival fibroblasts. J Periodont Res 2013, 48:66−73
44. Sawa T, Nishimura F, Ohyama H, Takahashi K, Takashiba S, Murayama Y: In vitro induction of activation-induced cell death in lymphocytes from chronic periodontal lesions by exogenous Fas ligand. Infect Immun 1999, 67:1450−1454
45. Chowdhury I, Tharakan B, Bhat GK: Current concepts in apoptosis: the physiological suicide program revisited. Cell Mol Biol Lett 2006, 11:506−525
46. Rahman MA, Shirai M, Aziz MA, Ushirokita R, Kubota S, Suzuki H, Azuma Y: An epistatic effect of apaf-1 and caspase-9 on chlamydial infection. Apoptosis 2015, 20:1271−1280
47. Halder UC, Bagchi P, Chattopadhyay S, Dutta D, Chawla-Sarkar M: Cell death regulation during influenza A virus infection by matrix (M1) protein: a model of viral control over the cellular survival pathway. Cell Death Dis 2011, 2:e197
48. Ke X, Lei L, Li H, Li H, Yan F: Manipulation of necroptosis by Porphyromonas gingivalis in periodontitis development. Mol Immunol 2016, 77:8−13
49. Riedl SJ, Renatus M, Schwarzenbacher R, Zhou Q, Sun C, Fesik SW, Liddington RC, Salvesen GS: Structural basis for the inhibition of caspase-3 by XIAP. Cell 2001, 104:791−800
50. Vasilikos L, Spilgies LM, Knop J, Wong WW: Regulating the balance between necroptosis, apoptosis and inflammation by inhibitors of apoptosis proteins. Immunol Cell Biol 2017, 95:160−165
51. Olsen I, Yilmaz O: Modulation of inflammasome activity by Porphyromonas gingivalis in periodontitis and associated systemic diseases. J Oral Microbiol 2016, 8:30385
52. Huck O, Elkaim R, Davideau J-L, Tenenbaum H: Porphyromonas gingivalis-impaired innate immune response via NLRP3 proteolysis in endothelial cells. Innate Immun 2015, 21:65−72
53. Zhao P, Liu J, Pan C, Pan Y: NLRP3 inflammasome is required for apoptosis of Aggregatibacter actinomycetemcomitans-infected human osteoblastic MG63 cells. Acta Histochem 2014, 116:1119−1124
54. Shi C-S, Kehrl JH: Cytochrome c negatively regulates NLRP3 inflammasomes. PLoS One 2016, 11:e0167636
55. Ong JD, Mansell A, Tate MD: Hero turned villain: NLRP3 inflammasome-induced inflammation during influenza A virus infection. J Leukoc Biol 2017, 101:863−874
56. Graves DT, Kang J, Andriankaja O, Wada K, Rossa C Jr: Animal models to study host-bacteria interactions involved in periodontitis. Front Oral Biol 2012, 15:117−132
57. Kocgozlu L, Elkaim R, Tenenbaum H, Werner S: Variable cell responses to P. gingivalis lipopolysaccharide. J Dent Res 2009, 88: 741−745
58. Elkaim R, Werner S, Kocgozlu L, Tenenbaum H: P. gingivalis regulates the expression of Cathepsin B and Cystatin C. J Dent Res 2008, 87:932−936
59. Soto C, Bugueño I, Hoare A, Gonzalez S, Venegas D, Salinas D, Melgar-Rodríguez S, Vernal R, Gamonal J, Quest AF, Pérez-Donoso JM, Bravo D: The Porphyromonas gingivalis O antigen is required for inhibition of apoptosis in gingival epithelial cells following bacterial infection. J Periodont Res 2015, 51:518−528
60. Murray DA, Wilton JM: Lipopolysaccharide from the periodontal pathogen Porphyromonas gingivalis prevents apoptosis of HL60-derived neutrophils in vitro. Infect Immun 2003, 71:7232−7235
61. Yang X, Zhang J, Ni J, Ouyang B, Wang D, Luo S, Xie B, Xuan D: Toll-like receptor 4-mediated hyper-responsiveness of gingival epithelial cells to lipopolysaccharide in high-glucose environments. J Periodontol 2014, 85:1620−1628
62. Lee K-I, Choi H-G, Son Y-J, Whang J, Kim K, Jeon HS, Park H-S, Back YW, Choi S, Kim S-W, Choi CH, Kim H-J: Mycobacterium avium MAV2052 protein induces apoptosis in murine macrophage cells through Toll-like receptor 4. Apoptosis 2016, 21:459−472
63. Tiwari B, Ramakrishnan UM, Raghunand TR: The Mycobacterium tuberculosis protein pair PE9 (Rv1088)-PE10 (Rv1089) forms heterodimers and induces macrophage apoptosis through Toll-like receptor 4. Cell Microbiol 2015, 17:1653−1669

CHAPITRE 2

Implication des microvésicules d'origine endothéliale induites par l'infection par *Porphyromonas gingivalis* dans l'inflammation endothéliale.

Bugueno I.M., El-Ghazouani F., Batool F., El Itawi H., Anglès-Cano E., Benkirane-Jessel N., Toti F., Huck O. *Porphyromonas gingivalis* triggers the shedding of inflammatory endothelial microvesicles that act as autocrine effectors of endothelial dysfunction**. *Article* accepté avec des révisions.**

Contexte et objectifs

La parodontite a été liée à plusieurs maladies systémiques, en particulier l'athérosclérose et l'infection chronique ont été décrites comme un mécanisme potentiel impliqué dans son aggravation (Linden et al., 2013 ; Huck et al., 2011 ; Lockhart et al., 2012). Il a été proposé un éventuel impact au niveau vasculaire de *P.gingivalis* et d'une grande variété de médiateurs inflammatoires agissant comme effecteurs cellulaires autocrines ou paracrines (Tonneti et al., 2007 ; Salhi et al., 2019)(Welsh et al., 2017 ; Van Tassell et al., 2013). Les MV, également appelées microparticules, sont des vésicules membranaires plasmatiques allant de 50 nm à 1 µm sécrétées par des cellules stimulées. Elles contiennent une grande variété de molécules actives telles que des lipides, des enzymes, des récepteurs (TLRs, ...), des microARN (miARN). La caractéristique principale des MV est leur exposition de la phosphatidylsérine (PhtdSer) sur leur membrane plasmique externe. Les EMV circulantes procoagulantes ont été démontrées comme biomarqueurs pertinents des atteintes vasculaires d'origine athérothrombotique, inflammatoire ou mécanique, y compris l'ischémie-reperfusion (Ridger et al., 2017 ; Meziani et al., 2010).

L'objectif de cette étude est de déterminer le rôle de *P.gingivalis* sur la production des EMV et d'évaluer leur impact sur la mort cellulaire endothéliale et l'inflammation favorisant l'acquisition d'un état athérothrombotique. Nous évaluerons ainsi les effets induits par *P.gingivalis* et son LPS sur la production des EMV *in vitro* dans des EC humaines et leur impact sur certains marqueurs inflammatoires et étapes clés de la souffrance endothéliale.

Résultats et discussion

Les EMV ont été purifiées à partir des ECs infectées par *P.gingivalis* (MOI 100) pendant 24h. Par la suite, des ECs naïves ont été stimulées par ces EMV et leur effet a été comparé à

celui provoqué par l'infection directe (*P.gingivalis*). L'impact sur la viabilité cellulaire, le type de mort et l'expression de l'ARNm et protéique concernant plusieurs molécules liées à la réponse inflammatoire, au stress oxydatif, au dysfonctionnement endothélial et au recrutement des cellules du système immunitaire, telles que TNF-α, VCam, ICam, Il-8, Il-6, P21, P53, SOD-1, CDK4, eNOS et iNOS, ont été évalués. Enfin, nous avons également étudié l'expression et la phosphorylation de 43 kinases humaines impliquées dans l'activation des principales voies associées à l'inflammation. Ainsi, la stimulation des ECs par les EMV_{Pg} induit un effet pro-inflammatoire et augmentent la mort cellulaire. Fait intéressant, l'analyse protéomique, a mis en évidence la modulation de plusieurs voies liées à l'inflammation suite à la stimulation par *P.gingivalis* ou par les EMV_{Pg}. Il est intéressant de noter que non seulement les voies de signalisation JNK / AKT mais aussi des voies STAT ont été stimulées par l'infection ou les EMV_{Pg}.

Conclusion

Cette étude contribue à démontrer que les EMV produites lors de l'infection bactérienne pourraient exacerber les lésions endothéliales par l'augmentation de la mort cellulaire, du stress oxydatif et de l'inflammation endothéliale. La connaissance de la composition des EMVs circulantes et leur impact biologique *in vivo* restent certes encore insuffisants. Les EMV pourraient ainsi être considérées comme des effecteurs autocrine et paracrine impliqués dans la relation entre parodontite et athérothrombose ayant une valeur pronostique ou diagnostique.

Porphyromonas gingivalis **triggers the shedding of inflammatory endothelial microvesicles that act as autocrine effectors of endothelial dysfunction**

Isaac Maximiliano Bugueno[1], Fatiha Zobairi El-Ghazouani[1], Fareeha Batool[1], Hanine El Itawi[1], Eduardo Anglès-Cano[2], Nadia Benkirane-Jessel[1], Florence Toti[1] and Olivier Huck[1,3]

1. INSERM (French National Institute of Health and Medical Research), UMR 1260, Regenerative Nanomedicine, Fédération de Médecine Translationnelle de Strasbourg (FMTS), Strasbourg, France.

2. Université de Paris, Innovative Therapies in Haemostasis, INSERM UMR_S 1140, F-75006, Paris, France.

3. Université de Strasbourg, Faculté de Chirurgie-dentaire, 8 rue Sainte-Elisabeth, 67000 Strasbourg, France.

Words: 4306

Figures: 5

Table: 1

Corresponding author: Pr Olivier HUCK, Department of Periodontology, Dental faculty, 8 rue Sainte-Elisabeth 67000 Strasbourg- FRANCE, Tel: 0033388116947; @: o.huck@unistra.fr

Abstract

A link between periodontitis and atherothrombosis has been highlighted. The aim of this study was to determine the influence of *Porphyromonas gingivalis* on endothelial microvesicles (EMV_{Pg}) shedding and their contribution to endothelial inflammation.

Endothelial cells (EC) were infected with *P.gingivalis* (MOI=100) for 24h. EMV_{Pg} were isolated and their concentration was evaluated by prothrombinase assay. EMV_{Pg} were significantly increased in comparison with EMV_{Ctrl} shedded by unstimulated cells. While EMV_{Ctrl} from untreated EC had no effect, whereas, the proportion of apoptotic EC was increased by 30nM EMV_{Pg} and viability was decreased down to 25%, a value elicited by *P.gingivalis* alone. Moreover, high concentration of EMV_{Pg} (30nM) induced a pro-inflammatory and pro-oxidative cell response including up-regulation of TNF-α, IL-6 and IL-8 as well as an altered expression of iNOS and eNOS at both mRNA and protein level. An increase of VCAM-1 and ICAM-1 mRNA expression (4.5 folds and 3 folds respectively (p<0.05 vs untreated) was also observed after EMV_{Pg} (30nM) stimulation whereas *P.gingivalis* infection was less effective, suggesting a specific triggering by EMV_{Pg}. Kinasome analysis demonstrated the specific effect induced by EMV_{Pg} on main pro-inflammatory pathways including JNK/AKT and STAT. EMV_{Pg} are effective pro-inflammatory effectors that may have detrimental effect on vascular homeostasis and should be considered as potential autocrine and paracrine effectors involved in the link between periodontitis and atherothrombosis.

Keywords: periodontitis ; infection ; endothelial ; microparticles ; *Porphyromonas gingivalis*

Introduction

Periodontitis is a group of infectious inflammatory diseases associated with soft tissue inflammation and destruction of the tooth-supporting tissues characterized by increased periodontal pocket depth, gingival bleeding and clinical attachment loss. Such disease impairs oral health related quality of life and is considered the main cause of dental mobility and tooth loss[1]. Periodontitis affects a large proportion of the worldwide population and prevalence of its severe forms is estimated to be around 11% with a peak incidence around 38 years of age[2]. The development of periodontitis is associated with the establishment of a dysbiosis characterized by the predominance of anaerobic species, including *Porphyromonas gingivalis* (*P.gingivalis*), and an imbalanced host-immune response inducing periodontal tissue destruction[3].

During the last decades, periodontal diseases were associated with various chronic diseases such as diabetes, rheumatoid arthritis, adverse pregnancy outcomes and cardiovascular diseases, suggesting a systemic impact[4–6] with an enhanced proportion of worsened cardiovascular outcomes[7–9]. Indeed, patients with periodontitis are more prone to endothelial dysfunction, aneurysmal disease progression[10], coronary artery narrowing, and an increased all-cause and cardio-vascular related mortality[11,12]. Moreover, in a clinical trial, intensive periodontal treatment of patients with severe periodontitis, improved at 6 months the endothelial dysfunction, a well-known marker of vascular injury[7] thereby strengthening the causative link.

Among the proposed biological mechanisms[3,5,10,13], the impact of oral and more specifically periodontal bacteria, on arterial homeostasis[14] is suggested by their eventual dissemination in blood flow from the periodontal pocket. Interestingly, they were detected in atheromatous plaques as well as in the wall of healthy vessels in patients suffering from mild to severe periodontitis[15,16]. *P.gingivalis*, an anaerobic bacteria considered as a keystone

periodontal pathogen, was demonstrated, *in vitro*[17–20] and *in vivo*[21,22] as a pro-inflammatory and pro-atheromatous mediator. Indeed, *P.gingivalis* exhibits a large number of virulence factors such as lipopolysaccharide (*Pg*-LPS), fimbriae or gingipaïns, contributing to the modulation of the innate immune response mainly through activation of Toll-Like-Receptors (TLRs)–dependent pathways[1,5,17,18]. Nevertheless, infection by *P.gingivalis* enhances endothelial inflammation or cell death in response to either low-density lipoprotein cholesterol (LDL) or pro-inflammatory cytokines (TNF-α), two circulating mediators associated with elevated cardiovascular risk, thus, highlighting a potential impact in the development of atherothrombosis[18]. However, the hypothesis of a detrimental effect solely induced by direct infection remains controversial as clinical trials assessing the preventative effect of antibiotic therapy did not show significant benefit in the secondary prevention of cardiovascular acute events in patients with history of myocardial infarction or myocardial ischemia[23]. Recently, the CANTOS trial pointed out inflammation as a key driver of atherothrombosis in patients with pro-inflammatory background. However, anti-interleukin-1β (IL-1β) antibodies although improving the cardiovascular outcomes failed to reduce cardiovascular mortality[24]. The eventual vascular impact of a variety of inflammatory mediators acting as autocrine or paracrine cellular effectors has been proposed[25,26]. Amongst them, microvesicles of endothelial origin (EMV) shed from the inflamed endothelium in response to infection could be the possible missing link between the infection-driven and the pro-thrombotic vascular responses.

Microvesicles (MV), also termed microparticles, are plasma membrane vesicles ranging from 50 nm to 1 µm released from stimulated cells. They contain a variety of active molecules such as lipids, enzymes, receptors and microRNAs. One characteristic feature of MV is that they expose phosphatidylserine (PhtdSer), an anionic phospholipid translocated from the inner to the outer leaflet of the plasma membrane. In addition, membrane proteins at

the surface of the mother cell allow the characterization of their cell origin in body fluids. Circulating procoagulant EMV have been demonstrated as relevant biomarkers of vascular insult of atherothrombotic, inflammatory or mechanical origin, including ischemia reperfusion. Regardless of their cell origin, circulating MV emerge as the new actors of cellular crosstalk acting as procoagulant, pro-inflammatory, apoptotic or senescent pathogenic messengers under pathological conditions. Verily, the initial cellular stress at the origin of the MV shedding appears of relevance in the induction of a specific cell dysfunction[27]. In the context of infectious disease, the shedding of $CD105^{+}$EMV has been proven to have a prognosis value in sepsis-induced coagulopathy[28], whereas circulating MV of platelet and leukocyte origin released upon inflammation favor the recruitment of leukocytes at the surface of the inflamed endothelium[29,30].

This study aims to determine *in vitro* the influence of *P.gingivalis* infection on EMV shedding (EMV_{Pg}) and to evaluate an eventual autocrine action of EMV_{Pg} as noxious effectors possibly contributing to the dissemination of endothelial cell inflammatory responses and dysfunction.

Materials and methods

Cell culture

Human umbilical vein endothelial cells (EC) (HUVEC, PromoCell, Heidelberg, Germany) were cultured in EGM2 medium (Promocell, Heidelberg, Germany) supplemented with 10% Fetal Bovine Serum at 37°C in a humidified atmosphere with 5% CO_2. Culture medium was changed each 3 days and no antibiotics were added to the medium.

Endothelial cell infection by P.gingivalis

P.gingivalis strain 33277 (ATCC, Manassas, VA, USA) was cultured under strict anaerobic conditions at 37°C in brain-heart infusion medium (Sigma-Aldrich, Saint-Quentin Fallavier, France) supplemented with hemin (5 µg/ml) and menadione (1 µg/ml) (Sigma-Aldrich). Bacteria were collected and counted as previously described[31]. Twenty-four hours before infection, $2x10^5$ EC/ml were seeded per well in a 24-well plate. EC were washed twice with PBS before infection with *P.gingivalis* at a multiplicity of infection (MOI) of 100. After 2h of infection, medium was removed and infected EC were washed three times with PBS to remove non-adherent and external bacteria. Then, metronidazole (200µg/mL) was added for 1h to kill external bacteria and, after washing, 1 mL of fresh medium was added in each well. For comparative purposes, in some experiments, EC were stimulated with *P.gingivalis* ultrapure lipopolysaccharide (*Pg*-LPS) (1 µg/ml) (InvivoGen, San Diego, CA, USA) for 24h.

Measurement of EMV released in EC supernatant

After 24h, supernatants from LPS-treated or *P.gingivalis*-infected EC were collected under sterile conditions. Detached EC and debris were discarded by low speed centrifugation (300g; 15 min). EMV were then concentrated after two successive centrifugations (14000g; 1h at 4°C), collected in 400 to 600 µl of HBSS (Hanks' Balanced Salt solution) (Sigma-

Aldrich) and stored at 4°C. EMV concentration was measured by prothrombinase assay of the MV ubiquitous Phtdser exposure as previously described. Briefly, EMV were captured onto insolubilized Annexin-V, a protein with high affinity for Phtdser, using streptavidin-coated microtitration plates (Roche Diagnostics, Germany). After three washings, EMV were measured by prothrombinase assay in which blood clotting factors and calcium concentrations ensure that the PhtdSer borne by EMV is the rate-limiting parameter in the generation of soluble thrombin from prothrombin. After 10 min of incubation at 37°C with human FXa (106pM, Hyphen Biomed, France), Factor Va (FVa, 250pM, Sekuisu, USA), prothrombin (FII, 3.5µM, Hyphen BioMed, Paris, France) and $CaCl_2$, thrombin generation was assessed in a multiplate spectrophotometer at 405nm (Versamax, Molecular Devices, Wokingam Berkshire, UK) using a chromogenic thrombin substrate (PNAPEP0216 1.52mM, Cryopep, Montpellier, France). Results were expressed as nanomolar PhtdSer equivalents (nM PhtdSer eq.) by reference to a standard curve established using liposomes of known composition and concentration[32].

Treatment of EC with EMV

EC were seeded in a 24-wells plate at $2x10^5$ cells/well. After 24h, attached EC were washed and incubated with 5 to 30 nM of EMV_{Ctrl} (unstimulated EC) or EMV_{Pg} according to the experiment.

Measurement of cell metabolic activity

Cell metabolic activity was determined using colorimetric AlamarBlue test (Life Technologies, Saint-Aubin, France) as described previously and according to manufacturer's instructions[33]. Briefly, after 24h of stimulation with EMV or *P.gingivalis*, 300 µl of cell

supernatants were transferred to 96-well plates and optical density was measured at 570 and 595 nm in order to determine the percentage of AlamarBlue reduction.

Determination of the cell viability

The cellular viability was evaluated using a fluorescence-based LIVE/DEAD® assay (LIVE/DEAD® Cell Imaging Kit, Molecular Probes™, Invitrogen) after 24h of either infection or EMV stimulation. Cells were washed twice with PBS before staining. The staining solution consisted of 0.5 µL/mL calcein AM reagent and 2 µL/mL EthD-1 reagent mixed in 2 mL PBS. Samples were incubated for 10 min before analysis using a 10x and 20x objective lens of a fluorescence microscope (Olympus BX53F, Tokyo, Japan), filters for fluorescein and Texas Red for calcein and EthD-1 staining and digital CCD color imaging system (Microscope Digital Camera DP72; CellSens Entry®, Olympus, Tokyo, Japan).

Measurement of cell apoptosis and necrosis

Annexin V-propidium iodide double staining was performed on washed trypsinized EC using the Annexin-V-FLUOS Staining Kit (Roche Applied Science, Meylan, France) according to manufacturer's instructions. For each condition, a total of $1x10^4$ isolated cells were analyzed by flow cytometry using a BD™ LSR II. The percentage of positive cells for IP^{PE} (necrosis), Annexin-V^{FITC} and IP^{PE} (late apoptosis), Annexin-V Positive Cells V^{FITC} (apoptosis), and unlabeled (viable cells) was determined from quadrant analysis.

RNA isolation, reverse transcription and quantitative real-time PCR analysis

Total RNAs from samples were extracted using Tri reagent (Sigma-Aldrich) according to the manufacturer's instructions. The total RNA concentration was quantified by spectrophotometry (NanoDrop 1000, Fischer Scientific, Illkirch, France) at 230nm. Reverse transcription was performed using the iScript Reverse Transcription Supermix kit (Biorad,

Miltry-Mory, France) according to the manufacturer's instructions. qPCR was performed on the cDNA samples and gene expression was further analyzed using the CFX Connect™ Real-Time PCR Detection System (Biorad, Miltry-Mory, France). Amplification reactions have been performed using iTAq Universal SYBR Green Supermix (Biorad, Miltry-Mory, France). β-actin was used as endogenous RNA control (housekeeping gene) in all samples. Primers related to β-actin, TNF-α, Il-6, Il-8, p21, p53, CDK4, eNOS, iNOS, SOD-1, VCAM-1, ICAM-1 and tissular factor (TF) were synthesized (ThermoFischer, Saint-Aubin, France) (Table 1). Expression level was calculated after normalization to the housekeeping gene expression.

Proteome profile array of phospho-kinases

Total protein extraction and purification were performed from cell lysates as previously described[20]. Briefly, cells were lysed for 5 min on ice in 200 µl of ice-cold RIPA buffer (65 mM Tris–HCl, pH 7.4, 150mM NaCl, and 0.5% sodium deoxycholate) supplemented with phosphatase inhibitor cocktails I and II and a protease inhibitor cocktail (Sigma, Darmstadt, Germany). Then, standardized concentration of total proteins was subjected to a Proteome Profiler Human Phospho-Kinase Array (R&D Systems, Lille, France) following manufacturer's instructions. The density of spots, corresponding to protein activation, was measured by MyImage™ Analysis Software 2.0 (Thermofisher) for each molecule and each condition.

Western blotting

Briefly, cells were lysed for 5 min on ice in 200 µl of ice-cold RIPA buffer (65 mM Tris–HCl, pH 7.4, 150mM NaCl, and 0.5% sodium deoxycholate) supplemented with phosphatase inhibitor cocktails I and II and a protease inhibitor cocktail (Sigma, Darmstadt,

Germany). Lysates were centrifuged at 10,000 g at 4°C for 10min, supernatants were collected for quantification using the Bradford protein assay (Bio-Rad, Hercules, CA, USA) and 20µg of cell lysates were loaded on a 12 % SDS-PAGE for each condition. Antibodies against human eNOS (1/1000, mouse IgG, BD Biosciences, Le Pont de Claix, France), P21 (1/1000, rabbit IgG, Abcam, Paris, France), P53 (1/1000, rabbit IgG, Santa Cruz Biotechnology, Heidelberg, Germany), VCAM (1/500, rabbit IgG, Abcam, Paris, France), ICAM-1 (1/1000, mouse IgG, Life technologies, Courtaboeuf, France), CDK4 (1/1000, rabbit IgG, Life technologies), SOD-1 (1/1000, rabbit IgG, Life technologies), iNOS (1/1000, rabbit IgG, Life technologies) and against β-actin (1/2000, mouse IgG) from Santa Cruz Biotechnology (Heidelberg, Germany) were used for immunolabelling. Secondary alkaline phosphatase conjugated antibodies (anti-mouse (1/3000) or anti-rabbit (1/5000)) were purchased from Bethyl Laboratories (Montgomery, Texas, USA).

Enzyme-linked immunosorbent assay

TNF-α secreted in the cell supernatant was assessed by a sandwich enzyme-linked immunosorbent assay (ELISA). Briefly, a goat anti-Human TNF-α antibody, (PeproTech, Rocky Hill, NJ, USA) was coated on a multi-well plate (4µg/mL). Then, supernatants were added overnight at 4°C. After washing with PBS, TNF-α was detected using a biotinylated goat anti-Human TNF-α (PeproTech). After 3 washing steps to discard unbound antibodies, HRP conjugated streptavidin (mix of solution A+B, as manufacturer instructions) was added and incubated for 20 to 30 minutes at room temperature. Finally, 100 µL of the stop solution (horseradish peroxidase and TMB substrate Solution, SS04, Life Technologies, Saint-Aubin, France) was added to each well for 5 to 30 min and then OD was measured by spectrophotometer (450nm). The concentration of TNF-α was calculated by reference to a standard curve obtained with recombinant human TNF-α (PeproTech).

Statistical analysis

Statistical analysis was performed using pair-wise Anova test and post-hoc Tukey's test. Statistical significance level was considered for $p<0.05$. Data were analyzed using PRISM 6.0 (GraphPad, La Jolla, CA, USA). All experiments have been performed at least three times from three different EC culture batches (biological and technical replicates).

Results

Endothelial microvesicles generated in response to P.gingivalis are pro-apoptotic endothelial effectors

P.gingivalis infection (MOI:100) led to a significant 2.8 fold in the shedding of EC after 24h (infected *vs.* untreated, $p<0.05$) (Figure 1A) whereas the ultrapure *Pg*-LPS alone (1 µg/ml) had no significant effect (Figure 1A). Interestingly, no MV shedding was detected in *P.gingivalis* culture supernatant (Supplementary informations Figure 1). The putative cytotoxic effect of EMV_{Pg} shed after *P.gingivalis* infection and of EMV_{Ctrl} shed from unstimulated cells was assessed after 24h of incubation with the endothelial monolayer. While no cytotoxic effect has been observed for EMV_{Ctrl}, increasing concentrations of EMV_{Pg} (5 to 30nM) led to a significant 10% and 25% concentration-dependent reduction of cell viability and survival respectively (Figure 1B-C-D, $p<0.05$ vs untreated cells), values measured after 30 nM EMV_{Pg} treatment reaching the range of those elicited by *P.gingivalis* alone (MOI:100). A nearly 2-fold enhancement in the proportion of EC showing late apoptosis was observed in response to *P.gingivalis* infection or to 20-30 nM EMV_{Pg} by flow cytometry and fluorescence microscopy (*P.gingivalis*-triggered 1.7-fold fold *vs* untreated; 20 nM EMV_{Pg} -induced 1.6-fold *vs* untreated and 30 nM EMV_{Pg} -induced 1.5-fold *vs* untreated), while, the proportion of EC with early apoptosis was unchanged at 20 nM and drastically increased by 30nM EMV_{Pg} suggesting a concentration threshold (Figure 1 E).

EMV_{Pg} switch the mRNA and protein expression profiles of endothelial cells to a characteristic pro-inflammatory pattern

The potential pro-inflammatory *P.gingivalis* or EMV_{Pg} -induced action was first assessed by the analysis of mRNA transcripts following a 24h incubation with 5-30nM EMV_{Pg}. An up-regulation in the expression of pro-inflammatory TNF-α, IL-6 and IL-8

cytokines mRNA was detected, reaching similar TNF-α expression after either *P.gingivalis* infection or 30 nM EMV_{Pg} (6.5 folds *P.gingivalis* or EMV_{Pg} -induced *vs* untreated) (Figure 2A). IL-6 mRNA expression was enhanced by 2.2 fold (*P.gingivalis* -induced *vs.* untreated; $p<0.05$) whereas, IL-8 mRNA was highly and solely enhanced by 30 nM EMV_{Pg} by 6-fold. This pro-inflammatory switch was further confirmed by ELISA assay. Increased TNF-α concentrations after *P.gingivalis* infection (2.3 fold; $p<0.05$) and EMV_{Pg} stimulation (2 folds; $p<0.05$) were measured after 24h of incubation (Figure 3A). Interestingly, proteome analysis showed that several inflammation-related pathways are modulated following *P.gingivalis* or EMV_{Pg} stimulation (Figure 4). Interestingly, not only did the JNK/AKT but also STAT were differentially up-regulated following endothelial infection or stimulation.

Because leukocyte recruitment at the surface of the inflamed endothelium is one of the initial steps for atherothrombosis[34], therefore, expression of endothelial VCAM-1 and ICAM-1 adhesion molecules that favor leukocyte attachment was also assessed. After 24h incubation, 30 nM EMV_{Pg} significantly augmented both VCAM-1 and ICAM-1 mRNA expression (4.5 folds and 3 folds respectively ($p<0.05$ vs untreated) whereas *P.gingivalis* infection was less effective at the chosen concentration, suggesting a specific triggering by EMV_{Pg} as compared to the above pro-inflammatory cytokines induction (Figure 5A). Nevertheless, infection by *P.gingivalis,* significantly increased the expression of tissue factor (TF), the cellular initiator of the coagulation cascade at the endothelial surface, and also a pro-inflammatory and pro-apoptotic inducer[35] after 24h. Interestingly, EMV_{Pg} incubation led to a concentration-dependent expression of TF mRNA, reaching values prompted by *P.gingivalis* infection (Figure 5A).

EMV_{Pg} modulate endothelial oxidative stress and promote endothelial dysfunction

Because nitric oxide is one of the major vasoprotectors released by endothelial cells under physiological conditions and a very diffusible mediator of vaso-relaxation, we investigated whether the expression of NO synthases would be altered by EMV_{Pg}. In this context, under conditions mimicking cardiovascular pathological conditions, like cytokine treatment or angiotensin II-induced endothelial dysfunction, iNOS, the inducible form of NO synthase (iNOS) is up-regulated, whereas, the constitutive eNOS expression remains unchanged[36]. Herein, 24h after *P.gingivalis* infection or 20-30 nM EMV_{Pg} EC treatment, the expression of eNOS was significantly reduced at both transcriptional and protein levels (2.1 folds; $p<0.05$) (Figure 3B, 4, 5B). At contrary, increased iNOS expression was induced by *P.gingivalis* and EMV_{Pg} and enhanced by 2 and 5.8 folds respectively ($p<0.05$ *vs.* untreated), thereby indicating endothelial dysfunction, eventually altered vascular function and possible eNOS uncoupling[37]. The expression of endothelial super oxide dismutase (SOD-1), an enzyme that rapidly inactivates superoxide anions, was also triggered by *P.gingivalis* and 30 nM EMV_{Pg} that both induced a 400% mRNA rise after 24h, emphasizing the importance of cytoprotective signaling pathways in the endothelial response to major oxidative stress (Figures 3B, 5B).

Because oxidative stress and the control of cell cycle are closely related, we also investigated whether *P.gingivalis* infection or EMV_{Pg} could also trigger regulators of the cell cycle. Indeed, both endothelial treatments targeted the oncosuppressor p53 and its downstream partner p21, a cyclin-dependent kinase inhibitor 1 and an inducer of senescence with a significant increase in p21 and p53 mRNA levels (4.7 and 14.3 folds respectively) (Figure 2B). Moreover, the p53 up-regulation was confirmed by western-blot and proteomic analysis (Figure 3B, 4). Conversely, a significant 2.3-fold decrease in the mRNA and protein expression of the cyclin-dependent kinase CDK4 was evidenced ($p<0.05$ vs untreated) (Figures 2B, 3B).

Altogether, these data strongly suggest that endothelial dysfunction in response to *P.gingivalis* infection or EMV_{Pg} stimulation is associated with oxidative stress and modulation of the cell cycle in a redox-dependent manner as reported in human and murine endothelial cells[36,38].

Discussion

This study demonstrates the autocrine pro-inflammatory properties of EMV_{Pg} shed from EC in response to *P.gingivalis* infection. Results indicate that after 24h of incubation, the shed EMV_{Pg} appear as key mediators of endothelial dysfunction, switching the cytoprotective phenotype of endothelial cells toward a pro-inflammatory, pro-coagulant, pro-apoptotic and, eventually, a pro-senescent phenotype. All such phenotypes are a hallmark of sustained periodontitis in periodontal vascularization and atherothrombosis progression in large arteries. Furthermore, most of the cell responses investigated were of comparable severity whether initiated by *P.gingivalis* or by high concentration of EMV_{Pg} .

Because MV are procoagulant owing to PhtdSer exposure and the eventual presence of TF when shed from monocytes, neutrophils and endothelial cells, their impact as pathogenic effectors in acute or chronic cardiovascular diseases and associated disorders such as myocardial infarction, atrial fibrillation, unstable angina, type-2 diabetes and their accumulation in the arteriosclerotic plaque has been extensively studied in relationship with the vascular inflammatory responses[27]. In blood, MV constitute a dynamic storage pool of vascular effectors, whereby, their cellular origin and concentration characterizing the severity of the disease or of organ damage. Of note, EMV, even circulating as a small proportion of the vascular pool were found of prognostic value in organ and cellular graft rejection[39], pulmonary hypertension[40], sepsis-induced coagulopathy[41] and cardiovascular diseases[42–45].

Strikingly, reports concerning infection-related MV shedding and how both host and pathogens produce MV are scarce. For instance, virulence factors, like LMP1 from the replicating Epstein-Barr virus, can be embedded in MV released from the infected cell and further spread virus through paracrine interactions with yet non-infected target cells. Similarly, Human immunodeficiency virus also promotes MV shedding to transfer CCR5, its co-receptor on macrophages, to non-exposing target cells, consequently, promoting its own

spreading[46]. MV hijacking by pathogens could also be the causative of link between periodontitis and cardiovascular disease, as strongly supported by our data and previous reports[47]. In congruence with our data, *Chlamydia pneumoniae* was also detected within atheromatous plaques and demonstrated to up-regulate the endothelial expression of the TF within 24h together with the release of TF^{+}-EMV that persisted for 1 week[48]. Most interestingly, we identified via proteomic and transcriptomic assays that the EMV shedding in response to *P.gingivalis* was associated with characteristic prerequisite pathways of the cytoskeleton proteolytic cleavage and plasma membrane remodeling preceding the MV release from the inflamed or stimulated endothelium[38]. Indeed, the p38 MAP kinase pathway that promotes the release of pro-inflammatory MV from human aortic endothelial cells in response to TNF-α[49] was activated in our infection- driven model of pathogenic MV generation.

In this study, we emphasized the role of EMV_{Pg} as systemic pro-inflammatory and pro-oxidant effectors of endothelial responses mediated by *P.gingivalis*. In our *in vitro* MV-mediated model, EMV_{Pg} at 30 nM acted as cytotoxic endothelial effectors to an extent that was similar to the sole *P.gingivalis* infection (MOI=100), via the activation of inflammatory pathways evidenced through Kinasome analysis. The up-regulation of TNF-α and IL-6 proinflammatory cytokines and their secretion eventually associated to an uncontrolled oxidative stress via the down-regulation of eNOS and the up-regulation of iNOS suggest NO synthase uncoupling. Therefore, our data altogether strengthen, the hypothesis of an EMV mediated *P.gingivalis* systemic response. This observation is strongly suggestive of a noxious role of $EMV_{Pg,}$ eventually disseminated in blood flow to target healthy endothelial cells, even under conditions where its pathogenic inducer *P.gingivalis* would remain sequestered in the periodontal tissues by cells of the innate immune response[50]. Endothelial inflammation via TNF-α, IL-1β, or IL-6 pro-inflammatory cytokines favors leukocyte recruitment, endothelial

dysfunction and activation of blood coagulation making interleukin-driven proatherothrombotic processes a potential pharmacological target explored in several clinical trials[51,52]. In view of the recent anti-interleukin therapy trials, that failed to demonstrate a benefit on cardiovascular outcome, circulating EMV released upon pathogen infection appear to be another target since EMV are able to concentrate at endothelial sites where flow disturbance favors enhanced interactions with MV, namely at artery branches prone to the development of atherotrombosis plaques. It was reported that MV sequestered in plaques act as paracrine endothelial up-regulators of pro-inflammatory ICAM-1 or VCAM-1 prompting leukocyte recruitment in the growing plaque[43,53]. Whether the plaque of patients subjected to chronic exposure of EMV released from distant endothelial infected sites undergo exaggerated endothelial inflammation remains to be demonstrated in specific animal models of atherothrombosis and in clinical trials. Nevertheless, we also showed that EMV_{Pg} triggered inflammation-related pathways. Indeed, the modulation of upstream NF-$_K$B activators but also of transcription factors such as STAT confirmed their pro-inflammatory effect, as STAT pathway is a major signaling route converting the cytokine signal into gene expression programs regulating the proliferation and differentiation of the immune cell[54].

P.gingivalis was previously demonstrated as a specific TLR4-dependent endothelial actor in pro-inflammatory TNF-α and IL-6 secretion following endothelial invasion or via its virulence factors such as LPS[55,56]. Moreover, several studies demonstrated the importance of NF-$_K$B pathways in *P.gingivalis* elicited inflammation in several cell types[57–60]. In a previous report, we were able to demonstrate that $TLR4^+$MV generated by *Pseudomonas* were true mediators of NF-$_K$B-dependent signaling in $TLR4^-$HEK engineered cells via I_KB phosphorylation[61]. In the present study, our data confirm and extend these observations, by showing that EMV released upon *P.gingivalis* infection are autocrine endothelial effectors possibly contributing to plaque endothelium inflammation and erosion[62]. Such effect appears

specific to the EMV shedding trigger as only EMV_{Pg} were able to induce a significant endothelial cell response while none was measured with EMV_{Ctrl}. This observation highlights the need of deep analysis of the EMV_{Pg} content, including mRNA, miRNA and proteins, as it was shown that such content is highly influenced by both triggers; the cellular environment and pre-existing conditions[63,64]. It also paves the way of future clinical trials aiming to determine MV phenotype in the context of variable periodontitis severity and *P.gingivalis* infection.

Accumulation of ROS and endothelial redox imbalance have been widely demonstrated in the atherothrombotic plaque *in vitro*, in animal models and in human vascular tissues[43,65]. Oxidative stress is up-regulated upon infection by *Escherichia coli* or *Salmonella typhimurium*[66–68]. Conversely, *in vitro* models indicate that eNOS endothelial activity is reduced upon TNF-α or LPS incubation[69] whereas experimental bacterial meningitis in engineered mice with iNOS invalidation support the hypothesis of a dual endothelial iNOS and eNOS up-regulation upon comparison with wild type individuals[70]. Here, EMV_{Pg} triggered oxidative stress via altered the expression of iNOS and eNOS at mRNA and protein levels, data altogether supporting eNOS uncoupling owing to major ROS accumulation and consecutive endothelial dysfunction, together with blunted cytoprotective signaling pathways against excessive inflammatory and pro-thrombotic responses. Interestingly, circulating MV in patients with coronary artery disease are elevated in comparison to that with healthy individuals and contain reduced functional eNOS. Furthermore, it was also demonstrated that a proportion of EMV circulating in such patients reduce the availability of NO in coronary artery endothelial cells and down regulate its expression[71]. Further studies are required to characterize a specific sub-population of endothelial MV eventually responsible for the systemic dissemination of the pathogen-driven inflammatory and pro-oxidant signals to

uninfected endothelial cells and possibly contributing to endothelial dysfunction in patients with cardiovascular disease.

In this study, *P.gingivalis* strain ATCC 33277 was used as a pathogenic model. It should be mentioned that this strain is not the most virulent and future studies should determine the pro-inflammatory impact of others strains or mutants lacking fimbriae or gingipaïns as it was demonstrated a significant impact of such virulence factors on experimental outcomes in different cell types [72,73]. Future studies should also determine the precise composition of EMV_{Pg} as their content is clearly influenced by the quantity and type of cellular stress trigger. Indeed, a specific insight should be made on mRNA, miRNA, proteins and membrane receptors [74-76].

In conclusion, *P.gingivalis*-induced EMV are effective pro-inflammatory effectors potentially involved in cardiovascular disease worsening. Nevertheless, autocrine and paracrine actions of EMV need further characterization of embedded noxious content, and of their cellular and subcellular molecular partners. Further studies are needed to understand the impact of sustained yet low bacterial or virulence factors as well as low grade cytokine dissemination. A specific emphasis should be done on more relevant *in vitro* models such as human aortic endothelial cells and *in vivo*. Causative links between periodontitis and cardiovascular diseases should be investigated to decipher the systemic routes of the periodontal pathogenic signal dissemination. Local EMV released at distance from the thrombogenic plaque are a good candidate.

Acknowledgments / Fundings

The authors declare no financial and non-financial conflicts of interest related to this study. This work was partly funded by Agence Nationale pour la Recherche (ANR ENDOPAROMP ANR-17-CE17-0024-01 and ANR COCERP ANR-16-CE29-0009-03).

Authors contributions

I.M. Bugueno, F. Zobairi El-Ghazouani, E. Anglès-Cano, F.Toti, O.Huck contributed to conception and design, data acquisition, analysis and interpretation, drafted and critically revised the manuscript. F. Batool, H. El Itawi, N. Benkirane-Jessel contributed to data analysis and critically revised the manuscript. All authors gave final approval and agree to be accountable for all aspects of the work.

References

1. Hajishengallis, G. & Lamont, R.J. Breaking bad: Manipulation of the host response by *Porphyromonas gingivalis*. *Eur. J. Immunol.*;44, 328–338 (2014).
2. Kassebaum, N.J., Bernabé, E., Dahiya, M., Bhandari, B., Murray, C.J.L. & Marcenes, W. Global burden of severe periodontitis in 1990-2010: a systematic review and meta-regression. *J. Dent. Res.* 93,1045–1053 (2014).
3. Hajishengallis G. Periodontitis: from microbial immune subversion to systemic inflammation. *Nat. Rev. Immunol.* 15, 30–44 (2015).
4. Linden, G.J., Lyons, A. & Scannapieco, F.A. Periodontal systemic associations: review of the evidence. *J. Clin. Periodontol.* 40, 8-19 (2014).
5. Huck, O., Elkaim, R., Davideau, J.L. & Tenenbaum, H. Evaluating periodontal risk for patients at risk of or suffering from atherosclerosis: recent biological hypotheses and therapeutic consequences. *Arch. Cardiovasc. Dis.* 104, 352–358 (2011).
6. Lockhart, P.B., Bolger, A.F., Papapanou, P.N., Osinbowale, O., Trevisan, M., Levison, M.E., Taubert, K.A., Newburger, J.W., Gornik, H.L., Gewitz, M.H., et al. Periodontal disease and atherosclerotic vascular disease: does the evidence support an independent association?: a scientific statement from the American Heart Association. *Circulation* 125, 2520–2544 (2012).
7. Tonetti, M.S., D'Aiuto, F., Nibali, L., Donald, A., Storry, C., Parkar, M., Suvan, J., Hingorani, A.D., Vallance, P. & Deanfield, J. Treatment of Periodontitis and Endothelial Function. *N. Engl. J. Med.* 356, 911–920 (2007).
8. Pothineni, N.V.K., Subramany, S., Kuriakose, K., Shirazi, L.F., Romeo, F., Shah, P.K. & Mehta, J.L. Infections, atherosclerosis, and coronary heart disease. *Eur. Heart J.* 38, 3195–3201 (2017).

9. Rosenfeld, M.E. & Campbell, L.A. Pathogens and atherosclerosis: update on the potential contribution of multiple infectious organisms to the pathogenesis of atherosclerosis. *Thromb. Haemost.* 106, 858–867 (2011).
10. Salhi, L., Rompen, E., Sakalihasan, N., Laleman, I., Teughels, W., Michel, J.B. & Lambert, F. Can Periodontitis Influence the Progression of Abdominal Aortic Aneurysm? A Systematic Review. *Angiology* 70, 479–491 (2019).
11. Xu, F. & Lu, B. Prospective association of periodontal disease with cardiovascular and all-cause mortality: NHANES III follow-up study. *Atherosclerosis* 218, 536–542 (2011).
12. Buhlin, K., Mäntylä, P., Paju, S., Peltola, J.S., Nieminen, M.S., Sinisalo, J. & Pussinen, P.J. Periodontitis is associated with angiographically verified coronary artery disease. *J. Clin. Periodontol*. 38(11):1007-14 (2011).
13. Liljestrand, J.M., Paju, S., Pietiäinen, M., Buhlin, K., Persson, G.R., Niemine, M.S., Sinisalo, J., Mäntylä, P. & Pussinen, P.J. Immunologic burden links periodontitis to acute coronary syndrome. *Atherosclerosis* 268, 177–184 (2018).
14. Zelkha, S.A., Freilich, R.W. & Amar, S. Periodontal innate immune mechanisms relevant to atherosclerosis and obesity. *Periodontol. 2000* 54, 207–221 (2010).
15. Elkaïm, R., Dahan, M., Kocgozlu, L., Werner, S., Kanter, D., Kretz, J.G. & Tenenbaum, H. Prevalence of periodontal pathogens in subgingival lesions, atherosclerotic plaques and healthy blood vessels: a preliminary study. *J. Periodontal Res.* 43, 224–231 (2008).
16. Amar, S. & Engelke, M. Periodontal Innate Immune Mechanisms Relevant to Atherosclerosis. *Mol. Oral Microbiol.* 30, 171–185 (2015).
17. Huck, O., Elkaim, R., Davideau, J.L. & Tenenbaum, H. *Porphyromonas gingivalis*-impaired innate immune response via NLRP3 proteolysis in endothelial cells. *Innate Immun.* 21, 65–72 (2015).

18. Bugueno, I.M., Khelif, Y., Seelam, N., Morand, D.N., Tenenbaum, H., Davideau, J.L. & Huck, O. *Porphyromonas gingivalis* Differentially Modulates Cell Death Profile in Ox-LDL and TNF-α Pre-Treated Endothelial Cells. *PLoS ONE* 11 (2016).
19. Huck, O., Al-Hashemi, J., Poidevin, L., Poch, O., Davideau, J.L., Tenenbaum, H. & Amar, S. Identification and Characterization of MicroRNA Differentially Expressed in Macrophages Exposed to *Porphyromonas gingivalis* Infection. *Infect. Immun.* 23;85(3) (2017).
20. Bugueno, I.M., Batool, F., Korah, L., Benkirane-Jessel, N. & Huck, O. *Porphyromonas gingivalis* Differentially Modulates Apoptosome Apoptotic Peptidase Activating Factor 1 in Epithelial Cells and Fibroblasts. *Am. J. Pathol.* 188, 404–416 (2018).
21. Velsko, I.M., Chukkapalli, S.S., Rivera, M.F., Lee, J.Y., Chen, H., Zheng, D., Bhattacharyya, I., Gangula, P.R., Lucas, A.R. & Kesavalu, L. Active invasion of oral and aortic tissues by *Porphyromonas gingivalis* in mice causally links periodontitis and atherosclerosis. *PloS One* 9, e97811 (2014).
22. Li, L., Messas, E., Batista, E.L., Levin, R.A. & Amar, S. *Porphyromonas gingivalis* infection accelerates the progression of atherosclerosis in a heterozygous apolipoprotein E-deficient murine model. *Circulation* 105, 861–867 (2002).
23. Song, Z., Brassard, P. & Brophy, J.M. A meta-analysis of antibiotic use for the secondary prevention of cardiovascular diseases. *Can. J. Cardiol.* 24, 391–395 (2008).
24. Lutgen, E., Atzler, D., Döring, Y., Duchene, J., Steffens, Weber, C. Immunotherapy for cardiovascular disease. *Eur. Heart J.* doi:10.1093/eurheartj/ehz283 (2019).
25. Welsh, P., Grassia, G., Botha, S., Sattar, N. & Maffia, P. Targeting inflammation to reduce cardiovascular disease risk: a realistic clinical prospect? *Br. J. Pharmacol.* 174, 3898–3913 (2017).

26. Van Tassell, B.W., Toldo, S., Mezzaroma, E. & Abbate, A. Targeting Interleukin-1 in Heart Disease. *Circulation* 128, 1910–1923 (2013).

27. Ridger, V.C., Boulanger, C.M., Angelillo-Scherrer, A., Badimon, L., Blanc-Brude, O., Bochaton-Piallat, M.L., Boilard, E., Buzas, E., Caporali, A., Dignat-George, F., et al. Microvesicles in vascular homeostasis and diseases. Position Paper of the European Society of Cardiology (ESC) Working Group on Atherosclerosis and Vascular Biology. *Thromb. Haemost.* 117, 1296–1316 (2017).

28. Meziani, F., Delabranche, X., Asfar, P. & Toti, F. Bench-to-bedside review: circulating microparticles--a new player in sepsis? *Crit. Care Lond. Engl.* 14, 236 (2010).

29. Barry, O.P., Praticò, D., Savani, R.C. & Fitzgeral G.A. Modulation of monocyte-endothelial cell interactions by platelet microparticles. *J. Clin. Invest.* 102, 136–144 (1998).

30. Mause, S.F., Von Hundelshausen , Zernecke, A., Koene, R.R. & Weber, C. Platelet microparticles: a transcellular delivery system for RANTES promoting monocyte recruitment on endothelium. *Arterioscler. Thromb. Vasc. Biol.* 25, 1512–1518 (2005).

31. Huck, O., Elkaim, R., Davideau, J.L. & Tenenbaum, H. *Porphyromonas gingivalis* and its lipopolysaccharide differentially regulate the expression of cathepsin B in endothelial cells. *Mol. Oral Microbiol.* 27, 137–148 (2012).

32. Jy, W., Horstman, L.L., Jimenez, J.J., Ahn, Y.S., Biró, E., Nieuwland, R., Sturk, A., Dignat-George, F., Sabatier, F., Camoin-Jau, L., et al. Measuring circulating cell-derived microparticles. *J. Thromb. Haemost.* 2, 1842–1851 (2004).

33. Keller, L., Idoux-Gillet, Y., Wagner, Q., Eap, S., Brasse, D., Schwinté, P., Arruebo, M. & Benkirane-Jessel, N. Nanoengineered implant as a new platform for regenerative nanomedicine using 3D well-organized human cell spheroids. *Int. J. Nanomedicine* 12, 447–457 (2017).

34. May, A.E., Langer, H., Seizer, P., Bigalke, B., Lindemann, S. & Gawaz, M. Platelet-Leukocyte Interactions in Inflammation and Atherothrombosis. *Semin. Thromb. Hemost.* 33, 123–127 (2007).

35. Cimmino, G. & Cirillo, P. Tissue factor: newer concepts in thrombosis and its role beyond thrombosis and hemostasis. *Cardiovasc. Diagn. Ther.* 8, 581–593 (2018).

36. Khemais-Benkhiat, S., Idris-Khodja, N., Ribeiro, T.P., Silva, G.C., Abbas, M., Kheloufi, M., Lee, J.O., Toti, F., Auger, C. & Schini-Kerth, V.B. The Redox-sensitive Induction of the Local Angiotensin System Promotes Both Premature and Replicative Endothelial Senescence: Preventive Effect of a Standardized Crataegus Extract. *J. Gerontol. A. Biol. Sci. Med. Sci.* 71, 1581–1590 (2016).

37. Bhagat, K., Hingorani, A.D., Palacios, M., Charles, I.G. & Vallance, P. Cytokine-induced venodilatation in humans in vivo: eNOS masquerading as iNOS. *Cardiovasc. Res.* 41, 754–764 (1999).

38. Burger, D., Montezano, A.C., Nishigaki, N., He, Y., Carter, A. & Touyz, R.M. Endothelial microparticle formation by angiotensin II is mediated via Ang II receptor type I/NADPH oxidase/ Rho kinase pathways targeted to lipid rafts. *Arterioscler. Thromb. Vasc. Biol.* 31,1898–1907 (2011).

39. Morel, O., Ohlmann, P., Epailly, E., Bakouboula, B., Zobairi, F., Jesel, L., Meyer, N., Chenard, M.P., Freyssinet, J.M., Bareiss, P., et al. Endothelial cell activation contributes to the release of procoagulant microparticles during acute cardiac allograft rejection. *J. Heart Lung Transplant.* 27, 38–45 (2008).

40. Bakouboula, B., Morel, O., Faure, A., Zobairi, F., Jesel, L., Trinh, A., Zupan, M., Canuet, M., Grunebaum, L., Brunette, A., et al. Procoagulant membrane microparticles correlate with the severity of pulmonary arterial hypertension. *Am. J. Respir. Crit. Care Med.* 177, 536–543 (2008).

41. Delabranche, X., Helms, J. & Meziani, F. Immunohaemostasis: a new view on haemostasis during sepsis. *Ann. Intensive Care* 7 (2017).

42. Amabile, N., Cheng, S., Renard, J.M., Larson, M.G., Ghorbani, A., McCabe, E., Griffin, G., Guerin, C., Ho, J.E., Shaw, S.Y., et al. Association of circulating endothelial microparticles with cardiometabolic risk factors in the Framingham Heart Study. *Eur. Heart J.* 35, 2972–2979 (2014).

43. Rautou, P.E., Leroyer, A.S., Ramkhelawon, B., Devue, C., Duflaut, D., Vion, A.C., Nalbone, G., Castier, Y., Leseche, G., Lehoux, S., et al. Microparticles from human atherosclerotic plaques promote endothelial ICAM-1-dependent monocyte adhesion and transendothelial migration. *Circ. Res.* 108, 335–343 (2011).

44. Yin, M., Loyer, X. & Boulanger C.M. Extracellular vesicles as new pharmacological targets to treat atherosclerosis. *Eur. J. Pharmacol.* 763, 90–103 (2015).

45. Boulanger, C.M. & Dignat-George, F. Microparticles: an introduction. *Arterioscler. Thromb. Vasc. Biol.* 31, 2–3 (2011).

46. Mack, M., Kleinschmidt, A., Brüh, H., Klier, C., Nelso, P.J., Cihak, J., Plachý, J., Stangassinger, M., Erfle, V. & Schlöndorff, D. Transfer of the chemokine receptor CCR5 between cells by membrane-derived microparticles: a mechanism for cellular human immunodeficiency virus 1 infection. *Nat. Med.* 6, 769–775 (2000).

47. Lai, F.W., Lichty, B.D. & Bowdish, D.M.E. Microvesicles: ubiquitous contributors to infection and immunity. *J. Leukoc. Biol.* 97, 237–245 (2015).

48. Ettelaie, C., Collier, M.E.W., James, N.J. & Li, C. Induction of tissue factor expression and release as microparticles in ECV304 cell line by *Chlamydia pneumoniae* infection. *Atherosclerosis* 190, 343–351 (2007).

49. Curtis, A.M., Wilkinson, P.F., Gui, M., Gales, T.L., Hu, E. & Edelberg, J.M. p38 mitogen-activated protein kinase targets the production of proinflammatory endothelial microparticles. *J. Thromb. Haemost.* 7, 701–709 (2009).

50. Cooper, P.R., Palmer, L.J. & Chapple, I.L.C. Neutrophil extracellular traps as a new paradigm in innate immunity: friend or foe? *Periodontol. 2000* 63, 165–197 (2013).

51. Ridker, P.M. Anticytokine Agents: Targeting Interleukin Signaling Pathways for the Treatment of Atherothrombosis. *Circ. Res.* 124, 437–450 (2019).

52. Ridker, P.M. Clinician's Guide to Reducing Inflammation to Reduce Atherothrombotic Risk: JACC Review Topic of the Week. *J. Am. Coll. Cardiol.* 72, 3320–3331 (2018).

53. Leroyer, A.S., Isobe, H., Lesèche, G., Castier, Y., Wassef, M., Mallat, Z., Binder, B.R., Tedgui, A. & Boulanger, C.M. Cellular origins and thrombogenic activity of microparticles isolated from human atherosclerotic plaques. *J. Am. Coll. Cardiol.* 49, 772–777 (2007).

54. Pfitzner, E., Kliem, S., Baus, D. & Litterst, C.M. The role of STATs in inflammation and inflammatory diseases. *Curr. Pharm. Des.* 10, 2839–2850 (2004).

55. Kocgozlu, L., Elkaim, R., Tenenbaum, H. & Werner, S. Variable cell responses to *P. gingivalis* lipopolysaccharide. *J. Dent. Res.* 88, 741–745 (2009).

56. Ho, Y.S., Lai, M.T., Liu, S.J., Lin, C.T., Naruishi, K., Takashiba, Y & Chou, H.H. *Porphyromonas gingivalis* fimbriae-dependent interleukin-6 autocrine regulation by increase of gp130 in endothelial cells. *J. Periodontal Res.* 44, 550–556 (2009).

57. Huck, O., You, J., Han, X., Cai, B., Panek, J. & Amar, S. Reduction of Articular and Systemic Inflammation by Kava-241 in *Porphyromonas gingivalis*-induced Arthritis Murine Model. *Infect. Immun.* doi:10.1128/IAI.00356-18 (2018).

58. Singh, S.P., Huck, O., Abraham, N.G. & Amar, S. Kavain Reduces *Porphyromonas gingivalis*-Induced Adipocyte Inflammation: Role of PGC-1α Signaling. *J. Immunol.* 201, 1491–1499 (2018).

59. Yuan, H., Gupte, R., Zelkh, S. & Amar, S. Receptor activator of nuclear factor kappa B ligand antagonists inhibit tissue inflammation and bone loss in experimental periodontitis. *J. Clin. Periodontol.* 38, 1029–1036 (2011).

60. Wan, M., Liu, J. & Ouyang, X. Nucleotide-binding oligomerization domain 1 regulates *Porphyromonas gingivalis*-induced vascular cell adhesion molecule 1 and intercellular adhesion molecule 1 expression in endothelial cells through NF-κB pathway. *J. Periodontal Res.* 50, 189–196 (2015).

61. Constantinescu, A.A., Gleizes, C., Alhosin, M., Yala, E., Zobairi, F., Leclercq, A., Stoian, G., Mitrea, I.L., Prévost, G., Toti, F., et al. Exocrine cell-derived microparticles in response to lipopolysaccharide promote endocrine dysfunction in cystic fibrosis. *J. Cyst. Fibros.* 13, 219–226 (2014).

62. Hansson, G.K., Libby, P. &Tabas, I. Inflammation and plaque vulnerability. *J. Intern. Med.* 278, 483–493 (2015).

63. Giannella, A., Radu, C.M., Franco, L., Campello, E., Simioni, P., Avogaro, A., de Kreutzenberg, S.V. & Ceolotto, G. Circulating levels and characterization of microparticles in patients with different degrees of glucose tolerance. *Cardiovasc. Diabetol.* 16, 118 (2017).

64. Enjeti, A.K., Ariyarajah, A., D'Crus, A., Seldon, M. & Lincz, L.F. Circulating microvesicle number, function and small RNA content vary with age, gender, smoking status, lipid and hormone profiles. *Thromb. Res.* 156, 65–72 (2017).

65. Loyer, X., Vion, A.C., Tedgui, A. & Boulanger, C.M. Microvesicles as cell-cell messengers in cardiovascular diseases. *Circ. Res.* 114, 345–353 (2014).

66. Chiang, S.M. & Schellhorn, H.E. Regulators of oxidative stress response genes in Escherichia coli and their functional conservation in bacteria. *Arch. Biochem. Biophys.* 525, 161–169 (2012).

67. Fu, J., Qi, L., Hu, M., Liu, Y., Yu, K., Liu, Q. & Liu, X. Salmonella proteomics under oxidative stress reveals coordinated regulation of antioxidant defense with iron metabolism and bacterial virulence. *J. Proteomics* 157, 52–58 (2017).

68. Farr, S.B. & Kogoma, T. Oxidative stress responses in Escherichia coli and Salmonella typhimurium. *Microbiol. Rev.* 55, 561–585 (1991).

69. Cardaropoli, S., Silvagno, F., Morra, E., Pescarmona, G.P. & Todros, T. Infectious and inflammatory stimuli decrease endothelial nitric oxide synthase activity in vitro. *J. Hypertens.* 21, 2103–2110 (2003).

70. Winkler, F., Koedel, U., Kastenbauer, S. & Pfister, H.W. Differential expression of nitric oxide synthases in bacterial meningitis: role of the inducible isoform for blood-brain barrier breakdown. *J. Infect. Dis.* 183, 1749–1759 (2001).

71. Abbas, M., Jesel, L., Auger, C., Amoura, L., Messas, N., Manin, G., Rumig, C., León-González, A.J., Ribeiro, T.P., Silva, G.C., et al. Endothelial Microparticles From Acute Coronary Syndrome Patients Induce Premature Coronary Artery Endothelial Cell Aging and Thrombogenicity: Role of the Ang II/AT1 Receptor/NADPH Oxidase-Mediated Activation of MAPKs and PI3-Kinase Pathways. *Circulation* 135, 280–296 (2017).

72. Jayaprakash, K., Demirel, I., Khalaf, H. & Bengtsson, T. Porphyromonas gingivalis-induced inflammatory responses in THP1 cells are altered by native and modified low-density lipoproteins in a strain-dependent manner. *APMIS*. 126, 667–677 (2018).

73. Rodrigues, P.H., Reyes, L., Chadda, A.S., Bélanger, M., Wallet, S.M., Akin, D., Dunn Jr, W. & Progulske-Fox, A. Porphyromonas gingivalis strain specific interactions with

human coronary artery endothelial cells: a comparative study. *PLoS One*. 7:e52606 (2012).

74. Madkhali, Y., Featherby, S., Collier, M.E., Maraveyas, A., Greenman, J. & Ettelaie, C. The Ratio of Factor VIIa:Tissue Factor Content within Microvesicles Determines the Differential Influence on Endothelial Cells. *TH Open*. 3:e132–e145 (2019).

75. Pasquier, J., Thomas, B., Hoarau-Véchot, J., Odeh, T., Robay, A., Chidiac, O., Dargham, S.R., Turjoman, R., Halama, A., Fakhro, K., Menzies, R., Jayyousi, A., Zirie, M., Al Suwaidi, J., Rafii, A., Malik, R.A., Talal, T. & Khalil, C.A. Circulating microparticles in acute diabetic Charcot foot exhibit a high content of inflammatory cytokines, and support monocyte-to-osteoclast cell induction. *Sci Rep* 7:16450 (2017).

76. Enjeti, A.K., Ariyarajah, A., D'Crus, A., Seldon, M. & Lincz L.F. Circulating microvesicle number, function and small RNA content vary with age, gender, smoking status, lipid and hormone profiles. *Thromb Res* 156:65–72 (2017).

Figures and table

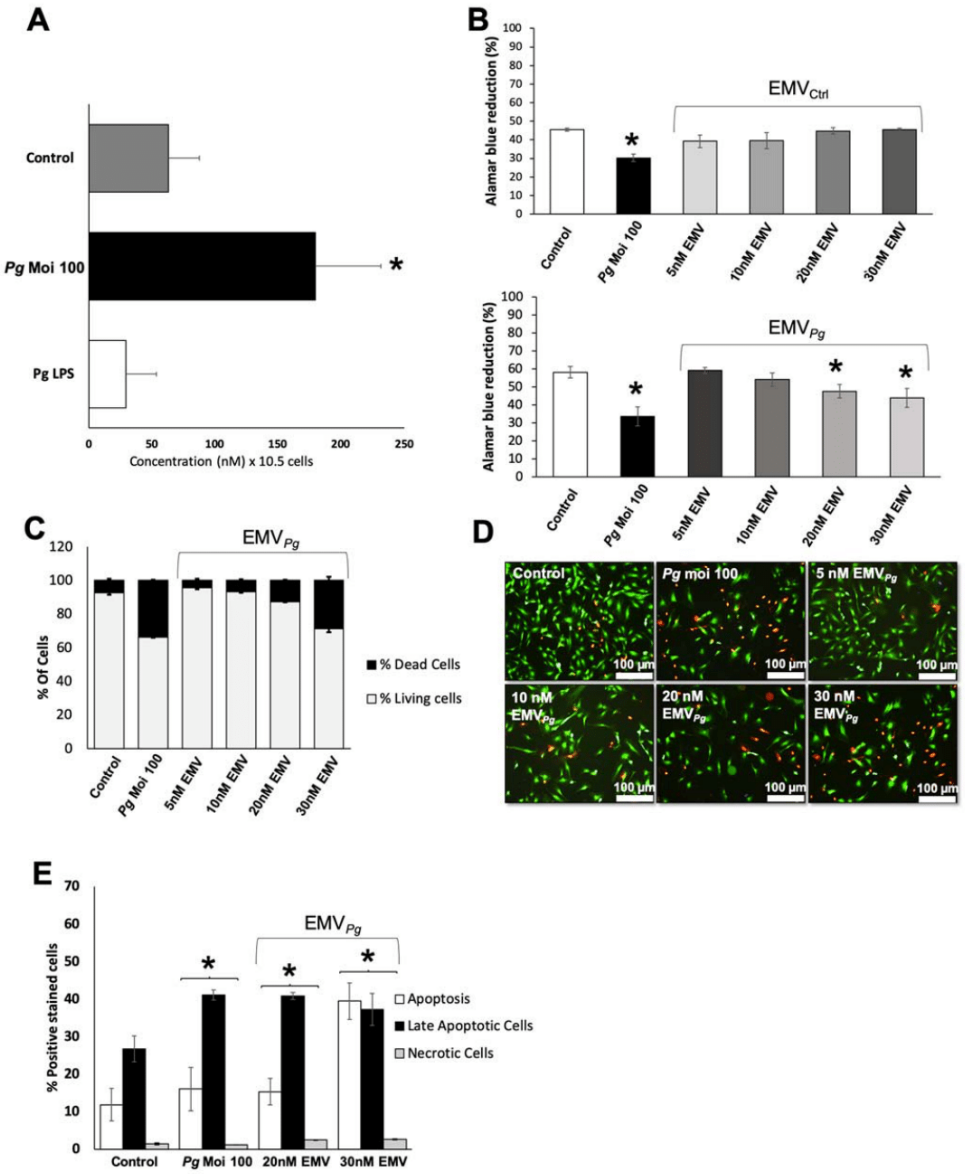

Figure 1. P.gingivalis promotes EMV shedding and alters endothelial cell viability.

(A) The generation of EMV from naïve EC (control) and following 24h of infection with *P.gingivalis* (*Pg)* (MOI=100) or stimulation with *Pg*-LPS (1µg/ml) was measured in the supernatant by prothrombinase assay. Concentrations are represented by mean +/- SD from 3 independent experiments; *:p<0.05 vs control (unstimulated EC). (B) Metabolic activity of EC infected with *Pg* (MOI=100) or exposed to EMV_{Ctrl} (upper panel) and EMV_{Pg} (lower

panel) (5, 10, 20 and 30 nM) for 24h measured by AlamarBlue assay. Results are expressed as mean+/- SD from 3 independent experiments; *:p<0.05 vs control (unstimulated EC). (C) Live-Dead assay to evaluate the ratio of live EC versus dead EC in cells exposed to *P.gingivalis* (*Pg*) (MOI:100) and EMV_{Pg} (5, 10, 20 and 30 nM) for 24h. Results are expressed as percentage of live and dead EC (mean+/-SD). (D) Immunofluorescence imaging of live-dead staining (green: live EC, red: dead EC) for each condition after 24 hours of exposure. (E) Evaluation of type of cell death by flow cytometry after *P.gingivalis* infection and EMV_{Pg} (20 and 30 nM) exposure for 24h. EC were labelled with Annexin-V FITC and propidium iodide (IPPE). All data were expressed as mean ± SD. *: (p <0.05 vs untreated cells).

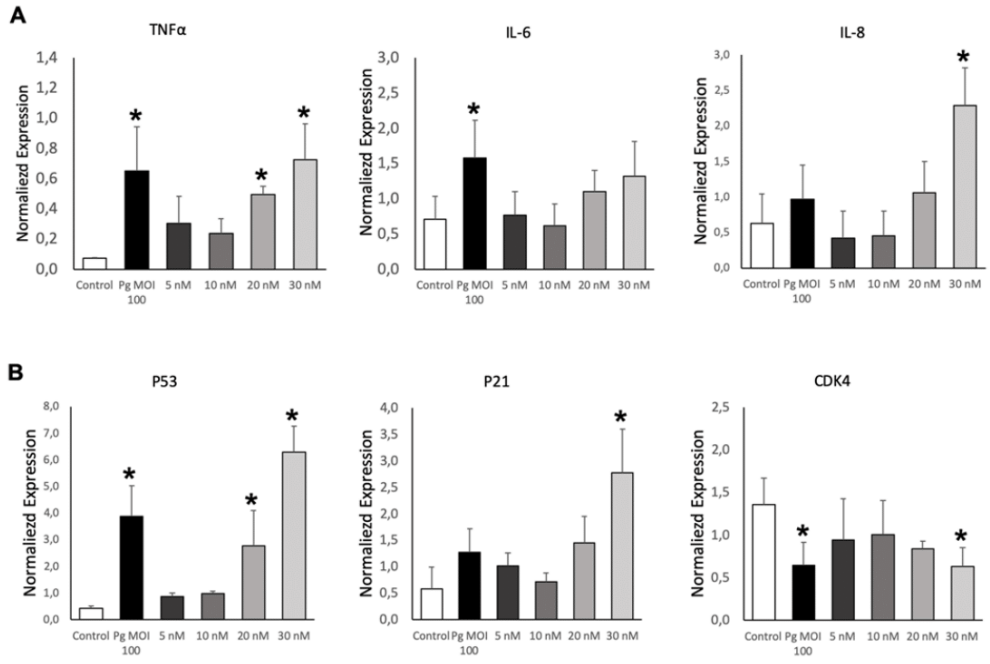

Figure 2. EMV_{Pg} trigger inflammatory endothelial response.

(A) The mRNA expression of inflammatory markers TNF-α, IL-6 and IL-8 in EC exposed to *P.gingivalis* (*Pg*) (MOI:100) and EMV_{Pg} (5, 10, 20 and 30 nM) for 24 h was measured by qRT-PCR. (B) The gene expression of cell cyle related markers p53, p21 and CDK4 EC in EC exposed to *P.gingivalis* (*Pg*) (MOI:100) and EMV_{Pg} (5, 10, 20 and 30 nM) for 24h. All

data were expressed as mean ± SD from 3 independent experiments *: p <0.05 between cells infected or stimulated against control (unstimulated cells).

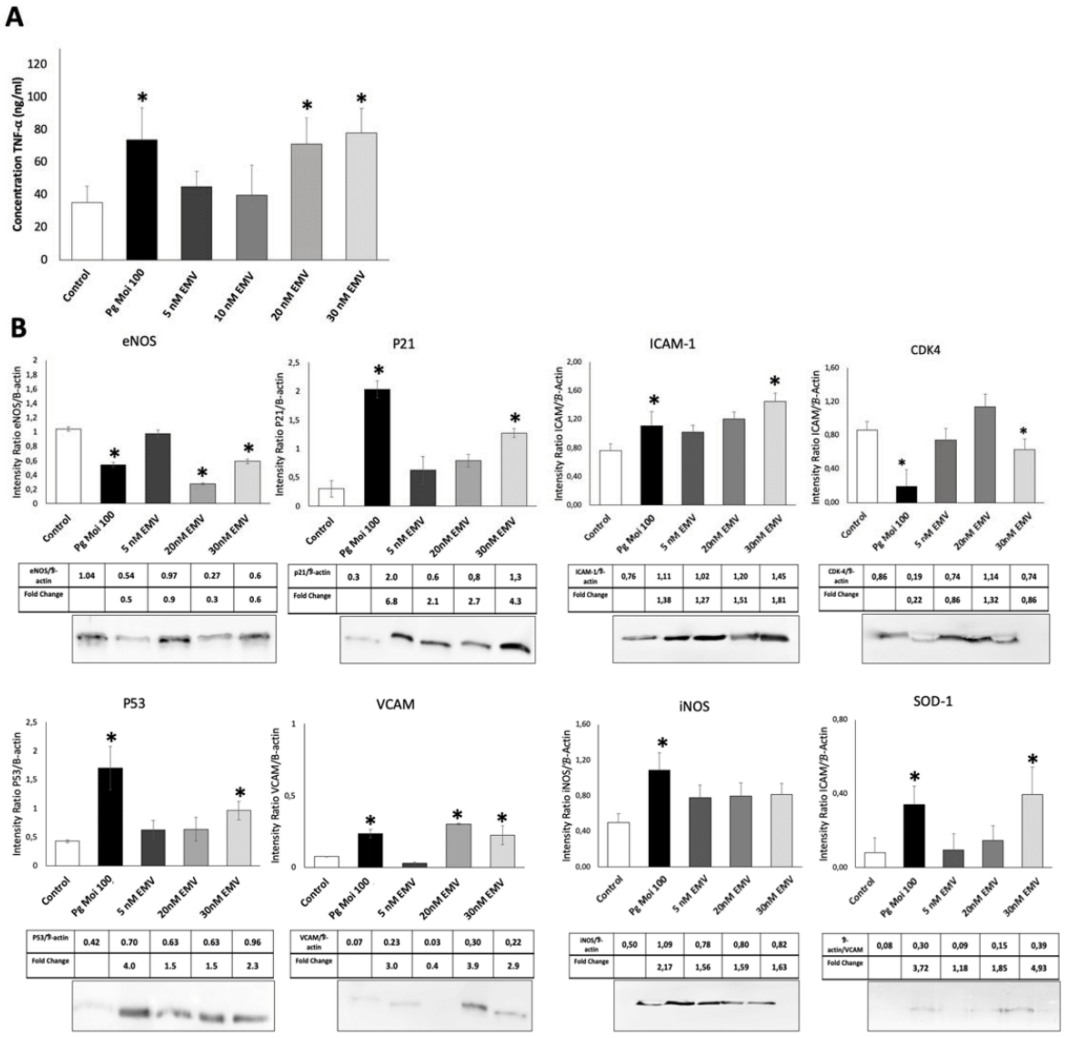

Figure 3. EMV_{Pg} induce pro-inflammatory and pro-oxidative protein expression similar to P.gingivalis infection.

(A) TNF-α secretion in supernatant by EC in response to *P.gingivalis* (*Pg*) (MOI:100) and EMV_{Pg} (5, 20 and 30 nM) for 24 h was measured by ELISA. (B) Intra-cellular protein expression of eNOS, P21, ICAM-1, CDK4, P53, VCAM, iNOS and SOD-1 in response to

P.gingivalis (*Pg*) (MOI:100) and EMV_{Pg} (5, 20 and 30 nM) for 24 h was evaluated by Western Blot. All data were expressed as mean ± SD from 3 independent experiments and normalized against internal control β-actin. *: p <0.05 between cells infected or stimulated against control (unstimulated cells).

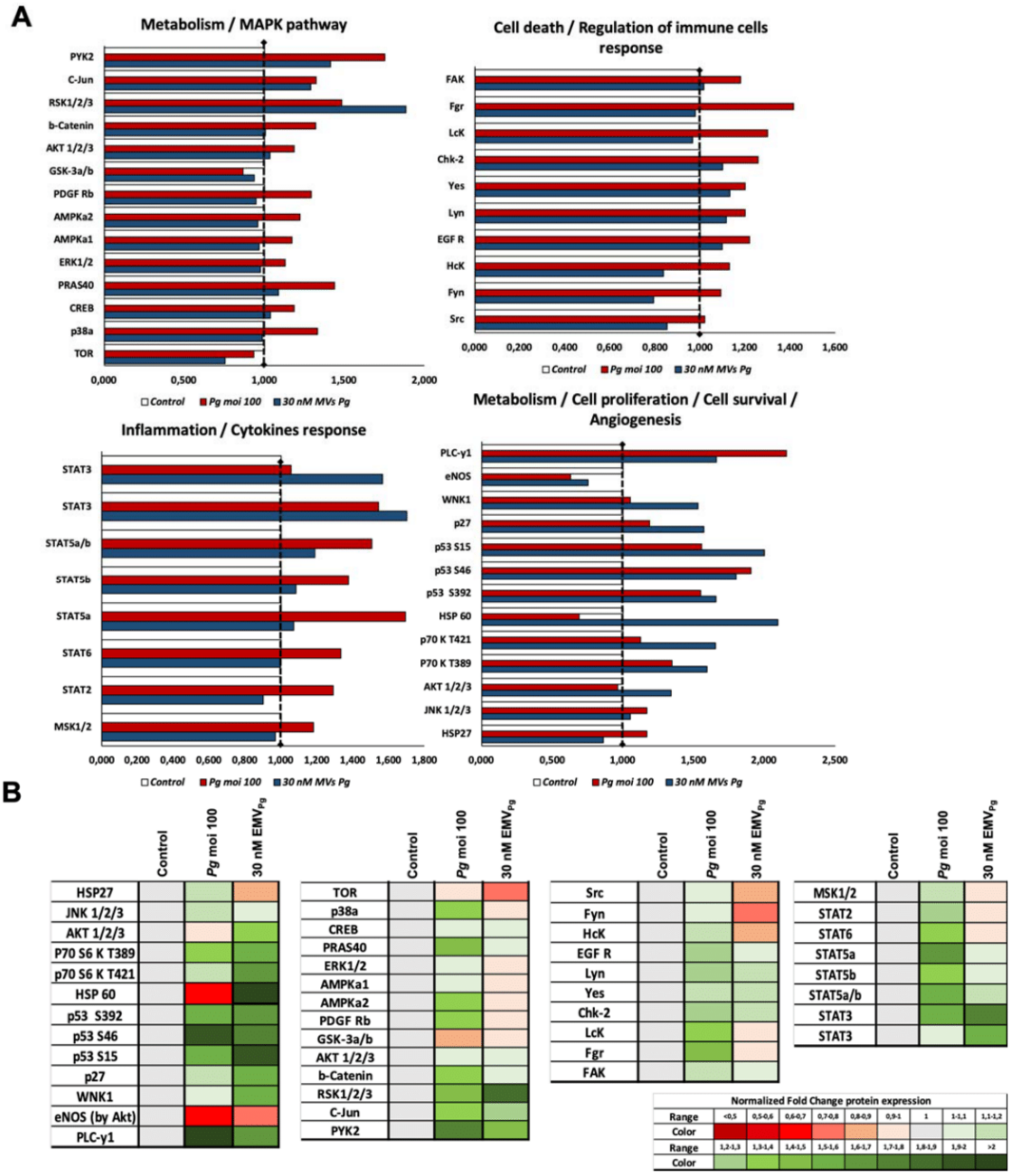

Figure 4: Exposure to EMV_{Pg} modulates significantly inflammatory pathways related to kinases activation.

Analysis of kinases activation induced by *P.gingivalis* infection (*Pg*) (MOI:100) and EMV_{Pg} (30 nM) for 24 h evaluated by phospho-kinase array. The density of spots was measured by MyImage™ Analysis Softwate 2.0 (Thermofisher) for each molecule and each condition. (A) Graphical representation of the kinases expression in untreated EC, in EC following *P.gingivalis* infection (*Pg*) (MOI:100) and EMV_{Pg} (30 nM) stimulation for 24 h. (B) Heat-map representation of the kinases expression normalized against untreated control (untreated EC).

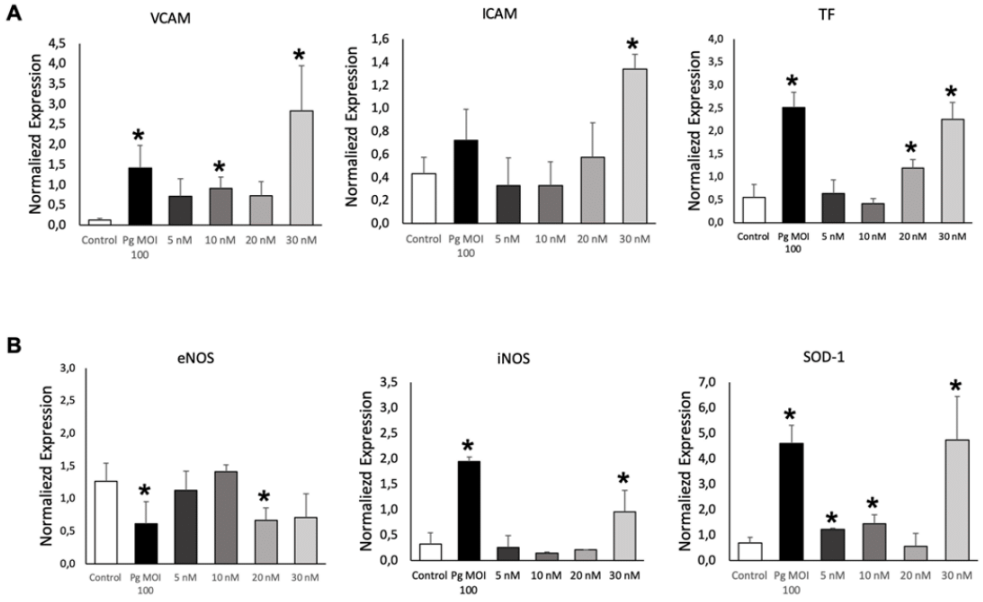

Figure 5: EMV_{Pg} induce expression of atherothrombosis and oxidative stress markers expression.

(A) The mRNA expression of endothelial markers VCAM, ICAM and Tissular factor (TF) in EC exposed to *P.gingivalis* (*Pg*) (MOI:100) and EMV_{Pg} (5, 10, 20 and 30 nM) for 24 h was measured by qRT-PCR. (B) The gene expression of oxydative stress markers eNOS, iNOS and SOD-1 in EC exposed to *P.gingivalis* (*Pg*) (MOI:100) and EMV_{Pg} (5, 10, 20 and 30 nM)

for 24h. All data were expressed as mean ± SD from 3 independent experiments *: $p < 0.05$ between cells infected or stimulated against control (unstimulated cells).

Gene (Human)	Sense strand	Sequences
β-actin	Forward Reverse	5'-AACGGCTCCGGCATGTGCAA-3' 5'-CTTCTGACCCATGCCCACCA-3'
TNF-α	Forward Reverse	5'-AGGCGCTCCCCAAGAAGACA-3' 5'-TCCTTGGCAAAACTGCACCT-3'
Il-6	Forward Reverse	5'-GCCTTCGGTCCAGTTGCCTT-3' 5'-GCAGAATGAGATGAGTTGTC-3'
Il-8	Forward Reverse	5'-ATGACTTCCAAGCTGGCCGTGGCT-3' 5'-TCTCAGCCCTCTTCAAAAACTTCTC-3'
P21	Forward Reverse	5'-TGGAGACTCTCAGGGTCGAAA-3' 5'-GGCGTTTGGAGTGGTAGAAATC-3'
P53	Forward Reverse	5'-AACGGTACTCCGCCACC-3' 5'-CGTGTCACCGTCGTGGA-3'
CDK4	Forward Reverse	5'-CATGTAGACCAGGACCTAAGG-3' 5'-AACTGGCGCATCAGATCCTAG-3'
eNOS	Forward Reverse	5'-CGGCATCACCAGGAAGAAGA-3' 5'-CATGAGCGAGGCGGAGAT-3'
iNOS	Forward Reverse	5'-TGGATGCAACCCCATTGTC-3' 5'-CCCGCTGCCCCAGTTT-3'
SOD-1	Forward Reverse	5'-TAAAGTAGTCGCGGAGACGGG-3' 5'-CGGCCTCGCAACACAAGCCT-3'
VCAM-1	Forward Reverse	5'-ATTGGGAAAAACAGAAAAGAG-3' 5'-GGCAACATTGACATAAAGT-3'
ICAM-1	Forward Reverse	5'-GGCCGGCCAGCTTATACAC-3' 5'-TAGACACTTGAGCTCGGGCA-3'
CD142 (TF)	Forward Reverse	5'-GACAATTTTGGAGTGGGAACCC-3' 5'-CACTTTTGTTCCCACCTG-3'

Table 1: Primers sequences

***Porphyromonas gingivalis* triggers the shedding of inflammatory endothelial microvesicles that act as autocrine effectors of endothelial dysfunction**

Isaac Maximiliano Bugueno, Fatiha Zobairi El-Ghazouani, Fareeha Batool, Hanine El Itawi, Eduardo Anglès-Cano, Nadia Benkirane-Jessel, Florence Toti and Olivier Huck

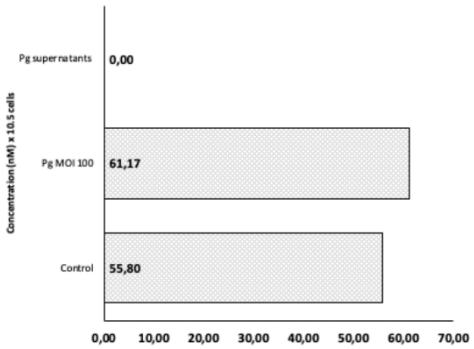

Supplemental Figure 1. EMV dosage. The generation of EMV from naïve EC (control), after 24h and of EC infected with *P.gingivalis* (*Pg*) (MOI=100) or *Pg* culture were measured in the supernatant by prothrombinase assay.

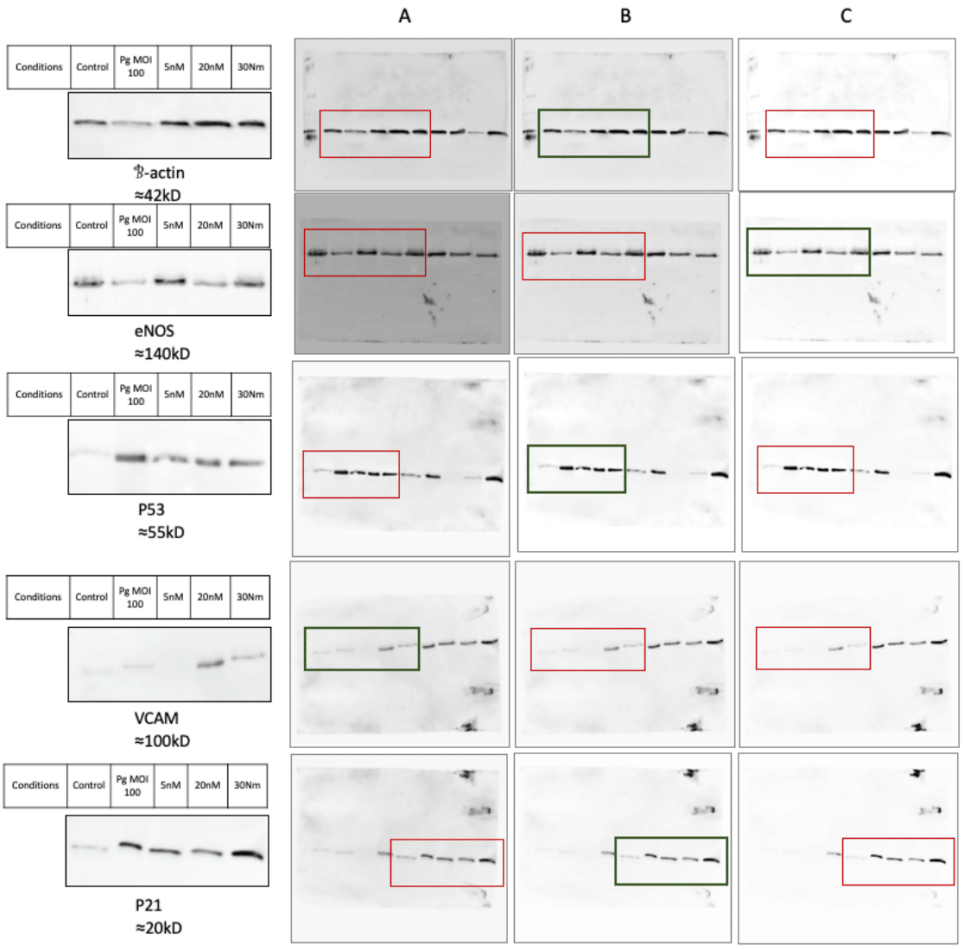

Supplemental Figure 2. Western Blots. The figure shows the original blots for ß-actin, eNOS, P53, VCAM and P21, that were cut to indicate only the conditions that were chosen (Control, *Pg*, EMV_{Pg} 5nM, 20nM and 30 nM). Brightness and contrast modifications were performed as shown in panels A, B and C. The green boxes show the area that was presented in the left panel of the figure, the red boxes indicate the same area but with a different time exposure.

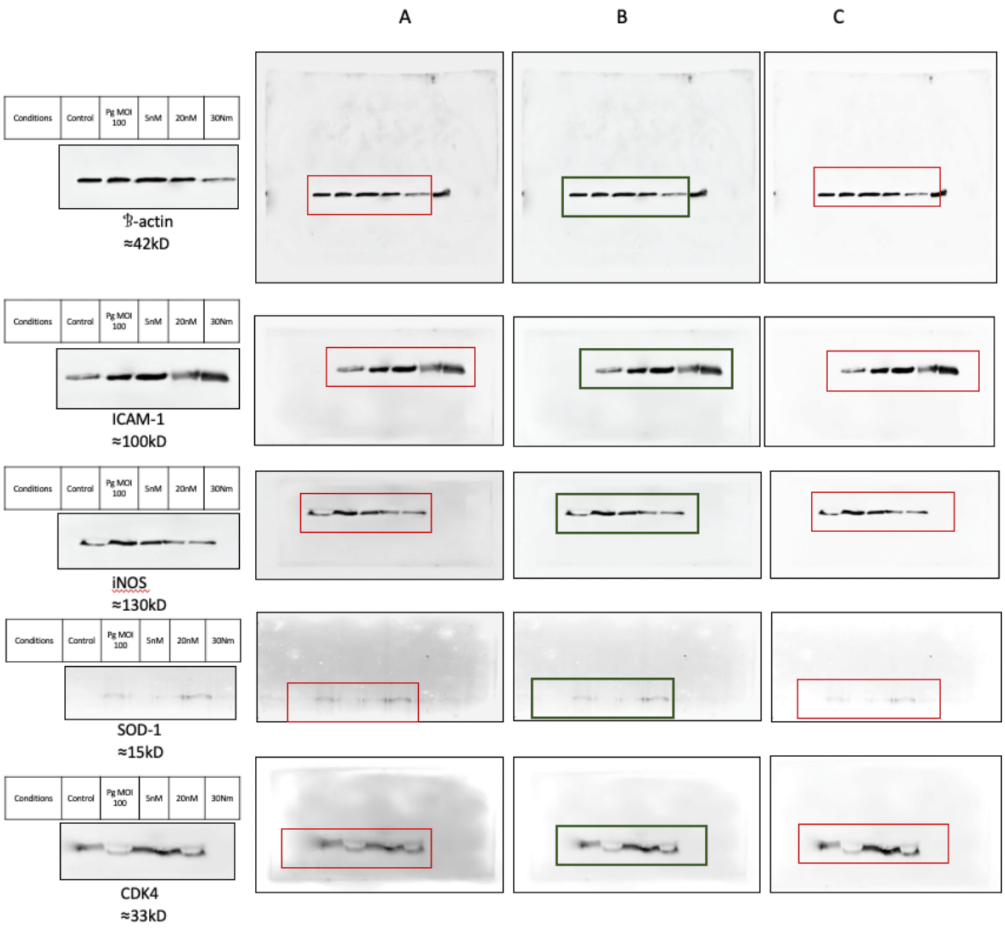

Supplemental Figure 3. Western blots. The figure shows the original blots for β-actin, ICAM-1, iNOS, SOD-1 and CDK-4, that were cut to indicate only the conditions that were chosen (Control, *Pg*, EMV_{Pg} 5nM, 20nM and 30 nM). Brightness and contrast modifications were performed as shown in panels A, B and C. The green boxes show the area that was presented in the left panel of the figure, the red boxes indicate the same area but with a different time exposure.

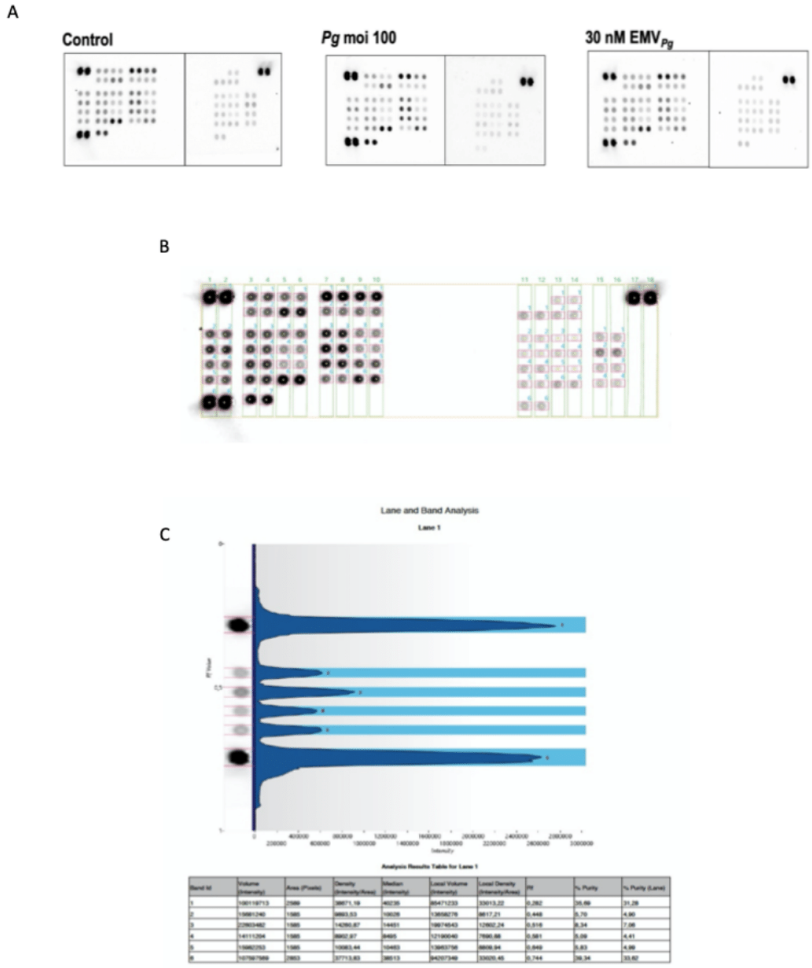

Supplemental Figure 4. Analysis of kinases activation induced by P.gingivalis infection (Pg) (MOI:100) and EMV$_{Pg}$ (30 nM) for 24 h evaluated by phospho-kinase array. (A) The density of spots was measured by MyImage^{TM} Analysis Software 2.0 (Thermofisher) for each molecule and each condition. (B-C) The figure shows how the analysis has been performed for each of the blots of the "Proteome Profiler Human Phopho-Kinase Array Assay" (R&D Systems, Lille, France). Each spot per column and per line was analyzed according to its intensity. This density of spots, corresponding to protein activation, was measured my MyImage^{TM} Analysis Software 2.0 (Thermofisher) for each molecule and each condition.

CHAPITRE 3

Développement d'un nouveau modèle 3D sphéroïde *in vitro* permettant l'évaluation de l'impact de l'infection par *P.gingivalis* sur les interactions épithélio-fibroblastiques.

❖ **Bugueno I.M**., Batool F., Keller L., Kuchler-Bopp S., Benkirane-Jessel N., Huck. O. *Porphyromonas gingivalis* bypasses epithelial barrier and modulates fibroblastic inflammatory response in an in vitro 3D spheroid model. **Scientific Reports 2018, (8):14914**.

Contexte et objectifs

Les GEC constituent la première ligne de défense de l'hôte contre les pathogènes oraux. Les GEC sont organisées en épithélium multicouches et sont constamment mises au défi par des agents pathogènes au niveau sulculaire. Les jonctions serrées, les hémi-desmosomes et les desmosomes sont les facteurs clés dans la mesure où ils interviennent dans les interactions cellule-cellule et cellule-matrice extracellulaire (Amano et al., 2007). Une inflammation soutenue au niveau des tissus mous sera impliquée dans la destruction de l'os alvéolaire sous-jacent (Yilmaz et al., 2006 ; Choi et al., 2014). Les modèles *in vitro* existants de culture cellulaire monocouche ont des limites car ils ne permettent pas de prendre en compte les interactions entre les différents types cellulaires. De plus, les cellules sont cultivées sur des surfaces synthétiques et peuvent former des attachements non naturels (Graves et al., 2008). Ces limitations impliquent la nécessité d'utiliser des modèles animaux qui, bien qu'ils soient les plus proches de la situation physiologique humaine, sont associés à des considérations éthiques et techniques (Kim et al., 2005 ; Artegiani et al., 2018). Par conséquent, pour pouvoir prendre en compte la complexité des tissus ou des organes, des modèles cellulaires 3D ont été développés (Artegiani et al., 2018 ; Pinnock et al., 2014 ; Bécavin et al., 2016). Les modèles 3D ont été décrits comme reproduisant plus fidèlement la physiologie et les phénotypes des tissus et des organes que les cellules cultivées en 2D (Amelian et al., 2017 ; Kuchler-Bopp et al., 2016). Ces modèles 3D ou multicellulaires ont déjà été utilisés pour étudier les mécanismes moléculaires associés aux infections, tels que *Neisseria gonorrheae* dans un modèle 3D de cellules épithéliales de l'endomètre (Laniewski et al., 2017) et dans des conditions pathologiques telles que le cancer (Birgerdotter et al., 2005 ; Chaddad et al., 2017).

Dans le contexte des maladies buccales, en particulier de la parodontite, certains modèles de muqueuse buccale ont été conçus pour imiter l'organisation tissulaire de l'épithélium multicouche et du tissu conjonctif sous-jacent (Pinnock et al., 2016 ; Andrian et al., 2004 ; Dabija et al., 2013). L'utilisation de ce type de modèle dans le contexte de l'infection par *P.gingivalis* a confirmé que ces modèles 3D sont plus pertinents que les cultures monocouches

2D *in vitro* car les réponses cellule / tissu observées dans celles-ci semblent plus proches de celles des modèles *in vivo* (Dabija et al., 2013). Les sphéroïdes 3D produits par auto-assemblage, dans un environnement sans échafaudage, reproduisent la fonction et l'architecture des tissus *in vivo*, soulignant ainsi leur rôle futur en tant que modèles *in vitro* (Achilli et al., 2012 ; Kelm et al., 2004) .

L'objectif de cette étude était donc de développer un modèle 3D *in vitro* sphéroïdal imitant la gencive afin de dépasser les limites des modèles existants et de prendre en compte les interactions épithélio-fibroblastiques. Un intérêt particulier a été porté à la dissémination de *P.gingivalis* et sur l'induction de la mort cellulaire et de l'inflammation.

Résultats et discussion

Des GEC et des FB ont été cultivés par la méthode de la goute suspendue pour générer des microtissus (MT) 3D. La structure 3D a été analysée sur des coupes histologiques et par microscopie électronique à balayage, en comparant un groupe non infecté et infecté par *P.gingivalis*. Les interactions entre cellules ont été observées à l'aide de la microscopie électronique à transmission et l'impact de l'infection par *P.gingivalis* (ATCC 33277) a été évalué au niveau moléculaire. Nous avons étudié l'impact de la bactérie sur divers marqueurs de la mort cellulaire (Apaf-1, caspase-3), des marqueurs inflammatoires (TNF-α, IL-6, IL-8) et les composants de la matrice extracellulaire (Col-IV, E-cadhérine, intégrine αv-β3) par immunohistochimie et RTqPCR.

Les MT formés ont présenté une organisation spatiale bien définie dans laquelle les EC se sont organisées dans une couche externe tandis que les FB ont constitué le noyau du MT. L'infection des MT a mis en évidence la capacité de *P.gingivalis* à traverser la barrière épithéliale en perturbant les structures jonctionnelles telles que les desmosomes pour atteindre le noyau fibroblastique. Un taux d'apoptose et de nécrose accru a été observé au niveau des FB, en corrélation avec une destruction du MT associée à la modulation des voies apoptotiques intrinsèques telles que l'activation de l'apoptosome Apaf-1. L'infection a induit une expression accrue de TNF-α, IL-6 et IL-8. Fait intéressant, la modulation de l'expression des gènes était légèrement différente de celle observée dans ces deux types cellulaires en monocouche.

Conclusion

La structure 3D des MT synthétisés imite la barrière épithélio-fibroblastique et permet d'étudier les effets induits par *P.gingivalis*. Le développement d'un tel modèle 3D *in vitro* pourrait être utile pour définir plus précisément le rôle des interactions épithélio-fibroblastiques sur la réponse immunitaire de l'hôte et également pour évaluer les propriétés thérapeutiques des médicaments anti-inflammatoires ou anti-infectieux.

SCIENTIFIC REPORTS

OPEN

Porphyromonas gingivalis bypasses epithelial barrier and modulates fibroblastic inflammatory response in an *in vitro* 3D spheroid model

Received: 8 February 2018
Accepted: 25 September 2018
Published online: 08 October 2018

Isaac Maximiliano Bugueno[1,2], Fareeha Batool[1,2], Laetitia Keller[1,2], Sabine Kuchler-Bopp[1], Nadia Benkirane-Jessel[1,2] & Olivier Huck[1,2,3]

***Porphyromonas gingivalis*-induced inflammatory effects are mostly investigated in monolayer cultured cells. The aim of this study was to develop a 3D spheroid model of gingiva to take into account epithelio-fibroblastic interactions. Human gingival epithelial cells (ECs) and human oral fibroblasts (FBs) were cultured by hanging drop method to generate 3D microtissue (MT) whose structure was analyzed on histological sections and the cell-to-cell interactions were observed by scanning and transmission electron microscopy (SEM and TEM). MTs were infected by *P. gingivalis* and the impact on cell death (Apaf-1, caspase-3), inflammatory markers (TNF-α, IL-6, IL-8) and extracellular matrix components (Col-IV, E-cadherin, integrin β1) was evaluated by immunohistochemistry and RT-qPCR. Results were compared to those observed *in situ* in experimental periodontitis and in human gingival biopsies. MTs exhibited a well-defined spatial organization where ECs were organized in an external cellular multilayer, while, FBs constituted the core. The infection of MT demonstrated the ability of *P. gingivalis* to bypass the epithelial barrier in order to reach the fibroblastic core and induce disorganization of the spheroid structure. An increased cell death was observed in fibroblastic core. The development of such 3D model may be useful to define the role of EC–FB interactions on periodontal host-immune response and to assess the efficacy of new therapeutics.**

Host-bacterial interactions are crucial in the onset and development of periodontitis, a chronic inflammatory disease of infectious origin affecting tooth supporting tissues[1]. At early stage of the disease, dysbiotic flora constituted by periodontal pathogens, including *Porphyromonas gingivalis*, interacts with the epithelial barrier[2] and induces a sustained inflammatory response[3]. Gingival epithelial cells (ECs) are the first line of host-defense challenged by oral pathogens. ECs are organized in multilayered epithelium and are challenged constantly by external pathogens at the sulcular level. Tight junctions, hemi-desmosomes and desmosomes are the key factors as they are involved in cell-to-cell and cell to extra-cellular matrix (ECM) interactions. During the establishment of the periodontal lesion, bacterial invasion or virulence factors and innate immune response activation impact such structures, leading to breakdown of the epithelial barrier and contributing to bacterial persistence within the periodontal tissues[4,5]. Sustained inflammation at the soft tissue level will be implicated in the crosstalk with underlying alveolar bone leading to its destruction[6].

Existing *in vitro* models of monolayer cell culture have limitations as they do not allow to take into consideration the cell-to-cell interactions as cells are grown on synthetic surfaces and may form unnatural cell attachments[7]. These limitations initiate the need of using animal models that, despite being the closest to human physiological situation, are associated with ethical and technical considerations[6]. Therefore, to be able to consider the complexity of tissues or organs, 3D cell models have been developed[8–11]. 3D models have been described as mimicking more closely the natural tissues and organs physiology and phenotypes than cells grown in 2D[10,12]. The spatial proximity of cells in such a model also enables interactions between adhesion molecules

[1]INSERM (French National Institute of Health and Medical Research), UMR 1260, Regenerative Nanomedicine (RNM), Fédération de Médecine Translationnelle de Strasbourg (FMTS), 11 rue Humann, Strasbourg, 67000, France. [2]Université de Strasbourg (UDS), Faculté de Chirurgie-dentaire, 8 rue Sainte-Elisabeth, Strasbourg, 67000, France. [3]Hôpitaux Universitaires de Strasbourg (HUS), Department of Periodontology, 1 place de l'Hôpital, Strasbourg, 67000, France. Correspondence and requests for materials should be addressed to O.H. (email: o.huck@unistra.fr)

and receptors maximizing cellular communication and signaling that is critical to cell function[13]. Also, cells can move, exert forces and migrate as they do *in vivo*[14]. Such 3D or multicellular models have already been used to investigate molecular mechanisms associated with infection such as for *Neisseria gonorrheae* in a 3D endometrial epithelial cell model[15] and in pathological conditions such as cancer[16,17]. In the context of oral diseases, especially periodontitis, some models of oral mucosa were engineered to mimic the tissular organization of the multilayered epithelium and underlying connective tissue[9,18,19]. For instance, an organotypic mucosal model was developed displaying a well-organized multi-layered epithelium and underlying connective tissue characterized by collagen-embedded fibroblasts. The use of this type of a model in the context of *P. gingivalis* infection confirmed that such 3D models are more relevant than the *in vitro* 2D monolayer cultures as the cell/tissue responses observed in them appear to be closer to that of the *in vivo* models[9].

P. gingivalis, a gram-negative anaerobic bacterium, is considered as a keystone pathogen as it modulates gene and protein expression compromising immune function at the periodontal level[20]. For instance, *P. gingivalis* is able to modulate inflammatory response, escape innate immunity and induce degradation of a large variety of proteins, resulting in tissue destruction. It also dampens immune response in various cell types through several mechanisms such as proteolysis as observed for NLRP3 inflammasome in endothelial cells[21], activation of NFkB and MAPK pathways in epithelial cells and macrophages[22,23], modulation of cell death[24] and increase of proteases activity as observed for cathepsins[25,26].

Mechanisms underlying intracellular invasion of epithelial cells are developed strategically by *P. gingivalis* to evade the host immune system and cause tissue damage, through its dissemination. It has been described that *P. gingivalis* influences tight junction and barrier function[27–29]. However, all mechanisms involved remain under investigation.

Therefore, the aim of this study was to develop a spheroid 3D *in vitro* model mimicking gingiva to overcome the limits of existing models and to take into account the epithelio-fibroblastic interactions. A special focus was made on *P. gingivalis* dissemination, induction of cell death and inflammation.

Materials and Methods

Gingival tissues. Gingival samples were obtained during periodontal surgeries (open access flap) or dental extractions from healthy patients (HP) and patients diagnosed with chronic periodontitis (CP)[30,31]. The healthy group consisted of nine patients (five men and four women; mean age, 37.8 ± 17.3 years), and the CP group consisted of eleven patients (four men and seven women; mean age, 62.4 ± 7.3 years). Samples were secured immediately in a sterile tube and stored at −80 °C until RNA extraction was carried out. All patients gave written and informed consent before enrollment. This study received approval from the Ethics Committee (French Ministry of Research, Bioethic department authorization. DC-2014-2220) and all subjects received information related to the study and gave written consent according to the Declaration of Helsinki and current French legislation.

Bacterial culture. *P. gingivalis* strain 33277 (ATCC, Manassas, VA, USA) was cultured under strict anaerobic conditions at 37 °C in brain-heart infusion medium (Sigma, Saint-Quentin Fallavier, France) supplemented with hemin (5 mg/ml) and menadione (1 mg/ml). On the day of infection, bacteria were collected and counted as previously described[26].

Experimental periodontitis. To induce experimental periodontitis, *P. gingivalis*-infected ligatures were placed along the cervical margins on palatal sides of the first and second maxillary molars of mice (C57/BL6, Charles River, L'Arbresle, France) (Fig. 1A). Ligatures were replaced twice a week for 30 days as described previously[32]. Mice were examined regularly to evaluate pain and stress. Moreover, their weight was monitored daily. Slides for immunofluorescence were treated as previously described by Saadi-Thiers *et al.*[33]. All experimental protocols fulfilled the authorization of the "Ministère de l'Enseignement Supérieur et de la Recherche" under the agreement number 01715.02. The Ethics Committee of Strasbourg named "Comité Régional d'Ethique en Matière d'Expérimentation Animale de Strasbourg (CREMEAS)" specifically approved this study.

Cell culture. Human oral epithelial cells (ECs) used in this study derived from the TERT-2 OKF-6 cell line (BWH Cell Culture and Microscopy Core, Boston, MA, USA) and were cultured in KSFM culture medium (serum-free medium for keratinocytes, Gibco, PromocellTM, Aachen, Germany) and human oral fibroblasts (FBs) were isolated from gingival biopsy and cultured in RPMI 1640 medium (Life Technologies, Saint-Aubin, France). This protocol has received approval of the local Ethical Committee (DC-2014-2220). To reduce the risk of contamination, 100 units/ml of penicillin and 100 µg/ml of streptomycin were added. Both were grown at 37 °C in a humidified atmosphere with 5% CO_2, as previously described[33].

Microtissues formation. To generate MTs, the hanging-drop culture method was used. MT is characterized by a 3D spheroid structure where cells are in direct contact, allowing cell-to-cell and cells-to-extracellular matrix components (ECM) interactions. This method can be used to co-culture two (or more) different cell populations to elucidate the role of cell-cell or cell-ECM interactions in a 3D environment[10,12] (Fig. 1B). It also allows the addition of very small quantities of any biological agent or drug in the cell culture medium. Initially, 3 different concentrations of FBs (3×10^3, 7×10^3 and 10×10^3) were cultured in suspension within a droplet of 40 µl of cells and medium in a 3D culture plate (GravityPLUS^{TM} 3D Culture, InSphero AG, Zürich, Switzerland) for 5 days, until the first true spheroid was visualized. Then, 20 µl of Defined Keratinocyte-SFM basal medium (KSFM) supplemented medium containing ECs (1.5×10^3, 5×10^3 and 7×10^3) was added in each droplet of the suspension for 5 more days respectively (Fig. 1B,C). After testing different MT sizes, a concentration of 7×10^3 FBs + 5×10^3 ECs was selected for further experiments. Every 2 days, 5 µl of both cell media were added to maintain the viability and physiological conditions of the cells, preventing the drop from desiccation and consequent disaggregation.

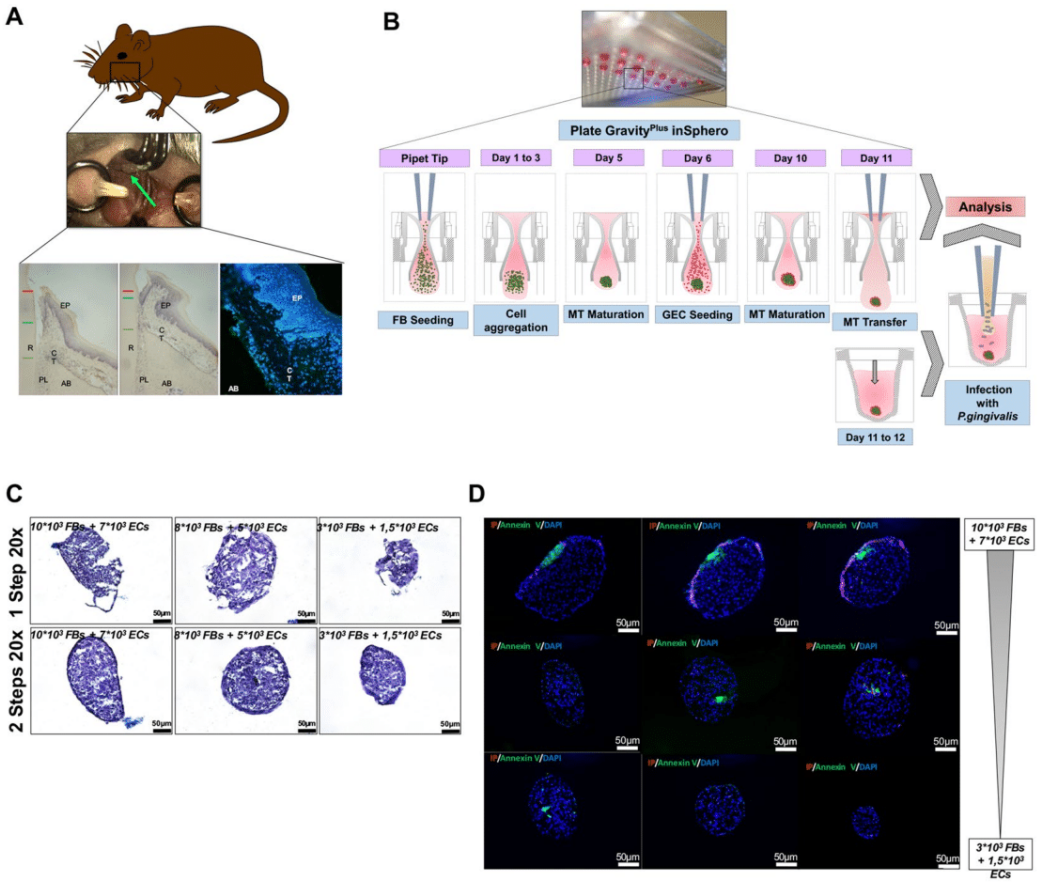

Figure 1. (**A**) Induction of experimental periodontitis. *P. gingivalis* infected ligatures were placed along the cervical margins on palatal sides of the maxillary first and second molars as described by Saadi-Thiers *et al.*[32]. (**B**) Microtissue spheroids formation diagram. Firstly, FBs were seeded in a droplet of culture medium for 5 days. After the formation of a spheroid, ECs were seeded over it. After 5 more days, two-cell types MTs were constituted. During all this procedure, cell culture medium was changed every 2 days. (**C**) Morphological characteristics of 1-Step and 2-Steps cell culture technique for MT spheroids. Three different cell concentrations (10×10^3 FBs $+ 7 \times 10^3$ ECs/8×10^3 FBs $+ 5 \times 10^3$ ECs/3×10^3 FBs $+ 1.5 \times 10^3$ ECs) were tested. In the 1-step procedure, both cell types were seeded simultaneously in a droplet while for the 2-steps procedure, each cell type was seeded in a time-specific manner. (**D**) Apoptosis quantification. Annexin V/IP staining of MTs at different cell concentrations showed a slight increase of cell death mainly located at the core of the MT, especially, in the biggest MT.

Infection with *P. gingivalis* and stimulation with its LPS and heat-killed *P. gingivalis*. Regarding monolayer infection, 2×10^5 cells were plated in each well of a 24-wells plate. At the day of the experiment, cells were washed twice with PBS and were either infected for 24 h with *P. gingivalis* at a multiplicity of infection (MOI) of 100 or stimulated with ultrapure *P. gingivalis* LPS (1 µg/ml) (InvivoGen, San Diego, CA, USA). To ensure that effects are induced by *P. gingivalis* invasion, after 2 h of infection, the medium was removed and replaced by the same volume of bacteria free culture medium.

Regarding MT infection and stimulation, MTs were first collected from 3D culture plate. Then, MTs were infected with *P. gingivalis* at MOI 100, heat-killed *P. gingivalis* or stimulated with its LPS (1 µg/ml) (InvivoGen, San Diego, CA, USA). To inactivate bacteria, *P. gingivalis* was incubated for 15 minutes at 85 °C prior to the experiment. The MTs suspended in a 96-Well plate (CytoOne, Orsay, France) were infected for 2 to 24 h. As described for monolayer cells infection, after 2 h, the medium was replaced by a bacteria-free culture medium. To ensure *P. gingivalis* invasion, after 2 h of contact with cells or MTs, cell medium was replaced with a *P. gingivalis*-free medium. Furthermore, an antibiotic protection assay has been performed (Supplementary Figure 1) that confirmed the invasiveness of *P. gingivalis* in both cell types and MT.

RNA isolation and reverse transcription. Total RNA from gingival samples and cells were extracted using the High Pure RNA Isolation Kit (Roche Diagnostics, Meylan, France) according to the manufacturer's instructions. The total RNA concentration was quantified using NanoDrop 1000 (Thermofisher, Illkirch, France). 25 ng of RNA from each sample were used for Reverse transcription. Reverse transcription was performed using iScript Reverse Transcription Supermix (Biorad, Miltry-Mory, France) according to the manufacturer's instructions.

Quantitative real-time PCR analysis. To quantify mRNA expression, qPCR was performed on the cDNA samples. PCR amplification and analysis were performed with CFX Connect™ Real-Time PCR Detection System (Biorad, Miltry-Mory, France). Amplification reactions were performed using iTAq Universal SYBR Green Supermix (Biorad, Miltry-Mory, France). Beta-actin was used as endogenous RNA control (housekeeping gene) in all samples. Primer sequences related to Bcl-2, Bax-1, Integrin β1, Apaf-1, Tnf-α, Il-6, Il-8, Col IV and β-actin were purchased from Qiagen, (Courtaboeuf Cedex, France) and ThermoFischer (Illkirch, France) (Supplementary Table 1). Expression level was calculated after normalization to the housekeeping gene expression.

Immunofluorescence. Immunofluorescence has been performed on sections of MTs and the tissues harvested from experimental periodontitis. After embedding MTs in OCT (Tissue-Tek, Sakura Finetek, Torrance, CA, USA), 15 µm sections were obtained using cryostat (Jung, CM3000) and fixed by immersion in 4% paraformaldehyde in PBS. Sections were incubated with primary antibody against vimentin (Polyclonal goat) (1:500), E-cadherin (Monoclonal rat) (1:500), Apaf-1 (Polyclonal rabbit) (1:200), collagen IV (Polyclonal goat) (1:200), Caspase-3 (Polyclonal rabbit) (1:200), integrin β1 (1:300) and anti-*P. gingivalis* (Polyclonal rabbit) (1:5000) respectively (Supplementary Table 1) at 4 °C for 24 h. After incubation, sections were incubated with the secondary antibody for 1 h at room temperature (1:250 to 1:500 of Alexa Fluor 594 or Alexa Fluor 488 (Invitrogen, Thermofisher, Illkirch, France)). Nuclei were stained with DAPI 200 nM (Euromedex, Souffelweyersheim, France) and actin was labeled with phalloïdin Alexa Fluor™ 546 (Thermofisher, Illkirch, France). Finally, sections were mounted (Dako, Trappes, France) and observed with a fluorescence microscope (Leica DM4000B).

Type of cell death assessment. Apoptosis and necrosis were visualized using Annexin-V-FLUOS Staining Kit according to the manufacturer's instructions (Roche Diagnostics, Meylan, France). A solution of DAPI 200 nM (Euromedex, Souffelweyersheim, France) was added for nuclear staining. Samples were observed under an epifluorescence microscope (Leica DM 4000 B) and a digital CCD color imaging system (Microscope Digital Camera DP72; CellSens Entry, Olympus, Tokyo, Japan).

Scanning electron microscopy (SEM). MTs were dehydrated in a series of alcohol solutions (50, 70, 90, 100%), dried and sputter-coated for 7 to 15 min with platinum using spray coating Technics Hummer II (Technics, Alexandria, VA). Images were captured using a scanning electron microscope Leica Cambridge Stereoscan 360 FE (Leica Cambridge Co., Cambridge, UK) and the software EDS 2006 (IXRF Systems Inc., Houston, TX).

Transmission electron microscopy (TEM). Samples were fixed by immersion in 2.5% glutaraldehyde and 2.5% paraformaldehyde in cacodylate buffer (0.1 M, pH 7.4), and post-fixed in osmium tetroxide 1% in 0.1 M cacodylate buffer for 1 h at 4 °C, dehydrated and then treated with propylene oxide for 30 min under stirring. Samples were incorporated into Epon 812. Semi-thin sections were cut at 2 µm with ultra-microtome (Leica Ultracut UCT), stained with toluidine blue and analyzed histologically by light microscopy (Microscope Digital Camera DP72; CellSens Entry, Olympus, Tokyo, Japan). The ultra-thin sections were cut at 70 nm and contrasted with uranyl acetate and lead citrate and examined at 70 kV with an electron microscope Morgagni 268 D. Images were captured digitally by Mega View III software (Soft Imaging System).

Statistical analysis. Statistical analysis was performed using pair-wise Anova test and post-hoc Tukey's test. Statistical significance level was considered for $p < 0.05$. Data were analyzed using PRISM 6.0 (GraphPad, La Jolla, CA, USA). All experiments have been performed at least in triplicate (biological and technical triplicates).

Results

Morphological characteristics of formed MT. To generate gingiva-like MTs, the hanging-drop method was used to sequentially seed the FBs in the first step followed by ECs as a second layer (Fig. 1B). This sequential seeding allows the formation of well-organized MT exhibiting two distinct layers at contrary to simultaneous seeding of both cell types (Fig. 1C). Different cell concentrations for FBs and ECs were also tested (Fig. 1D) to assess impact on MT size and cell death at the core of the MT. The increase of the number of cells seeded at each step increased MT size. However, this increased size (until 200–300 µm) did not induce significant cell death at the core of the MT as observed with immunostaining with Annexin V (Fig. 1D). Formed MT exhibited a well-defined spatial organization where ECs were organized in an external cellular multilayer while FBs constituted the core of the MT (Fig. 2A,B). This distinct cellular pattern was confirmed by immunostaining with E-cadherin, pan cytokeratin and cytokeratin 14 observed at the periphery, while vimentin was mainly detected at its core (Fig. 2I–K,N,O). In addition, laminin αV was localized mainly at the ECs layer (Fig. 2M).

The expression and localization of the same proteins were evaluated in an experimental periodontitis model (Fig. 3C–H). In healthy site, collagen IV and integrin β1 were localized from the epithelium-connective tissue interface until the alveolar bone border (Fig. 3C–H). Laminin αV was mainly detected at the epithelium-connective tissue interface (Fig. 3M,N). Vimentin was used as a connective tissue marker and was mainly expressed in connective tissue (Fig. 3K,L). These results confirmed the relevance of the 3D model to evaluate the mechanisms involved at the epithelial-fibroblast interface during periodontitis.

***P. gingivalis* influenced epithelial barrier integrity.** Invasion of *P. gingivalis* was evaluated by immunofluorescence in both 3D and monolayer culture. In spheroid model, invasion of MT by *P. gingivalis* was detected after 24 h (Fig. 2R,S). Interestingly, *P. gingivalis* was not only detected in the epithelial compartment but also within the fibroblastic core, demonstrating the ability of *P. gingivalis* to bypass the epithelial barrier and to disseminate within MT (Fig. 2S), hence, confirming the capability of *P. gingivalis* to invade both cell types (Fig. 2U–X) as

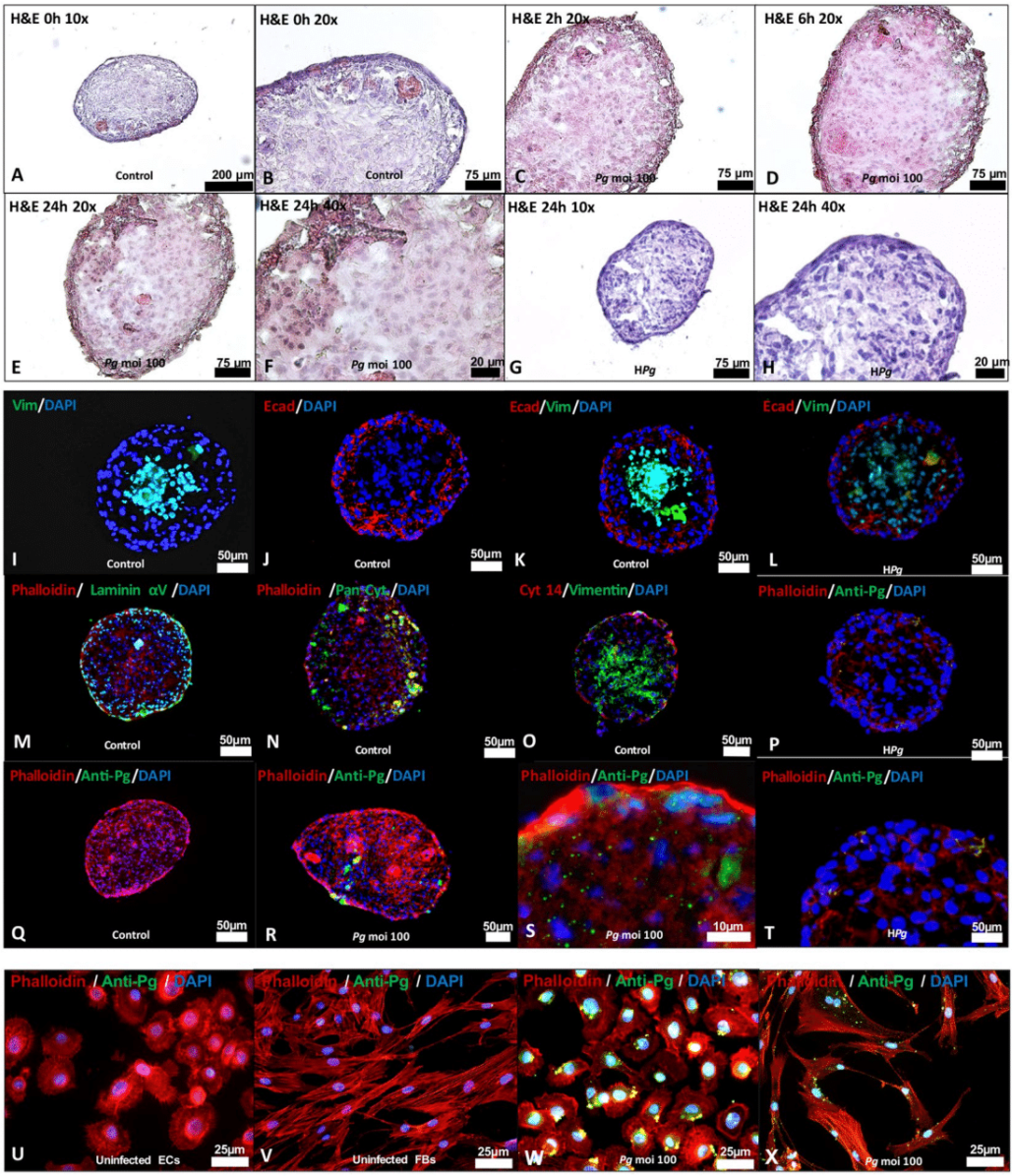

Figure 2. Morphological characteristics of MT spheroids mimicking gingival soft tissues. (**A**–**H**) Histological hematoxylin-eosin images under optic microscopy at 0, 2, 6 and 24 h at different magnifications (10x: **A**,**G**; 20x: **B**,**C**,**D**,**E**; 40x: **F**,**H**) of uninfected MTs (**A**,**B**), of MTs infected with *P. gingivalis* (**C**–**F**) and heat-inactivated *P. gingivalis* (**G**,**H**). (**I**–**L**) Immunofluorescence staining of uninfected MTs (**I**–**K**) and infected with heat-killed *P. gingivalis* (**L**) (Green: Vimentin, Red: E-cadherin, Blue: DAPI – nuclear staining-) (20x magnification). (**M**–**O**) Immunofluorescence staining of uninfected MTs (Green: Laminin α5; Pan Cytokeratin; Vimentin, Red: E-cadherin, Cytokeratin 14, Blue: DAPI – nuclear staining-) (20x magnification). (**P**–**T**) Immunofluorescence staining of uninfected, infected with *P. gingivalis* and heat-killed *P. gingivalis* infected MTs (Green: *P. gingivalis* immunostaining, Red: Phalloidin, Blue: DAPI – nuclear staining). (**U**–**X**) Immunofluorescence staining of uninfected, infected with *P. gingivalis* and heat-killed *P. gingivalis* infected ECs and FBs (Green: *P. gingivalis* immunostaining, Red: Phalloidin, Blue: DAPI – nuclear staining). Magnification was 20x for I-R and 40x for (**S**–**X**).

observed *in situ* (Fig. 3O,P). Interestingly, localization of inactivated *P. gingivalis* (HPg) was not observed within the core of the MT highlighting the role of invasion in this process (Fig. 2L,P,T).

Infection of MTs with *P. gingivalis* induced disorganization and destruction of the spheroid structure. To evaluate the effect of *P. gingivalis* infection on MT structure, 3D morphometric changes were followed after infection (Fig. 4) and compared to uninfected MT at 6 and 24 h. SEM analysis showed that *P.gingivalis* was able to adhere and colonize the external epithelial surface of the MT and to be internalized

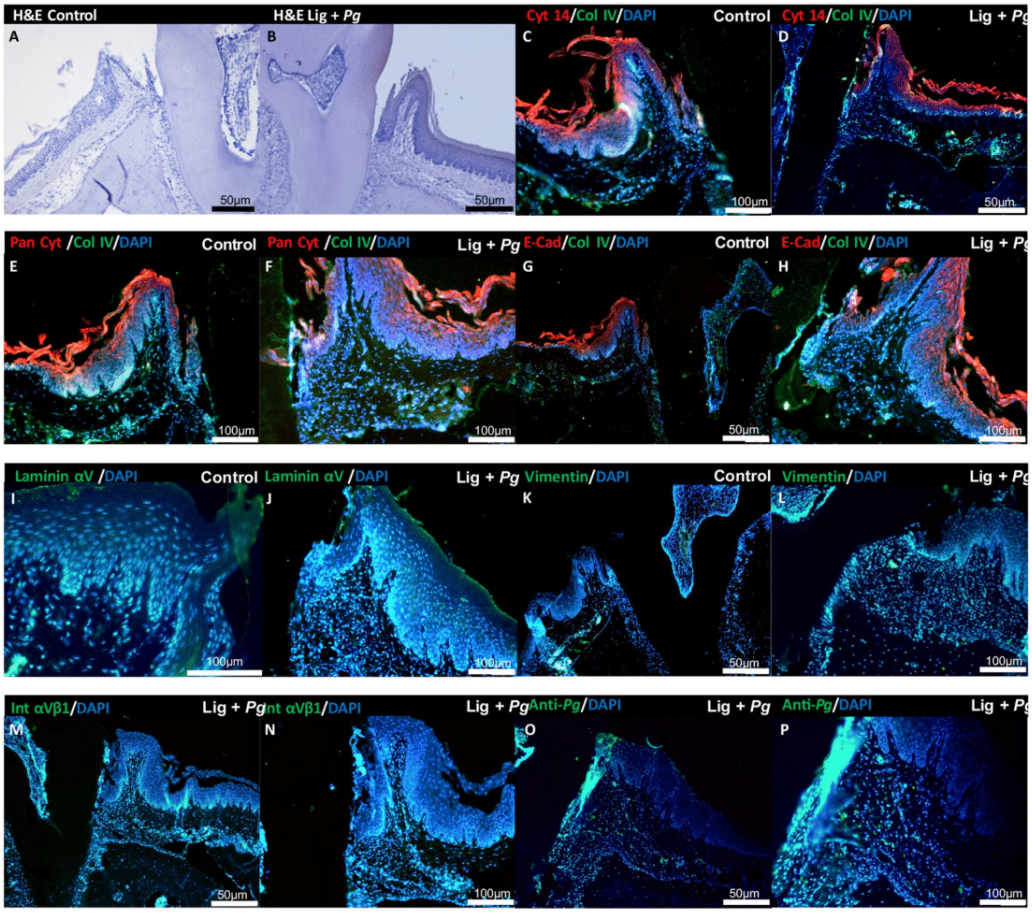

Figure 3. *P. gingivalis*-induced experimental periodontitis. (**A**) Histological hematoxylin-eosin staining of periodontium of non-treated site on the first molar of mice (Hematoxylin & Eosin) (10x magnification). (**B**) Morphological characteristics of periodontium of *P. gingivalis* ligature treated site on the first molar of mice (Hematoxylin & Eosin) (10x magnification). (**C**–**H**) Immunofluorescence staining for localization of Cytokeratin 14, Pan Cytokeratin and E-cadherin expression in epithelial tissue (red) and Collagen IV expression (green) in the periodontium (10x magnification). (**I**–**P**) Immunofluorescence staining for localization of Integrin β1, vimentin, laminin α5 and anti-*P. gingivalis* expression in the periodontium (green) at diseased site (10x magnification: **I**–**M** and **O**; 20x magnification: **N**,**P**). In all immunofluorescence images, nucleus has been stained by DAPI in blue.

(Fig. 4C). Furthermore, bacterial infection induced EC exfoliation (Fig. 4D). At 6 and 24 h, infected MT exhibited a collapsed shape associated with signs of cell injury and cell death illustrated by the detection of apoptosis (Fig. 4G,H). This observed collapsed shape seemed to be associated with the destruction of the core of the MT. Interestingly, at 24 h, infected MT exhibited signs of total destruction and some FBs could be observed even at the surface of the MT (Fig. 4H). Such destruction was not observed when MT were only stimulated with *P. gingivalis*-LPS even though structural modifications could be observed at the surface (Fig. 4F).

Changes induced by infection on structural organization of the MT were also observed using TEM. Uninfected MT displayed several hallmarks of a fibroblastic core surrounded by a healthy epithelial barrier (Fig. 5A–D). Several epithelial junctions have been observed such as desmosomes, *adherens* junctions and long tight junctions between ECs (Fig. 5C,D). However, infection of MT by *P. gingivalis* induced cellular stress highlighted by the presence of apoptotic bodies correlated with bacterial invasion of ECs at 2 h (Fig. 3E–H). The effect of the infection was also visible on the integrity of the epithelial barrier illustrated by the reduction of the number of cell junctions, especially located at the most external and superficial part of ECs (Fig. 5H). At 24 h, the full disruption of the epithelial barrier, multiple apoptotic cells and an acute cellular stress in all *strata* of the MT could be observed (Fig. 5M–P). This was confirmed by immunofluorescence staining of integrin β1 which demonstrated a decreased expression at the epithelial level in response to infection (Fig. 6J,K). This pattern of expression was directly correlated to the *P. gingivalis* invasion pattern that has been shown previously by immunofluorescence and SEM (Figs 3M–O and 4).

MT collapse correlated with *P. gingivalis*-induced apoptosis. To determine how *P. gingivalis* affects the different compartments of the MT, a focus was made on induced cell death using Annexin V/ IP staining. In comparison with the uninfected MT, at 24 h, a strong Annexin V staining was observed within the fibroblastic

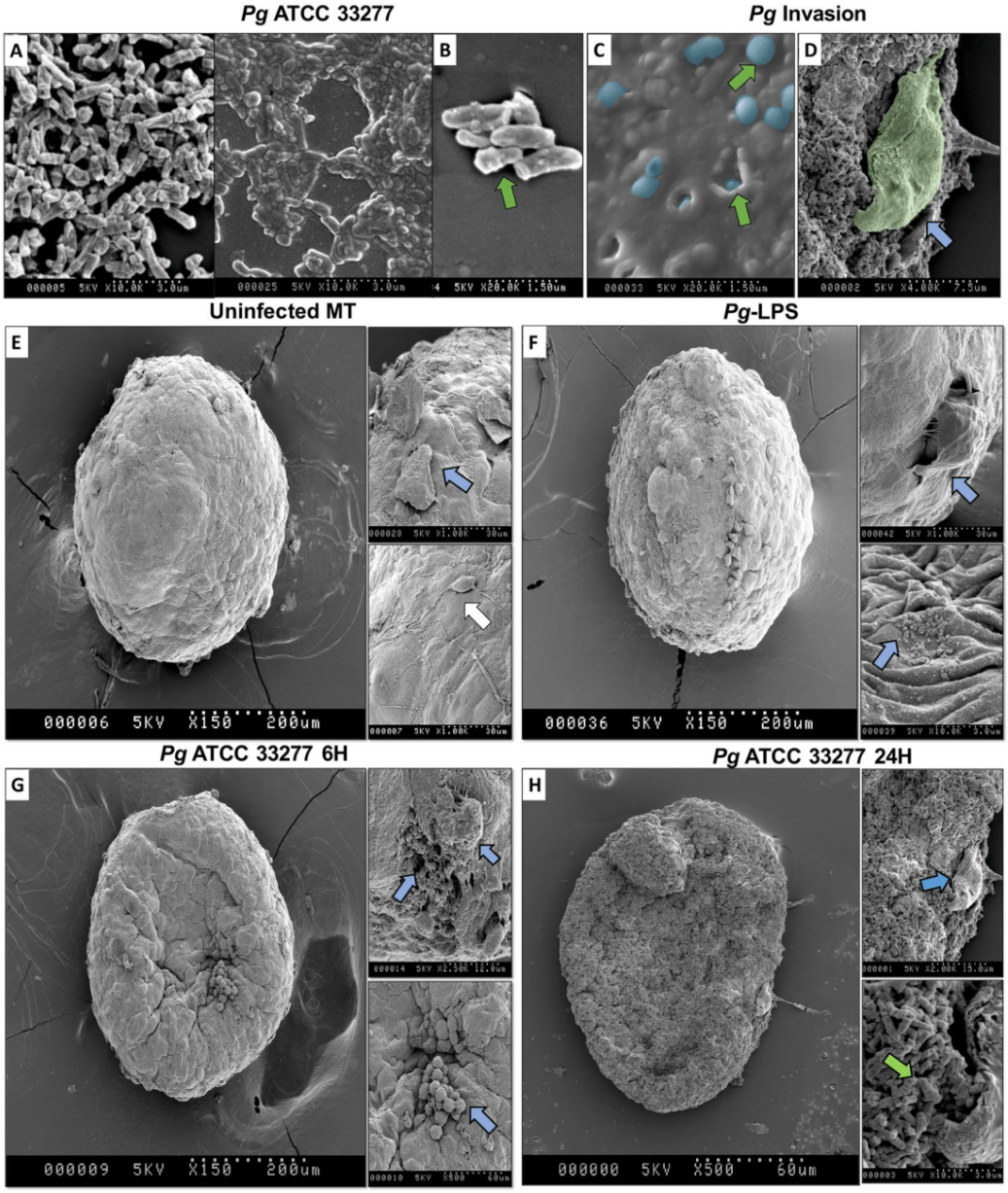

Figure 4. *P. gingivalis* bypasses the epithelial barrier to reach FBs located at the core of the MT leading to MT destruction. SEM imaging of (**A**,**B**) *P. gingivalis* culture, (**C**) *P. gingivalis* infection and intracellular invasion of the MT surface, (**D**) *P. gingivalis* proliferating on MT surface and EC exfoliation, (**E**) uninfected MT, (**F**) MT stimulated with LPS, (**G**) MT infected with *P. gingivalis* for 6 h and (**H**) for 24 h. Green arrows indicate *P. gingivalis* infection in MT and/or cell invasion; blue arrows indicate the disruption of epithelial barrier, multiple apoptotic cells and an acute cellular injury in all strata of the MT – EC and FB-; white arrow indicates proliferating EC at the surface of MT.

core (Fig. 6B) explaining the observed collapse (Figs 4 and 5). Interestingly, a differential expression of apoptosome APAF-1 and caspase-3 was simultaneously observed (Fig. 6C–H). Herein, in *P. gingivalis*-infected MT, an increased APAF-1 and caspase-3 expression was observed in FBs that emphasized the role of APAF-1 apoptosome in the activation of apoptosis. At contrary, APAF-1 detection within the ECs layer in infected MT was low (Fig. 4D,F).

Infection with *P. gingivalis* modulated differentially the inflammation and apoptosis associated gene expression. To evaluate the pattern of gene expression associated with inflammation, apoptosis and epithelial integrity, mRNA expression in MT in response to *P. gingivalis* infection was measured and compared to that of monolayer cell culture. Regarding inflammation, infection of MT increased TNF-α, IL-6 and IL-8 expression (Fig. 7A–C). Interestingly, same trend of results was observed in monolayer cell cultures. Effect on

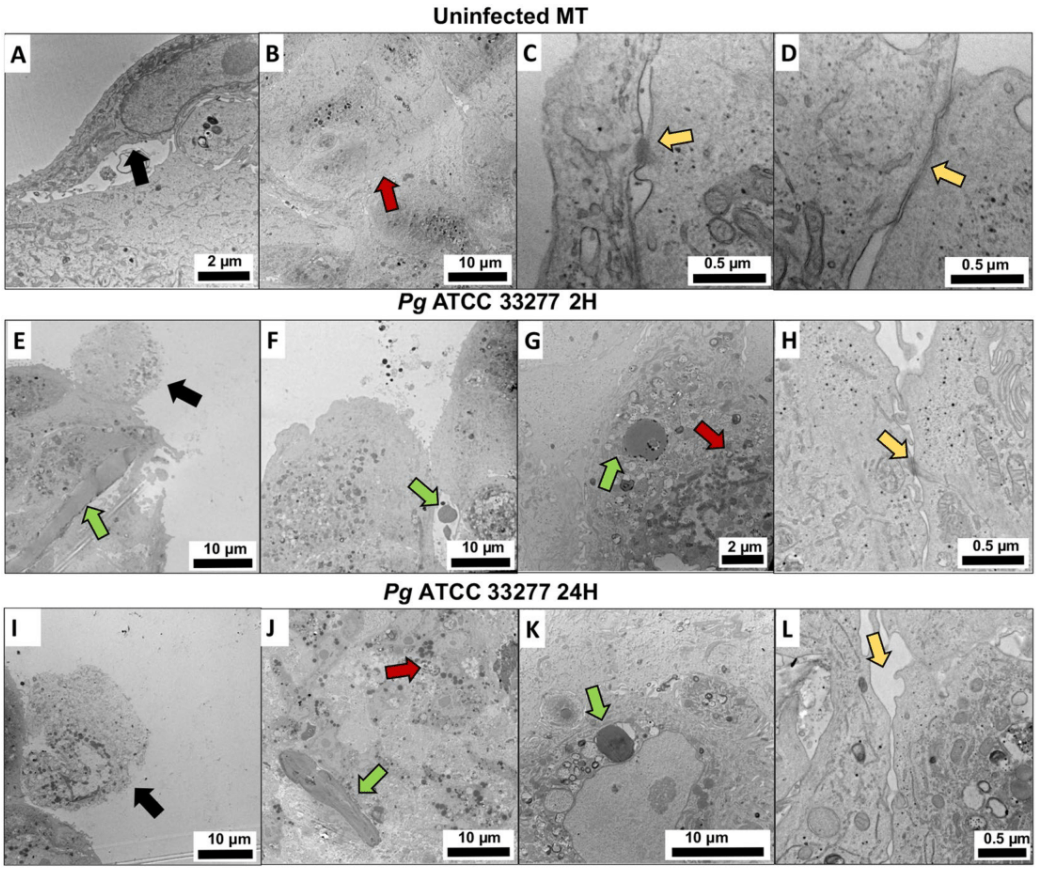

Figure 5. *P. gingivalis* induces fibroblastic stress and disruption of EC layer. TEM imaging of (**A**–**D**) uninfected MT, (**E**–**H**) MT infected with *P. gingivalis* for 2 h, (**M**–**O**) MT infected with *P. gingivalis* for 24 h. Green arrows indicate *P. gingivalis* bacterial infection and intercellular/intracellular invasion; black arrows indicate apoptotic cells and signs of acute cellular stress; red arrows indicate an acute cellular stress in FBs and the presence of lysosomes and apoptosis correlated with bacterial invasion; yellow arrows indicate several epithelial junctions such as desmosomes, long and short tight junctions between ECs.

apoptosis has also been evaluated focusing on Bcl-2/Bax-1 and Apaf-1. In ECs, infection with *P. gingivalis* displayed anti-apoptotic effects through a decrease of Bax-1 and Apaf-1 and an increase of anti-apoptotic Bcl-2 expression in EC (Fig. 7D–F). In FBs, *P. gingivalis* infection induced opposite effects as it increased the expression of pro-apoptotic markers (Fig. 7D–F). The gene expression of MT was closer to that of FBs. The breakdown of the epithelial barrier was also confirmed as mRNA expression of integrin-β1 was significantly decreased by infection (Fig. 7G).

To evaluate if the mRNA expression pattern observed in infected MT was comparable to that expressed in diseased tissues, mRNA expression of the same genes was evaluated in human gingival tissues harvested from healthy (H) and chronic periodontitis (CP) patients (Fig. 8). Analysis revealed that the expression of TNF-α, IL-6, IL-8, Bax-1 and Apaf-1 mRNAs was significantly increased in the CP group (TNF-α, 4.7-folds; IL-6, 3.85-folds; IL-8, 2.5-folds; Bax-1, 3-folds; Apaf-1, 3.9-folds) ($p < 0.05$) (Fig. 8A–D,F) while the anti-apoptotic Bcl-2 expression was decreased (1.9-folds) (Fig. 8E). As observed in MT, mRNA expression of integrin β1 was also increased significantly in CP (Fig. 8G). These results confirmed that the modulation of mRNA expression by *P. gingivalis* in MT is similar to the one observed in human diseased tissues.

Discussion

In this study, we designed a spheroid 3D *in vitro* model of gingival tissue and assessed the destructive effects associated with *P. gingivalis* infection. The well-organized 3D structure of the synthesized MT mimicked the epithelial-fibroblastic barrier and allowed investigation of the *P. gingivalis*-induced effects associated with bacterial invasion and to focus on the epithelial barrier disruption and inflammation.

It has already been described that the synthesis of 3D MT using hanging-drop method is a reliable technique to generate homogenous organs or tissue-like structures at low-cost without requiring specific growth factors or complicated technical procedures. This type of spheroid model has been used previously to determine the physiopathological processes associated with diseases such as cancers, cellular organization during embryogenesis, drug testing and also as potential therapeutics such as demonstrated in the context of dental pulp regeneration[10,17,34–36]. The use of this model is of interest to evaluate the effects associated with the infection by *P. gingivalis* or by other

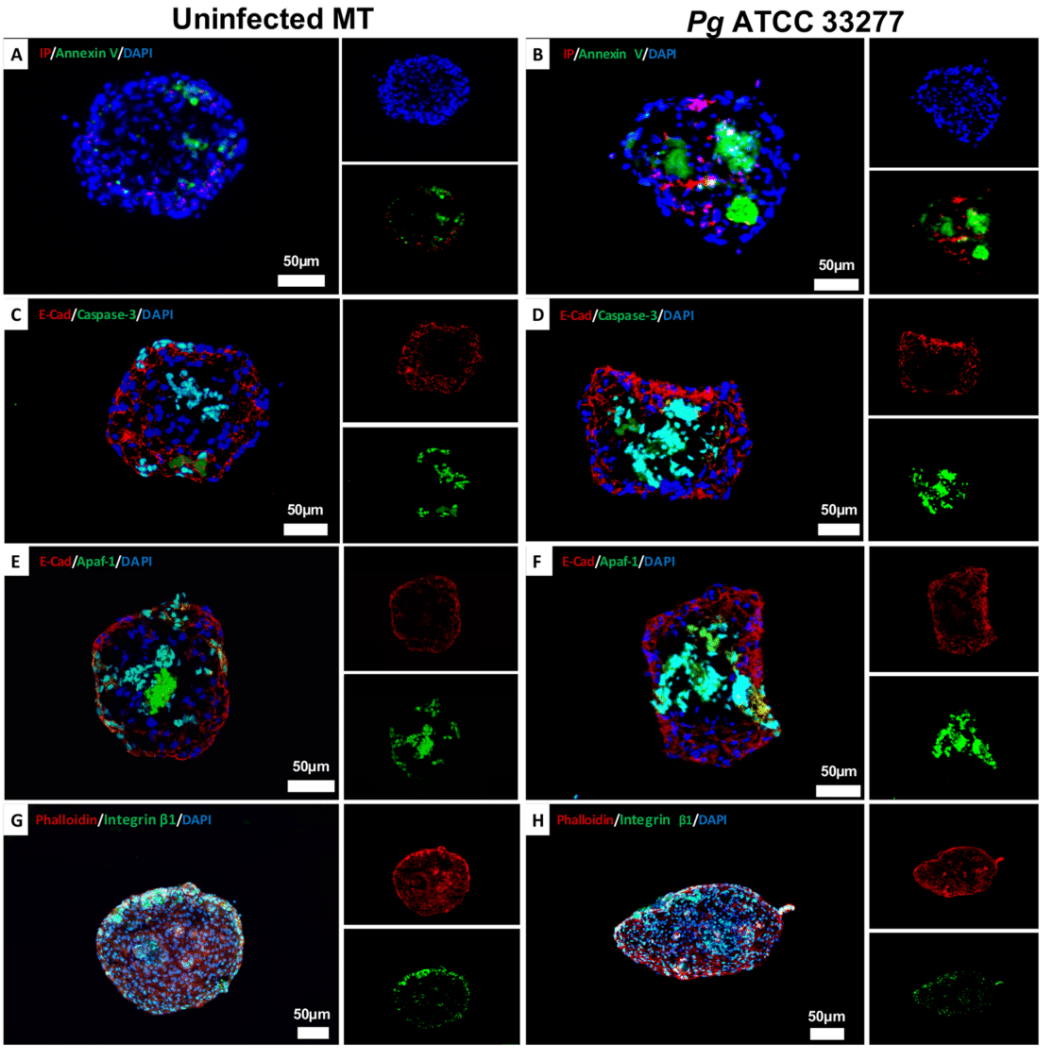

Figure 6. *P. gingivalis* infection induces an inflammatory response in MT correlated to an increased cell death. (**A**) Annexin V/IP fluorescence staining image in uninfected MT, (**B**) Annexin V/IP fluorescent staining images of MT infected with *P. gingivalis* for 24 h, (**C**,**D**) Immunofluorescence staining of uninfected MT (**C**) and infected with *P. gingivalis* (**D**) for 24 h (green: caspase-3, red: E-cadherin, blue: DAPI – nuclear staining), (**E**,**F**) Immunofluorescence staining of uninfected MT (**E**) and infected with *P. gingivalis* (**F**) for 24 h (green: APAF-1, red: E-cadherin, blue: DAPI – nuclear staining). (**G**,**H**) Immunofluorescence staining of uninfected MT (**G**) and infected with *P. gingivalis* (**H**) for 24 h (green: integrin β1, red: E-cadherin, blue: DAPI – nuclear staining). All images were acquired at 20x magnification.

periodontal pathogens while taking into account the epithelio-fibroblastic interactions. This coupling in 3D maximizes cell-to-cell communication and signaling that is critical to cell function. Furthermore, the phenotype or function of cells grown in 3D is more complex and closer to the functions of human tissues compared to the cells grown in 2D[37]. Hypoxia can be a physiologically relevant phenomenon considered as a major characteristic of 3D microenvironments both *in vitro* and *in vivo*. Oxygen concentration in 3D tissues depends on the balance between oxygen delivery and consumption[38]. In cancer models, hypoxic conditions need to be included in the 3D scaffold design and this can be done by strictly regulating the size of the MT. It has been shown that oxygen can diffuse across 100–200 µm of tissue thickness and it is generally desirable to maintain the optimal aggregate size of approximately 250 µm to prevent hypoxia[39]. In this study, the number of cells seeded was standardized to an ideal size for which the cells in the core of the uninfected MT remained healthy and unaffected by hypoxia. However, a modification of the protocol of MT synthesis may be done, through an increase in the number of the cells seeded, to evaluate the effect of hypoxia on cells response to infection as this phenomenon was demonstrated to be deleterious to oral health[40]. Such 3D model may also be interesting in the future to evaluate the effects of anti-infectious or anti-inflammatory drugs while considering tissular penetration.

Several other 3D models of oral mucosa have already been developed[9,41–43]. Most of them are collagen-based oral mucosal models (OMM) and displayed efficiently the characteristics of para-keratinized tissue. Interestingly, the feasibility of combining such engineered mucosa with engineered alveolar bone was also established[43]. The use

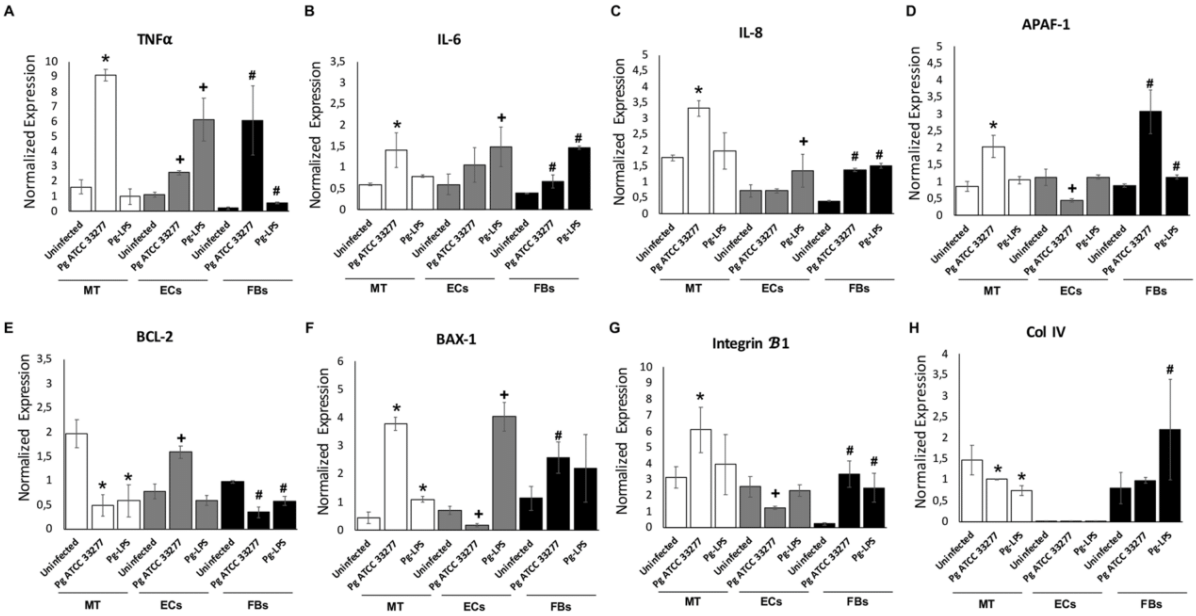

Figure 7. *P. gingivalis* infection induces an inflammatory and pro-apoptotic cell death response in MT correlated to increased gene expression. (**A**–**F**) Gene expression of inflammatory and pro-apoptotic cell death response related genes: TNF-α, IL-6, IL-8, Bax-1, Bcl-2 and Apaf-1 in MT; monolayer cell culture of ECs and FBs infected with *P. gingivalis* at MOI 100 for 24 h; (**G**,**H**) Gene expression of integrin β1 and collagen IV. *Differences between infected or stimulated MT vs control ($p < 0.05$). $^{+}$Differences between infected or stimulated ECs vs control ($p < 0.05$). $^{\#}$Differences between infected or stimulated FBs vs control ($p < 0.05$).

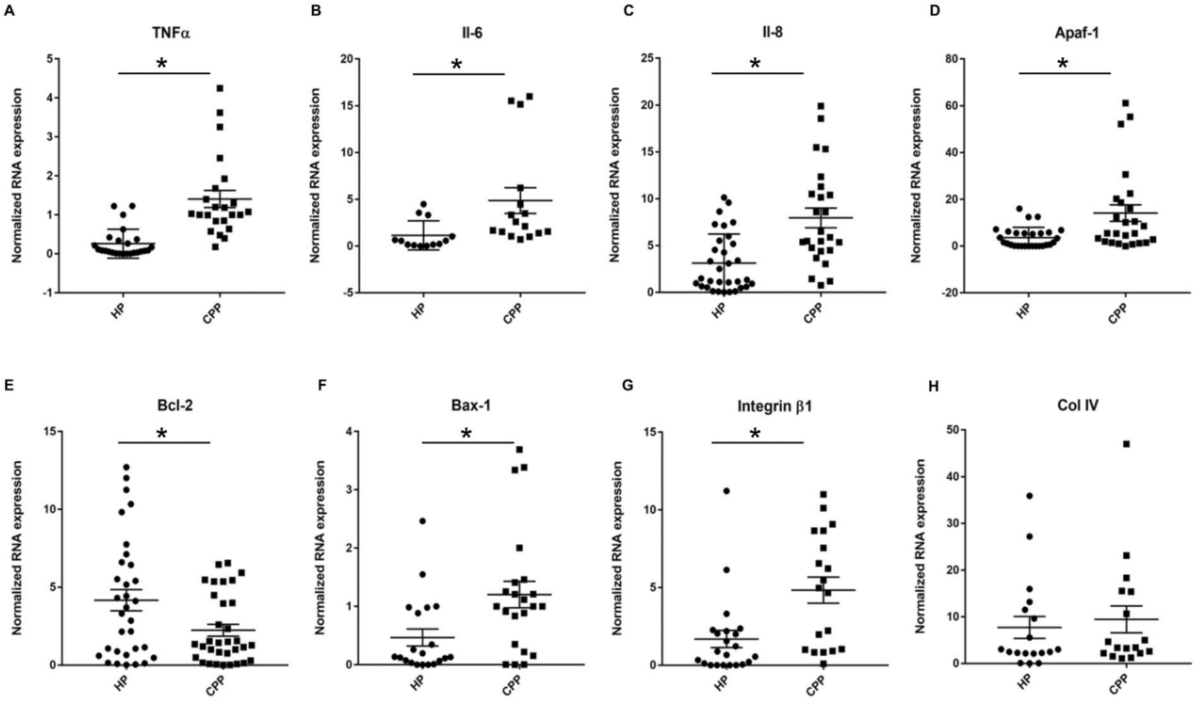

Figure 8. Inflammatory and pro-apoptotic cell death related gene expression is increased in chronic periodontitis samples. (**A**–**F**) Gene expression of inflammatory and pro-apoptotic cell death response related genes: TNF-α, IL-6, IL-8, Apaf-1, Bcl-2 and Bax-1 from mRNA extracted from chronic periodontitis patients (CPP) (11 patients) and healthy patients (HP) (9 patients); (**G**,**H**) Gene expression of integrin β1 and collagen IV from mRNA extracted from chronic periodontitis patients (CPP) (11 patients) and healthy patients (HP) (9 patients). *Differences between CPP and HP samples ($p < 0.05$).

of such models confirmed the need of 3D models to investigate inflammatory processes and also host-response to pathogens, such as *P. gingivalis*, as differential effects between 3D and 2D models were highlighted, especially, regarding inflammatory cytokines (IL-8, IL-1α) secretion[9]. In our 3D MT model, same discrepancies related to the mRNA expression of inflammatory markers were also observed in comparison with monolayer cultures. Furthermore, the gene expression of the non-infected and *P. gingivalis*-infected MT was similar to that measured in healthy and diseased gingival tissues respectively, confirming the similarity between MT and gingival tissue. It should be mentioned that one limitation of the MT model is the absence of keratinization that could be obtained and controlled in OMM after exposure of the cell layers to air[9,43,44].

In MT, the external localization of ECs mimics the epithelial barrier, a key element of the host-defense and innate immune response due to its implication in host-bacterial crosstalk[45]. At the junctional epithelium, ECs are connected to each other by a variety of specialized transmembrane proteins including tight junctions, *adherens* junctions, gap junctions and desmosomes[27,28] that constitute a thin structure. Adhesion structures are the key to maintain epithelial integrity and are also involved in the coordination of several signaling and trafficking molecules, thereby, regulating cell differentiation, proliferation, and polarity[46–48]. In our 3D model, ECs were characterized by the presence of E-cadherin observable at the periphery of the MT and localized at the epithelial level, confirming an architecture similar to that of the junctional epithelium. Following *P. gingivalis* infection, we observed *in vivo* and in MT, the bacterial ability to invade ECs, as demonstrated previously, and also to bypass the epithelial barrier to reach the underlying tissue. Invasion is a rapid process and is accompanied by cytoskeletal modifications, calcium ion fluxes, modulation of MAP kinase and apoptotic pathways, and downregulation of IL-8 expression[49,50] contributing *in vivo* to bacterial persistence and progression of the chronic aspects of periodontitis[51]. Several studies demonstrated that *P. gingivalis* induces proteolysis of adhesion structure components and modulates related gene expression[52,53]. Here, we focused on integrins due to their involvement in binding and invasion of *P. gingivalis* as demonstrated in several cell types[54,55]. In this study, *P. gingivalis* strain 33277 was used as it is a well-described invasive strain exhibiting several virulence factors such as fimbriae and our laboratory has significant experience using this strain[24,56,57]. Future studies should explore the precise role of each virulence factor in the invasion process and inflammatory response observed in MT model.

Modulation of apoptosis is a key feature of innate immune response subversion elicited by *P. gingivalis*, especially at the epithelial level[33,58]. In MT, the expression of apoptotic markers (caspase-3, Bax-1/Bcl-2, Apaf-1) was differentially measured according to cell type as observed previously[33]. In MT, APAF-1 related apoptosome was mostly expressed in fibroblastic core and its expression within epithelial layer was decreased following *P. gingivalis* infection. The inhibition of apoptosis in ECs is a well-described mechanism involved in *P. gingivalis* pathogenesis. Several studies demonstrated the targeting of cells with a rapid turnover, such as junctional epithelial cells, by *P. gingivalis*[59] and its ability to decrease epithelial apoptosis. Therefore, the use of MT model will be useful to evaluate indirect impact of *P. gingivalis* on connective tissue following ECs stimulation.

In conclusion, this 3D *in vitro* model of gingival tissue may be used to analyze pathophysiological processes involved in periodontitis especially molecular mechanisms related to either innate immune response, role of bacterial virulence factors occurring at the epithelium-connective tissue interface and therapeutic properties of potential anti-inflammatory or anti-infective drugs. The potential of adding a third cell type at the core of the MT, such as osteoblasts, may be of interest to investigate the influence of soft tissue infection and inflammation on soft tissue-bone crosstalk.

References

1. Hajishengallis, G. Periodontitis: from microbial immune subversion to systemic inflammation. *Nat. Rev. Immunol.* **15**, 30–44 (2015).
2. Amano, A. Disruption of epithelial barrier and impairment of cellular function by *Porphyromonas gingivalis*. *Front. Biosci. J. Virtual Libr.* **12**, 3965–3974 (2007).
3. Wang, H. *et al*. *Porphyromonas gingivalis*-Induced Reactive Oxygen Species Activate JAK2 and Regulate Production of Inflammatory Cytokines through c-Jun. *Infect. Immun.* **82**, 4118–4126 (2014).
4. Yilmaz, O., Verbeke, P., Lamont, R. J. & Ojcius, D. M. Intercellular spreading of *Porphyromonas gingivalis* infection in primary gingival epithelial cells. *Infect. Immun.* **74**, 703–710 (2006).
5. Choi, Y. S., Kim, Y. C., Ji, S. & Choi, Y. Increased bacterial invasion and differential expression of tight-junction proteins, growth factors, and growth factor receptors in periodontal lesions. *J. Periodontol.* **85**, e313–322 (2014).
6. Graves, D. T., Fine, D., Teng, Y. A., Van Dyke, T. E. & Hajishengallis, G. The Use of Rodent Models to Investigate Host-Bacteria Interactions Related to Periodontal Diseases. *J. Clin. Periodontol.* **35**, 89–105 (2008).
7. Kim, J. B. Three-dimensional tissue culture models in cancer biology. *Semin. Cancer Biol.* **15**, 365–377 (2005).
8. Artegiani, B. & Clevers, H. Use and application of 3D-organoid technology. *Hum. Mol. Genet*. **ddy187** (2018).
9. Pinnock, A., Murdoch, C., Moharamzadeh, K., Whawell, S. & Douglas, C. W. I. Characterisation and optimisation of organotypic oral mucosal models to study *Porphyromonas gingivalis* invasion. *Microbes Infect.* **16**, 310–319 (2014).
10. Bécavin, T. *et al*. Well-organized spheroids as a new platform to examine cell interaction and behaviour during organ development. *Cell Tissue Res.* **366**, 601–615 (2016).
11. Amelian, A., Wasilewska, K., Megias, D. & Winnicka, K. Application of standard cell cultures and 3D *in vitro* tissue models as an effective tool in drug design and development. *Pharmacol. Rep.* **69**, 861–870 (2017).
12. Kuchler-Bopp, S. *et al*. Three-dimensional Micro-culture System for Tooth Tissue Engineering. *J. Dent. Res.* **95**, 657–664 (2016).
13. Antoni, D., Burckel, H., Josset, E. & Noel, G. Three-dimensional cell culture: a breakthrough *in vivo*. *Int. J. Mol. Sci.* **16**, 5517–5527 (2015).
14. Achilli, T.-M., Meyer, J. & Morgan, J. R. Advances in the formation, use and understanding of multi-cellular spheroids. *Expert Opin. Biol. Ther.* **12**, 1347–1360 (2012).
15. Łaniewski, P., Gomez, A., Hire, G., So, M. & Herbst-Kralovetz, M. M. Human Three-Dimensional Endometrial Epithelial Cell Model To Study Host Interactions with Vaginal Bacteria and *Neisseria gonorrhoeae*. *Infect. Immun.* **85**, e01049–16 (2017).
16. Birgersdotter, A., Sandberg, R. & Ernberg, I. Gene expression perturbation *in vitro*–a growing case for three-dimensional (3D) culture systems. *Semin. Cancer Biol.* **15**, 405–412 (2005).
17. Chaddad, H. *et al*. Combining 2D angiogenesis and 3D osteosarcoma microtissues to improve vascularization. *Exp. Cell Res.* **15**, 138–145 (2017).

18. Andrian, E., Grenier, D. & Rouabhia, M. *In vitro* models of tissue penetration and destruction by *Porphyromonas gingivalis*. *Infect. Immun.* **72**, 4689–4698 (2004).
19. Dabija-Wolter, G., Bakken, V., Cimpan, M. R., Johannessen, A. C. & Costea, D. E. *In vitro* reconstruction of human junctional and sulcular epithelium. *J. Oral Pathol. Med. Off. Publ. Int. Assoc. Oral Pathol. Am. Acad. Oral Pathol.* **42**, 396–404 (2013).
20. Hajishengallis, G. & Lamont, R. J. Breaking bad: Manipulation of the host response by *Porphyromonas gingivalis*. *Eur. J. Immunol.* **44**, 328–338 (2014).
21. Huck, O., Elkaim, R., Davideau, J.-L. & Tenenbaum, H. *Porphyromonas gingivalis*-impaired innate immune response via NLRP3 proteolysis in endothelial cells. *Innate Immun.* **21**, 65–72 (2015).
22. Huck, O. *et al*. Reduction of Articular and Systemic Inflammation by Kava-241 in *Porphyromonas gingivalis*-induced Arthritis Murine Model. *Infect. Immun.* **AIA.00356-18** (2018).
23. Groeger, S., Jarzina, F., Domann, E. & Meyle, J. *Porphyromonas gingivalis* activates NFκB and MAPK pathways in human oral epithelial cells. *BMC Immunol.* **18**, 1 (2017).
24. Bugueno, I. M., Batool, F., Korah, L., Benkirane-Jessel, N. & Huck, O. *Porphyromonas gingivalis* Differentially Modulates Apoptosome Apoptotic Peptidase Activating Factor 1 in Epithelial Cells and Fibroblasts. *Am. J. Pathol.* **188**, 404–416 (2018).
25. Elkaim, R., Werner, S., Kocgozlu, L. & Tenenbaum, H. *P. gingivalis* regulates the expression of Cathepsin B and Cystatin C. *J. Dent. Res.* **87**, 932–936 (2008).
26. Huck, O., Elkaim, R., Davideau, J. L. & Tenenbaum, H. *Porphyromonas gingivalis* and its lipopolysaccharide differentially regulate the expression of cathepsin B in endothelial cells. *Mol. Oral Microbiol.* **27**, 137–148 (2012).
27. Groeger, S., Doman, E., Chakraborty, T. & Meyle, J. Effects of *Porphyromonas gingivalis* infection on human gingival epithelial barrier function *in vitro*. *Eur. J. Oral Sci.* **118**, 582–589 (2010).
28. Katz, J., Sambandam, V., Wu, J. H., Michalek, S. M. & Balkovetz, D. F. Characterization of *Porphyromonas gingivalis*-induced degradation of epithelial cell junctional complexes. *Infect. Immun.* **68**, 1441–1449 (2000).
29. Guo, W., Wang, P., Liu, Z.-H. & Ye, P. Analysis of differential expression of tight junction proteins in cultured oral epithelial cells altered by *Porphyromonas gingivalis*, *Porphyromonas gingivalis* lipopolysaccharide, and extracellular adenosine triphosphate. *Int. J. Oral Sci.* **10**, e8 (2018).
30. Armitage, G. C. Development of a classification system for periodontal diseases and conditions. *Ann. Periodontol.* **4**, 1–6 (1999).
31. G Caton, J. *et al*. A new classification scheme for periodontal and peri-implant diseases and conditions - Introduction and key changes from the 1999 classification. *J. Periodontol.* **89**(Suppl 1), S1–S8 (2018).
32. Saadi-Thiers, K. *et al*. Periodontal and systemic responses in various mice models of experimental periodontitis: respective roles of inflammation duration and *Porphyromonas gingivalis infection*. *J. Periodontol.* **84**, 396–406 (2013).
33. Bugueno, I. M. *et al*. *Porphyromonas gingivalis* Differentially Modulates Cell Death Profile in Ox-LDL and TNF-α Pre-Treated Endothelial Cells. *PLoS ONE* **11** (2016).
34. Kelm, J. M., Timmins, N. E., Brown, C. J., Fussenegger, M. & Nielsen, L. K. Method for generation of homogeneous multicellular tumor spheroids applicable to a wide variety of cell types. *Biotechnol. Bioeng.* **83**, 173–180 (2003).
35. Dissanayaka, W. L., Zhu, L., Hargreaves, K. M., Jin, L. & Zhang, C. Scaffold-free Prevascularized Microtissue Spheroids for Pulp Regeneration. *J. Dent. Res.* **93**, 1296–1303 (2014).
36. Weiswald, L.-B., Bellet, D. & Dangles-Marie, V. Spherical cancer models in tumor biology. *Neoplasia N. Y. N* **17**, 1–15 (2015).
37. Edmondson, R., Broglie, J. J., Adcock, A. F. & Yang, L. Three-Dimensional Cell Culture Systems and Their Applications in Drug Discovery and Cell-Based Biosensors. *Assay Drug Dev. Technol.* **12**, 207–218 (2014).
38. Asthana, A. & Kisaalita, W. S. Microtissue size and hypoxia in HTS with 3D cultures. *Drug Discov. Today* **17**, 810–817 (2012).
39. Griffith, L. G. & Swartz, M. A. Capturing complex 3D tissue physiology *in vitro*. *Nat. Rev. Mol. Cell Biol.* **7**, 211–224 (2006).
40. Terrizzi, A. R., Fernandez-Solari, J., Lee, C. M., Conti, M. I. & Martínez, M. P. Deleterious effect of chronic continuous hypoxia on oral health. *Arch. Oral Biol.* **72**, 1–7 (2016).
41. Garzon, I. *et al*. *In vitro* cytokeratin expression profiling of human oral mucosa substitutes developed by tissue engineering. *Int. J. Artif. Organs* **32**, 711–719 (2009).
42. Basso, F. G. *et al*. Phenotypic markers of oral keratinocytes seeded on two distinct 3D oral mucosa models. *Toxicol. Vitro Int. J. Publ. Assoc. BIBRA* **51**, 34–39 (2018).
43. Almela, T., Al-Sahaf, S., Bolt, R., Brook, I. M. & Moharamzadeh, K. Characterization of Multilayered Tissue-Engineered Human Alveolar Bone and Gingival Mucosa. *Tissue Eng. Part C Methods* **24**, 99–107 (2018).
44. Xiao, L., Okamura, H. & Kumazawa, Y. Three-dimensional Inflammatory Human Tissue Equivalents of Gingiva. *J. Vis. Exp. JoVE* **134** (2018).
45. Pöllänen, M. T., Laine, M. A., Ihalin, R. & Uitto, V.-J. Host-Bacteria Crosstalk at the Dentogingival Junction. *International Journal of Dentistry* **2012**, 821383 (2012).
46. Yeager, M. Structure of cardiac gap junction intercellular channels. *J. Struct. Biol.* **121**, 231–245 (1998).
47. Troyanovsky, S. Cadherin dimers in cell-cell adhesion. *Eur. J. Cell Biol.* **84**, 225–233 (2005).
48. Niessen, C. M. Tight junctions/adherens junctions: basic structure and function. *J. Invest. Dermatol.* **127**, 2525–2532 (2007).
49. Nakhjiri, S. F. *et al*. Inhibition of epithelial cell apoptosis by *Porphyromonas gingivalis*. *FEMS Microbiol. Lett.* **200**, 145–149 (2001).
50. Watanabe, K., Yilmaz, O., Nakhjiri, S. F., Belton, C. M. & Lamont, R. J. Association of mitogen-activated protein kinase pathways with gingival epithelial cell responses to *Porphyromonas gingivalis* infection. *Infect. Immun.* **69**, 6731–6737 (2001).
51. Rudney, J. D., Chen, R. & Sedgewick, G. J. Intracellular *Actinobacillus actinomycetemcomitans* and *Porphyromonas gingivalis* in buccal epithelial cells collected from human subjects. *Infect. Immun.* **69**, 2700–2707 (2001).
52. Belibasakis, G., Thurnheer, T. & Bostanci, N. *Porphyromonas gingivalis*. *Virulence* **5**, 463–464 (2014).
53. Hintermann, E., Haake, S. K., Christen, U., Sharabi, A. & Quaranta, V. Discrete proteolysis of focal contact and adherens junction components in *Porphyromonas gingivalis*-infected oral keratinocytes: a strategy for cell adhesion and migration disabling. *Infect. Immun.* **70**, 5846–5856 (2002).
54. Yilmaz, O., Watanabe, K. & Lamont, R. J. Involvement of integrins in fimbriae-mediated binding and invasion by *Porphyromonas gingivalis*. *Cell. Microbiol.* **4**, 305–314 (2002).
55. Zhang, B. *et al*. The periodontal pathogen *Porphyromonas gingivalis* changes the gene expression in vascular smooth muscle cells involving the TGFbeta/Notch signalling pathway and increased cell proliferation. *BMC Genomics* **14**, 770 (2013).
56. Baek, K. J., Ji, S., Kim, Y. C. & Choi, Y. Association of the invasion ability of *Porphyromonas gingivalis* with the severity of periodontitis. *Virulence* **6**, 274–281 (2015).
57. Huck, O. *et al*. Identification and Characterization of MicroRNA Differentially Expressed in Macrophages Exposed to *Porphyromonas gingivalis* Infection. *Infect. Immun.* **85** (2017).
58. Mao, S. *et al*. Intrinsic apoptotic pathways of gingival epithelial cells modulated by *Porphyromonas gingivalis*. *Cell. Microbiol.* **9**, 1997–2007 (2007).
59. Al-Taweel, F. B., Douglas, C. W. I. & Whawell, S. A. The Periodontal Pathogen *Porphyromonas gingivalis* Preferentially Interacts with Oral Epithelial Cells in S Phase of the Cell Cycle. *Infect. Immun.* **84**, 1966–1974 (2016).

Acknowledgements
Authors thanks Dr Valérie Demais for her technical help in TEM and SEM experiments. This study was funded by authors institutions and Agence Nationale de la Recherche (ANR ENDOPAROMP). The authors declare no financial and non-financial conflicts of interest related to this study.

Author Contributions
I.M. Bugueno, O. Huck contributed to conception and design, data acquisition, analysis and interpretation, drafted and critically revised the manuscript; F. Batool contributed to data analysis, drafted the manuscript; L. Keller, S. Kuchler-Bopp, N. Benkirane-Jessel contributed to conception and design, critically revised the manuscript. All authors gave final approval and agree to be accountable for all aspects of the work.

Additional Information
Supplementary information accompanies this paper at https://doi.org/10.1038/s41598-018-33267-4.

Competing Interests: The authors declare no competing interests.

Publisher's note: Springer Nature remains neutral with regard to jurisdictional claims in published maps and institutional affiliations.

***Porphyromonas gingivalis* bypasses epithelial barrier and modulates fibroblastic inflammatory response in an *in vitro* 3D spheroid model**

Isaac Maximiliano Bugueno, Fareeha Batool, Laetitia Keller, Sabine Kuchler-Bopp, Nadia Benkirane-Jessel, Olivier Huck

A) Primers		
Gene	**Primer Sequence 5' – 3' (Forward)**	**Primer Sequence 5' – 3' (Reverse)**
Bcl-2 *	--	--
Bax-1 *	--	--
Integrin Β-1 *	--	--
Apaf-1 ^	3'-GTCTGCTGATGGTGCAAGGA-5'	5'-GATGGCCCGTGTGGATTTC-3'
Tnf-α ^	3'-TCTTCTCCTTCCTGATCGTG-5'	5'-GAAGATGATCTGACTGCCTG-3'
Il-6 ^	3'-AATCATCACTGGTCTTTTGGAG-5'	5'-GCATTTGTGGTTGGGTCA-3'
Il-8 ^	3'-GAACCATCTCACTGTGTGTAAA-5'	5'-CACTCCTTGGCAAAACTG-3'
Β-actin ^	3'-TTGGCAATGAGCGGTT-5'	5'AGTTGAAGGTAGTTTCGTGGAT-3'
Col IV	3'-ATGGGGCCCCGGCTCAGC-5'	5'-ATCCTCTTTCACCTTTCAATAGC-3'

B) Antibodies	
Target	**Characteristics**
CYTOKERATIN 14	Santa Cruz Biotechnologies Goat Polyclonal
PAN CYTOKERATIN (AE1.AE3)	Santa Cruz Biotechnologies Goat Polyclonal
INTEGRIN αVΒ1	Chemicon International Alexa Fluor™ 488
LAMININ αV	Santa Cruz Biotechnologies Goat Polyclonal
VIMENTIN	Abcam Rabbit polyclonal
E-CADHERIN	Takara Bio Europe Rat monoclonal
COLLAGEN IV	Santa Cruz Biotechnologies Goat Polyclonal
ANTI-*Pg*	Provided for Dr Richard Lamont, USA Rabbit polyclonal
APAF-1	Thermofischer Rabbit polyclonal
CASPASE-3	Thermofischer Rabbit polyclonal
PHALLOÏDIN	Thermofisher Alexa Fluor™ 594

Supplementary Table 1. (A) Sequence of primers used for real-time quantitative RT-qPCR;

(*) Primer sequences were not provided by the manufacturer. (B) Antibodies used for immunofluorescence staining.

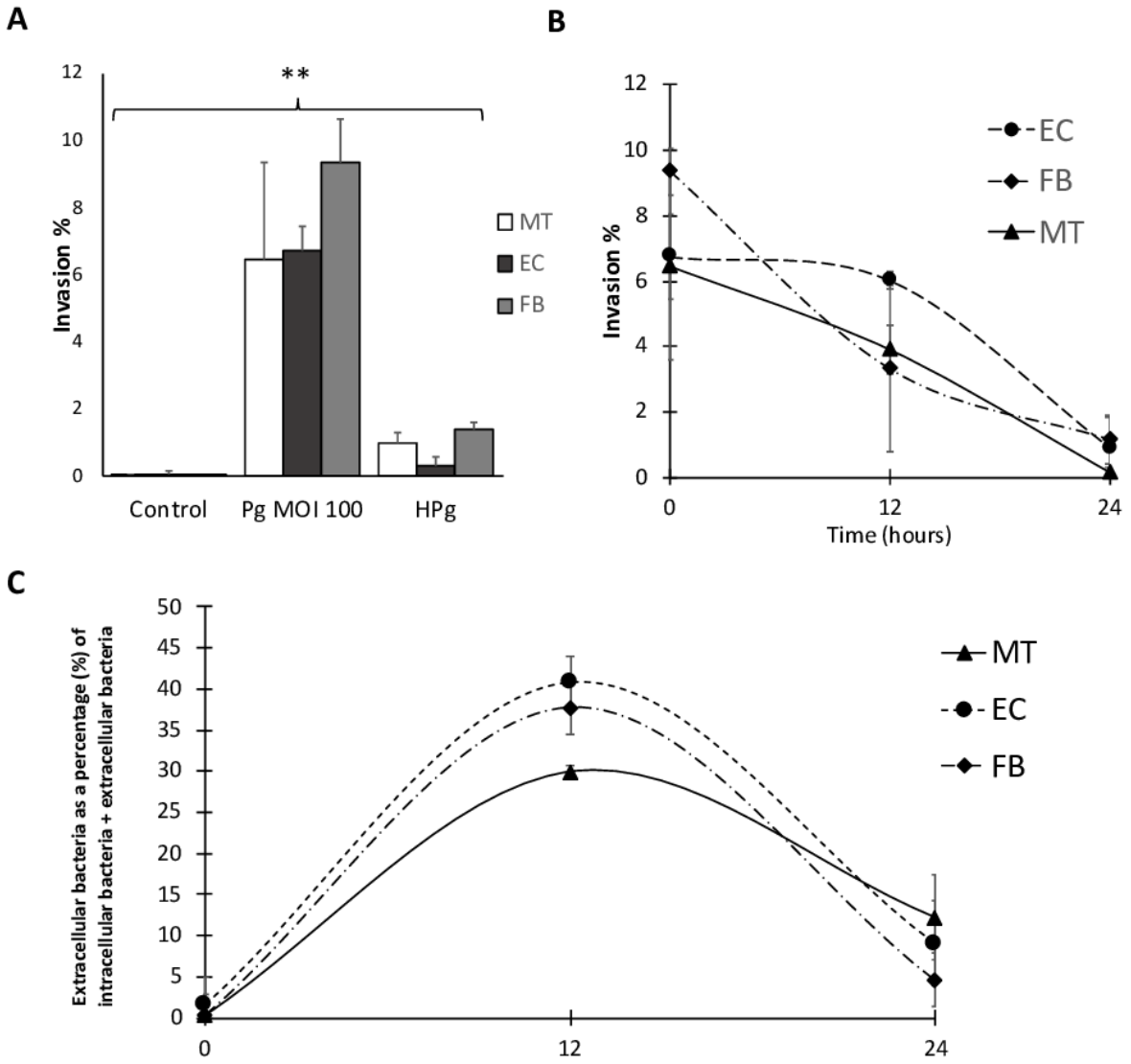

Supplementary Figure 1. Percentage of invasion evaluated by antibiotic protection assay. After monolayers ECs, FBs and MT culture, infection with *P. gingivalis* ATCC 33277 was performed at a multiplicity of infection (MOI) of 100 (for monolayers) or $1*10^7$ bacteria/ml (for MT; determined to be an equivalent of MOI 100 for a total of 10 MT; 1 MT = ~$1*10^4$ cells) suspended in the KSFM culture medium (serum-free medium for keratinocytes, Gibco, PromocellTM, Aachen, Germany) for ECs, in RPMI 1640 medium (Life Technologies, Saint-

Aubin, France) for FBs and in KSFM/RPMI medium (1:1) for MT. After 1.5 (monolayers) or 2h (MT) of infection at 37°C, monolayers and MT were washed three times with PBS to remove non-adherent and external bacteria, then metronidazole (200μg/mL) was added for 1h to kill the external bacteria. Intracellular bacteria were released by osmotic lysis using sterile distillated water and scraping the cells. Just after lysis, the number of bacteria was quantified by TaqMan Real-Time PCR (Suzuki et al., 2005). Primer sequences used were: universal 16S rRNA (Forward, TCC TAC GGG AGG CAG CAG T, Reverse, GGA CTA CCA GGG TAT CTA ATC CTG TT), *P. gingivalis* (Forward, CCT ACG TGT ACG GAC AGA GCT ATA, Reverse, AGG ATC GCT CAG CGT AGC ATT). The number of intracellular bacteria is expressed as the percentage of the infecting inoculum (MOI 100). Graphs show mean and SD of three independent experiments performed in triplicate, $^{**}p < 0.01$.

(A) Invasion of monolayer ECs and FBs, and MT infected with *P. gingivalis* ATCC 33277 and heat-inactivated *P.gingivalis*. (B) The line charts show invasion of monolayer ECs and FBs, and MT, cultured using EC + FB, infected with *P. gingivalis* ATCC 33277 at 0, 12 and 24 hours after antibiotic treatment. (C) The number of bacteria released from the cells on monolayers or MT, which is presented as the percentage of extracellular bacteria of the intracellular + extracellular bacteria estimated by TaqMan Real-Time PCR quantification.

Reference:

Suzuki, N., Yoshida, A. & Nakano, Y. Quantitative analysis of multi-species oral biofilms by TaqMan Real-Time PCR. *Clin. Med. Res.* **3**, 176-185 (2005).

CHAPITRE 4

Impact de *P.gingivalis* sur la modulation des protéines « TIR-domain-containing adaptors» dans la signalisation médiée par les « Toll-like receptors ».

Modulation of TIR-domain-containing adaptors proteins in Toll-like receptor signaling by *P.gingivalis*. **(Article en préparation).**

Contexte et objectifs

La reconnaissance des agents pathogènes dépend en grande partie des récepteurs TLRs et la signalisation intracellulaire n'est déclenchée que par l'activation et le recrutement des adaptateurs contenant le domaine TIR (TIR). On pense que les TLRs sont présentés en dimères et sont pré-assemblés dans un complexe de faible affinité avant la liaison du ligand. Cette dimérisation symétrique va associer les domaines TIR cytosoliques de manière symétrique et les contraindre par conséquent à se réorganiser structurellement, créant ainsi la plateforme de signalisation nécessaire au recrutement d'adaptateurs. Une fois que la signalisation est initiée, chaque adaptateur conduira finalement à l'activation de facteurs de transcription spécifiques (tels que NF-$_K$B ou IRF) (O'Neill et al., 2007).

Le but de cette étude était d'évaluer les effets de l'infection par *P.gingivalis* sur l'expression et les interactions protéine-protéine parmi les cinq protéines adaptatrices TIR, au niveau épithélial et endothélial, dans la recherche de nouvelles cibles thérapeutiques dirigées contre les parodontopathogènes.

Résultats et discussion

Des GEC et des EC ont été cultivées puis infectées par *P.gingivalis* (ATCC 33277) à une MOI 10 et 100 ou stimulées avec son lipopolysaccharide. Les effets de l'infection sur l'inflammation ont été évalués par dosage ELISA (TNF-α). L'expression génique des cinq adaptateurs contenant le domaine TIR (Myd88, MAL, TRIF, TRAM et SARM), de TLR-2, TLR-4 et du suppresseur de la protéine de signalisation de cytokine 1 (SOCS-1) a été évalué par RTqPCR. Enfin, les interactions protéine-protéine de TLR-2/4 et les différents TIR et inhibiteurs (tels que SOCS-1) ont été évalués par co-immunoprécipitation et par WB. Enfin, une transfection de siRNA ciblant les 2 adaptateurs les plus détectés a été réalisée afin d'inhiber leur action.

Après avoir confirmé un effet pro-inflammatoire dans les deux types cellulaires induits par *P.gingivalis*, et caractérisé par une augmentation significative de la sécrétion de TNF-α, nous avons observé une augmentation significative de l'expression de l'ARNm et protéique de MAL, Myd88, TRIF et TRAM, à la fois dans les GEC et les EC. De manière correspondante,

l'expression de TLR-4 et TLR-2 a augmenté significativement tant au niveau de la transcription que de la protéine, dans les deux types cellulaires. L'expression de TLR-4 était significativement plus élevée et était principalement associée à l'interaction protéique avec les adaptateurs MAL -Myd88 et très légèrement au complexe TRIF-TRAM, tant dans les GEC que dans les EC. Enfin, cette activation des protéines TIR, principalement via TLR-4, a conduit à une activation de l'adaptateur SARM et à une inhibition de la protéine SOCS-1 après infection par *P.gingivalis*. Lorsque nous avons réalisé l'inhibition transitoire par siRNA des adaptateurs, la viabilité des cellules, la réponse inflammatoire et la mort cellulaire étaient significativement moins influencées par l'infection par *P.gingivalis* et ses effets délétères étaient quasiment absents lorsque MAL ou TRAM étaient ciblés.

Conclusion

Ce travail permet d'établir que *P.gingivalis* est capable de moduler les cascades de signalisation intracellulaires activées par sa reconnaissance *via* TLR-4/2 dans les GEC et les EC et de moduler l'expression des protéines adaptatrices TIR, associées principalement à la signalisation *via* TLR-4. Cela nous a également permis d'observer que l'interaction protéine-protéine MAL -Myd88 associée à TLR-4 était la principale voie activée lors de l'infection par *P.gingivalis*. Par conséquent, l'infection pourrait moduler deux inhibiteurs de la réponse médiée par les cytokines induites par l'activation des complexes MAL / Myd88 et TRIF/ TRAM, SARM et SOCS-1. Enfin, il pourrait être utile de définir plus précisément le rôle de ces interactions TIR sur la réponse immunitaire de l'hôte dans le contexte des parodontites *in vivo*.

Article en préparation

Title: Modulation of TIR-domain-containing adaptors proteins in Toll-like receptor signaling by *P.gingivalis*.

Periodontal diseases are infectious inflammatory diseases associated to periodontal tissue inflammation and destruction of the tooth-supporting tissues characterized by increased periodontal pocket depth, gingival bleeding and clinical attachment loss. Such diseases impair oral health related quality of life and are considered the main cause of dental mobility and tooth loss [2]. Globally, most children have signs of gingivitis and, among adults, the initial stages of periodontal diseases are prevalent. Severe periodontitis, which may result in tooth loss, is found in around 11% of most populations. This prevalence increases gradually with age with a peak around 38 years of age [3]. Severe periodontitis, affecting individuals during puberty that leads to premature tooth loss, affects about 2% of youth[1].

The development of periodontitis is associated with dysbiotic microbiome characterized by the predominance of anaerobic species, including *Porphyromonas gingivalis* (*P.gingivalis*), and by imbalance with host-immune response directly involved in the periodontal tissue destruction [4]. The first line of host defense challenged by oral pathogens is the epithelial barrier. Once periodontal pathogens manage to disseminate via the systemic circulation, bacteria are also capable of facing the vascular endothelium. The host-bacterial interactions are therefore crucial in the onset and development of periodontitis and its links to systemic diseases. This dysbiotic flora induces an inflammatory response which contributes to the destruction of the periodontal tissues and their systemic dissemination at distance [5–7].

Any alterations in the balance of the oral ecosystem, as well as the pathological process of periodontal pocket formation, will create a favorable environment for the growth of anaerobic microorganisms, such as *P.gingivalis* [8]. Although the precise mechanisms of bacterial

pathogenesis are not entirely described, *P.gingivalis* has been shown to be able to invade, *in vitro*, a range of human epithelial cell lines, as well as to persist and to replicate intracellularly, which would prevent detection by the immune system [9–13]. Given the importance of this step in the infection of *P.gingivalis*, many studies attempted to clarify the mechanisms involved in the internalization of the bacterium by the host cell and those involved in the escape from immune system. Intracellular persistence is a strategy developed by the bacterium to escape the immune response, thus contributing to the pathological process of periodontitis [14,15]. Indeed, *P.gingivalis* is also able to modulate the cell cycle and programmed cell death in order to avoid response of the host cell [16,17,18]. The interaction between gingival epithelial cells (GECs) and periodontal bacteria would determine whether the colonization process would succeed or not. Thus, it has been observed that epithelial invasion of *P.gingivalis* regulates apoptosis and stimulates cell proliferation by modulating several molecular cascades involving p53 and JaK kinase / Stat and Apaf-1 apoptosome [5,9,11,21]. However, the precise mechanisms involved in the entry of this bacterium and the activation of these multiples signaling pathways, remain to be determined.

During the last decades, studies have demonstrated that periodontitis is therefore considered to be part of cardiovascular risk factors in clinical studies [22–24]. Several biological mechanisms have been proposed to explain this link [4,25,26]. The direct influence of bacterial spreading from periodontal pocket on arterial walls homeostasis has been evidenced [27] as periodontal bacteria could be detected in atheromatous plaque samples or in healthy vessels [28,29]. Several works have demostrated that *P.gingivalis* is able to induce pro-inflammatory and pro-atheromatous pathways, *in vitro* [6,30,31] and *in vivo* [32,33] models. In addition, *P.gingivalis* harvest multiple virulence factors contributing to the modulation of the innate immune response through activation of different molecular pathways involved in tissue remodeling, especially through the activation of Toll-Like-Receptors (TLRs) related pathways [2,6,7,30]. Nevertheless, it has also been observed that infection with *P.gingivalis* amplify the inflammation or cell death

in several cell types such as endothelial cells [30] or epithelial cells [9,11,21].

Toll-like receptors (TLRs) play a key role in initiating innate immunity against invading pathogens [34,35]. TLRs activate a potent immunostimulatory response, which induces the expression of pro-inflammatory genes, inflammatory cytokines such as IL-1B, IL-6, TNF-α, NF-$_{K}$B, and other molecules involved in cell death [34,36]. The signal transmitted by TLRs must therefore be tightly controlled, and it is clearly established that if TLRs are over-activated, infectious and inflammatory diseases may develop [37–39]. For instance, antigen O region of the LPS of *P.gingivalis* (*Pg*-LPS) is required to increase the viability of gingival epithelial cells during bacterial infection and this increase is attributable to a reduction of apoptosis [40]. In addition, although bacterial internalization is necessary, the observed effects are not due to alterations in adhesion, invasion, or intracellular survival of *P.gingivalis*. Interestingly, inhibition of apoptosis is correlated with increased TLR-4 expression, suggesting a role for TLR-4 in this process [40,41].

Finally*, P.gingivalis* is able to activate or modulate signaling pathways initiated by TLRs and this represents a crucial role in inflammation and activation and / or inactivation of other processes, such as apoptosis, in different lineages cell. Numerous studies have shown the effects of *P.gingivalis* infection on the activation of pro-inflammatory pathways via TLR-2 and TLR-4 [42,43]. TLRs signaling involves a family of five adapter proteins, which interact with downstream protein kinases and ultimately lead to the activation of transcription factors such as nuclear factor-$_{K}$B (NF-kB) and members of the interferon (IFN) regulatory factor (IRF) [35]. A key signaling domain, unique to the TLRs system, is the Toll / interleukin-1 (IL-1) receptor (TIR) domain, located on the cytosolic side of each TLR as well as in adapters [35,45,46]. Similar to TLRs, adapters are conserved in many species [47]. These adapters are MyD88, MyD88-adaptor-like (MAL, also known as TIRAP), an adapter protein containing an IFN-inducing TIR

domain (TRIF, also known as TICAM1), a molecule TRIF-related adapter (TRAM, also known as TICAM2), and a protein called sterile α- and armadillo-motif-containing protein (MRSA) [45].

The aim of this study was to evaluate the effects of *P.gingivalis* infection on the expression and protein-protein interactions among the five TIR domains in the TLR-2/TLR-4 signalling pathways, in epithelial and endothelial cells.

Materials and methods

Ethics Statement, study population and collection of gingival tissue samples

For the analysis of *ex-vivo* biopsied samples, a total of 19 patients accepted to participate in this study that received approval from Ethic Committee (French Ministry of Research, Bioethic department authorization DC-2014-2220). All patients gave written and informed consent prior to enrollment. Complete medical and dental histories were taken from all the subjects. Criteria for including these patients were considered. None of the patients had systemic diseases or cigarette smoking habit and had not taken any prior medications such as antibiotics in the last 3 months. Clinical periodontal examination included measurement of pocket probing depth and bleeding on probing at six sites around each tooth with a manual periodontal probe. The healthy group (H) consisted of 9 patients (5 males and 4 females, mean age 37.8 +/- 17.3) and the chronic periodontitis group (CP) of 11 patients (4 males and 7 females, mean age 62.4 +/- 7.3). Periodontal diagnosis was based on the past 1999 International World Workshop for a Classification of Periodontal Disease and Conditions [48,49] (Clinical examination of patients during 2015/2016). During periodontal surgeries (open access flap) or 3th molar extractions, gingival biopsied samples were obtained. Biopsies were inserted immediately in a sterile tube and stored at -80°C until RNA extraction.

Porphyromonas gingivalis culture

P.gingivalis strain 33277 (ATCC, Manassas, VA, USA) was cultured under strict anaerobic conditions at 37°C in brain-heart infusion medium (Sigma, Saint-Quentin Fallavier, France) supplemented with hemin (5 mg/ml) and menadione (1 mg/ml). On the day of infection, bacteria were collected and counted as previously described[44].

Cell culture

Human oral epithelial cells (EC) used in this study derived from the TERT-2 OKF-6 cell line (BWH Cell Culture and Microscopy Core, Boston, MA, USA) and were cultured in KSFM culture medium (serum-free medium for keratinocytes, Gibco, PromocellTM, Aachen, Germany) and Human umbilical vein endothelial cells (EC) (C-12200, PromoCell, Heidelberg, Germany) were cultured in EGM2 medium (Promocell, Heidelberg, Germany) supplemented with 10% Fetal Bovine Serum. Culture medium was changed each 3 days and no antibiotics were added to the medium. To reduce the risk of contamination, 100 units/ml of penicillin and 100 µg/ml of streptomycin were added to the KSFM culture medium and no antibiotics were added to the medium for endothelial cells. Both were grown at 37°C in a humidified atmosphere with 5% CO_2, as previously described [9,30].

Infection with P.gingivalis and stimulation with its lipopolysaccharide

For both cell types, *P.gingivalis* strain 33277 (ATCC, Manassas, VA, USA) was cultured under strict anaerobic conditions at 37°C in brain-heart infusion medium (Sigma-Aldrich, Saint-Quentin Fallavier, France) supplemented with hemin (5 mg/ml) and menadione (1 mg/ml) (Sigma-Aldrich). On the day of infection, bacteria were collected and counted as previously described [44]. Twenty-four hours before the experiment, $2x10^5$ cells were seeded in a 24-well plate. At the day of the experiment, GEC and EC were washed twice with PBS and infected for 24h with *P.gingivalis* at a multiplicity of infection (MOI) of 100 or 10. After 2h of infection, medium was removed and cells were washed three times with PBS to remove non-adherent and external bacteria. Then, metronidazole (200µg/mL) was added for 1h to kill the external bacteria and, after washing, fresh bacteria free medium was added in each well. To assess the effect of LPS, cells were stimulated with ultrapure *P.gingivalis* LPS (*Pg*-LPS) (InvivoGen, San Diego, CA, USA) at a concentration of 1 µg/ml for 24h.

RNA isolation, reverse transcription and quantitative Real-time PCR analysis

Total RNAs from samples were extracted using Tri reagent (Sigma-Aldrich) according to the manufacturer's instructions. The total RNA concentration was quantified using NanoDrop 1000 (Fischer Scientific, Illkirch, France). Reverse transcription was performed using iScript Reverse Transcription Supermix (Biorad, Miltry-Mory, France) according to the manufacturer's instructions. To quantify mRNA expression, qPCR was performed on the cDNA samples. PCR amplification and analysis were performed with CFX Connect™ Real-Time PCR Detection System (Biorad, Miltry-Mory, France). Amplification reactions have been performed using iTAq Universal SYBR Green Supermix (Biorad, Miltry-Mory, France). β-actin was used as endogenous RNA control (housekeeping gene) in all samples. Primer related to β-actin, TNF-α, Il-6, TLR-2, TLR-4 and to the 5 TIR (Myd88, Mal, Tram, Trif, Sarm) were synthesized (ThermoFischer, Saint-Aubin, France) (Table 1). Expression level was calculated after normalization to the housekeeping gene expression.

Pull-down assay

For pull-down assay, a tagged or labeled bait protein is coupled to a resin to capture a prey protein contained in the cell lysates. Through this technique, we can identify novel interactions between the known protein (we have chosen the adaptors Mal and Tram) and the others TIR domains (Myd88, Trif, Sarm, TLR-2, TLR-4 or others). The kit used, contains the EZ-Link Sulfo-NHS-LC-Desthiobiotin enzyme to label target proteins on primary amines (Ref: 16138, Thermofisher Scientific, Illkirch-Graffenstaden, France). Desthiobiotin is a biotin analogue that binds to streptavidin with less affinity than biotin. The soft release characteristics of desthiobiotin minimize the isolation of naturally biotinylated molecules that can interfere with results and also eliminate the use of harsh elution conditions that can disassociate complexes and/or damage the target protein or cell. To start, we calculated the appropriate

extent of desthiobiotin labeling and the exact quantity of 10mM EZ-Link Sulfo-NHS-LC-Desthiobiotin required. Then, a buffer exchange into PBS and removal of excess desthiobiotin reagent of the starting samples (initially in an amine-containing buffer) was performed, by desalting the samples in Zeba Spin Desalting Columns 7K (Ref: 89891, Thermofisher). Then the coupling of the desthiobiotinylated Bait protein to the streptavidin resin was performed and this complex was incubated with the cell lysates at least 1 hour to finally elute the desthiobiotinylated bait protein and any captured protein interactions. All the final samples were analysed by SDS-PAGE and stained by Coomassie Blue G-250 was performed (Thermofisher).

Co-immunoprecipitation for the TIR-domain-containing adaptors interaction

To identify interactions between the 5 TIR domains (Myd88, Mal, Trif, Tram, Sarm) and TLR-2 and TLR-4, co-immunoprecipitation using Dynabeads^{TM} Protein G (Thermofisher), was performed. Dynabeads^{TM} Protein G contains 30 mg/mL of magnetic beads in PBS, pH 7.4, with 0.01% Tween^{TM} 20 and 0.09% sodium azide as a preservative. Antibodies for TLR-2 (SC-10741, anti-rabbit, Santa Cruz Biotechnology), TLR-4 (SC-10739, anti-rabbit, Santa Cruz Biotechnology), Myd88 (PA1-9072, anti-goat, Thermofisher), Mal (PA1-12815, anti-rabbit, Thermofisher), Trif (PA5-20030, anti-rabbit, Thermofisher), Tram (PA5-23115, anti-rabbit, Thermofisher) and Sarm (PA5-20059, anti-rabbit, Thermofisher) were added to the Dynabeads^{TM} Protein G, and bind to the magnetic beads via their Fc-region during a short incubation. The tube is placed on a magnet, and the beads adhere to the side of the tube facing the magnet, allowing easy removal of the supernatant. The bead-bound antibodies are then used for immunoprecipitation in presence of cell lysates. Bound material is easily collected utilizing the unique magnetic properties of the Dynabeads^{TM} magnetic beads to be finally analyzed by Western Blotting.

Small Interfering RNA Transfection

One day prior to the transfection, $5x10^6$ of GEC or EC were seeded in a 6-wells plate. Transfection with 5 nM of Silencer™ Select Pre-Designed small interfering RNA (siRNA) targeted against Mal (ID: s195607, Ref: 4392420, Thermofisher), Tram (ID: s51477, Ref: 4392420, Thermofisher) or with negative control (contained in the kit), was performed using Lipofectamine 300 and the Silencer™ siRNA Transfection II Kit (Ref: AM1631, Thermofisher), according to the manufacturer's protocol. Transfected cells were then infected with *P.gingivalis* according to experimental design.

Western blotting

In order to detect protein level of TLR-2, TLR-4, Myd88, Mal, Trif, Tram, Sarm and SOCS-1, western blot was performed. SDS-PAGE followed by immunoblotting were performed in conditions previously described (Elkaim et al., 2008). Briefly, cells were lysed for 5 min on ice in 200 µl of ice-cold RIPA buffer (65 mM Tris–HCl, pH 7.4, 150mM NaCl, and 0.5% sodium deoxycholate) supplemented with phosphatase inhibitor cocktails I and II and a protease inhibitor cocktail (Sigma, Darmstadt, Germany). Lysates were centrifuged at 10,000 g at 4°C for 10min and supernatants were collected or the samples obtained from co-immunoprecipitation assay were used. Both lysates or samples were quantified using the Bradford protein assay (Bio-Rad, Hercules, CA, USA). To perform SDS-PAGE and immunoblotting, 15 to 25µg of proteins were used for each condition. Antibodies against TLR-2 (SC-10741, anti-rabbit, Santa Cruz Biotechnology), TLR-4 (SC-10739, anti-rabbit, Santa Cruz Biotechnology), Myd88 (PA1-9072, anti-goat, Thermofisher), Mal (PA1-12815, anti-rabbit, Thermofisher), Trif (PA5-20030, anti-rabbit, Thermofisher), Tram (PA5-23115, anti-rabbit, Thermofisher), Sarm (PA5-20059, anti-rabbit, Thermofisher) and SOCS-1 (38-5200, Anti-rabbit, Thermofisher) were used. Secondary alkaline phosphatase conjugated antibodies

(anti-goat [1:3000]; anti-rabbit [1:5000]) were purchased from Bethyl Laboratories (Montgomery, Texas, USA) or Thermofisher. All antibodies were used at the dilutions recommended by the manufacturer.

Enzyme-linked immunosorbent assay

In order to detect secreted TNF-α, a sandwich enzyme-linked immunosorbent assay (ELISA) was performed. Briefly, a first step involved attachment of a capture antibody to the microplate (Goat anti-Human TNF-α, PeproTech, Rocky Hill, NJ, USA). Then, samples containing unknown amount of TNF-α were added and bound to the capture antibody. After washing, a detection antibody (Biotinylated Goat anti-Human TNF-α, PeproTech) was added to the wells, and this antibody bind to the immobilized protein captured during the first incubation. Then, washing steps to rid the microplate of unbound non-linked substances and to remove excess detection antibody were performed and an HRP conjugate (streptavidin) was added and bind to the protein-antibodies sandwich. Finally, a substrate solution was added and was converted by the enzyme (HRP) for detection using a spectrophotometer set at 450nm. The intensity of this signal was compared to a standard curve (Recombinant Human TNF-α, PeproTech).

Statistical analysis

Statistical analysis was performed using pair-wise Anova test and post-hoc Tukey's test. Statistical significance level was considered for $p<0.05$. Data were analyzed using PRISM 6.0 (GraphPad, La Jolla, CA, USA). All experiments have been performed at least in triplicate (biological and technical replicates).

Results

P.gingivalis significantly increased TNF-α releasing and inflammatory response in both cell types and in clinical samples

As it has been shown, IL-6 is the major factor involved in the acute phase of the systemic inflammatory response [50]. Accordingly, IL-6 and TNF-α levels are considered reliable indicators of inflammation. TNF-α determines strength, effectiveness and duration of inflammatory reactions [51,52]. Interindividual differences in TNF-α regulation may be critical with respect to the final outcome of an inflammatory response [53]. The pro-inflammatory effect of *P.gingivalis* infection was confirmed in GEC and EC showing a significant increase in TNF-α secretion after 24 hours at MOI 100. The mRNA expression of TNF-α and IL-6 was significantly increased in clinical samples from CP patients in comparison to healthy ones **(Figure n°1)**.

Impact of P.gingivalis in the expression of TLR-2 and TLR-4

As it has been described previously, only two of the TLRs family, TLR-2 and TLR-4, have been identified as the principal signaling receptors for bacterial components [54]. For instance, TLR-4 recognizes LPS from gram-negative bacteria and TLR-2 recognizes a wide variety of PAMP, from both gram-positive and -negative bacteria [55–57]. Recently, the presence of TLR-2 and TLR-4 has been shown to be primordial for the progression of periodontitis in animal models and human patients [58,59]. Regarding the expression of these two TLRs, at the mRNA level, a significant increase was observed in CP group (Fold change 2.8 and 2.2 respectively). Interestingly, TLR-4 and TLR-2 expression increased significantly in both cell types at the transcriptional or protein level **(Figure n°1,2,3).**

Increased mRNA expression of TIR domains in CP patients and in P.gingivalis-infected cells.

After confirming an activation of the TLR-2 and TLR-4 signalling pathways in our cell lines and in the CP group, a significant increase of Myd88, Mal and Tram was observed in patients with periodontitis (Fold changes 2.4, 2.8 and 2.3 respectively). An increased mRNA expression of the five adapters was also observed in both cells types after infection by *P.gingivalis* MOI 100. Interestingly, Mal and Tram showed a high increase in both cell types **(Figure n°1,2)**.

Co-localization of increased expression of TIR domains and TLR-2/TLR-4 in both cells types after P.gingivalis infection

When a component of a gram-negative bacteria, as *P.gingivalis*, is recognized by the TLR-2 and TLR-4, the TIR domains must be activated and linked to the cytosolic internal part of the TLR dimer. Among the five components of this family of TIR domains associated with the response mediated by TLRs, the interaction between Myd88 and Mal, and between Trif and Tram must be evaluated. Therefore, the expression of these different TIR and TLR-2 and 4 was evaluated by immunofluorescence. The expression of Mal / Myd88 and Trif / Tram colocalized with the expression of TLR-2 and TLR-4, after *P.gingivalis* MOI 100 infection, in both types of cells **(Figure n°5 and table 2).**

Mal/Myd88 and Tram/Trif complexes are necessary mainly when TLR-4 signaling pathway is activated after P.gingivalis infection in GEC and EC.

We have observed a significant increase of the TLR-2 and TLR-4 mRNA and protein level in our cells, then both receptors were isolated by immunoprecipitation and we looked into the different protein-protein interactions with each of the 5 TIR domains using Pull-down assay

and Co-IP **(Figure n°5)**. The TLR-2 and TLR-4 activation were mainly associated with the increased Mal and Myd88 adapters interaction and protein expression (evaluated through the presence on the co-immunoprecipitated protein complex) and very slightly with Trif and Tram adapters, both in GEC and EC **(Figure n°5 and table 2)**. Interestingly, the activation of TIR domains, mainly *via* TLR-4, led to an activation of the Sarm adapter and the inhibition of SOCS-1 protein after *P.gingivalis* infection **(Figure n°5 B)**.

Mal and Tram targeted-inhibition was associated with cell protection against P.gingivalis-related effects.

When transient siRNA inhibition of the adapters Mal and/or Tram was achieved **(Figure n°6A)**, *P.gingivalis* infection was not able, respectively, to increase or decrease significantly cell viability in both cell types **(Figure n°6B)**. Further, inflammatory response was significantly decreased in transfected cells following *P.gingivalis* infection **(Figure n°6C)**.

Discussion

As described, different mechanisms associated with periodontal infection in different cell or animal models, have identified novel virulence mechanisms of *P.gingivalis*. This has allowed us to highlight certain mechanisms of invasion and the activation of the inflammatory response at the local periodontal level [5,9] or its systemic association, concerning the endothelium infection, identifying several molecular pathways involved [9,30,33,44]. Here, we demonstrated that this pathogen is able to modulate the cell signaling *via* TLR-2 and TLR-4, through the modulation of the expression of the receptor, as well as different TIR domains adaptors, mainly Mal and Tram. This novel mechanism can represent one of the main pathways associated with the modulation of the inflammatory response, related to the activation of transcription factors, such as NF-KB, the activation of the NLRP3 inflammasome, the secretion of RANK-L and other cytokines and interleukins, such as Il-33 or Il-36 [60,61]. The use of the CRISPR / Cas9 technique on Mal and Tram in GEC and EC will allow us to confirm these results and to propose new molecular targets for future targeted treatments in periodontitis.

This work establishes that *P.gingivalis* is able to modulate the intracellular signaling cascades activated by its recognition via TLR-4 and slightly TLR-2 in GEC and EC and to modulate differentially the expression of TIR domains, mainly associated with TLR-4 signaling pathway. It has also allowed us to observe that TLR-4-associated Mal-Myd88 protein-protein interaction was the primary pathway activated during *P.gingivalis* infection. Therefore, the infection is able to modulate two inhibitors of the cytokine mediated response induced by Mal / Myd88 and Trif / Tram, Sarm and SOCS-1 proteins. Finally, it may be useful to define more precisely the role of these TIR protein-protein interactions on the host immune response in the context of periodontitis pathogenesis, as well as to evaluate therapeutics targeting some of these adapters, such as Mal.

Here, the design of the study may be related to some limitations. The use of a mono-infection model allows us to evaluate in a simplified way, very complex mechanisms implicated in the physiopathology of infectious diseases such as periodontitis. However, it is important to consider the multifactorial aspect of periodontitis and the great bacterial diversity present in the periodontal pocket [2,4,8], in order to get as close as possible to the clinical situation. Thus, complementary experiments taking into account *in vivo* and biofilms assessments, should be carried out in order to corroborate the results observed with *P.gingivalis* infection.

Furthermore, it has been shown that this periodontal pathogen, highly prevalent in patients with severe periodontitis, harvests multiple virulence factors capable of activating inflammation and immune system response, resulting in the destruction of the periodontium. *P.gingivalis* is able to modulate major biological processes in cell life, such as apoptosis, the cell cycle, inflammation, allowing it to escape the immune system [9,11,17,40,41]. All these mechanisms contribute to the development of periodontal lesions and to spreading of the pathogen.

We still need to confirm the observed results on other types of immune cells and polymicrobial infection. Altogether, these results can help us to improve or establish new targeted therapies.

References

1. Petersen, P. E. & Ogawa, H. The global burden of periodontal disease: towards integration with chronic disease prevention and control. *Periodontol. 2000* 60, 15–39 (2012).
2. Hajishengallis, G. & Lamont, R. J. Breaking bad: Manipulation of the host response by *Porphyromonas gingivalis*. *Eur. J. Immunol.* 44, 328–338 (2014).
3. Kassebaum, N. J. *et al.* Global burden of severe periodontitis in 1990-2010: a systematic review and meta-regression. *J. Dent. Res.* 93, 1045–1053 (2014).
4. Hajishengallis, G. Periodontitis: from microbial immune subversion to systemic inflammation. *Nat. Rev. Immunol.* 15, 30–44 (2015).
5. Bugueno, I. M., Batool, F., Korah, L., Benkirane-Jessel, N. & Huck, O. *Porphyromonas gingivalis* Differentially Modulates Apoptosome Apoptotic Peptidase Activating Factor 1 in Epithelial Cells and Fibroblasts. *Am. J. Pathol.* 188, 404–416 (2018).
6. Huck, O., Elkaim, R., Davideau, J.-L. & Tenenbaum, H. *Porphyromonas gingivalis*-impaired innate immune response via NLRP3 proteolysis in endothelial cells. *Innate Immun.* 21, 65–72 (2015).
7. Huck, O. *et al.* Evaluating periodontal risk for patients at risk of or suffering from atherosclerosis: recent biological hypotheses and therapeutic consequences. *Arch. Cardiovasc. Dis.* 104, 352–358 (2011).
8. Abusleme, L. *et al.* The subgingival microbiome in health and periodontitis and its relationship with community biomass and inflammation. *ISME J.* 7, 1016–1025 (2013).
9. Bugueno, I. M., Batool, F., Korah, L., Benkirane-Jessel, N. & Huck, O. *Porphyromonas gingivalis* Differentially Modulates Apoptosome Apoptotic Peptidase Activating Factor 1 in Epithelial Cells and Fibroblasts. *Am. J. Pathol.* (2017). doi:10.1016/j.ajpath.2017.10.014
10. Inaba, H. *et al. Porphyromonas gingivalis* invades human trophoblasts and inhibits proliferation by inducing G1 arrest and apoptosis. *Cell. Microbiol.* 11, 1517–1532 (2009).

11. Mao, S. *et al.* Intrinsic apoptotic pathways of gingival epithelial cells modulated by *Porphyromonas gingivalis*. *Cell. Microbiol.* 9, 1997–2007 (2007).
12. Yilmaz, O. The chronicles of *Porphyromonas gingivalis*: the microbium, the human oral epithelium and their interplay. *Microbiol. Read. Engl.* 154, 2897–2903 (2008).
13. Yilmaz, O., Watanabe, K. & Lamont, R. J. Involvement of integrins in fimbriae-mediated binding and invasion by P*orphyromonas gingivalis. Cell. Microbiol.* 4, 305–314 (2002).
14. Lamont, R. J., Koo, H. & Hajishengallis, G. The oral microbiota: dynamic communities and host interactions. *Nat. Rev. Microbiol.* 16, 745 (2018).
15. Lamont, R. J. & Jenkinson, H. F. Life below the gum line: pathogenic mechanisms of *Porphyromonas gingivalis*. *Microbiol. Mol. Biol. Rev. MMBR* 62, 1244–1263 (1998).
16. Furuta, N., Takeuchi, H. & Amano, A. Entry of *Porphyromonas gingivalis* outer membrane vesicles into epithelial cells causes cellular functional impairment. *Infect. Immun.* 77, 4761–4770 (2009).
17. Pan, C., Xu, X., Tan, L., Lin, L. & Pan, Y. The effects of *Porphyromonas gingivalis* on the cell cycle progression of human gingival epithelial cells. *Oral Dis.* 20, 100–108 (2014).
18. Amano, A. Disruption of epithelial barrier and impairment of cellular function by *Porphyromonas gingivalis. Front. Biosci. J. Virtual Libr.* 12, 3965–3974 (2007).
19. Tribble, G. D. & Lamont, R. J. Bacterial invasion of epithelial cells and spreading in periodontal tissue. *Periodontol. 2000* 52, 68–83 (2010).
20. Tsuda, K. *et al.* Molecular dissection of internalization of *Porphyromonas gingivalis* by cells using fluorescent beads coated with bacterial membrane vesicle. *Cell Struct. Funct.* 30, 81–91 (2005).
21. Kuboniwa, M. *et al. P. gingivalis* accelerates gingival epithelial cell progression through the cell cycle. *Microbes Infect.* 10, 122–128 (2008).

22. Pothineni, N. V. K. *et al.* Infections, atherosclerosis, and coronary heart disease. *Eur. Heart J.* 38, 3195–3201 (2017).

23. Rosenfeld, M. E. & Campbell, L. A. Pathogens and atherosclerosis: update on the potential contribution of multiple infectious organisms to the pathogenesis of atherosclerosis. *Thromb. Haemost.* 106, 858–867 (2011).

24. Tonetti, M. S. *et al.* Treatment of Periodontitis and Endothelial Function. *N. Engl. J. Med.* 356, 911–920 (2007).

25. Liljestrand, J. M. *et al.* Immunologic burden links periodontitis to acute coronary syndrome. *Atherosclerosis* 268, 177–184 (2018).

26. Salhi, L. *et al.* Can Periodontitis Influence the Progression of Abdominal Aortic Aneurysm? A Systematic Review. *Angiology* 70, 479–491 (2019).

27. Zelkha, S. A., Freilich, R. W. & Amar, S. Periodontal innate immune mechanisms relevant to atherosclerosis and obesity. *Periodontol. 2000* 54, 207–221 (2010).

28. Amar, S. & Engelke, M. Periodontal Innate Immune Mechanisms Relevant to Atherosclerosis. *Mol. Oral Microbiol.* 30, 171–185 (2015).

29. Elkaim, R., Werner, S., Kocgozlu, L. & Tenenbaum, H. *P. gingivalis* regulates the expression of Cathepsin B and Cystatin C. *J. Dent. Res.* 87, 932–936 (2008).

30. Bugueno, I. M. *et al. Porphyromonas gingivalis* Differentially Modulates Cell Death Profile in Ox-LDL and TNF-α Pre-Treated Endothelial Cells. *PLoS ONE* 11, (2016).

31. Huck, O. *et al.* Identification and Characterization of MicroRNA Differentially Expressed in Macrophages Exposed to *Porphyromonas gingivalis* Infection. *Infect. Immun.* 85, (2017).

32. Li, L., Messas, E., Batista, E. L., Levine, R. A. & Amar, S. *Porphyromonas gingivalis* infection accelerates the progression of atherosclerosis in a heterozygous apolipoprotein E-deficient murine model. *Circulation* 105, 861–867 (2002).

33. Velsko, I. M. *et al.* Active invasion of oral and aortic tissues by *Porphyromonas gingivalis* in mice causally links periodontitis and atherosclerosis. *PloS One* 9, e97811 (2014).
34. Akira, S. TLR signaling. *Curr. Top. Microbiol. Immunol.* 311, 1–16 (2006).
35. O'Neill, L. A. J. & Bowie, A. G. The family of five: TIR-domain-containing adaptors in Toll-like receptor signalling. *Nat. Rev. Immunol.* 7, 353–364 (2007).
36. Sobrino, T. *et al.* Higher Expression of Toll-Like Receptors 2 and 4 in Blood Cells of Keratoconus Patiens. *Sci. Rep.* 7, 1–7 (2017).
37. Maekawa, T. *et al.* P*orphyromonas gingivalis* manipulates complement and TLR signaling to uncouple bacterial clearance from inflammation and promote dysbiosis. *Cell Host Microbe* 15, 768–778 (2014).
38. Nativel, B. *et al.* P*orphyromonas gingivalis* lipopolysaccharides act exclusively through TLR4 with a resilience between mouse and human. *Sci. Rep.* 7, (2017).
39. Wang, J. *et al.* The functional effects of physical interactions among Toll-like receptors 7, 8, and 9. *J. Biol. Chem.* 281, 37427–37434 (2006).
40. Soto, C. *et al.* The *Porphyromonas gingivalis* O antigen is required for inhibition of apoptosis in gingival epithelial cells following bacterial infection. *J. Periodontal Res.* 51, 518–528 (2016).
41. Díaz, L. *et al.* Changes in lipopolysaccharide profile of *Porphyromonas gingivalis* clinical isolates correlate with changes in colony morphology and polymyxin B resistance. *Anaerobe* 33, 25–32 (2015).
42. Kocgozlu, L., Elkaim, R., Tenenbaum, H. & Werner, S. Variable cell responses to P. gingivalis lipopolysaccharide. *J. Dent. Res.* 88, 741–745 (2009).
43. Singh, A. *et al.* The Capsule of *Porphyromonas gingivalis* Leads to a Reduction in the Host Inflammatory Response, Evasion of Phagocytosis, and Increase in Virulence ▿. *Infect. Immun.* 79, 4533–4542 (2011).

44. Huck, O., Elkaim, R., Davideau, J. l. & Tenenbaum, H. *Porphyromonas gingivalis* and its lipopolysaccharide differentially regulate the expression of cathepsin B in endothelial cells. *Mol. Oral Microbiol.* 27, 137–148 (2012).

45. O'Neill, L. A. J. The interleukin-1 receptor/Toll-like receptor superfamily: 10 years of progress. *Immunol. Rev.* 226, 10–18 (2008).

46. O'Neill, L. A. J., Fitzgerald, K. A. & Bowie, A. G. The Toll-IL-1 receptor adaptor family grows to five members. *Trends Immunol.* 24, 286–290 (2003).

47. Rast, J. P., Smith, L. C., Loza-Coll, M., Hibino, T. & Litman, G. W. Genomic insights into the immune system of the sea urchin. *Science* 314, 952–956 (2006).

48. Armitage, G. C. Development of a classification system for periodontal diseases and conditions. *Ann. Periodontol.* 4, 1–6 (1999).

49. Caton, J. G. *et al.* A new classification scheme for periodontal and peri-implant diseases and conditions – Introduction and key changes from the 1999 classification. *J. Clin. Periodontol.* 45, S1–S8 (2018).

50. Khan, K. *et al.* Clinical and pathological significance of interleukin 6 overexpression in systemic sclerosis. *Ann. Rheum. Dis.* 71, 1235–1242 (2012).

51. Lio, D. *et al.* Inflammation, genetics, and longevity: further studies on the protective effects in men of IL-10 -1082 promoter SNP and its interaction with TNF-alpha -308 promoter SNP. *J. Med. Genet.* 40, 296–299 (2003).

52. Lio, D. *et al.* IL-10 and TNF-alpha polymorphisms and the recovery from HCV infection. *Hum. Immunol.* 64, 674–680 (2003).

53. Giovannini, S. *et al.* Interleukin-6, C-reactive protein, and tumor necrosis factor-alpha as predictors of mortality in frail, community-living elderly individuals. *J. Am. Geriatr. Soc.* 59, 1679–1685 (2011).

54. Takeuchi, O. *et al.* Differential roles of TLR2 and TLR4 in recognition of gram-negative and gram-positive bacterial cell wall components. *Immunity* 11, 443–451 (1999).
55. Beutler, B. Innate immunity: an overview. *Mol. Immunol.* 40, 845–859 (2004).
56. Takeda, K. & Akira, S. Toll-like receptors. *Curr. Protoc. Immunol.* 109, 14.12.1–10 (2015).
57. Willcocks, S., Offord, V., Seyfert, H.-M., Coffey, T. J. & Werling, D. Species-specific PAMP recognition by TLR2 and evidence for species-restricted interaction with Dectin-1. *J. Leukoc. Biol.* 94, 449–458 (2013).
58. Berdeli, A. *et al.* TLR2 Arg753Gly, TLR4 Asp299Gly and Thr399Ile gene polymorphisms are not associated with chronic periodontitis in a Turkish population. *J. Clin. Periodontol.* 34, 551–557 (2007).
59. Song, B. *et al.* The role of Toll-like receptors in periodontitis. *Oral Dis.* 23, 168–180 (2017).
60. Lapérine, O. *et al.* Interleukin-33 and RANK-L Interplay in the Alveolar Bone Loss Associated to Periodontitis. *PLoS ONE* 11, (2016).

Figures and legends

Primers		
Gene	**Forward sequence 5'-3'**	**Reverse sequence 5'-3'**
β-actin	*AAGAGAGGCATCCTCACCCT*	*TACATGGCTGGGGTGTTGAA*
TNF-α	*GGT GCC TAT GTC TCA GCC TCT-*	*CAT CGG CTG GCA CCA CTA GTT*
Tlr2	*TCT GGG CAG TCT TGA ACA TTT*	*AGA GTC AGG TGA TGG ATG TCG*
Tlr4	*CAA GGG ATA AGA ACG CTG AGA*	*GCA ATG TCT CTG GCA GGT GTA*
Il-6	*CCAGCTATGAACTCCTTCTC*	*GCTTGTTCCTCACATCTCTC*
Tirap (Mal)	*CCAGCCTTTCACAGGAGAAG*	*ATATTCGGGATCTGGGGAAG*
Myd88	*GAGCGTTTCGATGCCTTCAT*	*CGGATCATCTCCTGCACAAA*
Trif (Ticam1)	*TGCCTTGAAGCCTTCAGTTATG TGCCTTGAAGCCTTCAGTTATG*	*CCAACCACCACCATGATGAG*
Tram (Ticam2)	*GGGAATTCATAATGGGTATCGGGAAGTC*	*GGCTGCAGGTTATATGTTTCATCTCAGGC*
Sarm	*GCGCGAATTCACTCCAGATGTCTTCATCAGC*	*GGCCTCTAGATTAGCGGCCCTGCAGGAA GCGG*

Table 1. (A) Sequence of primers used for real-time quantitative RT-qPCR.

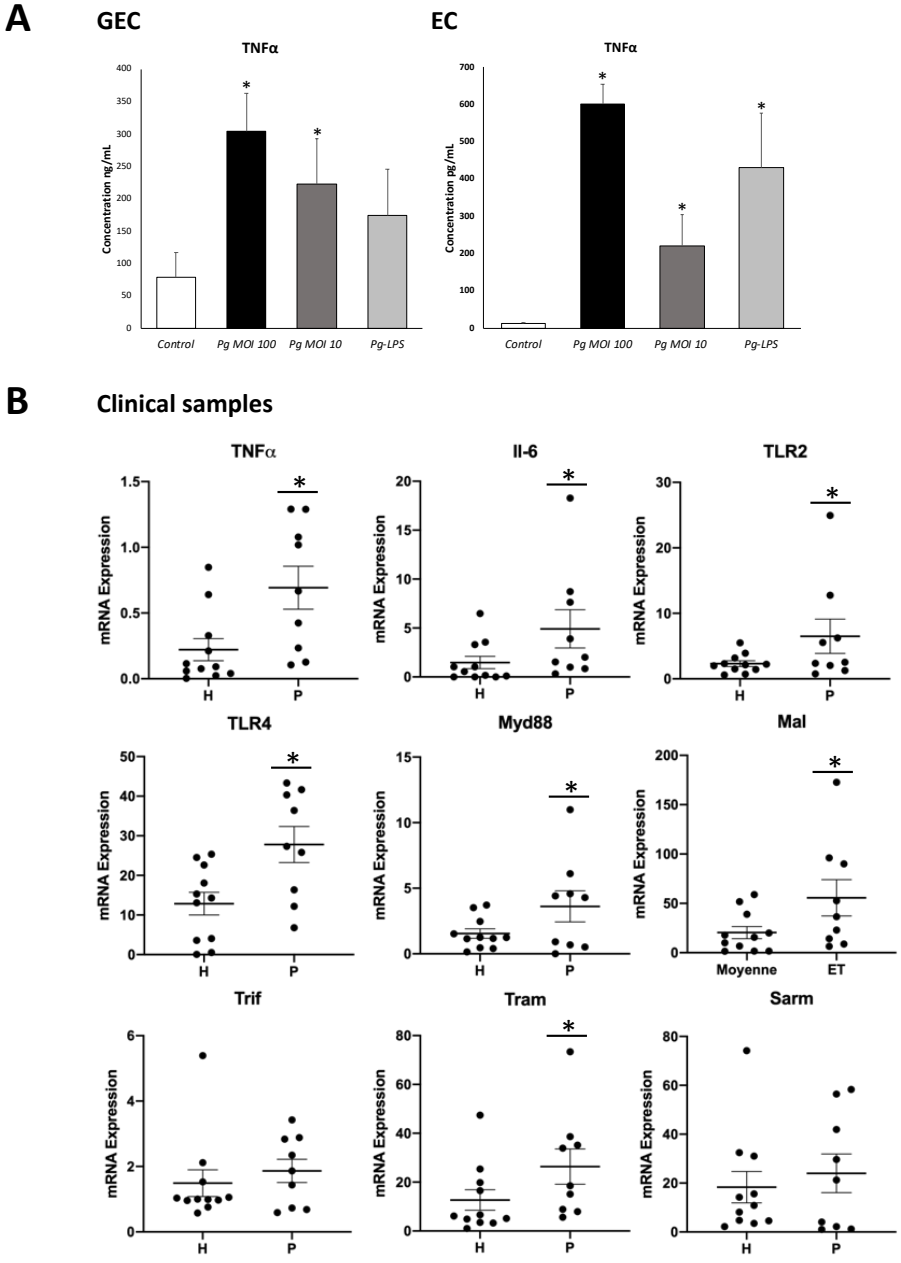

Figure 1. *P. gingivalis* infection induces an inflammatory response *via* TLR-2/TLR-4 and their TIR domains in GEC, EC and clinical samples, correlated to increased gene expression. **(A)** TNF-α secretion in supernatant of GEC and EC, in response to *P.gingivalis* (*Pg*) (MOI:100) for 24 h was measured by ELISA. **(B)** Gene expression of inflammatory response related genes: TNF-α and IL-6 and TLR-2, TLR-4, Myd88, Mal, Trif, Tram and Sarm by RTqPCR from mRNA extracted from chronic periodontitis patients (CP) and healthy patients (H). All data were expressed as the mean mRNA expression normalized with the β-

actin expression ± SD from 3 independent experiments *: p <0.05 between cells infected or stimulated against control (unstimulated cells) or differences between CP and H samples.

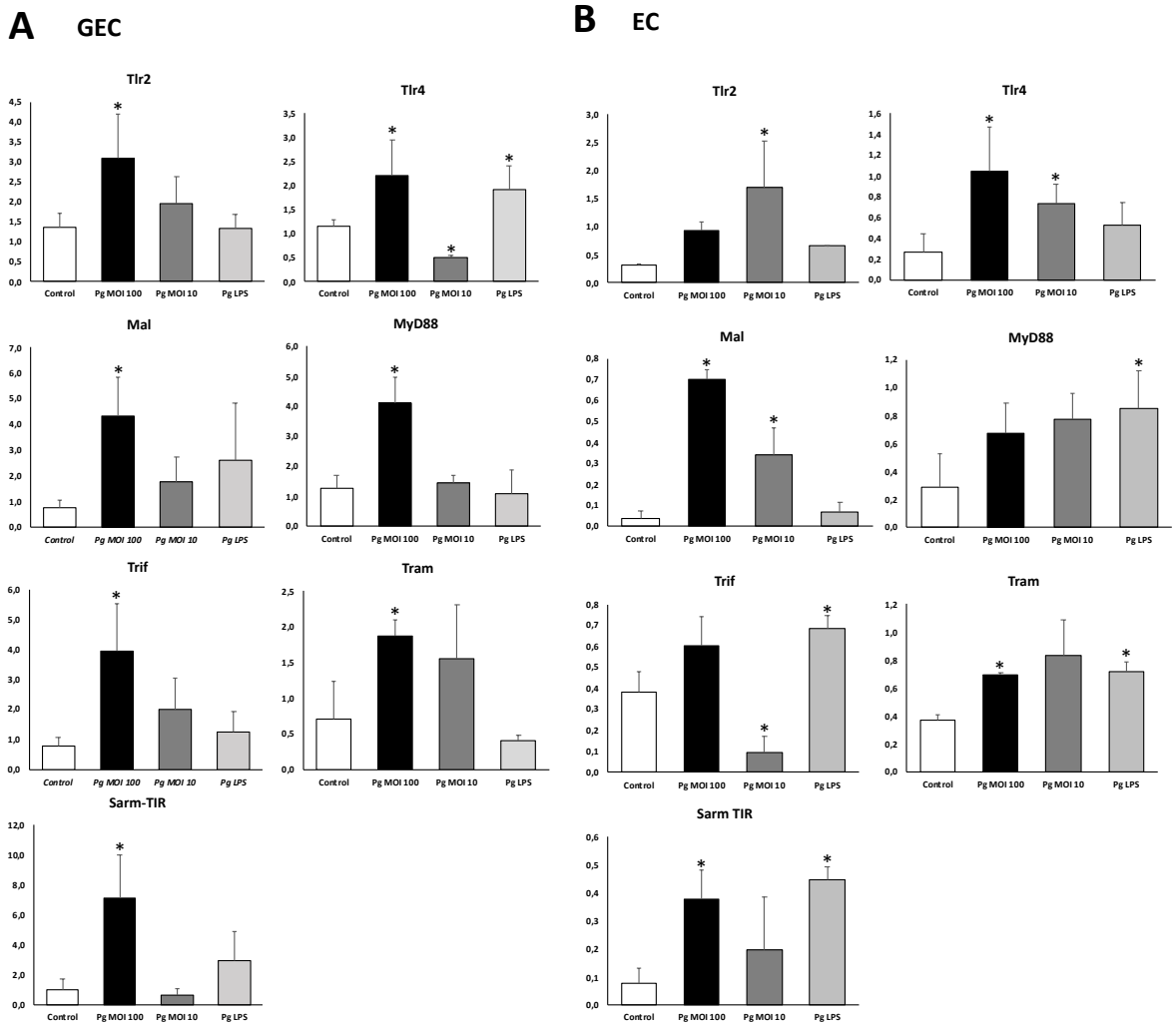

Figure 2. *P.gingivalis* significantly increased mRNA expression of TIR domains in both infected cell types. (A) The mRNA expression of both TLR-2 and TLR-4 and the five TIR domains: Myd88, Mal, Trif, Tram and Sarm in GEC infected with *P.gingivalis* (*Pg*) (MOI:100 and MOI:10) and stimulated with its lipopolysaccharide (*Pg*-LPS, 1µg/mL) for 24 h was measured by qRT-PCR. The mRNA expression of both TLR-2 and TLR-4 and the five TIR domains: Myd88, Mal, Trif, Tram and Sarm in EC infected with *P.gingivalis* (*Pg*) (MOI:100 and MOI:10) and stimulated with its lipopolysaccharide (*Pg*-LPS, 1µg/mL) for 24 h was measured by qRT-PCR.

All data were expressed as the mean mRNA expression normalized with the β-actin expression ± SD from 3 independent experiments *: p <0.05 between cells infected or stimulated against control (unstimulated cells).

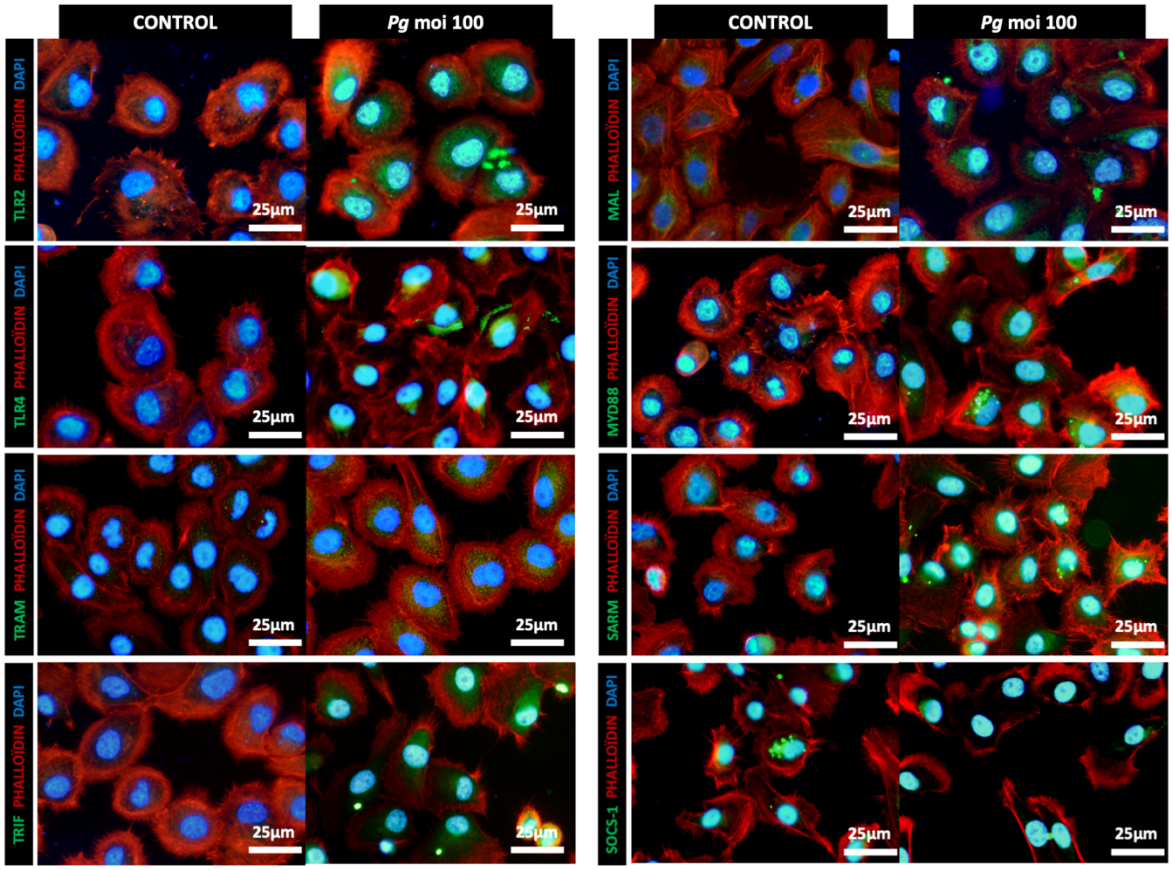

Figure 3. *P.gingivalis* infection induces an increased expression and co-localization of TLR-2, TLR-4 and the five TIR domains. Immunofluorescence staining of uninfected and infected GEC with *P. gingivalis* (*Pg*) (MOI:100) for 24 h. In green: TLR-2, TLR-4, Myd88, Mal, Trif, Tram, Sarm and SOCS-1, in red: Phalloïdin and in blue: DAPI (nuclear staining). All images were acquired at 20x magnification.

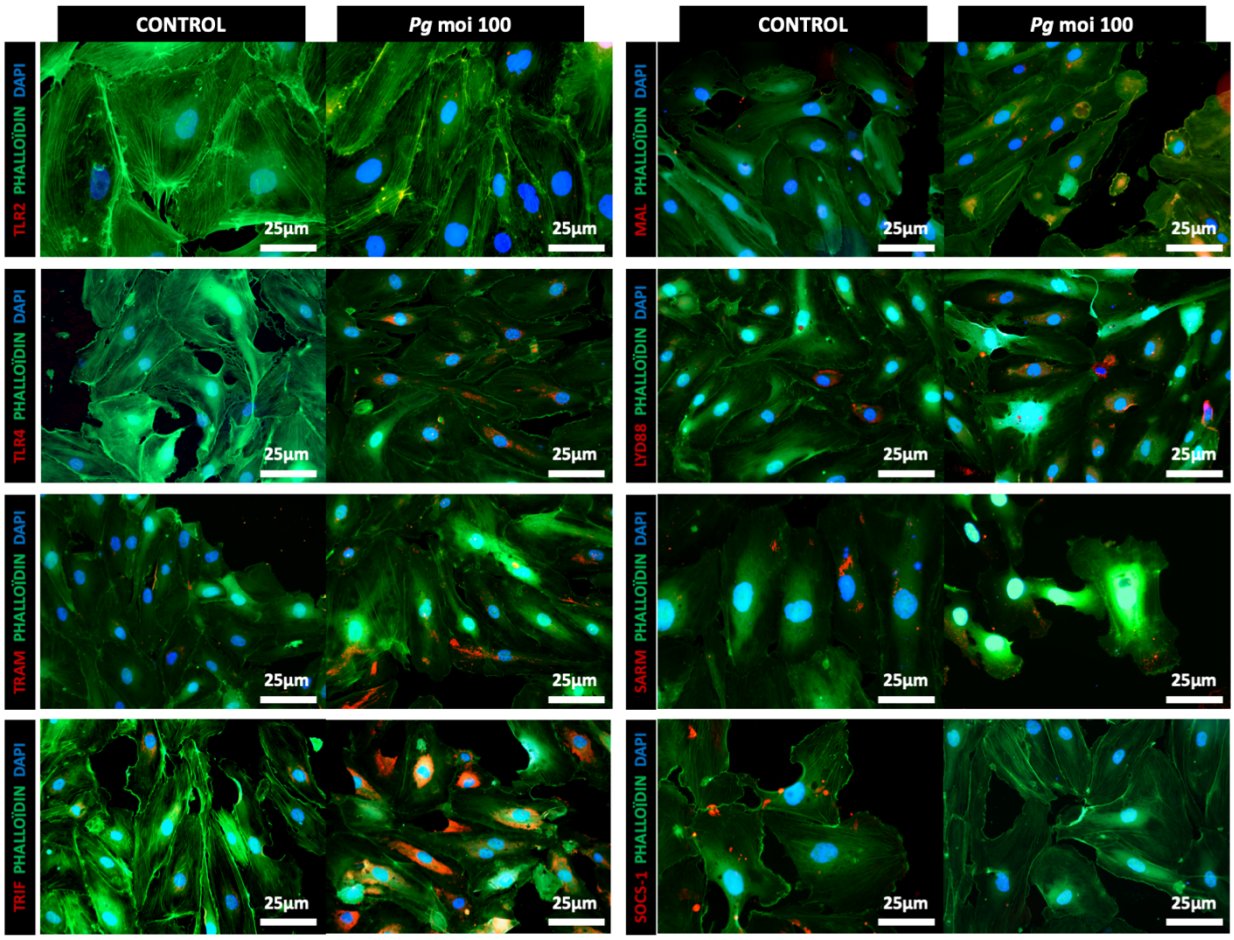

Figure 4. *P.gingivalis* infection induces an increased expression and co-localization of TLR-2, TLR-4 and the five TIR domains. Immunofluorescence staining of uninfected and infected EC with *P. gingivalis* (*Pg*) (MOI:100) for 24 h. In green: TLR2, TLR4, Myd88, Mal, Trif, Tram, Sarm and SOCS-1, in red: Phalloïdin and in blue: DAPI (nuclear staining). All images were acquired at 20x magnification.

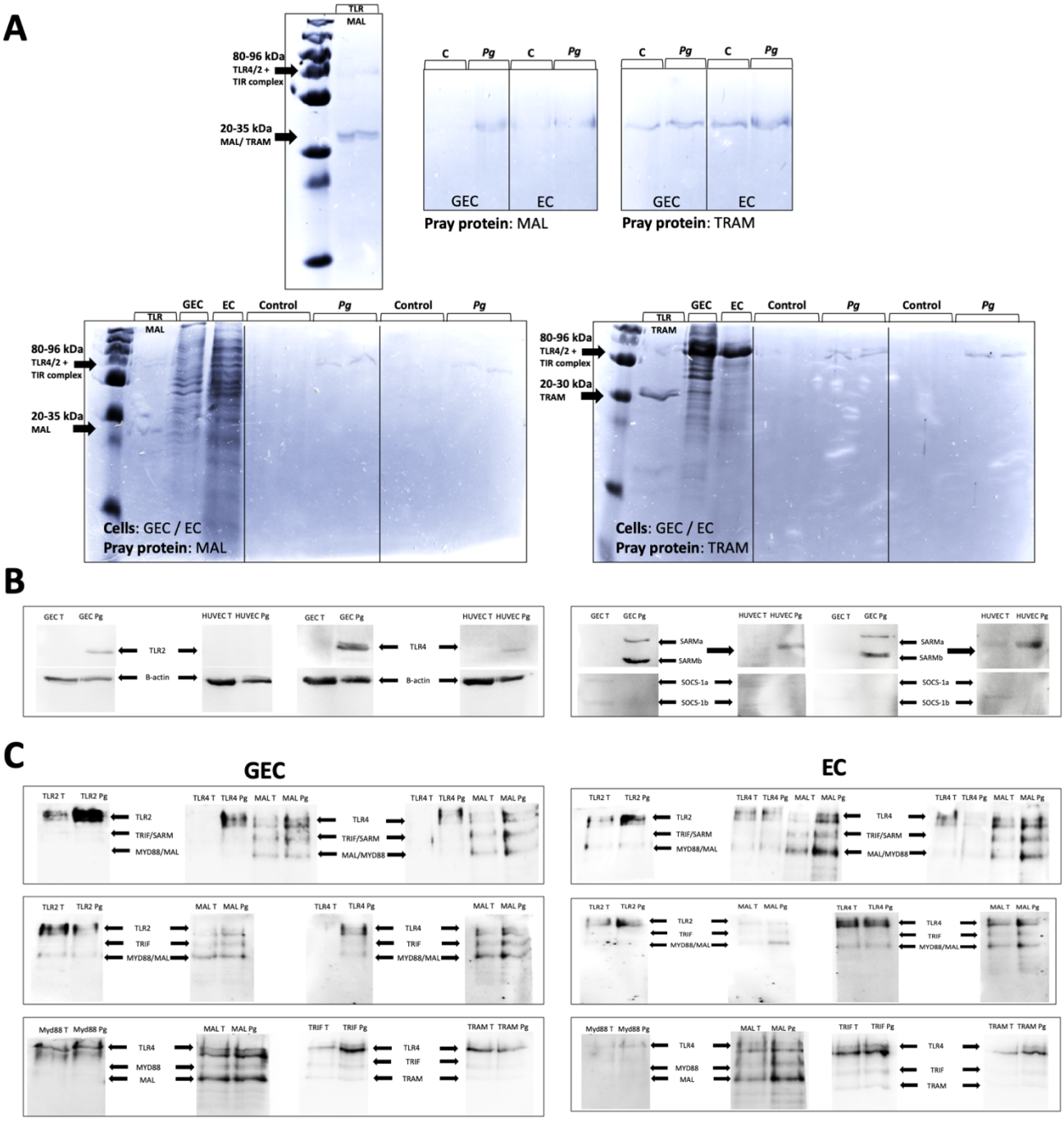

Figure 5. *P.gingivalis* infection activates Mal/Myd88 and Tram/Trif complexes via TLR-4 signaling pathway in GEC and EC. **(A)** Analysis of Pull-down assay of GEC and EC lysates untreated and infected with *P.gingivalis* (*Pg*) (MOI:100), considering the coupling of the desthiobiotinylated bait proteins Mal and Tram to the streptavidin resin. All the final samples are analyzed by SDS-PAGE and stained by Coomassie Blue G-250 after pulling down proteins. (B) Protein expression of TLR-2, TLR-4, Sarm and SOCS-1 in response to

P.gingivalis (*Pg*) (MOI:100) for 24 h was evaluated by Western Blot. All bands were compared and normalized with β-actin expression. (C) Co-immunoprecipitated proteins using Dynabeads™ Protein G, identifying interactions between the five TIR domains (Myd88, Mal, Trif, Tram, Sarm) and TLR-2 and TLR-4, by SDS-PAGE and blotting the protein complexes. On each column of bands, the primary precipitated protein by the capture antibody is indicated in the upper part. Then, in each band, the presence and expression of the different proteins that are interacting at the time of precipitation are indicated with the arrows.

A

GECs				
Protein	Expression From Total cell lysates	CO-IP protein	Expression from Co-IP protein	Conclusion
After *P.gingivalis* MOI 100 infection				
TLR2	Increased ++	TLR2	Increased +++	
		MAL	Increased +	
TLR4	Increased +++	TLR4	Increased +++	
		MAL	Increased ++	
		MYD88	Increased +	
		TRIF	Increased ++	
		TRAM	ND	
MYD88	Increased ++	TLR2	ND	
		TLR4	Increased +	
		MAL	Increased ++	
		MYD88	ND	
MAL/TIRAP		TLR2	ND	
		TLR4	Increased ++	
		MYD88	ND	
		MAL	Increased ++	
TRIF		TLR2	ND	
		TLR4	Increased ++	
		TRIF	Increased +	
		TRAM	ND	
		MAL	Increased +	
TRAM		TRIF	Increased +	
		TRAM	ND	
SARM	Increased +++	ND	ND	
SOCS-1	Decreased -	ND	ND	

B

HUVECs				
Protein	Expression From Total cell lysates	CO-IP protein	Expression from Co-IP protein	Conclusion
After *P.gingivalis* MOI 100 infection				
TLR2	ND	TLR2	Increased ++	
		MAL	Increased +	
TLR4	Increased +++	TLR4	+/-	
		MAL	Increased +++	
		MYD88	Increased ++	
		TRIF	Increased +++	
		TRAM	+/-	
MYD88	Increased ++	TLR2	+/-	
		TLR4	Increased +	
		MAL	Increased ++	
		MYD88	ND	
MAL/TIRAP		TLR2	Increased +	
		TLR4	Increased +	
		MYD88	ND	
		MAL	Increased +++	
TRIF		TLR2	Increased +	
		TLR4	Increased +	
		TRIF	Increased +++	
		TRAM	ND	
		MAL	Increased +	
TRAM		TRIF	Increased +	
		TRAM	Increased +	
SARM	Increased +++	ND	ND	
SOCS-1	Decreased -	ND	ND	

Table 2. (A) Summary of Western Blot, pull-down assay and co-immunoprecipitation results, on GEC (A) and EC (B) lysates untreated and infected with *P.gingivalis* (*Pg*) (MOI:100), for 24 h. All the final samples were analyzed by SDS-PAGE and stained by Coomassie Blue G-250 after pulling down proteins or Western Blot. +++ when the protein was highly increased, ++ when proteins were moderately increased, + when proteins were slightly increased or +/- not significantly increased. ND: not determined.

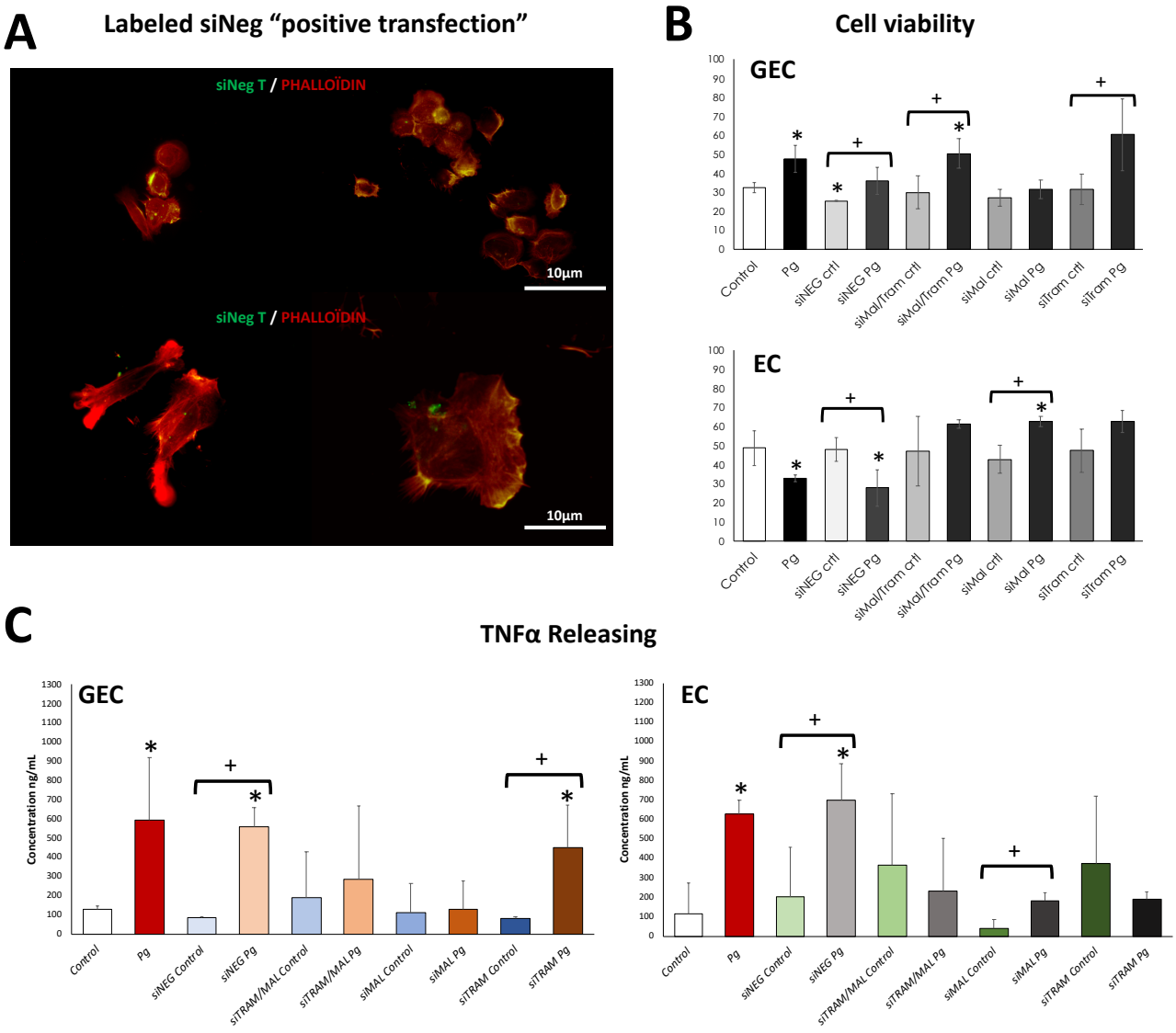

Figure 7. Decrease of P.gingivalis effects on GEC and EC through Mal and Tram targeted-inhibition. (A) Immunofluorescence staining of siRNA trasnfected GEC and EC for 6 to 8 hours. In green: siRNA fluorescence negative control and in red: phalloïdine. All images were acquired at 40x magnification. **(B)** Metabolic activity of GEC and EC transfected with siRNA against Mal, Tram or both and then infected with *P.gingivalis* (*Pg*) at MOI of 100 for 24 hours. **(C)** TNF-α secretion in supernatants of GEC and EC, in response to *P.gingivalis* (*Pg*) (MOI:100) for 24 h was measured by ELISA after trasnfection with siRNA against Mal, Tram or both. $P < 0.05$ for differences between pretreated and nontreated cells.

4. DISCUSSION ET PERSPECTIVES

Les maladies parodontales sont des maladies inflammatoires d'origine infectieuse et multifactorielles représentant un défi dans leur prise en charge tant par leur complexité locale que leur implication systémique. Les théories et les différents modèles évoqués dans l'initiation des lésions parodontales ont évolué rapidement au cours de cette dernière décennie. Bien que les traitements parodontaux soient associés à une amélioration des paramètres cliniques, certaines formes pathologiques, notamment les plus sévères, sont plus difficiles à traiter. La compréhension des mécanismes physiopathologiques impliqués permettrait, à terme, le développement de nouvelles stratégies thérapeutiques. Par exemple, le séquençage à grande échelle du code génétique de l'Homme et d'innombrables espèces, dont les bactéries, ont permis de développer une approche plus personnalisée de prise en charge pour certaines maladies chroniques, infectieuses et / ou inflammatoires. Dans le domaine parodontal, un intérêt grandissant est observé pour l'identification de nouvelles cibles moléculaires spécifiques permettant le développement de thérapies ciblées.

Au cours de cette thèse, différents mécanismes associés à l'infection parodontale dans différents modèles ont permis d'identifier des mécanismes de virulence originels mis en place par *P.gingivalis*. Ceci nous a notamment permis de mettre en évidence certains mécanismes d'invasion, d'activation de la réponse inflammatoire au niveau parodontal et endothélial et d'identifier les voies moléculaires impliquées (Bugueno et al., 2016; Bugueno et al., 2017; Bugueno et al., 2018). L'ensemble de ces données permet de mieux appréhender la pathogénie des parodontites et le rôle clé joué par l'infection. Nous avons pu démontrer le rôle de *P.gingivalis* sur l'apoptose via la modulation de l'apoptosome Apaf-1, via l'induction de molécules pro-apoptotiques, mais également en inhibant les protéines inhibitrices tel que XIAP (Bugueno et al., 2017). Ce pathogène est également capable de moduler la signalisation *via* TLR-2 et TLR-4, à travers la modulation de l'expression du récepteur, ainsi que de ses protéines adaptatrices liées au domaine TIR, principalement MAL et TRAM. Ces dernières pourraient représenter l'une des principales voies associées à la modulation de la réponse inflammatoire, liées à l'activation de facteurs de transcription, tels que NF-$_K$B, l'activation de l'inflammasome NLRP3, la sécrétion de RANK-L et d'autres cytokines et interleukines, telles que Il-33 ou Il-36 (Lapérine et al., 2017; Cloitre et al., 2019). L'utilisation de la technique CRISPR / Cas9 portant sur MAL et TRAM dans les cellules épithéliales et endothéliales, nous permettra de confirmer ces résultats et de proposer de nouvelles cibles moléculaires pour de futurs traitements ciblés dans la parodontite.

D'autre part, nos travaux ont également porté sur l'étude de modèles alternatifs pour l'étude de la physiopathologie des maladies parodontales. Cela nous a permis d'établir un nouveau modèle *in vitro* utile dans l'étude des interactions hôte-pathogène au niveau des tissus mous parodontaux (Bugueno et al., 2018). La mise en place de ce modèle a permis de contrôler la quantité et la distribution des deux types de cellules conduisant à la formation d'un MT bien organisé imitant l'interface épithélium-tissu conjonctif. Ainsi, il nous a permis d'évaluer plus précisément le rôle des interactions GEC-FB dans la réponse immunitaire innée de l'hôte dans le contexte de l'infection par *P.gingivalis* et de confirmer les résultats observés précédemment (Bugueno et al., 2017; Bugueno et al., 2018). Nous poursuivons actuellement ces travaux en établissant un modèle multicellulaire 3D, comportant une partie tissus mous (représentée par les cellules GEC et FB) et une partie tissu dur (l'os) au centre du MT (représentée par des ostéoblastes et une matrice minéralisée).

Enfin, en ce qui concerne la sécrétion autocrine et paracrine des cellules, lors d'un stress cellulaire induit, de nombreuses études ont démontré un rôle pour les MV dans la coagulation sanguine et la thrombose, à la fois *in vitro* et *in vivo* (Nieri et al., 2016). Les MV ont le potentiel de porter sur leur surface et d'inclure dans leur cytoplasme, d'autres molécules dérivées des cellules d'origine, y compris des protéines, de l'ADN, de l'ARN et des microARNs participant à l'entretien de l'homéostasie et à la pathogenèse (Hugel et al., 2005). Les MV ont rapidement été considérées comme des biomarqueurs et des cibles potentielles pour des interventions thérapeutiques et plus récemment comme des effecteurs pathogènes (Dignat-George et al., 2011). Récemment, il a été proposé que le rôle pathogène associé à l'infection pourrait être la répercussion de la réponse cellulaire paracrine médiée par certaines cytokines mais également par certaines EMV. Dans nos travaux, nous avons pu démontrer un lien entre la réponse cellulaire paracrine des cellules endothéliales *in vitro* et l'infection par *P.gingivalis*. En conséquence, il est possible d'établir que les EMV peuvent être considérées comme des structures complexes impliquées dans les mécanismes précoces de souffrance endothéliale mais également dans l'établissement d'une réaction inflammatoire. Différents mécanismes cellulaires de réparation, de défense et de maintien de l'homéostasie sont continuellement activés au cours de la vie. Ils permettent d'établir un équilibre temporaire face aux agressions successives endogènes et exogènes. L'endothélium vasculaire est dynamique et très sensible au stress oxydant. Nous pouvons donc proposer que *P.gingivalis* et les EMVs produites par l'infection ont un effet de stress important sur l'endothélium pouvant contribuer au développement et à la maturation de la plaque d'athérome. De ce fait, afin de mieux comprendre

les mécanismes impliqués dans l'altération de la fonction endothéliale au niveau vasculaire, il devient intéressant d'étudier les MVs générées i*n vivo* dans des conditions physiopathologiques, par exemple, dans un modèle expérimental d'athérosclérose chez la souris ApoE -/-, des souris développant des lésions athérosclérotiques spontanées. Au final, la connaissance de la composition des MV circulantes et de leurs effets biologiques *in vivo* restent certes encore insuffisantes, mais les nombreux travaux en cours, qui tendent à une meilleure compréhension de ces mécanismes, permettront dans un avenir proche l'utilisation en routine des MVs en clinique voire en thérapeutique.

Dans l'ensemble de nos travaux, nous avons choisi d'étudier l'impact de *P.gingivalis*. L'utilisation d'une mono-infection comme modèle d'étude nous permet d'évaluer de manière simplifiée les mécanismes pouvant entrer en jeu dans la pathologie. Cependant, il est important de prendre en compte l'aspect multifactoriel des parodontites et la grande diversité bactérienne présente au niveau du microbiote parodontal (Hajishengallis et al., 2012 ; Abusleme et al., 2013), ceci afin de se rapprocher au plus près de la situation clinique. Ainsi, des expériences complémentaires prenant en compte des modèles pluribactériens et des biofilms devront être effectuées afin de corroborer les résultats observés avec *P.gingivalis*.

Il est également important de considérer que même si ces travaux effectués nous ont permis de suggérer une réponse à plusieurs hypothèses relatives à l'infection parodontale, les types de cellules utilisés pourraient également être considérés comme une limite. En effet, les réponses observées au niveau de la barrière épithéliale, du tissu conjonctif ou de l'endothélium (représentées dans les monocultures de GEC / FB et EC), peuvent être considérées comme restreintes du fait de la diversité des types cellulaires retrouvée au niveau parodontal ou vasculaire **(Figure n°18)**. Par exemple, l'étude des effets au niveau des voies de signalisation TLRs et l'activation de processus tels que l'apoptose ou la sécrétion de MVs dans d'autres types de cellules du système immunitaire, comme les macrophages, les lymphocytes ou les neutrophiles, permettrait d'appréhender la problématique dans sa globalité et sa complexité.

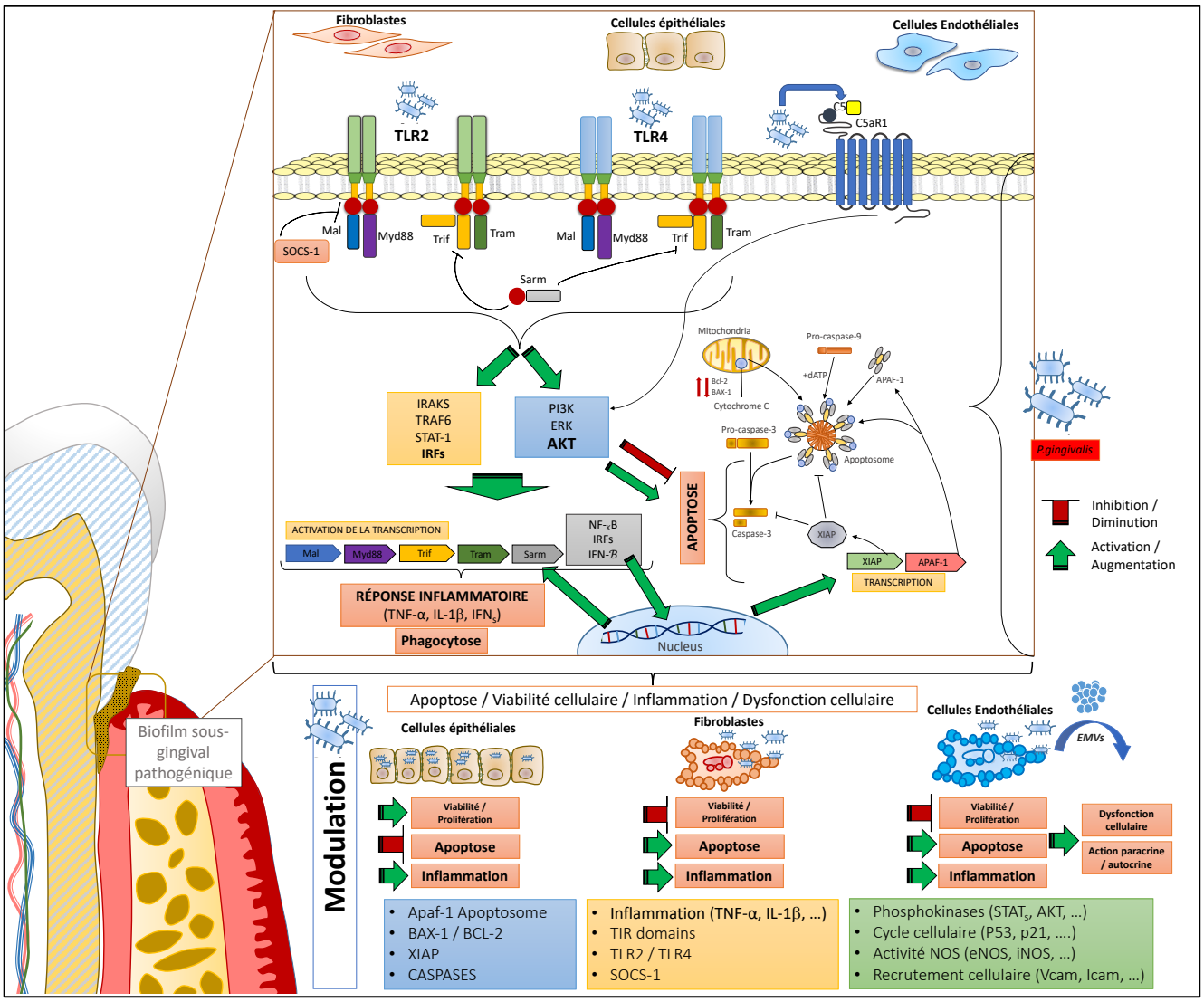

Figure n°18. Schéma des mécanismes moléculaires modulés par *P.gingivalis*.

5. CONCLUSIONS

L'ensemble des travaux effectués au cours de cette thèse nous a permis d'approfondir nos connaissances concernant l'impact de *P.gingivalis* sur la réponse cellulaire et moléculaire.

Premièrement, il a été démontré que ce parodontopathogène, de prévalence élevée chez les patients atteints de parodontite sévère, possède des facteurs de virulence multiples capables d'activer l'inflammation et la réponse du système immunitaire, entraînant la destruction du parodonte. *P.gingivalis* est capable de moduler différemment des processus biologiques primordiaux dans la vie cellulaire, tels que l'apoptose, le cycle cellulaire, l'inflammation, lui permettant d'échapper au système immunitaire. L'ensemble de ces mécanismes contribuent au développement de la lésion parodontale et à la dissémination du pathogène. Ces résultats ont aussi été validés dans un nouveau modèle 3D de MT *in vitro*, tout en validant le modèle lui-même, ses avantages sur les cellules cultivées en monocouche et en même temps, c'est qui nous a permis d'étudier la réponse inflammatoire des cellules face à l'infection par *P.gingivalis*, en présence d'une matrice extracellulaire et au contact d'autres cellules tri-dimensionnellement, ce qui est encore plus proche des modèles *in vivo*.

Ainsi, *P.gingivalis* est capable de se propager *via* la circulation sanguine, d'envahir l'endothélium et de franchir cette barrière, en modulant l'apoptose, en augmentant l'inflammation et en modulant plusieurs voies de signalisation liées à la fonction endothéliale, de façon directe (l'infection bactérienne) ou indirecte, par action cellulaire autocrine et paracrine (EMV libérées lors de l'infection). Ce mécanisme original met l'accent sur la relation entre la parodontite, la propagation systémique d'agents pathogènes oraux et leur participation à la physiopathologie de maladies systémiques telle que l'athérosclérose.

Ces travaux restent pour la plupart des études *in vitro*, même si beaucoup d'entre eux ont été confirmés dans un modèle 3D des MT, dans un modèle expérimental de la parodontite expérimentale chez la souris et dans les biopsies gingivales de patients atteints ou non de parodontite. Nous devons encore confirmer ces effets sur d'autres types de cellules immunitaires et en utilisant un modèle d'infection polymicrobienne. Ensemble, ces résultats peuvent nous aider à améliorer ou à établir de nouvelles thérapies ciblées, lors de la régénération parodontale guidée et / ou encore mieux en envisageant des traitements préventifs.

6. RÉFÉRENCES

1. Abusleme, L., Dupuy, A.K., Dutzan, N., Silva, N., Burleson, J.A., Strausbaugh, L.D., Gamonal, J., Diaz, P.I. The subgingival microbiome in health and periodontitis and its relationship with community biomass and inflammation (2013). ISME J. 7, 1016–1025.
2. Achilli, T.-M., Meyer, J. & Morgan, J. R. Advances in the formation, use and understanding of multi-cellular spheroids (2012). *Expert Opin. Biol. Ther.* **12**, 1347–1360.
3. Akcali, A., Huck, O., Tenenbaum, H., Davideau, J.L., Buduneli, N. Periodontal diseases and stress: a brief review (2013). J. Oral Rehabil. 40, 60–68.
4. Akira, S. TLR signaling (2006). Curr. Top. Microbiol. Immunol. 311, 1–16.
5. Amano, A. Disruption of epithelial barrier and impairment of cellular function by *Porphyromonas gingivalis* (2007). Front. Biosci. J. Virtual Libr. 12, 3965–3974.
6. Amar, S., Engelke, M. Periodontal Innate Immune Mechanisms Relevant to Atherosclerosis (2015). Mol. Oral Microbiol. 30, 171–185.
7. Amelian, A., Wasilewska, K., Megias, D. & Winnicka, K. Application of standard cell cultures and 3D *in vitro* tissue models as an effective tool in drug design and development (2017). *Pharmacol. Rep.* **69**, 861–870.
8. Andrian, E., Grenier, D. & Rouabhia, M. *In vitro* models of tissue penetration and destruction by *Porphyromonas gingivalis* (2004). *Infect. Immun.* 72, 4689–4698.
9. Angelillo-Scherrer, A. Leukocyte-derived microparticles in vascular homeostasis (2012). Circ. Res. 110, 356–369.
10. Antoni, D., Burckel, H., Josset, E. & Noel, G. Three-dimensional cell culture: a breakthrough *in vivo* (2015). *Int. J. Mol. Sci.* **16**, 5517–5527 (2015).
11. Armitage, G.C. Periodontal diagnoses and classification of periodontal diseases (2004). Periodontol. 2000 34, 9–21.
12. Armitage, G.C. Development of a classification system for periodontal diseases and conditions (1999). Ann. Periodontol. 4, 1–6.
13. Artegiani, B. & Clevers, H. Use and application of 3D-organoid technology (2018). *Hum. Mol. Genet*. 1;27(R2):R99-R107
14. Auriol. Histologie du parodonte (2000). EMC Chirurgie orale et maxillo-faciale Doi : 10.1016/S1283-0852(13)55778-8
15. Asman, B., Gustafsson, A., Bergström, K. Gingival crevicular neutrophils: membrane molecules do not distinguish between periodontitis and gingivitis (1997). J. Clin. Periodontol. 24, 927–931.
16. Barros, S.P., Williams, R., Offenbacher, S., Morelli, T. Gingival Crevicular as a Source of Biomarkers for Periodontitis (2016). Periodontol. 2000 70, 53–64.
17. Bécavin, T. *et al*. Well-organized spheroids as a new platform to examine cell interaction and behaviour during organ development (2016). *Cell Tissue Res.* **366**, 601–615.
18. Bell, J.K., Askins, J., Hall, P.R., Davies, D.R., Segal, D.M. The dsRNA binding site of human Toll-like receptor 3 (2006). Proc. Natl. Acad. Sci. U. S. A. 103, 8792–8797.
19. Berglundh, T., Lindhe, J., Ericsson, I., Marinello, C.P., Liljenberg, B., Thomsen, P. The soft tissue barrier at implants and teeth (1991). Clin. Oral Implants Res. 2, 81–90.
20. Birck, M.M., Saraste, A., Hyttel, P., Odermarsky, M., Liuba, P., Saukko, P., Hansen, A.K., Pesonen, E. Endothelial cell death and intimal foam cell accumulation in the

coronary artery of infected hypercholesterolemic minipigs (2013). J Cardiovasc. Transl. Res. 6, 579–587.
21. Birgersdotter, A., Sandberg, R. & Ernberg, I. Gene expression perturbation *in vitro*–a growing case for three-dimensional (3D) culture systems (2005). *Semin. Cancer Biol.* 15, 405–412.
22. Bosshardt, D.D. The periodontal pocket: pathogenesis, histopathology and consequences (2018). Periodontol. 2000 76, 43–50.
23. Bosshardt, D.D., Lang, N.P. The junctional epithelium: from health to disease (2005). J. Dent. Res. 84, 9–20.
24. Bosshardt, D.D., Schroeder, H.E. Initiation of acellular extrinsic fiber cementum on human teeth. A light- and electron-microscopic study (1991). Cell Tissue Res. 263, 311–324.
25. Bostanci, N., Belibasakis, G.N. *Porphyromonas gingivalis*: an invasive and evasive opportunistic oral pathogen (2012). FEMS Microbiol. Lett. 333, 1–9.
26. Bourgeois, D., Bouchard, P., Mattout, C. Epidemiology of periodontal status in dentate adults in France, 2002–2003 (2007). J. Periodontal Res. 42, 219–227.
27. Bratton, S.B., Salvesen, G.S. Regulation of the Apaf-1–caspase-9 apoptosome (2010). J. Cell Sci. 123, 3209–3214.
28. Bratton, S.B., Walker, G., Srinivasula, S.M., Sun, X.M., Butterworth, M., Alnemri, E.S., Cohen, G.M. Recruitment, activation and retention of caspases-9 and -3 by Apaf-1 apoptosome and associated XIAP complexes (2001). EMBO J. 20, 998–1009.
29. Brozovic, S., Sahoo, R., Barve, S., Shiba, H., Uriarte, S., Blumberg, R.S., Kinane, D.F. *Porphyromonas gingivalis* enhances FasL expression via up-regulation of NFkappaB-mediated gene transcription and induces apoptotic cell death in human gingival epithelial cells (2006). Microbiol. Read. Engl. 152, 797–806.
30. Brunelle, J.K., Letai, A. Control of mitochondrial apoptosis by the Bcl-2 family (2009). J. Cell Sci. 122, 437–441.
31. Bugueno, I.M., Khelif, Y., Seelam, N., Morand, D.-N., Tenenbaum, H., Davideau, J.-L., Huck, O (2016). *Porphyromonas gingivalis* Differentially Modulates Cell Death Profile in Ox-LDL and TNF-α Pre-Treated Endothelial Cells. PLoS ONE 11.
32. Buhlin, K., Gustafsson, A., Håkansson, J., Klinge, B. Oral health and cardiovascular disease in Sweden (2002). J. Clin. Periodontol. 29, 254–259.
33. Byrne, S.J., Dashper, S.G., Darby, I.B., Adams, G.G., Hoffmann, B., Reynolds, E.C. Progression of chronic periodontitis can be predicted by the levels of *Porphyromonas gingivalis* and Treponema denticola in subgingival plaque (2009). Oral Microbiol. Immunol. 24, 469–477.
34. Cain, K. Chemical-Induced Apoptosis: Formation of the Apaf-1 Apoptosome (2003). Drug Metab. Rev. 35, 337–363.
35. Casarin, R.C.V., Ribeiro, E.D.P., Mariano, F.S., Nociti, F.H., Casati, M.Z., Gonçalves, R.B. Levels of *Aggregatibacter actinomycetemcomitans, Porphyromonas gingivalis,* inflammatory cytokines and species-specific immunoglobulin G in generalized aggressive and chronic periodontitis (2010). J. Periodontal Res. 45, 635–642.

36. Castrillo, A., Pennington, D.J., Otto, F., Parker, P.J., Owen, M.J., Boscá, L. Protein kinase Cepsilon is required for macrophage activation and defense against bacterial infection (2001). J. Exp. Med. 194, 1231–1242.
37. Caton, J.G., Armitage, G., Berglundh, T., Chapple, I.L.C., Jepsen, S., Kornman, K.S., Mealey, B.L., Papapanou, P.N., Sanz, M., Tonetti, M.S. A new classification scheme for periodontal and peri-implant diseases and conditions – Introduction and key changes from the 1999 classification (2018). J. Clin. Periodontol. 45, S1–S8.
38. Chaddad, H. *et al*. Combining 2D angiogenesis and 3D osteosarcoma microtissues to improve vascularization (2017). *Exp. Cell Res.* **15**, 138–145.
39. Chavrier, C. Elastic system fibers of healthy human gingiva (1990). J. Parodontol. 9, 29–34.
40. Choi, Y. S., Kim, Y. C., Ji, S. & Choi, Y. Increased bacterial invasion and differential expression of tight-junction proteins, growth factors, and growth factor receptors in periodontal lesions (2013). *J. Periodontol.* 85, e313–322.
41. Choy, J.C., Granville, D.J., Hunt, D.W., McManus, B.M. Endothelial cell apoptosis: biochemical characteristics and potential implications for atherosclerosis (2001). J. Mol. Cell. Cardiol. 33, 1673–1690.
42. Costalonga, M., Herzberg, M.C. The oral microbiome and the immunobiology of periodontal disease and caries (2014). Immunol. Lett. 162, 22–38.
43. Crawford, J.M., Hopp, B. Junctional epithelium expresses the intercellular adhesion molecule ICAM-1 (1990). J. Periodontal Res. 25, 254–256.
44. Dabija-Wolter, G., Bakken, V., Cimpan, M. R., Johannessen, A. C. & Costea, D. E. *In vitro* reconstruction of human junctional and sulcular epithelium (2013). J. Oral Pathol. Med. Off. Publ. Int. Assoc. Oral Pathol. Am. Acad. Oral Pathol. 42, 396–404.
45. Dale, B.A. Periodontal epithelium: a newly recognized role in health and disease (2002). Periodontol. 2000 30, 70–78.
46. Degterev, A., Boyce, M., Yuan, J. A decade of caspases (2003). Oncogene 22, 8543–8567.
47. Díaz, L., Hoare, A., Soto, C., Bugueño, I., Silva, N., Dutzan, N., Venegas, D., Salinas, D., Pérez-Donoso, J.M., Gamonal, J., Bravo, D. Changes in lipopolysaccharide profile of *Porphyromonas gingivalis* clinical isolates correlate with changes in colony morphology and polymyxin B resistance (2015). Anaerobe 33, 25–32.
48. Dignat-George, F., Boulanger, C.M. The Many Faces of Endothelial Microparticles (2011). Arterioscler. Thromb. Vasc. Biol. 31, 27–33.
49. Dimmeler, S. Cardiovascular disease review series (2011). EMBO Mol. Med. 3, 697.
50. Dunn, S.R., Schnitzler, C.E., Weis, V.M. Apoptosis and autophagy as mechanisms of dinoflagellate symbiont release during cnidarian bleaching: every which way you lose (2007). Proc. R. Soc. B Biol. Sci. 274, 3079–3085.
51. El-Awady, A.R., Lapp, C.A., Gamal, A.Y., Sharawy, M.M., Wenger, K.H., Cutler, C.W., Messer, R.L.W. Human periodontal ligament fibroblast responses to compression in chronic periodontitis (2013). J. Clin. Periodontol. 40, 661–671.
52. El-Awady, A.R., Messer, R.L.W., Gamal, A.Y., Sharawy, M.M., Wenger, K.H., Lapp, C.A. Periodontal Ligament Fibroblasts Sustain Destructive Immune Modulators of Chronic Periodontitis (2010). J. Periodontol. 81, 1324–1335.

53. Elkaim, R., Werner, S., Kocgozlu, L., Tenenbaum, H. P. gingivalis regulates the expression of Cathepsin B and Cystatin C (2008). J. Dent. Res. 87, 932–936.
54. Elmore, S. Apoptosis: A Review of Programmed Cell Death (2007). Toxicol. Pathol. 35, 495–516.
55. Fadeel, B., Orrenius, S. Apoptosis: a basic biological phenomenon with wide-ranging implications in human disease (2005). J. Intern. Med. 258, 479–517.
56. Filipowska, J., Tomaszewski, K.A., Niedźwiedzki, Ł., Walocha, J.A., Niedźwiedzki, T. The role of vasculature in bone development, regeneration and proper systemic functioning (2017). Angiogenesis 20, 291–302.
57. Florencio-Silva, R., Sasso, G.R. da S., Sasso-Cerri, E., Simões, M.J., Cerri, P.S. Biology of Bone Tissue: Structure, Function, and Factors That Influence Bone Cells (2015). BioMed Res. Int. 2015.
58. Foster, B.L., Ao, M., Salmon, C.R., Chavez, M.B., Kolli, T.N., Tran, A.B., Chu, E.Y., Kantovitz, K.R., Yadav, M., Narisawa, S., Millán, J.L., Nociti, F.H., Somerman, M.J. Osteopontin regulates dentin and alveolar bone development and mineralization (2018). Bone 107, 196–207.
59. Furuta, N., Takeuchi, H., Amano, A. Entry of *Porphyromonas gingivalis* outer membrane vesicles into epithelial cells causes cellular functional impairment (2009). Infect. Immun. 77, 4761–4770.
60. Goodson, J.M., 2003. Gingival crevice fluid flow (2003). Periodontol. 2000 31, 43–54.
61. Graves, D. T., Fine, D., Teng, Y. A., Van Dyke, T. E. & Hajishengallis, G. The Use of Rodent Models to Investigate Host-Bacteria Interactions Related to Periodontal Diseases (2008). *J. Clin. Periodontol.* 35, 89–105.
62. Graves, D.T., Kang, J., Andriankaja, O., Wada, K., Rossa, C. Animal Models to Study Host-Bacteria Interactions Involved in Periodontitis (2012). Front. Oral Biol. 15, 117–132.
63. Greenberg, E.F., McColl, K.S., Zhong, F., Wildey, G., Dowlati, A., Distelhorst, C.W. Synergistic killing of human small cell lung cancer cells by the Bcl-2-inositol 1,4,5-trisphosphate receptor disruptor BIRD-2 and the BH3-mimetic ABT-263 (2015). Cell Death Dis. 6, e2034–e2034.
64. Griffin, C.J. Vascular hyperplasia of the periodontal membrane (1965). Aust. Dent. J. 10, 121–125.
65. Griffin, C.J., Harris, R. Innervation of human periodontium. I. Classification of periodontal receptors (1974a). Aust. Dent. J. 19, 51–56.
66. Griffin, C.J., Harris, R. Innervation of human periodontium. I. Classification of periodontal receptors (1974b). Aust. Dent. J. 19, 51–56.
67. Griffin, C.J., Spain, H. Organization and vasculature of human periodontal ligament mechanoreceptors (1972). Arch. Oral Biol. 17, 913–921.
68. Gruenheid, S., Finlay, B.B. Microbial pathogenesis and cytoskeletal function (2003). Nature 422, 775–781.
69. Gupta, S., Kass, G.E.N., Szegezdi, E., Joseph, B.. The mitochondrial death pathway: a promising therapeutic target in diseases (2009). J. Cell. Mol. Med. 13, 1004–1033. https://doi.org/10.1111/j.1582-4934.2009.00697.x

70. Haffajee, A.D., Socransky, S.S. Microbiology of periodontal diseases: introduction (2005). Periodontol. 2000 38, 9–12.
71. Hajishengallis, G. Periodontitis: from microbial immune subversion to systemic inflammation (2015a). Nat. Rev. Immunol. 15, 30–44.
72. Hajishengallis, G. Periodontitis: from microbial immune subversion to systemic inflammation (2015b). Nat. Rev. Immunol. 15, 30–44.
73. Hajishengallis, G., Lamont, R.J. Breaking bad: Manipulation of the host response by *Porphyromonas gingivalis* (2014). Eur. J. Immunol. 44, 328–338.
74. Hajishengallis, G., Lamont, R.J. Beyond the red complex and into more complexity: the polymicrobial synergy and dysbiosis (PSD) model of periodontal disease etiology (2012). Mol. Oral Microbiol. 27, 409–419.
75. Handfield, M., Mans, J.J., Zheng, G., Lopez, M.C., Mao, S., Progulske-Fox, A., Narasimhan, G., Baker, H.V., Lamont, R.J. Distinct transcriptional profiles characterize oral epithelium-microbiota interactions (2005). Cell. Microbiol. 7, 811–823.
76. Hienz, S.A., Paliwal, S., Ivanovski, S. Mechanisms of Bone Resorption in Periodontitis (2015). J. Immunol. Res. 2015, 615486.
77. Higa, K., Satake, Y., Shimazaki, J. The characterization of human oral mucosal fibroblasts and their use as feeder cells in cultivated epithelial sheets (2017). Future Sci. OA 3(4), FSO243.
78. Ho, J.-T., Wu, J., Huang, H.-L., Chen, M.Y., Fuh, L.-J., Hsu, J.-T. Trabecular bone structural parameters evaluated using dental cone-beam computed tomography: cellular synthetic bones (2013). Biomed. Eng. OnLine 12, 115.
79. Hopkins, P.N. Molecular biology of atherosclerosis (2013). Physiol. Rev. 93, 1317–1542.
80. Horng, T., Barton, G.M., Flavell, R.A., Medzhitov, R. The adaptor molecule TIRAP provides signalling specificity for Toll-like receptors (2002). Nature 420, 329–333.
81. How, K.Y., Song, K.P., Chan, K.G. *Porphyromonas gingivalis*: An Overview of Periodontopathic Pathogen below the Gum Line (2016). Front. Microbiol. 9;7:53.
82. Hristov, M., Erl, W., Linder, S., Weber, P.C. Apoptotic bodies from endothelial cells enhance the number and initiate the differentiation of human endothelial progenitor cells *in vitro* (2004). Blood 104, 2761–2766.
83. Huck, O., Elkaim, R., Davideau, J. l., Tenenbaum, H. *Porphyromonas gingivalis* and its lipopolysaccharide differentially regulate the expression of cathepsin B in endothelial cells (2012). Mol. Oral Microbiol. 27, 137–148.
84. Huck, O., Elkaim, R., Davideau, J.-L., Tenenbaum, H. *Porphyromonas gingivalis*-impaired innate immune response via NLRP3 proteolysis in endothelial cells (2015). Innate Immun. 21, 65–72.
85. Huck, O., Saadi-Thiers, K., Tenenbaum, H., Davideau, J.-L., Romagna, C., Laurent, Y., Cottin, Y., Roul, J.G. Evaluating periodontal risk for patients at risk of or suffering from atherosclerosis: recent biological hypotheses and therapeutic consequences (2011). Arch. Cardiovasc. Dis. 104, 352–358.
86. Huynh, J., Scholz, G.M., Aw, J., Reynolds, E.C. Interferon Regulatory Factor 6 Promotes Keratinocyte Differentiation in Response to *Porphyromonas gingivalis* (2017). Infect. Immun. 85, e00858-16.

87. Inaba, H., Kuboniwa, M., Bainbridge, B., Yilmaz, Ö., Katz, J., Shiverick, K.T., Amano, A., Lamont, R.J. *Porphyromonas gingivalis* invades human trophoblasts and inhibits proliferation by inducing G1 arrest and apoptosis (2009). Cell. Microbiol. 11, 1517–1532.
88. Jain, M., Kasetty, S., Udyavara Sridhara, S., Jain, N., Khan, S., Desai, A. Apoptosis and Its Significance in Oral Diseases: An Update (2013). J. Oral Dis 13; 401049: 11.
89. Jeyaseelan, S., Manzer, R., Young, S.K., Yamamoto, M., Akira, S., Mason, R.J., Worthen, G.S. Toll-IL-1 Receptor Domain-Containing Adaptor Protein Is Critical for Early Lung Immune Responses against *Escherichia coli* Lipopolysaccharide and Viable *Escherichia coli* (2005). J. Immunol. 175, 7484–7495.
90. Jönsson, D., Nebel, D., Bratthall, G., Nilsson, B.-O. The human periodontal ligament cell: a fibroblast-like cell acting as an immune cell (2011). J. Periodontal Res. 46, 153–157.
91. Jung, H., Jung, S.M., Rim, Y.A., Park, N., Nam, Y., Lee, J., Park, S.-H., Ju, J.H. Arthritic role of *Porphyromonas gingivalis* in collagen-induced arthritis mice (2017). PLoS ONE 30;12(11):e0188698.
92. Karki, R., Kim, S.-B., Kim, D.-W.. Magnolol inhibits migration of vascular smooth muscle cells via cytoskeletal remodeling pathway to attenuate neointima formation (2013). Exp. Cell Res. 319, 3238–3250.
93. Karring, T., Lang, N.P., Löe, H. The role of gingival connective tissue in determining epithelial differentiation (1975). J. Periodontal Res. 10, 1–11.
94. Kassebaum, N.J., Bernabé, E., Dahiya, M., Bhandari, B., Murray, C.J.L., Marcenes, W. Global burden of severe periodontitis in 1990-2010: a systematic review and meta-regression (2014). J. Dent. Res. 93, 1045–1053.
95. Katafuchi, M., Matsuura, T., Atsawasuwan, P., Sato, H., Yamauchi, M. Biochemical characterization of collagen in alveolar mucosa and attached gingiva of pig (2007). Connect. Tissue Res. 48, 85–92.
96. Kelm, J. M., Timmins, N. E., Brown, C. J., Fussenegger, M. & Nielsen, L. K. Method for generation of homogeneous multicellular tumor spheroids applicable to a wide variety of cell types (2003). Biotechnol. Bioeng. **83**, 173–180.
97. Kim, K., Lee, C.H., Kim, B.K., Mao, J.J. Anatomically Shaped Tooth and Periodontal Regeneration by Cell Homing (2010). J. Dent. Res. 89, 842–847.
98. Kocgozlu, L., Elkaim, R., Tenenbaum, H., Werner, S. Variable cell responses to P. gingivalis lipopolysaccharide (2009). J. Dent. Res. 88, 741–745.
99. Koeppel, M., Garcia-Alcalde, F., Glowinski, F., Schlaermann, P., Meyer, T.F. *Helicobacter pylori* Infection Causes Characteristic DNA Damage Patterns in Human Cells (2015). Cell Rep. 11, 1703–1713.
100. Koga, H., Sugiyama, S., Kugiyama, K., Watanabe, K., Fukushima, H., Tanaka, T., Sakamoto, T., Yoshimura, M., Jinnouchi, H., Ogawa, H. Elevated levels of VE-cadherin-positive endothelial microparticles in patients with type 2 diabetes mellitus and coronary artery disease (2005). J. Am. Coll. Cardiol. 45, 1622–1630.
101. Kooijman, R. Regulation of apoptosis by insulin-like growth factor (IGF)-I (2006). Cytokine Growth Factor Rev. 17, 305–323.

102. Korah, L., Amri, N., Valdebenito, I.M.B., Hotton, D., Tenenbaum, H., Huck, O., Berdal, A., Davideau, J.-L. Experimental periodontitis in Msx2 mutant mice induces alveolar bone necrosis (2019). J. Periodontol. https://doi.org/10.1002/JPER.16-0435
103. Kuboniwa, M., Hasegawa, Y., Mao, S., Shizukuishi, S., Amano, A., Lamont, R.J., Yilmaz, O. *P. gingivalis* accelerates gingival epithelial cell progression through the cell cycle (2008). Microbes Infect. 10, 122–128.
104. Kuchler-Bopp, S. *et al*. Three-dimensional Micro-culture System for Tooth Tissue Engineering (2016). *J. Dent. Res.* **95**, 657–664.
105. Lalla Evanthia, Lamster Ira B., Hofmann Marion A., Bucciarelli Loredana, Jerud Adrienne P., Tucker Sid, Lu Yan, Papapanou Panos N., Schmidt Ann Marie. Oral Infection With a Periodontal Pathogen Accelerates Early Atherosclerosis in Apolipoprotein E–Null Mice (2003). Arterioscler. Thromb. Vasc. Biol. 23, 1405–1411.
106. Lamont, R.J., Jenkinson, H.F. Life below the gum line: pathogenic mechanisms of *Porphyromonas gingivalis* (1998). Microbiol. Mol. Biol. Rev. MMBR 62, 1244–1263.
107. Lamont, R.J., Koo, H., Hajishengallis, G. The oral microbiota: dynamic communities and host interactions (2018). Nat. Rev. Microbiol. 16, 745.
108. Lapérine, O., Cloitre, A., Caillon, J., Huck, O., Bugueno, I.M., Pilet, P., Sourice, S., Le Tilly, E., Palmer, G., Davideau, J.-L., Geoffroy, V., Guicheux, J., Beck-Cormier, S., Lesclous, P. Interleukin-33 and RANK-L Interplay in the Alveolar Bone Loss Associated to Periodontitis (2016). PLoS ONE 11(12): e0168080.
109. Lawen, A. Apoptosis-an introduction (2003). BioEssays News Rev. Mol. Cell. Dev. Biol. 25, 888–896.
110. Ledgerwood, E.C., Morison, I.M. Targeting the Apoptosome for Cancer Therapy (2009). Clin. Cancer Res. 15, 420–424.
111. Lee, H.-H., Paudel, K.R., Kim, D.-W. Terminalia chebula Fructus Inhibits Migration and Proliferation of Vascular Smooth Muscle Cells and Production of Inflammatory Mediators in RAW 264.7 (2015). Evid.-Based Complement. Altern. Med. ECAM ;2015:502182.
112. Lézot, F., Davideau, J.-L., Thomas, B., Sharpe, P., Forest, N., Berdal, A. Epithelial Dlx-2 Homeogene Expression and Cementogenesis (2000). J. Histochem. Cytochem. 48, 277–283.
113. Liljestrand, J.M., Paju, S., Pietiäinen, M., Buhlin, K., Persson, G.R., Nieminen, M.S., Sinisalo, J., Mäntylä, P., Pussinen, P.J. Immunologic burden links periodontitis to acute coronary syndrome (2018). Atherosclerosis 268, 177–184.
114. Linden, G.J., Lyons, A., Scannapieco, F.A. Periodontal systemic associations: review of the evidence (2013). J. Clin. Periodontol. 40 Suppl 14, S8-19.
115. Lockhart, P.B., Bolger, A.F., Papapanou, P.N., Osinbowale, O., Trevisan, M., Levison, M.E., Taubert, K.A., Newburger, J.W., Gornik, H.L., Gewitz, M.H., Wilson, W.R., Smith, S.C., Baddour, L.M., American Heart Association Rheumatic Fever, Endocarditis, and Kawasaki Disease Committee of the Council on Cardiovascular Disease in the Young, Council on Epidemiology and Prevention, Council on Peripheral Vascular Disease, and Council on Clinical Cardiology (2012). Periodontal disease and atherosclerotic vascular disease: does the evidence support an independent association?:

a scientific statement from the American Heart Association. Circulation 125, 2520–2544.
116. Loesche, W.J., Grossman, N.S. Periodontal Disease as a Specific, albeit Chronic, Infection: Diagnosis and Treatment (2001). Clin. Microbiol. Rev. 14, 727–752.
117. Lopez, A., Dooner, J.J., Porter, K. Histologic Study of Elastin-Like Fibers in the Attached Gingiva (1976). J. Periodontol. 47, 444–449.
118. Lorencini, M., Silva, J. a. F., Almeida, C.A., Bruni-Cardoso, A., Carvalho, H.F., Stach-Machado, D.R. A new paradigm in the periodontal disease progression: gingival connective tissue remodeling with simultaneous collagen degradation and fibers thickening (2009). Tissue Cell 41, 43–50.
119. Madianos, P.N., Papapanou, P.N., Sandros, J. *Porphyromonas gingivalis* infection of oral epithelium inhibits neutrophil transepithelial migration (1971). Infect. Immun. 65, 3983–3990.
120. Maekawa, T., Krauss, J.L., Abe, T., Jotwani, R., Triantafilou, M., Triantafilou, K., Hashim, A., Hoch, S., Curtis, M.A., Nussbaum, G., Lambris, J.D., Hajishengallis, G. *Porphyromonas gingivalis* manipulates complement and TLR signaling to uncouple bacterial clearance from inflammation and promote dysbiosis (2014). Cell Host Microbe 15, 768–778.
121. Mahanonda, R., Seymour, G.J., Powell, L.W., Good, M.F., Halliday, J.W. Effect of initial treatment of chronic inflammatory periodontal disease on the frequency of peripheral blood T-lymphocytes specific to periodontopathic bacteria (1991). Oral Microbiol. Immunol. 6, 221–227.
122. Maiolino, G., Rossitto, G., Caielli, P., Bisogni, V., Rossi, G.P., Calò, L.A. The role of oxidized low-density lipoproteins in atherosclerosis: the myths and the facts (2013). Mediators Inflamm. 2013, 714653.
123. Mao, S., Park, Y., Hasegawa, Y., Tribble, G.D., James, C.E., Handfield, M., Stavropoulos, M.F., Yilmaz, O., Lamont, R.J. Intrinsic apoptotic pathways of gingival epithelial cells modulated by *Porphyromonas gingivalis* (2007). Cell. Microbiol. 9, 1997–2007.
124. Markiewicz, M., Richard, E., Marks, N., Ludwicka-Bradley, A. Impact of Endothelial Microparticles on Coagulation, Inflammation, and Angiogenesis in Age-Related Vascular Diseases (2013). J. Aging Res. 2013, e734509.
125. McGettrick, A.F., Brint, E.K., Palsson-McDermott, E.M., Rowe, D.C., Golenbock, D.T., Gay, N.J., Fitzgerald, K.A., O'Neill, L.A.J. Trif-related adapter molecule is phosphorylated by PKCε during Toll-like receptor 4 signaling (2006). Proc. Natl. Acad. Sci. U. S. A. 103, 9196–9201.
126. Mori, G., D'Amelio, P., Faccio, R., Brunetti, G. Bone-Immune Cell Crosstalk: Bone Diseases (2015). J. Immunol. Res. 2015:108451.
127. Moutsopoulos, N.M., Konkel, J.E. Tissue-Specific Immunity at the Oral Mucosal Barrier (2018). Trends Immunol. 39, 276–287.
128. Murray, D.A., Wilton, J.M.A. Lipopolysaccharide from the Periodontal Pathogen *Porphyromonas gingivalis* Prevents Apoptosis of HL60-Derived Neutrophils *In Vitro* (2003). Infect. Immun. 71, 7232–7235.

129. Naiki, Y., Michelsen, K.S., Zhang, W., Chen, S., Doherty, T.M., Arditi, M. Transforming growth factor-beta differentially inhibits MyD88-dependent, but not TRAM- and TRIF-dependent, lipopolysaccharide-induced TLR4 signaling (2005). J. Biol. Chem. 280, 5491–5495.
130. Nakhjiri, S.F., Park, Y., Yilmaz, O., Chung, W.O., Watanabe, K., El-Sabaeny, A., Park, K., Lamont, R.J. Inhibition of epithelial cell apoptosis by *Porphyromonas gingivalis* (2001). FEMS Microbiol. Lett. 200, 145–149.
131. Napoli, C. Oxidation of LDL, atherogenesis, and apoptosis (2003). Ann. N. Y. Acad. Sci. 1010, 698–709.
132. Nativel, B., Couret, D., Giraud, P., Meilhac, O., d'Hellencourt, C.L., Viranaïcken, W., Da Silva, C.R. *Porphyromonas gingivalis* lipopolysaccharides act exclusively through TLR4 with a resilience between mouse and human (2017). Sci. Rep. 7: 15789.
133. Noiri, Y., Ozaki, K., Nakae, H., Matsuo, T., Ebisu, S. An immunohistochemical study on the localization of *Porphyromonas gingivalis*, *Campylobacter rectus* and *Actinomyces viscosus* in human periodontal pockets (1997). J. Periodontal Res. 32, 598–607.
134. Olsson, M., Lindhe, J. Periodontal characteristics in individuals with varying form of the upper central incisors (1991). J. Clin. Periodontol. 18, 78–82.
135. O'Neill, L.A.J. The interleukin-1 receptor/Toll-like receptor superfamily: 10 years of progress (2008). Immunol. Rev. 226, 10–18.
136. O'Neill, L.A.J., Bowie, A.G. The family of five: TIR-domain-containing adaptors in Toll-like receptor signalling (2007). Nat. Rev. Immunol. 7, 353–364.
137. O'Neill, L.A.J., Fitzgerald, K.A., Bowie, A.G. The Toll-IL-1 receptor adaptor family grows to five members (2003). Trends Immunol. 24, 286–290.
138. Palmer, R.M., Lubbock, M.J. The soft connective tissues of the gingiva and periodontal ligament: are they unique? (1995). Oral Dis. 1, 230–237.
139. Pan, C., Xu, X., Tan, L., Lin, L., Pan, Y. The effects of *Porphyromonas gingivalis* on the cell cycle progression of human gingival epithelial cells (2014). Oral Dis. 20, 100–108.
140. Patz, S., Trattnig, C., Grünbacher, G., Ebner, B., Gülly, C., Novak, A., Rinner, B., Leitinger, G., Absenger, M., Tomescu, O.A., Thallinger, G.G., Fasching, U., Wissa, S., Archelos-Garcia, J., Schäfer, U. More than cell dust: microparticles isolated from cerebrospinal fluid of brain injured patients are messengers carrying mRNAs, miRNAs, and proteins (2013). J. Neurotrauma 30, 1232–1242.
141. Paudel, K.R., Panth, N., Kim, D.-W. Circulating Endothelial Microparticles: A Key Hallmark of Atherosclerosis Progression (2016). Scientifica 2016, 8514056.
142. Perricone, C., Ceccarelli, F., Saccucci, M., Di Carlo, G., Bogdanos, D.P., Lucchetti, R., Pilloni, A., Valesini, G., Polimeni, A., Conti, F. *Porphyromonas gingivalis* and rheumatoid arthritis (2019). Curr. Opin. Rheumatol. 31, 517–524.
143. Petersen, P.E., Ogawa, H. The global burden of periodontal disease: towards integration with chronic disease prevention and control (2012). Periodontol. 2000 60, 15–39.
144. Pihlstrom, B.L., Michalowicz, B.S., Johnson, N.W. Periodontal diseases (2005). Lancet Lond. Engl. 366, 1809–1820.

145. Pinnock, A., Murdoch, C., Moharamzadeh, K., Whawell, S. & Douglas, C. W. I. Characterisation and optimisation of organotypic oral mucosal models to study *Porphyromonas gingivalis* invasion (2014). *Microbes Infect.* **16**, 310–319.
146. Pirillo, A., Norata, G.D., Catapano, A.L. LOX-1, OxLDL, and Atherosclerosis (2013). Mediators Inflamm. 2013, e152786.
147. Plančak, D., Musić, L., Puhar, I. Quorum Sensing of Periodontal Pathogens (2015). Acta Stomatol. Croat. 49, 234–241.
148. Pöllänen, M.T., Laine, M.A., Ihalin, R., Uitto, V.-J. Host-Bacteria Crosstalk at the Dentogingival Junction (2012). Int. J. Dent.
149. Pöllänen, M.T., Salonen, J.I., Uitto, V.-J. Structure and function of the tooth-epithelial interface in health and disease (2003). Periodontol. 2000 31, 12–31.
150. Pothineni, N.V.K., Subramany, S., Kuriakose, K., Shirazi, L.F., Romeo, F., Shah, P.K., Mehta, J.L. Infections, atherosclerosis, and coronary heart disease (2017). Eur. Heart J. 38, 3195–3201.
151. Preshaw, P.M., Alba, A.L., Herrera, D., Jepsen, S., Konstantinidis, A., Makrilakis, K., Taylor, R. Periodontitis and diabetes: a two-way relationship (2012). Diabetologia 55, 21–31.
152. Rafiei, M., Kiani, F., Sayehmiri, K., Sayehmiri, F., Tavirani, M., Dousti, M., Sheikhi, A. Prevalence of Anaerobic Bacteria (*P.gingivalis*) as Major Microbial Agent in the Incidence Periodontal Diseases by Meta-analysis (2018). J. Dent. 19, 232–242.
153. Rakoto-Alson, S., Tenenbaum, H., Davideau, J.-L.. Periodontal diseases, preterm births, and low birth weight: findings from a homogeneous cohort of women in Madagascar (2010). J. Periodontol. 81, 205–213.
154. Rast, J.P., Smith, L.C., Loza-Coll, M., Hibino, T., Litman, G.W. Genomic insights into the immune system of the sea urchin (2006). Science 314, 952–956.
155. Riedl, S.J., Salvesen, G.S. The apoptosome: signalling platform of cell death (2007). Nat. Rev. Mol. Cell Biol. 8, 405–413.
156. Ripamonti, U., Petit, J.-C., Teare, J. Cementogenesis and the induction of periodontal tissue regeneration by the osteogenic proteins of the transforming growth factor-beta superfamily (2009). J. Periodontal Res. 44, 141–152.
157. Rodrigues, P.H., Reyes, L., Chadda, A.S., Bélanger, M., Wallet, S.M., Akin, D., Dunn, W., Progulske-Fox, A. *Porphyromonas gingivalis* strain specific interactions with human coronary artery endothelial cells: a comparative study (2012). PloS One 7, e52606.
158. Romanos, G.E., Bernimoulin, J.P. [Collagen as a basic element of the periodontium: immunohistochemical aspects in the human and animal. Gingiva and alveolar bone (1990). Parodontol. Berl. Ger. 1, 363–375.
159. Rosenfeld, M.E., Campbell, L.A. Pathogens and atherosclerosis: update on the potential contribution of multiple infectious organisms to the pathogenesis of atherosclerosis (2011). Thromb. Haemost. 106, 858–867.
160. Roth, G.A., Ankersmit, H.J., Brown, V.B., Papapanou, P.N., Schmidt, A.M., Lalla, E. *Porphyromonas gingivalis* infection and cell death in human aortic endothelial cells (2007). FEMS Microbiol. Lett. 272, 106–113.

161. Rydén, L., Shahim, B., Mellbin, L. Clinical Implications of Cardiovascular Outcome Trials in Type 2 Diabetes: From DCCT to EMPA-REG (2016). Clin. Ther. 38, 1279–1287.
162. Saffar, J.L., Lasfargues, J.J., Cherruau, M. Alveolar bone and the alveolar process: the socket that is never stable (1997). Periodontol. 2000 13, 76–90.
163. Sakallioğlu, E.E., Ayas, B., Sakallioğlu, U., Açikgöz, G., Cağlayan, F. Osmotic pressure and vasculature of gingiva in periodontal disease: an experimental study in rats (2006). Arch. Oral Biol. 51, 505–511.
164. Salhi, L., Rompen, E., Sakalihasan, N., Laleman, I., Teughels, W., Michel, J.-B., Lambert, F. Can Periodontitis Influence the Progression of Abdominal Aortic Aneurysm? A Systematic Review (2019). Angiology 70, 479–491. https://doi.org/10.1177/0003319718821243
165. Salonen, J., Santti, R. Ultrastructural and immunohistochemical similarities in the attachment of human oral epithelium to the tooth *in vivo* and to an inert substrate in an explant culture (1985). J. Periodontal Res. 20, 176–184.
166. Sandros, J., Papapanou, P.N., Nannmark, U., Dahlén, G. *Porphyromonas gingivalis* invades human pocket epithelium *in vitro* (1994). J. Periodontal Res. 29, 62–69.
167. Savill, J. Apoptosis in resolution of inflammation (1997). J. Leukoc. Biol. 61, 375–380.
168. Schroeder, H.E., Listgarten, M.A. The gingival tissues: the architecture of periodontal protection (1997). Periodontol. 2000 13, 91–120.
169. Schwartz, Z., Goultschin, J., Dean, D.D., Boyan, B.D. Mechanisms of alveolar bone destruction in periodontitis (1997). Periodontol. 2000 14, 158–172.
170. Seo, B.-M., Miura, M., Gronthos, S., Mark Bartold, P., Batouli, S., Brahim, J., Young, M., Gehron Robey, P., Wang, C.Y., Shi, S. Investigation of multipotent postnatal stem cells from human periodontal ligament (2004). The Lancet 364, 149–155.
171. Shiozaki, E.N., Chai, J., Rigotti, D.J., Riedl, S.J., Li, P., Srinivasula, S.M., Alnemri, E.S., Fairman, R., Shi, Y. Mechanism of XIAP-mediated inhibition of caspase-9 (2003). Mol. Cell 11, 519–527.
172. Singh, A., Wyant, T., Anaya-Bergman, C., Aduse-Opoku, J., Brunner, J., Laine, M.L., Curtis, M.A., Lewis, J.P. The Capsule of *Porphyromonas gingivalis* Leads to a Reduction in the Host Inflammatory Response, Evasion of Phagocytosis, and Increase in Virulence (2011). Infect. Immun. 79, 4533–4542. https://doi.org/10.1128/IAI.05016-11
173. Slots, J., Chen, C. The oral microflora and human periodontal disease, in: Tannock, G.W. (Ed.), Medical Importance of the Normal Microflora (1999). Springer US, Boston, MA, pp. 101–127. https://doi.org/10.1007/978-1-4757-3021-0_5
174. Sobrino, T., Regueiro, U., Malfeito, M., Vieites-Prado, A., Pérez-Mato, M., Campos, F., Lema, I. Higher Expression of Toll-Like Receptors 2 and 4 in Blood Cells of Keratoconus Patiens (2017). Sci. Rep. 7, 1–7.
175. Socransky, S.S., Haffajee, A.D. Dental biofilms: difficult therapeutic targets. Periodontol (2002). 2000 28, 12–55.
176. Somerman, M.J., Young, M.F., Foster, R.A., Moehring, J.M., Imm, G., Sauk, J.J. Characteristics of human periodontal ligament cells *in vitro* (1990). Arch. Oral Biol. 35, 241–247.

177. Song, L., Yao, J., He, Z., Xu, B. Genes related to inflammation and bone loss process in periodontitis suggested by bioinformatics methods (2015). BMC Oral Health 15:105.
178. Soto, C., Bugueño, I., Hoare, A., Gonzalez, S., Venegas, D., Salinas, D., Melgar-Rodríguez, S., Vernal, R., Gamonal, J., Quest, A.F.G., Pérez-Donoso, J.M., Bravo, D. The *Porphyromonas gingivalis* O antigen is required for inhibition of apoptosis in gingival epithelial cells following bacterial infection (2016). J. Periodontal Res. 51, 518–528.
179. Srivastava, B., Chandra, S., Jaiswal, J.N., Saimbi, C.S., Srivastava, D. Cross-sectional study to evaluate variations in attached gingiva and gingival sulcus in the three periods of dentition (1990). J. Clin. Pediatr. Dent. 15, 17–24.
180. Stathopoulou, P.G., Galicia, J.C., Benakanakere, M.R., Garcia, C.A., Potempa, J., Kinane, D.F. *Porphyromonas gingivalis* induce apoptosis in human gingival epithelial cells through a gingipain-dependent mechanism (2009). BMC Microbiol. 9, 107.
181. Tang, Y., Zhang, Y.-C., Chen, Y., Xiang, Y., Shen, C.-X., Li, Y.-G. The role of miR-19b in the inhibition of endothelial cell apoptosis and its relationship with coronary artery disease (2015). Sci. Rep. 5, 15132.
182. Taylor, J.J., Preshaw, P.M. Gingival crevicular fluid and saliva (2016). Periodontol. 2000 70, 7–10.
183. Tenenbaum, H., Tenenbaum, M. A clinical study of the width of the attached gingiva in the deciduous, transitional and permanent dentitions (1986). J. Clin. Periodontol. 13, 270–275.
184. Tonetti, M.S., D'Aiuto, F., Nibali, L., Donald, A., Storry, C., Parkar, M., Suvan, J., Hingorani, A.D., Vallance, P., Deanfield, J. Treatment of Periodontitis and Endothelial Function (2007). N. Engl. J. Med. 356, 911–920.
185. Tribble, G.D., Lamont, R.J. Bacterial invasion of epithelial cells and spreading in periodontal tissue (2010). Periodontol. 2000 52, 68–83.
186. Tsuda, K., Amano, A., Umebayashi, K., Inaba, H., Nakagawa, I., Nakanishi, Y., Yoshimori, T. Molecular dissection of internalization of *Porphyromonas gingivalis* by cells using fluorescent beads coated with bacterial membrane vesicle (2005). Cell Struct. Funct. 30, 81–91.
187. Urnowey, S., Ansai, T., Bitko, V., Nakayama, K., Takehara, T., Barik, S. Temporal activation of anti- and pro-apoptotic factors in human gingival fibroblasts infected with the periodontal pathogen, *Porphyromonas gingivalis*: potential role of bacterial proteases in host signalling (2006). BMC Microbiol. 6, 26.
188. VanWijk, M.J., VanBavel, E., Sturk, A., Nieuwland, R. Microparticles in cardiovascular diseases (2003). Cardiovasc. Res. 59, 277–287.
189. Vernal, R., León, R., Silva, A., van Winkelhoff, A.J., Garcia-Sanz, J.A., Sanz, M. Differential cytokine expression by human dendritic cells in response to different Porphyromonas gingivalis capsular serotypes (2009). J. Clin. Periodontol. 36, 823–829.
190. Vignery, A., Baron, R. Dynamic histomorphometry of alveolar bone remodeling in the adult rat (1980). Anat. Rec. 196, 191–200.
191. Vitkov, L., Krautgartner, W.D., Hannig, M. Bacterial internalization in periodontitis (2005). Oral Microbiol. Immunol. 20, 317–321.

192. Vítková, V., Živný, J., Janota, J., 2018. Endothelial cell-derived microvesicles: potential mediators and biomarkers of pathologic processes (2018). Biomark. Med. 12, 161–175.
193. Wang, J., Shao, Y., Bennett, T.A., Shankar, R.A., Wightman, P.D., Reddy, L.G. The functional effects of physical interactions among Toll-like receptors 7, 8, and 9 (2006). J. Biol. Chem. 281, 37427–37434.
194. Weber, C., Noels, H. Atherosclerosis: current pathogenesis and therapeutic options (2011). Nat. Med. 17, 1410–1422.
195. Wu, R.-Q., Zhang, D.-F., Tu, E., Chen, Q.-M., Chen, W. The mucosal immune system in the oral cavity-an orchestra of T cell diversity (2014). Int. J. Oral Sci. 6, 125–132.
196. Xu, F., Lu, B. Prospective association of periodontal disease with cardiovascular and all-cause mortality: NHANES III follow-up study (2011). Atherosclerosis 218, 536–542.
197. Yamada, K., Asai, K., Nagayasu, F., Sato, K., Ijiri, N., Yoshii, N., Imahashi, Y., Watanabe, T., Tochino, Y., Kanazawa, H., Hirata, K. Impaired nuclear factor erythroid 2-related factor 2 expression increases apoptosis of airway epithelial cells in patients with chronic obstructive pulmonary disease due to cigarette smoking (2016). BMC Pulm. Med. 16, 27.
198. Yamamoto, M., Sato, S., Hemmi, H., Sanjo, H., Uematsu, S., Kaisho, T., Hoshino, K., Takeuchi, O., Kobayashi, M., Fujita, T., Takeda, K., Akira, S. Essential role for TIRAP in activation of the signalling cascade shared by TLR2 and TLR4 (2002). Nature 420, 324–329.
199. Yao, L., Jermanus, C., Barbetta, B., Choi, C., Verbeke, P., Ojcius, D.M., Yilmaz, Ö. P*orphyromonas gingivalis* infection sequesters pro-apoptotic Bad through Akt in primary gingival epithelial cells (2010). Mol. Oral Microbiol. 25, 89–101.
200. Yilmaz, Ö. The chronicles of *Porphyromonas gingivalis*: the microbium, the human oral epithelium and their interplay (2008). Microbiol. Read. Engl. 154, 2897–2903.
201. Yilmaz, O., Verbeke, P., Lamont, R.J., Ojcius, D.M. Intercellular spreading of *Porphyromonas gingivalis* infection in primary gingival epithelial cells (2006). Infect. Immun. 74, 703–710.
202. Yilmaz, O., Watanabe, K., Lamont, R.J. Involvement of integrins in fimbriae-mediated binding and invasion by *Porphyromonas gingivalis* (2002). Cell. Microbiol. 4, 305–314.
203. Yilmaz, O., Young, P.A., Lamont, R.J., Kenny, G.E. Gingival epithelial cell signalling and cytoskeletal responses to *Porphyromonas gingivalis* invasion (2003). Microbiol. Read. Engl. 149, 2417–2426.
204. Yu, F., Cui, Y., Zhou, X., Zhang, X., Han, J. Osteogenic differentiation of human ligament fibroblasts induced by conditioned medium of osteoclast-like cells (2011). Biosci. Trends 5, 46–51.
205. Yuan, S., Akey, C.W. Apoptosome structure, assembly, and procaspase activation (2013). Struct. Lond. Engl. 1993 21, 501–515.
206. Zamaraev, A.V., Kopeina, G.S., Zhivotovsky, B., Lavrik, I.N. Cell death controlling complexes and their potential therapeutic role (2015). Cell. Mol. Life Sci. 72, 505–517.
207. Zelkha, S.A., Freilich, R.W., Amar, S. Periodontal innate immune mechanisms relevant to atherosclerosis and obesity (2010). Periodontol. 2000 54, 207–221.

208. Zhang, Y., Xie, Y., You, S., Han, Q., Cao, Y., Zhang, X., Xiao, G., Chen, R., Liu, C. Autophagy and Apoptosis in the Response of Human Vascular Endothelial Cells to Oxidized Low-Density Lipoprotein (2015). Cardiology 132, 27–33.
209. Zou, H., Henzel, W.J., Liu, X., Lutschg, A., Wang, X. Apaf-1, a human protein homologous to *C. elegans* CED-4, participates in cytochrome c-dependent activation of caspase-3 (1997). Cell 90, 405–413.

7. ANNEXES

I. Liste de publications scientifiques

- **Bugueno I.M.**, El-Ghazouani F., Batool F., El Itawi H., Anglès-Cano E., Benkirane-Jessel N., Toti F., Huck O. *Porphyromonas gingivalis* triggers the shedding of inflammatory endothelial microvesicles that act as autocrine effectors of endothelial dysfunction. Scientific Reports 2019, under review.

- **Bugueno I.M.**, Batool F., Keller L., Kuchler-Bopp S., Benkirane-Jessel N., Huck. O. *Porphyromonas gingivalis* bypasses epithelial barrier and modulates fibroblastic inflammatory response in an in vitro 3D spheroid model. Scientific Reports 2018, (8):14914.

- **Bugueno I.M.**, Batool F. , Benkirane- Jessel N., Huck N. "*Porphyromonas gingivalis* differentially modulates apoptosome APAF-1 in epithelial cells and fibroblasts", The American Journal of Pathology 2017, 188(2): 404-416.

- **Bugueno I.M.**, Khelif Y., Seelam N., Morand DN., Tenenbaum H., Davideau JL., Huck O. *"Porphyromonas gingivalis* Differentially modulates Cell death profile in Ox-LDL and TNF-a pre-treated Endothelial Cells". PLoS One 2016, 11(4): e0154590.

- Korah L., Amri N., **Bugueno I.M.,** Hotton E., Tenenbaum H., Huck O., Berdal A., Davideau J.L. Experimental periodontitis in Msx2 mutant mice induces alveolar bone necrosis. Journal of Periodontology 2019, Doi:10.1002/JPER.16-0435.

- Petit C., Batool F., **Bugueno I.M.**, Schwinté P., Benkirane-Jessel N., Huck O. Contribution of Statins towards Periodontal Treatment: A Review. Mediators of Inflammation 2019, (2019):6367402.

- Cloitre A., Halgand B., Sourice S., Caillon J., Huck O., **Bugueno I.M.**, Batool F., Guicheux J., Geoffroy V., Lesclous P. " IL-36γ is a pivotal inflammatory player in periodontitis-associated bone loss", Scientific Reports 2019, under peer-review.

- Mendez K., Hoare A., Soto C., **Bugueno I.M.**, Olivera M., Meneses C., Pérez-Donoso J.M., Castro-Nallar E., Bravo D. Variability in Genomic and Virulent Properties of *Porphyromonas gingivalis* Strains Isolated From Healthy and Severe Chronic Periodontitis Individuals. Front Cell Infect Microbiol. 2019 Jul 10;9:246

- Batool F., Strub M., Petit C., **Bugueno I.M.,** Bornert F., Clauss F., Huck O., Kuchler-Bopp S., Benkirane-Jessel N. "Periodontal Tissues, Maxillary Jaw Bone, and Tooth Regeneration Approaches: From Animal Models Analyses to Clinical Applications". Nanomaterials 2018, 8, 337.

- Batool F., Morand D., Thomas L., **Bugueno I.M.**, Aragon J., Irusta S., Keller L., Benkirane-Jessel N., Tenenbaum H., Huck O. "Synthesis of a Novel Electrospun Polycaprolactone Scaffold Functionalized with Ibuprofen for Periodontal Regeneration: An *In Vitro* and In *Vivo Study"*. Materials 2018, 11, 580.

- Elkaim R., **Bugueno I.M.**, Benkirane-Jessel N., Tenenbaum H. "*Porphyromonas gingivalis* and its lipopolysaccharide differentially regulate the expression of peptidyl arginine deiminases in human chondrocytes". Innate Immunity 2017, 23 (5): 175342591771626.

- Elkaim R., **Bugueno I.M.**, Benkirane-Jessel N., Tenenbaum H. "*Porphyromonas gingivalis* and its lipopolysaccharide differently modulate epidermal growth factor–dependent signaling in human gingival epithelial cells". Journal of Oral Microbiology 2017, 9 (1):1334503.

- Lapérine O., Cloitre A., Caillon J., Huck O., **Bugueno I.M.**, Pilet P., Sourice S., Le Tilly E., Palmer G., Davideau JL., Geoffroy V., Guicheux J., Cormier S., Lesclous P. "Interleukin-33 and RANK-L Interplay in the Alveolar Bone Loss Associated to Periodontitis". PLos One 2016, 11(12); e0168080.

II. Conférences scientifiques nationales et internationales

- **Bugueno I.M.**, Benkirane-Jessel N., Huck O. *Porphyromonas Gingivalis* Modulates TIR-domain-containing Adaptors Proteins Expression in Epithelial and Endothelial Cells. CED-IADR/NOF Oral Health Research Congress, 9-21 septembre 2019, Madrid, Espagne.

- **Bugueno I.M.**, F. Batool, F. El-Ghazouani, E. Anglès-Cano, N., Benkirane-Jessel, F. Toti, O. Huck. Implication des microvésicules d'origine endothéliale induites par l'infection par *Porphyromonas gingivalis* dans l'inflammation endothéliale. Congrès de la SFPIO - Société Française de Parodontologie et d'Implantologie Orale, 13-15 juin 2019, Paris, France.

- **Bugueno I.M.**, Keller L., Batool F., Kuchler-Bopp S., Benkirane-Jessel N., Huck O. "A new 3D *in vitro* model of gingival tissue to assess host-pathogen interactions". EuroPerio9, 20-23 juin 2018, Amsterdam, Pays Bas.

- **Bugueno I.M.**, Batool F., Benkirane-Jessel N., Huck O. Endothelial-derived Microvesicles Induced by *Porphyromonas gingivalis* Activate Endothelial Inflammatory Response. 96th General Session of the IADR, 25-28 juillet 2018, Londres, Anglaterre.

- **Bugueno I.M.**, Keller L., Batool F., Kuchler-Bopp S., Benkirane-Jessel N., Huck O. "Assessment of host-periodontal pathogens interactions in a new in-vitro 3D spheroid model". 103th Annual meeting American Academy of Periodontology. 5-12 septembre 2017, Boston, USA.

- **Bugueno I.M.**, Khelif Y., Seelam N., Tenenbaum H., Davideau JL., Huck O. *"Porphyromonas gingivalis* modulates Ox-LDL pre-treated endothelial cell death". 26es Journées Européennes de la Societé Française de Cardiologie (JESFC). 14-16 janvier 2016, Paris, France.

- **Bugueno I.M.**, Davideau JL., Tenenbaum H., Jessel N., Huck O. “La survie intracellulaire de *Porphyromonas gingivalis* à travers l'inhibition de l'apoptose”. Congrès de la Société Française de Parodontologie et d’Implantologie Orale (SFPIO). 6-9 Juin 2016. Lyon, France.

- **Bugueno I.M.**, Davideau JL., Tenenbaum H., Jessel N., Huck O. « Modulation de la voie liée à l’apoptosome Apaf-1 par *Porphyromonas gingivali ».* Journées en parodontologie et/ou implantologie au CNEP. 14-15 septembre 2016. Nice, France.

- **Bugueno I.M.**, Davideau JL., Tenenbaum H., Jessel N., Huck O. “Survival of Gingival Epithelial Cells Infected by *Porphyromonas gingivalis*”. 47th Meeting of Continental European Division of the International Association for Dental Research. 13-16 octobre 2015. Antalya, Turquie.

III. Annexe n°1

Bugueno IM., Khelif Y., Seelam N., Morand DN., Tenenbaum H., Davideau JL., Huck O. *"Porphyromonas gingivalis* Differentially modulates Cell death profile in Ox-LDL and TNF-a pre- treated Endothelial Cells". **PLoS One 2016, 11(4): e0154590.**

PLOS | ONE

RESEARCH ARTICLE

Porphyromonas gingivalis Differentially Modulates Cell Death Profile in Ox-LDL and TNF-α Pre-Treated Endothelial Cells

Isaac Maximiliano Bugueno[1], Yacine Khelif[1], Narendra Seelam[1,2], David-Nicolas Morand[1,2], Henri Tenenbaum[1,2], Jean-Luc Davideau[1,2], Olivier Huck[1,2]*

1 INSERM 1109 « Osteoarticular & Dental Regenerative Nanomedicine », Fédération de Médecine Translationnelle de Strasbourg (FMTS), Strasbourg, France, **2** Université de Strasbourg, Faculté de Chirurgie-dentaire, Department of Periodontology, Strasbourg, France

* huck.olivier@gmail.com

OPEN ACCESS

Citation: Bugueno IM, Khelif Y, Seelam N, Morand D-N, Tenenbaum H, Davideau J-L, et al. (2016) *Porphyromonas gingivalis* Differentially Modulates Cell Death Profile in Ox-LDL and TNF-α Pre-Treated Endothelial Cells. PLoS ONE 11(4): e0154590. doi:10.1371/journal.pone.0154590

Editor: Maria Fiammetta Romano, Federico II University, Naples, ITALY

Received: January 13, 2016

Accepted: April 17, 2016

Published: April 28, 2016

Data Availability Statement: All relevant data are within the paper.

Funding: This study was supported by INSERM.

Competing Interests: The authors have declared that no competing interests exist.

Abstract

Objective

Clinical studies demonstrated a potential link between atherosclerosis and periodontitis. *Porphyromonas gingivalis* (*Pg*), one of the main periodontal pathogen, has been associated to atheromatous plaque worsening. However, synergism between infection and other endothelial stressors such as oxidized-LDL or TNF-α especially on endothelial cell (EC) death has not been investigated. This study aims to assess the role of *Pg* on EC death in an inflammatory context and to determine potential molecular pathways involved.

Methods

Human umbilical vein ECs (HUVECs) were infected with *Pg* (MOI 100) or stimulated by its lipopolysaccharide (*Pg*-LPS) (1μg/ml) for 24 to 48 hours. Cell viability was measured with AlamarBlue test, type of cell death induced was assessed using Annexin V/propidium iodide staining. mRNA expression regarding caspase-1, -3, -9, Bcl-2, Bax-1 and Apaf-1 has been evaluated with RT-qPCR. Caspases enzymatic activity and concentration of APAF-1 protein were evaluated to confirm mRNA results.

Results

Pg infection and *Pg*-LPS stimulation induced EC death. A cumulative effect has been observed in Ox-LDL pre-treated ECs infected or stimulated. This effect was not observed in TNF-α pre-treated cells. *Pg* infection promotes EC necrosis, however, in infected Ox-LDL pre-treated ECs, apoptosis was promoted. This effect was not observed in TNF-α pre-treated cells highlighting specificity of molecular pathways activated. Regarding mRNA expression, *Pg* increased expression of pro-apoptotic genes including caspases-1,-3,-9, Bax-1 and decreased expression of anti-apoptotic Bcl-2. In Ox-LDL pre-treated ECs, *Pg* increased significantly the expression of Apaf-1. These results were confirmed at the protein level.

Conclusion

This study contributes to demonstrate that *Pg* and its *Pg*-LPS could exacerbate Ox-LDL and TNF-α induced endothelial injury through increase of EC death. Interestingly, molecular pathways are differentially modulated by the infection in function of the pre-stimulation.

Introduction

Periodontal diseases are chronic inflammatory diseases affecting the tooth-supporting tissues. Pathogenesis of periodontitis is associated with dysbiosis of the periodontal microbiota. This dysbiosis is characterized by a shift from a symbiotic microbial community to a pathogenic one composed mainly of anaerobic bacteria resulting in alteration of the host-microbe cross-talk [1,2]. Periodontitis has been linked to several systemic diseases, especially atherosclerosis [3,4] while infection has been described as a potential mechanism involved in atherosclerosis worsening [4,5]. Interestingly, potential synergism has already been proposed for some risk factors of atherosclerosis, for instance periodontitis and obesity [6].

The role of infection in atherosclerosis has been proposed and several infective agents have been identified such as *Chlamydia pneumoniae*, *Helicobacter pylori* and *Porphyromonas gingivalis* (*Pg*) [3,7]. However, many aspects of the effects associated to infection, especially in an inflammatory context, remain unclear.

Pg is a gram-negative asaccharolytic bacterium implicated in periodontitis [1,7]. *Pg* is also considered as a keystone pathogen while it modulates gene and protein expression compromising immune function at the periodontal level [1,4]. Periodontal pathogens, including *Pg*, spread from periodontal pockets to general circulation and have been associated to atherosclerosis [4,8]. It has been detected in clinical human atheromatous plaque samples [8,9] and is able to worsen atheosclerosis in murine models [9,10]. Viable *Pg* has been detected in aorta of mice infected orally with *Pg* where it modulates innate immune response [10,11].

Endothelial cells (ECs) are key cells in vascular homeostasis and their dysfunction is associated with atherosclerotic process [11,12]. Due to their specific localization at the interface between inner part of the vessel and blood stream, ECs are under influence of several stressors such as bacterial pathogens including *Pg*. This bacterium, through its virulence factors such as lipopolysaccharide (*Pg*-LPS) is able to modify several molecular pathways associated to Toll-Like Receptors and innate immune response [12,13], activation of enzymes such as cathepsin B [13,14] and secretion of pro-inflammatory cytokines [14,15]. Interestingly, effects induced by the *Pg* infection in ECs appear to be strain-dependent [15,16].

ECs apoptosis has been observed in atheromatous plaque and may be involved in early phase of atherogenesis [16,17]. It increases vascular permeability, coagulation and promotes proliferation of smooth muscle cells [17,18]. Furthermore, non-phagocytosed apoptotic cells may undergo secondary necrosis contributing to vascular inflammation [18,19]. Several pathways have been described that are activated in ECs death, especially apoptosis, including caspase related pathways[19,20]. Apoptosis is a highly regulated mechanism activated through death receptors or perturbation of the mitochondria releasing cytochrome c that will induce pro-apoptotic factors activation [20,21]. Caspases are first synthesized as inactive pro-caspases that consist of a prodomain, which once initiated, activate a downstream or "effector" caspase such as caspase -3. Interestingly, the activation of caspase-9 is under the influence of the apoptosome complex constituted by apoptotic protease-activating factor-1 (Apaf-1). Apoptosome complex regulates apoptosis related cell death. However, its activation is under the control of

several physiological mechanisms. Recently, apoptosome has been recognized as a potential therapeutic target in several diseases including diabetes and obesity [21,22]. Its implication in atherosclerosis has been recently proposed [22,23].

Several pro-atherogenic factors such as oxidized low-density lipoproteins (Ox-LDL) and TNF-α influence death of ECs, smooth muscle cells and macrophages, promoting necrotic core development [23,24]. Ox-LDL is an essential atherosclerotic risk factor that induce the expression of adhesion molecules, morphological changes of ECs [24,25] and apoptosis [22,25,26]. TNF-α is an inflammatory cytokine that worsen atherosclerotic development. This cytokine affects several vascular cell types, including ECs, and induces inflammatory, proliferative, cytostatic and cytotoxic effects. It has also been described as an inductor of ECs apoptosis [22,26,27]. Interestingly, some pathogens such as *Chlamydiae pneumoniae (C.pneumoniae)* modulate ECs death by promoting necrosis and reducing apoptosis[27,28].

The aim of our study was to evaluate the effects induced by *Pg* and its LPS on Ox-LDL and TNF- α induced cell death to assess the potential co-influence of atherosclerosis risk factors.

Materials and Methods

Bacterial culture

The *Pg* strain (ATCC 33277) was purchased from the American Type Culture Collection (ATCC, Manassas, VA, USA). Bacterial culture was performed under strict anaerobic conditions at 37°C in Brain-Heart Infusion medium supplemented with hemin (5mg/ml) and menadione (1mg/ml) purchased from Sigma (St. Louis, MO, USA). The day of the infection, bacterial culture was centrifuged and bacteria were washed twice with Phosphate Buffer Saline (PBS) and counted as previously described [16,28]. Heat-killed *Pg* (H*Pg*) was heated for 10 min at 85°C before the experimentation.

Commercial ultrapure *Pg*-LPS and *Escherichia coli*-LPS (*E.Coli*-LPS) were purchased from InvivoGen (San Diego, CA, USA).

Cell culture

Human umbilical vein ECs (HUVECs) (C-12200, PromoCell, Heidelberg, Germany) were cultured in EGM2 medium (Promocell, Heidelberg, Germany) supplemented with 10% Fetal Bovine Serum at 37°C in a humidified atmosphere with 5% CO_2. To investigate the effect of infection on cytotoxicity mediated by Ox-LDL and TNF-α, HUVECS were pre-treated 24h before challenge with either bacteria or LPS. For this purpose, 50μg/ml of Ox-LDL (Tebu-Bio, Le Perray en Yvelines, France) [27] or 10ng/ml TNF-α [29] (Tebu-Bio, Le Perray en Yvelines, France) has been added to cell culture medium.

Infection of ECs with *Pg* and stimulation by LPS

Twenty-four hours before the experiment, $2x10^5$ cells were plated in each well of a 24-well plate. At the day of the experiment, HUVECs were washed twice with PBS and infected for 24 to 48h with *Pg* at a multiplicity of infection (MOI) of 100 bacteria/cell and stimulated by *Pg*-LPS (1μg/ml) and *E.Coli*-LPS (1μg/ml) for 24 to 48h.

Cell viability

Cell viability was determined using colorimetric AlamarBlue test (Life Technologies). After 24 and 48h, 300 μl of incubation media were transferred to 96-well plates and measured at 570 and 600 nm in order to determine the percentage of AlamarBlue reduction.

Live/Dead staining

The viability of HUVECs in all conditions was assessed using a fluorescence-based LIVE/DEAD® assay (LIVE/DEAD® Cell Imaging Kit, Molecular Probes™, Invitrogen) at 24h. Cells were washed twice with phosphate-buffered saline (PBS; Fisher Scientific, Fair Lawn, NJ, USA) before staining. The staining solution consisted of 0.5 μL/mL calcein AM reagent and 2 μL/mL EthD-1 reagent mixed in 2 mL of PBS. Samples were incubated for 10 min and imaged using a 10x and 20x objective lens of a fluorescence microscope (Olympus BX53F, Tokyo, Japan) and filters for fluorescein and Texas Red for calcein and EthD-1 stains, and a digital CCD color imaging system (Microscope Digital Camera DP72; CellSens Entry®, Olympus, Tokyo, Japan).

Type of cell death assessment

Apoptosis/necrosis ratio was analyzed using Annexin-V-FLUOS Staining Kit according to the manufacturer's instructions (Roche Diagnostics, Meylan, France) at 24h. Cells were washed twice with PBS before staining. Cells were incubated with 100 μl of buffer solution, 5 μl of annexin V-FITC and 5 μl of propidium iodide (PI) for 15 min in the dark at room temperature. 50 μl of a solution of DAPI 200nM (Sigma-Aldrich Co., St Louis, MO, USA) was added for nuclear staining. Samples were imaged using a 10x and 20x objective lens of a fluorescence microscope (Olympus BX53F, Tokyo, Japan) and filters for fluorescein and Texas Red for calcein and EthD-1 stains, and a digital CCD color imaging system (Microscope Digital Camera DP72; CellSens Entry®, Olympus, Tokyo, Japan).

RNA Isolation and Reverse Transcription

After cell lysis, total RNA was extracted using the High Pure RNA isolation kit (Roche Applied Science, Meylan, France) according to the manufacturer's instructions. The extracted total RNA concentration was quantified using NanoDrop 1000 (Fischer Scientific, Illkirch, France). Reverse transcription was performed with the iScript Reverse Transcription Supermix (Bio-Rad Laboratories, Hercules, CA, USA) according to the manufacturer's instructions.

Quantitative Real-Time PCR Analysis

To quantify RNA expression, qPCR was performed on the cDNA samples. PCR amplification and analysis were achieved using the CFX Connect™ Real-Time PCR Detection System (Bio-rad, Miltry-Mory, France). Amplification reactions have been performed using iTaq Universal SYBR Green Supermix (Bio-rad, Miltry-Mory, France). Beta-actin was used as endogenous RNA control (housekeeping gene) in the samples. Primers sequences related to Bcl-2, Bax-1, Caspase-1, Caspase-3, Caspase-9 were purchased from Qiagen (Les Ulis, France) and sequence for Apaf-1 (3'-GTCTGCTGATGGTGCAAGGA-5'; 5'-GATGGCCCGTGTGGATTTC-3') was synthesized (ThermoFischer, Saint-Aubin, France). The specificity of the reaction was controlled using melting curves analysis. The expression level was calculated using the comparative Ct method ($2^{-\Delta\Delta Ct}$) after normalization to the housekeeping gene (β-actin). All PCR assays were performed in triplicate and results were represented by the mean values.

Caspase activity fluorogenic assays

To determine caspase-1, -3 and -9 activity, cells were sonicated and lysates were incubated with 200 μL of substrate solution (20 mM HEPES, pH 7.4, 2 mM EDTA, 0.1% CHAPS, 5 mM DTT and 0.75 μM of caspase substrate) for 1 h at 37°C as previously described [30] [31]. The activities of caspase-1, -3 and -9 were calculated from the cleavage of the respective specific fluorogenic substrate (Ac-YVAD-AMC for caspase-1, AC-DEVD-AMC for caspase-3 and

AC-LEHD-AMC for caspase-9) (Bachem, Bobendorf, Switzerland). Substrate cleavage was measured with a fluorescence spectrophotometer with excitation wavelength of 360 nm and emission at 460 nm. The data were calculated as fluorescence units/mg of total protein.

Western blotting

In order to detect the protein level of Apaf-1, Western blot was performed. SDS-PAGE followed by immunoblotting were performed in conditions previously described [28]. Briefly, ECs collected from infection with *Pg* and from stimulation by *Pg*-LPS were lysed for 5 min on ice in 200 μl of ice-cold RIPA buffer (65 mM Tris–HCl, pH 7.4, 150mM NaCl, and 0.5% sodium deoxycholate) supplemented with phosphatase inhibitor cocktails I and II and a protease inhibitor cocktail (Sigma, Darmstadt, Germany). Lysates were centrifuged at 10,000 g at 4°C for 10min, and supernatants were collected for quantification using the Bradford protein assay (Bio-Rad, Hercules, CA, USA). To perform SDS-PAGE and immunoblotting, 25μg of proteins was used for each condition. The antibody against Apaf-1 (Rabbit) was purchased from ThermoFischer (Illkirch, France) (REF: PA5-19894) and against β-actin (Mouse) from Santa Cruz Biotechnology (Heidelberg, Germany) (REF:SC-130301). Secondary antibodies alkaline phospahatase conjugated (anti-mouse REF: A120-101AP; anti-rabbit REF: A90-116-AP) were purchased from Bethyl Laboratories (Montgomery, Texas, USA). All antibodies were used at the dilutions recommended by the manufacturer.

Statistical analysis

All experiments were repeated at least 3 times and statistical analysis was performed using pairwise Anova test. Tukey's post-hoc test was used to perform multiple comparisons. Data were analysed using PRISM 6.0 (GraphPad, La Jolla, CA, USA). Statistical significance was considered for $p<0.05$.

Results

Effect of Pg and its *Pg*-LPS on cell viability in ECs

Cell viability was evaluated at 24 and 48h. At each time point, infection with *Pg* and stimulation by all tested LPS significantly decreased ECs metabolic activity (25% decrease for *Pg* infection versus control at 24h and 32% at 48h; 44% decrease for *Pg*-LPS stimulation versus control at 24h and 48h). No differences were observed between infection and *Pg*-LPS stimulation at 24 and 48h. Interestingly, ECs death was more important after *E.coli*-LPS stimulation at 48h. No effect on EC viability was observed with H*Pg* at 24 and 48h, highlighting a potential role of bacterial invasion in this process (Fig 1A). Regarding the impact of Ox-LDL and TNF-α, both stressors also significantly decreased cell viability at 24 and 48h (Fig 1B). For instance, Ox-LDL decreased EC viability up to 15% at 24h and 31% at 48h. This effect was amplified by *Pg* infection resulting in a decrease of EC viability up to 34% at 24h and 59% at 48h highlighting a cumulative effect between Ox-LDL and infection. This effect was not observed when TNF-α pre-treated cells were infected. A cumulative effect was only observed at 24h for *E.coli*-LPS in TNF-α pre-treated cells but not for *Pg*-LPS. These results were confirmed by Live/Dead staining (Fig 2).

Modulation of type of cell death by *Pg*

Type of cell death induced by each stressor was analyzed using Annexin V/ propidium iodide staining at 24h. Infection with *Pg* alone and stimulation by its LPS reduced apoptosis/necrosis ratio (Fig 3A and 3B). A specific effect was observed regarding the type of LPS used, *E.coli*-LPS

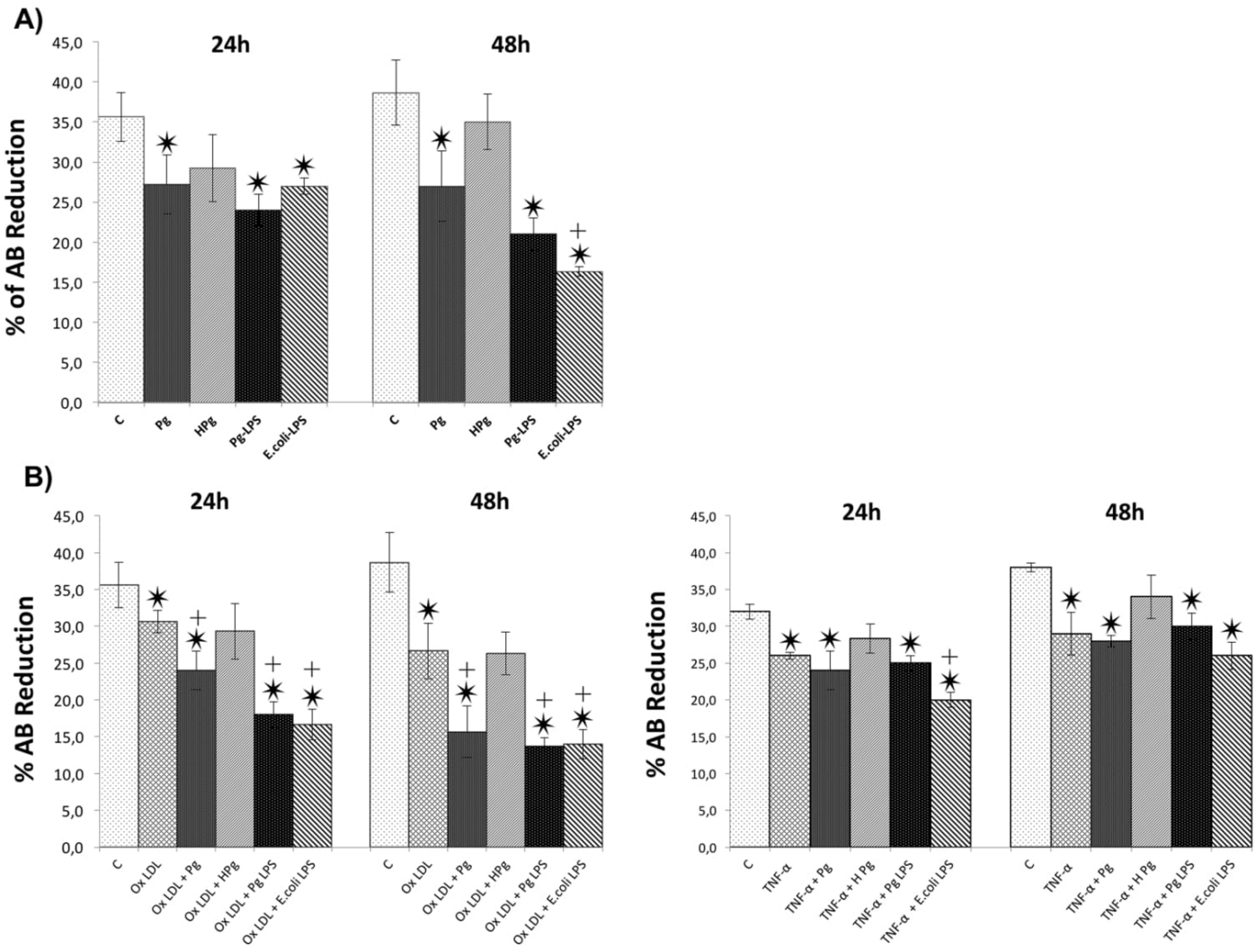

Fig 1. *Pg* ant its LPS increase ECs death. (A) Viability of HUVECs infected with *Pg* at a MOI of 100 or Heat-inactivated *Pg* (H*Pg*) and stimulated by *Pg*-LPS (1μg/ml) or *E.Coli*-LPS (1μg/ml) for 24h to 48h was measured using AlamarBlue test. **(B)** Viability of Ox-LDL (50μg/ml) and TNF- α (10ng/ml) pre-treated HUVECs with *Pg* at a MOI of 100 or Heat-inactivated *Pg* (H*Pg*) and stimulated by *Pg*-LPS (1μg/ml) or *E.Coli*-LPS (1μg/ml) for 24h to 48h. Data were expressed as mean ± SD. *: difference between non-stimulated/infected and stimulated/infected cells, $p < 0.05$, ┼: difference between non pre-treated/ stimulated/infected and treated cells, $p < 0.05$.

doi:10.1371/journal.pone.0154590.g001

seemed to induce more necrosis than *Pg*-LPS. In cells pre-treated by Ox-LDL and TNF-α, apoptosis was also the main type of cell death (Fig 4). Interestingly, an amplification of the apoptotic cell count was observed in Ox-LDL pre-treated cells infected with *Pg*. Such effect seemed to be independent of *Pg*-LPS, this virulence factor inducing mainly necrosis as it appeared with *E. coli*-LPS (Fig 4A and 4B). In TNF-α pre-treated cells, the same effect was not observed at 24h, where *Pg* infection induced an increase of necrosis in the same range as *Pg*-LPS and *E.coli*-LPS stimulation (Fig 4C and 4D).

Modulation of cell death related mRNA expression

Cell death related gene expression was measured at 24h. Infection with *Pg* significantly increased expression of genes related to cell death including Bax-1, caspase-1, -3 and -9 and

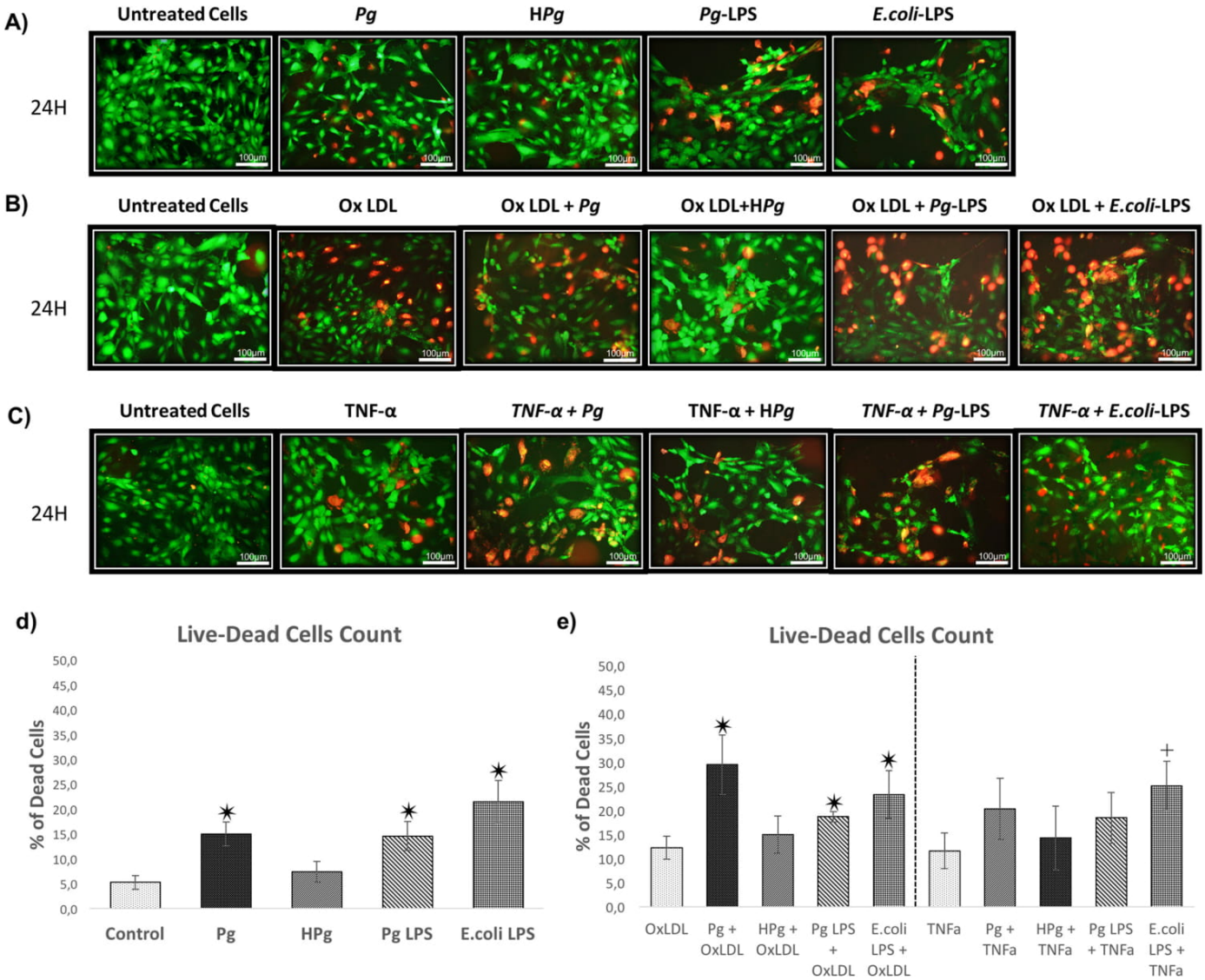

Fig 2. Qualitative evaluation of the EC death. (A) Viability of HUVECs infected with *Pg* at a MOI of 100 or Heat-inactivated *Pg* (H*Pg*) and stimulated by *Pg*-LPS (1μg/ml) or *E.Coli*-LPS (1μg/ml) at 24h. All different conditions have been evaluated quantitatively and qualitatively by Live-Dead staining assays. **(B)** Viability of Ox-LDL (50μg/ml) pre-treated HUVECs on cell cultures infected with *Pg* or H*Pg* at a MOI of 100 and stimulated by *Pg*-LPS (1μg/ml) or *E.Coli*-LPS (1μg/ml) at 24h. **(C)** Viability of TNF- α (10ng/ml) pre-treated HUVECs on cell cultures infected with *Pg* or H*Pg* at a MOI of 100 and stimulated by *Pg*-LPS (1μg/ml) or *E.Coli*-LPS (1μg/ml) at 24h. **(D)** Percentage of dead cells infected with *Pg* or H*Pg* and stimulated by *Pg*-LPS (1μg/ml) or *E.Coli*-LPS (1μg/ml) at 24h. **(E)** Percentage of dead cells in OxLDL qnd TNF- α pre-treated HUVECs. All images were acquired under fluorescence microscopy (in green: viable cells; in red: dead cells). All scale bars indicate 100 μm.

doi:10.1371/journal.pone.0154590.g002

decreased expression of anti-apoptotic Bcl-2 (2-fold). An increase of Apaf-1 expression was already observed after *Pg* infection (1.45 fold) (Figs 5A and 6A). Interestingly, *Pg*-LPS induced similar modulation of gene expressions while *E.coli*-LPS did not modify significantly Apaf-1 related gene expression (Fig 5A). These results highlighted some cell death related pathways modulated during infection and may explain the decrease of cell viability induced by infection.

In Ox-LDL pre-treated cells, similar effects were observed regarding the expression of Bcl-2, Bax-1 and caspase-3. Infection with *Pg* increased significantly caspase-3, -9, Bax-1 and Apaf-1

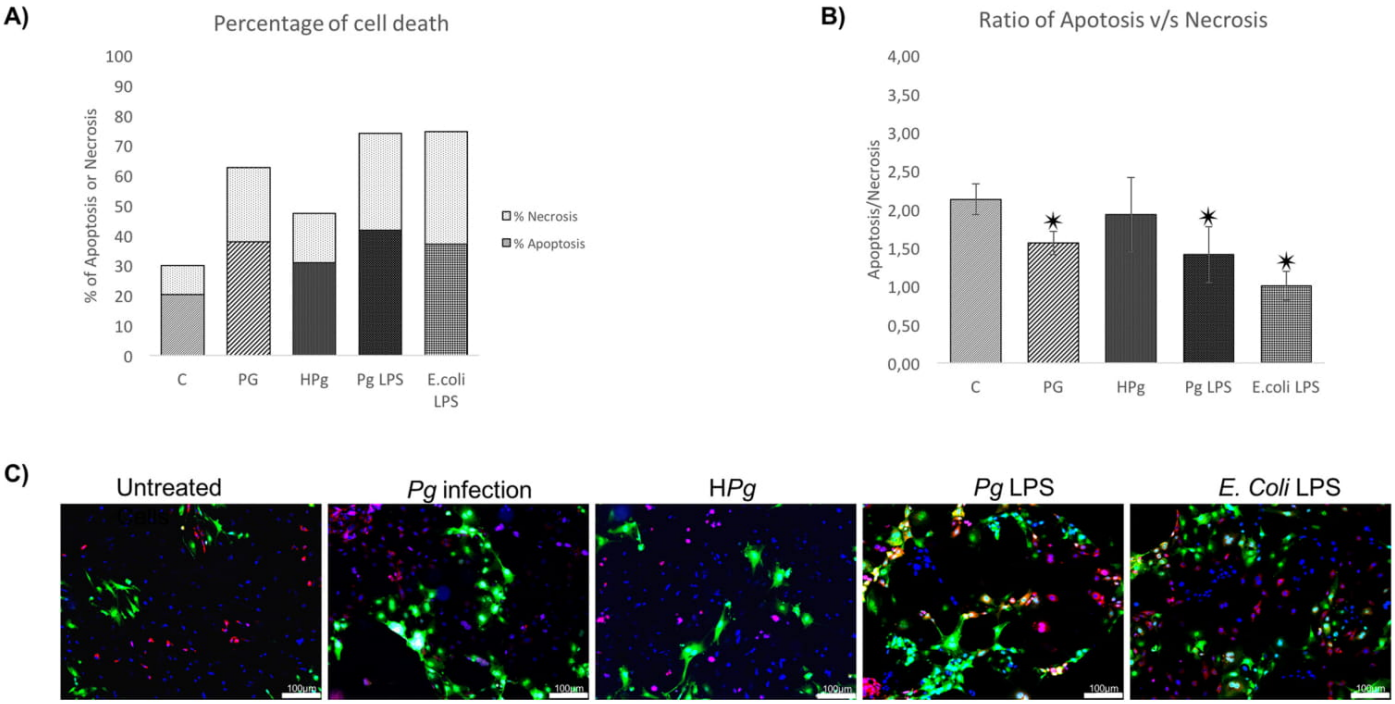

Fig 3. Infection of ECs leads to cell death mediated by apoptosis. (A) Percentage of cell death of ECs infected with *Pg* or Heat inactivated *Pg* (H*Pg*) at a MOI of 100 and stimulated by *Pg*-LPS (1μg/ml) or *E.Coli*-LPS (1μg/ml). Each percentage was calculated on account of total cells counted in triplicate for each experiment. **(B)** The apoptosis/necrosis ratio of ECs infected with *Pg* or Heat inactivated *Pg* (H*Pg*) at a MOI of 100 and stimulated by *Pg*-LPS (1μg/ml) or *E. Coli*-LPS (1μg/ml). Each value was calculated from the ratio between the total number of apoptotic cells and necrotic cells and for each count nine images were used of each experimentation. Data were expressed as mean ± SD. ✶: difference between non pre-treated/stimulated/infected and infected/stimulated cells, $p < 0.05$; **(C)** Infected and stimulated HUVECs cell death was evaluated for each condition qualitatively using Annexin V-IP staining at 24h (in green: Annexin V positive staining; in red: Iodure propidium positive staining; in blue: DAPI nuclear staining) Images were acquired under fluorescence microscopy (10x) after Annexin V-IP and DAPI staining for all previously described condition. All scale bars indicate 100 μm.

doi:10.1371/journal.pone.0154590.g003

expression and decreased Bcl-2 expression in comparison with Ox-LDL pre-treated cells (Figs 5B and 6B). This result corroborated the increase of apoptosis rate previously observed. Stimulation with *Pg*-LPS and *E.coli*-LPS decreased expression of Bcl-2 and increased expression of caspase-1. Only *Pg*-LPS increased expression of Bax-1 and caspase-3 (Figs 5B and 6B).

In TNF-α pre-treated cells, only Bcl-2 and caspase-1 were differentially expressed after *Pg* infection in comparison with TNF-α pre-treatment cells. Interestingly, *E.coli*-LPS significantly increased expression of caspase-3 (Figs 5C and 6C).

Caspases activity

To confirm the results observed at the mRNA level, enzymatic activities of the caspase-1, -3, and -9 were measured. Infection with *Pg* increased significantly the enzymatic activity of caspase-1, -3 and -9 (Fig 7A). Interestingly, Ox-LDL and TNF-α did not affect caspases activity in comparison with untreated cells (Fig 7). In Ox-LDL pre-treated ECs, a synergism between Ox-LDL and *Pg* infection has been highlighted regarding the activation of caspase-3 only (Fig 7B). Interestingly, in TNF-α pre-treated ECs, a synergy was observed regarding caspase-1 activity demonstrating the impact of one stressor on the potential molecular pathway activated by *Pg* (Fig 7C). A specific response was also observed, according to the pre-treatment with Ox-LDL or TNF-α, regarding the effects induced by *Pg*-LPS stimulation (Fig 7B and 7C).

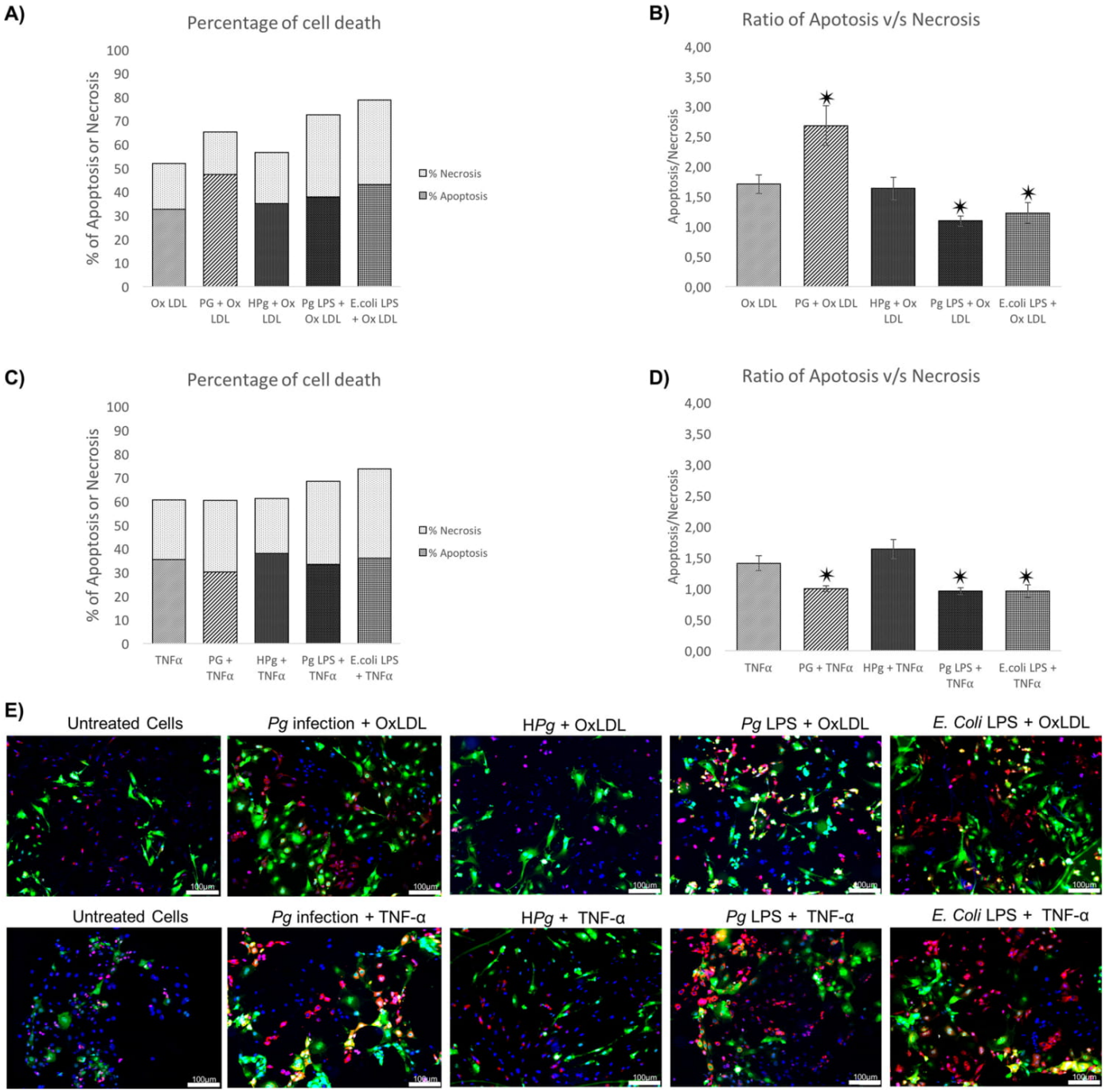

Fig 4. Pre-treatment of EC leads to different types of cell death induced by *Pg*. (A) Percentage of cell death of Ox-LDL (50µg/ml) pre-treated ECs infected with *Pg* at a MOI of 100 or Heat-inactivated *Pg* (H*Pg*) and stimulated by *Pg*-LPS (1µg/ml) or *E.Coli*-LPS (1µg/ml) for 24h. **(B)** The apoptosis/necrosis ratio of Ox-LDL (50µg/ml) pre-treated ECs with *Pg* at a MOI of 100 or Heat-inactivated *Pg* (H*Pg*) and stimulated by *Pg*-LPS (1µg/ml) or *E.Coli*-LPS (1µg/ml) for 24h. **(C)** Percentage of cell death of TNF-α (10ng/ml) pre-treated ECs infected with *Pg* at a MOI of 100 or Heat-inactivated *Pg* (H*Pg*) and stimulated by *Pg*-LPS (1µg/ml) or *E.Coli*-LPS (1µg/ml) for 24h. **(D)** The apoptosis/necrosis ratio of TNF- α (10ng/ml) pre-treated ECs infected with *Pg* at a MOI of 100 or Heat-inactivated *Pg* (H*Pg*) and stimulated by *Pg*-LPS (1µg/ml) or *E.Coli*-LPS (1µg/ml) for 24h. Data were expressed as mean ± SD. ✳: difference between non pre-treated/stimulated/infected and infected/stimulated cells, $p < 0.05$; **(E)** Infected and stimulated Ox-LDL (50µg/ml) and TNF- α (10ng/ml) pre-treated HUVECs cell death was evaluated for each condition qualitatively using Annexin V-IP staining at 24h and 48h (in green: Annexin V positive staining; in red: Iodure propidium positive staining; in blue: DAPI nuclear staining). Images were acquired under fluorescence microscopy (10x) after Annexin V-IP and DAPI staining for all previously described condition. All scale bars indicate 100 µm.

doi:10.1371/journal.pone.0154590.g004

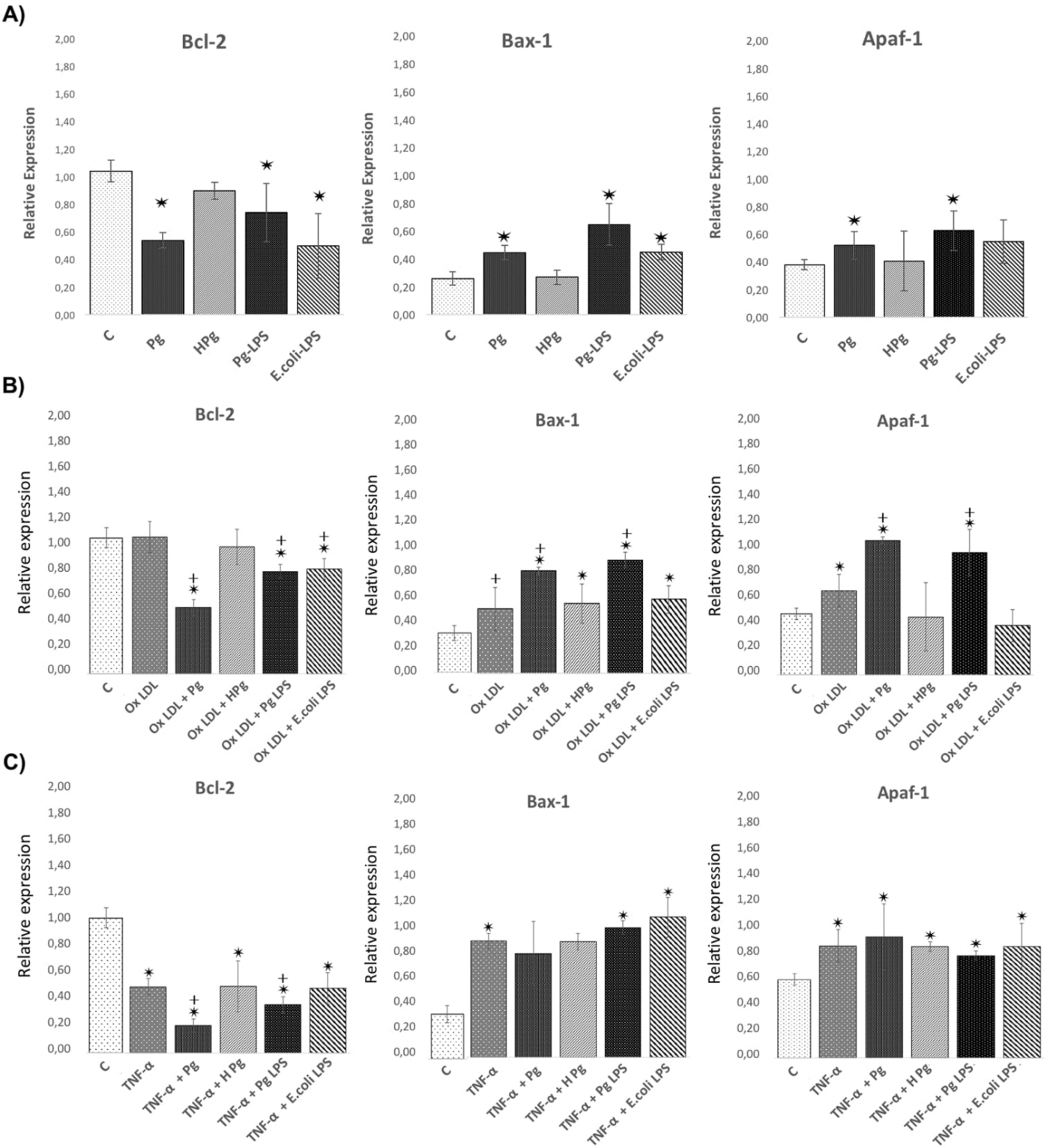

Fig 5. *Pg* and its LPS modulate the expression of EC death related gene expression. (A) Gene expression of Bcl-2, Bax-1, and Apaf-1 in HUVECs infected with *Pg* at a MOI of 100 or with heat inactivated *Pg* and stimulated by *Pg*-LPS (1μg/ml) or *E.Coli*-LPS (1μg/ml) at 24h. **(B)** Gene expression for the same described genes in Ox-LDL (50μg/ml) pre-treated HUVECs infected with *Pg* at a MOI of 100 or with heat inactivated *Pg* and stimulated by *Pg*-LPS (1μg/ml) or *E.Coli*-LPS (1μg/ml) at 24h. **(A)** Gene expression for the same described genes in TNF- α (10ng/ml) pre-treated HUVECs infected with *Pg* at a

MOI of 100 or with heat inactivated *Pg* and stimulated by *Pg*-LPS (1μg/ml) or *E.Coli*-LPS (1μg/ml) at 24h. Data were expressed as mean ± SD. *: difference between non-stimulated/infected and stimulated/infected cells, $p < 0.05$, ┼: difference between non pre-treated/stimulated/infected and treated cells, $p < 0.05$.

doi:10.1371/journal.pone.0154590.g005

Pg and its LPS increase Apaf-1 protein expression

Regarding the effect on the Apaf-1 mRNA expression, an increase was observed with *Pg* infection especially in Ox-LDL pre-treated ECs (Fig 5B). This result was confirmed at the protein level (Fig 8). In Ox-LDL pre-treated ECs, *Pg* infection increased significantly the concentration of Apaf-1 (X2.5 vs Ox-LDL alone) (Fig 8B). Such effect was not observed in TNF-α pre-treated ECs as observed at the mRNA level (Fig 5C). These results were specific to live *Pg* as no modifications were observed when H*Pg* was used.

Regarding the *Pg*-LPS, a significant protein expression increase was observed following the stimulation in Ox-LDL pre-treated ECs (Fig 8).

Discussion

The role of infection, especially with *Pg*, in atherosclerosis still needs to be clarified. Several risk factors have been identified for atherosclerosis including dyslipidemia [32] and systemic inflammation [33]. Some studies already demonstrated a synergism between risk factors as demonstrated for infection with *Pg* on endothelial injury in an obese mouse model [34]. However, mechanisms underlying this effect need to be determined.

In this study, we showed that infection with *Pg* increased EC death. As hypothesized, the pre-stimulation by another stressor, such as Ox-LDL amplified this cell mortality. However, no cumulative effect was observed after TNF-α pre-treatment. Interestingly, the type of cell death induced by *Pg* infection seemed to be under the influence of the inflammatory state of ECs, illustrating the cumulative influence of atherosclerotic risk factors on ECs survival.

ECs death was observed in early phases of atherogenesis [16,35] and several molecular risk factors could activate cell death related pathways. It has already been described that Ox-LDL, one of the most important atherosclerosis risk factors, was able to induce apoptosis in ECs in a concentration-dependent manner [27,35] and necrosis depending on Ox-LDL concentration and LDL oxidation level [5,27].

Infection with several periodontal pathogens, especially *Pg*, has been proposed as one of the potential mechanisms contributing to chronic inflammation of the atheromatous plaque [5,36] and also promoting lipid deposition within arterial wall [27,36]. Several bacteria have been described as being able to worsen atherosclerosis through induction of ECs death including *C. pneumoniae*, as demonstrated *in vitro* [27,37] and *in vivo* [37,38]. Regarding periodontal pathogens, especially *Pg*, it has been shown that this bacterium was able to mediate EC death in a dose-dependent manner [34,38] and to amplify endothelial injury through EC apoptosis induced by other molecules such as free fatty acids [27,34]. However, no data regarding the effects induced by *Pg* in the context of Ox-LDL or TNF-α pre-treated ECs were available. A cumulative effect between Ox-LDL and *Pg* infection on cell viability has been observed as demonstrated for *C.pneumoniae* [27,39]. *Pg*-LPS is one of the major virulence factors of *Pg* and endotoxemia has been considered to induce systemic inflammation contributing to atherosclerosis worsening [14,39]. In ECs, *Pg*-LPS has been described to induce secretion of several pro-inflammatory cytokines [13,14] and to activate different types of enzymes such as cathepsin B contributing to inflammation [13,40]. In our study, we showed that *Pg*-LPS decreased EC viability similar to *E.coli*-LPS. Interestingly, the impact on cell viability was higher in Ox-LDL and TNF-α pre-treated ECs. This synergism between *Pg*-LPS and Ox-LDL effect has already been observed in several cell types such as THP-1 [34,40], foam cells [41] and in hTERT-

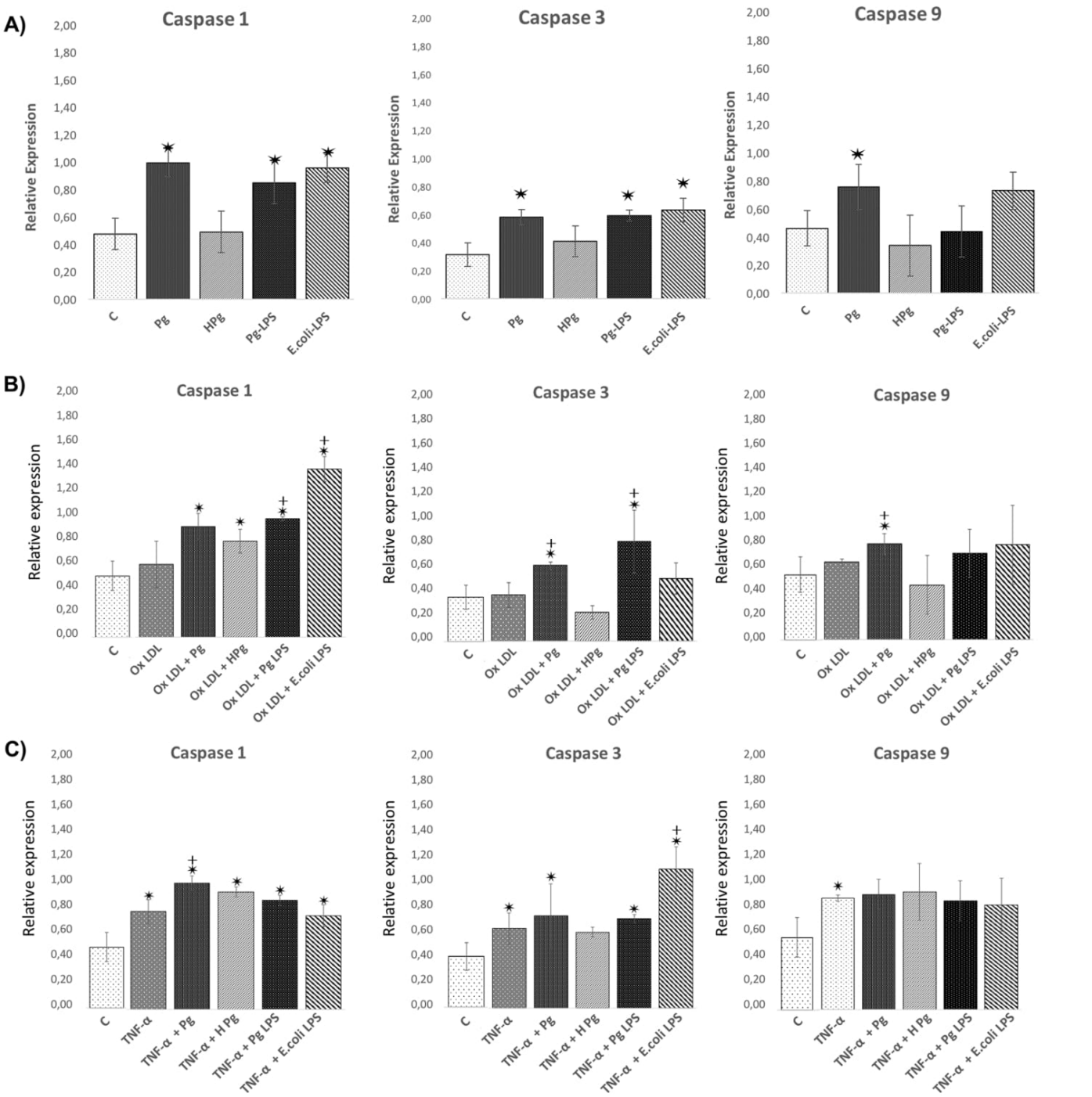

Fig 6. Differential modulation of the EC death related gene expression with *Pg* and its LPS in Ox-LDL and TNF-α pre-treated cells. (A) Gene expression of Caspase-1,-3 and -9 in HUVECs infected with *Pg* at a MOI of 100 or with heat inactivated *Pg* and stimulated by *Pg*-LPS (1μg/ml) or *E.Coli*-LPS (1μg/ml) at 24h. **(B)** Gene expression for the same described genes in Ox-LDL pre-treated HUVECs at 24h. **(C)** Gene Expression for the same described genes in TNF- α pre-treated HUVECs at 24h. Data were expressed as mean ± SD. *: difference between non-stimulated/infected and stimulated/infected cells, $p < 0.05$, ┼: difference between non pre-treated/stimulated/infected and treated cells, $p < 0.05$.

doi:10.1371/journal.pone.0154590.g006

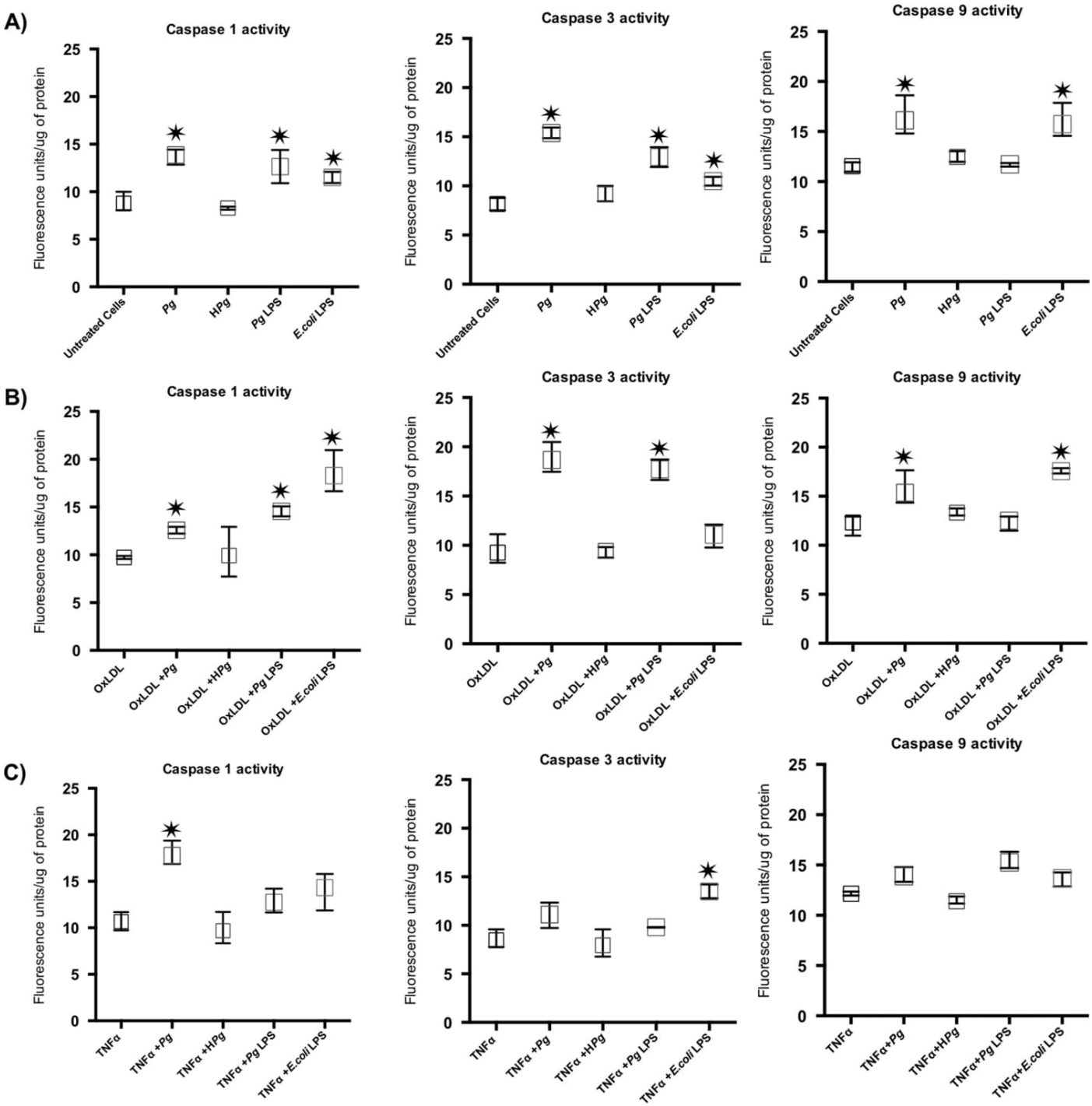

Fig 7. Differential modulation of the EC death related caspase activity after infection with *Pg* and its LPS in Ox-LDL and TNF-α pre-treated cells. (A) Enzymatic activity of Caspase-1, -3 and -9 in HUVECs infected with *Pg* at a MOI of 100 or with heat inactivated *Pg* and stimulated by *Pg*-LPS (1μg/ml) or *E. Coli*-LPS (1μg/ml) at 24h. **(B)** Enzymatic activity of Caspase-1, -3 and -9 in Ox-LDL pre-treated HUVECs at 24h. **(C)** Enzymatic activity of Caspase-1, -3 and -9 in in TNF- α pre-treated HUVECs at 24h. Data were expressed as mean ± SD. *: difference between non-stimulated/infected and stimulated/infected cells, $p < 0.05$.

doi:10.1371/journal.pone.0154590.g007

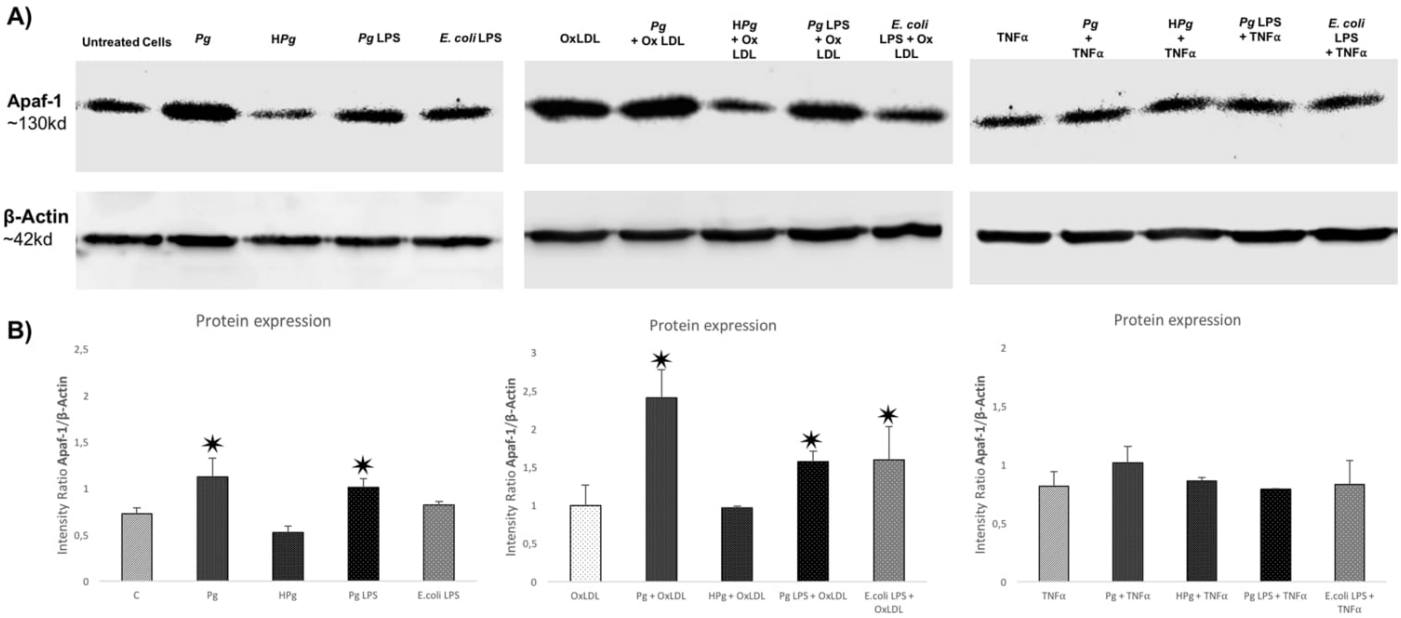

Fig 8. Differential modulation of Apaf-1 protein expression after infection with *Pg* and its LPS in Ox-LDL and TNF-α pre-treated cells. (A) Western blot analysis for Apaf-1 protein in HUVECs infected with *Pg* at a MOI of 100 or with H*Pg* and stimulated by *Pg*-LPS (1μg/ml) or *E.Coli*-LPS (1μg/ml) and pre-treated with Ox-LDL (50μg/ml) or TNF- α (10ng/ml) at 24h. **(B)** Density tracing was used to illustrate the quantitative differences in western blot analysis for Apaf-1 protein. Data were expressed as mean ± SD. *: difference between non-stimulated/infected and stimulated/infected cells, $p < 0.05$.

doi:10.1371/journal.pone.0154590.g008

immortalized human umbilical vein endothelial cells (HuhT1) [34,42]. Nevertheless, its impact seemed to be cell-dependent as it was also showed that it inhibits apoptosis in epithelial cells [42,43] illustrating the complexity of cell responses to bacterial infection and endotoxemia.

In this study, we analysed the type of cell death induced by infection. Our results showed that cell death associated with *Pg* infection was both apoptosis and necrosis. Necrosis could be considered to be more pro-inflammatory than apoptosis. However, the significant increase of apoptosis was also detrimental to the organism [34,43]. Interestingly, the type of cell death induced was under the influence of EC pre-treatment. In Ox-LDL pre-treated ECs, *Pg* and its *Pg*-LPS significantly increased the apoptosis rate at 24h. This result was already observed in another EC model [34,44]. On the contrary, an increase of the necrosis rate was observed in TNF-α pre-treated ECs. This first observation illustrates the need of the use of complex cell models to mimic specifically the different processes involved in a vascular disease. In our study, type of cell death was determined by cells counting microscopically. A more precise evaluation could be achieve using flow-cytometry.

Apoptosis is considered as a programmed cell death. Recently, many other forms of programmed cell death have been described including pyroptosis. Pyroptosis is part of the host defense against infection and is dependent on the caspase-1 activation. This type of cell death is involved in several diseases characterized by inflammation [44,45]. *In vitro* evaluation of these processes seemed to be difficult and their roles have not been well defined *in vivo*. For instance, several features of pyroptosis seemed to overlap with apoptosis and pyroptosis and apoptosis shared a positive annexin V staining. Annexin V binds to phosphatidyl serine that is normally restricted to the inner leaflet of the cell membrane. During pyroptosis, pores are open in cell membrane allowing annexin V to enter the cell and stain [44,45]. In our study, *Pg* infection increased caspase-1 expression that could be considered as a potential trigger of pyroptotic cell death promoting inflammation [44,46].

Several pathways have been related to cell death, especially apoptosis. These pathways involved caspases that could be considered as the effectors and other complexes such as apoptosome that are activated after release of cytochrome c (cyt c) from the mitochondria. This process is under the influence of Bcl-2 and Bax [46]. In ECs, *Pg* increased cell death related gene expressions of Bax-1, caspase -1, -3, -9 and Apaf-1. To our knowledge, this is the first time that an influence of *Pg* on apoptosome related Apaf-1 gene expression was described. Furthermore, these modifications at the mRNA level were confirmed at the protein level. Caspase-1, -3 and -9 enzymatic activity was increased following the infection. Others studies showed influence of *Pg* on intrinsic apoptotic pathways, especially in epithelial cells [47,48].

Apaf-1 apoptosome is implicated in the intrinsic cell death pathway. Pro-apoptotic stimuli induce the release of cyt c that will act on this complex leading to activation of procaspase-9 and -3 and contributing to apoptosis [49]. Other bacteria have been described as being able to regulate apoptosis through Apaf-1/caspase-9 modulation [50]. Interestingly, in this study, Apaf-1 expression, at both mRNA and protein levels, was increased especially in Ox-LDL pretreated ECs infected with *Pg* and also observed after stimulation by *Pg*-LPS highlighting a potential role for this virulence factor in this process and subsequently implication of TLR-4 related pathways [14].

In summary, this study contributes to demonstrate that *Pg* and its *Pg*-LPS could exacerbate Ox-LDL and TNF-α induced endothelial injury through increase of EC cell death. These results strengthen the hypothesis that periodontitis should be considered as a risk factor for atherosclerosis progression, especially in patients at-risk such as dyslipidemic and obese patients. This also highlights the need of strong collaboration between periodontists and cardiologists to diagnose and treat periodontal diseases to prevent atherosclerosis worsening.

Acknowledgments

Authors thank Fareeha Batool for her help in the preparation of the manuscript.

Author Contributions

Conceived and designed the experiments: OH HT JLD. Performed the experiments: IMB YK NS OH. Analyzed the data: IMB OH. Contributed reagents/materials/analysis tools: IMB YK NS DNM OH. Wrote the paper: IMB HT JLD OH.

References

1. Hajishengallis G, Lamont RJ. Breaking bad: manipulation of the host response by Porphyromonas gingivalis. Eur J Immunol. 2014; 44: 328–338. doi: 10.1002/eji.201344202 PMID: 24338806
2. Hajishengallis G. Periodontitis: from microbial immune subversion to systemic inflammation. Nat Rev Immunol. 2015; 15: 30–44. doi: 10.1038/nri3785 PMID: 25534621
3. Lockhart PB, Bolger AF, Papapanou PN, Osinbowale O, Trevisan M, Levison ME, et al. Periodontal Disease and Atherosclerotic Vascular Disease: Does the Evidence Support an Independent Association?: A Scientific Statement From the American Heart Association. Circulation. 2012; 125: 2520–2544. doi: 10.1161/CIR.0b013e31825719f3 PMID: 22514251
4. Huck O, Saadi-Thiers K, Tenenbaum H, Davideau J-L, Romagna C, Laurent Y, et al. Evaluating periodontal risk for patients at risk of or suffering from atherosclerosis: recent biological hypotheses and therapeutic consequences. Archives of Cardiovascular Diseases. 2011; 104: 352–358. doi: 10.1016/j.acvd.2011.02.002 PMID: 21693372
5. Rosenfeld ME, Campbell LA. Pathogens and atherosclerosis: update on the potential contribution of multiple infectious organisms to the pathogenesis of atherosclerosis. Thromb Haemost. 2011; 106: 858–867. doi: 10.1160/TH11-06-0392 PMID: 22012133
6. Zelkha SA, Freilich RW, Amar S. Periodontal innate immune mechanisms relevant to atherosclerosis and obesity. Periodontol 2000. 2010; 54: 207–221. doi: 10.1111/j.1600-0757.2010.00358.x PMID: 20712641

7. Yilmaz O. The chronicles of Porphyromonas gingivalis: the microbium, the human oral epithelium and their interplay. Microbiology (Reading, Engl). 2008; 154: 2897–2903. doi: 10.1099/mic.0.2008/021220-0
8. Elkaim R, Dahan M, Kocgozlu L, Werner S, Kanter D, Kretz JG, et al. Prevalence of periodontal pathogens in subgingival lesions, atherosclerotic plaques and healthy blood vessels: a preliminary study. J Periodont Res. 2008; 43: 224–231. PMID: 18326058
9. Li L, Messas E, Batista EL, Levine RA, Amar S. Porphyromonas gingivalis infection accelerates the progression of atherosclerosis in a heterozygous apolipoprotein E-deficient murine model. Circulation. 2002; 105: 861–867. PMID: 11854128
10. Velsko IM, Chukkapalli SS, Rivera MF, Lee J-Y, Chen H, Zheng D, et al. Active invasion of oral and aortic tissues by Porphyromonas gingivalis in mice causally links periodontitis and atherosclerosis. PLoS ONE. 2014; 9: e97811. doi: 10.1371/journal.pone.0097811 PMID: 24836175
11. Bach LA. Endothelial cells and the IGF system. J Mol Endocrinol. 2015; 54: R1–R13. doi: 10.1530/JME-14-0215 PMID: 25351818
12. Huck O, Elkaim R, Davideau J-L, Tenebaum H. Porphyromonas gingivalis-impaired innate immune response via NLRP3 proteolysis in endothelial cells. Innate Immunity. 2015; 21: 65–72. doi: 10.1177/1753425914523459 PMID: 24583910
13. Huck O, Elkaim R, Davideau J-L, Tenenbaum H. Porphyromonas gingivalis and its lipopolysaccharide differentially regulate the expression of cathepsin B in endothelial cells. Molecular Oral Microbiology. 2012;: no–no. doi: 10.1111/j.2041-1014.2012.00638.x
14. Kocgozlu L, Elkaim R, Tenenbaum H, Werner S. Variable cell responses to P. gingivalis lipopolysaccharide. J Dent Res. 2009; 88: 741–745. doi: 10.1177/0022034509341166 PMID: 19734462
15. Rodrigues PH, Reyes L, Chadda AS, Bélanger M, Wallet SM, Akin D, et al. Porphyromonas gingivalis strain specific interactions with human coronary artery endothelial cells: a comparative study. PLoS ONE. 2012; 7: e52606. doi: 10.1371/journal.pone.0052606 PMID: 23300720
16. Choy JC, Granville DJ, Hunt DW, McManus BM. Endothelial cell apoptosis: biochemical characteristics and potential implications for atherosclerosis. J Mol Cell Cardiol. 2001; 33: 1673–1690. doi: 10.1006/jmcc.2001.1419 PMID: 11549346
17. Pirillo A, Norata GD, Catapano AL. LOX-1, OxLDL, and atherosclerosis. Mediators Inflamm. 2013; 2013: 152786. doi: 10.1155/2013/152786 PMID: 23935243
18. Hopkins PN. Molecular Biology of Atherosclerosis. Physiol Rev. 2013; 93: 1317–1542. doi: 10.1152/physrev.00004.2012 PMID: 23899566
19. Napoli C. Oxidation of LDL, atherogenesis, and apoptosis. Ann N Y Acad Sci. 2003; 1010: 698–709. PMID: 15033814
20. Czabotar PE, Lessene G, Strasser A, Adams JM. Control of apoptosis by the BCL-2 protein family: implications for physiology and therapy. Nat Rev Mol Cell Biol. 2014; 15: 49–63. doi: 10.1038/nrm3722 PMID: 24355989
21. Gupta S, Kass GEN, Szegezdi E, Joseph B. The mitochondrial death pathway: a promising therapeutic target in diseases. J Cell Mol Med. 2009; 13: 1004–1033. doi: 10.1111/j.1582-4934.2009.00697.x PMID: 19220575
22. Tang Y, Zhang Y-C, Chen Y, Xiang Y, Shen C-X, Li Y-G. The role of miR-19b in the inhibition of endothelial cell apoptosis and its relationship with coronary artery disease. Sci Rep. 2015; 5: 15132. doi: 10.1038/srep15132 PMID: 26459935
23. Maiolino G, Rossitto G, Caielli P, Bisogni V, Rossi GP, Calò LA. The role of oxidized low-density lipoproteins in atherosclerosis: the myths and the facts. Mediators Inflamm. 2013; 2013: 714653. doi: 10.1155/2013/714653 PMID: 24222937
24. Ross R. The pathogenesis of atherosclerosis: a perspective for the 1990s. Nature. 1993; 362: 801–809. doi: 10.1038/362801a0 PMID: 8479518
25. Qin B, Cao Y, Yang H, Xiao B, Lu Z. MicroRNA-221/222 regulate ox-LDL-induced endothelial apoptosis via Ets-1/p21 inhibition. Mol Cell Biochem. 2015; 405: 115–124. doi: 10.1007/s11010-015-2403-5 PMID: 25893733
26. Rastogi S, Rizwani W, Joshi B, Kunigal S, Chellappan SP. TNF-α response of vascular endothelial and vascular smooth muscle cells involve differential utilization of ASK1 kinase and p73. Cell Death Differ. 2012; 19: 274–283. doi: 10.1038/cdd.2011.93 PMID: 21738216
27. Nazzal D, Cantero A-V, Therville N, Segui B, Negre-Salvayre A, Thomsen M, et al. Chlamydia pneumoniae alters mildly oxidized low-density lipoprotein-induced cell death in human endothelial cells, leading to necrosis rather than apoptosis. J Infect Dis. 2006; 193: 136–145. doi: 10.1086/498617 PMID: 16323142

28. Elkaim R, Werner S, Kocgozlu L, Tenenbaum H. P. gingivalis regulates the expression of Cathepsin B and Cystatin C. J Dent Res. 2008; 87: 932–936. PMID: 18809746

29. Petrache I, Birukov K, Zaiman AL, Crow MT, Deng H, Wadgaonkar R, et al. Caspase-dependent cleavage of myosin light chain kinase (MLCK) is involved in TNF-alpha-mediated bovine pulmonary endothelial cell apoptosis. FASEB J. 2003; 17: 407–416. doi: 10.1096/fj.02-0672com PMID: 12631580

30. Hasegawa J, Kamada S, Kamiike W, Shimizu S, Imazu T, Matsuda H, et al. Involvement of CPP32/Yama(-like) proteases in Fas-mediated apoptosis. Cancer Res. 1996; 56: 1713–1718. PMID: 8620480

31. Rosado JA, Lopez JJ, Gomez-Arteta E, Redondo PC, Salido GM, Pariente JA. Early caspase-3 activation independent of apoptosis is required for cellular function. J Cell Physiol. 2006; 209: 142–152. doi: 10.1002/jcp.20715 PMID: 16791842

32. Hendrani AD, Adesiyun T, Quispe R, Jones SR, Stone NJ, Blumenthal RS, et al. Dyslipidemia management in primary prevention of cardiovascular disease: Current guidelines and strategies. World J Cardiol. 2016; 8: 201–210. doi: 10.4330/wjc.v8.i2.201 PMID: 26981215

33. Wilson PWF. Evidence of systemic inflammation and estimation of coronary artery disease risk: a population perspective. Am J Med. 2008; 121: S15–20. doi: 10.1016/j.amjmed.2008.06.012 PMID: 18926165

34. Ao M, Miyauchi M, Inubushi T, Kitagawa M, Furusho H, Ando T, et al. Infection with Porphyromonas gingivalis exacerbates endothelial injury in obese mice. PLoS ONE. 2014; 9: e110519. doi: 10.1371/journal.pone.0110519 PMID: 25334003

35. Zhang Y, Xie Y, You S, Han Q, Cao Y, Zhang X, et al. Autophagy and Apoptosis in the Response of Human Vascular Endothelial Cells to Oxidized Low-Density Lipoprotein. Cardiology. 2015; 132: 27–33. doi: 10.1159/000381332 PMID: 26021729

36. Hayashi C, Viereck J, Hua N, Phinikaridou A, Madrigal AG, Gibson FC, et al. Porphyromonas gingivalis accelerates inflammatory atherosclerosis in the innominate artery of ApoE deficient mice. Atherosclerosis. 2011; 215: 52–59. doi: 10.1016/j.atherosclerosis.2010.12.009 PMID: 21251656

37. Birck MM, Saraste A, Hyttel P, Odermarsky M, Liuba P, Saukko P, et al. Endothelial Cell Death and Intimal Foam Cell Accumulation in the Coronary Artery of Infected Hypercholesterolemic Minipigs. J of Cardiovasc Trans Res. 2013; 6: 579–587. doi: 10.1007/s12265-013-9463-2

38. Roth GA, Ankersmit HJ, Brown VB, Papapanou PN, Schmidt AM, Lalla E. Porphyromonas gingivalis infection and cell death in human aortic endothelial cells. FEMS Microbiol Lett. 2007; 272: 106–113. doi: 10.1111/j.1574-6968.2007.00736.x PMID: 17459112

39. Pussinen PJ, Tuomisto K, Jousilahti P, Havulinna AS, Sundvall J, Salomaa V. Endotoxemia, immune response to periodontal pathogens, and systemic inflammation associate with incident cardiovascular disease events. Arterioscler Thromb Vasc Biol. 2007; 27: 1433–1439. doi: 10.1161/ATVBAHA.106.138743 PMID: 17363692

40. Park E, Na HS, Song Y-R, Shin SY, Kim Y-M, Chung J. Activation of NLRP3 and AIM2 inflammasomes by Porphyromonas gingivalis infection. Infect Immun. 2014; 82: 112–123. doi: 10.1128/IAI.00862-13 PMID: 24126516

41. Lei L, Li H, Yan F, Li Y, Xiao Y. Porphyromonas gingivalis lipopolysaccharide alters atherosclerotic-related gene expression in oxidized low-density-lipoprotein-induced macrophages and foam cells. J Periodont Res. 2011; 46: 427–437. doi: 10.1111/j.1600-0765.2011.01356.x PMID: 21418223

42. Soto C, Bugueño I, Hoare A, Gonzalez S, Venegas D, Salinas D, et al. The Porphyromonas gingivalis O antigen is required for inhibition of apoptosis in gingival epithelial cells following bacterial infection. J Periodont Res. 2015. doi: 10.1111/jre.12331

43. Leist M, Jäättelä M. Four deaths and a funeral: from caspases to alternative mechanisms. Nat Rev Mol Cell Biol. 2001; 2: 589–598. doi: 10.1038/35085008 PMID: 11483992

44. Duprez L, Wirawan E, Vanden Berghe T, Vandenabeele P. Major cell death pathways at a glance. Microbes Infect. 2009; 11: 1050–1062. doi: 10.1016/j.micinf.2009.08.013 PMID: 19733681

45. Brennan MA, Cookson BT. Salmonella induces macrophage death by caspase-1-dependent necrosis. Mol Microbiol. 2000; 38: 31–40. PMID: 11029688

46. Gortat A, Sancho M, Mondragón L, Messeguer À, Pérez-Payá E, Orzáez M. Apaf1 inhibition promotes cell recovery from apoptosis. Protein Cell. 2015; 6: 833–843. doi: 10.1007/s13238-015-0200-2 PMID: 26361785

47. Mao S, Park Y, Hasegawa Y, Tribble GD, James CE, Handfield M, et al. Intrinsic apoptotic pathways of gingival epithelial cells modulated by Porphyromonas gingivalis. Cell Microbiol. 2007; 9: 1997–2007. doi: 10.1111/j.1462-5822.2007.00931.x PMID: 17419719

48. Stathopoulou PG, Galicia JC, Benakanakere MR, Garcia CA, Potempa J, Kinane DF. Porphyromonas gingivalis induce apoptosis in human gingival epithelial cells through a gingipain-dependent mechanism. BMC Microbiol. 2009; 9: 107. doi: 10.1186/1471-2180-9-107 PMID: 19473524

49. Yuan S, Akey CW. Apoptosome structure, assembly, and procaspase activation. Structure. 2013; 21: 501–515. doi: 10.1016/j.str.2013.02.024 PMID: 23561633

50. Rahman MA, Shirai M, Aziz MA, Ushirokita R, Kubota S, Suzuki H, et al. An epistatic effect of apaf-1 and caspase-9 on chlamydial infection. Apoptosis. 2015; 20: 1271–1280. doi: 10.1007/s10495-015-1161-x PMID: 26290316

IV. Annexe n°2

Korah L., Amri N., **Bugueno I.M**., Hotton E., Tenenbaum H., Huck O., Berdal A., Davideau J.L. Experimental periodontitis in Msx2 mutant mice induces alveolar bone necrosis. **Journal of Periodontology 2019, Doi:10.1002/JPER.16-0435.**

Experimental periodontitis in *Msx2* mutant mice induces alveolar bone necrosis

Linda KORAH Scientist[*], Nawel AMRI DDS[†], Isaac Maximiliano BUGUENO VALDEBENITO DDS[*], Dominique HOTTON Engineer[†], Henri TENENBAUM Professor[*‡],

Olivier HUCK Professor[*‡], Ariane BERDAL Professor[†], Jean-Luc DAVIDEAU Professor[‡]

[*]INSERM (French National Institute of Health and Medical Research), UMR 1109, Osteoarticular and Dental Regenerative Nanomedicine laboratory, Faculté de Médecine, FMTS (Federation of Translational Medicine Strasbourg), Strasbourg, France.

[†]INSERM UMR 1138, Laboratory of Oral Molecular Physiopathology, Institut des Cordeliers, Paris, France

[‡]Department of Periodontology, Dental Faculty, University of Strasbourg, France

Linda KORAH, Nawel AMRI, Isaac Maximiliano BUGUENO VALDEBENITO, Dominique HOTTON, Olivier HUCK, and Jean-Luc DAVIDEAU substantially contributed to conception and design, or acquisition, analysis, or interpretation of data. Jean-Luc DAVIDEAU drafted the article and Henri TENENBAUM, Olivier HUCK, Ariane BERDAL revised it the critically the article for important intellectual content. All authors gave the final approval of the version to be published, and agreed to be accountable for all aspects of the work in ensuring that questions related to the accuracy or integrity of any part of the work are appropriately investigated and resolved.

Corresponding author: Jean-Luc Davideau, Department of Periodontology, Dental Faculty of Strasbourg, 1 place de l'Hôpital, 67000 Strasbourg, France.

Tel/Fax number: +33(0)388116947 E-mail: jean-luc.davideau@chru-strasbourg.fr (e-mail address could be published)

Words: 3560

Figures: 6

References: 47

Running title: *Msx2* and periodontitis

Sentence summary: *Msx2* mutation effects on periodontitis suggested that *Msx2* was involved in the control of periodontal tissue destruction.

ABSTRACT

Background: *Msx2* homeoprotein is a key transcription factor of dental and periodontal tissue formation and is involved in many molecular pathways controlling mineralized tissue homeostasis such as Wnt/sclerostin pathway. This study evaluated the effect of *Msx2*-null mutation during experimental periodontitis in mice. **Methods**: Experimental periodontitis was induced for 30 days in wild type and *Msx2* knock-in Swiss mice using *Porphyromonas gingivalis* infected ligatures. In knock-in mice, *Msx2* gene was replaced by *n-LacZ* gene encoding β-galactosidase. Periodontal tissue response was assessed by histomorphometry, TRAP histoenzymology, β-galactosidase, sclerostin immunochemistry and TUNEL assay. Expression of *Msx2* gene expression was also evaluated in human gingival biopsies using RT-qPCR. **Results**: During experimental periodontitis osteonecrosis area and osteoclast number were significantly elevated in knock-in mice compared to wild type mice. Epithelial downgrowth and bone loss was similar. Sclerostin expression in osteocytes appeared to be reduced during periodontitis in knock-in mice. *Msx2* expression was detected in healthy and inflamed human gingival tissues. **Conclusion**: These data indicated that *Msx2* pathway influenced periodontal tissue response to experimental periodontitis and appeared to be a protective factor against alveolar bone osteonecrosis. As shown in other inflammatory processes such as atherothrombosis, genes initially characterized in early development could also play an important role in human periodontal pathogenesis.

Keywords: periodontitis, mice, osteonecrosis, *Msx2*, human

INTRODUCTION

Msx2 is a member of the Muscle segment homeobox gene (*Msx*) family.[1] *Msx2* gene encodes homeoprotein that acts as transcriptional factor binding specific DNA sequences and plays an important role during early skeletal development.[2,3] In human, gain-and loss-of-function associated with *Msx2* mutations are correlated to premature cranial suture fusion (Boston-type2 craniosynostosis) and impaired suture closing in the parietal foramina.[4] Besides this major skeletal manifestations, in *Msx2* transgenic mouse model, tooth root abnormalities and delayed tooth eruption are observed in addition to enamel and cranial suture defects.[5–7] Dental root epithelium and cellular cementum appear hyperplasic and radicular dentinogenesis is prematurely stopped leading to short and deformed roots.[6,8] These defects appear root and tooth specific while a gradient of deformities is observed from the first to the third molars. Furthermore, alveolar bone resorption is impaired and the number of osteoclasts reduced.[8] These data suggest that *Msx2* is involved in the periodontal tissue formation and homeostasis. Indeed, in vitro and in vivo studies show that *Msx2* is expressed in periodontal and dental cells[9], such as osteoblasts[10], osteoclasts[8], odontoblasts[11], periodontal ligament fibroblasts[12], root epithelial cells and ameloblasts[6]. In these cells, interactions of *Msx2* with others transcription factors influence cell differentiation via the control of matrix and bio-mineralization protein expression, such as osteocalcin[10], amelogenins[6], and other proteins essential for periodontal tissue formation and/or homeostasis such as alkaline phosphatase[13], dentin sialophosphoprotein[11], bone sialoprotein BSP[14], laminine-5α3[5], and cytokeratin 5[6]. *Msx2* is also a key element of the BMP-2[3] and the Wnt-βcatenin/sclerostin pathways which regulate bone homeostasis[7,16,17]. Wnt/βcatenin signaling pathways are involved in normal periodontal tissue formation.[18-19] Sclerostin acts as an antagonist of Wnt-βcatenin canonical pathway and reduces bone formation.[20] Inhibition of sclerostin action in periostin null mutant mice[21] or injected sclerostin antibodies after experimental periodontitis[22] have been shown to decrease or reverse bone loss. Interestingly, *Msx2* is also involved in inflammatory processes and its upregulation by TNF-α has been shown to impaired osteoblast differentiation[23] and to increase vessel wall calcification[24].

Regarding the role of *Msx2* during tooth and root development, tissue homeostasis, and its regulation by inflammatory cytokines, the aim of this study was to determine the involvement of *Msx2* pathways in the local response to experimental periodontitis.

MATERIALS AND METHODS

Msx2 KI mice (generation, genotyping)

Knock-in mice were produced by insertion of the bacterial *n-lacZ* gene within the *Msx2* gene, replacing the coding sequence.[8] Heterozygous males and females were mated using a CD1 Swiss genetic background. Their litters were used to compare wild-type (*Msx2*+/+), transgenic heterozygous (*Msx2*+/-) and homozygous (*Msx2*-/-) mice. Each experimental group comprised at least 3 mice, for a total number of 15 animals. For genotyping, primers were selected for PCR analysis of genomic DNA extracted from the tails in order to determine the genotype.[6] Amplification conditions were 95 °C (10 s), 65 °C (30 s) and 72 °C (1 min) for 30 cycles. Amplification products were identified on 2% agarose gels.

Animals

To avoid any potential effects of estrogen, we used only male mice (n=15, Swiss) 12 weeks old. Sample size calculation was based on previous experiments results on mean attachment level and observed standard deviation in different model of experimental periodontitis at different times.[25] The mean attachment level was 0.16mm with 0.02mm standard deviation. A difference of 0.1mm between groups was chosen based on comparable studies.[26] The minimal estimated[§] number of mice per group was 3. All animals were fed a regular diet and were kept in the same environment. All experiments were performed in accordance with the French National Consultative Bioethics

[§] G*Power 3.1.9.2, University of Dusseldorf, Germany

Committee for Health and Life Science, following ethical guidelines for animal care (A-75-06-12). Mice were inspected in order to evaluate pain stress and their weight was monitored on a daily basis.

Induction of experimental periodontitis

Experimental periodontitis was induced as previously described.[25] Briefly, twelve-week-old mice were intraperitoneally anaesthetized with a mixture of ketamine (80 mg/kg) and xylazine (10 mg/kg) . Sterilized black braided 6.0 silk threads[¶] were soaked in *Porphyromonas gingivalis* strain ATCC 33277 in an anaerobic chamber for one day and were placed at the cervical palatal site of the first maxillary molars on the right side. Contra-lateral molars were left without ligatures as control. In order to facilitate the first ligature placement, a slight incision to the bone crest contact was made at the junction between the gum and the tooth along the first and second molars. The thread was then blocked with a drop of glass ionomer[#]. The ligatures were inspected and replaced without incision twice a week in order to maintain a ligature for 30 days before euthanasia.

Tissues preparation

Mice were euthanized with an intra-peritoneal lethal injection of pentobarbital (100 mg/kg) . Intra-cardiac perfusion with a fixative solution containing 4% paraformaldehyde in Phosphate Buffer Saline (PBS) pH 7.4 was then performed. Maxillae were then dissected and post-fixed by immersion in the same fixative solution overnight at 4°C. After rinsing in PBS for 24 h, maxillae were processed

---

Centravet, Velaine en Haye, France

[¶] Ethicon, Auneau, France

[#] Fugi II GC GC France, Bonneuil sur Marne, France

for histologic analysis by decalcification at 4°C for 6 weeks in a pH 6.7 solution containing 4.13% EDTA[**] changed twice a week with constant stirring. After extensive washing in PBS, the samples were dehydrated in increasing concentrations of ethanol and toluene and finally embedded in paraffin Paraplast plus. Serial frontal sections of the maxilla were cut with a microtome. Computerized images were analyzed for the different calculations and countings using ImageJ 1.36b[††].

Histomorphometric analysis

For histomorphometric evaluation, 7-µm-thick sections were deparaffinized, rehydrated and stained with hematoxylin. After dehydration, slides were mounted with DPX resin and observed and photographed on a DMRB microscope[‡‡]. Three frontal sections of palatal root and mesial and distal furcation areas of the first molar were examined. The zone of interest was the palatal aspect of first molar periodontium (1mm long and 500µm width area). The level of attachment/extension of the apical down-growth of epithelium and the level of alveolar bone crest resorption were evaluated from the cemento-enamel junction at 400X magnification[25,27] in the first molar mesial furcation and root palatal zones using ImageJ software.

[**] Sigma, Saint Quentin Fallavier, France

[††] Wayne Rasband, National Institutes of Health, Bethesda, MD, USA

[‡‡] RM 2145; Leica, Rueil-Malmaison, France

Tartrate-resistant acid phosphatase (TRAP) activity assay

TRAP activity assay was performed as previously described.[25] Paraffin frontal sections were rehydrated, fixed for 5 min in fixative solution and rinsed in water before staining in pH 5.2 acetate buffer containing 2.5 mM Naphtol-AS-TR-Phosphate, 0.36 MN–NDimethyl-formamide, 0.1 M sodium tartrate and 4 mM Fast Red TR Salt . After staining, sections were rinsed in water and mounted with Clearmount[§§]. TRAP-positive cells were counted on the alveolar bone crest surface at the palatal root and the mesial and distal furcation aspects of the first molar using standardized views. The number of TRAP-positive cells was divided by the bone soft connective tissue linear surface length.[28]

Immunocytochemistry of β-galactosidase and sclerostin

All washings and incubations were performed at room temperature with PBS pH 7.4 solutions in humidified chamber. Sections were deparaffinized and hydrated, and endogenous peroxidases were inhibited by incubation for 10 min in a freshly made solution of 3% H_2O_2 in deionized water. For β-galactosidase immunodetection, nonspecific protein binding was blocked by incubation for 1 hour in 10% normal goat serum in PBS. Specimens were incubated for 1 hour with a polyclonal chicken anti-β-galactosidase antibody AB 9361 at a dilution of 1:300. Sections were then washed extensively three times in PBS at room temperature before treatment for 1 hour at room temperature with the horseradish peroxidase goat anti-chicken antibody[¶¶] at a dilution of 1:200, washed with PBS and stained with DAB chromogen[##]. For sclerostin immunodetection, non-specific binding was blocked by incubation 1 hour in 2.5% normal horse serum in PBS. Specimens were

---

[§§] Euromedex, Souffelweyerscheim, France

Abcam, Cambridge, UK

[¶¶] Bethyl Laboratories Inc, Montgomery, TX, USA

[##] Dako France SA, Les Ulis, France

incubated for 12 hours at 4°C with a polyclonal goat anti-mouse sclerostin at a dilution of 1:40[***] as previously described.[7] Immunostaining was revealed using cell and tissue staining goat kit HRP-DAB system[†††]. After dehydration, slides were mounted with DPX. The number of sclerostin immunonegative/positive osteocytes per μm^2 in the palatal crestal zone was calculated in an area corresponding to a square of 52500μm^2 in periodontitis and contralateral control sites. Codetection of sclerostin immunostaining and TRAP activity has been performed using a protocol design previously described.[25] TRAP activity assay was performed on hydrated sections after sclerostin immunostaining.

Osteonecrosis quantification

Osteonecrosis quantification method was based on methods described in mice [29] and rat [30] and adapted to the observed specific morphological aspect of bone response in the presented models. Alveolar bone crest zones containing more than three contiguous empty lacunae and bone fragments with empty lacunae and without bone lining cells were defined as areas of osteonecrosis (see supplementary Figure S1 in online Journal of Periodontology). Areas were marked at palatal root, distal furcation, and mesial aspects of the first molar using standardized views. The total osteonecrosis area was calculated.

[***] R&D systems, Wiesbaden, Germany

[†††] R&D systems, Wiesbaden, Germany

TUNEL assay

Apoptotic gingival cells, including inflammatory cells and fibroblasts, and bone-lining cells were detected by Terminal deoxynucleotidyl transferase-mediated dUTP nickend labeling (TUNEL) assay, with the use of an *in situ* cell death detection kit[‡‡‡], performed according to the manufacturer's instructions after heated treatment of slides at 80°C during 30min in citrate buffer pH 6. TUNEL was performed on the section adjacent to that used for histomorphometric evaluation stained with hematoxylin. TUNEL osteocytes and total osteocytes were counted manually within 1mm adjacent to osteonecrotic foci or (if osteonecrosis was not present) within a 1mm along the palatal aspect of alveolar bone.[30] TUNEL-positive gingival and bone lining cells were counted. The data are presented as the number of apoptotic cells related to the same surface of analysis corresponding to a square of 52500µm^2.

Collection of gingival tissue samples

Samples of gingival tissues, including sulcus/pocket epithelium and underlying connective tissues were collected from patients attending periodontal treatments at the department of periodontology of the Strasbourg Dental Faculty. All participants signed an informed consent form. Tissue collection received approval from the Ethics Committee (DC-2014-2131) in accordance with the Declaration of Helsinki, as revised in 2008. Samples of gingival tissues were taken during flap surgery at sites with pocket depth >5mm in 5 patients suffering from chronic periodontitis or during crown-lengthening and plastic surgeries at non-inflammatory sites in 5 patients without periodontitis. Directly after harvesting, biopsies were stored at -80°C for subsequent RNA analysis.

‡‡‡ Roche Applied Science, Meylan, France

RNA isolation and reverse transcription

Total RNA from gingival samples was extracted using Tri reagent[§§§] according to the manufacturer's instructions. The Total RNA concentration was quantified using NanoDrop 1000[‖‖‖]. Reverse transcription was performed with the iScript Reverse Transcription Supermix[¶¶¶] according to the manufacturer's instructions. GAPDH was used as endogenous RNA control (housekeeping gene) in the samples, and primers sequences related to *Msx2* were the following: M2humP1→5'-CTCATGTCCGACAAGAAGCC-3' M2humP4→ 5'-GTACATGCCATATCCCACTG-3'. The expression level was calculated by the comparative Ct method ($2^{-\Delta\Delta Ct}$) after normalization to the housekeeping gene. All PCR assays were performed in triplicate and results are represented by the mean values.

Data analysis

The differences were tested for significance using one-way ANOVA with Tukey's test to allow comparison between groups. Student's *t-test*[###] analysis between two groups was also performed. Statistical significance was considered for p-value <0.05.

[§§§] Sigma, Saint Quentin Fallavier, France

[‖‖‖] Fischer Scientific, Illkirch, France

[¶¶¶] Bio-rad, Miltry-Mory, France

[###] XLSTAT, Addinsoft France, Paris, France

RESULTS

Msx2 expression

During the 30 days of follow-up, the weight gains were comparable in the different groups of mice. *Msx2-/-* mice were smaller than the litters and displayed hair follicle defects. Crown and root defects, such as marked crown wearing, shortened roots, cellular cementum hyperplasia, and an increase of epithelial rests of Malassez size were observed in *Msx2-/-* mice. These defects were more pronounced in second and third molars than in the first maxillary molar. Epithelial rests of Malassez were mainly observed around vestibular roots in wild type and mutant mice. *Msx2* gene expression pattern revealed by β-galactosidase immunodetection was similar in heterozygote and *Msx2-/-*. *Msx2* expression was mainly observed in epithelial rests of Malassez and dental pulp cells (Figures 1A through 1D), in hair follicle and enamel organ of continuously growing incisor (data not shown). *Msx2* was also expressed in palatal oral epithelium, especially in keratinocyte of granular layers, and some basal cells. At experimental periodontitis sites, expression pattern of *Msx2* was similar, however *Msx2* positive cells were also observed in inflamed pocket epithelium (Figure 1C).

Periodontal tissue responses to experimental periodontitis

Significant epithelial downgrowth and alveolar bone loss were observed at periodontitis sites compared to control counterparts in the different groups of mice ($P < 0.05$) (Figures 2A through 2F). However, no significant difference was observed between *Msx2+/+, Msx2+/-,* and *Msx2-/-* mice in comparable areas (Figure 2G). Interestingly, the distance between the alveolar bone crest and the cemento-enamel junction was significantly increased in *Msx2-/-* control teeth compared to *Msx2+/+* and *Msx2+/-* control teeth ($P < 0.05$) (Figure 2H).

Bone necrosis and osteoclast distributions

In *Msx2+/-* and *Msx2-/-* mice, bone osteonecrosis areas characterized by contiguous empty osteocyte lacunae were only observed in alveolar bone crest. Nevertheless, many necrotic fragments of alveolar bone were observed in inflamed connective tissue. Some of them were in contact or surrounded by pocket epithelium. In *Msx2+/+*, sparse and small bone fragments were inconstantly observed (Figures 3A through 3C). In *Msx2+/-* and *Msx2-/-* mice, alveolar bone necrosis was significantly ($P < 0.05$) more pronounced than in *Msx2+/+* mice at periodontitis sites (Figure 3J). Interestingly, no bone necrosis was observed at control sites. The number of osteoclastic cells increased with periodontitis (Figures 3D through 3I). In *Msx2-/-* mice, the number of osteoclastic cells was significantly higher than in *Msx2+/+*, and *Msx2+/-* mice ($P < 0.05$) (Figure 3K).

TUNEL positive cell distribution

TUNEL positive cells were mainly observed in inflamed gingiva and keratinocytes of the granular layer of palatal epithelium (Figures 4A through 4F). TUNEL positive bone lining cells and osteocytes were also detected especially in alveolar bone around teeth with experimental periodontitis (Figures 4E and 4F). No significant difference in the number of TUNEL positive osteocytes was observed between mice/teeth groups (Figure 4G), while TUNEL positive gingival and bone lining cells were significantly increased during periodontitis and in *Msx2+/+* mice ($P < 0.05$) (Figure 4H).

Sclerostin expression

Sclerostin was mainly detected in osteocytes except in those next to the bone surface, and in cementocytes of cellular cementum but less constantly. In *Msx2+/+* mice, sclerostin expression pattern in alveolar bone was comparable in control and periodontitis sites and its expression was not detected in osteoid areas (Figures 5A through 5D). In *Msx2-/-* mice a trend of decrease of sclerostin expression in osteocytes was observed during periodontitis compared to contralateral control sites ($P < 0.1$) (Figures 5E through 5G).

Expression of MSX2 in human gingival tissues

MSX2 expression was detected in healthy and inflamed human gingival tissues. No difference of *MSX2* relative expression was observed between periodontitis and healthy gingival tissues (Figure 6).

DISCUSSION

The data presented here showed that *Msx2* pathways could influence periodontal tissue response to experimental periodontitis in mouse. Furthermore, the first detection of *MSX2* expression in human gingiva in patients with healthy periodontium and suffering from periodontitis suggested that these pathways could be also involved in human periodontitis onset and development. *MSX2* gain or loss of function mutations induced relative rare human syndromes mainly characterized by craniofacial suture closure disorders, and in some cases, enamel malformations.[1,2] Clinical dental and periodontal structures have not been studied so far in these specific syndrome features. In mice, *Msx2* knock-out[5,31] and knock-in[6–8,32] homozygous mutations are associated to pronounced tooth defects, especially root defects. The presence of anatomical defects, such as flattened crowns, shortened roots and hyperplasia of cellular cementum and epithelial rests of Malassez in first and second maxillary molars appeared to be tooth, root and site specific.[5,8] Albeit

these anatomical defects, the histological aspect of connective attachment and alveolar bone of *Msx2* knock-in mutant mice were quite similar to wild type and *Msx2* heterozygous mice. These data showed that periodontal tissue homeostasis was not noticeably impacted by the absence of *Msx2* expression despite tooth and root anatomical defects. In periodontal tissue of adult mice, *Msx2* was mainly expressed in epithelial rest of Malassez[6], as also observed during root formation and tooth eruption[8,9,32]. Using knock-in *Msx2/LacZ* transgenic mice, *Msx2* expression was not observed in other tissue compartments of periodontium, while *Msx2* mRNA expression has been detected by RT-PCR in adult mice periodontium.[1] Furthermore, in vitro studies have shown that *Msx2* is also expressed in osteoblasts[23] and periodontal ligament cells[12], suggesting that they expressed *Msx*2 in situ at a too low level to be detected in knock-in *Msx2/LacZ* transgenic mice by β-galactosidase immunocytochemistry[6] and histoenzymology[8]. In inflamed periodontal tissues, the observed expression pattern of *Msx2* was similar. *Msx2* positive cells were detected in pocket epithelium while its expression was not observed in non-inflamed sulcular epithelium[6], suggesting that *Msx2* expression in inflamed epithelium could be induced or that cells from epithelial rest of Malassez could migrate or be incorporated within pocket epithelium as observed in skin with the migration of *Msx2* positive hair follicle cells in epithelial wound edges.[33]

The response of alveolar bone to a 30 days experimental periodontitis appeared to be impaired in *Msx2* mutant mice. Studies using the same periodontitis model demonstrated that this period appeared optimum to investigate chronic alveolar bone loss.[25,34,35] A significant increase of bone necrosis in alveolar bone crest was observed in *Msx2* mutant mice compared to wild type mice. The increase of bone necrosis defined here as the presence of contiguous empty osteocyte lacunae has been infrequently reported in studies using the same experimental mice periodontitis model,[34,35] or mice model with non-infected ligature,[27] but was described at a lesser extent in rat ligature model.[36] Larger osteonecrosis of alveolar bone processes has been observed during experimental periodontitis in studies on bisphosphonate-related osteonecrosis of jaws (BRONJ) in rat.[30,37]

Interestingly, *Msx*1 expression was specifically reduced in jaw osteonecrosis in rat[38] and human[39] suggesting that *Msx* pathways are involved in jaw bone osteonecrosis.

Studies on BRONJ suggested that altered bone remodeling and delayed osteoclastogenesis impaired alveolar bone response to periodontitis and may induce osteonecrosis.[30,37] Indeed, bisphosphonates reduced osteoclast differentiation and its consecutive osteogenic and angiogenic influence.[40] Previous studies have shown that *Msx2* is expressed in osteoclasts and the number of osteoclasts is reduced in *Msx2-/-* mice during tooth formation and eruption.[6,8] This consecutive delayed tooth eruption could be partly balanced by RANKL overexpression in osteoclasts.[32] These data suggested that *Msx2* could be directly involved in the physiological remodeling process of alveolar bone. This decrease of osteoclast number was not observed during experimental periodontitis in *Msx2* mutant mice and the absence of *Msx2* detection in osteoclasts, suggested that control of osteoclast recruitment by osteoblastic cells could be different in adult mice. Interestingly, an increase of osteoclast number during periodontitis was rather observed in *Msx2-/-* mice and could be explained by the presence of bone osteonecrosis while osteocytes apoptosis has been shown to induce local bone resorption.[41] A parallel progressive increase of osteoclast and apoptotic osteocyte numbers has been observed for BRONJ.[37] However, no significant difference of osteocyte apoptosis could be evidenced using TUNEL in wild type and *Msx2* mutant mice, such result may be due to the limit of TUNEL detection method in bone and/or bone response kinetic to experimental periodontitis.[37] Despite a higher number of osteoclast in *Msx2-/-*, no significant difference of alveolar bone loss was observed between wild type and *Msx2* mutant mice. Previous studies on BRONJ have shown that osteonecrosis was not associated to a significant increase of alveolar bone loss during experimental periodontitis apparently due to a reduced/delayed osteoclastic response.[30,37] All These data suggested that *Msx*2 was involved in bone response to experimental periodontitis in mice via the control of bone catabolism, i.e osteocyte viability and bone resorption.

Msx2 is also involved in bone formation directly controlling gene transcription and expression during osteoblast differentiation, especially via Wnt signaling.[16] During ligature induced experimental periodontitis, the blockage of SFRPI and Wnt-βcatenin pathway leads to an increase of bone loss.[26] *Msx2* appears necessary to osteoblastic cells proliferation but detrimental to osteoblast terminal differentiation.[42] Derived *Msx2-/-* osteoblastic cell culture showed a higher level of mineralization and expression of bone differentiation markers.[43] In the present study, sclerostin was mainly expressed in osteocytes and cementocytes of cellular cementum, as previously shown.[7,36,44] However, sclerostin expression was reduced in the closest osteocytes to alveolar bone surface. In *Msx2-/-* mice, sclerostin expression pattern in periodontal healthy tissues was globally the same as previously shown.[7] In wild type mice, the ratio between sclerostin-negative and -positive osteocytes was similar in periodontitis and control. In other study on ligature induced periodontitis in rat, the number of sclerostin positive osteocytes was increased during the acute bone resorption phase at 3 days but decreased at 20 days during alveolar bone restoration phase compared to control.[36] This difference of observed expression pattern could be due to the continuous aspect of bone resorption with few new bone formation in the present model. Interestingly, in *Msx2-/-* mice, a decrease of sclerostin-positive osteocytes was observed at periodontitis site. The expression of pro-inflammatory cytokines, such as TNF-α was increased during experimental periodontitis[45] and TNF-α has been shown to increase sclerostin expression in osteoblasts.[46] Moreover, *Msx2* has been shown to relay TNF-α dedifferentiation action on osteoblast[42], suggesting that in absence of *Msx2*, sclerostin expression in osteocytes could not be stimulated by inflammation.

Considering the limitations of this study, the data suggested that *Msx2* pathways were involved in experimental periodontitis pathogenesis. *Msx2* expression was detected in healthy and inflamed gingiva of patients. From a clinical point of view, *MSX2* mutations are very rare, and even *MSX2* polymorphism has been shown to be associated to ankylosing spondylitis[47], emphasizing that *MSX2* could not appear nowadays as a periodontal diagnosis therapeutic target itself. However, this

study highlighted the potential role of genes initially characterized in early development and tooth patterning in periodontal homeostasis.

ACKNOWLEDGMENTS

The authors report no conflict of interest related to this study.

The authors wish to thank Stéphane Petit PhD for *MSX2* primers designing and supplying and Dr. Ibtissam Senoussi DDS PhD, INSERM U1138 for mice supplying. Authors thank Dr Benoit Robert, PhD Institut Pasteur Paris, Unité de Génétique Moléculaire de la Morphogenèse for providing *Msx2* KI mouse line.

REFERENCES

1. Berdal A, Molla M, Hotton D, et al. Differential impact of MSX1 and MSX2 homeogenes on mouse maxillofacial skeleton. *Cells Tissues Organs (Print)*. 2009;189:126-132.

2. Alappat S, Zhang ZY, Chen YP. Msx homeobox gene family and craniofacial development. *Cell Res*. 2003;13:429-442.

3. Nishimura R, Hata K, Matsubara T, Wakabayashi M, Yoneda T. Regulation of bone and cartilage development by network between BMP signalling and transcription factors. *J Biochem*. 2012;151:247-254.

4. Plaisancié J, Collet C, Pelletier V, et al. MSX2 Gene Duplication in a Patient with Eye Development Defects. *Ophthalmic Genet*. 2015;36:353-358.

5. Bei M, Stowell S, Maas R. Msx2 controls ameloblast terminal differentiation. *Dev Dyn*. 2004;231:758-765.

6. Molla M, Descroix V, Aïoub M, et al. Enamel protein regulation and dental and periodontal physiopathology in MSX2 mutant mice. *Am J Pathol*. 2010;177:2516-2526.

7. Amri N, Djolé SX, Petit S, et al. Distorted Patterns of Dentinogenesis and Eruption in Msx2 Null Mutants: Involvement of Sost/Sclerostin. *Am J Pathol*. 2016;186:2577-2587.

8. Aïoub M, Lézot F, Molla M, et al. Msx2 -/- transgenic mice develop compound amelogenesis imperfecta, dentinogenesis imperfecta and periodental osteopetrosis. *Bone*. 2007;41:851-859.

9. Yamashiro T, Tummers M, Thesleff I. Expression of bone morphogenetic proteins and Msx genes during root formation. *J Dent Res*. 2003;82:172-176.

10. Matsubara T, Kida K, Yamaguchi A, et al. BMP2 regulates Osterix through Msx2 and Runx2 during osteoblast differentiation. *J Biol Chem*. 2008;283:29119-29125.

11. Cho Y-D, Yoon W-J, Woo K-M, Baek J-H, Park J-C, Ryoo H-M. The canonical BMP signaling pathway plays a crucial part in stimulation of dentin sialophosphoprotein expression by BMP-2. *J Biol Chem*. 2010;285:36369-36376.

12. Yoshizawa T, Takizawa F, Iizawa F, et al. Homeobox protein MSX2 acts as a molecular defense mechanism for preventing ossification in ligament fibroblasts. *Mol Cell Biol*. 2004;24:3460-3472.

13. Kim Y-J, Lee M-H, Wozney JM, Cho J-Y, Ryoo H-M. Bone morphogenetic protein-2-induced alkaline phosphatase expression is stimulated by Dlx5 and repressed by Msx2. *J Biol Chem*. 2004;279:50773-50780.

14. Foster BL, Soenjaya Y, Nociti FH Jr, et al. Deficiency in acellular cementum and periodontal attachment in bsp null mice. *J Dent Res*. 2013;92:166-172.

15. Ryan MC, Lee K, Miyashita Y, Carter WG. Targeted disruption of the LAMA3 gene in mice reveals abnormalities in survival and late stage differentiation of epithelial cells. *J Cell Biol*. 1999;145:1309-1323.

16. Cheng S-L, Shao J-S, Cai J, Sierra OL, Towler DA. Msx2 exerts bone anabolism via canonical Wnt signaling. *J Biol Chem*. 2008;283:20505-20522.

17. Yu L, van der Valk M, Cao J, et al. Sclerostin expression is induced by BMPs in human Saos-2 osteosarcoma cells but not via direct effects on the sclerostin gene promoter or ECR5 element. *Bone*. 2011;49:1131-1140.

18. Bae CH, Lee JY, Kim TH, et al. Excessive Wnt/β-catenin signaling disturbs tooth-root formation. *J Periodont Res*. 2013;48:405-410.

19. Kuchler U, Schwarze UY, Dobsak T, et al. Dental and periodontal phenotype in sclerostin knockout mice. *Int J Oral Sci*. 2014;6:70-76.

20. Monroe DG, McGee-Lawrence ME, Oursler MJ, Westendorf JJ. Update on Wnt signaling in bone cell biology and bone disease. *Gene*. 2012;492:1-18.

21. Ren Y, Han X, Ho SP, et al. Removal of SOST or blocking its product sclerostin rescues defects in the periodontitis mouse model. *FASEB J*. 2015;29:2702-2711.

22. Taut AD, Jin Q, Chung J-H, et al. Sclerostin antibody stimulates bone regeneration after experimental periodontitis. *J Bone Miner Res*. 2013;28:2347-2356.

23. Lee H-L, Woo KM, Ryoo H-M, Baek J-H. Tumor necrosis factor-alpha increases alkaline phosphatase expression in vascular smooth muscle cells via MSX2 induction. *Biochem Biophys Res Commun*. 2010;391:1087-1092.

24. Shao J-S, Aly ZA, Lai C-F, et al. Vascular Bmp Msx2 Wnt signaling and oxidative stress in arterial calcification. *Ann N Y Acad Sci*. 2007;1117:40-50.

25. Saadi-Thiers K, Huck O, Simonis P, et al. Periodontal and Systemic Responses in Various Mice Models of Experimental Periodontitis: Respective Roles of Inflammation Duration and Porphyromonas Gingivalis Infection. *J Periodontol*. 2013;84:396-406.

26. Li CH, Amar S. Inhibition of SFRP1 reduces severity of periodontitis. *J Dent Res*. 2007;86:873-877.

27. de Molon RS, de Avila ED, Boas Nogueira AV, et al. Evaluation of the host response in various models of induced periodontal disease in mice. *J Periodontol*. 2014;85:465-477.

28. Marques MR, dos Santos MCLG, da Silva AF, Nociti FH Jr, Barros SP. Parathyroid hormone administration may modulate periodontal tissue levels of interleukin-6, matrix metalloproteinase-2 and matrix metalloproteinase-9 in experimental periodontitis. *J Periodont Res*. 2009;44:744-750.

29. Bi Y, Gao Y, Ehirchiou D, et al. Bisphosphonates cause osteonecrosis of the jaw-like disease in mice. *Am J Pathol*. 2010;177:280-290.

30. Aghaloo TL, Kang B, Sung EC, et al. Periodontal disease and bisphosphonates induce osteonecrosis of the jaws in the rat. *J Bone Miner Res*. 2011;26:1871-1882.

31. Satokata I, Ma L, Ohshima H, et al. Msx2 deficiency in mice causes pleiotropic defects in bone growth and ectodermal organ formation. *Nat Genet*. 2000;24:391-395.

32. Castaneda B, Simon Y, Jacques J, et al. Bone resorption control of tooth eruption and root morphogenesis: Involvement of the receptor activator of NF-kappaB (RANK). *J Cell Physiol*. 2011;226:74-85.

33. Yeh J, Green LM, Jiang T-X, et al. Accelerated closure of skin wounds in mice deficient in the homeobox gene Msx2. *Wound Repair and Regeneration*. 2009;17:639–648.

34. Lapérine O, Cloitre A, Caillon J, et al. Interleukin-33 and RANK-L Interplay in the Alveolar Bone Loss Associated to Periodontitis. *PLoS ONE*. 2016;11(12):e0168080.

35. Bugueno IM, Batool F, Korah L, Benkirane-Jessel N, Huck O. Porphyromonas gingivalis Differentially Modulates Apoptosome Apoptotic Peptidase Activating Factor 1 in Epithelial Cells and Fibroblasts. *Am J Pathol*. 2018;188:404-416.

36. Kim J-H, Lee D-E, Cha J-H, Bak E-J, Yoo Y-J. Receptor activator of nuclear factor-κB ligand and sclerostin expression in osteocytes of alveolar bone in rats with ligature-induced periodontitis. *J Periodontol*. 2014;85:370-378.

37. Aguirre JI, Akhter MP, Kimmel DB, et al. Oncologic doses of Zoledronic acid induce osteonecrosis of the jaw-like lesions in rice rats (oryzomys palustris) with periodontitis. *Journal of Bone and Mineral Research*. 2012;27:2130-2143

38. Xuan B, Yang P, Wu S, Li L, Zhang J, Zhang W. Expression of Dlx-5 and Msx-1 in Craniofacial Skeletons and Ilia of Rats Treated With Zoledronate. *J Oral Maxillofac Surg*. 2017;75:994.e1-994.e9.

39. Wehrhan F, Hyckel P, Amann K, et al. Msx-1 is suppressed in bisphosphonate-exposed jaw bone analysis of bone turnover-related cell signalling after bisphosphonate treatment. *Oral Dis*. 2011;17:433-442.

40. Gao S-Y, Zheng G-S, Wang L, et al. Zoledronate suppressed angiogenesis and osteogenesis by inhibiting osteoclasts formation and secretion of PDGF-BB. *PLoS ONE*. 2017;12:e0179248.

41. O'Brien CA, Nakashima T, Takayanagi H. Osteocyte control of osteoclastogenesis. *Bone*. 2013;54:258-263.

42. Lee H-L, Yi T, Woo KM, Ryoo H-M, Kim G-S, Baek J-H. Msx2 mediates the inhibitory action of TNF-α on osteoblast differentiation. *Exp Mol Med*. 2010;42:437-445.

43. Marijanović I, Kronenberg MS, Erceg Ivkosić I, Lichtler AC. Comparison of proliferation and differentiation of calvarial osteoblast cultures derived from Msx2 deficient and wild type mice. *Coll Antropol*. 2009;33:919-924.

44. Jäger A, Götz W, Lossdörfer S, Rath-Deschner B. Localization of SOST/sclerostin in cementocytes in vivo and in mineralizing periodontal ligament cells in vitro. *J Periodont Res*. 2010;45:246-254.

45. de Molon RS, Park CH, Jin Q, Sugai J, Cirelli JA. Characterization of ligature-induced experimental periodontitis. *Microsc Res Tech*. 2018;81:1412-1421.

46. Heiland GR, Zwerina K, Baum W, et al. Neutralisation of Dkk-1 protects from systemic bone loss during inflammation and reduces sclerostin expression. *Ann Rheum Dis*. 2010;69:2152-2159.

47. Furuichi T, Maeda K, Chou C-T, et al. Association of the MSX2 gene polymorphisms with ankylosing spondylitis in Japanese. *J Hum Genet*. 2008;53:419-424.

Figure Legends

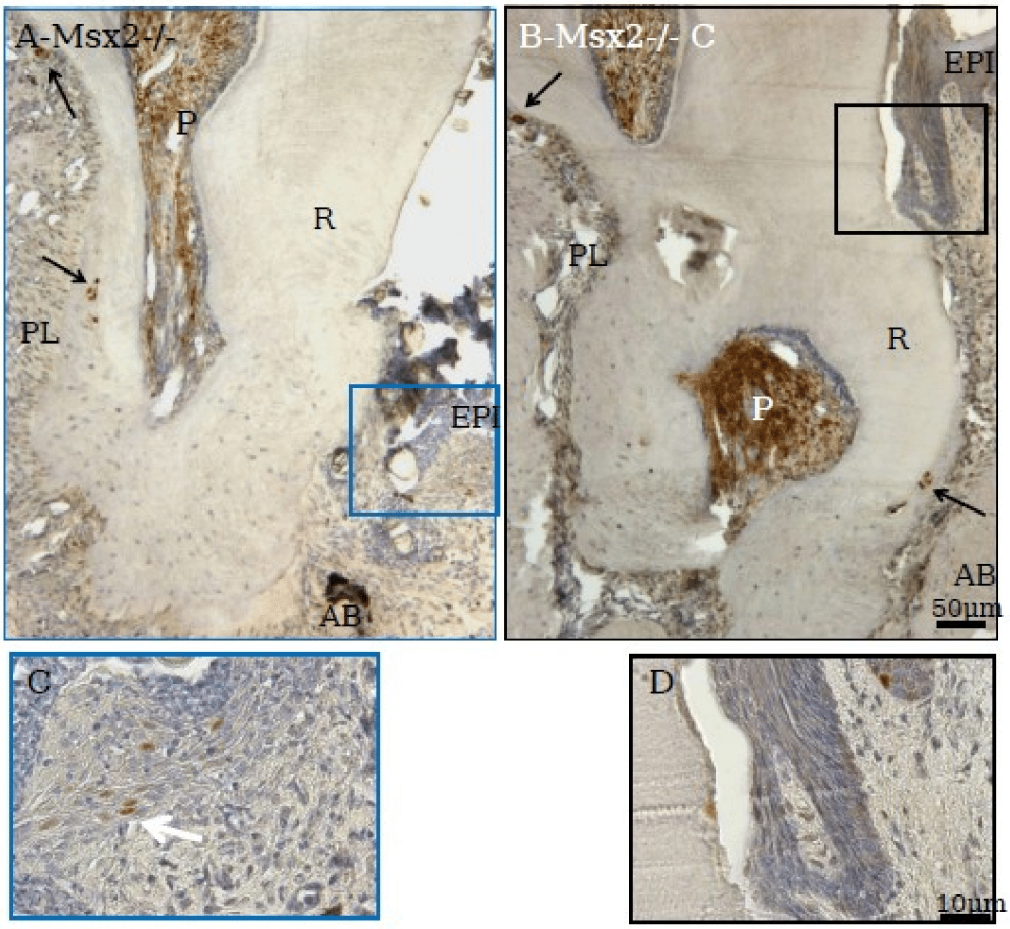

Figure 1: Immunolocalization of β-galactosidase protein in *Msx2-/-* periodontal tissues: frontal sections of palatal root aspect. The morphology of the tooth crown and root was altered in *Msx2-/-* mice. *Msx2* gene expression was revealed by brown staining. In tooth with experimental periodontitis **(A and C)** and control **(B and D)**, the strongest staining was observed in dental pulp cells and epithelial rests of Malassez (black arrows). Some basal cells of palatal epithelium were also stained. Magnified areas showed some stained epithelial cells in inflamed pocket epithelium (white arrow) **(C and D)**. EPI = oral epithelium, AB = alveolar bone, PL = periodontal ligament, R = root, P = dental pulp.

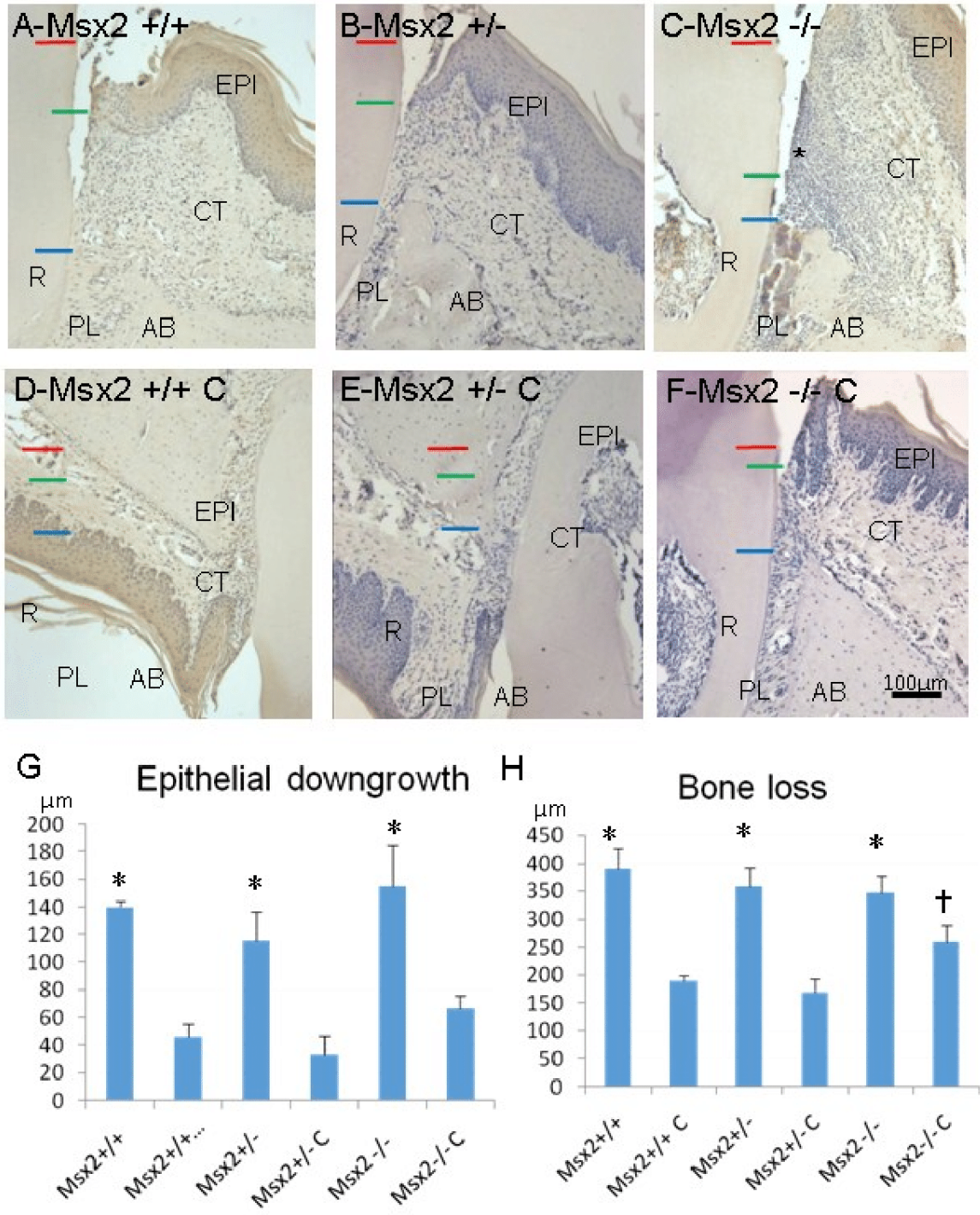

Figure 2: Hematoxylin stained histological views of the first maxillary molars: frontal sections of palatal root aspect. The gingiva is thicker and the epithelium apical down-growth is more noticeable in site with experimental periodontitis **(A, B and C)**, compared to control site **(D, E and F)**. The levels of attachment (green line) and alveolar bone crest (blue line) were evaluated from the cemento-

enamel junction (red line) in the different groups of mice and their controls. Epithelial down-growth **(G)** corresponds to the distance from the cemento-enamel junction (CEJ) to the most apical epithelium down-growth, bone loss **(H)** to the distance from cement-enamel junction to the most cervical part of alveolar bone crest. Bars represent mean values + SD/2. Statistically significant differences *P *<0.05* with corresponding controls, and †P *<0.05* between *Msx2-/-* control and control of other groups. EPI = oral epithelium, CT = gingival connective tissue, AB = alveolar bone, PL = periodontal ligament, R = root.

Figure 3

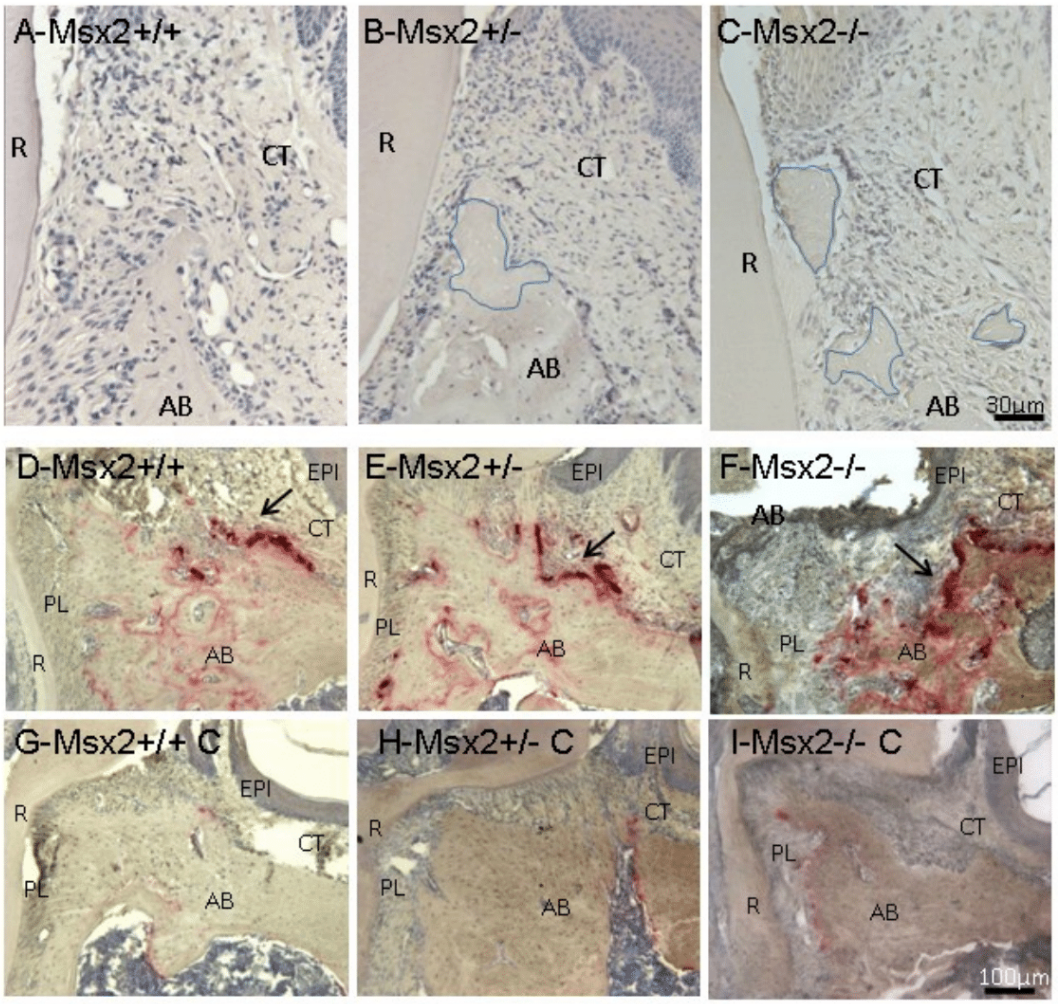

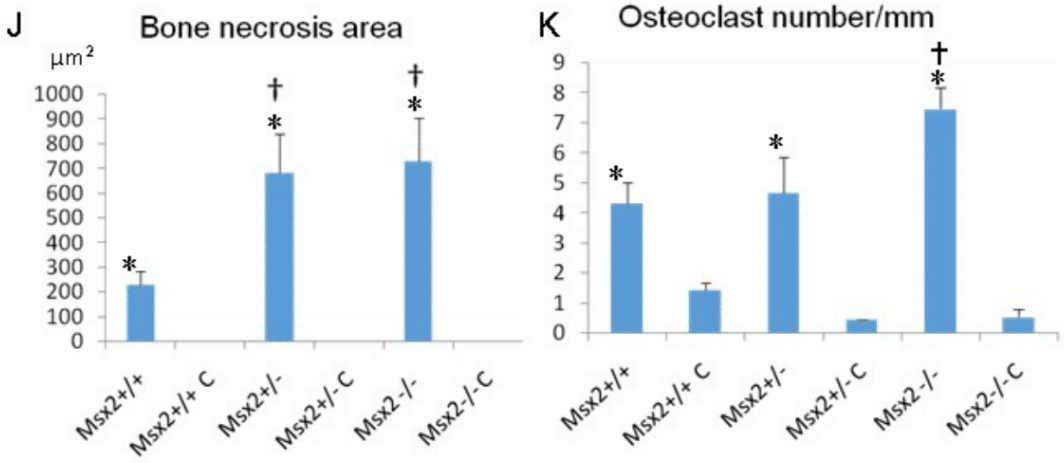

Figure 3: Bone necrosis **(A through C and J)** and TRAP enzymology **(D through I and K)** evaluation: frontal sections of palatal root **(A through C)** and distal furcation **(D through I)** and of the first maxillary molars. In *Msx2+/-* **(B)** and *Msx2-/-* **(C)**, empty lacunae and mice necrotic bone fragments were observed close to pocket epithelium, while no necrotic zone was observed in *Msx2+/+* **(A)**. In *Msx2+/-* and *Msx2-/-*, empty lacunae and mice necrotic bone fragments were observed close to pocket epithelium. Areas of osteonecrosis defined with more than 3 contiguous empty lacunae and bone fragments defined by empty lacunae and the absence of bone lining cells were surrounded by blue lines. Quantification of osteonecrosis zones **(J)**. Osteoclasts were stained in red. A strong staining was observed on the palatal surface (black arrow) of AB **(D through F)**. In control, only a few osteoclasts were seen **(G through I)**. Osteoclast number/mm corresponds to the number of TRAP-positive cells per mm of alveolar bone linear surface **(K).** Bars represent mean values + SD/2. Statistically significant differences * P <0.05 with corresponding controls, † P ≤ 0.05 with *Msx2+/+*. EPI = oral epithelium, CT = gingival connective tissue, AB = alveolar bone, PL = periodontal ligament, R = root.

Figure 4

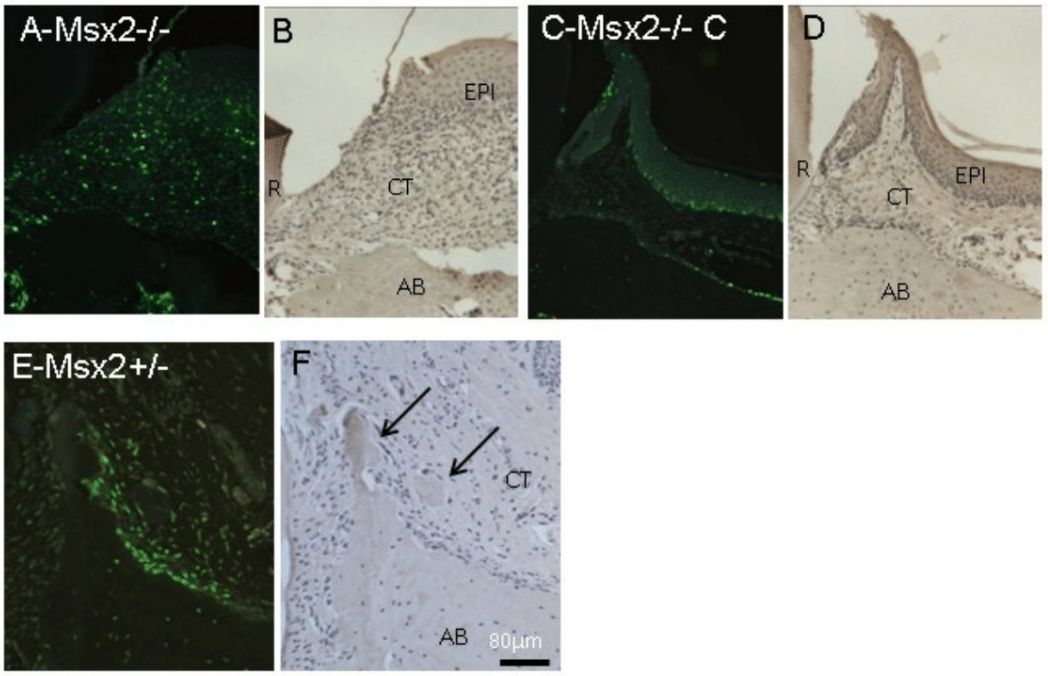

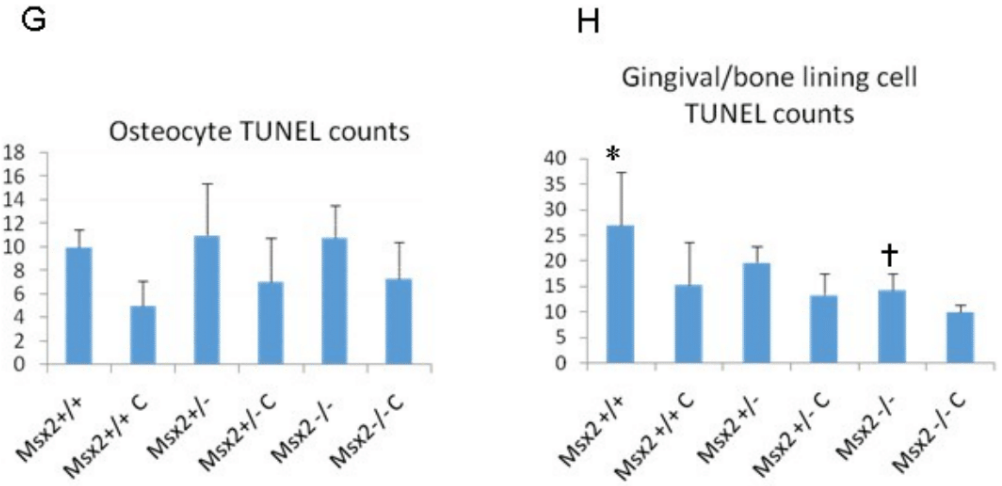

Figure 4: TUNEL staining: frontal sections of mesial **(A through D)** and palatal root **(E and F)** aspect. Green TUNEL positive cells were mainly observed in gingival and bone lining cells. In site with experimental periodontitis, bone cells around necrotic bone were marked (arrows). No statistical difference was observed for TUNEL positive osteocytes **(G)** while TUNEL positive gingival and bone lining cells were significantly increased in Msx2+/+ mice during periodontitis **(H)**. EPI = oral epithelium, CT = gingival connective tissue, AB = alveolar bone, R = root. Statistically significant differences *P *<0.05* with corresponding control, †P *<0.05* with *Msx2+/+*.

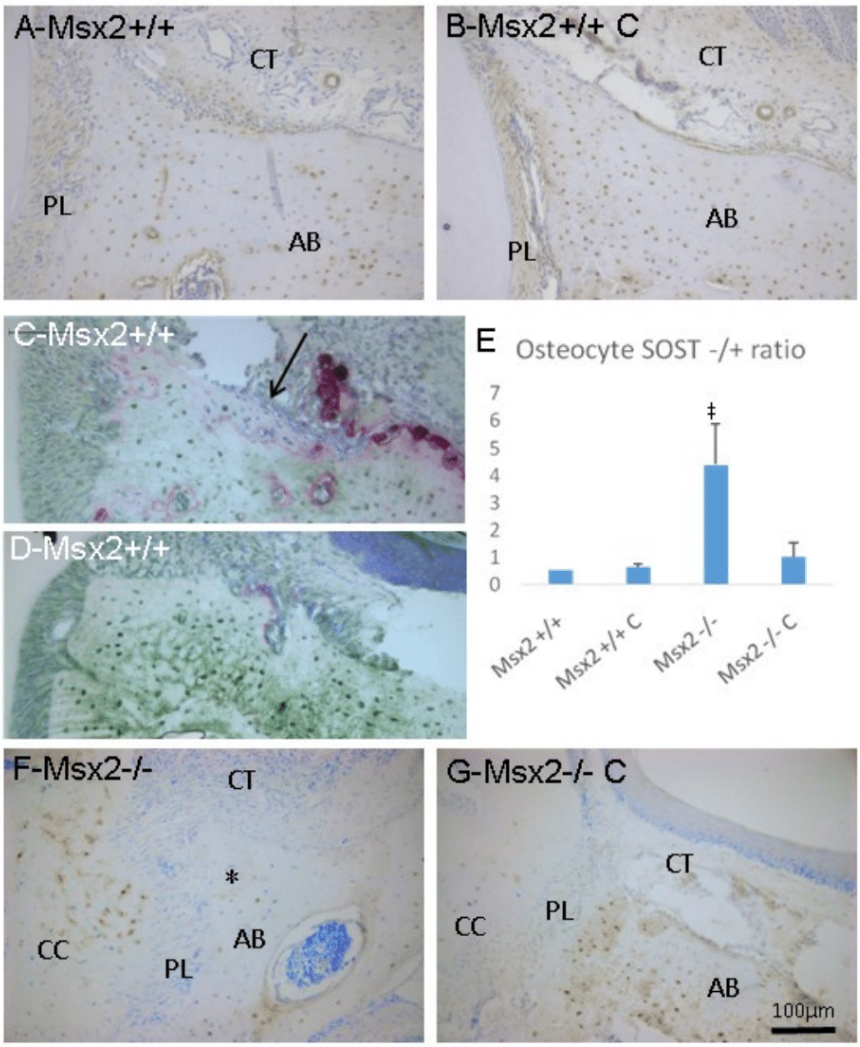

Figure 5: Sclerostin immunochemistry **(A, B, F, and G)** and TRAP codetection **(C and D)** views of the first maxillary molars: frontal sections of palatal and distal furcation root aspect. Sclerostin immunostaining was mainly observed in osteocytes in sites with periodontitis **(A, C, and F)** and controls **(B, D, and G**) and in cementocytes of cellular cementum **(F and G)**. Osteocytes near bone surface and in osteoid bone (black arrow) were not stained **(C)**. In *Msx2-/-* mice, the number of sclerostin positive osteocytes decreased in periodontitis (asterisk) site compared to contralateral control site **(F, G and E).** CT = gingival connective tissue, AB = alveolar bone, PL = periodontal ligament, CC: cellular cementum**.** Statistically significant differences ‡ P <0.1 with Msx2+/+ periodontitis and control groups.

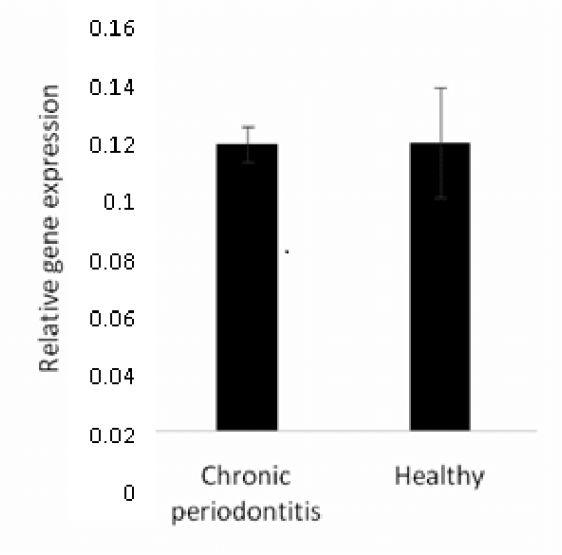

Figure 6: *MSX2* relative gene expression in human gingival tissues. Bars represent mean values + SD/2.

V. Annexe n°3

Lapérine O., Cloitre A., Caillon J., Huck O., **Bugueno I.M.,** Sourice S., Le Tilly E., Palmer G., Davideau J.L., Geoffroy V., Guicheux J., Beck-Cornier S., Lesclous P. "Interleukin-33 and RANK-L Interplay in the Alveolar Bone Loss Associated to Periodontitis", **PLoS ONE 11(12): e0168080. doi:10.1371/journal.pone.0168080.**

PLOS ONE

RESEARCH ARTICLE

Interleukin-33 and RANK-L Interplay in the Alveolar Bone Loss Associated to Periodontitis

Olivier Lapérine[1,2,3‡], Alexandra Cloitre[1,2,3,4‡], Jocelyne Caillon[5], Olivier Huck[6,7], Isaac Maximiliano Bugueno[6], Paul Pilet[1,2,3,4], Sophie Sourice[1,2,3], Elodie Le Tilly[1,2,3], Gaby Palmer[8,9], Jean-Luc Davideau[6,7], Valérie Geoffroy[10,11], Jérôme Guicheux[1,2,3,4]*, Sarah Beck-Cormier[1,2,3], Philippe Lesclous[1,2,3,4]*

1 INSERM, U791, LIOAD, Nantes, France, **2** Université de Nantes, UMR-S 791, LIOAD, Nantes, France, **3** UFR Odontologie, Nantes, France, **4** ONIRIS, UMR-S 791, LIOAD, Nantes, France, **5** EA 3826 Thérapeutiques cliniques et expérimentales des infections, Nantes, France, **6** INSERM, U1109 Osteoarticular & Dental Regenerative Nanomedicine, Fédération de Médecine Translationnelle de Strasbourg (FMTS), Strasbourg, France, **7** Département de Parodontologie, Faculté de Chirurgie Dentaire, Université de Strasbourg, Strasbourg, France, **8** Division of Rheumatology, Department of Internal Medicine Specialties, University Hospitals of Geneva, Geneva, Switzerland, **9** Department of Pathology-Immunology, University of Geneva, School of Medicine, Geneva, Switzerland, **10** INSERM U1132 BIOSCAR, Hôpital Lariboisière, Paris, France, **11** Université Paris Diderot, Sorbonne Paris Cité, Paris, France

‡ These authors are co-first authors on this work.
* jerome.guicheux@inserm.fr (JG); philippe.lesclous@univ-nantes.fr (PL)

Citation: Lapérine O, Cloitre A, Caillon J, Huck O, Bugueno IM, Pilet P, et al. (2016) Interleukin-33 and RANK-L Interplay in the Alveolar Bone Loss Associated to Periodontitis. PLoS ONE 11(12): e0168080. doi:10.1371/journal.pone.0168080

Editor: Özlem Yilmaz, Medical University of South Carolina, UNITED STATES

Received: September 20, 2016

Accepted: November 27, 2016

Published: December 19, 2016

Data Availability Statement: All relevant data are within the paper and its Supporting Information files.

Funding: Support was provided by Région des pays de la Loire (grant 2012-05775-05776) [http://www.paysdelaloire.fr/]. The funders had no role in study design, data collection and analysis, decision to publish, or preparation of the manuscript.

Competing Interests: The authors have declared that no competing interests exist.

Abstract

Introduction

Chronic Periodontitis (CP) is an inflammatory disease of bacterial origin that results in alveolar bone destruction. *Porphyromonas gingivalis* (*Pg*), one of the main periopathogens, initiates an inflammatory cascade by host immune cells thereby increasing recruitment and activity of osteoclasts, the bone resorbing cells, through enhanced production of the crucial osteoclastogenic factor, RANK-L. Antibodies directed against some cytokines (IL-1β, IL-6 and TNF-α) failed to exhibit convincing therapeutic effect in CP. It has been suggested that IL-33, could be of interest in CP.

Objective

the present study aims to analyze whether and how IL-33 and RANK-L and/or their interplay are involved in the bone destruction associated to CP.

Material and Methods

mRNAs and protein expressions of IL-33 and RANK-L were analyzed in healthy and CP human gingival samples by immunohistochemistry (IHC) and RT-qPCR. Murine experimental periodontitis (EP) was induced using *Pg* infected ligature and *Pg* free ligature around the first maxillary molar. Alveolar bone loss was recorded by μCT. Mouse gingival explants were stimulated for 24 hours with IL-33 and RANK-L mRNA expression investigated by RT-qPCR. Human oral epithelial cells were infected by *Pg* for 6, 12; 24 hours and IL-33 and RANK-L mRNA expressions were analyzed by RT-qPCR.

Results

IL-33 is overexpressed in gingival epithelial cells in human affected by CP as in the murine EP. In human as in murine gingival cells, RANK-L was independently induced by *Pg* and IL-33. We also showed that the Pg-dependent RANK-L expression in gingival epithelial cells occured earlier than that of IL-33.

Conclusion

Our results evidence that IL-33 overexpression in gingival epithelial cells is associated with CP and may trigger RANK-L expression in addition to a direct effect of *Pg*. Finally, IL-33 may act as an extracellular alarmin (danger signal) showing proinflammatory properties in CP perpetuating bone resorption induced by *Pg* infection.

Introduction

Periodontitis refers to an inflammatory disease of bacterial origin that affects tissues surrounding and supporting the tooth ie gingiva, periodontal ligament, cementum and alveolar bone. The hallmark of periodontitis is a destruction of alveolar bone resulting ultimately in extended tooth loss and oral disability [1]. Growing evidence indicates that periodontitis is highly prevalent in adult population according to a 2012 US survey underlining that 47% of this population is affected by periodontitis, 8.5% in its severe form. This rate increased to 64% in aging persons older than 65 years and is expected to increase with age [2]. Periodontitis is a major health challenge particularly affecting the elderly where the disease is the primary cause of tooth loss but also because periodontitis interplays with systemic health, particularly by increasing the patients' risk and morbidity for atherosclerosis, rheumatoid arthritis (RA) and diabetes mellitus [3, 4]

An anaerobic bacterium, *Porphyromonas gingivalis* (*Pg*), is traditionally considered a major causative agent of periodontitis, based on its virulence properties and strong association with diseased sites. However, *Pg*-induced periodontitis required the presence of commensal microbiota for the onset of periodontitis [5]. In a recently proposed definition, periodontitis may result not from individual pathogens, but rather from polymicrobial synergy and dysbiosis, a condition characterized by an imbalance in the relative abundance or influence of species within a microbial community [3].

It is now well acknowledged that the presence of bacterial species is necessary but not sufficient for the onset and progression of periodontitis. The recognition of microbial components as "danger signals" by host immune cells and subsequent production of inflammatory mediators is an essential step in periodontitis pathogenesis [6]. Production of pro-inflammatory cytokines (including IL-1β, IL-6, and TNF-α) by resident and recruited inflammatory cells acting synergistically seemed to be of particular importance in this process. Indeed, these cytokines increase the recruitment and activity of the bone resorbing cells, the osteoclasts, through enhanced production of a crucial osteoclastogenic factor, the Receptor Activator of Nuclear Factor κ B Ligand (RANK-L) and favor bone destruction [7]. However antibodies directed against these 3 cytokines did not exhibit a convincing therapeutic effect in periodontitis, thereby strongly suggesting that others mediators could be involved in the pathogenesis of this disease [8]. Recently, it has been suggested that among inflammatory mediators involved in

chronic periodontitis (CP), a member of the IL-1 family, IL-33, could play a role in the initiation and the progression of CP [9].

IL-33 has been described to regulate innate and adaptive immunity [10]. IL-33 is constitutively expressed as a nuclear factor in many cell types including epithelial cells, fibroblasts and endothelial cells. Sequestrated in the nucleus of these cells, IL-33 is considered as an endogenous molecule that allows the maintenance of the crucial transcription factor NFκB and thus reduces the expression of genes encoding for proinflammatory cytokines thereby ensuring tissue homeostasis. When released in the extracellular medium upon cell damage or stress, IL-33 acts as an alarmin (also known as danger signal) showing proinflammatory properties [11–13]. IL-33 acts through its ST2 receptor, widely expressed on many cell types of innate and adaptive immunity such as mastocytes, Th2 lymphocytes and B cells leading to pro-inflammatory cytokines production [10, 14, 15]. Interestingly, some studies have highlighted a potential role for IL-33 in the regulation of inflammatory process related to RA, a disease sharing many immunopathological similarities with periodontitis [16]. In mice, inhibition of IL-33 signaling with a soluble isoform of ST2 (sST2) acting as a decoy receptor or deletion of ST2 has been shown to attenuate the severity of induced arthritis in part by blocking RANK-L expression [17]. However, ST2 deletion in a mouse model of K/BxN serum transfer-induced arthritis did not protect animals from inflammation and bone resorption [18]. These contradictory results suggest that the role of IL-33 in inflammatory process leading to bone destruction is highly questionable, probably local or even focal and timely regulated depending of the inflammatory microenvironment.

The potential role for IL-33 in the onset and progression of periodontal disease is emerging and mostly considered as a proinflammatory factor. In a rat model of ligature induced-periodontitis, IL-33 expression was upregulated concomitantly to RANK-L [19]. In human, high IL-33 overexpression was recorded in the gingiva of patients affected by CP and may act as a triggering factor for the recruitment of B and T lymphocytes expressing RANK-L [20]. But in gingival crevicular fluid (an inflammatory exudate collected in the periodontal pocket) conflicting results regarding IL-33 levels have been reported in patients affected by CP [21–23]. Interestingly, *Pg* has been described to upregulate IL-33 mRNA expression in gingival epithelial cells through the PAR-2 signaling pathway [24]. But to date, it is still unclear whether bacterial or pro-inflammatory stimulus first triggers IL-33 expression in the gingival tissue. Contrasting with its positive effect on RANK-L expression, IL-33 has also been reported to inhibit osteoclast differentiation *in vitro*, suggesting a protective effect on bone [25–27]. Taken together, these data suggest a multiple and contrasting role for IL-33 during inflammatory diseases associated to bone resorption such as CP that need to be clarified.

In periodontitis, multiple sources of RANK-L have been proposed such as osteoblasts, B and T lymphocytes or epithelial cells [28, 29]. Interestingly, gingival epithelial cells, the first-line cell population in contact with periopathogens, can produce various pro-inflammatory cytokines and basal level of RANK-L to support osteoclastogenesis [30–32]. Malcolm et al described an increased expression of IL-33 in gingival epithelial cells from patient affected by CP. However, the contribution of this cell type cell to the onset and the progression of the disease through RANK-L expression have not been elucidated.

The present study aims to analyze whether and how IL-33 and RANK-L and/or their interplay are involved in the bone destruction associated to CP.

We showed in this study that IL-33 is overexpressed in gingival epithelial cells in human affected by CP as in a murine model of experimental periodontitis (EP). Moreover, in human as in murine gingival cells, we showed that RANK-L expression can be independently induced by *Pg* and IL-33. These results strengthen a potent role for IL-33 in the pathogenesis of

periodontitis and suggest that both *Pg* and IL-33 induce overexpression of RANK-L and subsequently increase alveolar bone loss.

Materials and Methods

Patients

The human study protocol, consent forms and consent procedure were reviewed and approved by the Institutional Medical Ethic Comittee of the Universitary Hospital of Nantes (SVTO:DC-2011-1399). All patients provided their written consent to participate to this study. Detailed medical and periodontal histories of each patient were recorded (Table 1). According to the American Association of Periodontology, criteria for CP, were i) probing pocket depth $>$ 5 mm, ii) clinical attachment level $>$ 3 mm and iii) bleeding on probing periodontal pockets [33].

In patients diagnosed for CP (n = 13), gingival samples between 5 to 8 mm sides and 3 to 5 mm deep were obtained during the surgical treatment, an open flap debridement combined with dental extractions and gingival regularization. Healthy gingival samples were harvested from patients (n = 9) without any periodontal diseases undergoing oral surgical procedures needing gingival regularization such as extraction of impacted third molars. No patients had taken any anti-inflammatory medication for 2 weeks before surgical procedures. The gingival samples were used for RT-qPCR and/or histology.

Murine model of alveolar bone loss

Animal studies were approved by the Ethic Committee for Animal Experiment of Pays de la Loire (CEEA 2012.187). Mice were housed in specific-pathogen-free facilities, and under light- (12h light/dark cycle), temperature- (22–25°C) and humidity- (50–60%) controlled conditions. To avoid any gingival effect of estrogens, we only used 12 week-old male CD1 Swiss mice (Janvier). All animals were fed with regular diet. A wash-out period was first performed in which mice were treated with water diluted sulfomethoxazole-trimethoprim 0.2mg/mL (Roche) for ten days followed by a 3 days antibiotic-free period [34]. For periodontal procedures, mice were anesthetized with intraperitoneal injection of ketamine (80 mg/kg, Imalgene

Table 1. Characteristics of the patients.

Variables	Chronic periodontitic patients		Healthy patients	
	Number	%	Number	%
Gender				
Male	10	76.9	3	33.3
Female	3	23.1	6	66.7
Age (years)	48.3 ± 8.5		20.33 ± 3.6	
Tobacco				
User	8	61.5	4	44.4
Non-user	5	38.5	5	55.6
Probing pocket depth (mm)	5.3 ± 1.9		NA*	
Clinical attachment level (mm)	7.8 ± 1.9		NA*	
Bleeding on probing	13	100	0	0

* NA: Not applicable

Variables: mean values [SD]

doi:10.1371/journal.pone.0168080.t001

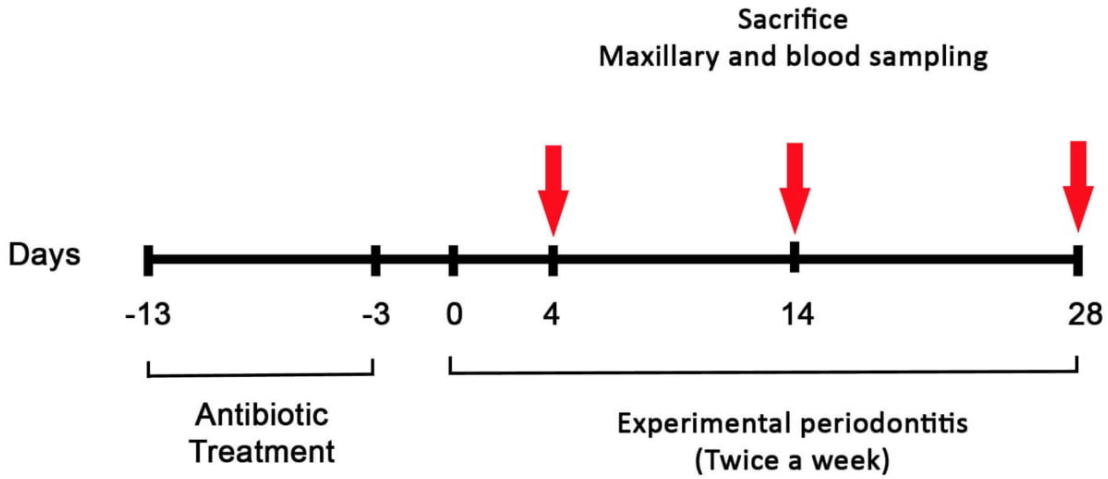

Fig 1. Study design of the murine model of experimental periodontitis.

doi:10.1371/journal.pone.0168080.g001

1000, Merial) and xylazine (10mg/kg, Rompun 2%, Bayer). *Pg*-infected and control mice were placed in separated cages and kept in the same environment. Mice were monitored in order to evaluate pain stress, and weighed on a daily basis.

A time course experiment was conducted with 90 animals randomly distributed in 9 experimental groups of 10 mice. EP was induced by placement of a 6.0 silk ligature soaked wih *Pg* (*Pg* Lig) or not (L) in the gingival crevice (so called sulcus) around the first maxillary molar for 4, 14 or 28 days. This procedure was repeated twice a week (Fig 1). Control mice received a slight incision into the sulcular epithelium to mimic the ligature placement (Sham). At every time periods, mice were sacrificed by cardiac exsanguination under the same anesthesia procedure as previously described for periodontal procedure.

Blood samples were collected by cardiac puncture and sera were prepared by centrifugation at 2000xg for 2 minutes.

Micro-computed tomography and histological analyses were performed on sampled maxilla fixed in 4% paraformaldehyde at 4˚C for 24 hours.

Bacterial and strain culture

Pg (ATCC 33277) was cultured at 37˚C on Shaedler agar plated with sheep blood (BD), in an oxygen-free atmosphere. After 10 days of culture, *Pg* colonies were selected and resuspended in brain-heart broth at 10^9 CFU/mL for ligature placement or at 10^5 CFU/mL for *Pg* injection. A 6–0 silk thread was placed in the suspension 24 hours before EP procedure.

Gingival explant culture

Palatal mucosa from 3 C57BL/6J mice was harvested and placed connective face in contact with plate for 1 hour to allow cell adhesion. Explants were then cultured in DMEM supplemented with 10% FCS, 50U/ml Penicillin and 50 mg/ml Streptomycin for 24 hours. They were then stimulated with 100ng/mL of recombinant murine IL-33 (3626-ML-010, R&D) in serum-free DMEM supplemented with 50U/ml Penicillin and 50 mg/ml Streptomycin for 24 hours. Three independent experiments were performed.

Micro-computed tomography (μCT)

Two and three dimensional analyses of the maxilla were performed using a Skyscan 1272 (Skyscan). Acquisition parameters were 60 kV, 80 mA, 0.25-mm aluminium filter. The NRecon software (Skyscan) was used for reconstruction. For the two-dimensional analyses, distance between the palatal cementum-enamel junction of the first molar and the alveolar bone crest (CEJ-ABC) was measured to assess alveolar bone loss on the coronal plan. Five sections per animal were analyzed when radicular canal for each tooth were fully visible. For the three-dimensional analyses, bone mineral volume/tissue volume (MBV/TV) was assessed in an elliptical region of interest (ROI) between CEJ and the root apices of the first molar in the axial plan. The fraction of MBV/TV was calculated using CTan software and data are presented as percentage of ROI area. Evaluations were performed by two independent operators.

Immunohistochemistry (IHC)

Fixed maxilla were decalcified in EDTA 0.5M at 4˚C for three weeks. Human and mouse samples were then dehydrated and embedded in paraffin. IHC were performed on 4 μm-thick sections. Antigens were retrieved by boiling slides for 30 minutes in citrate buffer pH 6. Sections were then incubated in blocking solution (S2022, Dako) for 45 minutes at RT. Incubation with primary antibodies was performed in the blocking solution at 4˚C over-night. Sections were rinsed three times (0.05% tween in PBS) and endogenous peroxydase activity was quenched with 3% H2O2 in PBS for 20 minutes. Specific binding was detected using DAB (Dako). Sections were counterstained with Harris Hematoxilin, dehydrated and mounted in Eukitt. Primary and secondary antibodies used are: polyclonal goat anti-IL-33 (AF3626 and AF3625; R&D systems), polyclonal goat anti-RANK-L (sc7628, clone N-19, 1/100; Santa Cruz) and monoclonal rat anti-human CD3 (clone CD3-12, 1/200; AbD Serotec), anti-goat HRP antibody (1:500; sc-2961, Santa Cruz Biotechnology), anti-rat HRP antibody (1:500, Jackson Immunoresearch inc,). Specificity of IL-33 antibody was assessed using maxilla samples from IL-33 KO mice. Automated whole slide imaging was performed using the NanoZoomer 2.0 (Hamamatsu). All analyses were performed in multiple randomly selected high-power microscopic fields (magnification x200). Staining quantification on four sections per sample was performed using Fiji software (NIH).

RT-qPCR

Total RNA was extracted from human gingival samples and mouse gingival explants using the Nucleospin RNA isolation kit (Macherey Nagel). cDNA were synthesized using SuperScript III First-strand Synthesis System (Life Technologies). Twenty nanograms of cDNA were used to assess mRNA expression by using TaqMan gene expression assays (Life technologies). The probe and primer sets for Human *IL33* (Hs01125943_m1), RANK-L (*Tnfsf11*, Hs00243522_m1), *TNF-α* (Hs01113624_g1), *IL-6* (Hs00985639_m1) and mouse RANK-L (*Tnfsf11*, Mm01313943_m1) and the normalizers human *Ppia* (Hs99999904_m1) and mouse *GusB* (Mm01197698_m1) were obtained from Applied Biosystems. Measurements were performed in triplicate. Relative quantification was determined using the Biorad CFX manager software (Biorad).

Enzyme-linked immunosorbent assay (ELISA)

Serum IL-33 concentrations were measured according to manufacturer's instructions (Kit duoset DY3626-05 ELISA R&D). Briefly, plates were coated with a goat anti-mouse IL-33 antibody overnight. Then samples were incubated during 1 hour. A biotinylated goat anti-mouse

IL-33 antibody was added for 2 hours. Streptavidin-HRP was added for 20 minutes and the reaction was visualized by the addition of 50 μl chromogenic substrate (TMB) for 30 minutes. The reaction was stopped with 100 μl H2SO4 and absorbance at 450 nm was measured using an ELISA plate reader (Victor3, Wallac 1420, PerkinElmer). All procedures were performed at room temperature.

Cell culture

Oral epithelial cells (OECs) derived from Human oral keratinocyte cell line TERT-2 OKF-6 (BWH Cell Culture and Microscopy Core) were cultured in defined Keratinocyte-SFM basal medium (KSFM) supplemented with growth supplements (Invitrogen).

Infection and stimulation of OECs. Twenty-four hours before infection with *Pg*, 3 x 10^5 cells per well were seeded in 24-well plate. On the day of the infection or stimulation, cells were washed with PBS and medium without antibiotics containing *Pg* (MOI 100:1 or MOI 10:1) was added for 24 hours.

Quantitative RT-qPCR analysis. RT-qPCR was performed to quantify RNA expression. PCR amplification and analysis were achieved using the CFX Connect ™ Real-Time PCR Detection System (Bio-Rad). Amplification was performed using iTaq Universal SYBR Green Supermix. Beta-actin was used as endogenous control in the samples. Primers sequences related to *IL-33* (5′-GGTGTTACTGAGTTATATGAG-3′, 3′-GGAGCTCCACAGAGTGTTCCTTG-5′) and RANKL (*Tnfsf11)* (5′-GCCAGTGGGAGATGTTAG-3′, 3′-CCCTTTTGAACGTCGATT-5′) were synthesized by Eurofins (Ebersberg).) Relative quantification was determined using the Biorad CFX manager software (Biorad). Three separate sets of experiments were performed for each procedure.

Statistical analysis

Data were compared using non-parametric tests (Kruskal-Wallis test followed, if significant, by group comparisons with the Mann-Whitney test or the unpaired student t-test. Differences were considered significant if $p \leq 0.05$. Results are given as means ± SEM or means ± SD for patient's characteristics.

Results

IL-33 and RANK-L are overexpressed in human chronic periodontitis

First, we analyzed clinical parameters to determine the inflammatory status of CP samples (Table 1) and expression of well documented inflammatory markers such as CD3, IL-6 and TNF-α by IHC. We observed a strong positive CD3 immunostaining in CP samples both in connective tissue and in gingival epithelium (Fig 2A). Expression mRNA of the pro-inflammatory cytokines TNF-α and IL-6 was investigated by RT-qPCR. Significant overexpression of mRNA encoding for both cytokines was recorded in CP compared to healthy samples ($p<0.05$) (Fig 2B). No differences were recorded according to the gender or the tobacco habit.

We then determine whether IL-33 and RANK-L can also be overexpressed in CP gingival samples when compared to healthy gingival samples. As indicated in Fig 3A, IL-33 mRNA was significantly increased in CP samples ($p<0.001$). Immunolabeling for IL-33 was also increased in CP compared to healthy samples ($p<0.001$) (Fig 3B). Interestingly, quantification of IL-33 positives cells revealed a drastic 8-fold increase in the gingival epithelium and a slighter but significant 1.5-fold increase in the connective tissue of CP samples ($p<0.01$). As expected, transcript coding for RANK-L was significantly higher in CP samples ($p<0.05$) (Fig 3C) and IHC revealed a 3-fold RANK-L overexpression in CP samples but only in the epithelial

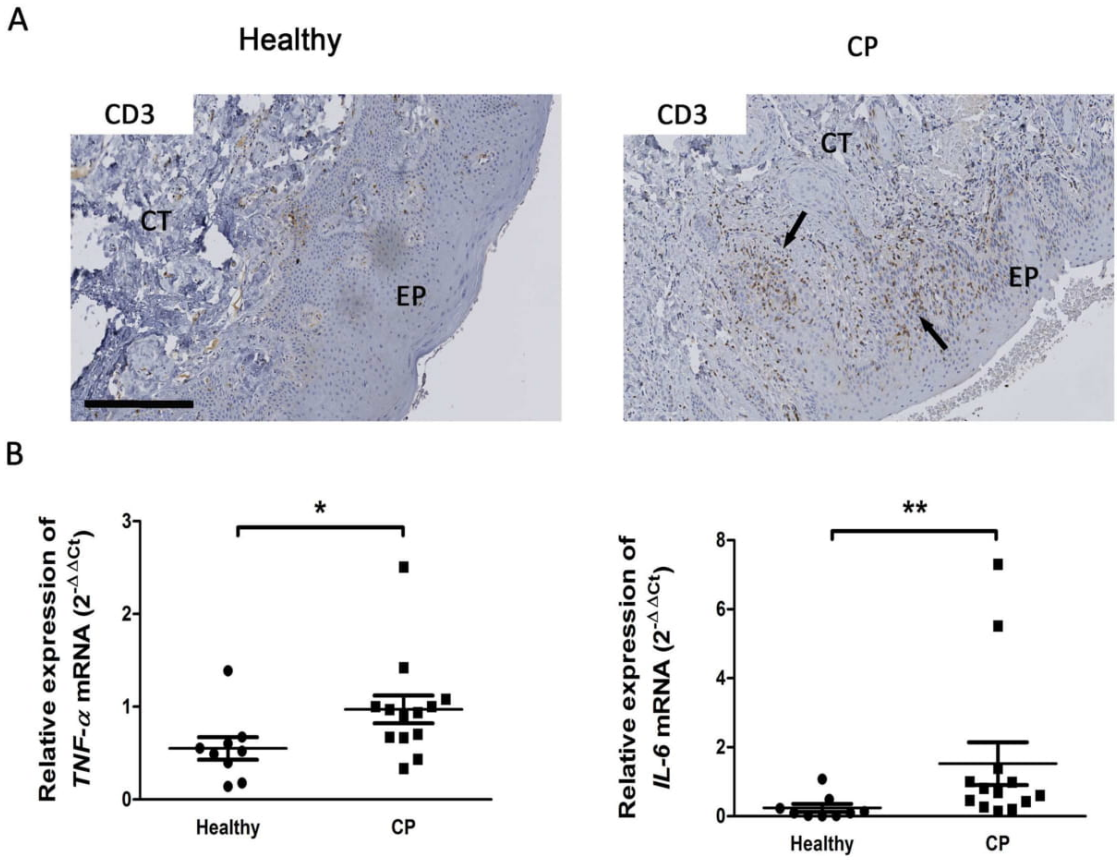

Fig 2. Characterization of human gingival samples in healthy and patients affected by chronic periodontitis. A. Samples were stained for the T lymphocytes marker CD3 (arrows). Sections were counterstained with Harris Hematoxylin staining. EP: Epithelium; CT: Connective Tissue. B. TNF-α and IL-6 expression in healthy and CP patients were measured by RT-qPCR. Data are shown as mean ± SD. Healthy samples n = 9; chronic periodontitis samples n = 13. Bar = 250μm. *p<0.05, **p<0.01.

doi:10.1371/journal.pone.0168080.g002

compartment ($p<0.05$) (Fig 3D). Interestingly, this epithelial RANK-L overexpression appeared in parallel with that of IL-33.

Bone loss is associated with IL-33 overexpression in a murine model of experimental periodontitis

We used a murine model of EP to determine whether IL-33 may be associated to the alveolar bone loss occurring in CP in a time course study with three experimental groups "*Pg* ligature" (*Pg* L), "Ligature" (Lig) and "Sham" mimicking the ligature apposition. Alveolar bone loss induced by *Pg* ligature was significant as early as 14 days following surgery and persisting until day 28 when compared to sham group ($p<0.05$) (Fig 4A and 4B). *Pg* free ligature failed to induce significant alveolar bone loss compared to sham group (Fig 4A and 4B). After having confirmed that *Pg* ligature induced significant alveolar bone loss, we further addressed if IL-33 may be implicated in this process. Immunostaining revealed an increase of IL-33 positive cells in the connective tissue of *Pg* ligature group when compared to sham group 4 days after surgery ($p<0.05$). We also recorded such higher IL-33 positive cells in ligature and *Pg* ligature groups when compared to sham at 28 days ($p<0.01$) (Fig 5A and 5B). Interestingly, increases

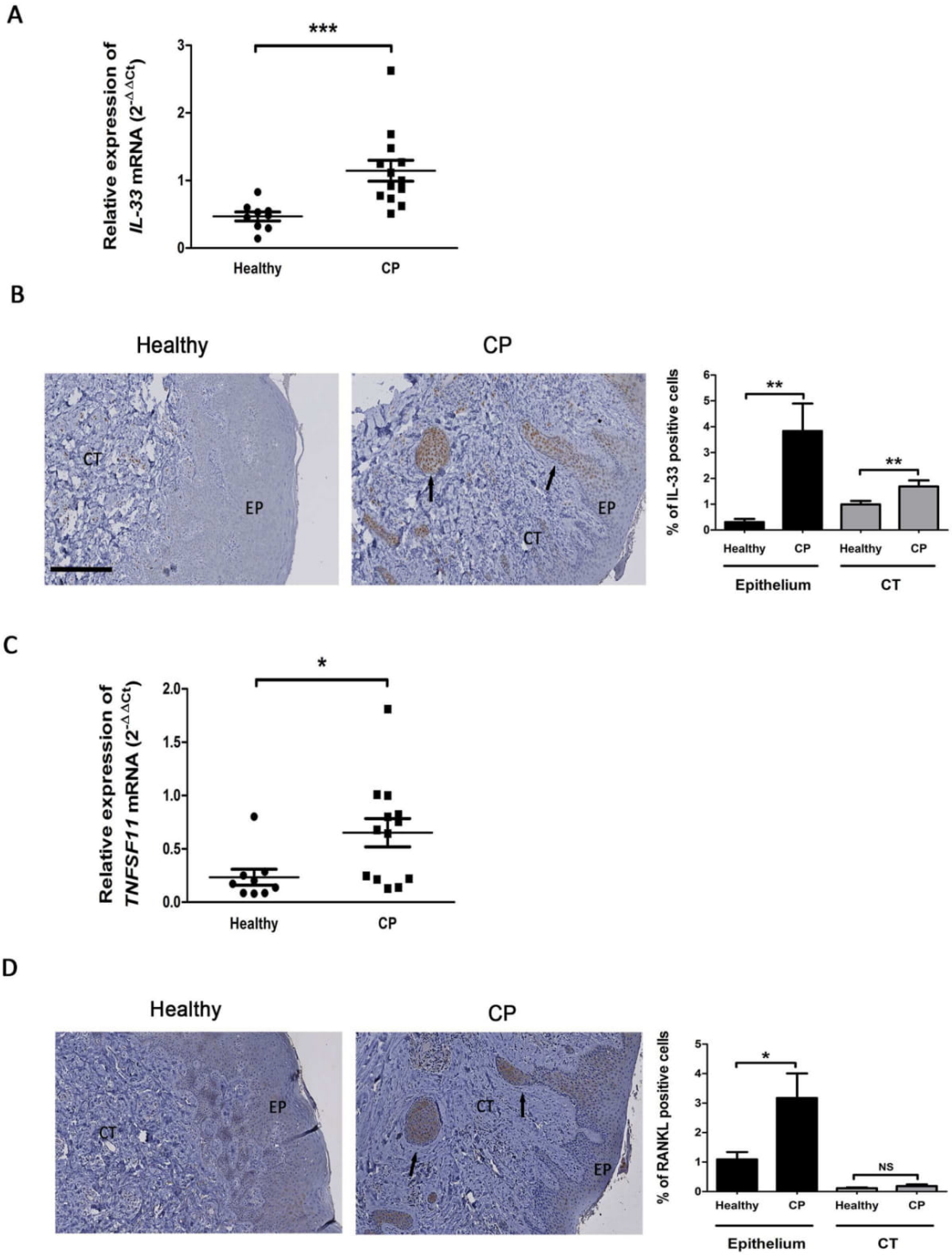

Fig 3. IL-33 and RANK-L expressions in gingival samples of healthy and patients affected by chronic periodontitis. A. mRNA encoding for IL-33 was quantified by RT-qPCR. B. Healthy and CP gingival samples were immunostained for IL-33 (arrows). The percentage of cells positive for IL-33 was quantified using Fiji software and defined as a percentage of DAB positive staining area per region of interest. C. mRNA encoding for RANK-L was quantified by RT-qPCR. D. Healthy and CP gingival samples were immunostained for RANK-L (arrows). The percentage of cells positive for RANK-L was quantified using Fiji software and defined as a percentage of DAB positive staining area per region of interest. EP: Epithelium; CT: Connective

Tissue. Data are shown as mean ± SEM. Healthy samples n = 9; Chronic periodontitis samples (CP) n = 13. Bar = 250μm. *p<0.05; **p<0.01; ***p<0.001.

doi:10.1371/journal.pone.0168080.g003

of IL-33 positive cells were also recorded in the gingival epithelium of the ligature and *Pg* ligature groups at 4 and 14 days after surgery ($p<0.05$ and $p<0.01$ respectively at 4 days; $p<0.05$ and $p<0.05$ respectively at 14 days) (Fig 5A and 5B). Significant increase of IL-33 positive cells was sustained in *Pg* ligature group at 28 days ($p<0.001$) but not in ligature group compared to sham at this time, indicating that *Pg* is necessary for a continuous expression of IL-33 in gingival cells (Fig 5A and 5B). Globally, our data indicates that IL-33 increased in mice in epithelial and in connective compartments, as observed in human samples, before the onset of alveolar bone loss and that *Pg* sustained IL-33 expression in gingival epithelial cells during EP.

IL-33 increased RANK-L expression in mouse gingival explants

To further analyze whether IL-33 can be involved in the increased alveolar bone loss associated to periodontitis, we used mouse gingival explants treated with IL-33 for 24 hours. RT-qPCR

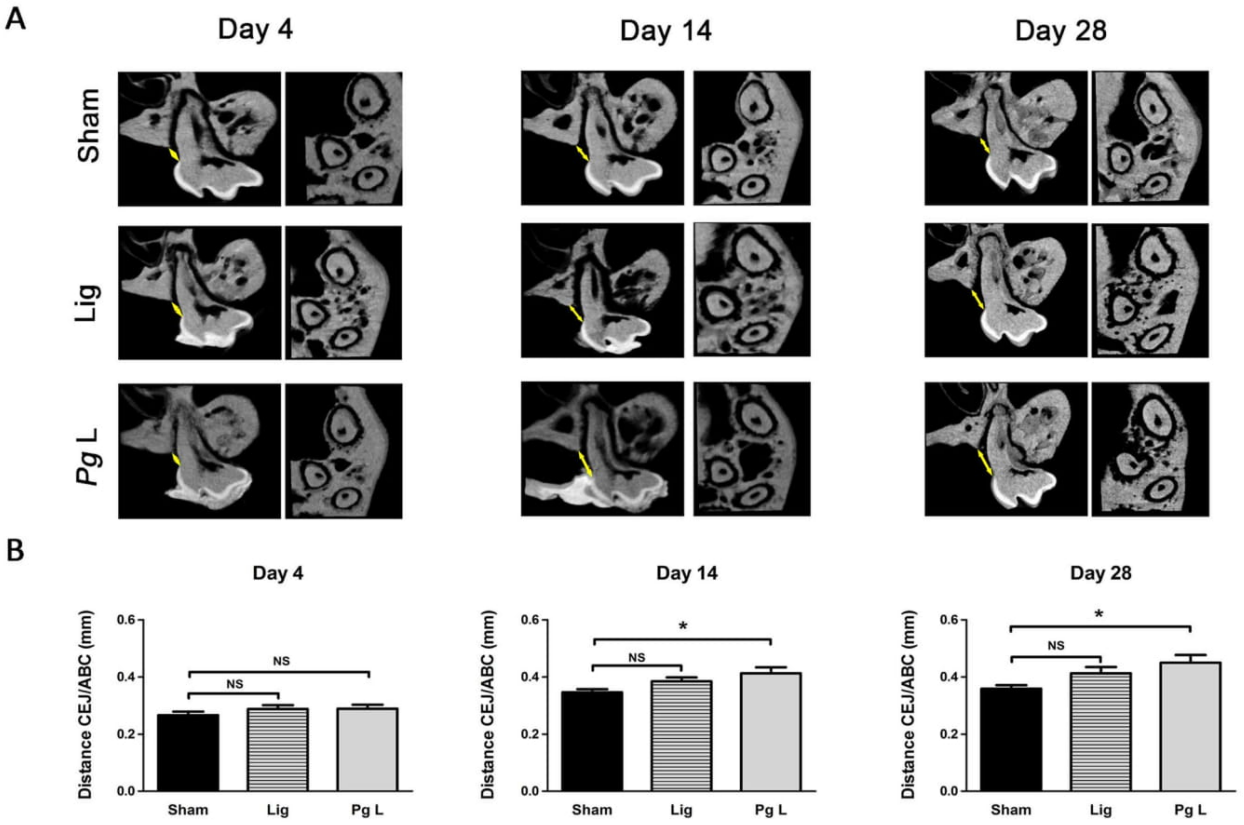

Fig 4. Time-course of alveolar bone loss in the ligature-induced murine model of experimental periodontitis. CD1 Swiss mice (n = 90) were subjected to experimental periodontitis for 4, 14 and 28 days. At each time point, animals were sacrificed and maxillary samples were harvested. A. After 4, 14 and 28 days, μCT analysis was performed. Longitudinal sections through the middle of the palatal root of the first maxillary molar (left images) and transversal sections from the apices of the three roots of the first maxillary molar to the summit of the alveolar bone crest (right images) are presented for each time points. B. Alveolar bone loss was assessed using 2D μCT. At each time point, data of ligatured groups (Lig and *Pg* L) were compared to their respective Sham groups. Data are shown as means ± SEM. * p<0.05.

doi:10.1371/journal.pone.0168080.g004

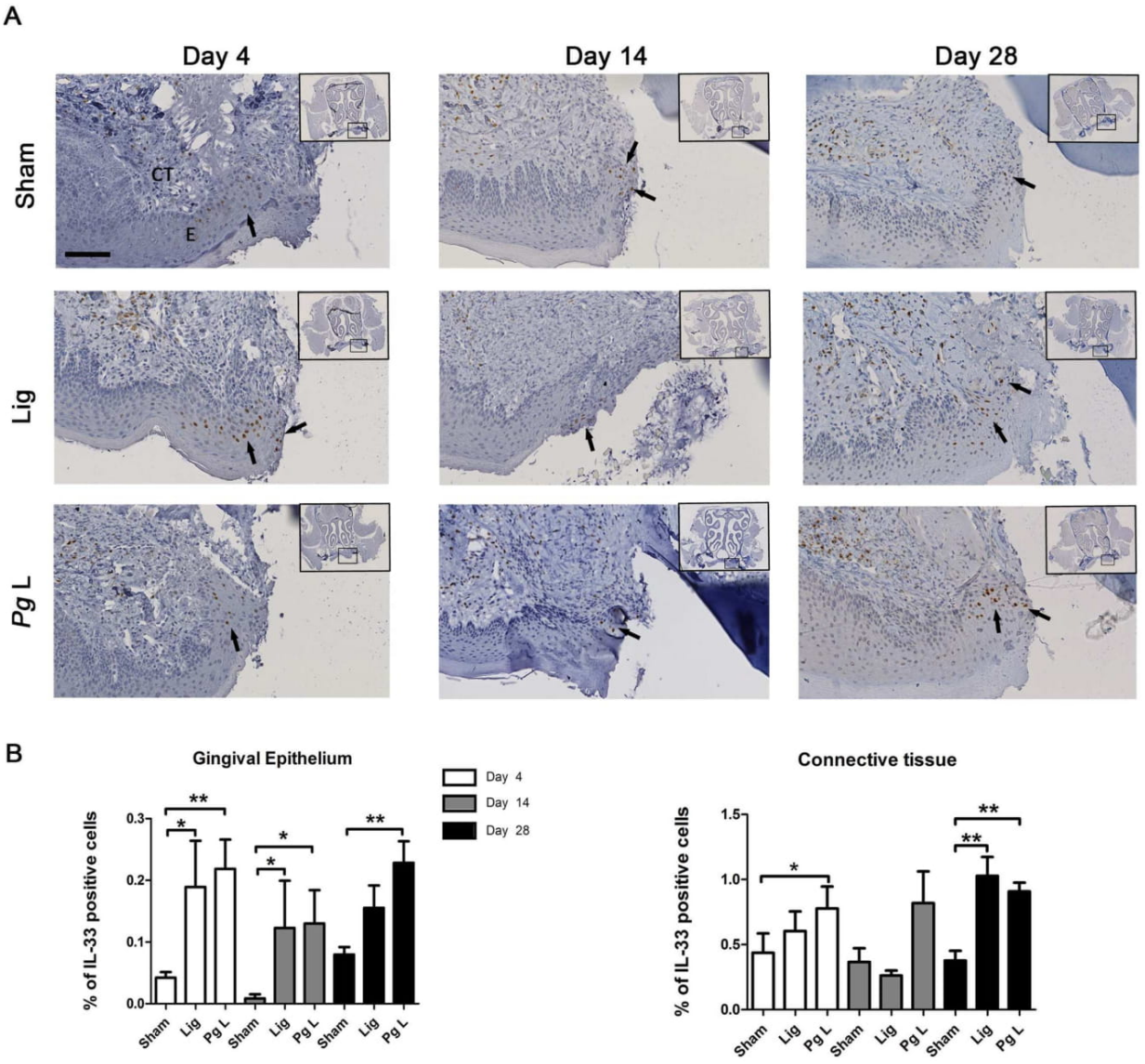

Fig 5. Time-course of IL-33 expression in the ligature-induced murine model of experimental periodontitis. A. IL-33 expression was assessed by IHC and sections were counterstained with Harris Hematoxylin staining (arrows). B. The percentage of IL-33 was quantified in gingival epithelium and in connective tissue using Fiji software and defined as a percentage of DAB positive staining area per region of interest. At each time point, data of ligatured groups (Lig and *Pg* L) were compared to their respective Sham groups. EP: Epithelium, CT: Connective tissue. Data are shown as means ± SEM. * p<0.05; **p<0.01. Scale bar = 100μm.

doi:10.1371/journal.pone.0168080.g005

analyses evidenced a significant increase of RANK-L mRNA expression 24 hours after IL-33 stimulation ($p<0.05$) (Fig 6). This demonstrates the ability of IL-33 to induce RANK-L expression in murine gingival cells.

Pg infection resulted in an overexpression of RANK-L mRNA but was a weak inducer of IL-33 mRNA in human oral epithelial cells

We also investigated whether *Pg* could be the triggering factor to induce IL-33 and RANK-L in human OECs. OECs were infected by *Pg* for 6, 12 and 24 hours at MOI of 10:1 or 100:1. RT-

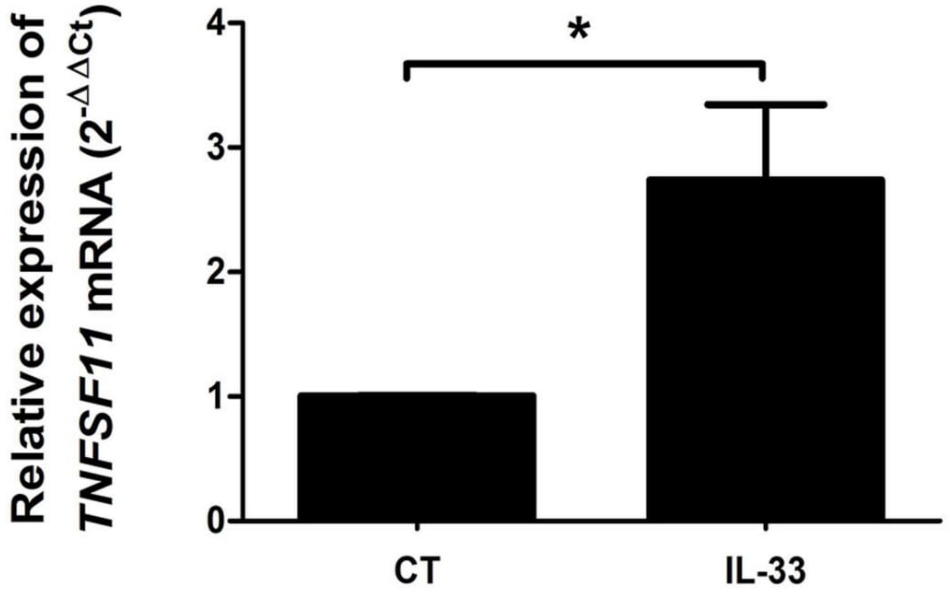

Fig 6. IL-33 induced RANK-L expression in mouse gingival explants. Explants from palatal mucosa of C57BL/6 mice were culture overnight at 37˚C. These explants were then stimulated with 100ng/mL of recombinant murine IL-33 for 24 hours. Total tissue RNA was extracted and RANK-L transcript was quantified by RT-qPCR. Three separate experiments were performed. Data are shown are means ± SEM. *p<0.05.

doi:10.1371/journal.pone.0168080.g006

qPCR analysis revealed that IL-33 mRNA expression was only significantly increased at MOI of 100:1 24 hours after *Pg* infection ($p<0.05$) (Fig 7A). Expression of RANK-L was stable throughout the experiment in control cells. After *Pg* infection, this RANK-L expression increased from 6 to 24 hours at MOI10:1 but was quite stable at MOI 100:1. A significant overexpression of RANK-L was evidenced for each time of infection (6 hours: MOI 100:1, $p<0.01$; 12 hours: MOI 100:1 and 10:1, $p<0.05$; 24 hours: MOI 10:1, $p<0.01$) (Fig 7B). These results suggest that *Pg* may trigger RANK-L expression in gingival epithelial cells but is a weak inducer of IL-33 expression.

Discussion

In this study, we demonstrated that gingival epithelial cells could play an undescribed role in the alveolar bone loss associated to periodontal disease throughout RANK-L production. We also evidenced that RANK-L overexpression could be mediated by *Pg* and/or through IL-33 expression in gingival epithelial cells.

IL-33 protein expression was increased in gingival epithelial cells both in human and mouse. IL-33 expression in CP in human has recently been described by Malcolm et al. in gingival epithelial cells and our results confirmed this observation [20]. This is of particular interest because differences of IL-33 expression in skin have been reported between species [35]. Notably in human and porcine keratinocytes, IL-33 expression is low but rapidly induced after skin wounding whereas it is the opposite in mice. Here, we evidenced in a murine model of EP induced by the apposition of a *Pg*-soaked ligature that IL-33 expression was increased in gingival epithelial cells similarly as in human CP. This sustains the reliability of this experimental model to mimic the alveolar bone loss related to periodontitis in human and so, to investigate the potent role of IL-33 in the inflammatory cascade associated to the CP pathogenesis.

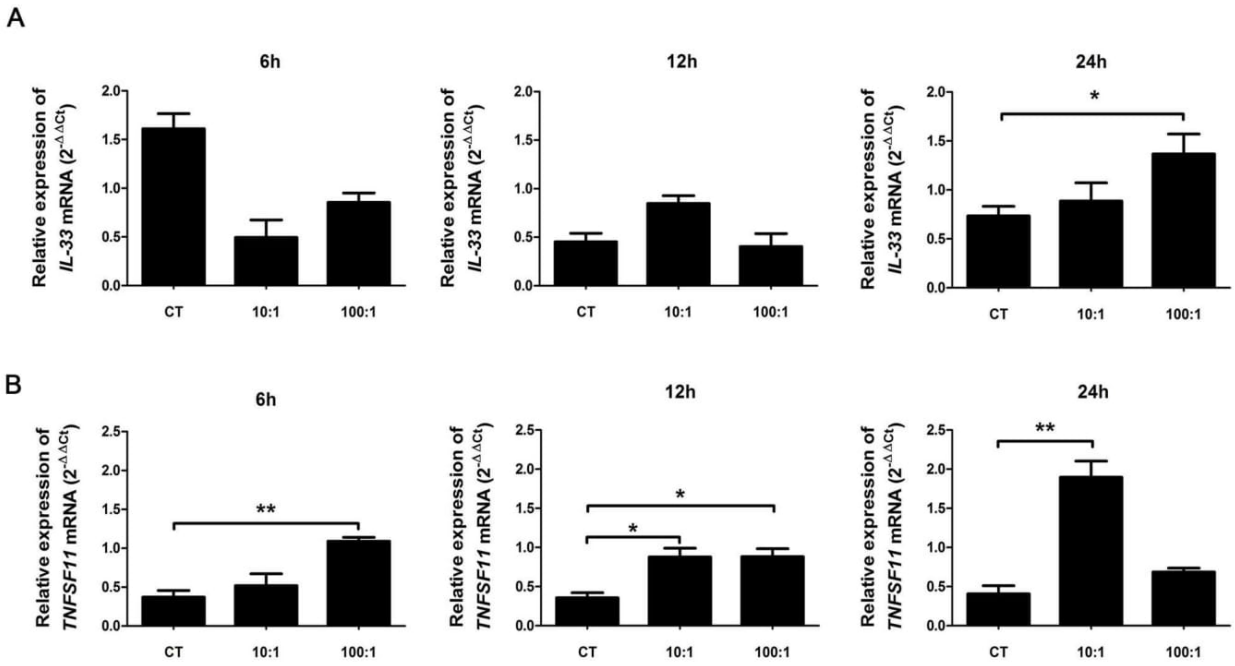

Fig 7. *Pg* infection increased the expression of RANK-L and IL-33 mRNAs in human oral epithelial cells. Human oral epithelial cells (OKF6/TERT2) were cultured with *Pg* at 10:1 or 100:1 MOI for 6, 12 or 24 hours. mRNAs encoding for IL-33 (A) and RANK-L ((B) were quantified by RT-qPCR. Three separate sets of experiment were performed. Data are shown as mean ± SEM. *p<0.05; **p<0.01.

doi:10.1371/journal.pone.0168080.g007

We have confirmed that IL-33 expression is increased in human gingiva from CP patients and we have also evidenced this increase in a ligature-induced model of EP. Two major models of EP are described in the literature. The oral gavage model is useful for addressing a wide variety of hypotheses related to periodontal pathogenesis, ranging from the role of the host response to virulence traits of pathogens and to the interconnections of those factors with systemic parameters. The silk ligature model is more relevant to investigate mechanistic and inflammatory aspects of the host immune response to bacterial stimulus and to identify potent therapeutic targets of particular interest in this inflammatory cascade [36]. This experimental model is also the most appropriate as it mimics the start point of periodontitis, a local gingival infection where oral epithelial cells are the first-line defense. Indeed, in our study, the inflammatory process seems strictly localized to the stimulated area because no alveolar bone loss was recorded elsewhere. We didn't evidence any increase in serum concentration of IL-33 in mice subjected to ligatures impregnated or not with *Pg*. This hardly suggests that IL-33 is not involved in a systemic inflammatory process but rather in a gingival localized one to possibly trigger alveolar bone loss.

The first key factor for the onset of periodontitis is the presence of pathogen species such as *Pg*. Increased expression of inflammatory cytokines and particularly IL-33 has been previously described *in vitro* after *Pg* infection of gingival epithelial cells [24, 31]. We also recorded such increase 24 hours after *Pg* infection of human epithelial cells. However, as we also recorded an increased IL-33 expression *in vivo* independently of *Pg* infection, it is tempting to speculate that the ligature apposition is an inflammatory stimulus sufficient to induce the increase of IL-33 expression in gingival epithelial cells, directly or throughout other pro-inflammatory cytokines such as TNF-α or IFN-γ [35, 37]. Consistently, we have also observed an IL-33 expression in Sham animals subjected to a slight incision suggesting that this mechanical

stimulus may trigger the production of IL-33 in gingival epithelial cell and that *Pg* may be not the major factor needed for IL-33 expression.

In CP, increased osteoclast activity is related to increased production of RANK-L. Several sources of RANK-L have been described notably B and T lymphocytes [28]. In our study, we showed a concomitant increase in CD3 and RANK-L positive cells and in RANK-L expression in gingival epithelial cells of patients affected by CP. RANK-L-producing lymphocytes are recruited towards inflammatory sites following *Pg* infection [38]. *Pg* can also stimulate RANK-L production by other cells such as bone alveolar osteoblasts and periodontal ligament fibroblasts notably via TLR2 signaling [39]. Mice deficient for TLR2 were protected from *Pg*-induced alveolar bone loss indicating that *Pg* is a crucial factor for the increase in RANK-L expression observed in CP [39]. Gingival epithelial cells, the first cells in contact with bacterial stimulus, are also able to produce RANK-L when stimulated by TNF-α [32]. In patients affected by CP, we recorded an increase in RANK-L expression in epithelial cells at the close vicinity of inflammatory sites, supporting a potential role to trigger the recruitment of osteoclast precursors, the osteoclast differentiation and activity as suggested by others [29].

IL-33-induced RANK-L expression in lymphocytes of the gingival tissue has been observed in EP induced by oral gavage and treatment with IL-33 [20]. We showed, using RT-qPCR quantification, that RANK-L was stimulated before IL-33 expression after *Pg* infection of gingival epithelial cells. This finding suggests that overexpression of RANK-L in CP is not primarily caused by IL-33 and that this cytokine may act as a secondary factor able to promote bone resorption through RANK-L after gingival infection by *Pg*. We can also hypothesize that IL-33 could be required for the perpetuation of alveolar bone loss in CP and we propose that alveolar bone loss related to CP is induced by the combination of *Pg* infection and IL-33.

EP applied to IL-33 knock-out mice will be needed to decipher the potent role of IL-33 in alveolar bone loss associated to CP. Taken together, these data highlight the ability of IL-33 to induce RANK-L expression in gingival cells and the interplay between both factors in CP.

Conclusion

Our results provide evidences that IL-33 overexpression in gingival epithelial cells is associated with CP and can trigger RANK-L expression in addition to the direct effect of *Pg*. Finally, IL-33 may act as an extracellular alarmin showing proinflammatory properties in CP by perpetuating bone resorption induced by *Pg* infection.

Acknowledgments

The authors were supported by the SFBTM (Société Française de Biologie des Tissus Minéralisés) for technical support, UTE-IRS-UN for animal facilities and "Région des pays de la Loire" (grant 2012-05775-05776).

Author Contributions

Conceptualization: PL JG.

Funding acquisition: PL.

Investigation: OL AC EL SS PP.

Methodology: OL SBC PP SS.

Project administration: JG.

Resources: OH IMB JLD JC GP.

Supervision: PL JG SBC VG.

Writing – original draft: OL AC.

Writing – review & editing: OL PL VG JG GP SBC.

References

1. Pihlstrom BL, Michalowicz BS, Johnson NW. Periodontal diseases. The Lancet. 2005; 366(9499): 1809–20.
2. Eke PI, Dye BA, Wei L, Thornton-Evans GO, Genco RJ, Cdc Periodontal Disease Surveillance workgroup: James Beck GDRP. Prevalence of periodontitis in adults in the United States: 2009 and 2010. Journal of dental research. 2012; 91(10):914–20. doi: 10.1177/0022034512457373 PMID: 22935673
3. Hajishengallis G. Periodontitis: from microbial immune subversion to systemic inflammation. Nature reviews Immunology. 2015; 15(1):30–44. doi: 10.1038/nri3785 PMID: 25534621
4. Eke PI, Dye BA, Wei L, Slade GD, Thornton-Evans GO, Borgnakke WS, et al. Update on Prevalence of Periodontitis in Adults in the United States: NHANES 2009 to 2012. Journal of periodontology. 2015; 86(5):611–22. doi: 10.1902/jop.2015.140520 PMID: 25688694
5. Hajishengallis G, Liang S, Payne MA, Hashim A, Jotwani R, Eskan MA, et al. Low-abundance biofilm species orchestrates inflammatory periodontal disease through the commensal microbiota and complement. Cell host & microbe. 2011; 10(5):497–506.
6. Graves DT, Oates T, Garlet GP. Review of osteoimmunology and the host response in endodontic and periodontal lesions. Journal of oral microbiology. 2011; 3:5304–19.
7. Hienz SA, Paliwal S, Ivanovski S. Mechanisms of Bone Resorption in Periodontitis. Journal of immunology research. 2015; 2015:615486–95. doi: 10.1155/2015/615486 PMID: 26065002
8. Preshaw PM, Taylor JJ. How has research into cytokine interactions and their role in driving immune responses impacted our understanding of periodontitis? Journal of clinical periodontology. 2011; 38 Suppl 11:60–84.
9. da Luz FA, Oliveira AP, Borges D, Brigido PC, Silva MJ. The physiopathological role of IL-33: new highlights in bone biology and a proposed role in periodontal disease. Mediators of inflammation. 2014; 2014:342410–7. doi: 10.1155/2014/342410 PMID: 24692848
10. Schmitz J, Owyang A, Oldham E, Song Y, Murphy E, McClanahan TK, et al. IL-33, an interleukin-1-like cytokine that signals via the IL-1 receptor-related protein ST2 and induces T helper type 2-associated cytokines. Immunity. 2005; 23(5):479–90. doi: 10.1016/j.immuni.2005.09.015 PMID: 16286016
11. Moussion C, Ortega N, Girard JP. The IL-1-like cytokine IL-33 is constitutively expressed in the nucleus of endothelial cells and epithelial cells in vivo: a novel 'alarmin'? PLoS One. 2008; 3(10):e3331. doi: 10.1371/journal.pone.0003331 PMID: 18836528
12. Byers DE, Alexander-Brett J, Patel AC, Agapov E, Dang-Vu G, Jin X, et al. Long-term IL-33-producing epithelial progenitor cells in chronic obstructive lung disease. The Journal of clinical investigation. 2013; 123(9):3967–82. doi: 10.1172/JCI65570 PMID: 23945235
13. Carriere V, Roussel L, Ortega N, Lacorre DA, Americh L, Aguilar L, et al. IL-33, the IL-1-like cytokine ligand for ST2 receptor, is a chromatin-associated nuclear factor in vivo. Proceedings of the National Academy of Sciences of the United States of America. 2007; 104(1):282–7. doi: 10.1073/pnas.0606854104 PMID: 17185418
14. Moulin D, Donze O, Talabot-Ayer D, Mezin F, Palmer G, Gabay C. Interleukin (IL)-33 induces the release of pro-inflammatory mediators by mast cells. Cytokine. 2007; 40(3):216–25. doi: 10.1016/j.cyto.2007.09.013 PMID: 18023358
15. Komai-Koma M, Gilchrist DS, McKenzie AN, Goodyear CS, Xu D, Liew FY. IL-33 activates B1 cells and exacerbates contact sensitivity. J Immunol. 2011; 186(4):2584–91. doi: 10.4049/jimmunol.1002103 PMID: 21239718
16. Liew FY, Pitman NI, McInnes IB. Disease-associated functions of IL-33: the new kid in the IL-1 family. Nature reviews Immunology. 2010; 10(2):103–10. doi: 10.1038/nri2692 PMID: 20081870
17. Palmer G, Talabot-Ayer D, Lamacchia C, Toy D, Seemayer CA, Viatte S, et al. Inhibition of interleukin-33 signaling attenuates the severity of experimental arthritis. Arthritis and rheumatism. 2009; 60(3): 738–49. doi: 10.1002/art.24305 PMID: 19248109
18. Martin P, Talabot-Ayer D, Seemayer CA, Vigne S, Lamacchia C, Rodriguez E, et al. Disease severity in K/BxN serum transfer-induced arthritis is not affected by IL-33 deficiency. Arthritis research & therapy. 2013; 15(1):R13.

19. Koseoglu S, Hatipoglu M, Saglam M, Enhos S, Esen HH. Interleukin-33 could play an important role in the pathogenesis of periodontitis. Journal of periodontal research. 2015; 50(4):525–34. doi: 10.1111/jre.12235 PMID: 25266494

20. Malcolm J, Awang RA, Oliver-Bell J, Butcher JP, Campbell L, Adrados Planell A, et al. IL-33 Exacerbates Periodontal Disease through Induction of RANKL. Journal of dental research. 2015; 94:968–75. doi: 10.1177/0022034515577815 PMID: 25808546

21. Kursunlu SF, Ozturk VO, Han B, Atmaca H, Emingil G. Gingival crevicular fluid interleukin-36beta (-1F8), interleukin-36gamma (-1F9) and interleukin-33 (-1F11) levels in different periodontal disease. Archives of oral biology. 2015; 60(1):77–83. doi: 10.1016/j.archoralbio.2014.08.021 PMID: 25247780

22. Papathanasiou E, Teles F, Griffin T, Arguello E, Finkelman M, Hanley J, et al. Gingival crevicular fluid levels of interferon-gamma, but not interleukin-4 or -33 or thymic stromal lymphopoietin, are increased in inflamed sites in patients with periodontal disease. Journal of periodontal research. 2014; 49(1): 55–61. doi: 10.1111/jre.12078 PMID: 23550893

23. Saglam M, Koseoglu S, Aral CA, Savran L, Pekbagriyanik T, Cetinkaya A. Increased levels of interleukin-33 in gingival crevicular fluids of patients with chronic periodontitis. Odontology / the Society of the Nippon Dental University. 2016;Odontology.

24. Tada H, Matsuyama T, Nishioka T, Hagiwara M, Kiyoura Y, Shimauchi H, et al. Porphyromonas gingivalis Gingipain-Dependently Enhances IL-33 Production in Human Gingival Epithelial Cells. PLoS One. 2016; 11(4):e0152794. doi: 10.1371/journal.pone.0152794 PMID: 27058037

25. Saidi S, Bouri F, Lencel P, Duplomb L, Baud'huin M, Delplace S, et al. IL-33 is expressed in human osteoblasts, but has no direct effect on bone remodeling. Cytokine. 2011; 53(3):347–54. doi: 10.1016/j.cyto.2010.11.021 PMID: 21190867

26. Kiyomiya H, Ariyoshi W, Okinaga T, Kaneuji T, Mitsugi S, Sakurai T, et al. IL-33 inhibits RANKL-induced osteoclast formation through the regulation of Blimp-1 and IRF-8 expression. Biochemical and biophysical research communications. 2015; 460(2):320–6. doi: 10.1016/j.bbrc.2015.03.033 PMID: 25795135

27. Palmer G, Gabay C. Interleukin-33 biology with potential insights into human diseases. Nature reviews Rheumatology. 2011; 7(6):321–9. doi: 10.1038/nrrheum.2011.53 PMID: 21519352

28. Kawai T, Matsuyama T, Hosokawa Y, Makihira S, Seki M, Karimbux NY, et al. B and T lymphocytes are the primary sources of RANKL in the bone resorptive lesion of periodontal disease. The American journal of pathology. 2006; 169(3):987–98. doi: 10.2353/ajpath.2006.060180 PMID: 16936272

29. Liu D, Xu JK, Figliomeni L, Huang L, Pavlos NJ, Rogers M, et al. Expression of RANKL and OPG mRNA in periodontal disease: possible involvement in bone destruction. International journal of molecular medicine. 2003; 11(1):17–21. PMID: 12469211

30. Usui M, Sato T, Yamamoto G, Okamatsu Y, Hanatani T, Moritani Y, et al. Gingival epithelial cells support osteoclastogenesis by producing receptor activator of nuclear factor kappa B ligand via protein kinase A signaling. Journal of periodontal research. 2015; 51(4):462–70. doi: 10.1111/jre.12323 PMID: 26432443

31. Zhao JJ, Feng XP, Zhang XL, Le KY. Effect of Porphyromonas gingivalis and Lactobacillus acidophilus on secretion of IL1B, IL6, and IL8 by gingival epithelial cells. Inflammation. 2012; 35(4):1330–7. doi: 10.1007/s10753-012-9446-5 PMID: 22382516

32. Fujihara R, Usui M, Yamamoto G, Nishii K, Tsukamoto Y, Okamatsu Y, et al. Tumor necrosis factor-alpha enhances RANKL expression in gingival epithelial cells via protein kinase A signaling. Journal of periodontal research. 2014; 49(4):508–17. doi: 10.1111/jre.12131 PMID: 24102429

33. Holtfreter B, Albandar JM, Dietrich T, Dye BA, Eaton KA, Eke PI, et al. Standards for reporting chronic periodontitis prevalence and severity in epidemiologic studies: Proposed standards from the Joint EU/USA Periodontal Epidemiology Working Group. Journal of clinical periodontology. 2015; 42(5):407–12. doi: 10.1111/jcpe.12392 PMID: 25808877

34. Saadi-Thiers K, Huck O, Simonis P, Tilly P, Fabre JE, Tenenbaum H, et al. Periodontal and systemic responses in various mice models of experimental periodontitis: respective roles of inflammation duration and Porphyromonas gingivalis infection. Journal of periodontology. 2013; 84(3):396–406. doi: 10.1902/jop.2012.110540 PMID: 22655910

35. Sundnes O, Pietka W, Loos T, Sponheim J, Rankin AL, Pflanz S, et al. Epidermal Expression and Regulation of Interleukin-33 during Homeostasis and Inflammation: Strong Species Differences. The Journal of investigative dermatology. 2015; 135(7):1771–80. doi: 10.1038/jid.2015.85 PMID: 25739051

36. Laperine O, Guicheux J, Lesclous P. Periostin-deficient mice, a relevant animal model to investigate periodontitis or not? BoneKEy reports. 2016; 5:794. doi: 10.1038/bonekey.2016.21 PMID: 27087940

37. Balato A, Di Caprio R, Canta L, Mattii M, Lembo S, Raimondo A, et al. IL-33 is regulated by TNF-alpha in normal and psoriatic skin. Archives of dermatological research. 2014; 306(3):299–304. doi: 10.1007/s00403-014-1447-9 PMID: 24522896

38. Han X, Lin X, Yu X, Lin J, Kawai T, LaRosa KB, et al. Porphyromonas gingivalis infection-associated periodontal bone resorption is dependent on receptor activator of NF-kappaB ligand. Infection and immunity. 2013; 81(5):1502–9. doi: 10.1128/IAI.00043-13 PMID: 23439308

39. Lin J, Bi L, Yu X, Kawai T, Taubman MA, Shen B, et al. Porphyromonas gingivalis Exacerbates Ligature-Induced, RANKL Dependent Alveolar Bone Resorption via Differential Regulation of Toll-Like Receptor 2 (TLR2) and TLR4. Infection and immunity. 2014; 82:4127–34. doi: 10.1128/IAI.02084-14 PMID: 25047844

VI. Annexe n°4

Cloitre A., Halgand B., Sourice S., Caillon J., Huck O., **Bugueno I.M.**, Batool F., Guicheux J., Geoffroy V., Lesclous P. “IL-36γ is a pivotal inflammatory player in periodontitis-associated bone loss”, **Scientific Reports** *(2019) 9:19257.*

SCIENTIFIC REPORTS
nature research

OPEN

IL-36γ is a pivotal inflammatory player in periodontitis-associated bone loss

Alexandra Cloitre[1,2,3], Boris Halgand[1,2,3], Sophie Source[1,2], Jocelyne Caillon[4], Olivier Huck[5,6,7], Isaac Maximiliano Bugueno[5,6], Fareeha Batool[5,6], Jérôme Guicheux[1,2,3*], Valérie Geoffroy[1,2,8] & Philippe Lesclous[1,2,3,8]

Periodontitis is a prevalent chronic inflammatory disease due to the host response (IL-1β, IL-6, TNF-α and IL-17A) to oral bacteria such as *Porphyromonas gingivalis*. The newer members of the IL-1 family, IL-36s (IL-36α/IL-36β/IL-36γ/IL-36Ra/IL-38) are known to be involved in host defense against *P. gingivalis* in oral epithelial cells (OECs) and are considered as key inflammatory mediators in chronic diseases. The aim of this study was to investigate the potential role of IL-36s in periodontitis. We showed here that *IL-36γ* mRNA gingival expression is higher in periodontitis patients, whereas *IL-36β* and *IL-36Ra* mRNA expression are lower compared to healthy controls. Interestingly, the elevated *IL-36γ* expression in patients is positively correlated with the *RANKL/OPG* ratio, an index of bone resorption. *In vitro*, *IL-36γ* expression was induced through TLR2 activation in primary OECs infected with *P. gingivalis* but not in gingival fibroblasts, the most widespread cell type in gingival connective tissue. In OECs, recombinant IL-36γ enhanced the expression of inflammatory cytokines (*IL-1β*, *IL-6*, *TNF-α* and *IL-36γ*), of *TLR2* and importantly, the *RANKL/OPG* ratio. These findings suggest that IL-36γ could be a pivotal inflammatory player in periodontitis by perpetuating gingival inflammation and its associated alveolar bone resorption and could be a relevant therapeutic target.

Periodontitis is a chronic multifactorial disease resulting from dysbiotic bacterial biofilms that compromise the integrity of the tooth-supporting tissue[1]. Hallmarks of periodontitis are gingival inflammation and irreversible destruction of the alveolar bone supporting the tooth, which may result in severe tooth loss. Periodontitis also contributes to systemic inflammation and increases the patients risk and morbidity associated with diseases such as diabetes mellitus[2], rheumatoid arthritis (RA)[3], atherosclerosis[4], asthma[5] and adverse pregnancy outcomes[6]. Controlling the disease should therefore have local and general benefits. But it implies a better understanding of the pathogenic mechanisms that are not fully deciphered.

Porphyromonas gingivalis is a Gram-negative anaerobic bacteria considered as a key pathogen in the pathogenesis of periodontitis (periopathogen)[7]. It is strongly associated with diseased sites, has various virulence factors such as lipopolysaccharide (LPS) and is able to induce dysbiosis in an ecologically balanced biofilm. Although the primary etiology of periodontitis is bacterial, the most of periodontal destruction is secondary to the host response to the bacterial challenge[8]. The recognition of pathogen-associated molecular patterns (PAMPs) such as LPS by toll-like receptors (TLRs) expressed by host cells stimulates the production of pro-inflammatory cytokines such as interleukin (IL)-1, IL-6, tumor necrosis factor-α (TNF-α), IL-17A and Receptor Activator of Nuclear Factor κ-B Ligand (RANKL), the most major pro-osteoclastogenic cytokine. These pro-inflammatory cytokines perpetuate local inflammation and subsequent alveolar bone resorption directly or indirectly. RANKL binds to its receptor RANK expressed by bone-resorbing cells, the osteoclasts, or their precursors from the monocyte-macrophage lineage, and enhances their recruitment, differentiation, fusion and activity. Osteoprotegerin (OPG), a soluble decoy receptor, inhibits osteoclastogenesis by competing with RANK

[1]Inserm, UMR 1229, RMeS, Regenerative Medicine and Skeleton, Université de Nantes, ONIRIS, Nantes, France. [2]Université de Nantes, UFR Odontologie, Nantes, France. [3]CHU Nantes, PHU4 OTONN, Nantes, France. [4]EA 3826 Thérapeutiques cliniques et expérimentales des infections, Nantes, France. [5]INSERM (French National Institute of Health and Medical Research), UMR 1260, Regenerative Nanomedicine (RNM), FMTS, Strasbourg, France. [6]Université de Strasbourg, Faculté de Chirurgie-dentaire, Strasbourg, France. [7]Hôpitaux Universitaires de Strasbourg, Pôle de médecine et chirurgie bucco-dentaire, Department of Periodontology, Strasbourg, France. [8]These authors jointly supervised this work: Valérie Geoffroy and Philippe Lesclous. *email: jerome.guicheux@inserm.fr

for interaction with RANKL. Therefore, the increase in the RANKL/OPG ratio is considered a good indicator of alveolar bone resorption activity notably in alveolar bone loss associated with periodontitis[9,10].

IL-36 cytokines (IL-36s) are new members of the IL-1 family that may play a key role in the immune response to *P. gingivalis* during periodontitis[11]. IL-36 cytokines include three agonists (IL-36α, IL-36β and IL-36γ) and two antagonists (IL-36Ra and IL-38)[12,13]. All these cytokines bind to IL-36R a widely expressed dimeric receptor. The antagonizing binding of IL-38 to this receptor has been shown only in one study[14]. But, unlike the other cytokines, IL-38 has been reported to bind several other receptors. IL-36 receptor is composed of the subunit IL-36R specific to IL-36 (IL-1Rrp2) and of the co-receptor IL-1R accessory protein (IL-1RAcP). This co-receptor is shared by the agonists of the IL-1 receptor family. IL-36 agonists induce an inflammatory response through the IL-36R and activate NF-κB and MAPK pathways, whereas IL-36 antagonists binding to IL-36R do not recruit its co-receptor and inhibit the IL-36 signaling pathway. IL-36s are mainly expressed by epithelial cells in barrier tissues and are involved in host immunity in both innate and acquired responses. A large body of evidence points to a key role of IL-36s in psoriasis, whereas their involvement in Crohn disease and RA is still currently debated[12,13,15]. Increasing evidence suggests that IL-36s are important regulators of host defense against pathogens in the oral mucosa[11,16–18]. In periodontitis, IL-36β and IL-36γ have been detected in the patient's gingival crevicular fluid, an inflammatory exudate collected within the gingival crevice[19]. *In vitro*, IL-36γ was strongly overexpressed in oral epithelial cells (OECs) in response to *P. gingivalis*[11]. IL-36γ stimulates OECs in an autocrine manner to induce expression of inflammatory mediators (IL-6, IL-8, CXCL1, CCL20), suggesting the presence of IL-36R on these cells[11]. While it has been suggested that IL-36γ, like other inflammatory cytokines including TNF-α and IL-33, may support osteoclastogenesis by enhancing the RANKL/OPG ratio, its role in the alveolar bone loss associated with periodontitis has not yet been investigated[20,21].

In this context, we hypothesize that IL-36s and IL-36γ in particular, could play a pivotal role in the pathogenesis of periodontitis. The aims of our work were (i) to show the gingival expression pattern of IL-36s and its role in periodontitis using human gingival samples and primary gingival cells, and (ii) to present evidence that IL-36γ support osteoclastogenesis by enhancing *RANKL/OPG* expression ratio in OECs.

Results

Analyses of IL-36s expression in patients with periodontitis. The demographic and clinical characteristics of 20 periodontitis and 16 healthy controls are summarized in Supplementary Table S1. Compared to healthy controls, periodontitis patients were older (average age 50.5 ± 2.2 vs 21.1 ± 1.2). This age discrepancy between patients and healthy controls, as often in periodontitis-based studies, is explained by the surgical procedure performed to harvest healthy gingival tissues during the extraction of impacted wisdom teeth, that is most often performed in young adults.

mRNA expression of inflammatory cytokines *IL-1β*, *IL-6*, *TNF-α* and the *RANKL/OPG* mRNA ratio were increased in periodontitis patients compared with gingival samples of healthy controls ($p < 0.05$) (Fig. 1), matching the clinical diagnosis of periodontitis (Supplementary Table S1).

Transcript analyses by RT-qPCR revealed that the five IL-36s were expressed in human gingival samples irrespective of their clinical status. Interestingly, *IL-36γ* mRNA expression was found to be the most altered by the clinical condition. A significant increase (3-fold, $p < 0.01$) in *IL-36γ* mRNA was observed in the gingiva of periodontitis as compared to healthy controls, whereas expression of *IL-36β* and *IL-36Ra* was significantly lower (0.4-fold, $p < 0.01$ for both) (Fig. 1). No difference was recorded for *IL-36α* and *IL-38* mRNA expressions.

To better assess the involvement of the IL-36 signaling in gingival samples from periodontitis patients, we calculated their induction rate (*IL-36* agonists to *IL-36Ra* antagonist). The majority of periodontitis patients (70%) exhibited a ratio over 3, illustrating that expression of *IL-36* agonists is higher than that of antagonists (Fig. 2) and suggesting the activation of the *IL-36* signaling pathway. Then, although the role of IL-38 as IL-36 receptor antagonist is debatable, the alternative ratio of *IL-36* agonists to *IL-36* antagonists, including *IL-36Ra* and *IL-38*, was calculated.in order to compare our results with literature[22]. Most of the patients (78.6%) that exhibit a *IL-36* agonists/ *IL-36Ra* ratio above 3 were also found to show an alternative *IL-36* agonists/ *IL-36* antagonists ratio (*IL-36Ra* and *IL-38*) above 1.5.

We next determined the correlation between the expression of *IL-36β*, *IL-36γ* and *IL-36Ra* in human gingiva and other inflammatory cytokines, receptors and bone resorption markers (Table 1). Of particular interest, in periodontitis patients, *IL-36γ* mRNA is positively correlated with archetypal inflammatory cytokines already known to be involved in periodontitis and inflammatory diseases, i.e., *IL-1β*, *IL-6*, *TNF-α* and *IL-17A* while *IL-36β* or *IL-36Ra* are not correlated with these cytokines. *IL-36γ* mRNA expression in patients was also correlated with those of *TLR2*, *RANKL*, *OPG* and the *RANKL/OPG* ratio, unlike *IL-36β* or *IL-36Ra* ($p > 0.05$). Altogether, these results evidenced that *IL-36γ* are correlated with other inflammatory cytokines, receptors and bone resorption markers unlike *IL-36β*/*IL-36Ra* which are not correlated to these factors (Table 1).

To further confirm mRNA expression data at the level of proteins, we sought to analyze IL-36γ protein expression and to determine its tissue distribution. As expected, immunohistochemistry analyses on gingival samples of periodontitis patients and healthy controls revealed an intense signal in the OECs of the gingival epithelium and a weaker one in the underlying gingival connective tissue mainly composed of GFs (Fig. 3).

These data suggest that variations of IL-36γ expression are representative of the IL-36 signaling activity and that IL-36γ could be worthy of further investigations in the pathogenesis of periodontitis.

Effect of *P. gingivalis* on IL-36γ expression in human OECs and potential role of TLR2. To further investigate the role of IL-36γ in periodontitis, we investigated the influence of *P. gingivalis* on human established and primary gingival cells (OKF6/TERT2 cell line, primary OECs, and primary GFs) in culture. We performed a time-course of infection over 24 h.

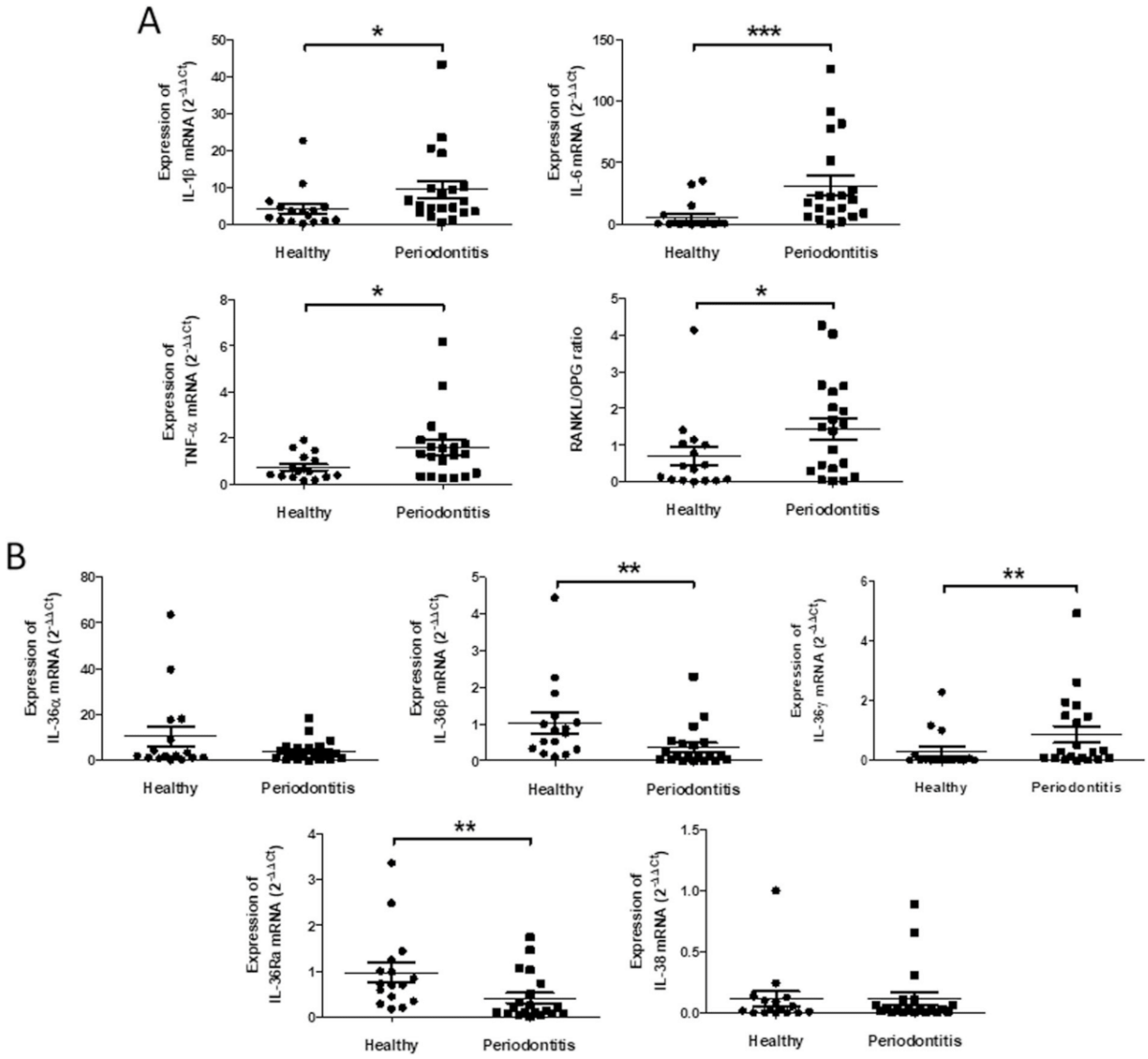

Figure 1. Expression of inflammatory cytokines and *RANKL*/*OPG* ratio in gingival samples of healthy controls and periodontitis patients. (**A**). *IL-1β*, *IL-6*, *TNF-α*, *RANKL* and *OPG* mRNA expression were measured in healthy controls and periodontitis patients by RT-qPCR. *RANKL/OPG* ratio was determined from quantification of *RANKL* and *OPG* expression. (**B**). Expression of the *IL-36* family members was measured by RT-qPCR. Data are shown as mean ± s.e.m; $n = 16$ healthy controls; $n = 20$ periodontitis patients; $^{*}p < 0.05$; $^{**}p < 0.01$; $^{***}p < 0.001$.

In OKF6/TERT2 cell line, *IL-36γ* mRNA expression was significantly increased by exposure to *P. gingivalis* from 1 h to 24 h at MOI 100:1 (maximum: 17.6-fold at 12 h) (Supplementary Fig. S1). *TNF-α* expression was used as positive control (maximum: 22.0-fold increase at 12 h). The increased expression of *IL-36γ* mRNA after *P. gingivalis* infection was further confirmed in primary OECs from 3 to 24 h at MOI 100:1 (maximum: 19.1-fold at 3 h) (Fig. 4A). TNF-α expression was also used as positive control (maximum: 99.1-fold increase at 24 h). Interestingly, the other IL-36 cytokines were not significantly affected by *P. gingivalis* infection. Of particular relevance to bone loss associated with periodontitis, *P. gingivalis* infection at MOI 100:1 also induced an increase in the *RANKL*/*OPG* ratio (3.5-fold) in primary human OECs, which occurred later than the increase in *IL-36γ* expression (3 h vs 24 h). This pattern of expression strongly suggests that *IL-36γ* is upstream in the signaling cascade and suggests that *IL-36γ* could participate in the increase in the *RANKL*/*OPG* expression ratio in human OECs infected by *P. gingivalis*. Finally, our Western blotting data confirm the presence of IL-36γ protein in the culture supernatant of primary OECs infected by *P. gingivalis* at MOI 100:1 for 24 h but not in that of cells not exposed to *P. gingivalis* (Fig. 4B). IL-36γ protein expression in the supernatant was only investigated at 24 h because it was not detectable before that time.

Because *P. gingivalis* is known to invade deep connective tissue[23], we finally sought to determine whether *P. gingivalis* infection could also affect the expression level of *IL-36γ* in human primary GFs. According to the lack of IL-36γ immunostaining in the connective tissue of gingival samples (Fig. 3), we found that *IL-36γ* expression was

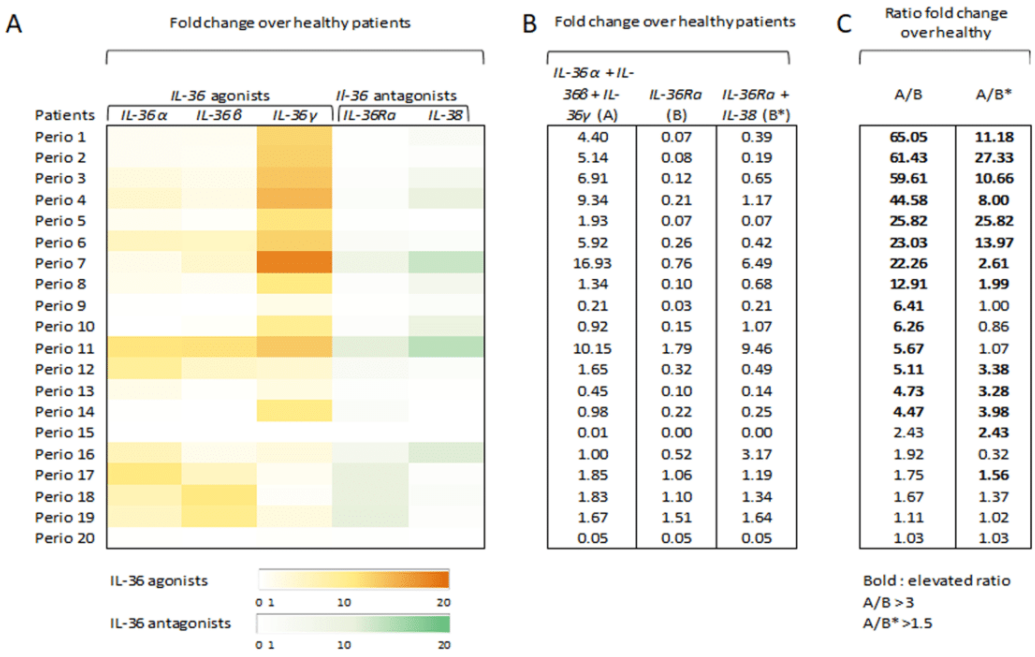

Figure 2. *Changes in IL-36* agonists and antagonists mRNA expression in gingival samples of periodontitis patients. Data are shown in individual patients ($n = 20$; Perio 1 to 20) as fold change over the mean value calculated from the 16 healthy controls. (**A**). *IL-36* agonists (*IL-36α, IL-36β* and *IL-36γ*) are presented in yellow and *IL-36* antagonists (*IL-36Ra* and *IL-38*) in green according to the color scale. (**B**). Sums of *IL-36* agonists (*IL-36α, IL-36β and IL-36γ*) (A), *IL-36Ra* (B) and sums of *IL-36* antagonists (*IL-36Ra* and *IL-38*) (B*) fold changes are presented. (**C**). *IL-36* agonists/ *IL-36Ra* ratio (A/B) and alternative IL-36 agonists/antagonists (*IL-36Ra* and *IL-38*) ratio (A/B*) are presented. A/B ratio over 3 and A/B* ratio over 1.5 are considered as elevated ratio and are in bold.

	IL-36β		*IL-36γ*		*IL-36Ra*	
	***p*-value**	**Spearman r**	***p*-value**	**Spearman r**	***p*-value**	**Spearman r**
Cytokines						
IL-1β	ns, $p = 0.4067$		*, $p = 0.0217$	r = 0.3815	ns, $p = 0.6783$	
IL-6	ns, $p = 0.1873$		***, $p = 0.0001$	r = 0.5935	ns, $p = 0.3478$	
TNF-α	ns, $p = 0.5050$		*, $p = 0.0171$	r = 0.3951	ns, $p = 0.8127$	
IL-17A	**, $p = 0.0091$	r = −0.4609	**, $p = 0.0035$	r = 0.5081	*, $p = 0.0164$	r = −0.4278
TLRs						
TLR2	ns, $p = 0.47647$		**, $p = 0.0031$	r = 0,5137	ns, $p = 0,3824$	
TLR4	ns, $p = 0.4607$		ns, $p = 0.0604$		ns, $p = 0,2349$	
Bone resorption markers						
RANKL	ns, $p = 0.0638$		***, $p < 0.0001$	r = 0,7431	ns, $p = 0,0736$	
OPG	ns, $p = 0.1679$		*, $p = 0.0459$	r = 0,3349	ns, $p = 0,3692$	
RANKL/OPG	ns, $p = 0.3393$		**, $p = 0.0073$	r = 0,4397	ns, $p = 0,2140$	

Table 1. Correlations between expression of *IL-36β*, *IL-36γ*, *IL-36Ra* and cytokines, receptors and bone resorption markers in gingival samples of healthy controls and periodontitis patients. Expression was measured by RT-qPCR. Data are shown as *p*-value and Spearman r coefficient. $n = 16$ healthy controls; $n = 20$ periodontitis patients. ns indicate nonsignificant *p*-values, significant *p*-values are indicated $*p < 0.05$, $**p < 0.01$, $***p < 0.001$.

lower in GFs as compared to OECs (average CT of *IL-36γ* mRNA, 33.7 in healthy control GFs vs 25.9 in healthy control OECs). In addition, our data revealed that *P. gingivalis* failed to significantly affect the expression level of *IL-36γ* in human GFs at MOI:100 (Fig. 4C).

Finally, to further decipher the mechanisms underlying the effects of *P. gingivalis* on *IL-36γ* expression levels, human primary OECs were stimulated with TLR agonizing and antagonizing ligands. After having confirmed that *TLR2* and *TLR4* mRNA were expressed in human primary OECs, cells were stimulated with TLR2 (Pam2CSK4, Fig. 5A) agonists. TLR2 agonist induced a significant increase in *IL-36γ* mRNA. In addition, when

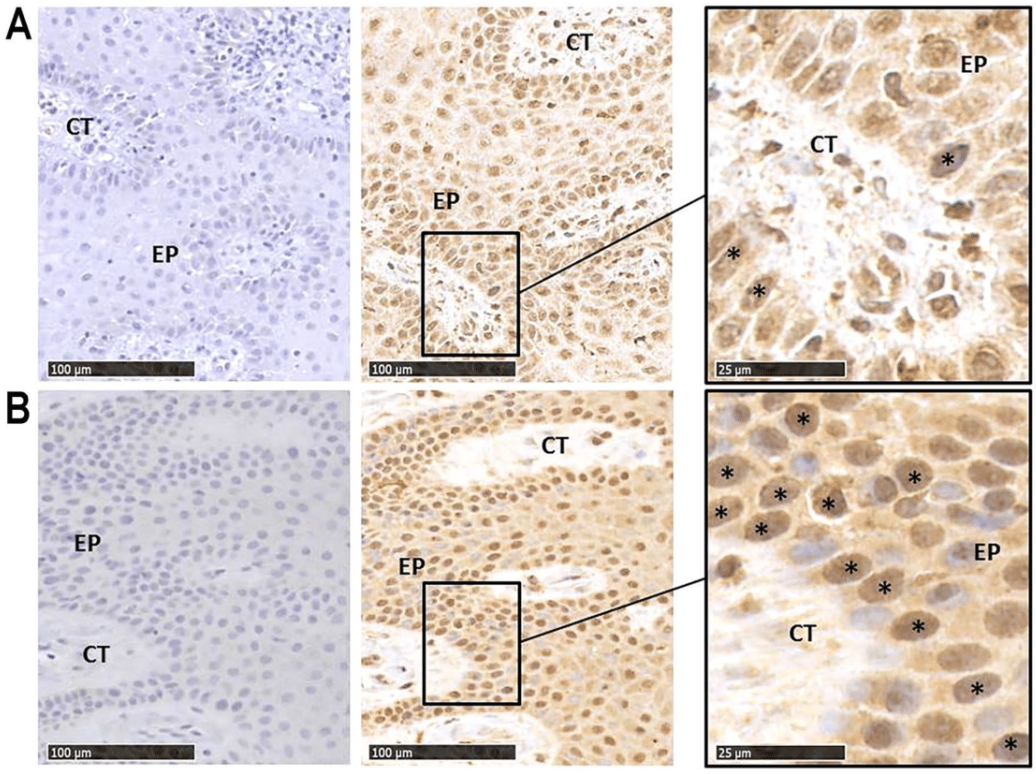

Figure 3. IL-36γ protein expression in gingival samples of healthy controls and periodontitis patients. Serial sections of gingival samples of healthy controls (**A**) and periodontitis patients (**B**) were immunostained with an isotype control antibody or with an anti-IL-36γ antibody. Secondary antibody goat anti-mouse was used. Specific binding was detected using 3,3-diaminobenzidine chromogen. Sections were counterstained with Harris hematoxylin. EP: epithelium; CT: connective tissue, * are positive cells. Scale bar = 100 µm and = 25 µm.

using a dual agonist of TLR2/TLR4 in the presence of a specific antagonist of TLR4, we also reported a significant increase in *IL-36γ* mRNA (Fig. 5B). Taken together, these data support the hypothesis that *P. gingivalis* increased *IL-36γ* expression at least through TLR2 activation in human OECs.

Effects of IL-36γ on the expression levels of inflammatory cytokines, *RANKL/OPG* ratio and *TLR2* in human OECs. To further elucidate the role of IL-36γ, we were interested in determining the effects of recombinant human IL-36γ (100 ng/ml; 24 h of treatment) on human primary OECs. The RT-qPCR analyses first demonstrated that IL-36γ acted on OECs by enhancing the expression of inflammatory cytokines, which have been clearly established as participating in the pathogenic mechanisms of periodontitis including *IL-1β*, *IL-6* and *TNF-α* with a 1.4-, 12.3- and 5.03-fold increase (Fig. 6A), respectively. In addition, we found that treatment with *IL-36γ* strongly enhanced the expression of *IL-36α* (3.5-fold increase; $p < 0.05$) and *IL-36γ* itself with the highest fold change among all of inflammatory cytokines analyzed in this study (18.4-fold increase; $p < 0.05$) (Fig. 6B). In addition, IL-36γ failed to alter the expression levels of *IL-36β* and those of all *IL-36* antagonists as well (data not shown). Interestingly, and as previously described for *P. gingivalis*, IL-36γ significantly increased the *RANKL*/*OPG* ratio in OECs (3.5-fold increase, $p < 0.05$) (Fig. 6C) as well as *TLR2* ($p < 0.05$, 1.3-fold increase) (Fig. 6D).

Discussion

In this study, we showed that a majority of periodontitis patients (70%) exhibited an elevated *IL-36* agonists/*IL-36Ra* antagonist mRNA ratio, suggesting the involvement of IL-36s cytokines in the pathogenesis of the disease. *IL-36γ* was the most highly expressed in the gingiva of patients and its expression was the most affected by periodontitis. Its expression was also increased in human primary OECs upon bacterial challenge with the key periopathogen *P. gingivalis* potentially through TLR2. IL-36γ could perpetuate gingival inflammation by increasing pivotal inflammatory cytokines in periodontitis (*IL-1β*, *IL-6* and *TNF-α*) and alveolar bone resorption through an increase of the *RANKL*/*OPG* ratio in OECs.

In the gingiva, all the *IL-36s* are expressed but only three of them have a modulated expression in periodontitis. Previously, only IL-36β and IL-36γ expressions have been reported *in vivo* in gingival crevicular fluid with a higher IL-36β level in aggressive compared to chronic periodontitis patients[19]. We found that a majority of periodontitis patients (70%) had a high *IL-36* agonists/*IL-36Ra* mRNA ratio. Although the role of IL-38 as IL-36 receptor antagonist is debatable, the alternative ratio of *IL-36* agonists to *IL-36* antagonists, including *IL-36Ra* and

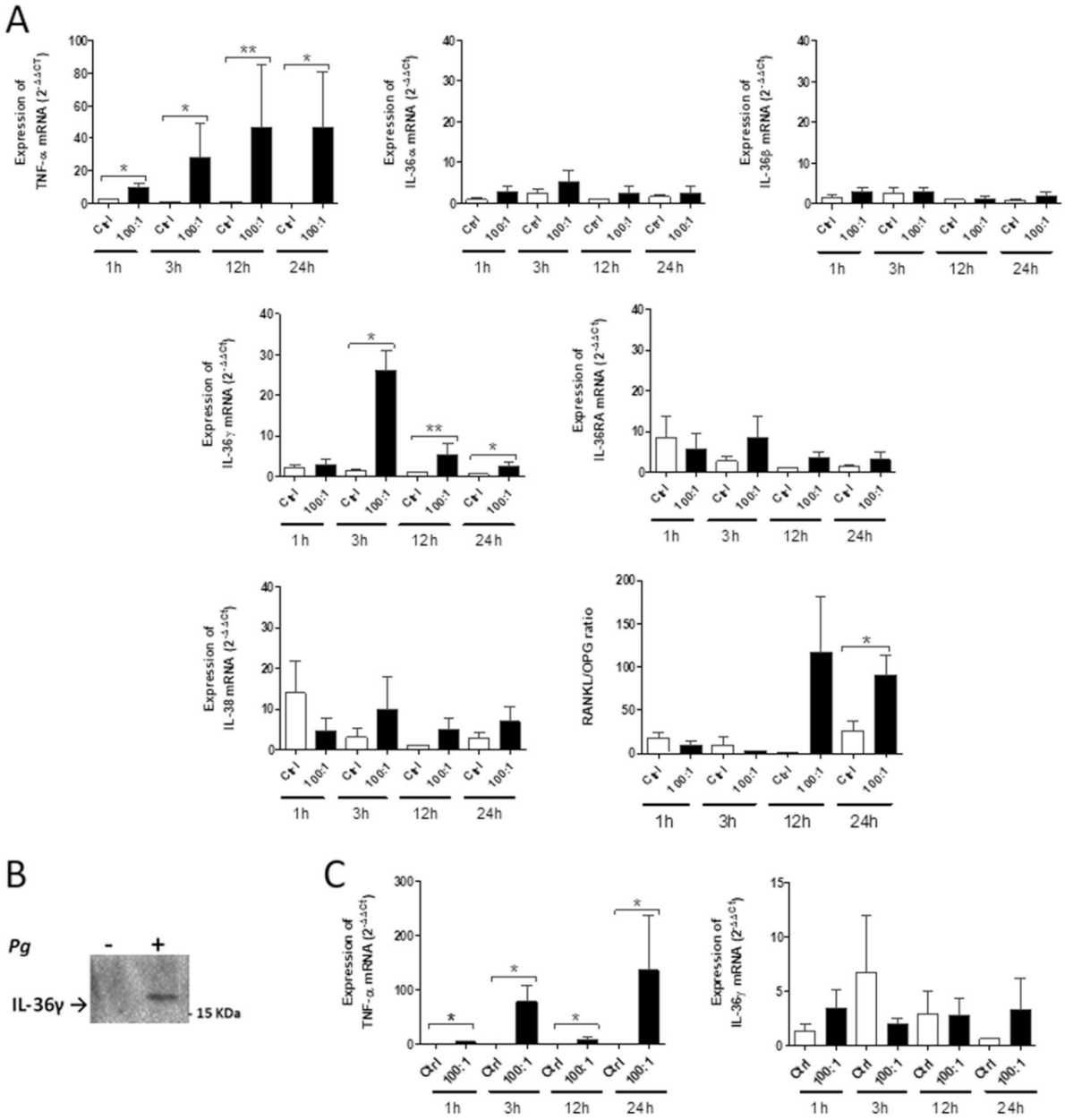

Figure 4. Effect of *Porphyromonas gingivalis* (*Pg*) infection on *IL-36γ* mRNA expression and *RANKL/OPG* expression ratio in human oral epithelial cells (OECs) and in human primary gingival fibroblasts (GFs). (**A**). Human primary OECs were cultured without *Pg* (control; Ctrl) or with *Pg* at 100:1 MOI for 1, 3, 12 or 24 h. *TNF-α* (positive control) and *IL-36γ* mRNA expressions were measured by RT-qPCR and *RANKL/OPG* was determined from quantification of *RANKL* and *OPG* mRNA expression. 4 biological replicates of primary OECs were used. n was used for statistical comparisons; $*p < 0.05$, $**p < 0.01$. (**B**). IL-36γ protein expression was assessed by Western blotting in the supernatants of human primary OEC culture. *Pg* – (Ctrl 24 h) and *Pg* + (100:1 MOI 24 h) supernatants were subjected to Western blotting with anti–IL-36γ. The Western blot presented is representative of two independent experiments.(See whole membrane in suplementary Fig. S3) (**C**). Human primary GFs were cultured without *Pg* (control Ctrl) or with *Pg* at 100:1 MOI for 1, 3, 12 or 24 h. *TNF-α* (positive control) and *IL-36γ* mRNA expressions were measured by RT-qPCR. Data are shown as mean ± s.e.m. 3 biological replicates were used for statistical comparisons.

IL-38, give a similar result. This alternative ratio permit us to compare the tissue expression of *IL-36s* in periodontitis with that of three other chronic inflammatory diseases reported in the literature[22] (Supplementary Table S2). Sixty-five percent of periodontitis patients exhibited an alternative *IL-36* agonists/antagonists ratio (*IL-36Ra* and *IL-38)* over 1.5. This is higher than in RA or Crohn's disease (29% and 25%, respectively) in which the role of IL-36s is currently debated, and smaller than in psoriasis (93%) in which IL-36s are key cytokines. This considerably strengthens the hypothesis of a promising role for IL-36s in periodontitis. The increased expression of *IL-36γ*

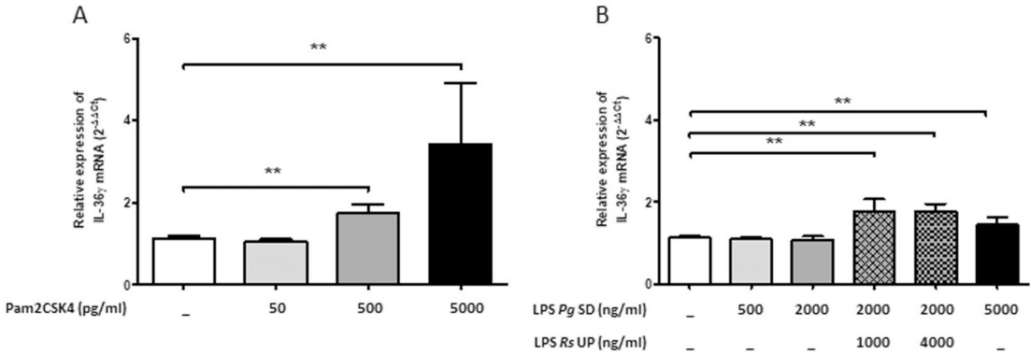

Figure 5. *IL-36γ* mRNA expression in human oral epithelial cells (OECs) stimulated with TLR2 or TLR2 TLR4 agonists with or without TLR4 antagonist for 24 h. Human primary OECs were cultured for 24 h with or without TLR2 agonist (Pam2CSK4) (**A**) and with or without TLR2/TLR4 agonist (LPS-Pg SD) and with or without pretreatment with TLR4 antagonist (LPS-Rs UP) 30 min before stimulation (**B**) at the concentrations indicated. IL-36γ mRNA expression was measured by RT-qPCR. Data are shown as mean ± s.e.m. 5 biological replicates were used for statistical comparisons; $^{**}p < 0.01$ vs CTL (white bar).

mRNA is the only common hallmark between these diseases. Within periodontitis, an inter-individual variability was observed. This probably limits the use of *IL-36γ* as a diagnostic biomarker, but this strongly suggests the existence of subgroups within periodontitis patients, which lays foundations for personalized medicine. This also raised the question of whether host modulation therapy blocking IL-36s could be relevant in the management of the disease in the subgroup of patients with an elevated *IL-36* agonists/*IL-36Ra* ratio.

OECs are the main gingival cells that express IL-36γ in periodontitis. These cells not only act as a physical barrier against periopathogen invasion, but are also immune contributors in initiating the innate immune defense of the host. In particular, they produce pivotal pro-inflammatory cytokines in periodontitis such as IL-1β, IL-6 and TNF-α in response to bacterial challenge with the key periopathogen *P. gingivalis* through the NFκB and MAPK signaling pathways[24,25]. In accordance with Huynh *et al.*[11], we reported that OEC infected by these bacteria strongly overexpressed IL-36γ not only in an established OEC line (OKF6 cells), but also in primary OECs isolated from human gingiva. Interestingly, this overexpression occurred early in the time course of infection, raising the hypothesis of a role for IL-36γ in the initiation of the host response to *P. gingivalis*. This hypothesis is in line with a recent report describing IL-36γ as an alarmin for surrounding cells with respect to its release by dying cells and its pro-inflammatory properties[26]. Unlike *IL-36γ*, the expression of other *IL-36 isoforms* by OECs remains unaffected by *P. gingivalis* infection, as previously shown[11]. The distinct variations of IL-36α, IL-36β and IL-36γ expression in inflammatory diseases are documented but not fully understood. Although these three isoforms are processed differentially by neutrophils and skin resident cell proteases[27,28], they act through the same receptor and seem to have redundant biological effects[12,29].

The other main gingival resident cells are GFs, which also participate in the immune response to oral bacteria by producing pro-inflammatory cytokines including IL-6 and IL-8[30]. In this study, we reported that *IL-36s* mRNA expression was not altered in human primary GFs infected with *P. gingivalis*. This is in accordance with our immunohistochemical findings, which indicated that GFs were not the main producers of *IL-36s* in the periodontitis gingiva. This is also in agreement with Jang *et al.*, who reported that in contrary to less pathogenic bacteria, *P. gingivalis* induced marginally or suppressed the inflammatory cytokine response in GFs, resulting in the persistence of bacteria within periodontal tissue that perpetuates the chronicity of periodontitis[23].

IL-36s expression has been shown to be induced by TLR signaling in several cell types including OECs[11,12]. *P. gingivalis* LPS can activate host cells to induce pro-inflammatory cytokines through TLR2 and/or TLR4[31–33]. In human gingival samples we showed that *IL-36γ* mRNA expression was positively correlated with *TLR2* but not with *TLR4* and that LPS *P. gingivalis* stimulates *IL-36γ* expression in primary OECs potentially via TLR2. Our results are in line with those of Huynh *et al.*, who reported that the stimulation of OECs with the TLR2 synthetic agonist FSL-1 resulted in an induction of IL-36γ expression upon the regulation of IRF6 and IRAK1[11]. We also showed that IL-36γ increases the expression of *TLR2* and the *RANKL*/*OPG* expression ratio in OECs. Interestingly, TLR2 is required for *P. gingivalis*-induced inflammatory bone loss in experimental periodontitis in mice[34–36]. Bone resorption associated with periodontitis is RANKL-dependent, as demonstrated *in vivo* by the anti-resorptive effects of a local anti-RANKL antibody administration[36]. Osteoblasts and macrophages have also been shown to be key TLR2-expressing cells driving alveolar bone resorption induced by *P. gingivalis*[35,37]. Activation of TLR2 in osteoblasts by *P. gingivalis* LPS increased RANKL production[37]. Adoptive transfer of TLR2-expressing macrophages into TLR2-deficient mice restored the ability of *P. gingivalis* to induce inflammatory bone *in vivo*, which is TNF-dependent[35].

Pivotal inflammatory cytokines in periodontitis, namely IL-1β, IL-6, TNF-α and IL-17A, mediate both periodontal inflammation and alveolar bone resorption[8]. We reported that gingival expression of *IL-36γ* in periodontitis patients was positively correlated with expression of these cytokines, suggesting its involvement in the pathogenesis of the disease. We also showed that IL-36γ could perpetuate inflammation in human primary OECs by increasing gene expression of inflammatory cytokines (*IL-1β*, *IL-6*, *TNF-α*, *IL-36α* and *IL-36γ* by

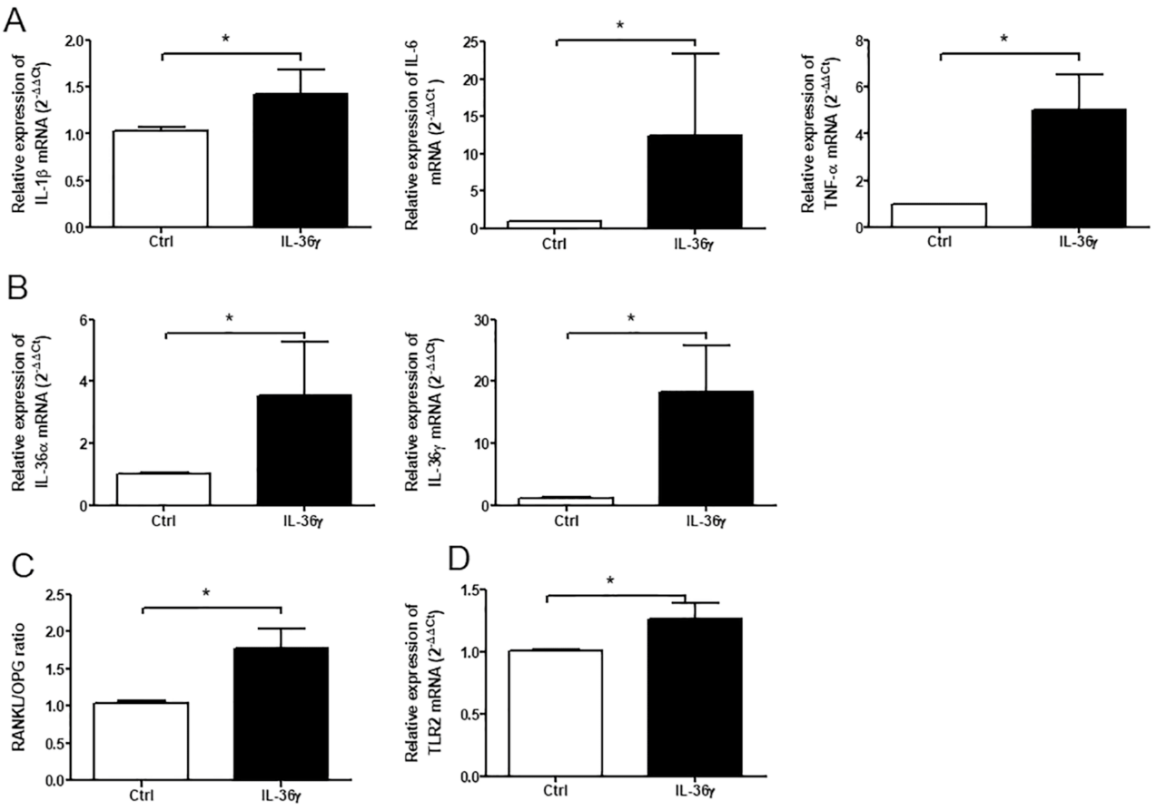

Figure 6. *IL-36γ* increased expression of inflammatory cytokines (*IL-1β, IL-6, TNF-α, IL-36α, IL-36γ*), *RANKL/OPG* ratio and TLR2 in primary human oral epithelial cells (OECs). Human primary OECs were cultured with or without 100 ng/ml of recombinant human IL-36γ for 24 h. *IL-1β, IL-6, TNF-α, IL-36α, IL-36γ, RANKL, OPG, TLR2* mRNA expression were measured by RT-qPCR. The *RANKL/OPG* ratio was determined from quantification of *RANKL and OPG* expression. Data are shown as mean ± s.e.m. 3 biological replicates were used for statistical comparisons; $*p < 0.05$.

self-amplification) and of *TLR2*. This is compatible with a starting action of IL-36γ in periodontitis and could lead to an uncontrolled inflammation cascade by increasing TLR2-induced cytokines. The effects of IL-36γ previously reported in the OEC line are the increase in the production of inflammatory cytokines (IL-6[11], IL-23p19/EBI3 (IL-39)[17]). It also stimulates the expression of neutrophil (IL-8, CXCL1) and Th17 cell chemokines (CCL20)[11] and PGLYRP2 antimicrobial proteins[16]. In addition IL-36γ is known to stimulate human dendritic cells and to a lesser extent macrophages to produce chemokines (IL-8, CXCL1, CCL20)[11]. It is noteworthy that, since IL-17A enhances the expression of IL-36γ in human OECs, a strong inflammatory axis between IL-17A and IL-36γ has been suggested in the oral mucosa[11]. The *in vivo* positive correlation evidenced in this study between *IL-36γ* and *IL-17A* mRNA expression corroborates this hypothesis. We have further reported that IL-36γ could perpetuate the alveolar bone resorption related to periodontitis through an increase in the *RANKL/OPG* ratio. In periodontitis, gingival expression of IL-36γ was positively correlated with the *RANKL/OPG* ratio. In primary OECs, *IL-36γ* was induced prior to the *RANKL/OPG* increase during *P. gingivalis* infection, suggesting that IL-36γ could act as an inducer. This was confirmed by stimulating these cells with IL-36γ. OECs produce a basal level of RANKL able to induce osteoclast formation in a co-culture assays with osteoclast precursor cells[38]. IL-36γ-dependent increase of the *RANKL/OPG* expression ratio in OECs could therefore contribute to increase osteoclast differentiation. Further analyses in a co-culture system (OECs/pre-osteoclasts) will be performed to decipher the effect of IL-36γ produced by OECs on the osteoclastogenesis. Regarding the direct effect of IL-36s on osteoclastogenesis, only IL-36α has been studied. Since IL-36 receptor is not present on mature osteoclasts, IL-36 isoforms have no direct effect on these mature cells[39].

The mechanisms of IL-36s in periodontitis could be multiple, as highlighted in Fig. 7. Additional studies are needed to better understand the role of IL-36 in periodontitis, and in particular experimental periodontitis in *IL-36R-* or *IL-36γ*-deficient mice could be useful in sustaining its importance in inflammatory bone loss[40]. Moreover, experimental periodontitis could allow the assessment of targeted therapies.

Overall, these findings from human gingival samples and primary gingival cells suggest a pathological involvement of IL-36s, IL-36γ in particular, in the pathogenesis of periodontitis. IL-36γ seems to play a pivotal role in the innate immune response to bacterial challenge with the key periopathogen *P. gingivalis*. IL-36γ is rapidly induced in OECs acting upstream of other cytokines considered as key mediators in periodontitis. Deciphering the mechanisms involving IL-36s in periodontitis is a prerequisite to the development of host modulation therapy

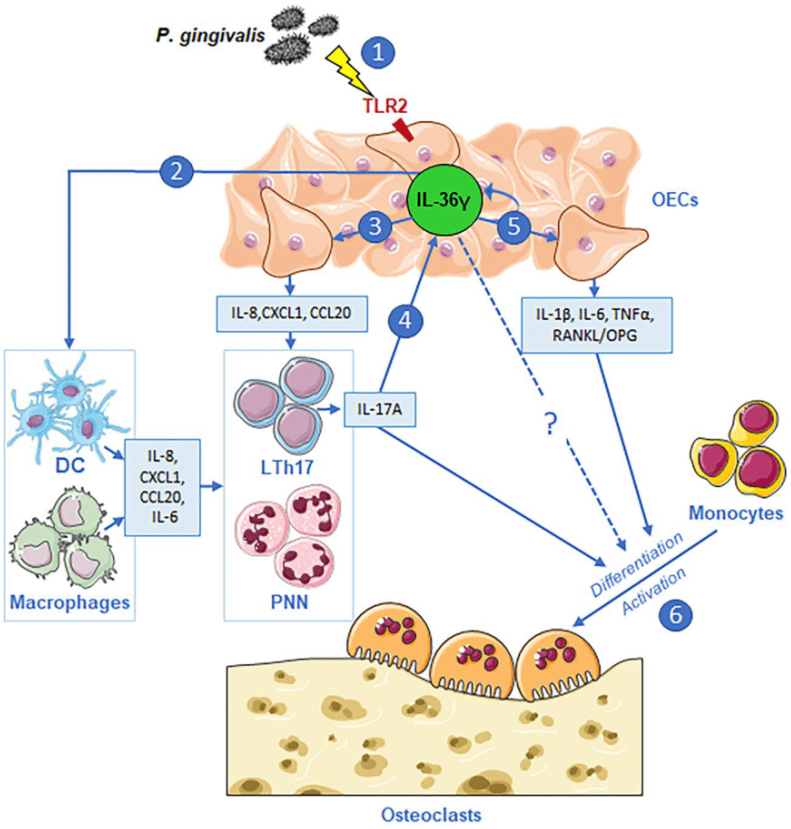

Figure 7. Involvement of IL-36γ in periodontitis pathogenesis. (**1**) *P. gingivalis* induces the expression of IL-36γ by OECs via TLR2 signaling. (**2**). IL-36γ acts on dendritic cells and macrophages to express chemokines attractant for neutrophils (IL-8, CXCL1) and LTh17 lymphocytes (CCL20) and IL-6. (**3**) IL-36γ also acts on OECs by inducing the expression of the same chemokines (IL-8, CXCL1, CCL20). (**4**) Th17 lymphocytes recruited on the inflammation site produce IL-17A, which increases IL-36γ expression by OECs, suggesting an inflammatory axis between these two cytokines. (**5**) IL-36γ also acts on OECs to induce its own expression and expression of IL-136γ, IL-6 and TNF-α, and to increase the RANKL/OPG ratio. (**6**) These cytokines promote the differentiation and activation of osteoclasts that perpetuate alveolar bone resorption. This figure was created using Servier Medical Art templates, which are licensed under a Creative Commons Attribution 3.0 Unported License; https://smart.servier.com.

blocking IL-36R signaling. The use of recombinant IL-36Ra or receptor-blocking monoclonal antibodies could be promising in periodontitis, as suggested for other inflammatory diseases[41].

Materials and Methods

Gingival sample collection. All enrolled patients provided their written informed consent for study participation. The study was approved by the Institutional Medical Ethics Committee of the Nantes University Hospital (SVTO:DC-2011-1399) and was conducted in accordance with the code of ethics of the World Medical Association (Declaration of Helsinki). The following characteristics were recorded: demography (gender, age), medical history (diseases, medications, tobacco use) and periodontal status (probing pocket depth (PPD), clinical attachment loss (CAL) and bleeding on probing (BOP)). According to the recent periodontal epidemiology working group, periodontitis was defined as PPD $\geq$ 4 mm, CAL $\geq$ 3 mm and presence of BOP[42]. Gingival samples were harvested just after an extraction when the mucosa was in excess. Patients were not included in the study if they suffered from systemic diseases that could affect periodontal health (such as diabetes mellitus, immunological disorders, human immunodeficiency virus infections, osteoporosis), or pregnant females and patients who were taking antibiotics, anti-inflammatory or immunosuppressive therapies in the 3 months prior to the dental extractions. The diagnosis of periodontitis was confirmed by RT-qPCR analyses of transcripts coding for inflammatory cytokines such as *IL-1β*, *IL-6*, *TNF-α* and the bone resorption markers *RANKL* and *OPG* (Supplementary Table S3 for primer sequences). The gingival samples were used for RT-qPCR analyses, histology and/or primary cell cultures.

Oral cell culture. Cell line**:** human OKF6/TERT2 OECs (BWH Cell Culture and Microscopy Core, USA) were amplified in defined keratinocyte-SFM basal medium (K-SFM) with growth supplements (Thermo Fischer Scientific, USA).

Primary cells: human OECs and gingival fibroblasts (GFs) were isolated from gingival samples of healthy controls using the direct explant technique as previously described for the skin[43]. Briefly, cells were characterized by their respective morphology and by RT-qPCR amplification of markers. OECs were tetrahedral and positive for keratin 14 (*KRT14*), whereas GFs were fusiform and positive for *CD90*. OECs were cultured in a serum-free keratinocyte growth medium CnT-07 (CELLnTEC, Switzerland) with 0.1% penicillin-streptomycin. GFs were cultured in Dulbecco's Modified Eagle's Medium (DMEM) glutaMAX® (Thermo Fischer Scientific, USA) supplemented with 10% FCS, 1% penicillin-streptomycin. OECs were used at passage 0 for all experiments except for challenging with TLR ligands (passage 1). GFs were used at passage 3.

Bacterial and strain culture. *P. gingivalis* (ATCC 33277) was cultured at 37 °C on Shaedler agar plated with sheep blood (Becton Dickinson, Germany) in an oxygen-free atmosphere. After 10 days in culture on the day of infection, *P. gingivalis* colonies were selected and resuspended in PBS for cell infection.

Challenging oral cells with viable *P. gingivalis*. Twenty-four hours before infection with viable *P. gingivalis*, oral cells were washed twice with HBSS and antibiotic-free media was added. The media for OECs was serum-free and the media for GFs was with heat-inactivated serum (30 min at 56 °C). The day of infection, cells were challenged with *P. gingivalis* at the multiplicity of infection (MOI) 10:1 or MOI 100:1.

Challenging oral cells with TLR ligands or recombinant IL-36γ. OECs were stimulated in a CnT-07 serum-free media with 0.1% penicillin-streptomycin for 24 or 48 h with:

- Pam2CSK4, a synthetic TLR2 agonist (tlrl-pm2s-1, InvivoGen, USA) at 0 to 5000 pg/ml,
- ultrapure LPS from *P. gingivalis* (LPS-*Pg* UP), a TLR4 agonist (tlrl-ppglps, InvivoGen, USA) at 0 to 5000 ng/ml,
- standard LPS from *P. gingivalis* LPS (LPS-*Pg* STD), TLR2 and TLR4 agonists (tlrl-pglps, InvivoGen, USA) at 0 to 5000 ng/ml,
- ultrapure LPS from *Rhodobacter sphaeroides* (LPS-RS), a strong TLR4 antagonist (tlrl-prslps, InvivoGen, USA) at 0 to 10,000 ng/ml with 30 min pretreatment before TLR stimulation,

Primary OECs were stimulated with 100 ng/mL of recombinant human IL-36γ (6835-IL, R&D, USA) in a CnT-07 serum-free media with 0.1% penicillin-streptomycin for 24 h.

RNA extraction and RT-qPCR analyses. Human gingival tissues were homogenized with the FastPrep® system (MP Biomedicals, USA). Total RNA was isolated from homogenized tissues or cells in culture using the Nucleospin® RNA II kit (Macherey-Nagel, Germany) according to the manufacturer's instructions. RNA quality and concentration were determined using a NanoDrop® 1000 spectrophotometer (Thermo Fisher Scientific, USA). RNA was reverse-transcribed using SuperScript®III (Thermo Fisher Scientific, USA) according to the manufacturer's instructions. Relative quantification of gene expression was performed on a CFX96 thermal cycler (BioRad, USA) using the SYBR®Select Master Mix (Applied Biosystems, USA). Primer sequences are indexed in Supplementary Table S3 and were synthesized by Eurofins Scientific® (Luxembourg). For the analyses, *SDHA*, *beta-actin*, and *B2M* were used as endogenous control and the relative gene expression levels were calculated with the $2^{-\Delta\Delta Ct}$ method.

The *IL-36* agonists/*IL-36Ra* ratio was calculated as follows: (*IL-36α* fold increase (mRNA expression in periodontitis vs healthy controls) + *IL-36β* fold increase + *IL-36γ* fold increase) / (*IL-36Ra* fold increase). A patient's ratio higher than 3 (three agonists/one antagonist) was considered elevated compared to samples of healthy controls. In order to compare with literature, an alternative ratio including *IL-36Ra* and *IL-38* i.e. (*IL-36α* fold increase (mRNA expression in periodontitis vs healthy controls) + *IL-36β* fold increase + *IL-36γ* fold increase) / (*IL-36Ra* fold increase + *IL-38* fold increase), was also calculated as previously described[22]. A patient's alternative ratio higher than 1.5 (three agonists/two antagonists) was considered elevated compared to samples of healthy controls.

Immunohistochemistry. Human gingival samples were fixed in PFA 4% for 48 h, dehydrated in an increasing percentage of ethanol and embedded in paraffin. Immunohistochemistry was performed on 4-µm-thick sections. Antigens were retrieved by boiling slides in Tris-EDTA buffer. Primary antibody mouse anti-human IL-36γ (1:50, Proteintech, UK) was incubated overnight at 4 °C. Secondary antibody goat anti-mouse (1:200, Dako, UK) was used (30 min at room temperature). Specific binding was detected using 3,3-diaminobenzidine chromogen (Dako, UK). Sections were counterstained with Harris hematoxylin and mounted in Eukitt®. Automated whole-slide imaging was performed using the NanoZoomer 2.0 (Hamamatsu, Japan). The negative control was done by omitting primary antibody.

Western blotting. Cells were washed twice with ice-cold PBS and then lysed in ice-cold lysis buffer (RIPA buffer: 50 mM Tris-HCl pH 7.5, 150 mM NaCl, 0.5% sodium deoxycholate 10%, 1% NP40, 0.1% SDS 20%) containing protease inhibitor cocktail (1:100, Sigma-Aldrich) on ice for 60 min. The lysate was centrifuged at 12,000 × *g* for 10 min at 4 °C and the supernatant containing the protein extracts was collected and stored at −80 °C until use.

For the protein isolation from cell culture media, supernatants were concentrated 25-fold using the Centricon® centrifugal filter (Millipore, USA). The protein concentration in the cell lysates and in the concentrated cell culture media was assessed using the Pierce® BCA Protein Assay Kit (Thermo scientific, USA). Protein extracts were diluted with Laemmli loading buffer containing β-mercaptoethanol before SDS-PAGE. Proteins were transferred to PVDF membrane and blocking was performed in blocking buffer (5% nonfat dry milk in

TBST) for 1 h at room temperature. Primary antibody rat anti-human IL-36γ (MAB 2320, 1:2,000, R&D, USA) was incubated in blocking buffer overnight at 4 °C. Then secondary horseradish peroxidase conjugate antibody donkey anti-rat (712-035-153, 1:10,000, Jackson Immuno Research, UK) was incubated for 1 h at room temperature. The signal was detected using SuperSignal® West Dura Extended Duration Substrate (Thermo Fisher Scientific, USA) and the ChemiDoc Imaging SystemTM (Bio-Rad, USA).

Statistical analysis. Results are given as means ± s.e.m. GraphPad Prism 5.0 software (GraphPad Software, USA) was used to perform nonparametric tests to compare data (the Kruskal-Wallis test followed, if significant, by group comparisons with the Mann-Whitney test) or for the Spearman correlation test. The n for statistical comparisons is the number of periodontitis patients or healthy controls includes in the *in vivo* studies as well as the number of healthy controls to extract primary cells and thus the number of *in vitro* biological replicates. The results were considered statistically significant if the *p*-value was less than 0.05. All experiments were repeated at least three times.

Data availability

The datasets used and/or analyzed during the current study are available from the corresponding author on reasonable request.

Received: 15 March 2019; Accepted: 30 November 2019;
Published online: 17 December 2019

References

1. Papapanou, P. N. *et al*. Periodontitis: Consensus report of workgroup 2 of the 2017 World Workshop on the Classification of Periodontal and Peri- Implant Diseases and Conditions. *J. Periodontol.* **45**, 286–291 (2018).
2. Löe, H. The sixth complication of diabetes mellitus. *Diabetes Care* **16**, 329–334 (1993).
3. Tang, Q. *et al*. A Possible Link Between Rheumatoid Arthritis and Periodontitis: A Systematic Review and Meta-analysis. *Int. J. Periodontics Restorative Dent.* **37**, 79–86 (2017).
4. Almeida, A. P. C. P. S. C., Fagundes, N. C. F., Maia, L. C. & Lima, R. R. Is There An Association Between Periodontitis And Atherosclerosis In Adults? A Systematic Review. *Curr. Vasc. Pharmacol.* 1–2 (2017).
5. Moraschini, V., de Albuquerque Calasans-Maia, J. & Diuana Calasans-Maia, M. Association Between Asthma and Periodontal Disease: A Systematic Review and Meta-Analysis. *J. Periodontol.* 1–20 (2017).
6. Corbella, S. *et al*. Adverse pregnancy outcomes and periodontitis: A systematic review and meta-analysis exploring potential association. *Quintessence Int.* **47**, 1–12 (2015).
7. Hajishengallis, G. Periodontitis: from microbial immune subversion to systemic inflammation. *Nat. Rev. Immunol.* **15**, 30–44 (2015).
8. Di Benedetto, A., Gigante, I., Colucci, S. & Grano, M. Periodontal disease: Linking the primary inflammation to bone loss. *Clin. Dev. Immunol.* **2013**, 1–7 (2013).
9. Crotti, T. *et al*. Receptor activator NF kappaB ligand (RANKL) and osteoprotegerin (OPG) protein expression in periodontitis. *J. Periodontal Res.* **38**, 380–387 (2003).
10. Bostancı, N. *et al*. Differential expression of receptor activator of nuclear factor-kB ligand and osteoprotegerin mRNA in periodontal diseases. *J. Periodontal Res.* **42**, 287–293 (2007).
11. Huynh, J. *et al*. IRF6 Regulates the Expression of IL-36γ by Human Oral Epithelial Cells in Response to Porphyromonas gingivalis. *J. Immunol.* **196**, 2230–8 (2016).
12. Bassoy, E. Y., Towne, J. E. & Gabay, C. Regulation and function of interleukin-36 cytokines. *Immunol. Rev.* **281**, 169–178 (2018).
13. van de Veerdonk, F. L., de Graaf, D. M., Joosten, L. A. & Dinarello, C. A. Biology of IL-38 and its role in disease. *Immunol. Rev.* **281**, 191–196 (2018).
14. van de Veerdonk, F. L. *et al*. IL-38 binds to the IL-36 receptor and has biological effects on immune cells similar to IL-36 receptor antagonist. *Proc. Natl. Acad. Sci.* **109**, 3001–3005 (2012).
15. Gabay, C. & Towne, J. E. Regulation and function of interleukin-36 cytokines in homeostasis and pathological conditions. *J. Leukoc. Biol.* **97**, 645–52 (2015).
16. Scholz, G. M., Heath, J. E., Aw, J. & Reynolds, E. C. Regulation of the peptidoglycan amidase PGLYRP2 in epithelial cells by IL-36γ. *Infect. Immun.* **IAI**, 00384–18 (2018).
17. Scholz, G. M., Heath, J. E., Walsh, K. A. & Reynolds, E. C. MEK-ERK signaling diametrically controls the stimulation of IL-23p19 and EBI3 expression in epithelial cells by IL-36γ. *Immunol. Cell Biol.* **1**, 1–10 (2018).
18. Verma, A. H. *et al*. IL-36 and IL-1/IL-17 Drive Immunity to Oral Candidiasis via Parallel Mechanisms. *J. Immunol.* ji1800515 (2018).
19. Kurşunlu, S. F., Oztürk, V. Ö., Han, B., Atmaca, H. & Emingil, G. Gingival crevicular fluid interleukin-36β (-1F8), interleukin-36γ (-1F9) and interleukin-33 (-1F11) levels in different periodontal disease. *Arch. Oral Biol.* **60**, 77–83 (2015).
20. Fujihara, R. *et al*. Tumor necrosis factor-α enhances RANKL expression in gingival epithelial cells via protein kinase A signaling. *J. Periodontal Res.* **49**, 508–517 (2014).
21. Lapérine, O. *et al*. Interleukin-33 and RANK-L interplay in the alveolar bone loss associated to periodontitis. *PLoS One* **11**, 1–17 (2016).
22. Boutet, M. A. *et al*. Distinct expression of interleukin (IL)-36α, β and γ, their antagonist IL-36Ra and IL-38 in psoriasis, rheumatoid arthritis and Crohn's disease. *Clin. Exp. Immunol.* **184**, 159–173 (2016).
23. Ji, S., Choi, Y. S. & Choi, Y. Bacterial invasion and persistence: Critical events in the pathogenesis of periodontitis? *J. Periodontal Res.* **50**, 570–585 (2015).
24. Sandros, J. *et al*. Cytokine responses of oral epithelial cells to Porphyromonas gingivalis infection. *J. Dent. Res.* **79**, 1808–1814 (2000).
25. Groeger, S., Jarzina, F., Domann, E. & Meyle, J. Porphyromonas gingivalis activates NFKB and MAPK pathways in human oral epithelial cells. *BMC Immunol.* **18**, 1–11 (2017).
26. Lian, L.-H., Milora, K. A., Manupipatpong, K. K. & Jensen, L. E. The double-stranded RNA analogue polyinosinic-polycytidylic acid induces keratinocyte pyroptosis and release of IL-36γ. *J. Invest. Dermatol.* **132**, 1346–53 (2012).
27. Henry, C. M. *et al*. Neutrophil-Derived Proteases Escalate Inflammation through Activation of IL-36 Family Cytokines. *Cell Rep.* **14**, 708–722 (2016).
28. Ainscough, J. S. *et al*. Cathepsin S is the major activator of the psoriasis-associated proinflammatory cytokine IL-36γ. *Proc. Natl. Acad. Sci.* **114**, E2748–E2757 (2017).
29. Towne, J. E., Garka, K. E., Renshaw, B. R., Virca, G. D. & Sims, J. E. Interleukin (IL)-1F6, IL-1F8, and IL-1F9 Signal Through IL-1Rrp2 and IL-1RAcP to Activate the Pathway Leading to NF-??B and MAPKs. *J. Biol. Chem.* **279**, 13677–13688 (2004).
30. Jang, J. Y., Song, I.-S., Baek, K. J., Choi, Y. & Ji, S. Immunologic characteristics of human gingival fibroblasts in response to oral bacteria. *J. Periodontal Res.* **52**, 447–457 (2017).

31. Darveau, R. P. *et al*. Porphyromonas gingivalis lipopolysaccharide contains multiple lipid A species that functionally interact with both toll-like receptors 2 and 4. *Infect. Immun.* **72**, 5041–5051 (2004).
32. Kirikae, T. *et al*. Lipopolysaccharides (LPS) of oral black-pigmented bacteria induce tumor necrosis factor production by LPS-refractory C3H/HeJ macrophages in a way different from that of Salmonella LPS. *Infect. Immun.* **67**, 1736–1742 (1999).
33. Nativel, B. *et al*. Porphyromonas gingivalis lipopolysaccharides act exclusively through TLR4 with a resilience between mouse and human. *Sci. Rep.* **7**, 1–12 (2017).
34. Burns, E., Bachrach, G., Shapira, L. & Nussbaum, G. Cutting Edge: TLR2 Is Required for the Innate Response to Porphyromonas gingivalis: Activation Leads to Bacterial Persistence and TLR2 Deficiency Attenuates Induced Alveolar Bone Resorption. *J. Immunol.* **177**, 8296–8300 (2006).
35. Papadopoulos, G. *et al*. Macrophage-Specific TLR2 Signaling Mediates Pathogen-Induced TNF-Dependent Inflammatory Oral Bone Loss. *J. Immunol.* **190**, 1148–1157 (2013).
36. Lin, J. *et al*. Porphyromonas gingivalis exacerbates ligature-induced, RANKLdependent alveolar bone resorption via differential regulation of Toll-like receptor 2 (TLR2) and TLR4. *Infect. Immun.* **82**, 4127–4134 (2014).
37. Kassem, A. *et al*. Porphyromonas Gingivalis Stimulates Bone Resorption by Enhancing RANKL through Activation of Toll- like Receptor 2 in Osteoblasts. *J. Biol. Chem.* **290**, jbc.M115.655787 (2015).
38. Usui, M. *et al*. Gingival epithelial cells support osteoclastogenesis by producing receptor activator of nuclear factor kappa B ligand via protein kinase A signaling. *J. Periodontal Res*. 462–470 (2015).
39. Derer, A. *et al*. Blockade of IL-36 receptor signaling does not prevent from TNF-induced arthritis. *PLoS One* **9**, 2–8 (2014).
40. Graves, D. T., Kang, J., Andriankaja, O., Wada, K. & Rossa, C. Animal models to study host-bacteria interactions involved in periodontitis. *Front. Oral Biol.* **15**, 117–132 (2012).
41. Walsh, P. T. & Fallon, P. G. The emergence of the IL-36 cytokine family as novel targets for inflammatory diseases. *Ann. N. Y. Acad. Sci*. 1–12 (2016).
42. Holtfreter, B. *et al*. Standards for reporting chronic periodontitis prevalence and severity in epidemiologic studies: Proposed standards from the Joint EU/USA Periodontal Epidemiology Working Group. *J. Clin. Periodontol.* **42**, 407–12 (2015).
43. Zuliani, T., Saiagh, S., Knol, A., Esbelin, J. & Dre, B. Fetal Fibroblasts and Keratinocytes with Immunosuppressive Properties for Allogeneic Cell-Based Wound Therapy. **8** (2013).

Acknowledgements

The authors thank Frédéric Blanchard and Claudine Blin for helpful comments and Marie-Astrid Boutet for technical support. This work was supported by Institut Français pour la Recherche Odontologique (IFRO), RFI Bioregate (Région Pays de la Loire) (Inflamos 38 Project) and by the School of Dentistry of Nantes.

Author contributions

A.C., V.G., J.G. and P.L. contributed to the conception or design of the work. A.C., B.H., S.S., J.C., I.M. and F.B. contributed to the investigation. A.C., V.G. and P.L. drafted the manuscript. A.C., B.H., S.S., J.C., O.H., I.M.B., F.B., J.G., V.G. and P.L. critically revised the manuscript.

Competing interests

The authors declare no competing interests.

Additional information

Supplementary information is available for this paper at https://doi.org/10.1038/s41598-019-55595-9.

Correspondence and requests for materials should be addressed to J.G.

Reprints and permissions information is available at www.nature.com/reprints.

Publisher's note Springer Nature remains neutral with regard to jurisdictional claims in published maps and institutional affiliations.

RÉSUMÉ

Les mécanismes impliqués dans l'initiation et le développement des parodontites, ainsi que la dissémination des parodontopathogènes via la circulation systémique et ses effets au niveau vasculaire, restent peu connus. L'infection chronique a été décrite comme un mécanisme potentiel impliqué dans l'aggravation de l'athérothrombose. A l'heure actuelle, le rôle joué par *Porphyromonas gingivalis (P.gingivalis)* est considéré comme majeur dans les phénomènes associés, tels que sa capacité à perturber la barrière épithéliale ainsi que l'endothélium vasculaire, l'induction d'une réponse inflammatoire soutenue contribuant à la destruction tissulaire. Dans ces travaux de thèse, nous avons évalué les effets de *P.gingivalis* sur l'apoptose et l'inflammation des cellules épithéliales (GEC), fibroblastiques (FB) et dans un modèle 3D de microtissus (MT), ainsi que dans des cellules endothéliales (EC). Finalement, nous avons évalué son rôle dans la réponse inflammatoire liée à la signalisation via les TLR-2 et TLR-4 et cinq protéines adaptatrices contenant le domaine du récepteur Toll/interleukine-1 (TIR). Nous avons mis en évidence que *P.gingivalis* est capable d'activer l'inflammation et la réponse du système immunitaire entraînant la destruction du parodonte en modulant différentiellement des processus biologiques primordiaux tels que l'apoptose (modulation de l'apoptosome Apaf-1 et son inhibiteur XIAP), le cycle cellulaire (P53, P21, CDK4), l'inflammation (modulation des TLR-2, TLR-4 et ses adaptateurs MAL et TRAM et des protéines inflammatoires telles que TNF-α), lui permettant d'échapper au système immunitaire, de contribuer à la destruction parodontale et sa dissémination systémique et d'exercer des effets sur l'endothélium. La mise en évidence de nouveaux mécanismes ou de nouvelles cibles cellulaires affectées par ce pathogène pourrons nous permettre de développer de nouvelles stratégies thérapeutiques.

ABSTRACT

The mechanisms involved in the initiation and development of periodontitis, as well as the dissemination of periodontal pathogens via the systemic circulation and their effects at the vascular level, remain poorly described. Chronic infection has been identified as a potential mechanism involved in atherothrombosis worsening. Indeed, *Porphyromonas gingivalis* (*P.gingivalis*) is considered to be a major periodontal pathogen involved in the onset and development of the diseases. Its ability to disrupt the epithelial barrier, as well as the endothelium barrier, and to induce a sustained inflammatory response contributes to tissue destruction. In this thesis, we evaluated the effects of *P.gingivalis* on apoptosis and inflammation of epithelial cells (GEC), fibroblasts (FB) and in a 3D model of microtissue (MT), as well as in endothelial cells (EC). Finally, we evaluated its role in the signaling-related inflammatory response via TLR-2 and TLR-4 and its five TIR-domain-containing adaptors proteins (TIR). We have shown that *P.gingivalis* is able to activate the inflammation and host-immune response, resulting in the destruction of the *periodontium* through modulation of primordial biological processes of various cell types, such as apoptosis (modulation of apoptosome Apaf-1 and its inhibitor XIAP), cell cycle (P53, P21, CDK4), inflammation (modulation of TLR-2, TLR-4, its MAL and TRAM adaptors proteins and inflammatory proteins such as TNF-α) , allowing it to escape from the immune system contributing to periodontal destruction and its systemic dissemination. The discovery of new mechanisms or new molecular targets affected by this pathogen will allow us to develop new therapeutic strategies.

Université de Strasbourg

Inserm
La science pour la santé
From science to health

Isaac Maximiliano BUGUENO VALDEBENITO

« Impact de l'infection par *Porphyromonas gingivalis* sur la réponse inflammatoire locale et systémique »

École Doctorale des Sciences de la Vie et de la Santé
STRASBOURG

Résumé

Les mécanismes impliqués dans l'initiation et le développement des parodontites, ainsi que la dissémination des parodontopathogènes via la circulation systémique et ses effets au niveau vasculaire, restent peu connus. L'infection chronique a été décrite comme un mécanisme potentiel impliqué dans l'aggravation de l'athérothrombose. A l'heure actuelle, le rôle joué par *Porphyromonas gingivalis (P.gingivalis)* est considéré comme majeur dans les phénomènes associés, tels que sa capacité à perturber la barrière épithéliale ainsi que l'endothélium vasculaire, l'induction d'une réponse inflammatoire soutenue contribuant à la destruction tissulaire. Dans ces travaux de thèse, nous avons évalué les effets de *P.gingivalis* sur l'apoptose et l'inflammation des cellules épithéliales (GEC), fibroblastiques (FB) et dans un modèle 3D de microtissus (MT), ainsi que dans des cellules endothéliales (EC). Finalement, nous avons évalué son rôle dans la réponse inflammatoire liée à la signalisation via les TLR-2 et TLR-4 et cinq protéines adaptatrices contenant le domaine du récepteur Toll/interleukine-1 (TIR). Nous avons mis en évidence que *P.gingivalis* est capable d'activer l'inflammation et la réponse du système immunitaire entraînant la destruction du parodonte en modulant différentiellement des processus biologiques primordiaux tels que l'apoptose (modulation de l'apoptosome Apaf-1 et son inhibiteur XIAP), le cycle cellulaire (P53, P21, CDK4), l'inflammation (modulation des TLR-2, TLR-4 et ses adaptateurs MAL et TRAM et des protéines inflammatoires telles que TNF-α), lui permettant d'échapper au système immunitaire, de contribuer à la destruction parodontale et sa dissémination systémique et d'exercer des effets sur l'endothélium. La mise en évidence de nouveaux mécanismes ou de nouvelles cibles cellulaires affectées par ce pathogène pourrons nous permettre de développer de nouvelles stratégies thérapeutiques.

Mots clés : *Porphyromonas gingivalis ; Parodontite ; Athérosclérose ; Apoptose ; Inflammation ; Cibles thérapeutiques.*

Résumé en anglais

The mechanisms involved in the initiation and development of periodontitis, as well as the dissemination of periodontal pathogens via the systemic circulation and their effects at the vascular level, remain poorly described. Chronic infection has been identified as a potential mechanism involved in atherothrombosis worsening. Indeed, *Porphyromonas gingivalis* (*P.gingivalis*) is considered to be a major periodontal pathogen involved in the onset and development of the diseases. Its ability to disrupt the epithelial barrier, as well as the endothelium barrier, and to induce a sustained inflammatory response contributes to tissue destruction. In this thesis, we evaluated the effects of *P.gingivalis* on apoptosis and inflammation of epithelial cells (GEC), fibroblasts (FB) and in a 3D model of microtissues (MT), as well as in endothelial cells (EC). Finally, we evaluated its role in the signaling-related inflammatory response via TLR-2 and TLR-4 and its five TIR-domain-containing adaptors proteins (TIR). We have shown that *P.gingivalis* is able to activate the inflammation and host-immune response, resulting in the destruction of the periodontium through modulation of primordial biological processes of various cell types, such as apoptosis (modulation of apoptosome Apaf-1 and its inhibitor XIAP), cell cycle (P53, P21, CDK4), inflammation (modulation of TLR-2, TLR-4, its MAL and TRAM adaptors proteins and inflammatory proteins such as TNF-α) , allowing it to escape from the immune system contributing to periodontal destruction and its systemic dissemination. The discovery of new mechanisms or new molecular targets affected by this pathogen will allow us to develop new therapeutic strategies.

Keywords: *Porphyromonas gingivalis; Periodontitis; Atherosclerosis; Apoptosis; Inflammation; Therapeutic targets.*